Functional characterisation of three transcription factors downstream of RIPENING INHIBITOR that control tomato plant morphology and fruit development and ripening

Jack Christian Gillan

This thesis was submitted for the degree of Doctor of Philosophy at Royal Holloway University of London, November 2018.

Declaration of Authorship

I, Jack Christian Gillan, hereby declare that the work presented in this thesis is original work of the author unless otherwise stated. Original material used in the creation of this thesis has not been previously submitted either in part or whole for a degree of any description from any institution.

Signed: 

Abstract

Tomato (*Solanum lycopersicum*) is one of the most extensively consumed fruit crops worldwide. Therefore, the identification of genes central to fruit development and ripening, which influence fruit quality, remains an important objective. Previously, the *RIPENING INHIBITOR* (*RIN*) transcription factor was shown to be a global ripening-regulator. Current breeding strategies have utilised the heterozygous *rin* mutation as fruits display reduced fruit softening, expanding distribution and storage opportunities, despite negatively impacting both fruit colour and flavour. Therefore, downstream targets of RIN have been identified in order to facilitate a more targeted approach for tomato improvement. Using Systems Biology outputs derived from transcriptomics performed over fruit development and ripening, three transcription factors were identified, including the direct RIN target *ZINC FINGER PROTEIN INDETERMINATE DOMAIN 2* (*ZFPIDD2*), and predicted indirect RIN targets: *ZINC-FINGER PROTEIN ZPR1* and *HEAT SHOCK TRANSCRIPTION FACTOR A3* (*HSFA2*). These transcription factors were manipulated through the insertion of a knock-down RNAi construct under constitutive control (CaM35S).

Down-regulation of *ZFPIDD2* resulted in several plant developmental differences, including reduced internode lengths, elevated non-vegetative biomass with increased fruit number, size and total yield. Fruits displayed a partial uncoupling of ripening: with significant reduction to fruit softening and potential extension to shelf-life, combined with elevated colour-associated ripening and carotenoid content. Therefore, the improvements of the *rin* mutation are maintained, while enhancing yield and colour development. Similar ripening-related improvements were demonstrated by *ZPR1* transgenic lines, containing the knock-down construct, with altered phenolics and less development and fruit yield-associated differences. *HSFA2* transgenic lines exhibited phenotypes similar to *hy5* down-regulation: including extended shoot growth during early development, paler leaves and reduced carotenoid content in ripe fruits. Despite not providing targeted improvements, all three transcription factors were shown to be important for development and fruit ripening-related quality traits. This study provides further insight into transcriptional control of tomato development and ripening, and future approaches to trait improvement using the emerging technologies associated with gene editing.

Acknowledgments

My PhD has proven to be an exciting and challenging adventure, which has enabled me to fulfil a personal ambition and to grow as a person.

I would like to thank my supervisor Prof. Paul Fraser for the opportunity to work within an exciting PhD project and in an excellent international laboratory. I am grateful for his support, expert knowledge, guidance and scientific discussions throughout. I would like to express my gratitude to my second supervisor, Dr Genny Enfissi, and my advisor, Prof. Peter Bramley for their encouragement and pertinent questions, also my lab colleagues for their friendship and willingness to help. I would also like to acknowledge my project collaborators Prof. Graham Seymour of Nottingham University and Syngenta for provision of material and support, and Royal Holloway for my Crosslands scholarship.

Finally, to my Mum and Dad who have been with me on every step of this journey. I thank them for their never wavering commitment and faith in me. Without their love and guidance I would not be where I am today and the person I have become.

I am extremely proud of this achievement, which has provided me with the strength, determination and resolve to succeed in life.

Jack

Table of Contents

List of Figures

List of Tables

List of Abbreviations

1-MCP	1-methylcyclopropene
ABA	Abscisic acid
Abs	Absorbance
AC	Ailsa craig
ACC	AMINOCYCLOPROPANE-1-CARBOXYLIC ACID
ACO	1-AMINOCYCLOPROPANE-1-CARBOXYLIC ACID OXIDASE
ACS	AMINOCYCLOPROPANE-1-CARBOXYLIC ACID SYNTHASE
ANN	Artificial neural network
AP2A	APETALA2
APRR2	TWO-COMPONENT RESPONSE REGULATOR-LIKE
ARF	AUXIN RESPONSE FACTORS
BSA	Bovine serum albumin
Br	Breaker stage
C	Carbon
°C	Celsius
Ca	Chlorophyll a concentration
CAB	CHLOROPHYLL A/B-BINDING PROTEIN
CAR	Carotenoid
Cas	CRISPR associated proteins
35S	Cauliflower mosaic virus 35S promoter
Cb	Chlorophyll b concentration
CHI	CHALCONE ISOMERASE
ChIP	Chromatin immunoprecipitation
CHS	CHALCONE SYNTHASE
CI	CYTOPLASMIC INVERTASE
CK	Cytokinin
CLP	CASEIN LYTIC PROTEINASE
CNR	COLOURLESS NON-RIPENING
CRISPR	Clustered regularly interspaced palindromic repeats
CRTB	BACTERIAL PHYTOENE SYNTHASE
CRTE	BACTERIAL GGPP SYNTHASE
CRTI	BACTERIAL PHYTOENE DESATURASE
CRTISO	CAROTENOID ISOMERASE
CRTR-B1	B-CAROTENE HYDROXYLASE 1
CRTR-B2	B-CAROTENE HYDROXYLASE 2
CRTW	BACTERIAL B-CAROTENE KETOLASE
CRTZ	BACTERIAL B-CAROTENE HYDROXYLASE
CRTY	BACTERIAL LYCOPENE CYCLASE
Ct	Cycle threshold
Cv	Cultivar
CWI	CELL WALL INVERTASE
Cx+c	Total carotenoid concentration
c-ZR	Cis-zeatin riboside
CYC-B	FRUIT SPECIFIC LYCOPENE β-CYCLASE
CYP97A	Haem-containing CYTOCHROME P450 β-RING HYDROXYLASE
CYP97C	Haem-containing CYTOCHROME P450 ε-RING HYDROXYLASE
DDB1	DAMAGED DNA BINDING PROTEIN 1
DET1	DE-ETIOLATED 1
DFR	DIHYDROFLAVONOL-4-REDUCTASE
DGDG	Digalactosyldiacylglycerol

dH_2O	Distilled water
DMAPP	Dimethylallyl diphosphate
DNA	Deoxyribonucleic acid
Dpa	Days post anthesis
Dpb	Days post breaker
DXP	1-DEOXY-D-XYLULOSE 5-PHOSPHATE
DXS	1-DEOXY-D-XYLULOSE 5-PHOSPHATE SYNTHASE
DXR	1-DEOXY-D-XYLULOSE 5-PHOSPHATE REDUCTOISOMERASE
DW	Dry weight
E8	ACC OXIDASE homolog
EDTA	Ethylenediaminetetraacetic acid
EIL	ETHYLENE INSENSITIVE 3-LIKE
EIN2	ETHYLENE INSENSITIVE 2
EMS	Ethyl methane sulfonate
ERF	ETHYLENE RESPONSE FACTOR
ERFC4	ETHYLENE RESPONSIVE TRANSCRIPTION FACTOR C4
ETR	ETHYLENE RESPONSE family
EXP	Expansin family
EXP1	EXPANSIN 1
F3H	FLAVANONE-3-HYDROXYLASE
F3’H	FLAVONOID-3′-HYDROSYLASE
FAOSTAT	Food and Agriculture Organisation of the United Nations
FID	Flame ionisation detector
FK	FRUCTOKINASE
FLC	FLACCA
FLIM	Fluorescence lifetime imaging microscopy
FLS	FLAVONOL SYNTHASE
FPP	Farnesyl diphosphate
FUL1	FRUITFULL 1
FUL2	FRUITFULL 2
FW	Fresh weight
GA3P	Glyceraldehyde-3-phosphate
GA	Gibberellic acid
GA4-Me	Gibberellic acid 4 – methyl ester
GA20ox	GA 20-oxidase
GC-MS	Gas Chromatography Mass Spectrometry
GGPP	Geranyl geranyl diphosphate
GGPPS	GERANYL GERANYL DIPHOSPHATE SYNTHASE
GID1	GIBBERELLIN INSENSITIVE DWARF1
GMO	Genetically modified organism
GPP	Geranyl diphosphate
GPPS	GERANYL DIPHOSPHATE SYNTHASE
GT	FLAVONOL-3-GLUCOSYLTRANSFERASE
GWAS	Genome-wide association study
h	Hour
HB-1	HD-ZIP 1
HCl	Hydrochloric acid
HDR	4-HYDROXY-3-METHYLBUT-2-ENYL DIPHOSPHATE REDUCTASE
B-HEX	β-D-N-ACETYLHEXOSAMINIDASE
HG	Homogalacturonan
HK	HEXOKINASE
HP-1	HIGH PIGMENT 1
HSFA2	HEAT STRESS TRANSCRIPTION FACTOR A3

HSP	HEAT SHOCK PROTEIN family
HSP4	HEAT SHOCK PROTEIN 4
HSP30	HEAT SHOCK PROTEIN 30
HSP70	HEAT SHOCK PROTEIN 70
HSP110	HEAT SHOCK PROTEIN 110
HY5	ELONGATED HYPOCOTYL 5
IAA	Indoleacetic acid
IDD	INDETERMINATE DOMAIN family
IDD2	INDETERMINATE DOMAIN 2
IPP	Isopentenyl diphosphate
ISPE	4-DIPHOSPHOCYTIDYL-2-C-METHYL-D-ERYTHRITOL KINASE
JA	Jasmonic acid
LB	Luria Broth medium
LCY-ε	LYCOPENE ε-CYCLASE
LCY-β	LYCOPENE β-CYCLASE
LC-MS	Liquid chromatography mass spectrometry
LIN5	SUCROSE INVERTASE CWIN1
LOX	LIPOXYGENASE family
LOXC	LIPOXYGENASE C
MADS-MC	MACROCALYX
A-MAN	α-MANNOSIDASE
MEP	2-C-Methyl-D-erythritol 4-phosphate
Min	Minute
MG	Mature green stage
MVA	Mevalonate pathway
NCED	9-*CIS*-EPOXYCAROTENOID DIOXYGENASE
NI	NEUTRAL INVERTASE
NOR	NON-RIPENING
NOT	NOTABILIS
NPQ	Non photochemical quenching
NPTII	NEOMYCIN PHOSPHOTRANSFERASE II
NR	NEVER RIPE
NXS	NEOXANTHIN SYNTHASE
OR	ORANGE
PCA	Principal component analysis
PCR	Polymerase chain reaction
PDA	Photo-diode array
PDS	PHYTOENE DESATURASE
PE	PECTINESTERASE
PG	ENDO-POLYGALACTURONASE
PG2A	POLYGALACTURONASE A
PIF	PHYTOCHROME-INTERACTING FACTOR family
PIF3	PHYTOCHROME-INTERACTING FACTOR 3
PL	PECTATE LYASE
PME	PECTIN METHYLESTERASE
PS	Phosphatidylserine
PSII	Photosystem II
PSY-1	FRUIT SPECIFIC PHYTOENE SYNTHASE 1
PSY-2	PHYTOENE SYNTHASE 2
PTGS	Post transcriptional gene silencing
qPCR	Quantitative PCR
QTL	Quantitative trait loci
RG-I	Rhamnogalacturonan I

RG-II	Rhamnogalacturonan II
RIN	RIPENING INHIBITOR
RNA	Ribonucleic acid
RGN	RNA-guided nucleases
RNAi	RNA interference
ROS	Reactive oxygen species
RT	FLAVONOL-3-GLUCOSIDE-RHAMNOSYLTRANSFERASE
RT-PCR	Reverse transcription PCR
RTqPCR	Quantitative real time reverse transcription
SBP	SQUAMOSA PROMOTER-BINDING PROTEIN
SCL3	SCARECROW-LIKE 3
SD	Standard deviation
SDS	Sodium dodecyl sulphate
Sec	Second
SEP	SEPALLATA
SGR1	SENESCENCE-INDUCIBLE CHLOROPLAST STAY-GREEN PROTEIN1
SK	Shikimate pathway
SlARF7	AUXIN RESPONSE FACTOR 7
SlERF6	ETHYLENE RESPONSE FACTOR 6
SUCR	SUCROSE ACCUMULATOR
T_0	Primary generation
T_1	Second generation
T_2	Third generation
T_3	Fourth generation
TAGL1	AGAMOUS-LIKE1
TB	Transfer buffer
TBG	β- GALACTOSIDASE
TILLING	Targeting Induced Local Lesions IN Genomes
Tm	Melting temperature
Tris	Tris-hydroxymethyl-aminomethane
t-ZR	Trans-zeatin riboside
UPLC	Ultra High Performance Liquid Chromatography
USDA	U.S. Department of Agriculture
UV	Ultraviolet
V	Volt
VDE-1	VIOLAXANTHIN DE-EPOXIDASE
VI	VACUOLAR INVERTASE
VIF	VACUOLAR INVERTASE INHIBITOR
VIGS	Virus-induced gene silencing
VTE	Vitamin E
WPTC	World Processing Tomato Council
WT	Wild-type
XET	XYLOGLUCAN XYLOGLUCOSYLTRANSFERASE
XTH	XYLOGLUCAN TRANSGLYCOSYLASE/HYDROLASE
ZEP-1	ZEAXANTHIN EPOXIDASE
ZFP	ZINC FINGER PROTEIN family
ZFPIDD2	ZINC FINGER PROTEIN INDETERMINATE DOMAIN 2
Z-ISO	15-C*IS*- Z -CAROTENE ISOMERASE

Chapter I: Introduction

1.1 The value of tomato

Tomato (*Solanum lycopersicum*) is the most extensively consumed fruit crop worldwide. Production has steadily increased from 130.5 to 177.1 million tonnes between 2006 and 2016 (FAOSTAT Database, 2018). The net production value has risen from $47.6 to $64.7 billion throughout the same period, making it the fifth most important crop in the world in terms of global net production value. Currently, Asia produces the largest share of tomatoes worldwide (60.1%) followed by the Americas (14.7%) and Europe (13.7%), although consumption was greatest in the Americas and Europe then Africa. Interestingly, the average annual fresh tomato consumption is 18 kg per European and 8 kg per capita in the US (Department of Agriculture US. Economic Research Service, Tomatoes, 2008; Raiola et al., 2014). Production is steadily rising, due to increasing demand for the fresh market fruit and processing products including soups, sauces, purees, canned, juices and powder forms (Raiola et al., 2014; Raiola et al., 2015) (Figure 1-1). In total the World Processing Tomato Council estimated that 40 million tonnes of tomatoes were processed worldwide (WPTC, 2015; Nour et al., 2018).

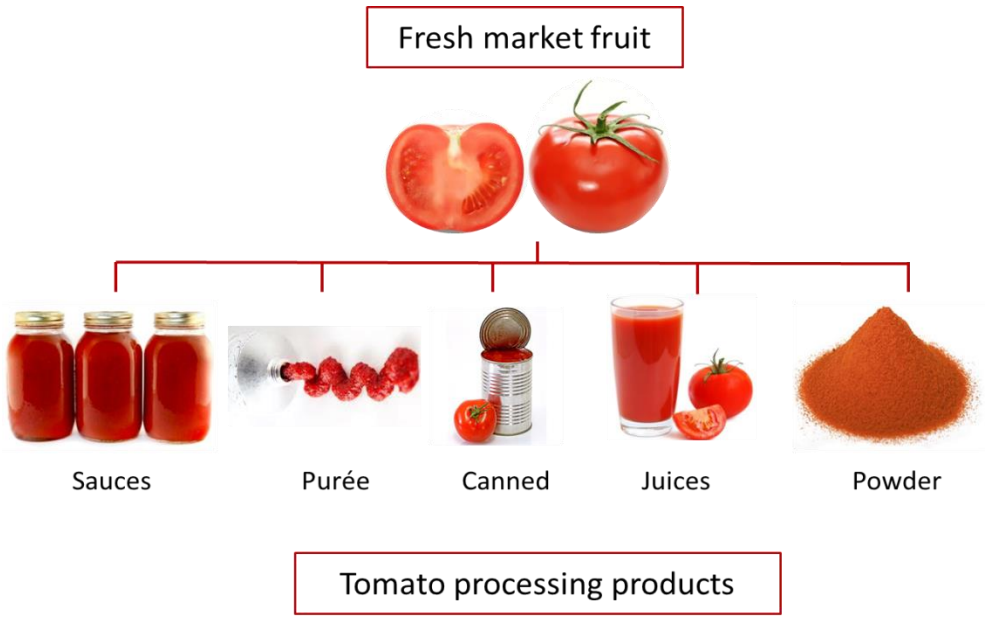

Figure 1-1 The wide ranging products of tomato fruits.

Being perennial, often self-fertile and tolerant to stresses, with short crop duration, high yields, combined with the capability of fruit production throughout the whole year using poly tunnels, fields or glasshouses have contributed to increased tomato cultivation. Field tomatoes are amenable to mechanical harvesting, thus allowing vast tonnages to be grown and processed economically. Similar to other plant species that are part of our diet, tomatoes are an important source of substances with known beneficial effects on health, including vitamins, organic acids, minerals, antioxidants and dietary fibre (USDA, 2018; Raiola et al., 2014).

Tomato is considered to be an important model system to study fleshy-fruit ripening (outlined in Karlova et al., 2014), due to its: diploid genetics, a range of well characterised single gene mutants, recombinant inbred lines, mapping populations and an excellent and well-annotated genome sequence (Giovannoni, 2004; The Tomato Genome, 2012). Furthermore, rich omics data resources including several databases are available for exploring genome and expressed sequence tag (EST) sequences (Sol Genomics Network; Mueller et al., 2005, Bombarely et al., 2011), and for gene expression analysis (Tomato Expression Database; Fei et al., 2006, Shinozaki et al., 2018). Advanced transcriptomic, metabolomic and proteomic platforms are established, while efficient transformation protocols have been developed.

Tomato was selected because of its agronomic value, its nutritional importance, whilst being a model crop species for studying fleshy-fruit ripening, thus any potential advancement through crop improvement would have a significant impact.

1.2 Tomato distribution and supply chains

Various factors from both local and global supply chains (Figure 1-2) dictate the maturity stage in which tomatoes are harvested, including distribution distances, storage and marketable life and overall fruit quality. Each stage at harvest has its own postharvest attribute that the fruit will exhibit. In many parts of the world, including the United States of America and China, tomatoes are generally picked at the mature green stage when fruits are still firm (Edan et al., 1997). Subsequently, costs are reduced because fewer harvests are necessary (Davis and Gardner, 1994); while the fruits themselves are able to withstand handling and transportation and have a longer

marketable shelf-life compared to other stages in order to limit losses (Moneruzzaman et al., 2009). Despite this, the nutritional values and appearance may be affected when harvesting at mature green stages (Cliff et al., 2009; Moneruzzaman et al., 2009). Fruits then undergo ripening simultaneously or with ethylene treatment prior to shipment to retailers (Wills and Ku, 2002). However, for European based markets fruits are often harvested later in development, as less time is required for ripe fruit to reach the acceptable conditions for consumers due to shorter transportation distances. Therefore, limiting the losses caused by excessive deterioration during holding and marketing of fruits. Harvesting at ripe also maximises their nutritional value and promotes greater sugar accumulation (Arah et al., 2015). Fruits destined for processing, for canning or juice extraction for instance, are harvested at the turning or ripe stages (Rama and Narasimham, 2003; Arah et al., 2015). The pH of fruits is an important parameter for the processing industry, where tomatoes are processed as high-acid foods. Therefore, there is a demand for fruits with a higher acidity (pH 4.25-4.4); hence fruits are often harvested at the turning stage prior to the rapid decline of acids as fruits ripen (Monti, 1979; Arah et al., 2015).

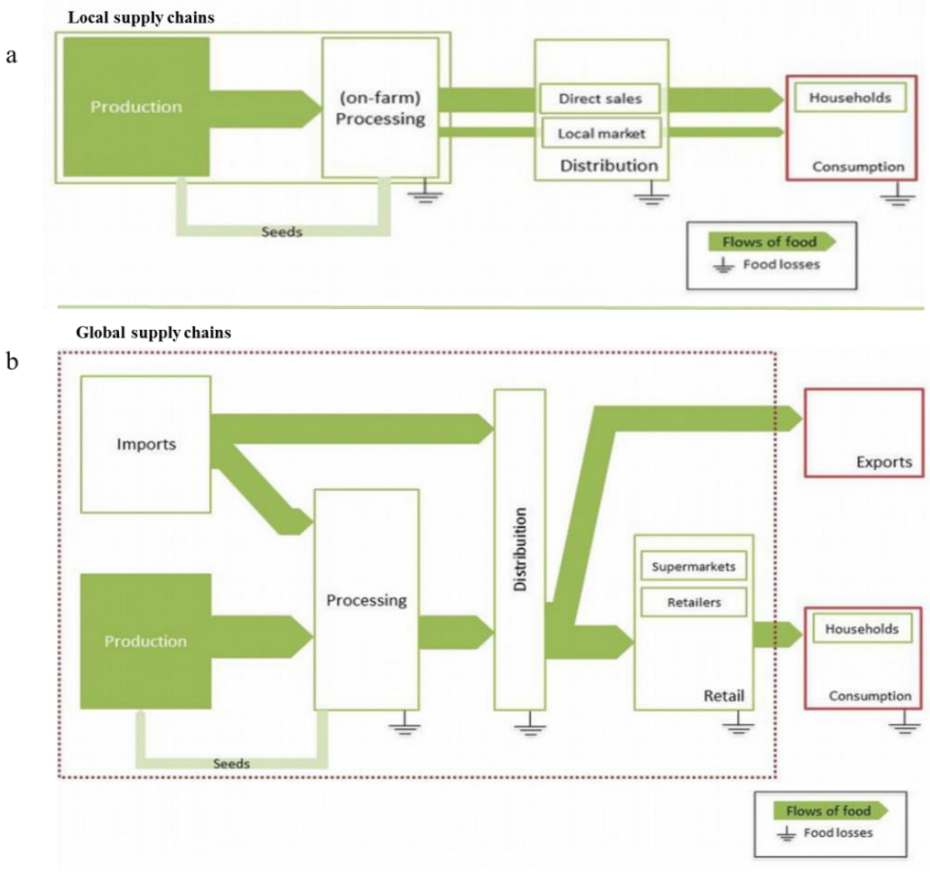

Figure 1-2 Comparison of local and global tomato supply chains. Adapted from (Gamboa et al., 2017).

1.3 Tomato development

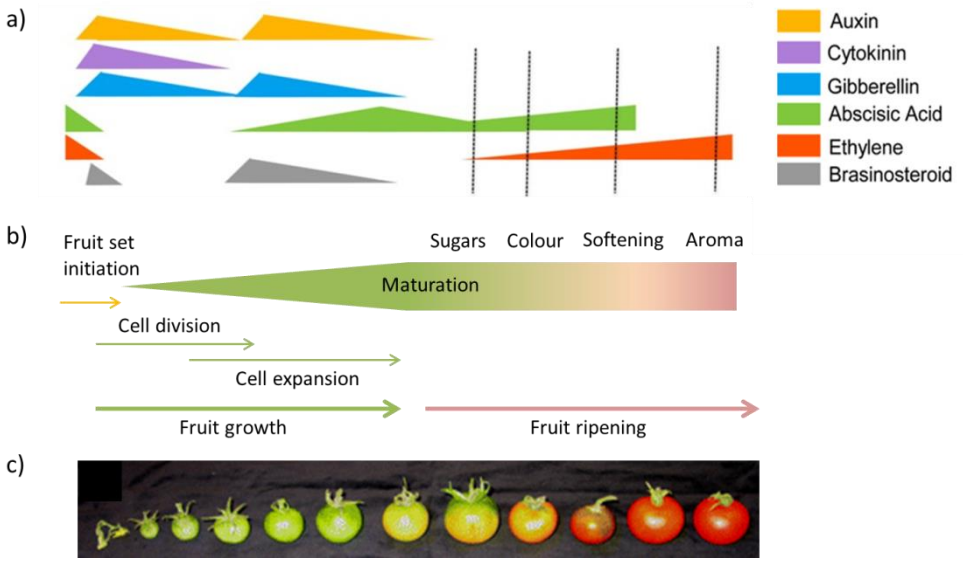

Figure 1-3 Hormonal and physiological changes during tomato development and ripening.

The hormonal (a) and physiological (b) changes during flower fertilisation, fruit set, development and ripening. A developmental and ripening time series is shown (c).

1.3.1 Tomato fruit set

Early fruit development consists of three distinct stages. In phase I, the ovary differentiates from the floral meristem and develops to a point where it is ready for fertilization, enabling fruit set. Fruit set represents the first step of fruit development, and is defined as the changeover from the static condition of the flower ovary to the rapidly growing condition of the young fruit, and is dependent on the completion of ovary fertilization (Gillaspy et al., 1993). Phase II encompasses fertilisation and subsequent cell division. Fertilization after pollination requires pollen germination on the pistil, forming a pollen tube. The penetration and growth of the pollen tube in the stylar tissue and ovular micropyle, enables the delivery of two sperm cells to the embryo sac for fusion with the egg cell. Double fertilisation occurs fertilizing the embryo and the endosperm (Raghavan, 2003; Hamamura et al., 2012). Consequently, both embryo and surrounding tissues may generate signals that stimulate the development of the ovary

into a fruit. Fruit growth continues during phase III, which primarily comprises of cell expansion rather than division.

Fruit set can be attributed to the action of three hormones, auxin, gibberellin and cytokinin that increase upon fruit set (Figure 1-3) (Srivastava and Handa, 2005; Mariotti et al., 2011; McAtee et al., 2013; Kumar et al., 2014). Individually, any of these hormones can initiate fruit development to a certain extent; when applied in combination normal fruit growth can be achieved in the absence of fertilisation (Nitsch, 1952; Crane, 1964; Gillaspy et al., 1993; Vivian-Smith and Koltunow, 1999; Wuddineh et al., 2015). The results demonstrates that interplay between these hormones is necessary for fruit set and fruit growth.

Gibberellin (GA) has been shown to be important for fruit set initiation in tomato. Disruption to GA biosynthesis by *gib1*, *gib2* and *gib3* mutations resulted in fruit failing to set or develop, while these defects were rescued with the application of GA (Bensen and Zeevaart, 1990). Furthermore, application of exogenous GA_3 to unpollinated ovaries increases fruit set, although fruits are parthenocarpic (seedless) with reduced sizes of locular tissues and fruits compared with pollinated fruits (Wuddineh et al., 2015; Chen et al., 2016). While application of GA biosynthesis inhibitors limits fruit set, fruits were also smaller than untreated pollinated fruits (Bünger-Kibler and Bangerth, 1982; Fos et al., 2000; Olimpieri et al., 2007; Serrani et al., 2007b). Serrani et al., (2007) identified GA_1 as the most effective modulator of fruit set induction, and GA 20-oxidases (GA20ox) activity is most likely a limiting factor in the control of GA_1 biosynthesis.

Interaction between auxin and GA signalling pathways is essential for the promotion of fruit set in fleshy fruits (Vivian-Smith and Koltunow, 1999; Srivastava and Handa, 2005; Serrani et al., 2008; de Jong et al., 2009a; Carrera et al., 2012; Ruan et al., 2012). Auxin appears to promote fruit set and growth, at least partly through GA, with the ability to induce GA biosynthesis early during fruit development (Serrani et al., 2008), although each hormone independently has specific functions. Auxin-induced fruit contain many more cells compared to GA-induced fruits, which contain fewer but larger cells (Bünger-Kibler and Bangerth, 1982). Characterisation of *AUXIN RESPONSE FACTOR* (*SlARF7*) at the molecular level, revealed it to be an important player in gibberellin–auxin crosstalk, controlling both auxin and GA signalling (de Jong et al., 2009b; de Jong et al., 2011). Silencing of *SlARF7* resulted in constitutive auxin responses, including parthenocarpic fruit formation, indicating that inactivation of *SlARF7* is important for fruit set initiation. The development of parthenocarpic fruit with thick pericarps and

large cells were consistent with GA-induced fruit, suggesting *SlARF7* also acts as a modifier of the GA response during early stages of fruit development. Further evidence for this was identified with a point mutation in a gene encoding the DELLA protein, which resulted in a constitutive GA response and parthenocarpic fruit in *procera* (*pro*) mutant lines (Carrera et al., 2012). Altered transcript levels of genes involved in GA and auxin pathways were identified by transcriptome analysis, including *SlARF7*, providing further evidence of *SlARF7* involvement in GA responses during fruit development. DELLA proteins have been shown to tightly regulate GA-mediated responses, and their degradation is required for GA signalling. Reductions to DELLA activity impacts fruit set, resulting in fruits that were smaller and parthenocarpic, highlighting its importance to fruit development (Marti et al., 2007).

Cytokinin levels also increase after pollination (Matsuo et al., 2012). Its levels directly correlated to fruit growth (Srivastava and Handa, 2005). Application of cytokinin also results in the formation of parthenocarpic fruit (Gillaspy et al., 1993; Srivastava and Handa, 2005; Mariotti et al., 2011; Matsuo et al., 2012). Cytokinin-treated tomato seedlings mimic the *diogeotropica* (*dgt*) mutant phenotype, with reduced shoot growth and apical dominance (Coenen et al., 2003). In *Arabidopsis*, cytokinins also have roles in fruit development, including the development of the medial region of the gynoecia and formation of valve margins (Marsch-Martinez et al., 2012). Several studies have highlighted potential interactions between cytokinin and auxin (Coenen et al., 2003; Murray et al., 2012), specifically cytokinin could act via inhibiting auxin responses during fruit set and growth.

Abscisic acid (ABA) and ethylene are expected to play an antagonistic role in fruit set (Kumar et al., 2014), keeping the ovary in a temporally protected and dormant state prior to fertilisation (Pascual et al., 2009). ABA levels decrease upon fruit set, consistent with the downregulation of ABA biosynthesis genes and upregulation of ABA degradation genes (Vriezen et al., 2008). While ethylene has been shown to inhibit fruit set in tomato by suppressing GA metabolism (Shinozaki et al., 2015). Reduced ethylene sensitivity triggers accumulation of GA; increasing bioactive GA biosynthesis and decreasing GA inactivation. This results in parthenocarpy accompanied by pollination-independent cell expansion in the ovary. Ethylene promotes senescence of ovaries that fail to set fruit in tomato, by promoting expression of the senescence-associated genes *SlSAG12* and *SlNAP* (Shinozaki et al., 2018a). Many factors contribute to the process of fruit set, but their exact action and relations still needs more investigation.

1.3.2 Tomato development

Fruit set is followed by the development of both fruit and seeds, including two consecutive fruit growth phases, which are controlled by a precise and genetically controlled process mediated by phytohormones (Gillaspy et al., 1993). Phase II involves a period of cell division for 10-14 days, during which most of the fruit cells are established. Phase III primarily comprises of cell expansion rather than division continuing for 3-5 weeks, and is responsible for attainment of the maximum fruit size. Developing seed continually send signals for surrounding tissues to expand, thus contributing to fruit growth, which is shown by a positive correlation between seed number and fruit size (McAtee et al., 2013). Hormones are expected to originate mostly from the seed, and have to be transported to the surrounding tissue and/or are synthesized directly in the expanding tissue, with the exception of auxin. In addition, fruit growth is dependent on signals from developing fruits to the plant to ensure sufficient nutrient supply is available.

GA has been shown to accumulate during fruit cell division and cell expansion at early developmental stages (Figure 1-3) (Srivastava and Handa, 2005). Pollination promotes the expression of GA 20-oxidases, the rate limiting step involved in the syntheses of the main bioactive GA forms, GA_1 and GA_4 (Serrani et al., 2007b). The same study used a GA inhibitor that reduced both fruit growth and GA_1 content, thus GA_1 proved to be the main active GA in developing fruits. The pericarp of GA-induced fruit contains fewer cells with a larger volume, demonstrating that cell expansion might be enhanced by GAs (Bünger-Kibler and Bangerth, 1982; Serrani et al., 2007a).

Auxin also displays a bimodal pattern of activity, with peaks of activity at 10 and 30 days after anthesis in developing tomato fruits (Figure 1-3). The latter suggest that the hormone is involved with the initiation of the cell expansion phase (phase III) and during the final embryo development (Gillaspy et al., 1993; Srivastava and Handa, 2005). Auxin plays an important role during the growth phase by influencing cell enlargement together with GAs (Csukasi et al., 2011). In tomato, auxin gradients are maintained by the precise localisation of auxin transporters, such as the PIN transporters, which are important for fruit growth (Pattison and Catalá, 2012). Whereby, auxin in the outer layer of placental cells stimulates the placental expansion to surround the seeds and fill the locular cavity. Several genes belonging to EXPANSINS, ENDO-XYLOGLUCAN TRANSFERASE and PECTATE LYASES families have been shown to be regulated by

either auxin and GA, or both (de Jong et al., 2011; Carrera et al., 2012). Furthermore, AUXIN RESPONSE FACTORS (ARFs) that regulate auxin responses, have been shown to be involved in the regulation of cell division, thus could be part of the molecular mechanism underlying fruit yield (Kumar et al., 2011; Devoghalaere et al., 2012).

Additionally, ABA has been implicated in the regulation of the expansion phase of fruit growth, and not with cell division (Figure 1-3) (Gillaspy et al., 1993; Nitsch et al., 2012). ABA-deficient mutants produce smaller fruit; all parts of mature fruits were reduced including the pericarp, locule and placenta. The reduction to fruit size is hypothesised to be due to water loss through elevated transpiration (Ariizumi et al., 2013). It has been shown that ABA promotes cell expansion in the pericarp by suppressing ethylene production (Nitsch et al., 2012).

Cytokinin (CK) and GA act antagonistically (Weiss and Ori, 2007; Harberd et al., 2009; Fleishon et al., 2011). CK accumulate five days post anthesis when cell division is active (Figure 1-3), indicating a link between CK and cell division (Bohner et al., 1988). Also, a correlation between cell number and CK levels in young developing fruits provides further evidence of CK involvement in cell division (Srivastava and Handa, 2005). Potentially, CK is secreted from developing seeds to promote cell division in the tissues surrounding seeds (Bohner and Bangerth, 1988; Gillaspy et al., 1993). The application of synthetic CK to pre-anthesis ovaries yielded parthenocarpic fruit by activating cell division, acting as a positive regulator of fruit growth (Matsuo et al., 2012).

1.3.3 Tomato maturation

Fruit maturation is the developmental stage where fruits have reached the competence to ripen. Auxin and potentially cytokinin have been shown to be the main regulators of fruit maturation (Figure 1-3), as the levels of these hormones are higher in the *ripening inhibitor* (*rin*) mutant at breaker stage compared with wild-type fruits (Davey and Van Staden, 1978). Furthermore, suppression of the *rin*-like MADS-box gene (*MADS8/9*) resulted in the maintenance of high levels of auxin through maturation, inhibiting the initiation ripening (Ireland et al., 2013; Schaffer et al., 2013). Auxin levels are highest in seeds compared with surrounding tissues. It is expected that as seeds become dormant, auxin biosynthesis or transport to the rest of the fruit is inhibited, enabling fruit to ripen

(Devoghalaere et al., 2012). The addition of auxin to mature fruit from other fruit species also delays ripening (Vendrell, 1985; Manning, 1994; Cohen, 1996; Giovannoni, 2007; Zaharah et al., 2012; Su et al., 2015; Li et al., 2016b). The GH3 class of proteins are required for auxin conjugation and have been shown to maintain the physiologically active concentrations of auxin. High levels of GH3 proteins have been detected during fruit maturation in multiple fruit-bearing species (Bottcher et al., 2010). Their involvement in maturation was highlighted with overexpression of a capsicum GH3 in tomato, which reduced auxin levels and is suspected to responsible for the early fruit-ripening phenotype of these transgenic tomatoes (Liu et al., 2005). Two ripening-associated GH3 genes in tomato were identified, further supporting the hypothesis that a decline in auxin is a prerequisite for the initiation of ripening (Devoghalaere et al., 2012; Kumar et al., 2012). GH3 has been shown to be partially under the control of ABA (Bottcher et al., 2010), which promotes ripening (Zhang et al., 2009b).

The role of CK during maturation is less documented. A CK-deficient mutant of *Arabidopsis* exhibited a non-synchronous ripening phenotype (Werner et al., 2003). Moreover, a reduction to the levels of free CK before ripening initiation in grape was identified (Bottcher et al., 2011).

1.4 Tomato ripening and senescence

Tomato ripening is a highly coordinated developmental process that coincides with seed maturation. It involves changes to the metabolic and physiological traits of a fruit to facilitate seed dispersal, by making fruit attractive to animals. The ripening process transforms the less palatable green fruit into a highly palatable, nutritionally rich, and coloured fruit. Fleshy fruits are physiologically classified as climacteric or non-climacteric. Climacteric fruits such as tomato show a concomitant increase in respiration and ethylene biosynthesis upon initiation of ripening (Figure 1-3). Ethylene synthesis is essential for normal ripening in these species, blocking ethylene synthesis or perception prevents ripening. Non-climacteric fruits such as citrus, grape, and strawberry do not require increased respiration and have a lower requirement of ethylene to ripen, with ABA having a stronger role (McAtee et al., 2013).

Ripening is associated with a colour change of fruits, achieved through the degradation of chlorophyll and production of secondary colour metabolites including both carotenoids and anthocyanins. Also, cell walls undergo textural changes, resulting in either dehiscence or softening, while complex carbohydrates are converted to sugars and flavour and aroma compounds accumulate (Klee and Giovannoni, 2011; Seymour et al., 2013b). The control of ripening is achieved predominantly by ABA and ethylene (Figure 1-3) (Giovannoni, 2004; McAtee et al., 2013; Kumar et al., 2014). Owing to its importance to climacteric fruit ripening, ethylene remains the most extensively hormone studied (Bapat et al., 2010). In climacteric fruit, two systems of ethylene biosynthesis operate during fruit development and ripening. System 1 is responsible for producing basal ethylene levels that are detected in all tissues, which is autoinhibitory and is reported to function during fruit growth. Ethylene production markedly increases in system 2, in an autocatalytic manner during ripening. System 2 is regulated in both an ethylene-dependent and ethylene-independent fashion (Van de Poel et al., 2012). Hormonal alteration, transcriptional regulation, metabolite production and cell wall changes will be reviewed in different sections.

1.4.1 Ripening-related quality traits

1.4.1.1 Biosynthesis of carotenoids

Carotenoids are isoprenoid molecules derived from isopentenyl diphosphate (IPP) (Figure 1-4). IPP can be synthesised via two distinct pathways, the mevalonate (MVA) pathway in the cytosol and mitochondria and the 2-C-methyl-Derythritol 4-phosphate (MEP) pathway in the plastid. IPP is then interconverted into dimethylallyl diphosphate (DMAPP) by isopentenyl diphosphate isomerase. DMAPP serves as the reactive starter molecule for subsequent condensation reactions with IPP. Condensation of further IPP/DMAPP molecules leads to the assembly of geranyl diphosphate (GPP), farnesyl diphosphate (FPP) and geranylgeranyl diphosphate (GGPP). Several isoprenoid families exist based upon the number of carbons and the precursor utilised for their biosynthesis, they include monoterpenes (C10, built from GPP), sesquiterpenes (C15, FPP), both are primarily found in the plastid (Bick and Lange, 2003), along with diterpenes (C20, GGPP), triterpenes (C30, FPP) and carotenoids (C40, GGPP).

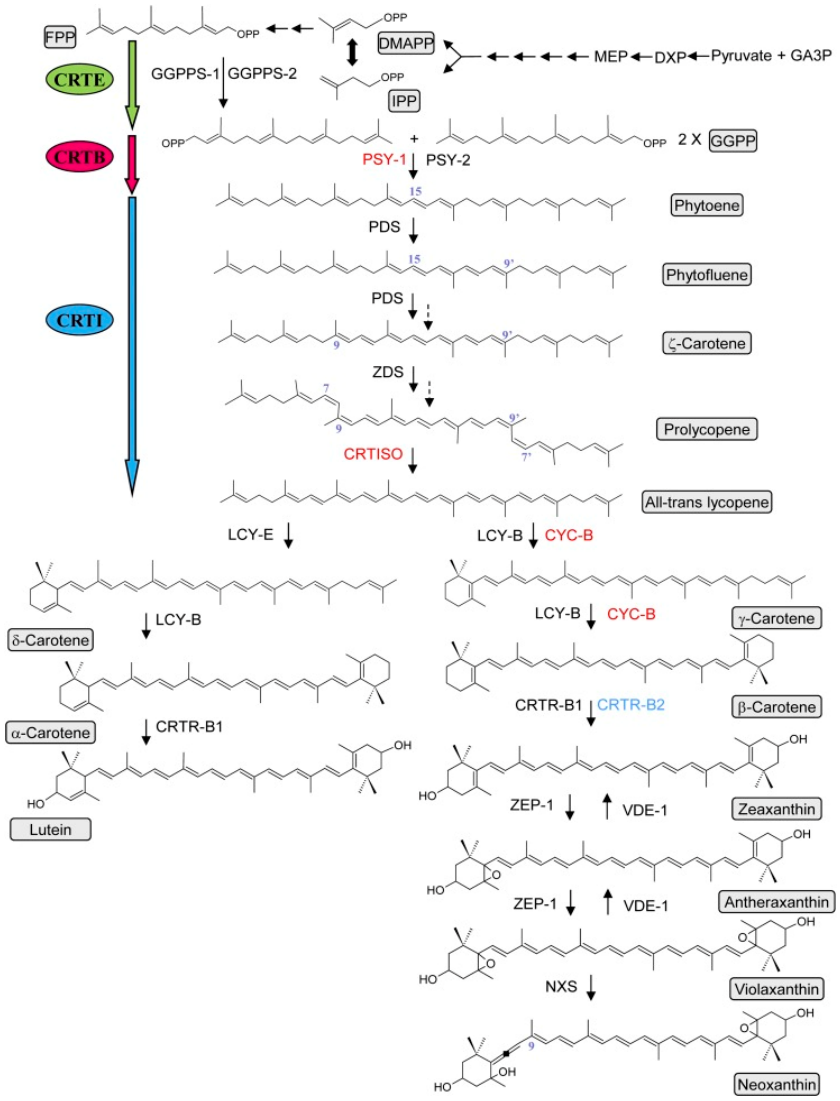

Figure 1-4 Carotenoid biosynthesis pathway in higher plants. Adapted from (Nogueira et al., 2013).

Enzymes displayed in red are tomato fruit ripening specific or enhanced, and those in blue are flower specific. GA3P, glyceraldehyde-3-phosphate; DXP, 1-deoxy-d-xylulose 5-phosphate; MEP, 2-C-methyl-d-erythritol 4-phosphate; IPP, isopentenyl diphosphate; DMAPP, dimethylallyl diphosphate; FPP, farnesyl diphosphate; GGPP, geranylgeranyl diphosphate; GGPPS-1 and -2, GERANYLGERANYL DIPHOSPHATE SYNTHASE; PSY-1, fruit-specific PHYTOENE SYNTHASE-1; PSY-2, PHYTOENE SYNTHASE-2; PDS, PHYTOENE DESATURASE; ZDS, ζ-CAROTENE DESATURASE; CRTISO, CAROTENE ISOMERASE; LCY-ε, ε-LYCOPENE CYCLASE; LCY-β, β-LYCOPENE CYCLASE; CYC-B, fruit-specific β-LYCOPENE CYCLASE; CRTR-B1, CAROTENE β-HYDROXYLASE 1; CRTR-B2, CAROTENE β-HYDROXYLASE 2 (flower specific); ZEP, ZEAXANTHIN EPOXIDASE; NXS, NEOXANTHIN SYNTHASE; VDE, VIOLAXANTHIN DEEPOXIDASE; CRTE, GERANYLGERANYL DIPHOSPHATE SYNTHASE; CRTB, PHYTOENE SYNTHASE; and CRTI, PHYTOENE DESATURASE.

The enzymes GPP SYNTHASE (GPS) and GGPP SYNTHASE (GGPS) add a supplemental IPP unit to IPP or DMAPP and GPP, respectively (Figure 1-4). Then PHYTOENE SYNTHASE (PSY) catalyses the condensation of two GGPP molecules to form 15-cis phytoene, the first committed step in the carotenoid pathway (Giuliano et al., 1993). Two variants of PHYTOENE SYNTHASE (PSY-1 and PSY-2) have been identified and characterised in tomato. PSY-1 is fruit and flower specific, while PSY-2 predominates in the chloroplasts of green tissues and is not involved in carotenogenesis in ripening fruit (Fraser et al., 1999; Fraser et al., 2000). Phytoene is converted to form phytofluene and then ζ-carotene by PHYTOENE DESATURASE (PDS), which catalyses two consecutive condensation reactions. An isomerisation catalysed by ζ-CAROTENE ISOMERASE (Z-ISO), transforms *tri-cis*-ζ-carotene to *di-cis* (Chen et al., 2010). Then *di-cis*- ζ-carotene undergoes two desaturation reactions to first become neurosporene and then *tetra-cis*-lycopene, both are catalysed by ζ-CAROTENE DESATURASE (ZDS). The second isomerisation, through the CAROTENE ISOMERASE (CRTISO), converts *tetra-cis*-lycopene to all-*trans*-lycopene (Isaacson et al., 2002; Isaacson et al., 2004).

Lycopene is the most abundant carotenoid in ripe tomato and lies at a junction of two distinct pathways. Cyclisation of lycopene creates a series of carotenes that have one or two rings of either the β- or ϵ- type (Figure 1-4). LYCOPENE β-CYCLASE (LCY-β) introduces two β-rings to form γ-carotene and β-carotene. While both LYCOPENE ϵ-CYCLASE (LCY-ε) and LYCOPENE β-CYCLASE add ε- and β-rings to lycopene, respectively, to produce δ-carotene and then α-carotene. Both cyclase enzymes are expected to act in complexes, bound to membranes within the plastid (Nogueira et al., 2013).

Xanthophylls are formed by the oxygenation of carotenes, typically by the addition of hydroxyl or epoxy groups (Figure 1-4). Hydroxylation of α-carotene and β-carotene result in the formation of α and β-cryptoxanthin, respectively. Hydroxylation of α and β-cryptoxanthin produces lutein and zeaxanthin, respectively. The introduction of hydroxyl groups into β-rings is catalysed by a haem-containing CYTOCHROME P450 β-RING HYDROXYLASE (CYP97A) or/and the CAROTENE β-HYDROXYLASE 1 and 2 (CRTR-B1 and CRTR-B2), while a haem-containing CYTOCHROME P450 ε-RING

HYDROXYLASE (CYP97C) hydroxylates ε-rings (Sun et al., 1996; Tian and DellaPenna, 2001; Tian et al., 2003; Tian et al., 2004; Kim and DellaPenna, 2006).

Zeaxanthin can be converted to antheraxanthin and then violaxanthin by the introduction of epoxy groups (Figure 1-4), both are catalysed by ZEAXANTHIN EPOXIDASE (ZEP-1). VIOLAXANTHIN DE-EPOXIDASE (VDE-1) action converts violaxanthin back to zeaxanthin. This partly reversible enzymatic process is known as the xanthophyll cycle. Rapid conversion of violaxanthin back to zeaxanthin protects thylakoid membranes against photo-oxidation caused by high light intensity (Demmig-Adams and Adams, 1996). Finally, violaxanthin is converted to neoxanthin by NEOXANTHIN SYNTHASE (NXS).

1.4.1.2 Biosynthesis of ketocarotenoids

Ketocarotenoids are almost exclusively biosynthesised in microorganisms, an overview of the reaction induced by CRTZ and CRTW is provided in Figure 1-5. β-carotene is the first carotenoid precursor for the ketocarotenoid pathway. Similar to plants, phytoene is synthesised by the condensation of two GGPP molecules, which is then converted to form β-carotene. The bacterial GGPP SYNTHASE and PHYTOENE SYNTHASE are called CRTE and CRTB, respectively. Only one bacterial enzyme, CRTI, is required to convert phytoene to lycopene, compared to the four enzymes in plants. CRTY then functions as a LYCOPENE CYCLASE in the formation of β-carotene (Misawa et al., 1990; Misawa et al., 1995b). The equivalent bacterial enzymes to plants are shown in Figure 1-4. CRTZ (CAROTENOID HYDROXYLASE) and CRTW (CAROTENOID KETOLASE) catalyse two steps of hydroxylation and ketolation, respectively. Both are involved in the synthesis of astaxanthin from β-carotene, a total of eight intermediates have been identified (Misawa et al., 1990; Misawa et al., 1995a; Misawa et al., 1995b; Fraser et al., 1997; Fraser et al., 1998; Masamoto et al., 1998; Misawa, 2009; Zhu et al., 2009). Also, both enzymes are bi-functional, with the ability to act prior or after ketolation and hydroxylation of the β-rings.

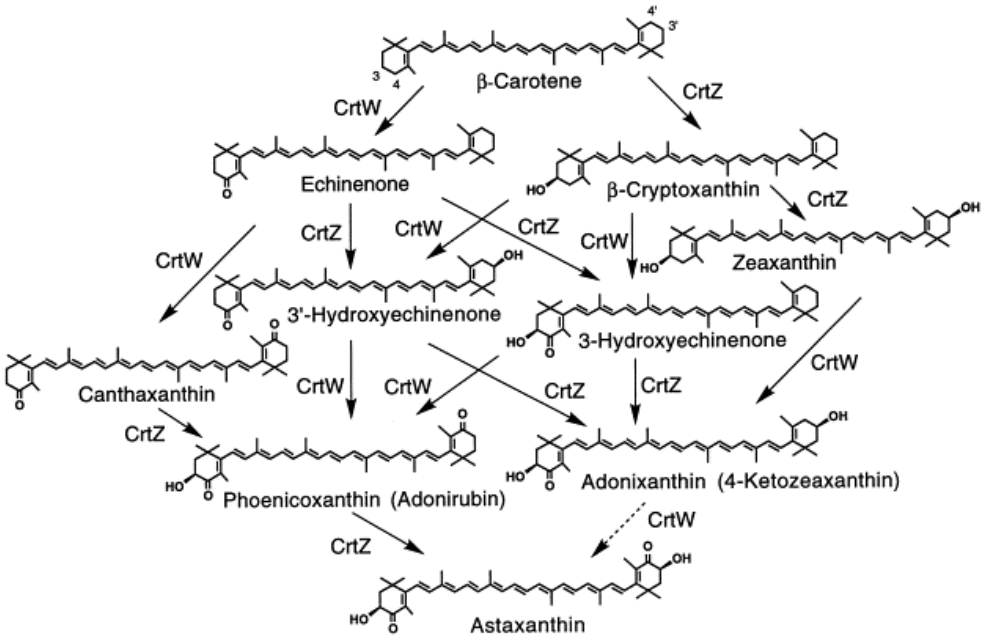

Figure 1-5 Ketocarotenoid biosynthesis pathway. Adapted from (Misawa and Shimada, 1998).

Functions of the genes CRTZ, CAROTENOID HYDROXYLASE; and CRTW, CAROTENOID KETOLASE in the ketocarotenoid biosynthesis pathway, with β-carotene or derived products as substrates and astaxanthin the final compound of this interactive pathway.

1.4.1.3 Chloroplast to chromoplast differentiation

Carotenoid production occurs in almost all types of plastid. Plastids are organelles unique to lower and higher plants, originating from endosymbiotic integration of a photosynthetic prokaryote, cyanobacterium (Gould et al., 2008). The ancestors of plastids, chloroplasts, then diversified into a variety of other plastid types with specialised functions.

Chloroplasts are the predominant plastid type in mature green fruit. In chloroplasts, carotenoids constitute photosynthetic complexes in thylakoid membranes (Cazzonelli and Pogson, 2010; Ruiz-Sola and Rodríguez-Concepción, 2012). However, upon the onset of ripening chloroplasts differentiate into chromoplasts (Figure 1-6). Mainly chromoplasts function as carotenoid synthesis and sequestration sites, responsible for the yellow, orange and red colours of many flowers and fruits. Chloroplast to chromoplast differentiation is characterised by the breakdown of photosynthetic machinery, including

thylakoid and chlorophyll, with simultaneous remodelling of the internal membrane system associated with the sequestration of carotenoids (Figure 1-6; Egea et al., 2010) . These new structures utilises the inner membrane envelope of the plastid, resulting in the formation of carotenoid-rich membranous sacs, the sight for the formation of carotenoid crystals (Harris and Spurr, 1969; Vishnevetsky et al., 1999; Simkin et al., 2007; Egea et al., 2010). Accumulation of carotenoids occurs in various sequestration structures, including crystals, globules and fibrils (LaBorde and Spurr, 1973; Grilli Caiola and Canini, 2004; Vasquez-Caicedo et al., 2006; Kim et al., 2010a). Tomato accumulates carotenoids predominantly in the form of lycopene crystalloids in membrane-shaped structures (Harris and Spurr, 1969).

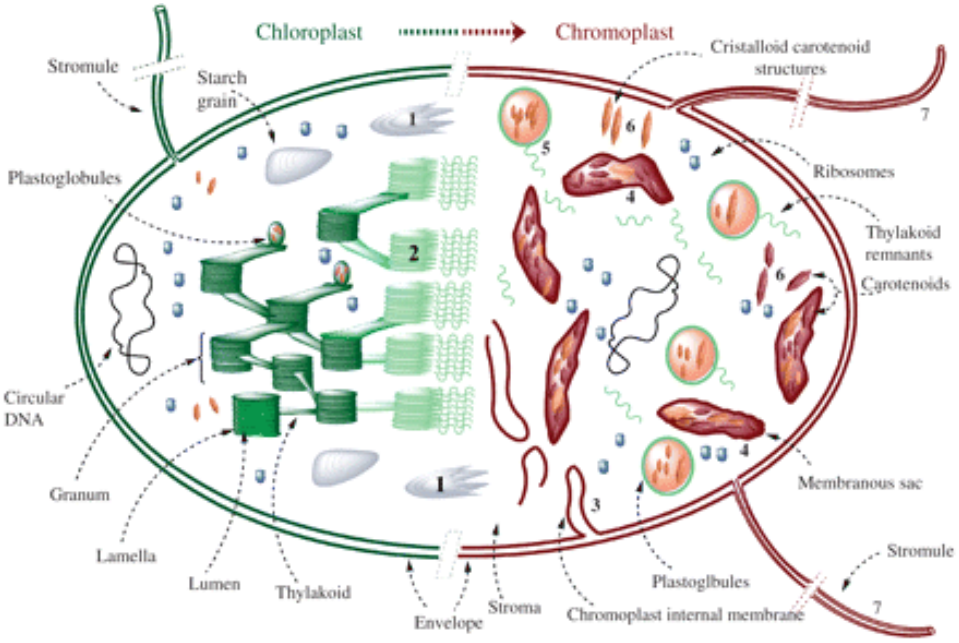

Figure 1-6 Chloroplast to chromoplast differentiation.

Schematic representation of the chloroplast–chromoplast transition. The scheme illustrates the breakdown of starch granules, grana, and thylakoids (1 and 2); the synthesis of sequestration structures from the inner membrane envelope of the plastid (3) resulting in the formation of carotenoid-rich membranous sacs (4); increasing number and size of plastoglobules during the differentiation that are no longer attached to the thylakoid (5); the appearance of carotenoid-containing crystalloids (6); increases to the number of protrusions emanating from the plastid envelope, called stromules (7) (Egea et al., 2010).

The *ORANGE* (*OR*) gene originally found in cauliflower, has been established as the only known gene that acts as a molecular switch to trigger the differentiation of non-coloured plastids into chromoplasts (Li et al., 2001). It has been shown to facilitate carotenoid accumulation in both cauliflower and potato, by generating a carotenoid deposition sink without affecting carotenoid biosynthesis (Li et al., 2001; Lu et al., 2006; Lopez et al., 2008). Therefore, *OR* remains an important regulator of carotenoid sequestration through plastid differentiation.

1.4.1.4 Roles of carotenoids and ketocarotenoids in plants

Carotenoids are the second most abundant naturally occurring pigments on earth consisting of more than 750 members, which are synthesised in all photosynthetic organisms (bacteria, algae, and plants as well as in some non-photosynthetic bacteria and fungi) (Nisar et al., 2015). Carotenoids are essential components of the light harvesting complexes and for photosynthesis. Carotenoids improve the effectiveness of light capture by absorbing light across a broad range of the spectral region that the sun emits, which is not efficiently absorbed by chlorophyll. Carotenoids then transfer this energy to chlorophyll and subsequently to the reaction centre. Together this initiates the primary photochemical events of photosynthesis (Polivka and Frank, 2010; Cazzonelli, 2011). Thus, having a variety of carotenoid and chlorophyll pigments maximises the absorption range of light within the light-harvesting antenna complexes, and consequently the excitation energy to the reaction centre.

Carotenoids also regulate the flow of energy within the photosynthetic apparatus. Importantly, they enable the plant to balance between absorbing sufficient light for photosynthetic processes, while protecting membranes and proteins from photo-oxidative damage caused by excess light absorption. Carotenoids are able to prevent damage to the photosynthetic apparatus due to the ability to quench the reactive triplet chlorophyll, reactive oxygen species (ROS) such as singlet oxygen by acting as an antioxidant, and xanthophyll-mediated non photochemical quenching (NPQ) to dissipate excess energy via thermal dissipation processes (Li et al., 2009; Cazzonelli, 2011; Jahns and Holzwarth, 2012). Xanthophyll carotenoids such as zeaxanthin, antheraxanthin and lutein have lower energy levels compared to those of chlorophylls, thus have a great capacity of energy dissipation (Demmig-Adams and Adams, 1996). Furthermore,

xanthophylls undergo very rapid light triggered concentration changes. With excess light VDE-1 activity in the thylakoid lumen catalyses the conversion of violaxanthin to zeaxanthin, and is strictly regulated by the pH of the lumen (Jahns et al., 2009). Under low light, zeaxanthin is converted back to violaxanthin. The precise role of zeaxanthin in NPQ is still debated, although it has been shown along with violaxanthin to strongly affect the thermodynamic parameters of membranes (Kostecka-Gugała et al., 2003; Jahns et al., 2009).

Further roles associated with their light absorbing properties are that they are responsible for the yellow to red colour spectrum in plants. Therefore, accumulation of carotenoids serves as powerful visual attractants for insects or animals; for pollination of flowers or seed dispersal (Cazzonelli, 2011). Furthermore, C_{40} carotenoid derivatives serve as substrates for carotenoid cleavage enzymes, resulting in the biosynthesis of plant volatile scents and aroma constituents, such as geranyl acetone and β-ionone (Simkin et al., 2004; Walter et al., 2010; Cazzonelli, 2011). These fragrant volatiles also can attract various types of animals for pollination and seed dispersal. The cleavage products of carotenoids can also act as phytohormones, such as abscisic acid and strigolactone, as well as other signalling molecules (Walter et al., 2010; Cazzonelli, 2011). ABA in particular plays critical roles in adaptive responses to biotic and abiotic stresses, notably the control of stomatal aperture and transpiration during drought, in addition to fruit development and ripening (Chinnusamy et al., 2008; Cazzonelli, 2011; Kumar et al., 2014; Leng et al., 2014; Lim et al., 2015; Mou et al., 2016).

1.4.1.5 Roles of carotenoids and ketocarotenoids in animals

Unlike plants, animals are unable to synthesise carotenoids *de novo* excluding some aphids (Fraser and Bramley, 2004; Moran and Jarvik, 2010), thus carotenoids are provided through their diet. Crop plants are the main source of carotenoids for humans (roots, leaves, shoots, seeds, fruit and flowers). Accumulation of carotenoids is related to camouflage, sexual behaviour, reproduction, and avoiding predation and parasitism. Particularly in fish and birds, the colours of the accumulated carotenoids can often result in preferential selection by potential sexual partners, as they boost both immune system and advertise health (McGraw et al., 2006; McGraw and Klasing, 2006; Pike et al.,

2007; Baron et al., 2008). The pink feather's from flamingos are due to carotenoid pigments, with possible cosmetic functions for mate choice (Cazzonelli, 2011).

Carotenoids have been shown to be beneficial to human health, due to their antioxidant, anti-inflammatory, hypolipidemic, and anti-carcinogenic activities in humans. Many diseases such as cancers and cardiovascular disease are caused by a concomitant increase and exposure to free radicals (e.g. superoxide anion, hydroxyl radical, alkoxy radical, peroxyl radical) and oxidative processes. Carotenoids are known to be very efficient neutralisers of singlet oxygen and reactive oxygen species, preventing oxidative damage to cellular components. The antioxidant activity of carotenoids related to their polyene chain, which stabilises the carotenoid radicals created by free radical quenching. The removal of free radicals limits irreversible oxidation and damage to lipids, nucleic acids, proteins and carbohydrates, reducing cell death along with the effects of ageing and degenerative, ageing-related diseases (Aruoma, 1994; Gülçin, 2012; Zhu et al., 2013).

The health benefits of carotenoid intake have been extensively studied; with provitamin A being the most established function of carotenoid activity in regard to human health. Provitamin A activity is conferred by 50 naturally occurring carotenoids with β-ring end groups, including β-carotene, zeaxanthin and β-cryptoxanthin (Fraser and Bramley, 2004; Grune et al., 2010). β-carotene is the most suitable and important precursor for vitamin A, and is present in tomato (Grune et al., 2010). Oxidative cleavage by a MONO-OXYGENASE (BCO) results in the formation of retinal (vitamin A) (Fraser and Bramley, 2004; Tang and Russell, 2009; Grune et al., 2010). Vitamin A deficiency has been linked with blindness and growth retardation, in addition to more severe diseases including respiratory and urinary infections, dysentery and immune responses (Britton, 2009). More than 230 million children have an inadequate intake of vitamin A, mainly in developing counties (Schweigert et al., 2003). A diet with vitamin A supplementation prevents deficiency related diseases and promotes human health by its immuno-stimulant and photoprotectant activities (Cazzonelli, 2011). It is estimated that 1-2 million deaths could be prevented annually among children (Ye et al., 2000). Therefore, Golden Rice which accumulates enhanced β-carotene levels was developed to combat vitamin A deficiency (Ye et al., 2000; Beyer et al., 2002; Paine et al., 2005). Only 100 g of Golden Rice would approximately fulfil the recommended daily intake of β-carotene.

Sources of lycopene are limited. However, it is the predominant carotenoid in tomato, and at least 85% of dietary lycopene comes from fresh tomatoes or tomato-based products (Fraser and Bramley, 2004). Lycopene has been shown to be a potent

antioxidant (Kim et al., 2010b; Kong et al., 2010). Consumption has been associated with decreased risk of chronic diseases such as cardiovascular disease, and several different types of cancer, including prostate, lung and stomach (Fraser and Bramley, 2004; Story et al., 2010; Viuda-Martos et al., 2014; Mozos et al., 2018). Supplementation with other carotenoids present in tomato such as lutein, α-carotene and zeaxanthin can also contribute to eye health, cognitive function, maternal and infant nutrition and fertility (Fraser and Bramley, 2004; Johnson et al., 2008; Mínguez-Alarcón et al., 2012; The Age-Related Eye Disease Study 2 Research, 2013; Eggersdorfer and Wyss, 2018). Tocopherols (vitamin E) are isoprenoids that are produced in sufficient amounts in tomato to impact health, their antioxidant ability also is associated with reduced risk of multiple diseases including cardiovascular disease and cancer (Rizvi et al., 2014; Raiola et al., 2015).

1.4.1.6 Economic value of carotenoids

The carotenoid market reached $1.5 billion in 2017 and is expected to reach $2.0 billion by 2022, at a compound annual growth rate (CAGR) of 5.7% for the period of 2017-2022 (FOD025F, 2018). The major applications for carotenoids in order of market volume are feed, food, supplements, pharmaceuticals and finally cosmetics.

The natural pigmentation of carotenoids enables use of these compounds as industrial colourants, especially in the aquaculture and poultry farming industries. Astaxanthin and canthaxanthin are the chosen carotenoids for the pigmentation of fish and shrimp, and the red tone in egg yolk, respectively (Johnson and Lewis, 1979). Also, lutein, lycopene, β-carotene and zeaxanthin supplementation increased carotenoid content in sampled egg yolks (Handelman et al., 1999; Karadas et al., 2006). Recently, tomatoes were engineered to produce ketocarotenoids (3.0 mg/g dry weight). The powder from these ripe fruit were mixed with fish feed. The resulting fish fillets were enriched with ketocarotenoids, with a two-fold retention of the main ketocarotenoids when compared to synthetic feed to colour trout flesh (Nogueira et al., 2017). Despite this advancement, chemical synthesis remains the production method of choice, but is linked to the chemical refining of fossil fuels. Furthermore, chemical synthesis remains expensive, has a detrimental environmental impact, and the final product contains reaction contaminants and a mixture of stereoisomers of which the non-natural form typically

predominates. Therefore, there is increasing consumer demand for non-artificial colourants; algal, fungal and bacterial platforms are used presently (Takaichi, 2011; Mata-Gómez et al., 2014; Mezzomo and Ferreira, 2016). Despite this, plant-based sources remain the most economically viable in terms of a production cost-basis, despite problems regarding seasonal and geographic variability that cannot be controlled (Mata-Gómez et al., 2014).

1.4.1.7 Fruit softening

Ripening is also associated with textural changes to cell walls resulting in fruit softening. Texture is an important driver of customer preference, thus alterations have been exploited by humans for crop domestication (Klee and Giovannoni, 2011; Seymour et al., 2013b). Texture also influences, and is a determinant of, shelf-life and transportability of fruits. The structural basis of fruit texture is complex, and depends on the capacity of the cell wall to maintain turgor pressure and mediate cellular adhesion. Remodelling of cell walls and the osmotic state of fruit tissues are the major causes of fruit softening. Despite this, more detailed mechanistic understanding has remained elusive and remains an active area of research. To date tomato has represented the primary model for fleshy fruit softening, and the control of softening has generally only been achieved through delay or attenuation of the entire ripening process (Seymour et al., 2013a; Wang et al., 2018), but uncoupling from other ripening-related quality traits remains desirable.

Softening is characterised by the extensive modification and altered mechanical properties of parenchyma cell walls, while middle lamella dissolution results in reduced cell adhesion. Cell wall modifying enzymes then catalyse cell wall and middle lamella modifications. Depolymerisation of matrix glycans, the solubilisation and depolymerisation of pectins, combined with the loss of neutral sugars from pectin side chains is responsible for the cell wall disassembly and subsequently softening (Brummell, 2006; Goulao and Oliveira, 2008; Paniagua et al., 2014). While the accumulation of apoplastic solutes (Wada et al., 2009), transpirational water loss through the cuticle (particularly in tomato which has fruits with thick and well developed cuticles; Saladié et al., 2007, Lara et al., 2014) and the cell wall modifications could all be influencing the loss turgor pressure during ripening (Thomas et al., 2008).

1.4.1.8 Cell wall structure

Cell walls are involved in support, controlling cell expansion and adhesion, generation of turgor pressure and protecting against mechanical stresses. Consistent with the majority of plant primary cell walls, those of tomato principally comprises of three classes of polysaccharide; consisting of cellulose fibrils being embedded in a matrix of hemicellulose and pectic polymers (Tucker et al., 2017). The cell wall also contains structural proteins, including extensin, hydroxyproline-rich, and arabinogalactan proteins. Complex compositional and structural cell wall changes occur during fruit development and ripening (Lunn et al., 2013).

1.4.1.9 Pectins

Pectins are the most complex polysaccharide, and are a highly abundant polymer in the middle lamella, with an important role in cell-to-cell adhesion (Willats et al., 2001a). The most pronounced changes occur to pectin during fruit softening, thus it has received the most sustained attention. Three major classes of pectins have been identified: homogalacturonan (HG), rhamnogalacturonan 1 (RG-I) and rhamnogalacturonan II (RG-II) that are interlinked in large pectic macromolecules (Figure 1-7). The latter (RG-II) is less abundant, but has a complex composition and is known for the existence of many different sugars (Bar-Peled et al., 2012). HG is made up of a backbone of 1,4-linked α-D-galacturonosyluronic acid residues. RG-I comprises of interspersed α-D-galacturonosyl and rhamnosyl residues, with side chains composed of arabinose and galactose. While RG-II generally exists as an RG-II borate diester dimer, ostensibly linking HG-connected pectin in the wall (Bar-Peled et al., 2012; Wang et al., 2018). Structural data indicates that the interconnected pectin structure consists of HG, RG-I, and RG-II connected by covalent linkages via their backbones (Bar-Peled et al., 2012; Wang et al., 2018). Despite this, it is not known whether these pectic polysaccharides are arranged in a specific order or what the representative lengths are for each domain within the larger pectin structure (Bar-Peled et al., 2012).

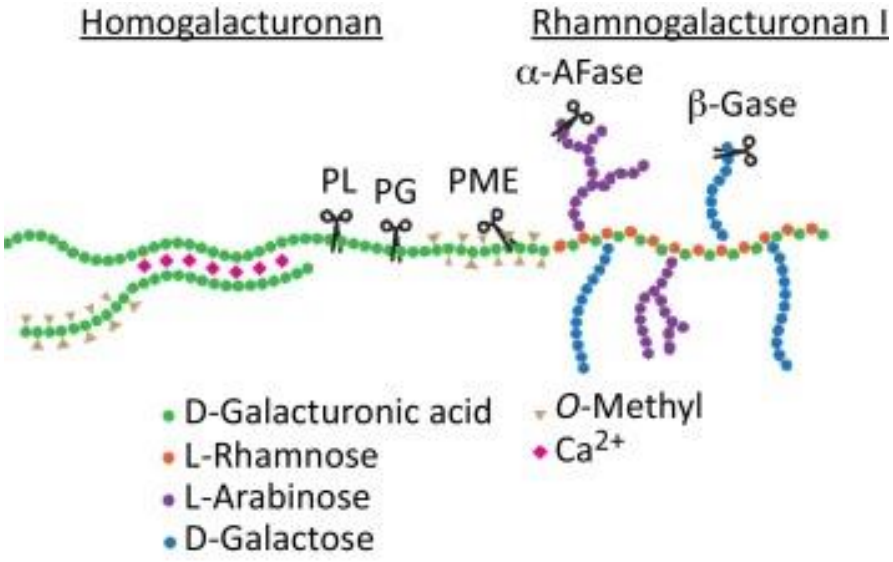

Figure 1-7 The structure of the major pectic polysaccharides and targets of ripening-related enzymes. Adapted from (Wang et al., 2018).

Structure of homogalacturonan and rhamnogalacturonan 1. Includes the enzymes in tomato that catalyse the pectin metabolism: PL, PECTATE LYASE; PG, ENDO-POLYGALACTURONASE; PME, PECTIN METHYLESTERASE; α-AFASE, A-ARABINOFURANOSIDASE; β-GASE, β-GALACTANASE.

1.4.1.10 Celluloses

Cellulose is highly stable and the cellulose fibril is generally conserved and well defined. Cellulose polymers consists of linear chains composed entirely of β-1,4 linked glucose residues, which are grouped together into fibrils (Somerville, 2006). It is generally accepted that between 24 and 36 polymers are found in each fibril, aligned parallel to each other and held together by hydrogen bonds yielding a crystalline structure that is very resistant to degradation. The fibrils also are aligned parallel to each other within each plane of the cell wall.

1.4.1.11 Hemicelluloses

Hemicelluloses are represented by a very diverse range of structural polymers: xyloglucans, glucomannans, and glucuronoxylans, with xyloglucans being the major hemicellulosic polysaccharide in primary plant cell walls in tomato (Scheller and Ulvskov, 2010). The basic structure of xyloglucan consists of a backbone of β-1,4 linked glucose, and is composed of a cellulose-like backbone branched by xylosyl residues. Furthermore, the xylose units can be substituted by several other monosaccharides such as galactose, fucose and arabinose (Fry, 1989). Hemicelluloses bind to cellulose by two mechanisms: by embedding themselves in the para-crystalline regions of the cellulose fibril, and hydrogen bonding to the surface of the cellulose fibrils (Scheller and Ulvskov, 2010; Tucker et al., 2017). Additionally, they may act as tethers between the adjacent cellulose fibrils. Xylans have a backbone of xylose residues. A common modification is the substitution with α-(1→2)-linked glucuronosyl and 4-O-methyl glucuronosyl residues, referred to as glucuronoxylans. Glucomannans are composed of a mixed glucose-mannose backbone.

1.4.1.12 Models of cell wall structure

Multiple models have been proposed in regards to how the major cell wall components (cellulose, hemicellulose, and pectin) interact to provide the biophysical properties associated with the cell wall. The most prevalent model was the ‘tethered network;’ composed of cross-linked hemicellulose and cellulose, forming a load-bearing network (Figure 1-8) (Cosgrove, 2005). While increasing evidence indicates that cellulose-pectin contacts are more prevalent, having a larger load-bearing and cross-linking role than previously predicted (Cosgrove, 2014). Recent studies demonstrate interactions between RG-I and xylan in both tomato and *Arabidopsis*, suggesting that xylans could function as the covalent connection between pectin and the hemicellulose-cellulose network or between pectin and cell wall proteins (Figure 1-8) (Tan et al., 2013; Ralet et al., 2016; Broxterman and Schols, 2018).

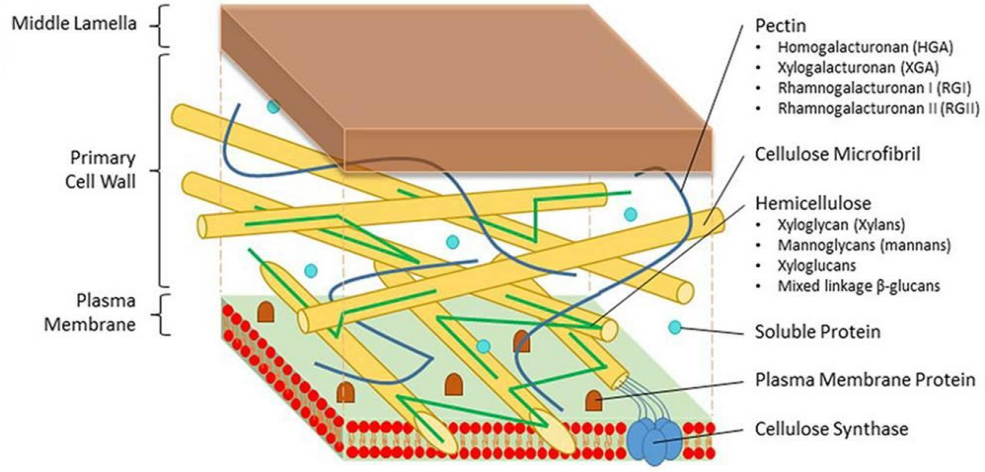

Figure 1-8 Structure and composition of the primary cell wall of plants. Adapted from (Loix et al., 2017).

The primary cell wall contains three polysaccharides: cellulose, hemicellulose and pectin. The cellulose fibrils are embedded in a matrix of hemicellulose and pectic polymers.

1.4.1.13 Cell wall changes during ripening

Softening is associated with changes to the structure and chemical composition of the majority of fruit cell wall polymers during ripening (Brummell, 2006). The middle lamella can be seen to swell during ripening, indicating hydration (Redgwell et al., 1997b). Further observations revealed reductions to neutral sugars such as galactose and arabinose from RG-I (Gross and Wallner, 1979), as well as a decline in methylation of pectins from 90% in green fruit to 35% in ripe fruit (Koch and Nevins, 1989). The latter is predicted to induce the swelling of the middle lamella, via Donan forces, caused by elevated negative charge on the pectin polymers. These changes are induced by enzymatic action within the cell wall.

1.4.1.14 Enzymes involved in cell wall metabolism during ripening

Activity from a range of enzymes has been associated with ripening, with the ability to modify the structure, physical and chemical properties of various cell wall components. Ripening-related softening is linked to secretion of numerous pectin-degrading enzymes

into the cell wall, their combined, sequential, and synergistic action results in solubilisation of pectic polysaccharides, along with their depolymerisation and loss of neutral sugar side-chains.

ENDO-POLYGALACTURONASE (referred to as PG here, which is distinct from an exo-acting POLYGALACTURONASE) was the main candidate predicted to be involved with pectin depolymerisation, resulting in middle lamella solubilisation, cell separation and tissue softening. This was due to its absence in green tomato fruit and the rapid accumulation of both PG transcript and protein upon the onset of ripening (Hobson, 1964; Grierson and Tucker, 1983; DellaPenna et al., 1986; DellaPenna et al., 1987). While *PG* expression and enzyme activity was reduced in *rin* (*ripening inhibitor*), *nor* (*non-ripening*) and *nr* (*never ripe*) ripening mutants, which exhibit reduced rates of fruit softening (DellaPenna et al., 1987; Lanahan et al., 1994). PG has been demonstrated to hydrolyse HG, by cleaving the α-1,4 linkage between galacturonic acids. Antisense suppression of the major ripening-associated PG isozyme, with activity to as low as 1% of normal levels, reduced pectin depolymerisation, but no significant reduction in pectin solubilisation was identified (Smith et al., 1990). Overall, several studies silencing *PG* demonstrated only minimal improvements in slowing the rate of fruit softening (Sheehy et al., 1988; Smith et al., 1988; Smith et al., 1990; Kramer et al., 1992; Langley et al., 1994). Therefore, it is apparent that PG's role is not initiating the fruit softening process.

The central role of pectin depolymerisation in tomato fruit softening was confirmed with the silencing of *PECTIN LYASE* (*PL*), which is involved in ripening-associated pectin-degradation (Uluisik et al., 2016). Sedimentation equilibrium experiments, uronic acid assays and microscopy revealed that *PL*-silenced fruits exhibited changes in the molecular weight, solubility, and distribution of pectic polysaccharides, respectively. *PL* is involved in the depolymerisation of HG, as *PL*-silenced fruits have greater amounts of de-esterified HGs in the tricellular junction zones and middle lamella region. De-esterified tricellular junction zones are predicted to contribute to intercellular adhesion, as biomechanical stresses that drive cell separation are concentrated at the cell corners (Willats et al., 2001b; Uluisik et al., 2016). This indicates that the major sites of *PL* action are tricellular junctions. These pectins usually undergo depolymerisation and solubilisation from the wall during ripening. In addition, *PL*-silenced fruits contained lesser amounts of water soluble pectins, thus it is predicted that more of the pectins are covalently associated with the wall matrix in transgenic lines. The water soluble pectins had a significantly higher average molecular weight in *PL*-silenced fruits, similar to

those reported in unripe tomato fruits. The action of PL and the breakdown of crosslinked HG polymers enable further degradation of the pectic polysaccharides in the cell wall by enzymes such as PG, inducing fruit softening (Uluisik et al., 2016).

PECTINESTERASE (PE) catalyses the de-esterification of galacturonic acid residues in HG forming free acid. PE is predicted to function in synergy with PG in the degradation of pectic cell wall components, as PG requires adjacent de-esterified residues for action (B. Seymour et al., 1987; Koch and Nevins, 1989; Tieman et al., 1992; Thakur et al., 1996). Unlike *PG*, *PE* is expressed in both development and ripening in tomato (Tucker et al., 1982; Harriman et al., 1991). However, suppression of *PE* to less than 10% of wild-type PE enzyme activity, with undetectable levels of PE protein and mRNA, had little effect on fruit firmness (Tieman et al., 1992). Additionally, it is predicted to be involved in the formation of blocks of de-esterified galacturonic acid residues in HG, promoting wall stability by the formation of calcium 'egg box' structures (Micheli, 2001; Tucker et al., 2017). Therefore, separate isoforms identified may be contributing to both wall strength and degradation during different phases of plant development.

β-GALACTOSIDASE (TBG) is an enzyme involved in side chain modification of pectins. β-GALACTOSIDASE, β-GALACTOSIDASE/exo-galactanase activity have the potential to remove galactose residues from the side chains of RG-I. TBG activity has been associated with softening across multiple fruit species, and reduced softening being associated with lower galactose content (Nakamura et al., 2003; Brummell et al., 2004; Mwaniki et al., 2005; Ogasawara et al., 2007; Paniagua et al., 2016). Seven *TBG* genes in tomato are expressed during fruit development and maturation (Smith and Gross, 2000), six were expressed during ripening and five were localised to the cell wall. Exo-galactanase activity increases up to 5-fold during ripening, and was correlated with the rise in free galactose (Pressey, 1983; Kim et al., 1991; Carey et al., 1995). Suppression of *TBG1* and *TBG3* individually failed to alter fruit firmness (Carey et al., 2001). While *TBG4* antisense lines yielded red-ripe fruits that were up to 40% firmer, combined with reduced exo-galactanase levels and high wall galactosyl content (Smith et al., 2002). Elevated mechanical strength due to increased content of pectic galactan side-chains, decreasing wall porosity and access of cell wall hydrolases to wall components, are predicted to be the mechanism for improved fruit firmness (Redgwell et al., 1997a; Brummell and Harpster, 2001; Smith et al., 2002). Finally, *TBG6* suppression increased fruit cracking, reduced locular space, and doubled the thickness of the fruit cuticle but failed to significantly impact fruit firmness (Moctezuma et al., 2003).

Ripening-related fruit softening is also correlated to increased *1,4-β-GLUCANASE* expression and activity (Brummell et al., 1994; Urbanowicz et al., 2007). Despite this, it is unclear whether 1,4-β-GLUCANASE depolymerises hemicellulose or cellulose. 1,4-β-GLUCANASE can hydrolyse β-1,4-linked glucose polymers, but action against cellulose is believed to be limited. Several studies have identified the substrate as xyloglucan, however in vitro hemicellulose is not readily hydrolysed (Urbanowicz et al., 2007).

XYLOGLUCAN TRANSGLYCOSYLASE/HYDROLASE (XTH) exhibits dual catalytic activity. XTH acts as XYLOGLUCAN XYLOGLUCOSYLTRANSFERASE (XET) that catalyses the transfer of a xyloglucan molecule fragment to another xyloglucan molecule, and/or xyloglucan endohydrolase (XEH), acting as a hydrolase to cleave the bond between adjacent glucose residues in xyloglucan, resulting in depolymerisation (Nishitani, 1997; Rose et al., 2002; Fry, 2004). A total of six XTHs have been reported during fruit development in tomato, only *XTH5* and *XTH8* expression has been associated with fruit ripening (Saladie et al., 2006; Miedes and Lorences, 2009). *XTH1*, *XTH5* and *XTH8* exhibit XET activity, with roles in cell wall turnover and maintenance rather than softening (Hiwasa et al., 2004; Nishiyama et al., 2007; Miedes et al., 2010). Overexpression of *XTH1* in tomato resulted in increased XET activity, which was responsible for reduced xyloglucan depolymerisation and softening (Miedes et al., 2010). The results highlighted that XET activity can be related to the maintenance of the structural integrity of the cell wall; influencing the xyloglucan structure and softening.

EXPANSINS (EXPs) are cell wall loosening proteins involved in cell enlargement and other developmental processes involved with cell wall modification (Cosgrove, 2000; Sampedro and Cosgrove, 2005). EXPs influence growth or shape change, by interacting at the junction of the cellulose fibril and by coating hemicellulose polymers to disrupt the hydrogen bonds. This enables cellulose microfibril slippage and cells to expand. The *EXPANSIN 1* (*EXP1*) gene was shown to contribute to ripening-related fruit softening, potentially through promoting cell wall loosening enabling hemicellulose depolymerisation (McQueen-Mason and Cosgrove, 1995; Brummell et al., 1999; Minoia et al., 2016). Silencing of *EXP1* reduced fruit softening in the early ripening stages, with limited cell wall pectin degradation without any effect on other cell wall matrix polysaccharides (Brummell et al., 1999). Overexpression exhibited elevated fruit softening and degradation of matrix glycans, including xyloglucans in green fruits.

The above studies show the complexity of ripening-related fruit softening. Few alterations to individual softening-related gene expression corresponded to differences to ripe fruit firmness and shelf-life, providing evidence for multiple enzymes working in concert to confer softening (Saladié et al., 2007; Lunn et al., 2013).

1.4.1.15 Fruit taste and aroma

The flavour of any food is the sum of interactions between taste and olfaction. Sugars and acids activate taste receptors, whereas a diverse set of volatile compounds activate olfactory receptors (Buttery et al., 1989; Baldwin et al., 2000; Tieman et al., 2012). Tomato taste is a result of a balance between sugars (mainly glucose and fructose), organic acids (citric, malic, and ascorbic acid) and glutamate, conferring sweetness, acidity and sourness, and savoury flavour, respectively. Significant quantities of both sugars and acids are required for flavour to be perceived as good and broadly accepted by consumers.

Volatiles define the unique flavour of a tomato and are essential for consumer liking (Baldwin et al., 2000; Tieman et al., 2012). Almost all the important volatiles related to flavour are derived from amino acids, carotenoids and lipids (Goff and Klee, 2006). Over 400 volatiles were detectable in tomato fruits, only 15–20 are produced in sufficient quantities and reach the odour thresholds to have an impact on human perception (Buttery et al., 1989; Baldwin et al., 2000). Interestingly, mutants deficient in carotenoid biosynthesis and therefore apocarotenoid volatiles (geranial, 6-methyl-5-hepten-2-one, and β-ionone), with normal levels of sugars, acids, and nonapocarotenoid volatiles, were perceived by consumers to be less sweet (Vogel et al., 2010). The results confirmed the positive correlation between geranial and perceived sweetness. Despite this, silencing of *13-LIPOXYGENASE* (*LOXC*) and the reduction to C6 volatiles (cis-3-hexenal, hexanal, cis-3-hexen-1-ol, hexyl alcohol, and hexylacetate), derived from 18:2 and 18:3 fatty acids, had no impact on consumer preference (Chen et al., 2004b; Tieman et al., 2012).

More recently, whole-genome sequencing and targeted metabolome quantification of flavour-associated chemicals in 398 modern, heirloom and wild accessions was performed (Tieman et al., 2017). A subset of accessions was evaluated by a consumer

panel and rated for overall liking and flavour intensity. The identification of metabolites linked to consumer liking formed the basis of a genome-wide association study (GWAS), to ascertain the genetic basis of flavour. Reduced levels of sugars, organic acids, and volatile compounds, including β-ionone, E-2-hexenal, 6-methyl-5-hepten-2-one, and phenylacetaldehyde were correlated to the poor flavour of modern varieties (Tieman et al., 2017; Wang and Seymour, 2017). Furthermore, the alleles associated with higher sugar content and flavour volatiles have been lost in modern varieties. Tieman et al., 2017 demonstrated that preferential selection for improved fruit size has resulted in the reduction to sugar content, confirming the inverse correlation between sugars and fruit size. GWAS enabled the identification of candidate loci capable of altering the chemicals contributing to consumer liking and overall flavor intensity of tomatoes. GWAS indicated that the extracellular *INVERTASE* (*LIN5*) was associated with sugar content, while the volatiles guaiacol and methylsalicylate were linked with ripening-related *ACC OXIDASE* homolog (*E8*). Many superior alleles were lost during modern breeding, the affects to many volatiles has resulted in overall flavour deterioration. Whereas, alleles associated with volatiles derived from carotenoids have been enriched, as breeders have selected deep-red fruits. Finally, the study suggests improvement to volatiles linked with sweetness, and the potential to improve sweetness perception without changing sugar concentration, thus avoiding the trade-off between higher sugar and smaller fruit size.

1.4.2 Ethylene biosynthesis and signalling

Ethylene biosynthesis starts with the formation of S-adenosyl-Met, then 1-AMINOCYCLOPROPANE-1-CARBOXYLIC ACID (ACC) SYNTHASE (ACS) and 1-AMINOCYCLOPROPANE-1-CARBOXYLIC ACID OXIDASE (ACO) catalyses a two-step process resulting in the production of ethylene. *ACS2* and *ACS4* are the main ACS family members expressed during tomato ripening (Oeller et al., 1991; Theologis et al., 1992; Van de Poel et al., 2012). *ACS1A*, *ACS11* and *ACS12* also exhibit ripening-related expression profiles (Barry et al., 2000; Liu et al., 2015b). While *ACO1* displays the most striking ripening-regulated pattern of expression (Nakatsuka et al., 1998; Van de Poel et al., 2012; Liu et al., 2015b). Furthermore, Van de Poel et al., (2012) demonstrated that *ACO3* and *ACO5* also have a ripening-related expression profile, while *ACO2* and *ACO4* transcript levels are highest during system 1 (Barry et al., 1996).

Whereas, Liu et al., (2015) identified that *ACO2* and *ACO4* were expressed upon ripening. While the transcript levels of *ACO3* and *ACO5* remains very low during ripening, and are not expected to contribute to climacteric ethylene production.

System 1 is responsible for producing basal ethylene levels that are detected in all tissues and relies on *ACS1A* and *ACS6* being negatively regulated by ethylene (Nakatsuka et al., 1998; Barry et al., 2000; Liu et al., 2015b). While the shift to the autocatalytic system 2 responsible for tomato ripening, is governed by the upregulation of *ACS2* and *ACS4* through positive feedback by ethylene (Van de Poel et al., 2012; Liu et al., 2015b). Furthermore, *ACO1* is involved in the transition to system 2.

Ethylene signalling can be regulated at several levels, including ethylene biosynthesis and its perception by ETHYLENE RESPONSE (ETR) genes. A total of seven ETRs receptors have been identified and shown to bind to ethylene. NEVER RIPE (NR) bears an altered allele of the ETHYLENE RECEPTOR gene *ETR3*, resulting in ethylene insensitivity and a non-ripening phenotype even when exposed to ethylene (Lanahan et al., 1994; Wilkinson et al., 1995; Yen et al., 1995). *ETR3* and *ETR4* are the main receptor genes expressed upon the initiation of tomato fruit ripening, antisense suppression of these results in phenotypes consistent with a constitutive ethylene response, including significantly earlier fruit ripening (Tieman et al., 2000; Kevany et al., 2007). *ETR7* also displays a ripening-regulated expression profile (Kevany et al., 2007; Klee and Giovannoni, 2011). GREEN RIPE (GR) is also suspected to regulate tomato ripening through ethylene signal transduction, as the *gr* mutant displayed reduced ethylene responsiveness and impaired fruit ripening (Barry and Giovannoni, 2006).

ETRs activate a signal transduction cascade through release of the block exerted by CONSTITUTIVE TRIPLE RESPONSE 1 (CTR1) on ETHYLENE INSENSITIVE 2 (EIN2) (Karlova et al., 2014). Subsequently, this release then activates *EIN3/EIN3*-like (*EIL*) primary transcription factor genes. The function of *CTR1* is to suppress the ethylene signalling pathway, as the *ctr1* loss-of-function mutation results in the constitutive activation of ethylene responses (Klee and Giovannoni, 2011). Four *CTR1* homologs have been identified in tomato, all with the ability to interact with one or more ethylene receptors (Zhong et al., 2008). Another component is EIN2, acting between CTR1 and the EIN3/EIL transcription factors (Alonso et al., 1999; Guo and Ecker, 2003). Its critical role in the ethylene signal transduction pathway was shown by down-regulation, resulting in ethylene insensitivity and ripening inhibition, associated with reduced expression of ethylene- and ripening-related genes (Fu et al., 2005; Hu et al.,

2010). EILs activate ethylene-responsive genes, while antisense knock-downs significantly reduced ethylene sensitivity. It has also been reported that the introduction of a *LeEIL1* overexpression construct restored ethylene responsiveness between various tissues of a *nr* mutant (Chen et al., 2004a). Finally, at the bottom of the signalling cascade is the ETHYLENE RESPONSE FACTOR (ERF) family of transcription factors. These are members of the AP2/ERF superfamily that are activated by the EIN3-like EILs. Expression profiling of *ERFs* revealed that a subset has enhanced expression at the onset of ripening, while several exhibited a ripening-associated decrease in expression. The results indicated that different ERFs may have contrasting roles in fruit ripening (Liu et al., 2016b). The specific roles of the ERFs in fruit ripening are still lacking due to functional redundancy. Overall, ERFs are involved in various processes, including hormonal signalling, biotic and abiotic stress responses, developmental processes, metabolic regulation, ethylene biosynthesis and fruit ripening (Liu et al., 2018a).

1.4.3 Transcriptional control of control of ripening

In tomato, ripening is regulated by a number of transcription factors in conjunction with the plant hormone ethylene, forming an intricate regulatory network (Figure 1-9). Characterisation of ripening defective tomato mutations have contributed to the elucidation of the network underlying the process, with several affecting ethylene signalling or transcription factor activity. Despite this, the network topology and internal interactions are far from understood. The MADS-domain protein RIPENING-INHIBITOR (RIN) (Vrebalov et al., 2002), an SBP transcription factor COLOURLESS NON-RIPENING (CNR) (Manning et al., 2006), and the NAC domain family transcription factor NON-RIPENING (NOR) (Martel et al., 2011) were shown to regulate the biosynthesis of ethylene and function early in the transcriptional activation cascade regulating ripening-related processes. Both *rin* and *cnr* mutations fail to ripen or produce ethylene, or respond to the exogenous form of the phytohormone (Manning et al., 2006).

For many years RIN has been considered the master regulator for tomato fruit ripening; demonstrated by the *rin* mutation that bears unripe fruit (Vrebalov et al., 2002). The *rin* mutation was determined to be a deletion extending over a part of the *RIN* gene and the intergenic region between *RIN* and the adjacent MADS box gene *MACROCALYX*

(*MADS-MC*) (Vrebalov et al., 2002). RIN is a homolog of *Arabidopsis thaliana SEPALLATA* (*SEP*), and has been shown to be one of the earliest acting key factors that initiate the fruit ripening cascade, including both ethylene-dependent and -independent processes (Vrebalov et al., 2002). Therefore, a severe ripening-defective phenotype is exhibited by *rin* mutants, whereby fruits fail to soften or accumulate lycopene, combined with the absence of the climacteric rise in respiration rate and ethylene. Other climacteric and nonclimacteric fruits have *SEP* homologs involved in fruit ripening (Elitzur et al., 2010; Seymour et al., 2011; Ireland et al., 2013; Schaffer et al., 2013).

RIN has been shown to directly bind to and positively regulate the expression of several important ripening-related transcription factors including *RIN* itself, *CNR* and *NOR* (Fujisawa et al., 2011; Martel et al., 2011; Fujisawa et al., 2012a; Fujisawa et al., 2013). As well as a member of the *AP2/ERF* family, *AP2A*, revealed to be a negative regulator of ethylene synthesis during ripening (Chung et al., 2010; Karlova et al., 2011). RIN directly regulates the expression of genes involved with ethylene production, softening and colour formation (Fujisawa et al., 2011; Martel et al., 2011; Fujisawa et al., 2012a; Fujisawa et al., 2013). RIN has been shown to induce ethylene biosynthesis by directly regulating the expression of *ACS2* and *ACS4*, while *ACO1* expression was demonstrated to be RIN dependant. Several carotenoid biosynthesis enzymes are positively regulated by RIN, including the rate-limiting enzyme for carotenoid biosynthesis, *PSY-1* (Fraser et al., 2002), which is a direct RIN target. Furthermore, RIN promotes *Z-ISO* and *CRTISO* directly, *ZDS* indirectly, resulting in the conversion of phytoene to lycopene. Multiple fruit softening enzymes have been shown to be directly regulated by RIN, including *POLYGALACTURONASE A* (*PG2A*), *β-GALACTOSIDASE 4* (*TBG4*), *ENDO-(1,4)-β-MANNANASE 4* (*MAN4*) and *EXPANSIN 1* (*EXP1*). RIN was also shown to regulate the GRAS gene, *FRUIT SHELF-LIFE REGULATOR* (*FSR*) (Zhang et al., 2018a). RIN directly induces the expression of the *LIPOXYGENASE* gene *TOMLOXC*, involved in formation of fatty acid-derived flavour volatiles (Chen et al., 2004b).

More recently, CRISPR/Cas9-mediated RIN-knockout mutation (*RIN-KO*) failed to repress the initiation of ripening (Ito et al., 2017). Compared to the *rin* mutation, *RIN-KO* fruits exhibited moderate red colouring and accumulated the red carotenoid lycopene and greater amounts of β-carotene, while displaying increased fruit softening and ethylene biosynthesis. Moderate expression of *PSY-1* coupled with elevated *PG2A* and *PL* expression in *RIN-KO* fruits are expected to contribute to the altered colour and softening phenotypes witnessed when compared with *rin* fruits. Similar rates of

softening were detected between *RIN-KO* and wild type fruits without alteration to *RIN*. Low but detectable levels of *ACS4* were detected in *RIN-KO* fruits, while stronger repression was exhibited by the *rin* mutation. A large increase to *ACS2* expression was detected, similar to wild type fruits. Elevated *ACS4* and *ACS2* are expected to contribute to elevated ethylene. Moreover, inactivation of the *rin* mutant allele partially restored the induction of ripening. Therefore, it was concluded that RIN is not necessary to induce fruit ripening, but RIN activity is required to complete normal ripening (Ito et al., 2017). The *rin* mutation is not a null mutation but a gain-of-function mutation that actively represses ripening. The results were not able to exclude that the truncated protein may have gained a novel function to stimulate ripening.

The *rin* mutation results in the fusion of two truncated transcription factors, *RIN* and *MC*, forming *RIN-MC*. The ripening-inhibited phenotype is attributed to the lack of a functional RIN protein, while *MC* has low expression in fruit. Nuclear localisation and interaction studies identified *RIN-MC* as a new transcriptional factor, with the ability to interact with other transcription factors such as *FUL1*, *FUL2*, *MADS1* and *TAGL1*. *RIN-MC* was shown to regulate other ripening-related genes including *ETR3/NR*; cell wall metabolism genes such as the *POLYGALACTURONASES PG2A* and *PGcat*, and the *PECTINESTERASES PME1.9*, and *PME2.1*; and genes involved in carotenoid formation including *PSY-1*, *PSY-2*, and *GGPPS2*. Overall, *RIN-MC* exhibits a distinct negative role in tomato ripening. Whereby, overexpression in transgenic wild-type cv Ailsa Craig tomato fruits impaired several ripening processes, while down-regulating *RIN-MC* expression in the *rin* mutant promoted the normal yellow mutant fruit to produce a weak red colour.

RIN has also been shown to interact with the MADS box FRUITFULL homologs FUL1 and FUL2, acting as key ripening regulators. Co-suppression of *FUL1* and *FUL2* revealed more diverse roles in ripening than RIN (Fujisawa et al., 2014), while highlighting their importance to lycopene accumulation and ripening-related ethylene production (Bemer et al., 2012; Shima et al., 2014). Co-suppression of *FUL1* and *FUL2* resulted in an orange ripe fruit with greatly reduced lycopene (Bemer et al., 2012; Shima et al., 2014), combined with very low levels of ethylene production due to suppression of both *ACS2* and *ACS4* (Shima et al., 2014). Expression of genes involved in cell wall modification, cuticle production, volatile production, and glutamate accumulation were also altered. In addition, FUL1 and FUL2 were shown to have redundant and independent functions, with the ability to function with and independently of RIN,

indicating divergence between the MADS-box proteins (Bemer et al., 2012; Fujisawa et al., 2014; Shima et al., 2014). With many key ripening-related genes being direct targets of RIN and either FUL1 or FUL2, or both, it is predicted that RIN functions as part of a DNA binding complex with the FUL homologs.

Another MADS box transcription factor *AGAMOUS-LIKE1* (*TAGL1*) plays an important role in both the development and ripening of fruit (Itkin et al., 2009; Vrebalov et al., 2009; Giménez et al., 2010; Zhao et al., 2018). TAGL1 activity in ripening is executed through direct activation of the ethylene biosynthesis gene *ACS2*, promoting both ethylene production and carotenoid biosynthesis. Overexpression lines resulted in fruits with enhanced lycopene, while loss of function yielded reduced carotenoid and ethylene levels, suppressed chlorophyll breakdown, and down-regulation of a set of ripening-associated genes. Suppression also resulted in reduced pericarp thickness and altered starch accumulation. Fujisawa et al., (2014) demonstrated the heterodimer formation of RIN-TAGL1consistent with previous studies (Leseberg et al., 2008; Martel et al., 2011; Bemer et al., 2012; Shima et al., 2013).

Due to the similar activities of RIN, FUL1, FUL2, and TAGL1 in tomato ripening, positively regulating ethylene and carotenoid biosynthesis, combined with their ability to form DNA binding complexes, these MADS-box transcription factors were proposed to form a higher-order complex (Bemer et al., 2012; Shima et al., 2013; Fujisawa et al., 2014; Shima et al., 2014; Wang et al., 2014). The tetramer complex is assumed to contain two RIN, one TAGL1 and one FUL homolog (Fujisawa et al., 2014; Ito, 2016). This complex regulates the expression of genes involved in the ripening-related phenomena through both ethylene-dependent and independent pathways (Ito, 2016).

COLOURLESS NON-RIPENING (*CNR*) is a major component in the regulatory network controlling fruit ripening. The *cnr* mutant is a result of an epigenetic change that alters the methylation of a gene encoding a putative *SQUAMOSA PROMOTER-BINDING PROTEIN* (*SBP*) (Manning et al., 2006; Osorio et al., 2011a). This results in pleiotropic ripening inhibition and reduced expression of ethylene-associated genes, such as *ACO1*, *E8*, and *NR* (Manning et al., 2006; Osorio et al., 2011a). The *cnr* mutants fail to produce ethylene. CNR was shown to positively regulate carotenoid biosynthesis, as the *cnr* mutant has a colourless, non-ripening phenotype, lacking detectable levels of phytoene and lycopene along with carotenoid precursors (Fraser et al., 2001). It was also implicated in the positive regulation of several ripening-related genes, including *PSY-1*, *LOX*.

The *nor* mutation was identified as a mutation in the gene encoding a member of NAC transcription factor family, resulting in a non-ripening phenotype similar to that observed in *rin* (Giovannoni, 2007). The *nor* mutation was suggested to have a more global effect on ethylene/ ripening-related gene expression than *rin*, potentially acting upstream of RIN in the transcriptional network controlling tomato fruit ripening (Osorio et al., 2011b).

HB-1 is an *HD-zip* transcription factor, which positively controls the expression of the ethylene-producing enzyme *ACO1* during fruit development and ripening (Lin et al., 2008b). Down-regulation of *HB-1* greatly inhibited both *ACO1* mRNA levels and ripening, while ectopic overexpression altered floral organ morphology. Another important ripening-related transcription factor is an *APETALA2* homolog (*AP2A*). *AP2A* is a negative regulator of ethylene synthesis and signalling, and ripening. Suppression of *AP2A* yielded alterations to fruit shape, differentiation of chromoplasts and carotenoid composition, producing orange ripe fruits, combined with elevated ethylene biosynthesis, senescence and deterioration (Chung et al., 2010; Karlova et al., 2011). Both *RIN* and *CNR* were shown to function upstream of *AP2A* and to positively regulate its expression.

Finally, the MADS-box gene *MADS1* in tomato was shown to be a negative regulator of fruit ripening (Dong et al., 2013). High *MADS1* expression is detected in mature green fruits, but declines during fruit ripening. Earlier and accelerated ripening was observed in *MADS1* RNAi-silenced plants, with enhanced *PSY-1* expression and carotenoid accumulation. Silenced lines also demonstrated elevated expression of ethylene biosynthetic genes (*ACS2*, *ACO1* and *ACO3*), combined with the ethylene-responsive genes *E4* and *E8*, which are involved in fruit ripening. This was associated with approximately 2- to 4-fold increases in ethylene production. An interaction between MADS1 and MADS-RIN may suggest that MADS1 reduces MADS-RIN activity.

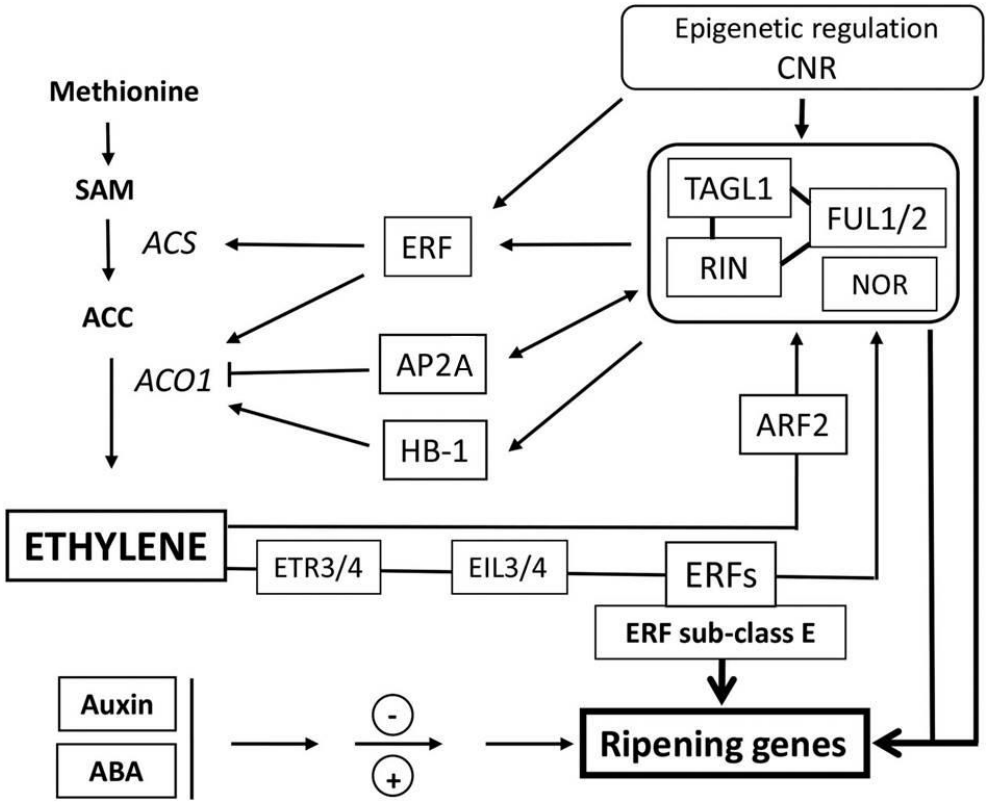

Figure 1-9 Schematic overview of the transcriptional control of ethylene biosynthesis and ripening. Adapted from (Liu et al., 2015b).

The master ripening regulators RIN**,** RIPENING INHIBITOR; TAGL1, AGAMOUS-LIKE 1; and FUL1/2, FRUITFULL homologs; are expected to form a higher order tetramer complex of MADS-box proteins, of varying composition, responsible for ethylene biosynthesis and ripening. Other master ripening regulators include NOR, NON-RIPENING; and CNR, COLORLESS NON-RIPENING. Together these transcription factors, along with the expression of ERFs; AP2A, APETALA2; and HB-1, HD-ZIP; regulate ethylene biosynthesis. Combined action of ETRs, ETHYLENE RESPONSE GENES; EILs, ETHYLENE INSENSITIVE 3-LIKE, EIN3-like; ERFs, ETHYLENE RESPONSE FACTORS; auxin and ABA, abscisic acid; and the master ripening regulator transcription factors regulate key ripening genes associated with fruit ripening.

1.5 Tomato breeding strategies

1.5.1 Conventional breeding strategies

For thousands of years, the primary method of plant breeding has been selection to provide crop improvement. Selection involves the detection of a desired trait among the

population, and the process of its breeding to produce a pure (homozygous) line. These homozygous lines can then be crossed, and plants containing the desirable traits are then selected for further breeding. Wild-type relatives can be one of the parents, to re-introduce genetic variety (e.g. disease resistance). However, this can result in linkage drag, which refers to the incorporation of undesirable traits along with the desirable trait, potentially resulting in a reduction to fitness. Removal of these undesirable traits can usually be accomplished through the time consuming process of repetitive backcrossing, to recover a competitive progeny. Conventional breeding is restricted by the sexual compatibility of the parent lines. Hybridisation is a type of conventional breeding frequently used for crop improvement. It involves cross pollination, which combines the desirable traits from two parent varieties (usually homozygous) creating a heterozygous F1 population with alleles from each parent. This can result in in hybrid vigour, or heterosis resulting in stronger offspring. The heterosis effect is often only visible in the first generation, thus new hybrid seed should be produced every year. Another conventional breeding method is polyploidy, producing lines with an increased number of chromosome sets. Polyploidy can occur spontaneously, or can be induced artificially using chemicals such as colchicine. Polyploid organisms often exhibit increased vigour and can outperform their diploid relatives in several aspects, thus have been the target for many breeders to improve plant cultivars (Sattler et al., 2016). Polyploidy has been shown to improve yields, product quality and tolerance to both biotic and abiotic stresses.

1.5.2 Modern breeding strategies

1.5.2.1 TILLING approaches

Diversity can be introduced in plants via induced-mutation approaches including TILLING (Targeting Induced Local Lesions In Genomes), which allows for the identification of an allelic series of mutants with a range of modified functions for desired genes. It is a reverse genetic tool that uses chemical mutagenesis (such as the ethyl methane sulfonate mutagenesis (EMS) method) for inducing variability and sensitive molecular screenings, for the identification of point mutations responsible for phenotype alteration. The mutagenesis strategy has the advantage of producing mutant

alleles directly for use in breeding programs as genetic sources or markers. The technology is considered straight forward and cost-effective, while being non-GMO. Therefore, it can be used to facilitate crop improvement without the GMO procedures and controversies, potentially alleviating consumer concerns and maximising commercialisation potential. TILLING has been successfully applied to a variety of crops. The technology has been applied to alter tomato fruit quality. TILLING was able to facilitate enhancement of carotenoids, resulting in a 2-fold increase to lycopene and total carotenoid content when applied to EMS-Red Setter tomato population for the lycopene cyclase locus (Minoia et al., 2010; Silletti et al., 2013). Similarly, mutations to genes encoding components of the tomato light signal transduction pathway, including *DEETIOLATED1* (*DET1*), resulted in resulted in elevated levels of both carotenoid and phenylpropanoid phytonutrients in ripe fruit (Jones et al., 2012). TILLING also resulted in the identification of the new allele of the *PSY-1* gene, providing important insights into carotenoid pathway regulation (Gady et al., 2012). Finally, mutant alleles of six ethylene receptor genes (*SlETR1–SlETR6*) delayed ripening and prolonged the shelf-life of tomato fruits, due to reduced ethylene responses (Okabe et al., 2011).

1.5.2.2 Genetic engineering strategies

Conventional breeding strategies including hybridisation and mutagenesis are often time consuming, unpredictable, and restricted to sexually compatible individuals. Therefore, more targeted approaches have been developed such as genetic engineering to help overcome these issues. One method is antisense RNA, which is a strand of nucleotides that binds to the mRNA to block the production of the protein based on its complementary properties (Hamilton and Baulcombe, 1999). The other is RNA interference (RNAi; also known as co-suppression) that has been an important functional genomics approach used for the identification and characterisation of genes with the ability to facilitate crop improvement. RNAi is a biological mechanism which leads to a post transcriptional gene silencing (PTGS) trigger, by the introduction of synthetic double stranded RNA (dsRNA) molecules to robustly supress the expression of specific endogenous genes (Younis et al., 2014). RNAi has proven to be more effective and specific than antisense strategies. RNAi technology has previously been used to characterise important genes involved in tomato ripening, including the *FRUITFULL*

homologs *FUL1* and *FUL2* (Shima et al., 2014), *MADS1* (Dong et al., 2013), *DET1* (Davuluri et al., 2005), *AP2A* (Karlova et al., 2011) and *FSR* (Zhang et al., 2018a).

1.5.2.3 Recent advances of CRISPR technologies

Clustered regularly interspaced palindromic repeats (CRISPR) had been found in bacteria and archaea, functioning as an adaptive immune system against invading viruses, phages and plasmids (Barrangou et al., 2007; Marraffini and Sontheimer, 2008; Wiedenheft et al., 2012).The bacteria are able to protect themselves using a series of CRISPR associated (Cas) proteins that cleave viral DNA. Pieces of viral DNA are inserted into their own genomes, forming CRISPR structures with spacer sequences that matched viral DNA, representing a memory of former infections. The bacteria then use certain Cas9 protein(s) paired with RNA transcribed from the viral DNA library to make targeted double-strand breaks in invading viral DNA. Engineering of nucleases such as Cas9 have enabled the domestication of CRISPR technology for targeted genome editing. Engineering of nucleases such as Cas9 and pairing with a synthetic single guide RNA (gRNA), results in the formation of RNA-guided nucleases (RGNs) with customizable specificities, enabling genome editing at any desired location (Sander and Joung, 2014; Malzahn et al., 2017). The emerging field of gene editing provides simplicity, precision, and a quicker, more powerful approach for crop improvement, without the incorporation of foreign transgenes. In tomato the CRISPR/Cas9 system has been utilised to induce mutations in the tomato *RIN* gene (Ito et al., 2015). The *RIN* silenced fruits exhibited incomplete-ripening and reduced ripening-related colour development, confirming the important role of RIN in ripening (Ito et al., 2015). The technology has also facilitated tomato improvements, through enrichment of lycopene (Li et al., 2018), extension to shelf-life (Yu et al., 2017), elevated fruit yield (Lin et al., 2016), and enhanced disease resistance (Nekrasov et al., 2017).

1.5.2.4 Systems Biology

Systems biology can be defined as the study of interactions among biological components, using models and/or networks to integrate genes, metabolites, proteins,

regulatory elements and other biological components (Yuan et al., 2008). The development of modern systems biology was driven by the need to assimilate the large amounts of data generated from different omics technologies such as genomics, proteomics, transcriptomics, interactomics and metabolomics into networks and models. It can define the interactions been genes and metabolites, plant interactome and protein interaction networks, gene and transcriptional regulatory networks, while modelling multigenic traits. Ultimately, plant systems biology has the potential to predict outcomes and provide crucial understanding of the regulatory networks controlling developmental, physiological and pathological processes in plants to help facilitate crop improvement. Systems biology approaches have been utilised in tomato to improve the understanding of tomato development and ripening (Alba et al., 2005; Lee et al., 2011; Osorio et al., 2011b; Osorio et al., 2012; Van de Poel et al., 2012; Pan et al., 2013).

1.6 Underlying scientific rationale of the project

Current breeding strategies have utilised the heterozygous *rin* mutation, due to reduced fruit softening and extension to shelf-life (Vrebalov et al., 2002). However, this has been at the expense of sensory quality with reduced ripening-related colour development, carotenoid accumulation, flavour and aroma. Therefore, it is important to identify transcription factors that compared to RIN are down-stream in the ripening cascade and other global ripening-regulators. This would provide further elucidation of the complex transcriptional control that governs fruit ripening and quality. Characterisation has previously been performed through the insertion of a knock-down 35S::RNAi construct under constitutive control into Ailsa Craig background. RNAi approaches have been utilised as they rarely lead to complete knock-down of gene expression, reducing the probability of mutant lethality. This strategy has proven successful both within the project with the identification of the fruit softening-related enzyme PECTATE LYASE, and a DEMETER-like DNA DEMETHYLASE (Liu et al., 2015c; Uluisik et al., 2016), in addition to determine the function of a variety of ripening-related transcription factors (Davuluri et al., 2005; Vrebalov et al., 2009; Bemer et al., 2012; Dong et al., 2013; Shima et al., 2014; Weng et al., 2015b).

1.7 The aim and objectives of this study

The aim of this project was to functionally characterise three transcription factors with ripening-related expression profiles, identified from system biology outputs to assess their effect on fruit quality. To date these transcription factors have not been characterised, system biology approaches revealed they are associated with known regulators of ripening.

Objective 1: Functional characterisation of the ZINC FINGER PROTEIN INDETERMINATE DOMAIN 2 (Solyc08g063040). To date this transcription factor had not been characterised but is a direct target of RIN and FUL1/2. To ascertain its function transgenic plants were made, they have been phenotyped over multiple generations, then molecular and biochemical techniques were used to elucidate the underlying principles (Chapter III).

Objective 2: Functional characterisation of the ZINC FINGER PROTEIN ZPR1 (Solyc02g069120). System biology outputs revealed that the transcription factor has a ripening-related expression profile and is expected to be downstream of multiple important ripening-regulators. To confirm a role in ripening, transgenic plants were made and phenotypic, molecular and metabolic approaches were utilised over multiple generations for functional characterisation (Chapter IV).

Objective 3: Functional characterisation of the HEAT STRESS TRANSCRIPTION FACTOR A3 (Solyc08g062960). The transcription factor was shown to interact with multiple ripening-related transcription factor hubs, identified previously using systems biology approaches. Despite this, its function has not been elucidated. Transgenic plants were made, and over multiple generations phenotypic, molecular and metabolic strategies were combined to establish its role (Chapter V).

Chapter II: Materials and methods

2.1 Plant cultivation and collection

2.1.1 Tomato cultivation

Tomato (*Solanum lycopersicum* Mill. cv. Ailsa Craig) plants were grown in pots containing M3 professional growing medium (Scotts Levington®, UK), and transferred to larger pots during development. Plants were cultivated to maturity under controlled greenhouse conditions, day and night time temperatures were approximately 25°C and 15°C, respectively. Humidity ranges were between 30-80%. A supplementary lighting regime of 16 h of light and 8 h of dark was used, to ensure at least 16,200 lux was achieved through a combination of natural daylight and growth lights.

2.1.2 Defining the stages of development and ripening

Tomato flowers were tagged at anthesis (once fully opened) to determine the age of developing fruits post anthesis. Mature green (MG) fruit are defined as being full size and green, prior to ripening. Fruits were also tagged at breaker stage, which represents the start of ripening and the initiation of ripening-related colour (orange/yellow) on predominantly green fruited tomatoes. Breaker stage was used to determine the ripening-related colour development and for accurate collection of fruit at different ripening stages. The main stages of ripening in this study are defined as breaker (Br), 3 days post breaker (3dpb), 7 days post breaker (7dpb), 14 days after breaker (14dpb).

2.1.3 Classification of individual lines

Each transcription factor studied was denoted by a number: zinc finger protein indeterminate domain 2 (10-), zinc finger protein ZPR1 (6-) and heat stress transcription factor A3 (4-). Lines were then classified based upon their progeny number through the several generations studied. For example 10-8-15-7-4 is a zinc finger protein indeterminate domain 2 transgenic line, the T_0 progeny number was 8, the T_1 progeny number was 15, the T_2 progeny number was 7 and the T_3 progeny number was 4.

2.1.4 Phenotypic characterisation

Various plant morphological phenotypic parameters were investigated for each plant (line) cultivated. Seedling growth was measured from soil to the top of the plant approximately three weeks post germination. Once the wild type Ailsa Craig (AC) background had formed five trusses, flower and truss phenotypes were assessed: including truss and flower number, number of flowers per truss and truss forking. Truss forking is defined by a singular truss axis that splits into multiple axes capable of yielding flowers. Then internode length and total plant height were measured once the Ailsa Craig (AC) wild type background had three or five trusses with fruit set. An internode length represents the distance between adjoining main stem nodes, which were randomly selected from the base of plant to the last node. The total plant height was measured from the soil to last node for each plant.

Several yield parameters were also studied, including fruit number, fruit size and total fruit yield, once the wild type AC background had formed five trusses with fruit set. All fruit weights were recorded individually postharvest and combined to determine total fruit yield. Non-vegetative biomass was determined by combining the following: the tallying of shoot cutting weights during development prior to senescing, and the remaining total leaf and stem weights post harvesting of all fruits. Shoot cuttings of older leaves were removed at regular intervals upon the first signs of senescence, which was identified visually by a loss of leaf pigmentation for example. Crop production efficiency or the harvest index was calculated by dividing total fruit yield by the non-vegetative biomass.

Further fruit phenotypic traits were evaluated. Fruit development time was determined by tagging flowers at anthesis (fully open flowers) and then recording the time taken to reach the onset of ripening at breaker stage. Fruits were then tagged at breaker to determine the number of days post breaker. The colour-associated ripening time was visually adjudicated, representing the time taken in days for fruits to transition from breaker to uniform red colour on the plant. A non-destructive method was used to determine fruit firmness and the rate of fruit softening. A Qualitest™ firmness meter with a 0.25cm^2 probe was used determine the firmness factor of fruits, immediately postharvest. The principle of the method is based on the millimetre of probe penetration into the fruit peel, producing a firmness percentage value. At each given time point between three and four measurements at different locations were recorded for each fruit

studied. Unless stated otherwise, a minimum of three fruit were studied per line. The individual lines were studied separately and were combined for each control genotype, while transgenic lines were kept separate.

2.1.5 Post-harvest assessment of ripening-associated fruit quality

Fruits were harvested at breaker stage and stored separately at room temperature in light conditions, but away from direct sunlight, following common commercial practices. Breaker stage was also chosen, as determining the maturity status of green fruits is difficult and would likely result in the harvesting of fruits at different developmental stages. Room temperature provided optimal ripening conditions for the fruits. This strategy limits the potential variation and ensured normal fruit ripening. Fruits were sterilised in 0.5% bleach for 10 min, prior to rinsing three times with sterile distilled water and then air-dried. Sterilising fruits ensured sterile and equal conditions for all samples tested. The ripening-related quality of post-harvest fruits was assessed, determining colour development and rate of softening.

Ripening time was evaluated visually by the number of days taken for fruits to reach a uniform red colouration. Colour development was monitored in more detail using a HunterLab's MiniScan XP colourimeter utilising the CIELAB sphere, defining colour along three perpendicular axes: L* (from white to black), a* (green to red) and b* (blue to yellow). Six time points throughout ripening from breaker (B+0) to breaker plus fourteen days (B+14) were chosen for this analysis. For each time point four colourimeter measurements were taken per fruit at different locations, thus the average was representative of the whole fruit. This strategy provided a quantitative approach to identify visual ripening-related colour changes. The rate of ripening-related softening was calculated by monitoring fruit firmness daily using the Qualitest™ firmness meter, providing an assessment of the storage potential of fruits. Firmness was quantified at four different points on the fruit to ensure the average is representative, measurements were taken from breaker to breaker plus twenty-one days. A total of five fruits were analysed per plant and a minimum of three individual plants from each line were combined for the analyses.

2.1.6 Probe penetration tests

Probe penetration tests enabled the investigation of the mechanical properties of fruit, the method used has been previously described (Chapman et al., 2012; Uluisik et al., 2016). The analysis determined whether the inner or outer pericarp tissue is the main contributor to increased fruit firmness. A 6-mm equatorial section of the outer and inner pericarp was cut from each fruit. Then a Lloyd Instrument LF, equipped with a 10-N load cell and 1.6-mm flat-head cylindrical probe, calculated maximum load required to penetrate the pericarp at 10 mm min^{-1}. The outer pericarp was defined as below the skin but before the vascular boundary, and the inner pericarp as the cells between the vascular boundary and the endodermis.

2.1.7 Tissue collection for DNA/RNA analysis

Leaf and fruit tissues were harvested. A total of four expanding leaves were harvested for each biological replicate. Younger leaves were preferentially chosen, from the top of developing plants. A minimum of three fruits from each biological replicate were harvested in situ at a predefined stage of ripening, four days post breaker (B+4). Both the seeds and jelly tissues were removed and the pericarp was cut in pieces. Once harvested, both leaf and fruit tissues were flash frozen and stored at -80°C, before grinding and subsequent nucleic acid extraction.

2.1.8 Tissue collection for metabolite analysis

Both leaf and fruit tissues for metabolite analysis were harvested in a similar manner to that described in section 2.1.7. Developing fruits were harvested at 20 days post anthesis. Ripening fruits were harvested at several stages: four, seven and fourteen days post breaker (B+4, B+7 and B+14). Leaves and fruits were subsequently freeze dried for one and three days, respectively, until completely dry. Material was then stored at -20°C, prior to grinding and extractions.

2.1.9 Seed collection

During fruit harvesting seeds were removed and treated in a hydrochloric acid solution (1:1 HCl (32%)/dH2O) within a plastic tray for between 30 and 60 min. Seeds were then thoroughly rinsed with water and dried on filter paper for one day. Seeds were then stored in a paper envelope at room temperature.

2.2 DNA and RNA molecular analysis

2.2.1 DNA extraction from plant tissues

The Qiagen DNeasy® Plant Mini Kit was used to extract and purify total cellular genomic DNA, following the manufacturer's instructions. A TissueLyser LT (Qiagen, UK) was used to grind the frozen leaf material collected, as detailed in section 2.1.7. Prior to grinding, the insert of the TissueLyser LT adapter was incubated on dry ice for 30 min. Up to 100 mg of frozen leaf material was weighed and placed into a pre-cooled 2 ml sterile sample tube RB (Qiagen, UK) with one 0.5 mm stainless steel bead (Qiagen, UK). Tissues were ground twice for 1 min at 50Hz, in between samples were placed on dry ice for 5 min.

Steel beads were removed, the frozen ground samples were lysed in AP1 buffer (400µl) and the RNA present was degraded using RNase A (4 µl). Samples were vigorously mixed by vortexing and then incubated at 65°C for 10 min, inverting several times during incubation to ensure that material were lysed. Then buffer P3 (130 µl) was added, samples were vortexed and incubated on ice for 5 min. The lysate was centrifuged for 5 min at 18,000 xg with an Eppendorf 5424 centrifuge. The supernatant was transferred to the QIAshredder Mini spin column in a 2 ml collection tube. The sample was then centrifuged for a further 2 min at 18,000 xg. The resultant flow-through was transferred to new sterile microcentrifuge tube, with care to not disturb the pellet, then buffer AW1 (1.5 x volume of lysate collected) was added and mixed thoroughly by pipetting. The sample was transferred to a DNeasy Mini spin column and then centrifuged at 6,000 xg for 1 min, the flow-through was discarded. The spin column was placed into a new sterile microcentrifuge tube. Then buffer AW2 (500 µl) was added to the column and

centrifuged for 1 min at 6,000 xg, the flow-through was discarded. The buffer AW2 wash step was repeated, but samples were centrifuged for 2 min at 18,000 xg. The spin column was then transferred to another sterile microcentrifuge tube and centrifuged again for 2 min at 18,000 xg to remove any remaining ethanol. The spin column is transferred to another sterile microcentrifuge tube and AE buffer (40 µl) was added. The sample was incubated for 5 min at room temperature, before being centrifuged for 1 min at 6,000 xg. This step was repeated, resulting in a final total of 80µl of eluted DNA. The concentration and purity (based upon the 260/280 ratio) was assessed using a NanoDrop 1000 spectrophotometer v3.7. A ratio of ~1.8 and ~2 are accepted as pure for DNA, these samples were selected. DNA solutions were stored at -20°C.

2.2.2 RNA extraction from plant tissues

The Qiagen RNeasy® Mini Kit and the RNase-Free DNase set (Qiagen, UK) were used to extract total cellular RNA from plant tissues, following the manufacturer's instructions. The fruits harvested and stored at -80°C, as detailed in section 2.1.7, and were ground in liquid nitrogen using a mortar and pestle. A minimum of three fruits were ground per biological replicate. Up to 100 mg of frozen powder was weighed and placed into pre-cooled 1.5 ml sterile microcentrifuge tube. Care was taken to ensure material stayed frozen throughout the grinding and weighing procedure. Then buffer RLT (450µl; containing β-mercaptoethanol) was added to the frozen material, followed by vigorous vortexing. The lysate was then transferred to a QIAshredder Mini spin column placed in a sterile 2 ml collection tube. The sample was then centrifuged for 2 min at maximum speed using an Eppendorf 5424 centrifuge. The supernatant of the flow-through was transferred to a sterile microcentrifuge tube, taking care not to disturb the cell-debris pellet in the collection tube. Then 100% ethanol (0.5 x volume of lysate collected) was added and mixed by pipetting. The sample was then transferred to an RNeasy Mini spin column placed in a sterile 2 ml collection tube, prior to centrifugation for 15 sec at 9,000 xg. The resultant flow-through was discarded. Buffer RW1 (350 µl) was added and the column was centrifuged for 15 sec at 9,000 xg and the flow-through was discarded. Then a DNaseI incubation mixture (80 µl) was prepared by mixing RDD buffer and DNaseI (7:1, v/v), this was added directly to the RNeasy spin column membrane and incubated at room temperature for 15 min. Three wash steps followed, the first with buffer RW1 (350 µl) followed by another wash with buffer RPE (500 µl).

The column was centrifuged for 15 sec at 9,000 xg and the flow-through was removed after each wash. A final wash with buffer RPE (500 µl) was performed and the column was centrifuged for 2 min at 9,000 xg. The RNeasy spin column was then transferred to a new sterile microcentrifuge tube, discarding the flow-through, and then centrifuged for 2 min at maximum speed to ensure all buffer RPE was removed from the column. The membrane was again placed into a sterile microcentrifuge tube. The RNA was eluted with RNase-free water (30µl, twice) by centrifugation for 1 min at 9,000 xg. Repeating the elution improved RNA yield. The concentration and purity of RNA samples were tested on the NanoDrop 1000 spectrophotometer v3.7. Samples with a 260/230 and a 260/280 ratio of ~1.8 and ~2.0 are accepted as pure for RNA. Gel electrophoresis was performed on an agarose gel (1%) to determine the integrity of RNA. The RNA samples were then diluted to desired concentration and aliquoted prior to storage at -80°C.

Samples sent for RNA-Seq were pooled after quantification and qualification. Then Biomatrica® RNAstabilizer (20µl) was added to each sample and mixed gently by pipetting. Samples were dried using a GeneVac Ez-2 Plus rotatory evaporator (UK) and stored in room temperature, following the manufacture guidance.

2.2.3 Molecular methods to detect the presence of the transgene

2.2.3.1 Primer design

Primer3web version 4.0.0 (http://primer3.ut.ee/) was used to design primers, while the sequence of the genes of interest was obtained from Sol Genomic Network (http://solgenomics.net/search/loci). The following specifications were used to design primers for PCR analysis: 18-23bp (optimal 20bp) for primer length, a percentage of GC content of 30-70% (optimal 50%) and a Tm of 57-62°C (optimal 59°C) with less than 5°C difference. For real-time PCR analyses, using the SYBR® Green system, primers were designed with different specifications: with an amplicon length of 100-150bp, primer length of 10-30bp, GC content of 40-60% and a Tm of 55-60°C with a maximal difference of 4°C between primers. Primers were supplied by Eurofins MWG Operon, UK. The sequences of the primers used in this work are listed in the appendix Table A1-1.

2.2.3.2 PCR

PCR was used determine the insertion of the 35s transgene by detecting the presence of the *NPTII* gene (Neomycin phosphotransferase II gene). Comparisons with AC wild type enabled the detection of transgenic lines and azygous (non-transgenic) controls. PCR reactions were carried out using Illustra™ puReTaq Ready-to-go PCR beads (GE Healthcare, UK), with the addition of both forward and reverse primers (10 pmol), genomic DNA (50 ng) and sterile molecular water (Sigma-Aldrich, UK) producing a final volume of 25 µl. PCR reactions were operated using a Techgene thermo cycler (Techne, UK). The tubes were incubated at 95°C for 5 min to denature the template DNA. PCR amplification followed, which included 30 cycles of: denaturation at 94°C for 30 sec, annealing at 55°C for 20 sec, extension at 72°C for 20 sec. Then a final incubation step at 72°C for 5 min completed the reaction.

2.2.4 Agarose gel electrophoresis

Agarose gel electrophoresis was performed for nucleic acid analysis, to determine the size of fragment and existence of PCR product, along with the integrity of DNA and RNA. Analysis was conducted on ~1% (w/v) agarose gels, depending on the size of the fragments of interest. Agarose powder was dissolved in TAE (Tris, acetic acid, and EDTA) through heating using a microwave. GelRed™ (Biotium, UK) was added at 10,000X dilution of stock. Once poured and set cast, the gel was then transferred to an electrophoresis tank filled with TAE. Samples were mixed with Blue/Orange Loading Dye (6X; Promega, UK) and loaded in gel wells. Also, depending on the nucleic acid analysed (DNA or RNA) and its size, an appropriate ladder (100 bp or 1kb; Promega) was run beside samples for size comparison. Gels were ran for between 20-40 min at 50-100 volts, and nucleic acids were visualized using a U:Genius3 gel imaging system (Syngene, UK).

2.2.5 Determination of the number of transgenes in plants

2.2.5.1 DNA purification

A Wizard® SV Gel and PCR Clean-Up System (Promega, UK) was used for the purification of the DNA from the PCR amplification and agarose gel, before cloning in to TOPO® vectors for real-time PCR analyses. Purification was carried out following the manufacturer's instructions. DNA purification from an agarose gel started with the excision of the DNA band containing the DNA fragment of interest, which was then placed in a microcentrifuge tube. Then 10 µl of Membrane Binding Solution was added per 10 mg of gel slice, the sample mixture was then vortex incubated at 50–65°C until the gel slice was completely dissolved. From this point, the same protocol was used for DNA purification from PCR amplification or agarose gel. Firstly, the Membrane Binding Solution was added to the PCR amplification in equal volumes, before mixing and transferring the sample mixture to a SV Minicolumn with a collection tube. This was then incubated for 1 min at room temperature, and then centrifuged at 18,000 xg for 1 min in an Eppendorf 5424 centrifuge. The flow-through was discarded, and the SV Minicolumn was reinserted into the collection tube. The SV Minicolumn was washed twice using the Membrane Wash Solution (700 µl and 500 µl, respectively), followed by centrifugation at 18,000 xg for 1 min and 5 min, respectively, and the flow-through was discarded. Residual ethanol was then allowed to evaporate by opening the lid of the microcentrifuge tube and centrifuging for a further 1 min at 18,000 xg. The SV Minicolumn was then transferred to a sterile 1.5 ml microcentrifuge tube, and 50 µl of Nuclease-Free Water was added directly to the centre of the column. Incubation for 1 min followed, before centrifugation for 1 min at 18,000 xg to elute the DNA, which was subsequently stored at -20°C. The purified DNA was used for cloning into TOPO® vectors, to use as a standard for real-time PCR analyses.

2.2.5.2 Media preparation

For plasmid amplification *Escherichia coli* strain DH5™ –T1R was used. Bacterial growth was maintained on Luria Broth (LB), which contained tryptone (1% (w/v)), yeast extract (0.5 % (w/v)) and NaCl (1% (w/v)). Solid LB media was made by the addition of agar (1.5% w/v). Media was autoclaved for 20 min at 121°C. Falcon tubes containing cooled LB and LB agar were supplemented with an appropriate antibiotic that had been prepared and filtered. LB agar was poured into Petri dishes to set inside a laminar flow hood at room temperature. *E. coli* were grown on solid and liquid media at 37°C, while liquid cultures were shaken at 180 rpm.

2.2.5.3 Cloning DNA in TOPO® vector

PCR products were ligated into vectors to allow amplicons to be cloned into pCR®2.1 TOPO® cloning vectors using the TOPO-TA DNA cloning® kit (Invitrogen, UK). The fresh PCR product (2 µl), salt solution (1 µl), TOPO vector (1 µl), and sterile water (2 µl; nuclease free) to a final volume of 6 µl were added to a sterile mircocentrifuge tube and gently mixed. The mixture was incubated at room temperature for 5-10 minutes, to allow the amplicon to become ligated with the vector. The tubes containing the TOPO® Cloning reaction mixture was then placed on ice, while One Shot®TOP10 chemically competent *E.coli* cells (DH5™ –T1R) were thawed on ice prior to use. Then the TOPO® Cloning reaction (2µl) was added to a vial of thawed One Shot TOPO10 chemically competent cells, which was then mixed gently and incubated on ice for 20 min. Competent cells were transformed by a heat shock treatment at 42°C for 30 sec followed by immediate incubation on ice. Room temperature S.O.C. medium (250 µl) was added to the tubes and then the transformation reaction was incubated at 200 rpm at 37°C for 1 h using a shaking incubator. Aliquots of the transformed cells (50-150 µl) were then spread on pre-warmed LB agar plates supplemented with kanamycin (50 µg/ml), and then incubated overnight at 37°C. The resulting colonies were used to inoculate LB medium (5 ml) containing kanamycin (50 µg/ml), the liquid cultures were incubated overnight in a shaking incubator at 37°C. Liquid cultures were used to make glycerol stocks, and for the isolation of plasmid DNA using the Wizard® Plus SV Miniprep DNA Purification System.

2.2.5.4 Glycerol stocks

Glycerol stocks of the transformed cells were prepared in a sterile manner by the addition of overnight liquid culture of bacteria (1.5 ml) to sterilised glycerol (100%; 0.5ml), in pre-autoclaved 2 ml screw-cap tubes. The stock was mixed well by pipetting and subsequently and placed at -80°C for long-term storage. Frozen bacterial cells were revived and re-cultured by scraping cells from the surface of frozen glycerol stocks, and streaked on to LB agar plates supplemented with an appropriate antibiotic, in a sterile manner. Plates were incubated at 37°C overnight up to two days to establish new colonies.

2.2.5.5 Plasmid DNA purification from bacterial culture

The Wizard® Plus SV Minipreps DNA Purification System (Promega, UK) was used to isolate the plasmid DNA from the bacterial cells, following the manufacturer's instructions. The bacterial overnight LB cultures were pelleted by centrifugation at 3,000 xg for 5 min using an Eppendorf centrifuge 5810R. The supernatant was discarded and the pellet was resuspended in Cell Resuspension Solution (250µl), prior to being transferred into a fresh 1.5 ml microcentrifuge tube. Then Cell Lysis Solution (250 µl) was added and tubes were inverted four times to mix. Alkaline Protease Solution (10 µl) was added before inverting a further four times to mix. The sample was incubated for 5 min at room temperature. The addition of Neutralization Solution (350 µl) followed, which was inverted four times to mix. The sample was then centrifuged at 18,000 xg for 10 min using an Eppendorf centrifuge 5424. The cleared lysate (supernatant) was then decanted into a Spin Column placed in a 2 ml collection tube, care was taken not to disturb the pellet. The column was then centrifuged at 18,000 xg for 1 min and the flow-through was discarded. Wash Solution (750 µl) was added and centrifuged for 1 min at 18,000 xg. The flow-through was discarded. This was repeated with 250µl and centrifuged for 2 min. The Spin Column was transferred to a sterile 1.5 ml microcentrifuge tube, then the DNA was eluted in Nuclease-Free Water (100µl) by centrifugation at 18,000 xg for 1 min. Both the quality and quantity of plasmid DNA was checked using a NanoDrop 1000 spectrophotometer v3.7 and agarose gel electrophoresis (section 2.2.1 and 2.2.6) before being stored at -20°C. Plasmid DNA was used as the standard template in both qPCR and RT-qPCR experiments.

2.2.5.6 Quantitative real-time PCR

Quantitative real-time PCR (qPCR) was used to verify the number of transgene inserts present. It relies on the relative amplification of the transgene compared to *PHYTOENE DESATURASE*, an endogenous single-copy gene utilised as a normaliser. A QuantiFast™ SYBR® Green RT-PCR kit (Qiagen, UK) and a thermal cycler of Research Rotor-Gene RG-3000 (Corbett Life Sciences, UK) were used for the qPCR analysis. DNA was extracted from leaves and quantified using a NanoDrop 1000 spectrophotometer v3.7 (section 2.2.1). DNA had been diluted and aliquoted to 25 ng/µl prior to use. A master mix was prepared for each gene separately, containing: 2X QuantiFast SYBR Green PCR Master Mix (10 µl), forward and reverse primers (1 µM), sterile RNA-free water, and QuantiFast RT Mix (0.2 µl) to a final volume of 19 µl. The master mix was mixed by inversion, spun down and stored on ice before aliquoting into wells. Then the amplicon DNA (25 ng) template were added (1 µl), thus the final reaction volume was 20 µl. Lids were placed onto qPCR tubes and placed in the Research Rotor-Gene RG-3000. Thermocycling conditions were, 95°C for 5 min for the activation of HotStarTaq DNA polymerase, followed by 35 cycles of 5 sec at 95°C for denaturation and 10 sec at 60°C for combined annealing and extension. To verify the specificity of the reactions, melt curve analysis was carried out. Calibration curves for each gene were run simultaneously with experimental samples, covering the complete range of expected expression for both the gene of interest and normaliser gene. They consisted of 4 or 5 points of dilution of TOPO® plasmids containing the DNA amplicon of interest (section 2.2.5.3). The standard curve was conducted in triplicate, while experimental reactions were conducted in duplicate. The linearity, reaction efficiency, sensitivity and reproducibility of the assay were determined by the standard curve. The efficiency of the PCR given by the Rotor-Gene software had to be between 0.9 and 1.1, and the R^2 value (which indicates how well the data points lie on the line) of more than 0.985, for the qPCR run to be considered acceptable.

The Rotor-Gene software enabled a direct comparison of *Ct* values between the target gene and the reference gene, which allows a relative quantification of the amount of DNA of interest in the experimental sample compared to the calibrator sample. Both the target and reference gene PCR efficiencies were between 90 and 110%, with a maximum difference of 10%. The target gene was the *NPTII* gene and the reference gene was

PHYTOENE DESATURASE (endogenous single-copy gene). The reference gene was divided by the target gene to determine the number of transgenes present.

2.2.5.7 Southern blot

Regular PCR and gel electrophoresis identified the presence of the transgene in tomato lines, and then Southern blotting was performed to determine the number of inserts present. DNA (~10 µg), was extracted from transgenic lines and AC wild type controls (untransformed plant), as described in section 2.2.1. The first step was the synthesis of a probe for the gene of interest, labelled with DIG-dUTP. Polymerase chain reaction was used to create the probe using the PCR DIG Probe synthesis kit (Roche, UK), following the manufacturer's instructions. A restriction enzyme was used to digest the DNA from experimental samples, along with both positive and negative controls. The restriction enzyme is required to cleave only once between the left and right border of the insert, but not in the gene of interest, while also being a high frequency enzyme. The restriction enzyme SacI (Promega, UK) was used for the digestion in accordance with the manufacturers' instructions. One unit is defined as the amount of enzyme required to digest 1 µg of lambda DNA in 1 hour at 37°C. The reactions contained DNA (~10 µg), enzyme buffer (10X), BSA (100X; bovine serum albumin), SacI (50 units) and nuclease free water to a final volume of 150 µl. Samples were gently mixed and then incubated at 37°C for 1 h. Due to the lower efficiency of SacI, more units of enzyme were used, and the addition of restriction enzyme and incubation step was repeated. The DNA was precipitated using ethanol. Sodium acetate pH 5.2, to 0.3 M was used to adjust the salt concentration of the digestion reaction, and then ethanol was added. Centrifugation at 20,000 xg for between 10-30 min at 4°C followed, using an Eppendorf centrifuge 5424. The supernatant was discarded, with care taken not to disturb the pellet. Room temperature 70% ethanol was then used to wash the DNA pellet, prior to centrifugation again at 20,000 xg for between 5-15 min at 4°C. Supernatant was discarded and the pellet was air-dried for 5 to 20 min. AE buffer (15 µl; Qiagen) was used to dissolve the DNA. Then a 0.8% agarose gel was prepared (section 2.2.6), and genomic DNA (~10 µg), plasmid (~1 ng; positive control) and 1 Kb ladder (Promega) were loaded onto the gel after being mixed with Blue/Orange Loading Dye (6X; Promega, UK). The gel was subsequently run at 25 V overnight (section 2.2.6), for optimal separation of the DNA bands. The digest was reviewed by post staining with gel red (33,000X) for 25 min. Post

visualisation, the gel was submerged in Denaturation solution (0.5 M NaOH, 1.5 M NaCl) for 15 min at room temperature, with gentle shaking, and then the solution was poured off. This step was repeated, before the gel was rinsed with sterile distilled water. Then the gel was submerged in Neutralisation solution (0.5 Tris-HCl, pH 7.5, 1.5M NaCl) for 15 min at room temperature with gentle shaking, solution was poured off and this was repeated. The gel was equilibrated for at least 10 minutes in 20x SSC (3M NaCl, 300mM sodium citrate, pH 7.0).

The blot transfer apparatus was then assembled, at the bottom a reservoir was filled with 20x SSC buffer. A glass plate was placed over the reservoir. A long sheet of Whatman paper (3MM paper; Whatman international Ltd) was cut, to cover the glass plate with both ends being in contact with the 20x SSC buffer in the reservoir to create a bridge. The gel was placed on top of the soaked Whatman paper. A positively charged nylon membrane (1417240.1; Roche, UK) was then placed over the gel. The Whatman paper on each side of the membrane was covered with parafilm. The blot assembly was completed with further sheets of Whatman paper laid on the membrane, followed by a stack of paper towels, another glass plate and several weights (200-500 g) distributed evenly. The assembly was left overnight ensuring that the DNA transferred from the gel to the membrane.

The blot transfer apparatus was then disassembled, and then each side of the wet membrane was exposed to UV light for 1 min at 120 mJ in a transilluminator (UVItec, UK). The membrane was then rinsed with molecular grade water (Sigma-Aldrich, UK), which is free from DNase, RNase and protease contamination. The membrane was air dried, and then placed in a mesh, which was rolled tightly and inserted into Hybaid tubes (Thermo Scientific, UK), containing pre-warmed pre-hybridisation buffer (20 ml of DIG Easy Hyb; Roche, UK). The Hybaid tube was then incubated in the Hybaid oven for at least 30 min at 49ºC. The hybridisation temperature depends on the sequence of the probe used. The hybridisation solution, containing DIG Easy Hyb (7 ml), with the appropriate PCR probe (21 µl) was prepared and incubated in a second Hybaid tube for 10 min at 68ºC in the oven. The pre-hybridisation buffer is then poured off from the first Hybaid tube and replaced by the pre-warmed hybridisation solution. The tube was then incubated in the oven rotating for 6 to 16 hours at 49ºC.

The hybridisation solution was then poured away and replaced with low stringency buffer (100 ml; 2X SSC (0.3 M NaCl, 30 mM sodium citrate, pH 7.0)) containing 0.1% (w/v) SDS. The tube is then incubated at room temperature for 5 min, with manual

rolling. Used buffer is then discarded and replaced with fresh low stringency buffer; the incubation step is then repeated. The low stringency buffer was poured off and pre-warmed high stringency buffer (100 ml; 0.1X SSC + 0.1% (w/v) SDS) was added. Incubation of the Hybaid tube followed for 15 min at 68ºC in the Hybaid oven under rotation. Again used buffer was discarded and replaced with fresh high stringency buffer, and the incubation was repeated. The membrane was placed into a washing solution (100 ml; 0.1 M maleic acid, 0.15 M NaCl, pH 7.5, 0.3% Tween 20) and incubated for 2 min with shaking at room temperature. The washing solution was replaced with blocking solution (100 ml; Roche) which was incubated for 30 min with shaking at room temperature. The blocking solution was discarded, and an antibody solution (Anti80 Digoxigenin-AP; Roche, 1:10,000 in blocking solution) was added. The membrane was incubated for 30 min with shaking at room temperature, before being rinsed with molecular grade water (Sigma-Aldrich, UK). Two further 15 min wash steps followed with the washing buffer (100 ml; 0.1 M maleic acid, 0.15 M NaCl, pH 7.5, 0.3% (v/v) Tween 20). The membrane was equilibrated for 3 min in 20 ml of detection buffer (20 ml; 0.1M Tris-HCl, 0.1M NaCl, pH 9.5), prior to being placed into a bag containing CSPD solution (1:100 in detection buffer; Roche; 4 ml). The membrane was then incubated for 5 min at room temperature. Excess CSPD solution was removed and the bag was sealed. To enhance the luminescence reaction, the bag was then incubated for 10 min at 37ºC in an incubator (Memmert, UK). The bag containing the membrane was then placed DNA face up into a cassette (Curix AGFA, UK), together with a Lumi-Film Chemiluminescent Detection Film (Roche, UK) and left for 30 min to 120 min. A developer (Photon Imaging Systems, UK) was used to develop the film. The number of bands present in each lane on the developed film corresponded to the number of inserts of transgenes in the plants.

2.2.6 Transcript level quantification

2.2.6.1 RT-PCR

Reverse-transcription PCR (RT-PCR) was used to produce a complementary DNA (cDNA) template of the genes of interest. Illustra™ Ready-to-go™ RTPCR beads (GE Healthcare, UK) and a Techgene thermo cycler (Techne, UK) were used for RT-PCR amplification. RNA was extracted from tomato plant tissues as described in section 2.2.2. Molecular grade water (Sigma-Aldrich, UK) was first added to the reaction, followed by oligo (dT) primer (2.5 pmol) and RNA template (~200 ng), the reaction was mixed by flicking tubes before being spun down. Tubes were then transferred to the thermocycler and incubated at 55°C for 5 min to denature the template. Then reverse transcription reaction followed at 42°C for 30 min and then a final incubation step at 95°C for 5 min to denature the reverse transcriptase. Forward and reverse primers were then added to the tubes and mixed. This was followed by 30 cycles of PCR amplification: with denaturation at 94°C for 30 sec; annealing at 48°C for 30 sec; and extension 72°C for 30 sec. The reaction was completed with a final incubation step of 5 min at 72°C. The PCR products were checked by agarose gel electrophoresis (section 2.2.4), and the DNA was purified (2.2.5.1). Then the desired gene was cloned into TOPO® vectors (section 2.2.5.3), and plasmid DNA was isolated using the Wizard® Plus SV Miniprep DNA Purification System (section 2.2.5.5) for real-time RT-qPCR.

2.2.6.2 RT-qPCR

Real-time qRT-PCR was performed to quantify the relative expression of genes of interest. A QuantiFast™ SYBR® Green RT-PCR kit (Qiagen, UK) and a thermal cycler of Research Rotor-Gene RG-3000 (Corbett Life Sciences, UK) were used for the RT-qPCR analysis. The RNA extracted had been diluted and aliquoted to 25 ng/µl and then stored at -80 °C prior to use (section 2.2.2). First a master mix was produced for both the gene of interest and reference gene. For each well the master mix consisted of: 2X QuantiFast SYBR Green RT-PCR Master Mix (10 µl), forward and reverse primers (1 µM), sterile RNA-free water and QuantiFast RT Mix (0.2 µl) to a final volume of 19 µl.

The master mix was mixed by inversion, spun down and stored on ice before aliquoting into wells. This step was conducted quickly due to sensitivity of QuantiFast RT Mix. Then the amplicon DNA and RNA template were added (1 µl), thus the final reaction volume was 20 µl. The amplicon DNA and RNA template are used to produce a standard curve and the determination of the transcript levels for the gene of interest, respectively. Lids were placed on the qPCR tubes, which were then spun down quickly and placed in the Research Rotor-Gene RG-3000. Thermo-cycling conditions were 10 min at 50°C for reverse transcription, followed by incubation for 5 min at 95°C for the activation of HotStarTaq DNA polymerase. Then 35 cycles of PCR amplification consisting of: 10 sec at 95°C for denaturation and 30 sec at 60°C for combined annealing and extension. To verify the specificity of the reactions, melt curve analysis was carried out. The calibration curves covered the complete range of expected expression for both the gene of interest and reference gene, consisting of 4 or 5 points of dilution of TOPO® plasmids containing the RNA amplicon of interest (section 2.2.6.1 and 2.2.5.3). The actin gene was used as the normaliser, due to similar expression throughout all growth stages. The standard curve was conducted in duplicate, while transcript levels were conducted in triplicate. The linearity, reaction efficiency, sensitivity and reproducibility of the assay were determined by the standard curve. The efficiency of the PCR given by the Rotor-Gene software had to be between 0.9 and 1.1, and the R^2 value (which indicates how well the data points lie on the line) of more than 0.985, for the RT-qPCR run to be considered acceptable.

Relative quantification of gene expression was performed by comparing *Ct* (cycle threshold) values between the target gene and the reference gene, given by the Rotor-Gene software. The *Ct* value is defined as the number of cycles required for the fluorescent signal to cross the threshold values, providing a number for the amount of copies of the transcript present. Relative quantification was followed by equation below:

ΔCt = Ct target – Ct reference gene

$\Delta\Delta Ct$ = (Ct target – Ct reference) calibrator – (Ct target – Ct reference) sample

2.3 Extraction and analysis of metabolites

2.3.1 Isoprenoid and phenolic extraction for UPLC analysis

Freeze dried fruits were used for extraction of pigments and tocopherols. Samples were ground into a fine homogenous powder using a TissueLyser II (Qiagen, UK) and one 0.5 mm stainless steel bead (Qiagen, UK). Sample powder (10 mg) was weighed in a microcentrifuge tube (2 ml). Metabolites were extracted by the addition methanol (250 µl) and chloroform (500 µl); samples were mixed vigorously using a vortex after the addition of both methanol and chloroform. Extractions were then incubated on ice for 20 min. Water (250 µl) was added and samples were vortexed, and then centrifuged at 18,000 xg for 5 min at 4°C using an Eppendorf centrifuge 5424. The organic phase (chloroform layer) was removed and added to a fresh microcentrifuge tube. Then the aqueous phase was re-extracted with chloroform (500µl). The organic phases were pooled together and dried using a GeneVac Ez-2 Plus rotatory evaporator (UK), before storing at -20°C prior to analysis.

Freeze dried fruits were also used for the extraction of phenolics. Extractions were made from sample powder (20 mg) in 2 ml microcentrifuge tubes. Methanol (2 ml) was added and the sample was vigorously mixed using a vortex, followed by incubation at 90°C for 1 h. Tube cap locks were used to prevent evaporation. Samples were placed on ice for 20 min and then centrifuged at 1,000 xg for 10 min at 4°C using an Eppendorf centrifuge 5424. The supernatant was transferred to a fresh microcentrifuge tube (1.5 ml) and dried using a GeneVac Ez-2 Plus rotatory evaporator (UK), before storing at -20°C. Prior to analysis samples were re-suspended in 20% MeOH containing 0.02mg/ml salicylic acid (200 µl), vigorously vortexed and centrifuged at maximum speed for 10 min at 4°C.

2.3.2 Spectrophotometric quantification of carotenoids

For many carotenoids the specific absorption coefficients for an absorbance of a 1% sample in a 1 cm path-width cuvette (A1% in a 1 cm light path) have been determined and published (Britton, 1995).

The following equation, using these coefficients, can be used to determine the weight (X; mg) of carotenoid in a sample solution (Y; ml):

X = (Abs x Y x 1000)/ absorbance coefficient x 100)

Purified carotenoids that were suspended in the appropriate solvents were quantified using the equation above. Absorbance (Abs) was then determined at the wavelength corresponding to the absorbance maxima (λmax) of the carotenoid in the given solvent, using a DU®800 Spectrophotometer (Beckman Coulter, UK). The equations below from Wellburn (1994) enable the calculation of chlorophyll a (Ca) and chlorophyll b (Cb) and total carotenoids concentrations in a mixed sample. The equations include the absorbance coefficient values of chlorophylls and carotenoids suspended in chloroform, and the absorbance (Abs) of a mixed sample measured at the λmax of Ca (666nm), Cb (648 nm) and Cx+c (480 nm).

Ca (chlorophyll a) = (10.91*Abs666) – (1.2*A648)

Cb (chlorophyll b) = (16.38*Abs648) – (4.57*Abs666)

Cx+c (total carotenoids) = (1000* Abs480 – 1.42*Ca – 46.09*Cb)/ 202

Sample (1 µl) was suspended in chloroform (1 ml), and a Beckman Coulter DU®800 spectrophotometer measured the Abs480, Abs648 and Abs666 which were used to quantify Ca, Cb and Cx+c, using the equations above.

2.3.3 Ultra High Performance Liquid Chromatography

Carotenoids and tocopherols were analysed by an Acquity™ system Ultra High Performance Liquid Chromatography (UPLC) with photo diode array detection (UPLC-PDA). Separation was performed using a reverse phase BEH C18 column (2.1 x 100 mm, 1.7 µm) with a BEH C18 VanGuard pre-column (2.1 x 50 mm, 1.7 µm). The mobile phase used consisted of A, methanol/water (50/50 by volume) and B, acetonitrile/ethyl acetate (75:25 by volume). Solvents used were HPLC grade from Fisher Scientific, and were filtered prior to use through a 0.2 µm filter. The following gradients used were A/B (30/70%) for 0.5 min, then A/B (0.1/99.9%) for 5.5 min, before returning to A/B (30/70%) for the last 2 min. The column temperature was maintained at 30°C, while

sample temperature was set at 8°C. An extended wavelength PDA (photo diode array; Waters, UK) was used to perform on-line scanning across the UV/Vis range, in a continuous manner from 250 to 600 nm. Isoprenoids were identified by the comparison of spectral properties and retention times to authentic standards and reference spectra. Quantification was performed using dose-response curves, by running different concentrations of authentic standards on the UPLC and determining peak areas. Different wavelengths were used to analyse the isoprenoids: 286 nm (phytoene, alpha-tocopherol, delta-tocopherol, and quinone) 350 nm (phytofluene), 400 nm (zeta-carotene), 450 nm (lutein, neurosporene, delta-carotene, gamma-carotene and beta-carotene) and 470 nm (lycopene).

Phenolic analysis was performed in a similar way to the isoprenoid analysis above, using the Acquity™ system UPLC-PDA. The mobile phase used consisted of A, formic acid (0.1%) and B, methanol (100%); solvents used were HPLC grade from Fisher Scientific, and filtered using a 0.2 μm filter prior to use. The following gradients used were A/B (88.5/ 11.5%) for 15 min, then A/B (50/50%) for 5 min, before returning to A/B (88.5/ 11.5%) for the last 1 min. The column temperature was maintained at 28°C, while sample temperature was set at 4°C. Comparison of spectral properties and retention times to authentic standards and reference spectra enabled phenolic identification. Relative quantification to the internal standard, salicylic acid, was performed.

2.3.4 Metabolite extraction and derivatisation for GC-MS analysis

Freeze-dried ground material (10 mg) was weighed in a microcentrifuge tube (2 ml), and then methanol (500 μl) and water (500 μl) were added. Samples were mixed vigorously using a vortex and then inverted at room temperature for 1 h. Chloroform (1 ml) was added and mixed vigorously with a vortex. Centrifugation at 9,000 xg for 5 min followed, to remove cell debris. The polar (upper) phase, containing methanol and water, was transferred to a fresh to a new microcentrifuge tube (2 ml). The non-polar (lower) phase was transferred to a new screw-cap glass vial (Agilent). Then the remaining pellet was saponified with the addition of 10% NaOH (w/v; 1 ml) and incubated in a sonicating water bath at room temperature for 10 min. NaOH was removed by centrifugation at 9,000 xg for 5 min. Methanol (300 μl) and chloroform (600 μl) were added and samples were vortexed, prior to partitioning with Tris-buffered saline (300 μl; 50 mM Tris-HCl,

NaCl 1M, pH 7.0). Samples were vortexed thoroughly and centrifuged at 9,000 xg for 5 min. The non-polar phases were pooled, and samples were spiked with D27-myristic acid (5 µl; 1 mg/ml in chloroform). Two aliquots of the polar extract (10 µl and 20µl) were transferred to glass vials (Agilent) and ribitol standard (10µl; 1 mg/ml in methanol) was added. A GeneVac Ez-2 Plus rotatory evaporator (UK) was used to dry down both polar and non-polar samples, which were stored at -20°C until derivatisation.

Derivatisation was performed firstly by the addition of methoxyamine-HCl (30 µl; Sigma-Aldrich, UK) prepared at a concentration of 20 mg/ml in pyridine, followed by incubation at 40°C for 1 h. Then N-methyltrimethylsilytrifluoroacetaminde (70 µl; Sigma-Aldrich, UK) was added and samples were incubated at 40°C for 2 h.

2.3.5 Gas chromatography-mass spectrometry

Metabolites from both the polar and non-polar phases were analysed using Gas Chromatography-Mass Spectrometry, as previously described (Enfissi et al., 2010), on an Agilent HP6890 (UK) gas chromatograph with a 5973MSD. Samples were injected (1µl) with a splitless injector at 280°C. Retention time locking to the internal standard was used. A temperature gradient was used where the gas chromatography oven was held for 3 min at 70°C, before ramping at 4°C/min to 325°C. The final temperature of 325°C was held for a further 1 min. The GC-MS interface was set at 250°C, the MS ran in full scan mode using 70 eV EI+ and scanned from 10-800 D. A mass spectral (MS) library, constructed from in-house standards for known tomato metabolites, and the NIST08 MS library was used for the identification of metabolites from chromatogram components found in the tomato profiles. In order to facilitate the determination of retention indices (RIs), a retention time calibration on all standards was performed. Each metabolite was identified by comparison of retention indices and MS to customised MS libraries. For polar (20 µl aliquots) and non-polar samples relative quantification to the internal standard was performed, for broad overview of alterations to metabolism. The polar (10 µl aliquots) were used to determine differences to the main tomato sugars (glucose, fructose and sucrose); absolute quantities for these sugars were determined using standard curves.

2.3.6 Liquid chromatography–mass spectrometry

Expanding leaf (non-senescing), developing fruits and turning fruits were selected for phytohormone analysis. Developing and turning fruits are defined as fruits harvested at 20 days post anthesis and 4 days post breaker, respectively. Material harvested was stored at -20°C, prior to being ground into a fine homogenous powder using a TissueLyser II (Qiagen, UK) and one 0.5 mm stainless steel bead (Qiagen, UK), and then lyophilised. Homogenised freeze-dried material (100 mg) was weighed in clean microcentrifuge tubes (2 ml) and transported to Syngenta on dry ice for quantification using liquid chromatography–mass spectrometry. Summary of plant hormone analysis carried out by the Metabolomics Skillset, Product Metabolism and Analytical Science, Jealott's Hill, Syngenta. Plant hormones, extracted in acidified methanol, were analysed using an Agilent 1290 liquid chromatography system with PAL HTS-xt autosampler connected to a Sciex QTRAP 5500 mass spectrometer. Analytes were separated by reverse phase gradient chromatography and detected using mass transitions specific for each analyte. Standards were used to identify chromatogram components: indole, indoleacetic acid, jasmonic acid, methyl-jasmonate, 6-(γ,γ-Dimethylallylamino) purine, 6-(γ,γ-Dimethylallylamino) purine riboside, salicylic acid, and trans-zeatin riboside standards were sourced from Sigma-Aldrich, UK (now Merck, UK). While abscisic acid, cis-zeatin riboside, dihydrozeatin, epibrassinolide, gibberellic acid forms (GA1, GA3, GA4, GA9, GA19, GA20, GA44, GA53), gibberellic acid methyl ester (GA1-Me, GA3-Me, GA4-Me) and trans-zeatin standards were sourced from OlChemIm s.r.o. Czech Republic. A 9 point mixed calibration standard was run bracketing the samples, ranging from 0.01 to 100 ng/ml, except for indole which is present in higher concentrations than most other plant hormones, which ranged from 0.1-1000 ng/ml. A quality control sample (created by pooling an aliquot from each sample), calibration check and suitable blanks dispersed throughout the samples to ensure data integrity. All of the analytes highlighted above were checked in the sample chromatograms, but only those detected were reported and non-detected analytes were removed. Once analysed, the quantified amounts were compared with and were found to be in accordance with the amounts reported using similar methods in literature for tomato (Buta and Spaulding, 1994; Fraser et al., 1995; Serrani et al., 2007b; Garcia-Hurtado et al., 2012; Matsuo et al., 2012; Pattison and Catalá, 2012; Breitel et al., 2016; Kumar et al., 2017; Sravankumar et al., 2018).

2.4 Statistical analysis

For each experiment a minimum of three biological and three technical replicates were analysed unless stated otherwise. Data was processed using Excel (Microsoft Office software), construction and formatting of graphs was performed using GraphPad Prism software v.7 (GraphPad Software, UK). Metabolite levels from the different technology platforms were combined. Normalised data was then analysed using PCA (principle component analysis), a statistical tool used to visualise the variance within the data set according to its principle components. SIMCA-P+ software v.15 (Umetrics, UK) was used to determine and display clusters derived from PCA analysis. Student's t-test and Dunnett's analysis were used to determine significant differences between the transgenic lines and both azygous (non-transgenic) and AC (wild type) controls. Statistical analysis was performed using the statistical software package SPSS (IBM SPSS-21, New York, USA). Where appropriate, $P < 0.05$, $P < 0.01$, and $P < 0.001$ are indicated by *, **, and ***, respectively.

Chapter III: Functional characterisation of the ZINC FINGER PROTEIN INDETERMINATE DOMAIN 2

3.1 Introduction

Zinc finger C2H2-type proteins play important roles in regulating various developmental processes or responses to abiotic stresses. Interestingly, there is growing evidence supporting the idea that this family of transcription factors are involved in fruit ripening, especially through phytohormonal control (Weng et al., 2015b; Han et al., 2016). A predicted C2H2-type zinc finger protein was identified using system biology outputs; the Sol Genomics Network denotes the genetic loci as the tomato locus IDD2. The INDETERMINATE DOMAIN (IDD) protein family's involvement in gibberellin signalling has been documented (Feurtado et al., 2011; Fukazawa et al., 2014; Yoshida et al., 2014). Despite this the functions of the IDD family in tomato remain unknown.

Previously, chromatin immunoprecipitation (ChIP) revealed that the *ZINC FINGER PROTEIN INDETERMINATE DOMAIN 2* (*ZFPIDD2*; Solyc08g063040) was a direct (RIPENING INHBITOR) RIN target, containing a single C-(A/T)-rich-G (CArG) box sequence that is a typical binding sequence for MADS-box proteins (Fujisawa et al., 2012b). The transcription factor was shown to be positively regulated by RIN, due to the reduced expression in turning fruits of the *rin* mutation (Fujisawa et al., 2013). The same study revealed that the expression of this gene failed to significantly change after treatment with the ethylene receptor inhibitor 1-methylcyclopropene (1-MCP), indicating that the zinc finger protein does not exhibit ethylene responsiveness. RNA-seq comparison between tomato cultivars with altered rates of maturity (Ailsa Craig and HG6-61) was able to correlate *ZFPIDD2* to fruit nutritional quality. Transcription abundance correlation analysis between structural genes from the carotenoid pathway and the zinc finger protein revealed that the transcription factor links to multiple genes putatively involved in carotenoid biosynthesis (Ye et al., 2015). Specifically, the zinc finger protein was correlated to phytoene, β-carotene and lycopene when comparing the metabolite and transcript abundances. The zinc finger protein was also demonstrated to be down-regulated by *SlMSI1*, a negative regulator of fruit ripening that potentially acts upstream of RIN (Liu et al., 2016a). Finally, Li et al., (2017) demonstrated that the transcription factor of interest was regulated by the fusion of adjacent truncated RIN and MC genes (RIN-MC) but not RIN in *rin* mutant fruits, which acts as negative regulator of ripening-related colour development. Despite remaining uncharacterised, *ZFPIDD2* has been included in numerous network and RNA-seq analyses, demonstrating potential roles in tomato fruit ripening.

Systems biology outputs revealed that in tomato *ZFPIDD2* has a ripening-related expression profile, and reduced expression in both *rin* and *nor* ripening mutants. Therefore, could be both RIN or NOR regulated. Additionally in the T_0 generation, carotenoid and chlorophyll profiles were altered in transgenic lines with the insertion of the knock-down 35S::RNAi construct. These results strengthen the prediction that the zinc finger protein has important ripening-related functions. To confirm a role in ripening and elucidate the underlying principles, detailed phenotypic and molecular characterisation with metabolic profiling was performed, enabling the assessment of how manipulation affected development, fruit ripening and fruit quality traits.

3.2 Results

3.2.1 Phenotypic and genotypic screening of the T_1 generation to identify potential functions of the *ZFPIDD2*

3.2.1.1 Screening for altered plant morphology and fruit development traits associated with transgenic lines

Once the carotenoid screen of ripe fruits established an increase in pigments, and previous data indicated a ripening-related function, suitable propagation was required to conduct broad phenotyping. Insertion events with increased carotenoid content were selected. Combined plant and fruit phenotyping would further characterise the function of the zinc finger protein, providing a selection process to reduce the number of individuals and genotypes. In total 220 plants were characterised across all three knockout constructs, which included 20 representative Alisa Craig (AC) wild type controls, thus fairly rapid phenotyping was required. A total of 65 *ZFPIDD2* transgenic lines were grown for the T_1 generation, including up to 20 lines per insertional event. Plants were randomly distributed and analysis combined all 20 of the AC wild type lines. Common commercial phenotypic parameters enabled assessment of quality and identified selectable markers that could be utilised by producers. Without knowing the insert number, zygosity and potential segregation within each insertion event, all transgenic lines were analysed separately.

The first observable phenotype of the transgenic lines was more condensed plant architecture. Upon visual determination of altered development, the average stem internode lengths and plant heights were measured. This provided a quantitative approach to confirm altered plant morphology. Measurements were recorded when the wild type controls had three trusses with fruit set. Internode lengths represent the average distance between four randomly selected leaf nodes, and the majority of transgenic lines displayed a reduced internode length (Figure 3-1a). In total 94% of transgenic lines had a reduction to the internode length in comparison with the wild type controls, with the average length being 5.7 cm compared to 7.1 cm of AC controls. Similarly plant height was also reduced (Figure3-1b), with 76% of transgenic lines showing a decrease in length from soil to the last node. On average transgenic lines were 17 cm shorter compared to the wild type lines. Interestingly, eight transgenic lines displayed a more severely perturbed development, whereby the height and average internode lengths were below 100 and 5 cm, respectively. The results from Figure 3-1 indicate that transgenic lines have altered plant morphology; therefore it can be predicted that the zinc finger protein likely functions in plant growth and development.

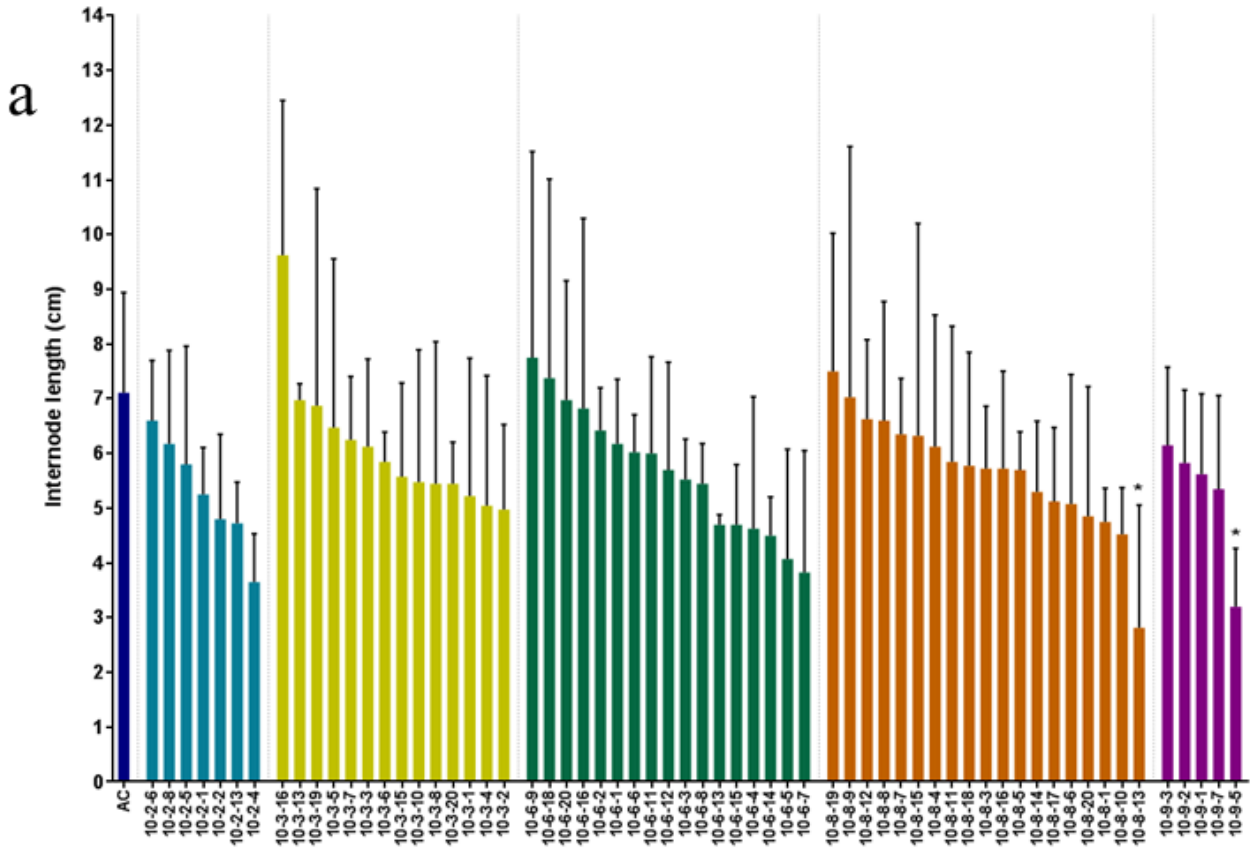
a
Internode length (cm)
0
1
2
3
4
5
6
7
8
9
10
11
12
13
14
AC
10-2-6
10-2-8
10-2-5
10-2-1
10-2-2
10-2-13
10-2-4
10-3-16
10-3-13
10-3-19
10-3-5
10-3-7
10-3-3
10-3-6
10-3-15
10-3-10
10-3-8
10-3-20
10-3-1
10-3-4
10-3-2
10-6-9
10-6-18
10-6-20
10-6-16
10-6-2
10-6-1
10-6-6
10-6-11
10-6-12
10-6-3
10-6-8
10-6-13
10-6-15
10-6-4
10-6-14
10-6-5
10-6-7
10-8-19
10-8-9
10-8-12
10-8-8
10-8-7
10-8-15
10-8-4
10-8-11
10-8-18
10-8-3
10-8-16
10-8-5
10-8-14
10-8-17
10-8-6
10-8-20
10-8-1
10-8-10
10-8-13
10-9-3
10-9-2
10-9-1
10-9-7
10-9-5

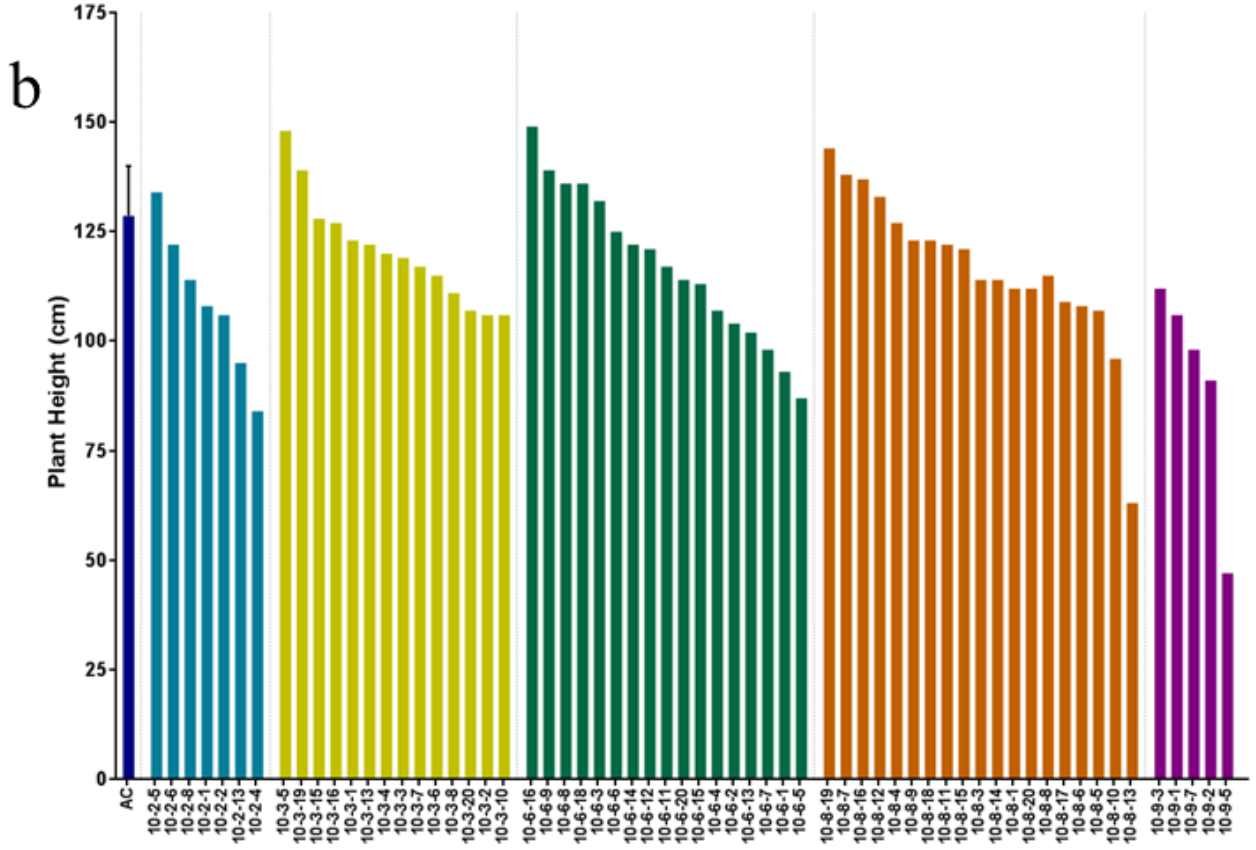

Figure 3-1 Using stem internode length and plant height as markers for altered plant morphology in transgenic lines.

Figure 3-1 Using stem internode length and plant height as markers for altered plant morphology in *ZFPIDD2* transgenic lines.

Stem internode length (a) and total plant height (b) were used to identify differences to plant development between Ailsa Craig (AC) and transgenic lines. Plant parameters were measured once the AC wild type background had three trusses with fruit set. Total plant height was measured from the soil to last node; four random internodes were measured from the base of the plant to the last node. Each transgenic individual is represented by a single column, for AC a total of nineteen lines were averaged ensuring enough wild type biological replicates were spread throughout the population. Statistical determinations are shown as mean ± SD, Dunnett's test analysis illustrates statistically significant differences between wild type background (AC) and the transgenic varieties, $P < 0.05$, $^{**}P < 0.01$, and $^{***}P < 0.001$ are designated by *, **, and ***, respectively.

Fruit development time was an important quality trait studied; representing the time fruits took to set from anthesis, until maturity and the onset of ripening. Transgenic lines exhibited an extended time to reach breaker, with fruits taking on average 52.7 days compared to just 45.1 days for the wild type lines (Figure 3-2a). Additionally, increased fruit size and total fruit yield were phenotypes identified in most transgenic lines (Figure 3-2b and c). Through weighing individual fruits, the average fruit size and fruit yield were increased by 23% and 22%, respectively. Significantly, a total of ten transgenic lines had an increase in yield of over 50%, rising up to 168% for the highest yielding line. Seventeen transgenic lines produced fruit that were on average 25% larger than AC lines, and 5 lines showing a 50% increase in weight. The results from Figure 3-2 imply that the transcription factor may potentially have important roles in the initiation of fruit set, as well as the transition through the developmental phases of cell division and expansion that contribute to fruit growth. Through either mechanism or a combination, the results indicate that potentially altered expression of the zinc finger protein can significantly improve crop productivity. Due to the fragility of fruit set and unfavourable conditions of a winter crop, the yield remained low, producing variation, thus further crops were required to confirm whether the transgenic lines do confer a yield increase. Progeny from the 10-8-9 insertion event failed to yield enough fruit, therefore no fruit phenotypes could be recorded.

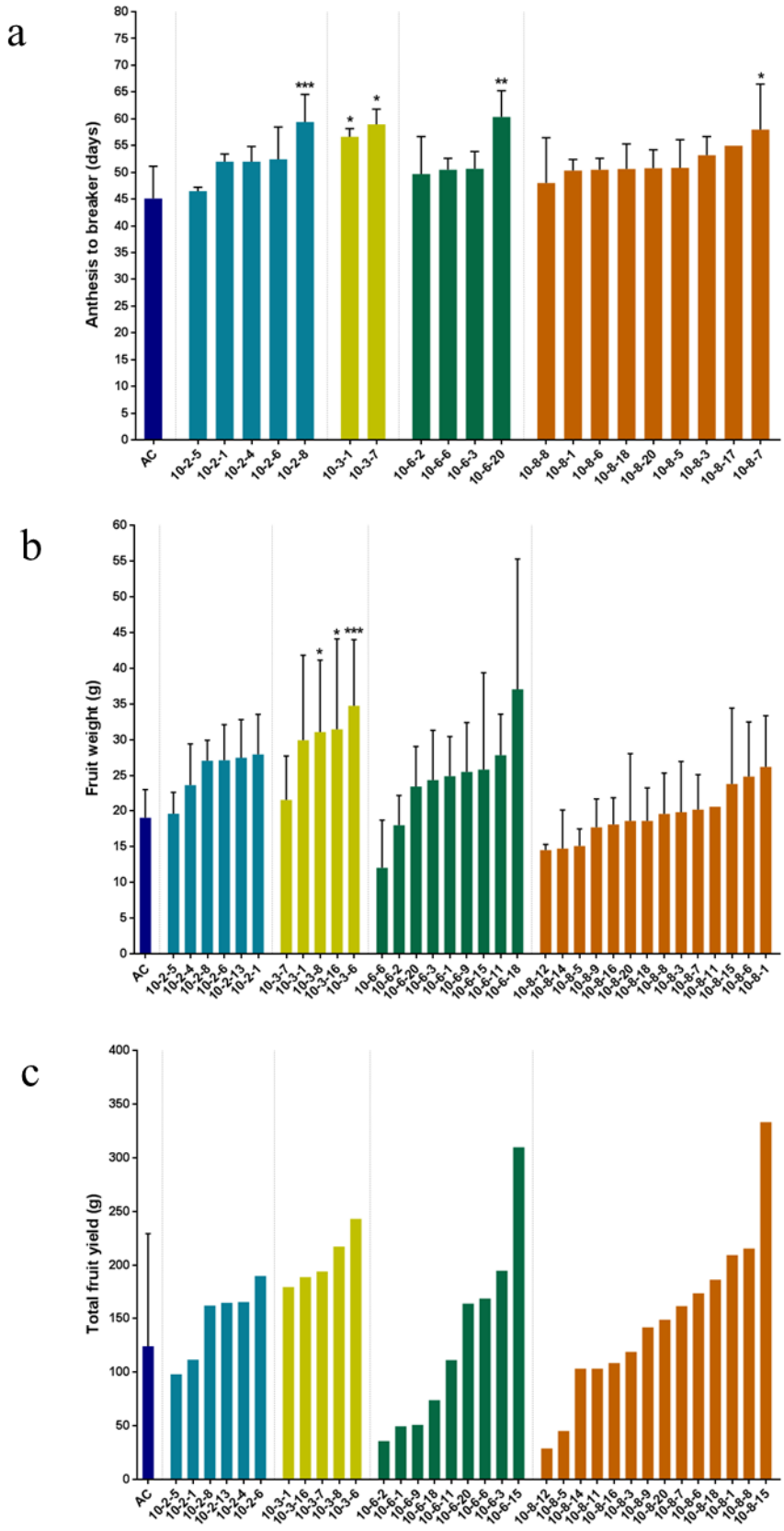

Figure 3-2 Measurement of the time from anthesis to breaker, average fruit weight and total fruit yield as markers for altered fruit set and development.

Figure 3-2 Measurement of the time from anthesis to breaker, average fruit weight and total fruit yield as markers for altered fruit set and development.

The maturity time from anthesis to breaker (a), average fruit weight (b) and total fruit yield (c) were recorded, to test whether transgenic lines exhibited altered fruit set and developmental phenotypes. Flowers were tagged at anthesis and the time taken to reach the onset of ripening at breaker stage was recorded. Fruit weights were determined individually postharvest and combined to determine total fruit yield. Fruit parameters were measured once the wild type AC background had formed five trusses. Each transgenic individual is represented by a single column, for AC up to a total of twelve lines were averaged, ensuring enough wild type biological replicates were spread throughout the population. Between two and twelve fruit measurements were recorded for each plant for either fruit maturity time or average fruit weight. Statistical determinations are shown as mean ± SD, Dunnett's test analysis illustrates statistically significant differences between wild type background (AC) and the transgenic varieties, $P < 0.05$, $^{**}P < 0.01$, and $^{***}P < 0.001$ are designated by *, **, and ***, respectively.

3.2.1.2 Using ripening-related colour development and softening as markers for altered ripening phenotypes associated with transgenic lines

With the predicted ripening-related function of the zinc finger protein, key ripening-associated fruit quality traits were evaluated. The first being the visual assessment of the rapidity of ripening-associated colour development. The time taken to transition from green to a uniform red colouration was consistently reduced in almost all the transgenic lines, on average taking 1.8 days less (Figure 3-3a). Syngenta confirmed a reduction to ripening time by a single day can significantly improve profitability, decreasing the time required before fruits are ready for purchase. In total nine transgenic lines took at least two days less to reach red ripe in terms of colour development. The second trait studied was fruit firmness that was measured at 14 days post breaker using a fruit firmness meter (Figure 3-3b). This time point was selected as fruits were expected to be approaching overripe, thus increased firmness at this stage could suggest an extended shelf-life. Interestingly, fruits from the transgenic lines were on average 11% firmer in comparison to the wild type controls, suggesting a reduced rate of softening. In total 80% of transgenic lines had firmer fruit than AC controls, with seven lines on average being 25% firmer and the largest increase to firmness was 43%.

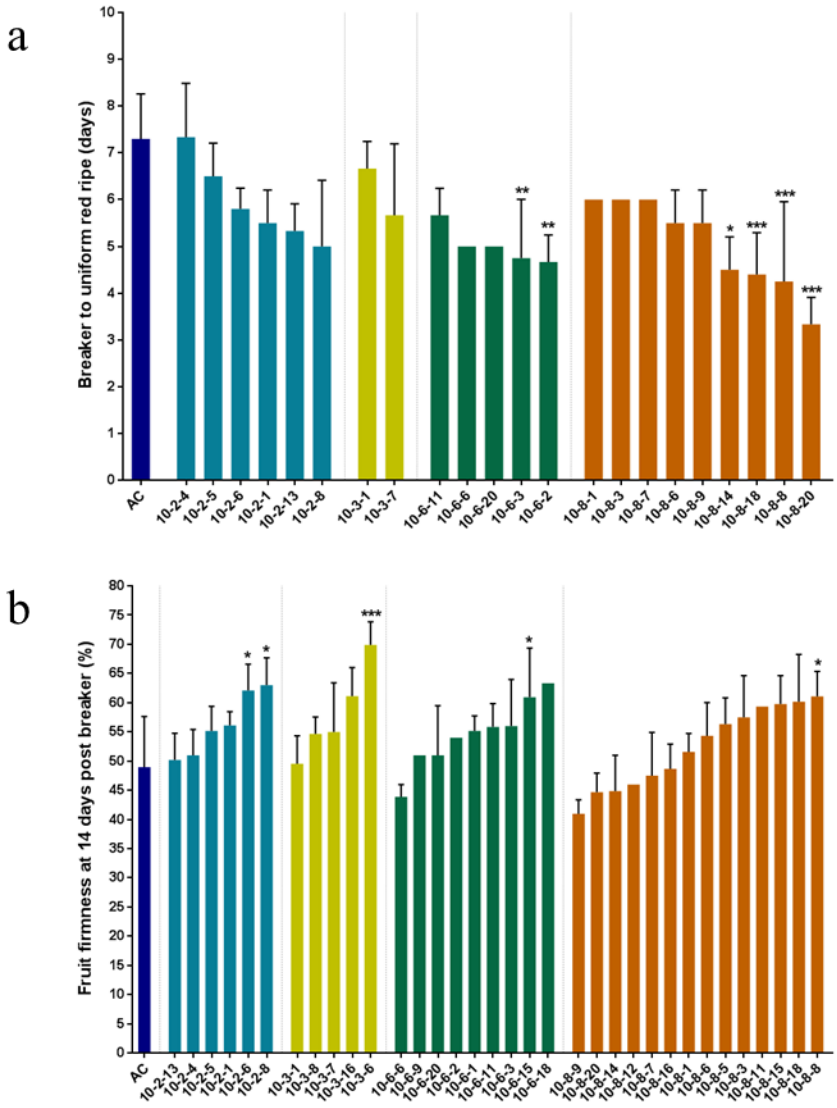

Figure 3-3 The study of colour development and fruit softening to identify changes to ripening associated fruit quality.

Colour related rapidity of ripening represents visual determination of the time taken for fruits to transition from breaker to uniform red (a). Fruit softening was measured in fruits at fourteen days post breaker using a fruit firmness meter; three measurements were taken per fruit (b). For both analyses between two and five fruits were studied. Each transgenic individual is represented by a single column, for AC a total of up to seven lines were averaged, ensuring enough wild type biological replicates were spread throughout the population. Statistical determinations are shown as mean ± SD, Dunnett's test analysis illustrates statistically significant differences between wild type background (AC) and the transgenic varieties, $P < 0.05$, $^{**}P < 0.01$, and $^{***}P < 0.001$ are designated by *, **, and ***, respectively.

End point levels of carotenoids were determined spectrophotometrically, in order to assess whether the altered ripening times seen in transgenic lines were due to an increase in pigment accumulation. As well as explaining why fruits from transgenic lines appeared to be darker in comparison to AC lines. Carotenoid extraction of freeze dried fruit material harvested at seven and fourteen days post breaker (7 dpb and 14 dpb, respectively) was performed (section 2.3.1). The extraction and spectrophotometer method performed is described in section 2.3.2. The wavelength of 470nm was used to quantify the levels of carotenoids, specifically lycopene, the predominant carotenoid in ripe tomato.

The reduced transition time from breaker to uniform red ripe was confirmed with the majority of lines displaying increases in carotenoid levels at 7 dpb (Figure 3-4a). The 10-8 lines presented the most consistent elevation to carotenoid content, on average showing a 1.2-fold increase to AC lines. As expected, the five lines with the most significantly elevated carotenoid levels (an average of 1.4-fold increase), had an average reduced colour-associated ripening time of 3 days (1.7-fold decrease). Indicating that increased carotenoid content was in part influencing the increased visual ripening-related colour transition phenotype witnessed in transgenic lines. Similarly, most transgenic lines exhibit increased pigmentation at 14 dpb, with 10-8 lines again proving to be most consistent for this trend (Figure 3-4b). Lines with the highest carotenoid content at 7 dpb showed further amplified pigmentation at 14 dpb, rising to 1.4-fold. This signified a sustained increased rate of carotenoid accumulation throughout the ripe stages of fruit ripening. The results confirm the potential of transgenic fruits to improve quality by increasing the rapidity of colour-related ripening, yielding darker fruit that are generally more popular to the consumer. Whilst demonstrating an increase to the predominant red carotenoid lycopene, that has been shown to be an important health-promoting compound in tomato fruits.

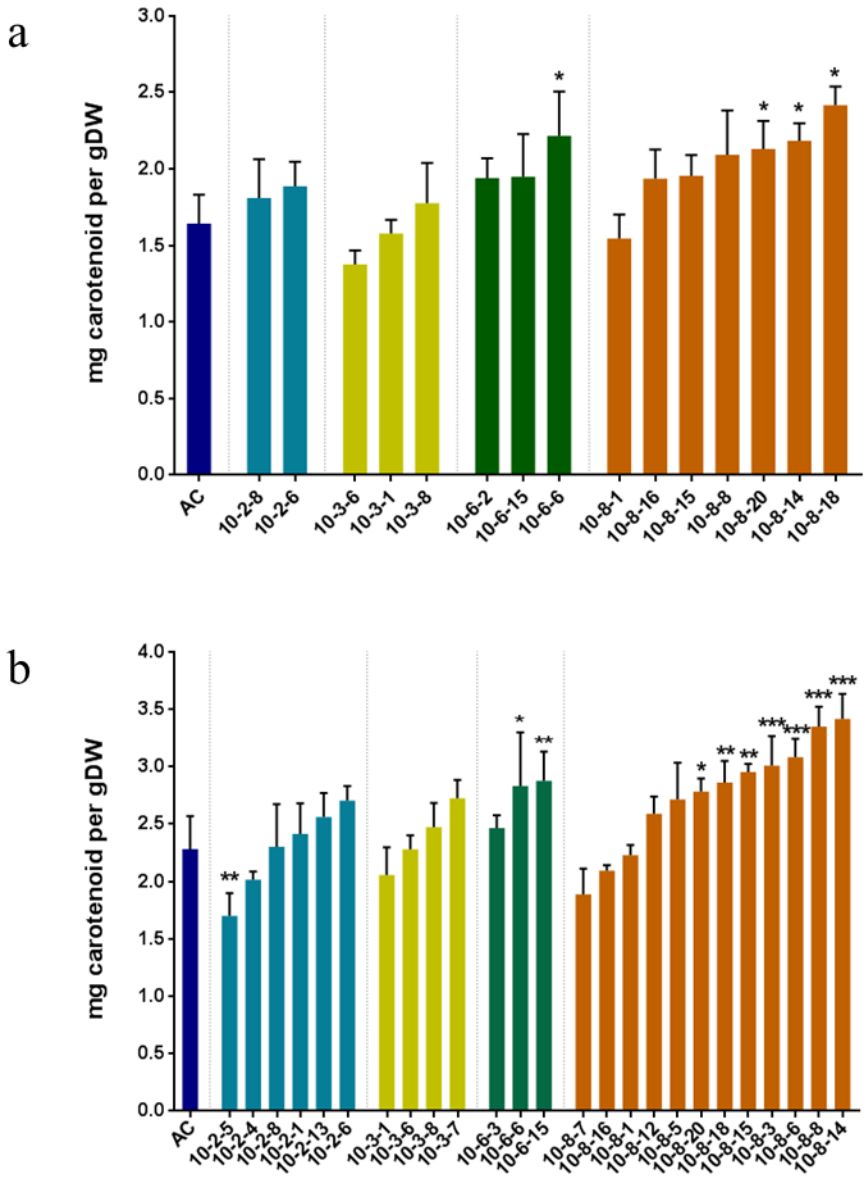

Figure 3-4 Spectrophotometer quantification of carotenoid content in ripe fruits.

Carotenoid content of two ripe fruit stages, seven (c) and fourteen days (d) post breaker, were quantified by spectrophotometer at 470 nm. Between two and four representative fruits were pooled per individual, then three technical and analytical determinations were made. Methods used for these determinations are described in section 2.3. Each transgenic individual is represented by a single column, for AC a total of up to seven lines were averaged, ensuring enough wild type biological replicates were spread throughout the population. Statistical determinations are shown as mean ± SD, Dunnett's test analysis illustrates statistically significant differences between wild type background (AC) and the transgenic varieties, $P < 0.05$, $^{**}P < 0.01$, and $^{***}P < 0.001$ are designated by *, **, and ***, respectively.

3.2.1.3 Molecular characterisation of transgenic lines by PCR, and Southern blotting to determine insert number

Lines with the most significantly improved phenotypes were selected for molecular characterisation, with the objective to identify individuals with the insertion of the knockout construct. DNA was extracted from previously harvested leaf material from young tomato plants (as described in section 2.2.1). Amplification of the *NEOMYCIN PHOSPHOTRANSFERASE II* (*NPTII*) gene by PCR verified the insertion of the transgene (section 2.2.3.2 and primers are described in appendix Table 1). On the resultant gel, transgenic lines were determined by the presence of the *NPTII* amplicon (Figure 3-5). As hoped the PCR indicated that the best lines were transgenic. However, few azygous lines were identified by a negative signal (absence of *NPTII* amplicon) identical to wild type controls. Real-time PCR was performed to confirm the number of inserts and potential zygosity of the transformants from several lines from multiple insertion events (method is described in section 2.2.5.6). Insert number was determined by the relative quantification ratios of *PHYTOENE DESATURASE* (endogenous single-copy gene) to the *NPTII* gene. The 10-8 transformation event produced the most consistent improved phenotype across all quality and yield associated traits, and therefore was considered most important to genotype. Similarly, 10-2 and 10-6 lines were also selected for genotyping. The 10-8-8 line was prioritised and the real-time PCR indicated a potential singular insert homozygous line. One to four inserts were predicted for the other selected 10-2 and 10-6 lines. From the 10-6 selected lines with a similar insert number to 10-8-8, the transformants proved to be low yielding.

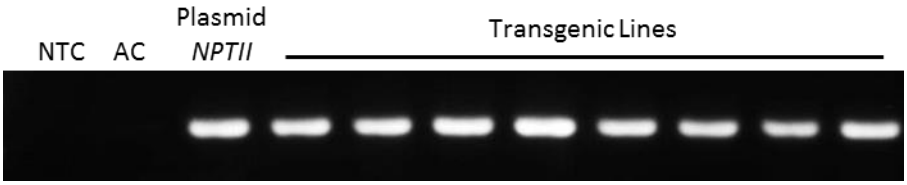

Figure 3-5 PCR confirmation of the presence of the knockout transgene in transgenic lines.

Amplification of the *NPTII* gene was performed by PCR on the majority of transgenic lines and visualised under UV light. DNA was extracted from a pool of 3 representative leaves of each plant. NTC: non template control**.**

To confirm the results found by both the original PCR and real-time PCR, a Southern blot was performed (as described in section 2.2.5.7) to determine the number of inserts from two individual lines, from two separate insertion events that had a positively altered phenotype. DNA from both 10-2-6 and 10-8-8 were used along with a pooled AC sample. The blot aimed to determine the number of inserts found in the best transgenic line from different insertion events, using a specific probe for the zinc finger protein knockout construct. First, the probe was created and tested, and then the Southern blot was performed using the DNA cut by the SacI restriction enzyme. The number of bands corresponded to the number of transgene inserts in each transgenic line. The autoradiograms, as shown by Figure 3-6, confirmed the presence of a singular band for both 10-2-6 (faint) and 10-8-8. Potentially there is a faint band at a higher bp than the most prominent band for 10-8-8, but the signal intensity is considerably lower on the autoradiogram. Taken together the combined PCR, real-time PCR and Southern blot indicated 10-8-8 was a singular insert line.

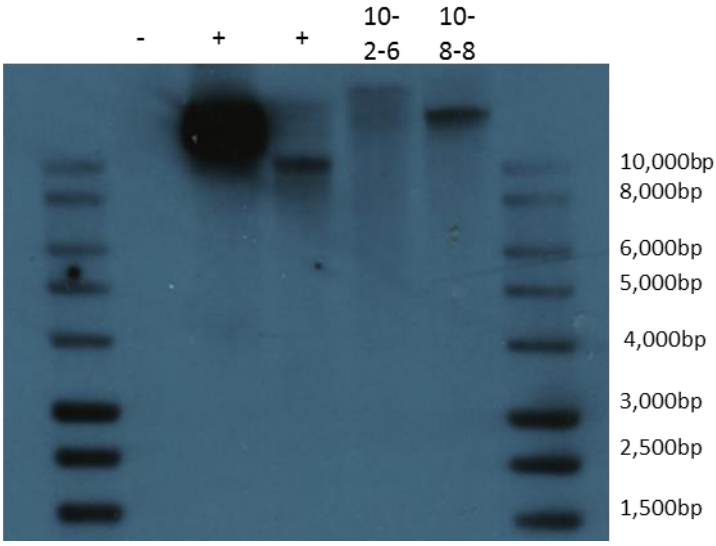

Figure 3-6 Autoradiograms of Southern blot used to determine the insert number of *ZFPIDD2* transgenic lines compared to a representative control.

The Southern blot used DNA from 10-2-6, 10-8-8 against pooled DNA from multiple AC lines. Digest was achieved using the SacI restriction enzyme and hybridisation was carried out using a specific probe to identify the transgene. The numbers correspond to the different plants tested. -, a negative control (DNA from the AC control) and +, positive control (DNA from the plasmid).

3.2.1.4 Combining results from the genotypic and phenotypic screen to select lines for further characterisation in the next generation

Phenotypic characterisation indicated a ripening-related function as predicted for the *ZFPIDD2*, in addition to several developmental roles. Interestingly, the majority of transgenic lines displayed increased carotenoid and ripening associated colour development, combined with reduced rate of softening. The partial uncoupling of ripening-related processes showed potential to provide significant improvement to the *rin* mutation currently utilised. A delay in the time to the onset of ripening combined with consistently increased fruit weight, suggested extension to either cell division or expansion phases of fruit growth. Together increased fruit size and fruit set produced lines with significantly higher yields in comparison the wild type controls. Furthermore, reduced internode and plant height could indicate the diversion of photosynthates from source tissues to fruit development and ripening, rather than plant growth. Ranking these traits enabled selection of the most consistently improved individuals, which included multiple 10-8 lines. The most improved line was 10-8-8: reaching a uniform red 3 days quicker with consistent increased rate of carotenoid accumulation at red ripe stages, fruits were 25% firmer and a 73% rise in fruit yield was recorded. Like 10-8-8, the transgenic line 10-2-6 had the most positively altered phenotype for its insertion event, and both lines were shown to be homozygous with a single insert. This provides greater evidence that the specific single insertion of the transgene is conferring the multiple phenotypes witnessed. Therefore, both 10-8-8 and 10-2-6 were selected for further analysis. Likewise, 10-8-15 was selected due to its significant potential to increase fruit size, yield and firmness. Whilst 10-8-18 was chosen for improving colour-related quality, with elevated carotenoid accumulation at 7 dpb and reduced colour associated ripening time. Furthermore, this line produced firmer fruits with an improved yield.

3.2.2 Identification of azygous individuals combined with more detailed characterisation in the T_2 generation

The lines selected from the T_1 generation (section 3.2.1) were propagated to achieve two objectives: firstly to genotype individuals and then to confirm the altered phenotypes witnessed in the previous crop, with the aim of further improving quality through selection of the best lines. The T_1 generation yielded few azygous lines and these individuals had a very low fruit set. Therefore, suitable propagation was required to ensure enough azygous lines could be produced through segregation within the population. With all three constructs (10, 6 and 4) being grown at the same time a feasible number of progeny would need to be chosen. For the zinc finger protein, a total of 10 progeny were grown for each of the selected lines mentioned in section 3.2.1. Therefore, 40 transgenic individuals were grown for comparison with 10 AC wild type lines. Additionally, a duplicate population was grown at the University of Nottingham. The specific aim of this parallel crop focused on confirming the yield increases seen in the previous crop across two separate facilities. Furthermore, probe penetration tests using a specialised Lloyd Instrument LF on both inner and outer pericarp tissues, could identify the main contributor conferring increases to fruit firmness.

3.2.2.1 Identification of azygous non-transgenic controls for true comparisons with transgenic lines

DNA was extracted from young tomato plant leaf material grown at Royal Holloway. The presence of the transgene was confirmed using PCR and specific primers to amplify the *NPTII* gene (section 2.2.3.2 and primers are described in appendix Table 1). Azygous lines were verified by the absence of *NPTII* amplicon (Figure 3-7). In total six azygous lines were identified by an absence of PCR product, yielding a negative signal identical the AC lines. A total of two azygous lines from the 10-2 and four from 10-8 insertion events were identified. With real-time PCR and Southern blotting across all three constructs not being feasible to determine insert number and zygosity, and the transgenic lines clearly still segregating, all lines that were verified to be positive for the transgene were kept separate in the subsequent analyses. Azygous lines are considered the non-transgenic true control as they have been through transformation and tissue culture. The

azygous lines from both insertion events were combined for this data analysis, as there were no statistically significant differences between their developmental and fruit quality traits outlined in sections 3.2.2.2, 3.2.2.3 and 3.2.2.4 (Dunnett's test).

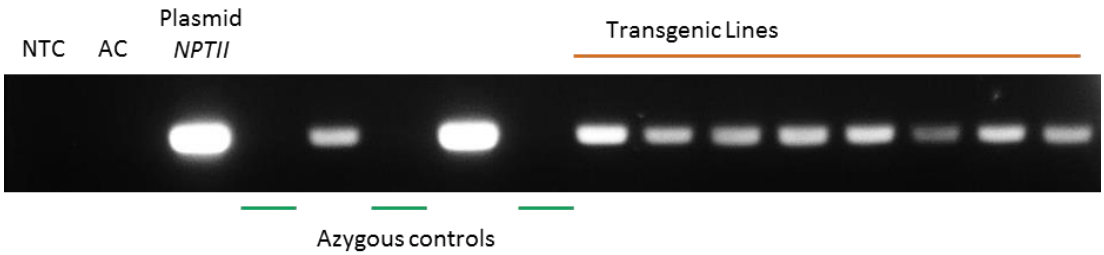

Figure 3-7 PCR confirmation to determine the presence of the knockout transgene in the transgenic lines and identification of azygous non-transgenic controls.
Amplification of the *NPTII* gene was performed by PCR on the majority of transgenic lines and visualised under UV light. Transgenic lines from the T_1 generation that yielded a negative signal identical to AC lines were identified as non-transgenic azygous controls (orange markers). DNA was extracted from a pool of 3 representative leaves of each plant. NTC: non template control**.**

3.2.2.2 Study of ripening-related and developmental traits to identify the extremes and most positively altered individuals for detailed characterisation

From the T_1 generation colour development, fruit firmness, fruit yield and internode length were consistently altered phenotypes in transgenic lines. Therefore, these traits were used as markers to identify and select the best lines. Comparison between the transgenic and AC lines demonstrates that these phenotypic differences are maintained into the T_2 generation. Transgenic lines exhibited altered plant morphology with the majority of lines showing a reduced internode length, on average being 2.6 cm shorter (Figure 3-8a). Significantly, on average, fruits transitioned from green to uniform red ripe 1.6 days earlier (Figure 3-9a), and fruits at 14 dpb were 26% firmer (Figure 3-9b). Once again showing the potential of transgenic lines to uncouple ripening-associated processes and provide improved fruit quality. Additionally, several transgenic lines displayed considerable increases to fruit yield, despite proving to be highly variable (Figure 3-8b).

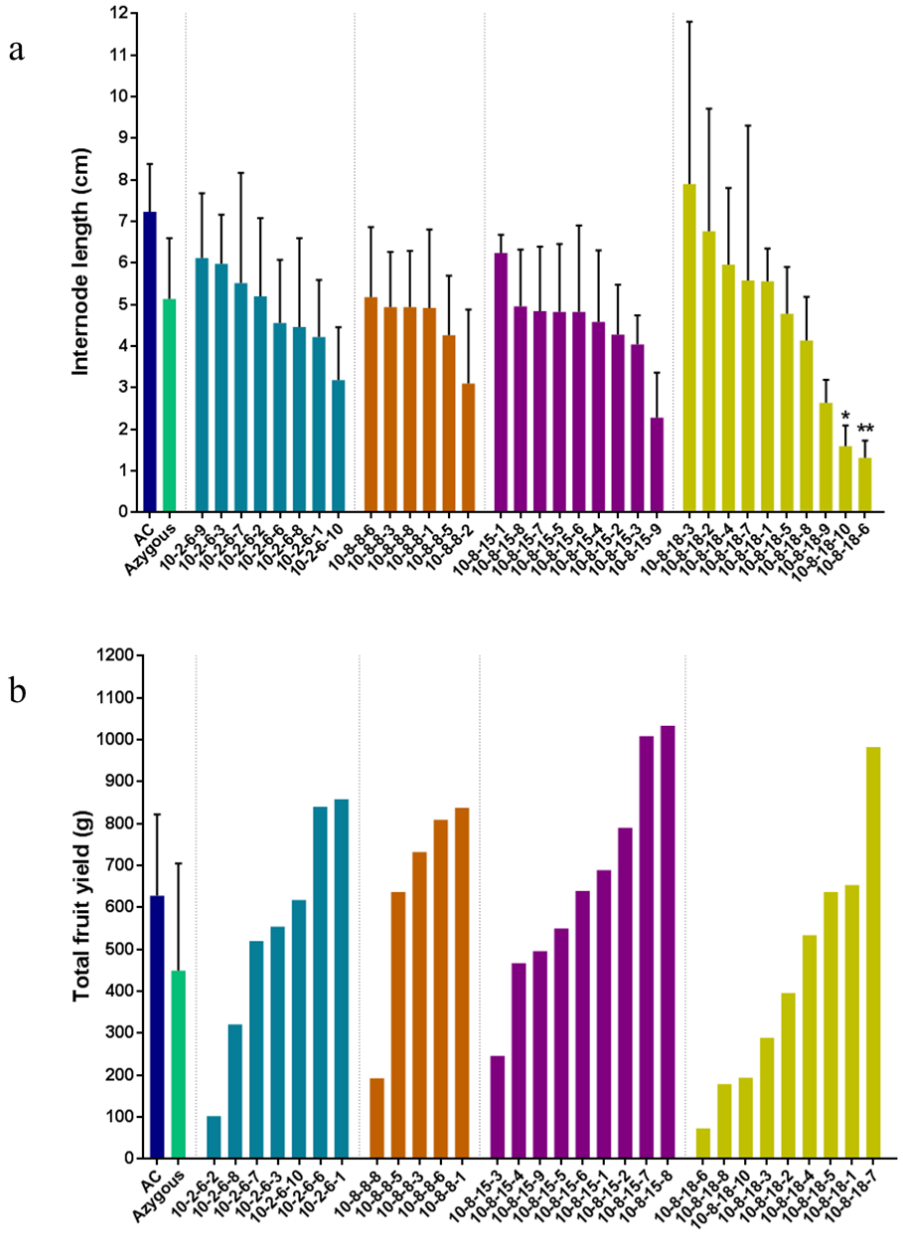

Figure 3-8 Internode length and total fruit yield screening of the T_2 population.

Internode lengths (a) and total fruit yield (b) of T_2 population enabled a screen for altered development. Phenotypic screening enabled the selection of extremes with the most positively altered phenotypes, and correlated with similar experiments conducted on the T_1 generation. Five random internodes were measured from the base of the plant to the last node. Fruit were weighed individually postharvest and combined to determine total fruit yield. Each transgenic individual is represented by a single column. A total of six and nine individuals were combined for azygous and AC controls, respectively. Statistical determinations are shown as mean ± SD, Dunnett's test analysis illustrates statistically significant differences between non-transgenic azygous controls and the transgenic varieties, $P < 0.05$, $^{**}P < 0.01$, and $^{***}P < 0.001$ are designated by *, **, and ***, respectively.

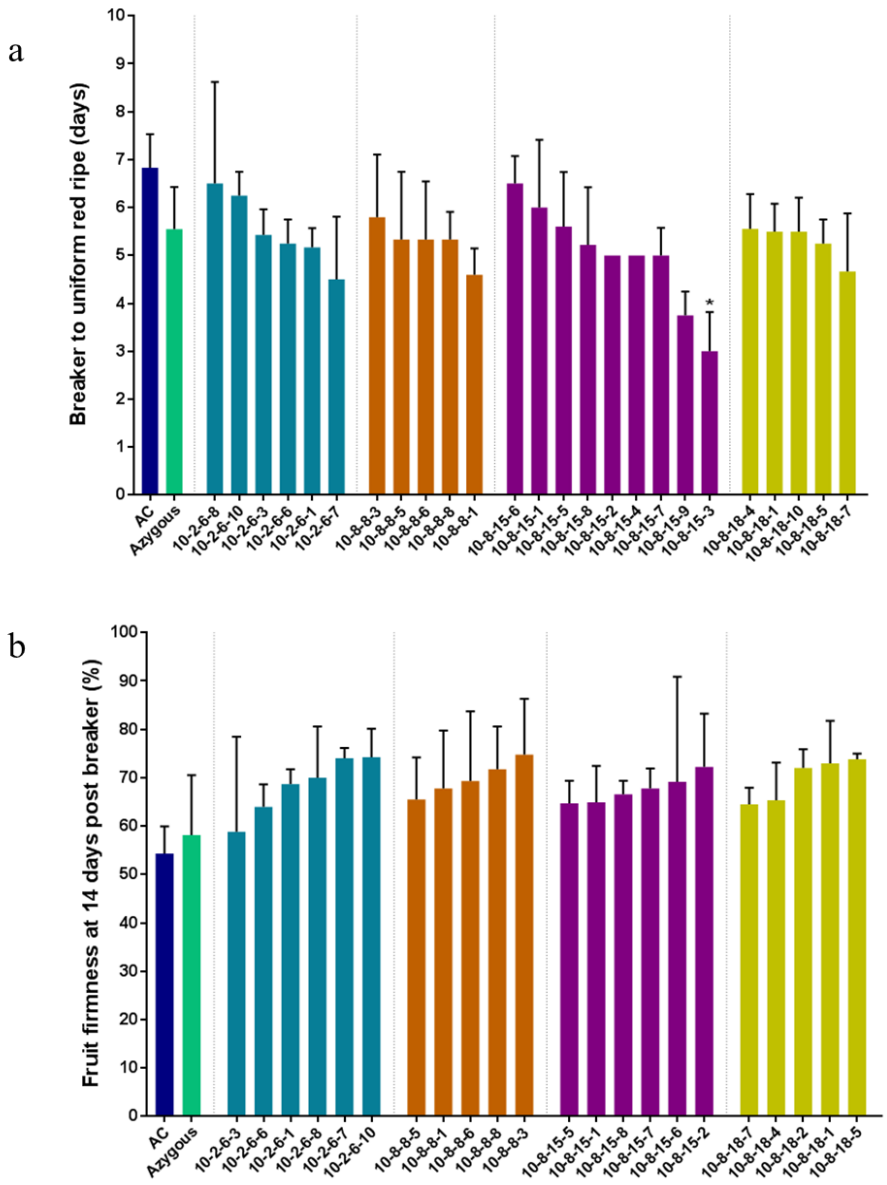

Figure 3-9 Ripening-related colour development and fruit firmness screening of the T_2 population.

Assessment of ripening-associated colour development (a) and fruit firmness (b) enabled the selection of the most improved lines, in addition to confirming the results obtained for the T_1 generation. Colour-related rapidity of ripening represents visual determination of the time taken for fruits to transition from breaker to uniform red. Fruit softening was measured at fourteen days post breaker using a fruit firmness meter; four measurements were taken per fruit. For both analyses between two and nine representative fruit were studied. Each transgenic individual is represented by a single column. A total of six and nine individuals were combined for azygous and AC controls, respectively. Statistical determinations are shown as mean ± SD, Dunnett's test analysis illustrates statistically significant differences between non-transgenic azygous controls and the transgenic varieties, $P < 0.05$, $^{**}P < 0.01$, and $^{***}P < 0.001$ are designated by *, **, and ***, respectively.

3.2.2.3 Detailed developmental-related phenotypic characterisation of most improved individuals

Figure 3-8 and Figure 3-9 were used to select the most consistently improved phenotypes, focusing on positively altered fruit quality and yield. For these lines more detailed phenotypic analysis was carried out to explain the differences seen. The selected lines had an improvement in fruit yield of 41% and 90% compared to AC and azygous controls, respectively. The 10-8-15 lines were most improved for this phenotype, averaging a 110% increase compared to azygous and 50% to AC controls. Transgenic fruit cluster away from both controls in terms of average mature fruit weight, producing fruit that were larger by 32% to AC and 30% to azygous controls (Figure 3-10a). These differences range from 15-54% and 14-52% to both AC and azygous lines, respectively.

Fruit set was investigated in Figure 3-10b, demonstrating that selected lines with elevated yield produce more flowers and fruits compared to the non-transgenic controls. On average, transgenic lines yielded 22 more flowers and 10 additional fruit compared to azygous lines. When compared to AC, transgenic lines produced similar numbers of fruit but had 16 more flowers. Specifically, 10-8-18-7 and 10-8-8-1 contributed most to the increased average flower number. Therefore, AC lines had the best fruit set at 36%, then transgenic lines at 30%, and azygous lines at 23%.

Consistent increases to average fruit weight, not fruit number, demonstrates that the larger fruit produced by the selected transgenic lines alone is conferring the elevated fruit yield when compared to AC controls. Whereas, elevated flower number, fruit number and fruit set, combined with the production of larger fruits, resulted in considerable fruit yield improvements when compared to azygous controls.

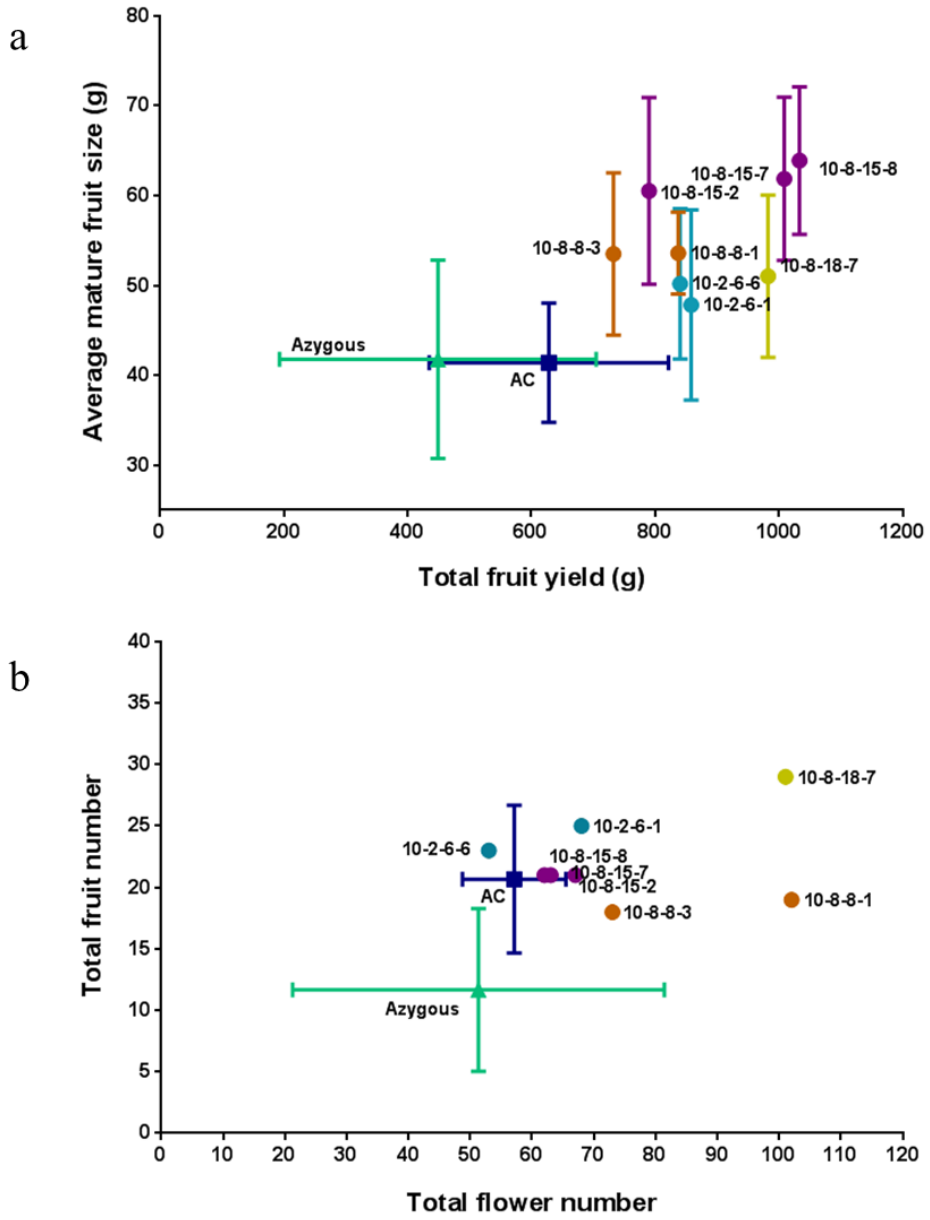

Figure 3-10 Assessment of fruit yield, size and set phenotypes for the most improved *ZFPIDD2* transgenic lines.

Total fruit yield and average ripe fruit size were correlated (a) to assess the fruit yield-related phenotypes. Fruit set was evaluated by determination of flower and fruit number (b). Only selected transgenic lines with the most improved yield and quality traits are shown. Ten representative fruits weights were combined for this analysis. Fruit weights were determined individually postharvest and combined to determine total fruit yield. Fruit parameters were measured once the wild type AC background had formed five trusses. Each transgenic individual is represented by a single point. A total of six and nine individuals were combined for azygous and AC controls, respectively. Statistical determinations are shown as mean ± SD.

Both the flowers per truss and truss forking parameters were studied, to investigate whether changes to truss morphology was influencing the increased flower number phenotype of transgenic lines. Figure 3-11 demonstrates that multiple transgenic lines have more flowers per truss. Later this was shown to be caused by increased truss forking. Transgenic lines 10-2-6-1, 10-8-8-1 and 10-8-18-7 trusses split on average 4.7, 2.0, 1.8 times, respectively, when compared to 1.3 times for both AC and azygous lines. Truss forking in this study is defined by a singular truss axis that splits into multiple axes capable of yielding more flowers. However, the other lines did not show a change in truss morphology, instead faster truss and flower development was observed. These lines either had an extra truss or more flowers on younger truss formations. Despite not proving conclusive, many transgenic lines display some form of altered truss development and morphology.

Another altered developmental related phenotype exhibited by transgenic lines compared to AC, was the reduction in plant height and internode length (Figure 3-12). AC lines had an increased height of 23 cm and internode length of 2.4 cm, compared to the selected transgenic lines. This proved to be an important marker to identify transgenic lines from AC, as these differences could be seen from around one month post germination. Conversely, azygous lines had a reduced average height (18 cm), and a slight increase to internode size (0.3 cm). Although, no significant differences were found to internode length between selected transgenic lines and azygous controls, the same would be expected with plant height.

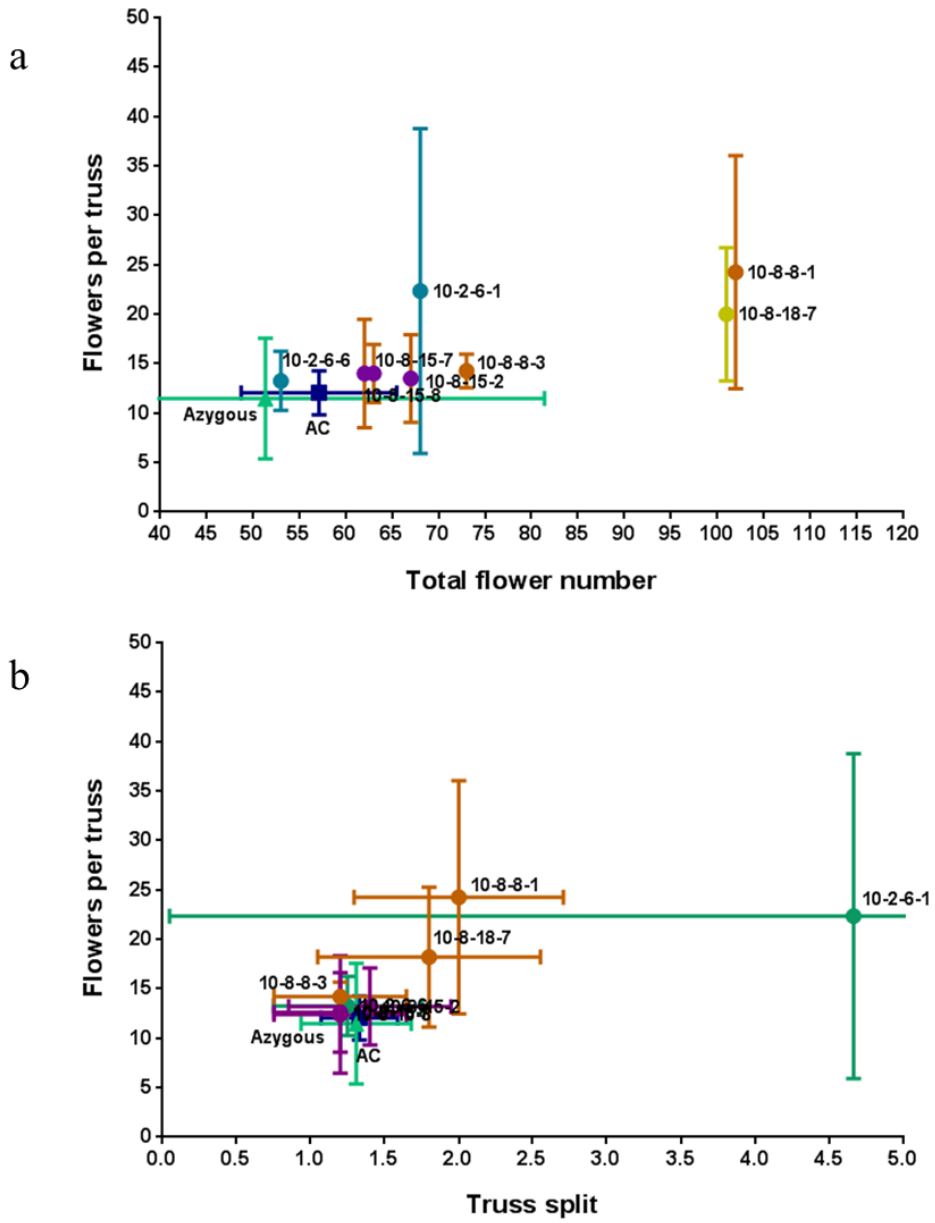

Figure 3-11 Phenotypic assessment of truss morphology for the most improved *ZFPIDD2* transgenic lines.

The number of flowers per truss and total flower number were correlated (a), and then flowers per truss and truss forking were compared (b). These phenotypic traits were used as markers for evaluating altered flower development in relation to truss architecture. Truss forking is defined by a singular truss axis that splits into multiple axes capable of yielding flowers. A minimum of four trusses were combined for both analyses. Fruit parameters were measured once the wild type AC background had formed five trusses. Each transgenic individual is represented by a single point. A total of six and nine individuals were combined for azygous and AC controls, respectively. Statistical determinations are shown as mean ± SD.

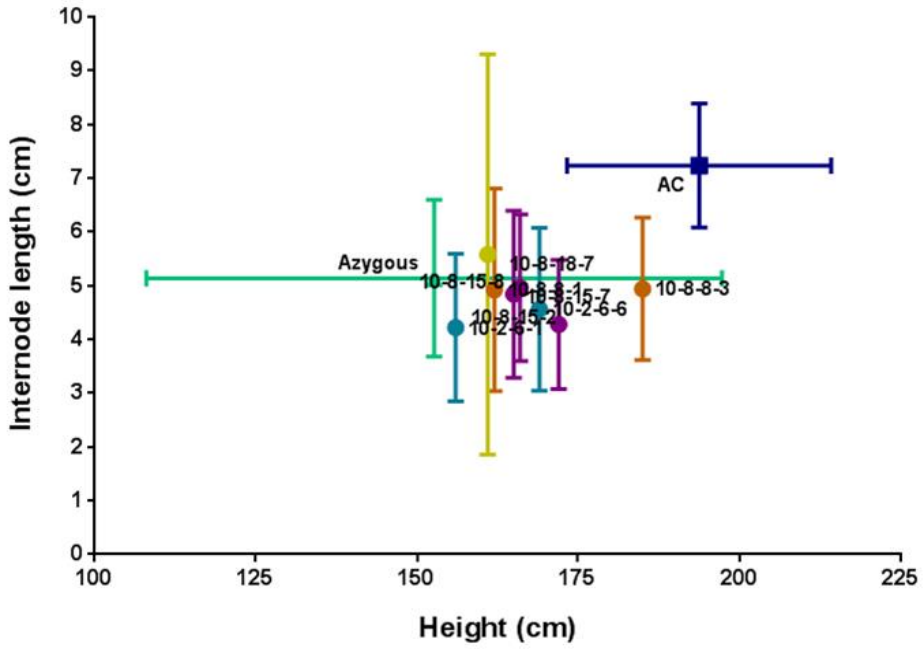

Figure 3-12 Phenotypic assessment of plant height and internode length for the most improved *ZFPIDD2* transgenic lines.

Both plant height and internode lengths were recorded once the wild type AC background had formed five trusses. Five random internodes were measured from the base of the plant to the last node. Each transgenic individual is represented by a single point. A total of six and nine individuals were combined for azygous and AC controls, respectively. Statistical determinations are shown as mean ± SD.

3.2.2.4 Elevated ripening-related colour and carotenoid accumulation combined with reduced fruit softening in most improved transgenic lines

As mentioned previously, increased rapidity of colour transition from green to red is a consistent phenotype displayed by transgenic lines. Fruits from selected transgenic lines took on average 1.6 days less compared to AC to appear ripe, shown by the presence of a uniform red colouration. Furthermore, a 0.5 day reduction to red ripe can be seen with azygous lines, although the differences rises to 1.2 and 1.1 days compared to 10-8-8-1 and 10-8-18-7, respectively. The results from Figure 3-13 confirm the results from T_1 generation, whilst demonstrating potential significant colour improvements against azygous lines.

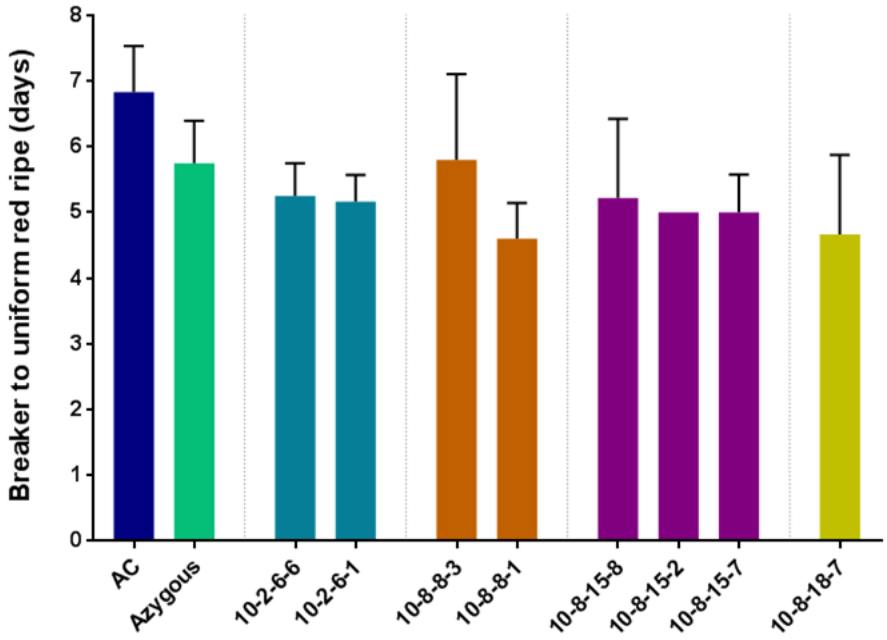

Figure 3-13 Ripening-related colour development for the most improved *ZFPIDD2* transgenic lines.

Colour related rapidity of ripening represents visual determination of the time taken for fruits to transition from breaker to uniform red. Between two and nine representative fruits were studied for each line. Each transgenic individual is represented by a single column. A total of six and nine individuals were combined for azygous and AC controls, respectively. Statistical determinations are shown as mean ± SD, Dunnett's test analysis illustrates statistically significant differences between non-transgenic (azygous) and the transgenic varieties, $P < 0.05$, $^{**}P < 0.01$, and $^{***}P < 0.001$ are designated by *, **, and ***, respectively.

More quantitative metabolite profiling of fruit pigments followed the visual confirmation of darker fruit phenotypes. In order to fully assess the role of the zinc finger protein in ripening-associated carotenoid accumulation, fruit tissue extracts from selected transgenic lines were screened by Ultra Performance Liquid Chromatography with on-line photo-diode array detection (UPLC-PDA). Analysis enabled the estimation of the level of carotenoids produced at two ripening stages (7 and 14 dpb) by transgenic lines, and azygous and wild type (AC) controls. Methods are described in section 2.3.

The UPLC profiles of transgenic fruits revealed significant qualitative differences at 14 dpb (Table 3-1). Quantification indicated that total carotenoid content had increased up to 1.4-fold to AC and 1.2-fold to azygous lines. Transgenic lines exhibited consistently

elevated lycopene levels at both ripening stages analysed, which correlated to the reduced colour associated ripening time to uniform red. Therefore, in terms of colour and carotenoid levels transgenic fruits were perceived as being more advanced. Additionally, phytoene levels were increased for all transgenic lines tested compared to both controls, although only four lines proved significant to azygous lines.

Transgenic lines displayed significant increases to lycopene ranging from 1.2 to 1.3-fold at 14 dpb. Likewise, on average phytofluene (1.1–fold) and phytoene (1.2-fold) levels were increased throughout all transgenic fruits, contributing to improved total carotenoid content at 14 dpb. More dramatic increases were identified in comparison to AC wild type controls at this stage. All transgenic lines exhibited significant increases to lycopene (1.1-1.6-fold), phytofluene (1.2-1.4-fold) and phytoene (1.4-1.9-fold), whilst β-carotene levels were slightly reduced (1.1-fold). Consequently, transgenic fruits display significant improvements to total carotenoid content up to 36% compared to AC controls. Lines from the 10-8 insertion event confer larger differences to lycopene and total carotenoid content than 10-2 lines. Lutein content remained unchanged throughout.

Differences to carotenoid content at 7 dpb are less pronounced compared to both controls (Table 3-1). No consistent change was observed between transgenic and azygous lines for any single carotenoid quantified. Only two lines 10-8-15-7 and 10-8-18-7 displayed significant improvement to lycopene content. However, on average elevated lycopene (1.2-fold), phytofluene (1.1-fold), phytoene (1.3-fold), combined with reduced β-carotene (1.1-fold) levels were shown when compared to AC controls. Overall, transgenic lines yielded a 10% increase to total carotenoid content compared to wild type AC lines at 7 dpb. As expected, lines with highest total carotenoid content at 7 dpb also had the most significant increases at 14 dpb, and higher levels of lycopene correlated to reduced colour associated ripening time.

Fruits at 7 days post breaker

	AC	Azygous	10-2-6-1	10-2-6-6	10-8-8-1	10-8-8-3	10-8-15-2	10-8-15-7	10-8-15-8	10-8-18-7
Lutein	697.8±15.0	695.6±14.7	708.4±30.5	688.8±13.6	691.1±13.1	712.7±11.1	688.6±16.0	694.7±21.2	704.2±13.7	688.9±11.4
Lycopene	1635.7±257.8	2063.4±95.0	2057.9±43.5	**1589.3±24.8*** **	2277.5±113.1	2083.3±37.3	1965.5±97.2	**2409.4±58.5** **	2010.2±83.1	**2345.5±63.3***
β-carotene	1091.0±46.9	1013.7±21.4	1056.6±41.7	1007.2±19.3	1014.8±14.8	1041.0±15.8	1015.6±22.8	1020.9±31.7	1033.4±20.5	1019.1±16.0
Phytofluene	414.6±31.7	462.6±25.6	456.4±12.4	436.1±6.6	482.2±2.6	467.6±6.3	**422.4±11.2***	470.3±11.7	446.3±6.4	484.3±6.4
Phytoene	232.9±46.5	311.3±29.6	277.5±5.9	288.9±3.4	338.2±8.1	303.1±3.9	**257.7±10.0***	324.6±8.3	280.5±7.4	326.1±9.2
Total CAR	4072.0±348.3	4546.5±164.6	4556.8±112.5	**4010.4±63.6** **	4803.8±94.5	4607.7±56.8	4350.0±150.4	4919.9±130.4	4474.6±118.6	4864.0±96.0

Fruits at 14 days post breaker

	AC	Azygous	10-2-6-1	10-2-6-6	10-8-8-1	10-8-8-3	10-8-15-2	10-8-15-7	10-8-15-8	10-8-18-7
Lutein	697.2±9.7	687.0±9.7	682.0±14.1	693.0±20.2	706.0±17.0	699.7±21.0	692.0±6.9	687.3±10.5	688.4±17.5	682.5±13.4
Lycopene	2531.5±286.7	3106.3±115.6	2891.5±112.8	3460.0±162.6	**4064.3±152.2*** **	**3805.3±130.6*** **	**3697.4±110.6** **	**3599.0±95.7** **	3331.1±133.3	**4125.7±116.0*** **
β-carotene	1096.9±17.5	1012.4±2.6	1008.2±21.5	1033.6±26.8	1029.6±27.5	1013.0±32.1	1014.7±9.9	1018.8±15.6	1017.2±25.6	1015.2±17.2
Phytofluene	456.7±27.1	522.2±49.1	547.4±16.4	**585.0±3.1***	**604.5±59.3** **	**626.7±12.7*** **	582.9±9.9	534.0±6.4	554.6±9.3	572.3±7.0
Phytoene	295.3±32.2	388.3±59.0	415.5±15.4	**510.4±13.4** **	**513.9±81.5*** **	**558.6±9.5*** **	**496.6±18.2** **	459.7±11.5	463.8±6.8	454.7±2.1
Total CAR	5077.6±315.8	5716.2±148.4	5544.6±178.6	**6282.0±136.4***	**6918.3±317.3*** **	**6703.3±158.7*** **	**6483.7±131.7*** **	**6298.7±105.9** **	6055.1±130.4	**6850.4±88.0*** **

Table 3-1 Comparison of carotenoid contents of multiple *ZFPIDD2* transgenic lines and both non-transgenic azygous and wild type AC controls.

Carotenoid contents are presented as µg/g DW. A minimum of three representative fruits were pooled and three determinations were made per sample. Transgenic individuals are displayed separately, therefore representing one biological replicate with three technical replicates. Between four and five AC control lines, and four and three azygous control lines were used for the analysis, ensuring a minimum of three biological and three technical replicates. Methods used for these determinations are described in section 2.3. The mean data are presented ± SD, with n=3 to15. Dunnett's test analysis illustrates statistically significant differences between non-transgenic azygous controls and the transgenic varieties, $P < 0.05$, $^{**}P < 0.01$, and $^{***}P < 0.001$ are designated by *, **, and ***, respectively.

Like colour development, fruit firmness increases were consistent from T_1 into the T_2 generation. Figure 3-14 shows a reduced rate of softening from breaker on the plant, until fruits are approaching overripe at 14 dpb compared to both controls. At 7 dpb, 10-8 fruits are 18% (1.3-fold) firmer than azygous lines, rising to 23% (1.4-fold) with AC controls. These differences are maintained as fruits progress to 14 dpb, where fruits from transgenic lines are 12% (1.2-fold) and 16% (1.3-fold) firmer compared to azygous and AC lines, respectively. Likewise, lines from the 10-2 insertion event also displayed a reduced rate of fruit softening. The results provide further evidence that transgenic lines improve fruit quality by potentially delaying fruit softening.

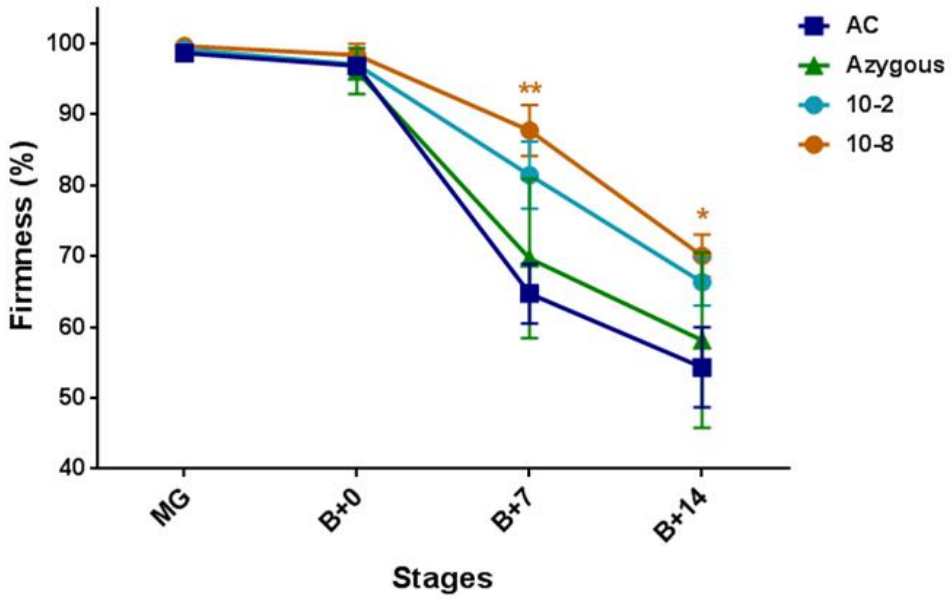

Figure 3-14 Monitoring fruit firmness during ripening.

Fruit firmness was recorded from mature green (MG) through to overripe stages (B+14). Between two and four representative fruits were studied for each line. Each transgenic individual is represented by a single column. A total of six and nine individuals were combined for azygous and AC controls, respectively. Statistical determinations are shown as mean ± SD, Dunnett's test analysis illustrates statistically significant differences between non-transgenic (azygous) and the transgenic varieties, $P < 0.05$, $^{**}P < 0.01$, and $^{***}P < 0.001$ are designated by *, **, and ***, respectively.

3.2.2.5 Parallel experiment to confirm yield improvements and probe penetration tests to establish differences to inner and outer pericarp firmness

Addition firmness experiments were undertaken by myself at Nottingham University, to ascertain whether there were any differences to the firmness of the outer or inner pericarp tissues of ripe fruit. Probe penetration tests using a Lloyd Instrument LF calculated the maximum load required to penetrate the pericarp tissues at 10 mm min^{-1} (section 2.1.6). The outer pericarp was demonstrated to be the main contributor to fruit firmness; on average transgenic lines showed a significant 143% increase compared to AC controls (Figure 3-15). Overall, 10-2-6 lines exhibited the largest increase to outer pericarp firmness (243%), followed by 10-8-15 (174%) and 10-8-8 (87%) lines. With all previous data being obtained using a fruit firmness meter that measured firmness on the exterior of fruit, reduced softening of the outer pericarp was expected and confirmed by the probe penetration tests. No consistent differences between inner pericarp tissues were observed, although 10-8-15 lines displayed a nonsignificant increase in firmness by 47%. The reduced softening of the outer pericarp highlights the potential of transgenic lines to provide improved shelf-life and fruit integrity, which could ultimately expand distribution opportunities, limit damage and disease, whilst extending fruit sensory quality and reducing waste.

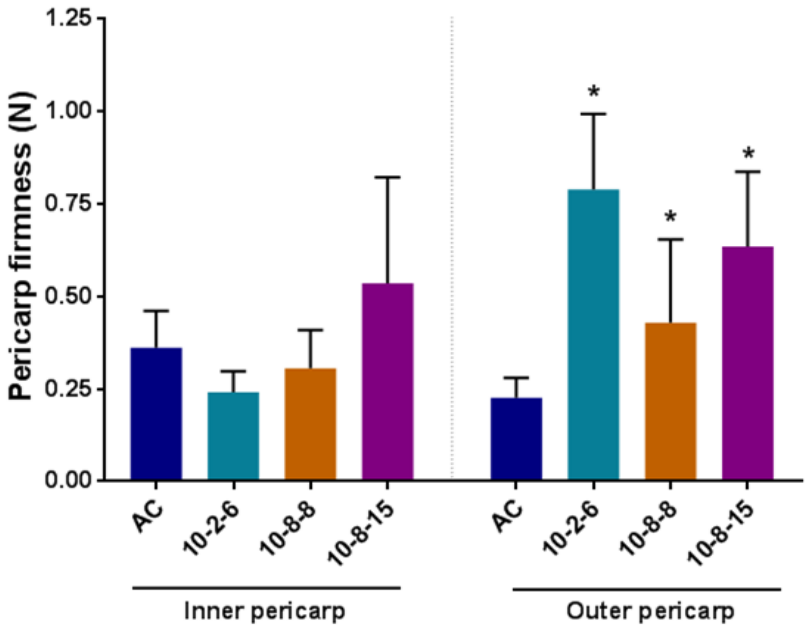

Figure 3-15 Probe penetrations tests on ripe pericarp tissues.

Probe penetration tests were conducted to assess the firmness of the outer and inner pericarp tissues. The best lines are grouped together based upon parental line number. For each line a minimum of three representative fruit were harvested. A 6-mm transverse section was cut from each fruit, probe penetration tests recorded the maximum load required to penetrate the pericarp tissue at 10 mm min−1. Measurements were taken separately from the outer and inner pericarp in duplicate. Outer pericarp tissues were defined as being below the skin but before the vascular boundary. Inner pericarp represents the cells between the vascular boundary and the endodermis. Method is described in section 2.1.6. Statistical determinations are shown as mean ± SD values. A *t test* analysis illustrates statistically significant differences (denoted $P < 0.05$) from the AC controls.

A parallel yield experiment conducted at University of Nottingham provided similar results to that recorded at Royal Holloway (Figure 3-8b). A total of 54% of transgenic lines exhibited improvements to fruit yield, showing the potential to almost double fruit biomass (Figure 3-16). Again, 10-8-15 transgenic lines were the highest yielding, whilst proving to be most consistent for producing larger fruits. Increased fruit size was again shown by the majority of transgenic lines (Figure 3-16). Importantly, the consistency between both crops grown at different locations provides further evidence that transgenic lines can significantly improve fruit size and yield.

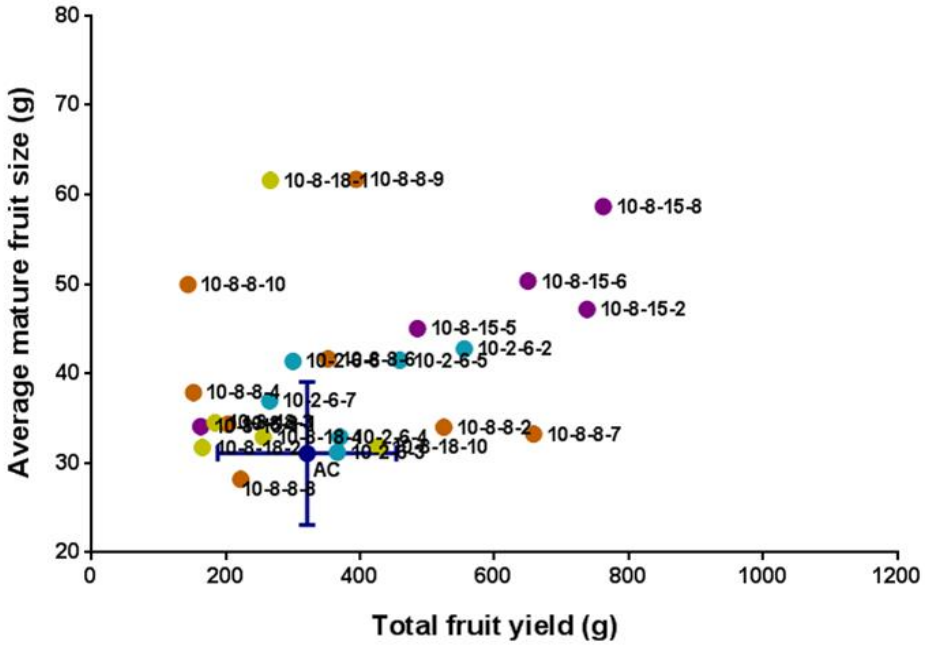

Figure 3-16 Parallel experiment to assess fruit size and weight at a separate location.

Total fruit yield and average ripe fruit weight were recorded for a parallel experiment at the University of Nottingham. Both traits were quantified when AC controls had reached five trusses with fruit set. Each transgenic individual is represented by a single point. A total of nine individuals were combined AC controls. Statistical determinations are shown as mean ± SD.

3.2.2.6 Selection of lines with most improved yield and ripening-related quality traits

The T_2 generation yielded consistent improvements to multiple phenotypes studied, confirming the results obtained in the previous generation. Indicating that the selection of the best lines from the T_1 generation was successful, providing more stable improvements that could be identified across the majority of transgenic lines. Furthermore, the identification of non-transgenic azygous individuals enabled a true comparison, allowing a more accurate characterisation of the *ZFPIDD2* transcription factor. Improvements to colour development, reduced fruit softening, fruit size and yield across two independent crops, all demonstrate the important developmental and ripening-related role of the transcription factor. Additionally, how potential manipulation of this gene can maintain the key *rin* associated quality of reduced softening, but provide improved ripening-related colour transition and yield. 10-8-8-1 was selected for further

analysis, as this line ranked highest, providing substantial improvements to yield and quality-related parameters. Whilst 10-8-15-7 and 10-8-15-8 were chosen for yield improvements, both lines produced significantly larger fruit. Finally, 10-2-6-1 was chosen as it produced the best overall phenotype from the 10-2 insertion event, with 10-2-6 lines showing considerable increases to outer pericarp firmness in the Nottingham probe penetration tests.

3.2.3 Confirming *ZFPIDD2* down-regulation in the T3 generation, combined with phytohormone and metabolite profiling, and evaluation of plant morphology, fruit development and post-harvest quality

3.2.3.1 Confirming *ZFPIDD2* down-regulation in transgenic lines with the most improved phenotypes

Regular PCR confirmed the presence of the transgene, enabling the identification of transgenic and azygous lines. Combined real-time PCR and Southern blotting indicated that the two insertion events carried forward, 10-8 and 10-2, were likely homozygous with a singular insert. This suggests that if the knock-down was successful, the specific single insertion of the transgene is conferring the multiple altered phenotypes witnessed. Therefore, confirming the down-regulation in transgenic lines was the next priority.

Normally the *ZINC FINGER PROTEIN INDETERMINATE DOMAIN 2* (*ZFPIDD2*) displays a relatively sharp rise in expression at breaker, peaking at four days post breaker (4 dpb). Due to the nature of the gene knock-down via 35s::RNAi, some endogenous gene expression is required to induce the down-regulation itself. With both factors in mind, turning fruits at 4 dpb was the stage chosen to compare transcript levels between transgenic lines to both azygous and AC controls. Fruits at breaker were tagged to ensure accurate selection of fruit for harvesting. The 10-8 insertion event was chosen due to the most consistently improved phenotype across all key traits, including colour and carotenoid content, firmness and yield. Once harvested and prior to flash freezing in liquid nitrogen, firmness was recorded for control and transgenic lines. Significant increases to transgenic fruit firmness, consistent with previous generations, indicated that

4 dpb was a suitable time point to determine altered zinc finger protein expression (appendix table A1-2).

Quantitative real-time RT-PCR was performed to confirm reduced expression of the *ZFPIDD2* in turning fruits, as described in section 2.2.6.2, with actin as the reference gene. Expression was screened for multiple azygous and AC lines, and no statistically significant differences were observed. Consequently, azygous controls were chosen for comparison with transgenic lines, as they are considered the true control because they have been through transformation and tissue culture. Multiple 10-8-8-1, 10-8-15-7 and 10-8-15-8 lines were chosen for comparison with azygous controls. Figure 3-17 demonstrates a significant reduction to transcript levels in turning fruits of transgenic lines, confirming the down-regulation. The 10-8-8-1 had the most improved phenotype overall in the T_2 generation and progeny demonstrated the largest down-regulation of 68%. Meanwhile, 10-8-15-8 and 10-8-15-7 lines displayed a down-regulation of 39% and 28%, respectively. With this confirmation, the altered phenotypes witnessed can be attributed to the down-regulation in transgenic lines, ultimately enabling accurate gene characterisation. Furthermore, this experiment indirectly confirms the down-regulation in parental lines, resulting in improved phenotypes that were used for selection of transgenic lines.

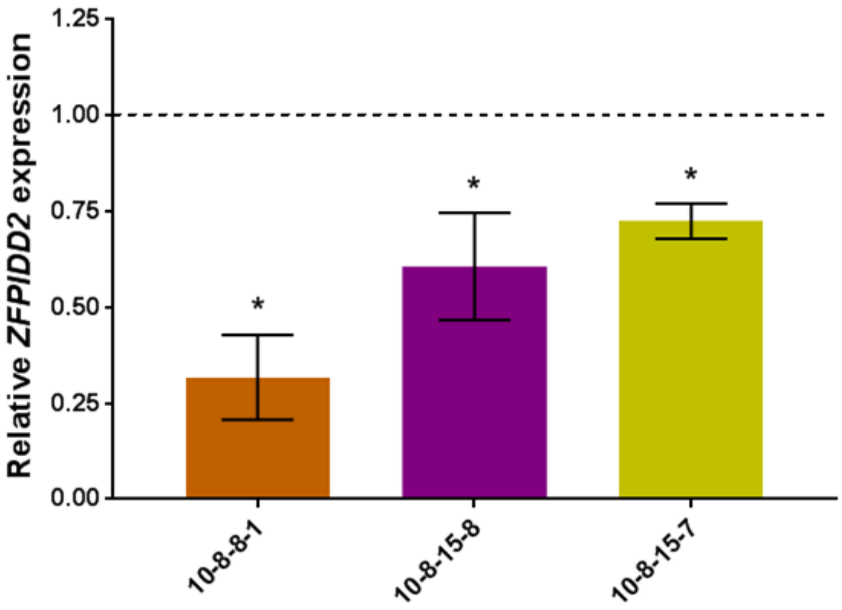

Figure 3-17 Profiling the relative *ZFPIDD2* expression in confirmed transgenic lines.

A minimum of three turning fruits, four days post breaker, were harvested and pulverised under liquid nitrogen into a homogenous powder, as described in section 2.1.6. For each genotype a minimum of three plants were used for expression analysis. Total RNA was extracted from an aliquot of the pooled material, qualitative real time qRT-PCR was performed using gene specific primers for the *ZINC FINGER PROTEIN INDETERMINATE DOMAIN 2* (*ZFPIDD2*) gene. A minimum of two determinations were made per biological replicate. Expression data were normalised to the reference gene actin. The expression values presented are relative and compared to the non-transgenic (azygous) controls, shown by dotted line. No statistically significant differences confirmed between the non-transgenic control and wild type (AC) background. Statistical determinations are shown as mean ± SD values, where n= 3 to 4. A *t test* analysis illustrates statistically significant differences (denoted $P < 0.05$) from the non-transgenic controls.

3.2.3.2 Assessment of phytohormone content in leaf and fruit tissues

Transgenic lines throughout have shown altered developmental and ripening-related phenotypes, due to nonspecific effects of the down-regulation, therefore differences to phytohormones were expected. Phytohormone analysis was conducted at Syngenta, utilising the liquid chromatography–mass spectrometry (LC-MS) platform and routine

screening protocols, for accurate determination of multiple hormones levels (section 2.3.6). A total of three fruits per plant were pooled, a representative aliquot from this powder was pooled with five other biological replicates. Each technical replicate ran then represents all material from one parental line with confirmed down-regulation: 10-8-8-1, 10-8-15-7 and 10-8-15-8. All material was grown, harvested and prepared at Royal Holloway University of London, along with the subsequent analysis of results. A limited number of samples were made available for analysis by Syngenta, so three tissue types were selected for screening: leaf, developing fruits and turning fruits.

Leaf material was studied to identify changes to phytohormones that could be influencing the darker leaf phenotype, altered plant development and morphology. Screening developing fruits (20 dpa) investigated the intricate interplay between multiple hormones governing fruit growth and expansion that control fruit size, which was identified as a major contributor to improved yield. Finally, turning fruits (4 dpb) were chosen to ascertain whether hormones could be contributing to the altered fruit ripening phenotypes. Flowers at anthesis were also harvested to investigate changes to hormones involved in fruit set, however these tissues could not be included due to small number of samples made available.

Good phytohormone coverage was achieved by the LC-MS analysis. A total of 12 quantified hormones from a potential 27 plant analytes were identified from previous analyses ran by Syngenta, across a variety of different crop species (Table 3-2). Principal component analysis (PCA) was used to evaluate the overall variance in phytohormone composition of transgenic lines and both AC and azygous controls, within the different tissues studied. Furthermore, the analysis identifies the contributions of each metabolite to the overall variance. As expected the PCA scatter plot, representing the score values for different tissues and genotypes, showed statistically different clusters for each tissue type (Figure 3-18). The loading scatter plot indicated that numerous metabolites have significant weightings, and the clusters from different tissues were due to multiple metabolites. For the two fruit stages, jasmonaic acid (JA), abscisic acid (ABA) as well as multiple gibberellin (GA) and zeatin-ribosides had the highest loading, leading to separation from leaf samples. Specifically, the zeatin-ribosides have the highest loading for turning fruits, whilst GA_4-Me, GA19, GA20 and JA had the highest loadings for developing fruits.

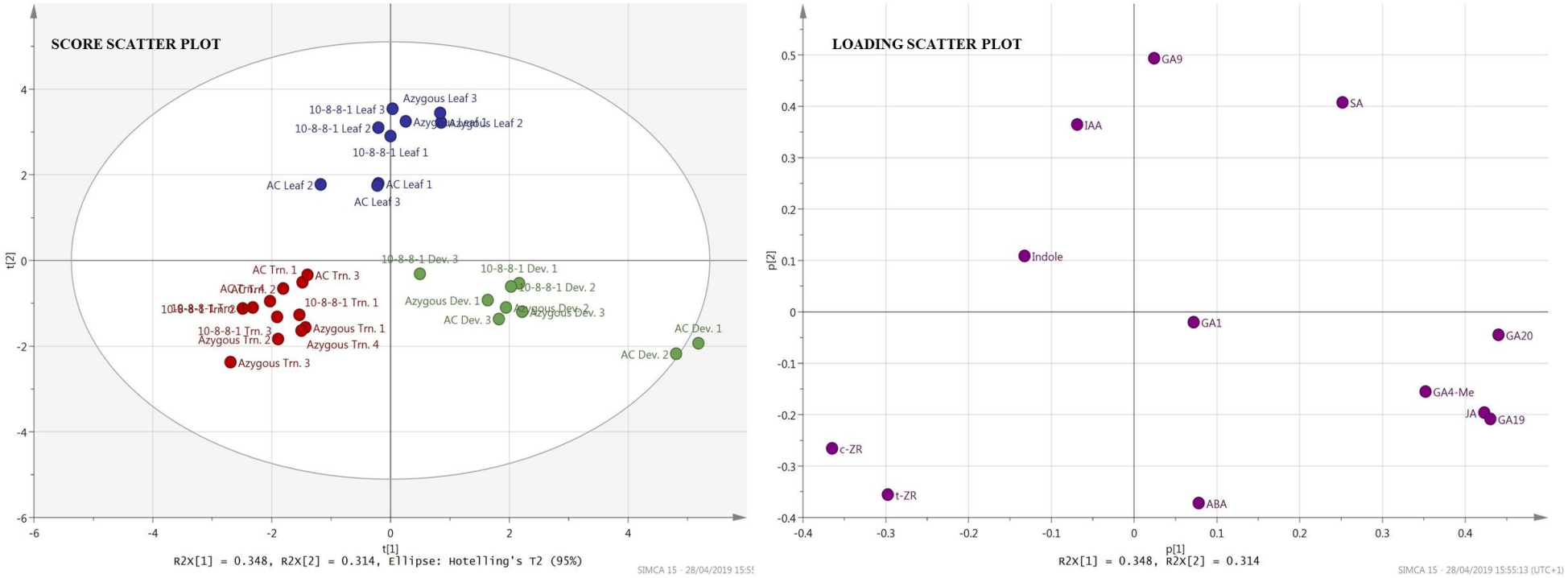

Figure 3-18 Principal component analysis of the phytohormones present in leaf, developing fruit and ripening fruit tissues.

Four representative leaves and three fruits per plant were pooled, a representative aliquot was taken and pooled with the other biological replicates. Material from five plants for each genotype was utilised for the analysis. Each technical replicate ran represent all material from one parental line, 10-8-8-1, 10-8-15-7 and 10-8-15-8. For the control, each technical replicate represents an aliquot of pooled control material. Therefore, five biological replicates were pooled for each genotype and three technical replicates were run. The method used to analyse the phytohormone content from different tissues is described in section 2.3.6, with the treatment and processing of data in section 2.4.

Young leaf material was harvested when truss formation, fruit set and changes to internode length could be identified. Hormonal changes could explain the altered growth, flower and fruit set phenotypes witnessed in transgenic lines, whilst improving the understanding of how the *ZFPIDD2* governs plant development. Compared to azygous controls, transgenic lines displayed a 2.8-fold reduction to JA; conversely cis-zeatin riboside (c-ZR) was elevated 1.3-fold. Compared to AC controls, gibberellin 9 (GA_9) and indoleacetic acid (IAA) was increased 1.4- and 1.5-fold, respectively. Additionally, GA_{20} was detected in both transgenic and azygous fruits, but not in AC controls. GA_{20} content was reduced 2.0-fold in transgenic lines compared to azygous controls, although due to variation between replicates the differences proved not to be statistically significant.

More accurate phytohormone screening was achieved in fruit tissues, with less of the detected analytes being close the limit of quantification (Table 3-2). Developing fruits were harvested at 20 days post anthesis. As expected based on Figure 1-2, multiple forms of gibberellin, as well as ABA and auxin were detected (Table 3-2). Changes to phytohormone content in these tissues could indicate a developmental shift or a delay through hormone induced fruit development, in addition to altered hormone ratios. Both of these could contribute to the increased fruit size of transgenic lines, and potentially the extended development time until the onset of ripening. Interestingly, ABA levels were significantly lower in transgenic lines compared to both controls, 1.3- and 1.2-fold for azygous and AC lines, respectively. Developing transgenic fruits also have altered levels of gibberellins, with an increase to GA_1, which was below the limit of quantification for both azygous and AC controls. Likewise, gibberellic acid 4 – methyl ester (GA_4-ME) could be detected in transgenic and AC lines, but not in azygous controls. Indole could only be detected in azygous controls. Transgenic lines also have a 2.0-fold reduction GA_{20} compared to AC controls. GA_{19} content in transgenic lines was reduced 1.6- and 2.6-fold to azygous and AC controls, respectively.

Finally, turning fruits (4 dpb) aimed to detect whether altered hormones, mainly auxin and ABA, could be triggering the increased accumulation of carotenoids or the reduced rate of fruit softening observed in transgenic lines. Consequently, both the down-regulation and hormone screen on ripening fruits were conducted at the same time point. IAA was detected in turning transgenic fruits, but not for either azygous or AC controls. Compared to the wild type AC controls: a 2.3-fold increase to ABA and a 1.5-fold

elevation to cis-zeatin riboside were displayed in transgenic lines. Finally, indole could not be detected in AC lines, but was present in other genotypes.

The results from the phytohormone screen indicate that the zinc finger protein can either directly or indirectly influence a number of key hormones, across all tissues studied, at different developmental time points. Also, it suggests that the *ZFPIDD2* is likely to be a central hub for hormone-controlled development and ripening, and can explain why many transgenic lines yield many nonspecific altered phenotypes. Gas chromatography with flame ionisation detector (GC-FID) was set up to quantify ethylene. However, all columns tested proved unsuccessful for the separation of compounds and ethylene could not be quantified. Separation therefore required a CP-PoraPLOT Q column, but due to time limitations ethylene screening could not be performed.

	Leaf			Developing Fruits			Turning		
Line	AC	Azygous	Transgenic	AC	Azygous	Transgenic	AC	Azygous	Transgenic
JA	4.8 ± 3.6	59.4 ± 3.9	**21.3 ± 14.3****	336.4 ± 63.4	338.5 ± 34.8	235.7 ± 91.1	16.1 ± 7.6	36.2 ± 13.2	21.7 ± 9.3
SA	2388.3 ± 652.1	3754.8 ± 511.5	3625.1 ± 831.3	2081.0 ± 239.6	2272.5 ± 149.4	2325.5 ± 634.0	928.6 ± 169.0	718.2 ± 185.9	972.1 ± 206.5
GA20	<LOQ	27.9 ± 11.3	13.7 ± 4.4	45.6 ± 7.3	26.4 ± 3.3	23.4 ± 4.3	<LOQ	<LOQ	<LOQ
GA4-Me	<LOQ	<LOQ	<LOQ	260.8 ± 144.0	<LOQ	132.7 ± 39.1	<LOQ	<LOQ	<LOQ
GA9	75.2 ± 11.9	132.8 ± 4.3	108.4 ± 14.1	<LOQ	<LOQ	<LOQ	<LOQ	<LOQ	<LOQ
GA19	<LOQ	<LOQ	<LOQ	71.8 ± 32.0	43.2 ± 8.7	27.5 ± 22.7	<LOQ	<LOQ	<LOQ
GA1	<LOQ	<LOQ	<LOQ	<LOQ	<LOQ	12.9 ± 2.2	<LOQ	<LOQ	<LOQ
ABA	2669.8 ± 54.3	2609.8 ± 95.2	2628.0 ± 99.2	4773.4 ± 254.6	5038.3 ± 141.3	**3911.8 ± 294.4****	2213.2 ± 150.6	4931.5 ± 185.9	4998.9 ± 425.7
Indole	195.3 ± 303.7	79.1 ± 16.6	86.1 ± 18.4	<LOQ	44.7 ± 30.2	<LOQ	<LOQ	72.5 ± 79.9	92.3 ± 74.2
IAA	10.7 ± 0.2	15.8 ± 1.7	16.2 ± 1.4	<LOQ	<LOQ	<LOQ	<LOQ	<LOQ	**13.5 ± 1.8****
t-ZR	1.4 ± 0.4	2.3 ± 0.4	2.2 ± 0.1	19.8 ± 11.4	17.6 ± 4.6	13.8 ± 2.5	44.2 ± 11.5	68.7 ± 21.8	50.3 ± 15.0
c-ZR	6.4 ± 0.4	5.1 ± 0.3	**6.7 ± 0.6****	14.1 ± 7.9	8.9 ± 2.0	7.1 ± 1.3	176.7 ± 55.4	182.5 ± 45.5	267.4 ± 44.5

Table 3-2 Phytohormone screen of leaf, developing fruits and ripening fruits.

The phyrohormones contents are presented as ng/g DW. Four representative leaves and three fruits per plant were pooled, a representative aliquot was taken and pooled with the other biological replicates. Material from five plants for each genotype was utilised for the analysis. Each technical replicate ran represent all material from one parental line, 10-8-8-1, 10-8-15-7 and 10-8-15-8. For the control, each technical replicate represents an aliquot of pooled control material. Therefore, five biological replicates were pooled for each genotype and three technical replicates were run. The mean data are presented ± SD. Dunnett's test analyses illustrates statistically significant differences between non-transgenic (azygous) controls and the transgenic varieties, $P < 0.05$, $^{**}P < 0.01$, and $^{***}P < 0.001$ are designated by *, **, and ***, respectively.

3.2.3.3 The effect of *ZFPIDD2* down-regulation on the spatial repartition of carotenoids within the different tissues of the tomato fruit

Both the exterior and interior of the fruit from down-regulated lines appear darker in comparison to both controls. In ripe fruit of the same age, carotenoids and tocopherols were quantified by UPLC analysis in pericarp, jelly and columella tissues. Comparison between down-regulated lines with both controls, revealed which tissues contributed most to the darker fruit phenotype witnessed. As expected, the analysis of wild type AC tissues demonstrate that on a DW basis per unit mass, pericarp tissue contained the most carotenoids. Pericarp tissues contained around 51% of the total carotenoid content, while columella and jelly sequestrated 12% and 37%, respectively. Both azygous controls and transgenic lines had comparable distribution of carotenoid content between compartments, particularly with pericarp tissues sequestering 50% of carotenoids. Whereas carotenoid distribution was shifted slightly towards jelly tissues, now around 20%, at the expense of columella content that fell to 30%. In transgenic lines, quantitative increases to carotenoid content were evident in all tissues studied, especially with significant increases found to both pericarp and jelly tissues.

Increased fruit pigmentation remains a key commercial trait. Through selection between generations, the project maximised the carotenoid potential of the transgenic lines. This is shown by carotenoid improvements in the T_3 generation, where extended differences between both controls and down-regulated lines can be seen. For example, total carotenoid content was elevated in pericarp tissues by 1.3-fold compared to azygous lines. A 1.5-fold increase to lycopene content drives the overall elevated carotenoid levels. Furthermore, significant increases were found upstream of lycopene in down-regulated transgenic lines, including phytoene (1.2-fold) and phytofluene (1.1-fold), combined with smaller increases for ζ-carotene and neurosporene. Post cyclisation of lycopene, small significant increases were identified for both γ-carotene and lutein against azygous lines. Transgenic lines also displayed elevated tocopherol content, due increases to both α-tocopherol (1.4-fold) and δ-tocopherol (1.1-fold). Phylloquinone content was also quantified, exhibiting a higher level (1.2-fold) compared to azygous lines.

Larger differences were detected to carotenoid and tocopherol contents in pericarp tissues when comparing down-regulated transgenic lines and AC controls. Transgenic lines displayed dramatic increases to phytoene (2.6-fold), phytofluene (2.2-fold) and

neurosporene, the latter could not be detected in AC lines. Small increases to ζ-carotene were observed, along with substantial increases to lycopene (2.7-fold) content. Similar to the previous generation, transgenic lines had a significant reduction to β-carotene (1.2-fold) compared to AC controls. Finally, δ-carotene was increased by 1.1-fold with no change to lutein. The dramatic increases in phytoene, phytofluene and lycopene primarily produced the 1.9-fold increase to the total carotenoid content. Total tocopherol levels were elevated due to a 1.6-fold increase to α-tocopherol, while no change was observed for δ-tocopherol. Moreover, elevated phylloquinones were found in transgenic lines (1.3-fold).

Similarly in jelly tissues, down-regulated lines were characterised by a higher lycopene (1.5-fold) and total carotenoid content (1.2-fold) compared to azygous controls. Greater amounts of phytoene (1.4-fold), phytofluene (1.1-fold) were detected, combined with smaller increases to δ-carotene. ζ-carotene remained unchanged, whilst β-carotene showed a significant reduction by 1.2-fold in transgenic lines. No change was detected to the total tocopherol content, but a small 1.2-fold decrease to δ-tocopherol was observed. Phylloquinone levels were increased 1.1-fold in down-regulated lines compared to azygous controls.

The comparison of jelly tissues between AC and down-regulated lines yielded the greatest differences to carotenoid content. Phytoene content was increased 2.3-fold. Phytofluene could not be detected in AC controls, while significant amounts were produced by transgenic lines. Substantial increases to lycopene (7.2-fold) were observed. Small increases to ζ-carotene, combined with elevated γ-carotene (1.3-fold) and δ-carotene (1.1-fold) also contribute to the 2.2-fold elevation to total carotenoid content in transgenic lines. As seen in the pericarp tissues, β-carotene was significantly reduced (1.3-fold). Interestingly, transgenic fruits have significantly less chlorophyll in jelly tissues, exhibiting a 10.2-fold decrease. Lutein remained unchanged in transgenic lines. Elevated tocopherol content was confirmed in down-regulated lines, with a 1.4-fold increase to α-tocopherol. While δ-tocopherol was significantly reduced 1.2-fold. No change to total phylloquinone level was detected.

Finally, the carotenoid content was measured in columella tissues. Fewer significant differences were established between down-regulated lines and both controls. A comparison between transgenic and azygous lines revealed no change to total carotenoid content. No observable differences were found for phytoene and phytofluene, while a small reduction to ζ-carotene was detected. Unlike other tissues, lycopene content

remained unchanged. Post cyclisation, small reductions to γ-carotene and lutein were observed in down-regulated lines, whilst no differences were detected for β-carotene and δ-carotene. The largest significant difference was a 1.1-fold reduction to α-tocopherol levels in down-regulated lines.

More significant differences were once again detected when comparing the columella tissues from down-regulated lines with AC controls. Transgenic lines exhibited increased phytoene (2.3-fold) and phytofluene (1.9-fold), with no observable differences to ζ-carotene and neurosporene. Lycopene levels were significantly elevated 1.4-fold. Downstream of lycopene, β-carotene was reduced by1.4-fold; smaller decreases were identified for γ-carotene. No change to δ-carotene was observed, while there was a small decrease to lutein. Together, the total carotenoid content of down-regulated lines was increased 1.2-fold. Small amounts of chlorophyll b were quantified in AC controls; however, these were not present in either transgenic or azygous lines. Total tocopherol content remained unchanged in down-regulated lines, displaying only a small significant reduction to δ-tocopherol (1.1-fold). Finally, no change to phylloquinone levels was detected.

	Pericarp			Jelly			Columella		
Line	AC	Azygous	10-8-8-1	AC	Azygous	10-8-8-1	AC	Azygous	10-8-8-1
Lutein	555.0 ± 6.0	541.4 ± 8.1	**553.8 ± 7.4***	262.8 ± 2.2	271.7 ± 6.9	**257.5 ± 3.3*****	361.6 ± 6.1	362.1 ± 7.4	**351.4 ± 2.0***
Neurosporene	0.0 ± 0.0	721.9 ± 10.1	**734.4 ± 4.5***	0.0 ± 0.0	0.0 ± 0.0	0.0 ± 0.0	496.8 ± 4.3	509.6 ± 6.3	502.2 ± 3.1
δ-Carotene	763.4 ± 6.8	784.2 ± 9.1	**828.3 ± 13.9*****	321.9 ± 3.1	357.1 ± 5.6	**367.5 ± 7.1***	496.9 ± 4.2	510.9 ± 7.4	503.3 ± 3.4
Lycopene	2759.3 ± 186.7	4892.9 ± 470.0	**7324.5 ± 795.1*****	368.4 ± 89.4	1823.7 ± 245.1	**2642.4 ± 245.0*****	2330.9 ± 129.0	3206.6 ± 235.2	3247.0 ± 161.8
γ-Carotene	221.5 ± 6.4	214.9 ± 6.7	221.2 ± 4.4	91.6 ± 2.0	113.9 ± 5.3	116.5 ± 5.1	498.2 ± 5.3	494.3 ± 5.9	**482.3 ± 3.3****
β-Carotene	971.2 ± 34.1	825.0 ± 29.3	841.7 ± 13.8	625.2 ± 35.8	599.5 ± 58.4	**488.0 ± 41.6****	747.0 ± 55.5	581.2 ± 14.9	548.8 ± 8.8
ζ-Carotene	736.8 ± 8.8	740.4 ± 9.9	**756.2 ± 4.4***	322.1 ± 3.2	328.4 ± 3.2	329.8 ± 5.6	494.1 ± 5.6	505.7 ± 7.4	**495.1 ± 3.3***
Phytofluene	290.4 ± 6.2	558.8 ± 28.5	**624.8 ± 30.8****	0.0 ± 0.0	120.3 ± 5.7	**135.5 ± 5.7*****	208.7 ± 6.9	413.7 ± 21.6	403.3 ± 25.7
Phytoene	175.6 ± 12.2	403.2 ± 9.8	**463.0 ± 32.8****	38.6 ± 2.4	70.2 ± 8.2	**97.0 ± 13.8****	140.9 ± 13.0	317.6 ± 31.0	326.2 ± 35.2
Total CAR	6473.1 ± 177.1	9682.8 ± 508.4	**12347.9 ± 862.0*****	2030.7 ± 123.5	3684.8 ± 198.6	**4434.2 ± 265.8*****	5775.2 ± 132.4	6901.7 ± 327.0	6859.6 ± 213.7
Total CHL	0.0 ± 0.0	0.0 ± 0.0	0.0 ± 0.0	213.6 ± 45.9	46.4 ± 8.8	20.9 ± 15.3	57.7 ± 10.3	0.0 ± 0.0	0.0 ± 0.0
α-Tocopherol	618.8 ± 12.8	703.3 ± 22.6	**966.6 ± 93.7*****	432.9 ± 30.5	611.1 ± 22.3	617.8 ± 22.6	495.3 ± 15.0	564.9 ± 33.8	**516.1 ± 14.8***
δ-tocopherol	312.6 ± 2.8	280.7 ± 14.1	**304.5 ± 16.2***	195.9 ± 11.9	194.6 ± 10.7	**169.2 ± 6.8****	200.8 ± 9.2	189.3 ± 8.7	180.4 ± 2.3
Total TOC	931.4 ± 10.5	984.0 ± 34.7	**1271.2 ± 103.9*****	628.9 ± 38.2	805.7 ± 18.2	787.0 ± 24.3	696.1 ± 23.4	754.2 ± 42.1	**696.5 ± 16.5***
Phylloquinone	448.0 ± 14.6	473.6 ± 23.4	**558.3 ± 17.3*****	288.8 ± 12.0	259.5 ± 19.8	**294.0 ± 23.1***	456.1 ± 20.2	495.4 ± 25.5	480.5 ± 18.7

Table 3-3 Carotenoid composition found in the pericarp, jelly and columella tissues of ripe fruit from down-regulated *ZFPIDD2* transgenic lines with both controls.

Carotenoid, tocopherol and phylloquinone contents are presented as μg/g DW. A minimum of five representative fruits were pooled. Determinations were made from the five independent pools of five fruits, each pool with three technical replicates, ensuring a minimum of five biological and three technical replicates. Methods used for these determinations are described in section 2.3. The mean data are presented ± SD, with n=15. Dunnett's test analysis illustrates statistically significant differences between non-transgenic azygous controls and the transgenic varieties, $P < 0.05$, $^{**}P < 0.01$, and $^{***}P < 0.001$ are designated by *, **, and ***, respectively.

3.2.3.4 Broader metabolism differences arising from *ZFPIDD2* down-regulation

The distinct uncoupled ripening-related phenotype of down-regulated lines suggested metabolite perturbations beyond the isoprenoid pathway. The broader effects to metabolism were screened using Gas Chromatography-Mass Spectrometry (GC-MS), generating a metabolite profile of ripe fruits. A combination of analytical platforms, with different phase extractions, coupled with different loadings enabled identification and quantification in a relative or absolute manner of over 65 metabolites. Metabolome comparisons were made between down-regulated lines and both non-transgenic azygous and wild type (AC) controls (as described in section 2.3). Statistical determinations were made to assess the differences between genotypes (as described in section 2.4). Significant (p-value <0.05) changes of metabolite levels were identified in most classes of compounds analysed (Table 3-3). The altered isoprenoid levels in different tissues of ripe fruits have been described in section 3.2.3.3. In down-regulated ripe fruit, most amino acids were elevated, around half of which proved significant to both azygous and AC controls. Consistent significant increases were seen for leucine, phenylalanine and threonine to both controls. Similarly, transgenic lines yielded greater glycerol and sorbitol/mannitol content, but inositol levels were reduced. Many organic acids were reduced in down-regulated fruits, with significantly less aconitic acid, citric acid and itaconic acid compared with azygous and AC lines. However, transgenic lines had elevated succinic acid content. Transgenic lines exhibited large reductions in glucaric acid content, with a 7.8-fold decrease compared to AC controls and a significant 20.3-fold reduction to azygous lines.

Fewer differences were detected for the different sugars forms. Interestingly, both galactose and sucrose levels were significantly reduced in transgenic lines. Galactose was reduced around 2.0-fold when compared to both controls. A 6.6- and 7.1-fold reduction to sucrose content was displayed by down-regulated lines in comparison to azygous and AC controls, respectively. Most fatty acids quantified were elevated in transgenic lines, however, significant alterations were found to C14:0, C18:2 cis9,12 and C20:0 when compared to AC controls. Overall the total fatty acid content of transgenic lines was significantly elevated when compared to AC controls, but remained unchanged to azygous controls. Likewise, glycerol-3-phosphate and free phosphate levels were significantly reduced in AC controls. Campesterol was significantly reduced in azygous

controls. No significant differences were identified for putrescine and the lipid gamma-aminobutyric acid (GABA).

	Ratio	
Metabolite	Transgenic to Azy	Transgenic to AC
Amino acid		
5-oxo-proline	0.84 ± 0.15	**1.87 ± 0.33**
Alanine	**1.60 ± 0.25**	1.23 ± 0.19
Aspartic acid	0.65 ± 0.11	**4.64 ± 0.75**
β-Alanine	1.11 ± 0.52	1.25 ± 0.58
Cysteine	2.00 ± 0.84	**10***
Glutamine	1.27 ± 0.14	**1.77 ± 0.19**
Glycine	**1.92 ± 0.56**	1.29 ± 0.38
Homocysteine	0.82 ± 0.08	0.92 ± 0.09
Isoleucine	**1.79 ± 0.47**	1.10 ± 0.29
Leucine	**1.98 ± 0.66**	**1.75 ± 0.58**
Methionine	1.45 ± 1.22	6.14 ± 5.16
Phenylalanine	**3.15 ± 0.89**	**9.40 ± 2.65**
Proline	0.59 ± 0.31	1.27 ± 0.66
Serine	**1.30 ± 0.14**	1.11 ± 0.12
Threonine	**1.43 ± 0.17**	**1.43 ± 0.17**
Valine	**1.78 ± 0.50**	1.05 ± 0.29
Fatty acid		
C12:0	1.64 ± 1.42	2.14 ± 1.85
C14:0	1.02 ± 0.15	**1.31 ± 0.19**
C16:0	0.99 ± 0.08	1.23 ± 0.10
C16:0	1.13 ± 0.46	1.11 ± 0.45
C18:0	1.01 ± 0.14	1.15 ± 0.16
C18:1cis9	0.75 ± 0.51	1.21 ± 0.82
C18:2 cis9,12	1.07 ± 0.06	**1.40 ± 0.07**
C18:2 trans9,12	1.12 ± 0.47	1.10 ± 0.46
C20:0	1.09 ± 0.13	**1.43 ± 0.16**
C22:0	0.88 ± 0.12	0.99 ± 0.13
C24:0	0.82 ± 0.13	0.70 ± 0.11
Glycero-1-C14:0	1.01 ± 0.21	1.22 ± 0.26
Glycero-1-C16:0	0.95 ± 0.12	1.14 ± 0.14
Glycero-1-C18:0	0.94 ± 0.12	1.15 ± 0.14
Glycero-2-C16:0	0.95 ± 0.11	1.08 ± 0.13
Glycero-2-C18:0	0.97 ± 0.11	1.13 ± 0.13
Isoprenoid		
Phytoene	**1.14 ± 0.09**	**2.62 ± 0.21**
Quinone	**1.16 ± 0.02**	**1.22 ± 0.02**
α-Tocopherol	**1.41 ± 0.12**	**1.61 ± 0.14**
δ-tocopherol	**1.10 ± 0.06**	0.98 ± 0.05
γ-Tocopherol	1.41 ± 0.77	1.58 ± 0.87
Phytofluene	**1.12 ± 0.06**	**2.15 ± 0.12**
ζ-Carotene	**1.02 ± 0.01**	**1.02 ± 0.01**
Lutein	**1.02 ± 0.02**	0.99 ± 0.02
β-Carotene	1.02 ± 0.02	**0.87 ± 0.02**
δ-Carotene	**1.06 ± 0.02**	**1.09 ± 0.02**
Neurosporene	**1.02 ± 0.01**	**10***
γ-Carotene	**1.03 ± 0.02**	1.01 ± 0.02

Lycopene	**1.54 ± 0.15**	**2.80 ± 0.26**
Lipid		
GABA	1.10 ± 0.35	0.73 ± 0.23
Non amino acid N-Containing compound		
Putrescine	1.80 ± 1.15	0.91 ± 0.58
Organic acids		
2-oxoglutaric acid	0.83 ± 0.18	1.07 ± 0.23
Aconitic acid	**0.56 ± 0.31**	**0.45 ± 0.25**
Citraconic acid	0.95 ± 0.27	0.89 ± 0.25
Citric acid	**0.75 ± 0.13**	**0.50 ± 0.09**
Fumaric acid	**1.35 ± 0.36**	**0.71 ± 0.19**
Glucaric acid	**0.05 ± 0.02**	0.13 ± 0.05
Gluconic acid	**0.87 ± 0.11**	0.94 ± 0.11
Itaconic acid	**0.80 ± 0.15**	**0.70 ± 0.13**
Lactic acid	1.04 ± 0.41	1.17 ± 0.46
Malic acid	1.40 ± 0.44	**0.58 ± 0.18**
Succinic acid	**2.70 ± 0.65**	**1.58 ± 0.38**
Phosphate		
Glycerol-3-phosphate	1.47 ± 0.25	**2.19 ± 0.37**
Phosphate	1.02 ± 0.12	**1.39 ± 0.17**
Phytosterol		
Campesterol	**3.26 ± 0.66**	1.11 ± 0.22
Sitosterol	1.30 ± 0.09	1.22 ± 0.08
Stigmasterol	1.32 ± 0.28	1.03 ± 0.22
Polyol		
Glycerol	**1.44 ± 0.28**	**1.54 ± 0.30**
Inositol	**0.73 ± 0.11**	**0.75 ± 0.11**
Sorbitol	**3.70 ± 2.57**	**2.84 ± 1.97**
Mannitol	**3.70 ± 2.57**	**2.84 ± 1.97**
Pyrimidone		
Dihydrouracil	**1.42 ± 0.30**	**1.98 ± 0.41**
Sugar		
Arabinose	1.00 ± 0.25	1.00 ± 0.25
Erythrose	1.11 ± 0.15	0.85 ± 0.12
Fructose	0.98 ± 0.09	0.98 ± 0.09
Galactose	**0.52 ± 0.15**	**0.40 ± 0.12**
Glucose	0.98 ± 0.18	0.96 ± 0.17
Ribose	1.00 ± 0.25	1.00 ± 0.25
Sucrose	**0.13 ± 0.09**	**0.14 ± 0.10**
Xylose	1.00 ± 0.25	1.00 ± 0.25
Xylulose	0.51 ± 0.46	0.69 ± 0.63

Table 3-4 Differences to metabolites occurring in *ZFPIDD2* transgenic ripe fruit compared to both azygous and AC controls.

Data has been compiled from multiple analytical platforms. Metabolites were quantified, then ratios were calculated and presented as mean ± SD. Student's t-test was performed, significant changes are represented in bold (p-value < 0.05). 10*, indicates the theoretical value when a metabolite is unique to transgenic at the concentration used, thus was not detected in control samples. GABA, gamma-aminobutyric acid, 5-oxo-proline, pyroglutamic acid.

Multivariate principal component analysis (PCA) used the quantified relative or absolute amounts to assess the overall variance in chemical composition of ripe fruits from down-regulated, azygous and AC lines, whilst identifying the contributions of each metabolite to the overall variance. A scatter plot that represents the score values for the PCA (Figure 3-19) showed that transgenic fruits corresponded to a statistically significant cluster, which separated away from both controls. Furthermore, a significant difference was identified between both azygous and AC controls, demonstrated by two separate clusters. Generally, the variability between technical replicates studied within biological samples remained low. Loading scatter plots demonstrates the numerous metabolites that have significant weightings, indicating that cluster separation was due to multiple metabolites from various metabolite classes. As expected, multiple isoprenoids including lycopene, ζ-carotene, δ-carotene, α-tocopherol and phylloquinonoes had the highest loading in down-regulated fruit. While phytoene, phytofluene and neurosporene loadings contributed to azygous and transgenic separation from AC controls, in addition to contributing to azygous and transgenic separation. β-carotene had the highest loading of any isoprenoid in AC controls. As expected, the variables with the greatest loading in down-regulated lines were multiple amino acids: including phenylalanine, cysteine, glutamine, threonine and leucine; as well as the polyols: glycerol and sorbitol/mannitol; and dihydrouracil.

Multiple fatty acids had the highest loading for azygous lines, with a total of twelve different forms contributing to the separation. Additionally, phosphate, homocysteine and an unknown had high loadings for the non-transgenic controls. Most of the highest loadings for AC controls were organic acids that included aconitic acid, citric acid, fumaric acid, itaconic acid and malic acid, in addition to the sugars erythrose, galactose and sucrose. GABA, inositol and an unknown were the other compounds that drove AC separation.

Interestingly, a PCA of metabolites quantified by GC-MS alone resulted in no clear separation between azygous and AC controls (not shown). This suggested that the carotenoid content drives the separation between both controls. Down-regulated lines still showed a clear separation to both controls, suggesting the separation was influenced by changes to broader metabolism and not just the isoprenoid pathway.

The visual alterations to sections of metabolism and interactions between metabolites were compared between transgenic lines and both controls, the relative changes in metabolite levels were painted onto biochemical pathway displays (Figure 3-20).

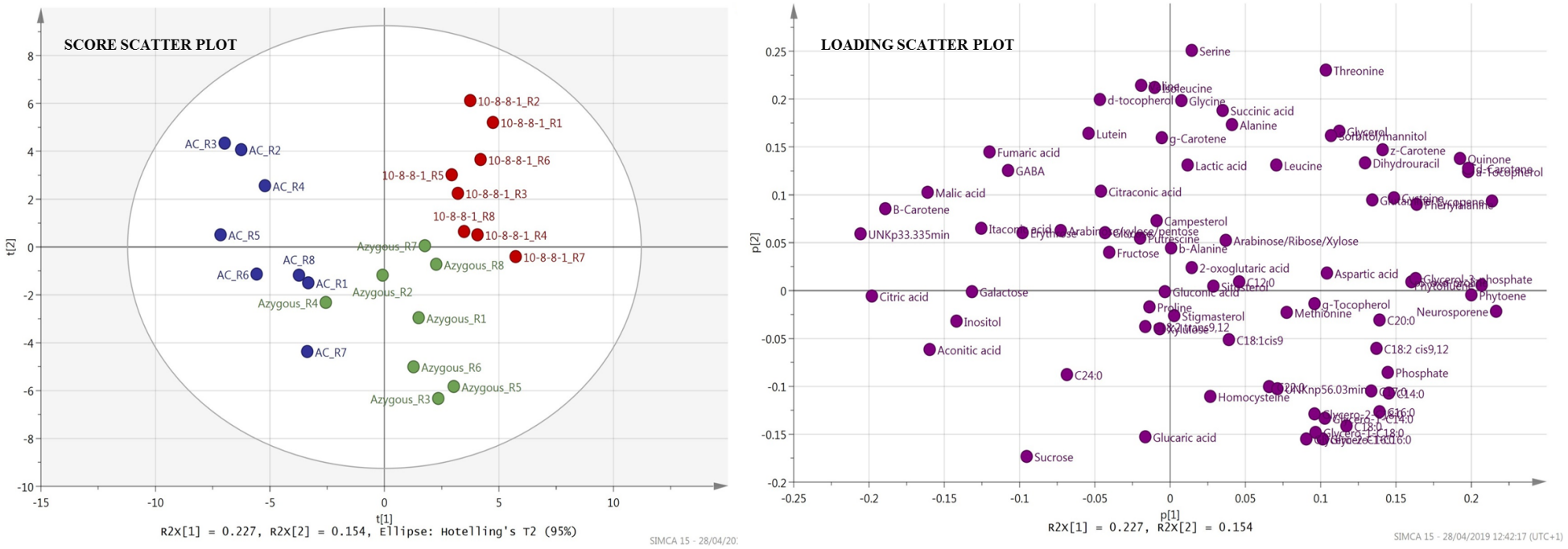

Figure 3-19 Principle component analysis of ripe fruit metabolism for *ZFPIDD2* down-regulated lines with both azygous and AC controls.

A minimum of four biological and two technical replicates were analysed for each experiment. Metabolite levels from the GC-MS and UPLC analytical platforms were combined. The UPLC method used to analyse isoprenoids, the GC-MS method to assess broader metabolism effects, and the treatment and processing of data are described in section 2.3.3, 2.3.5 and 2.4, respectively.

a

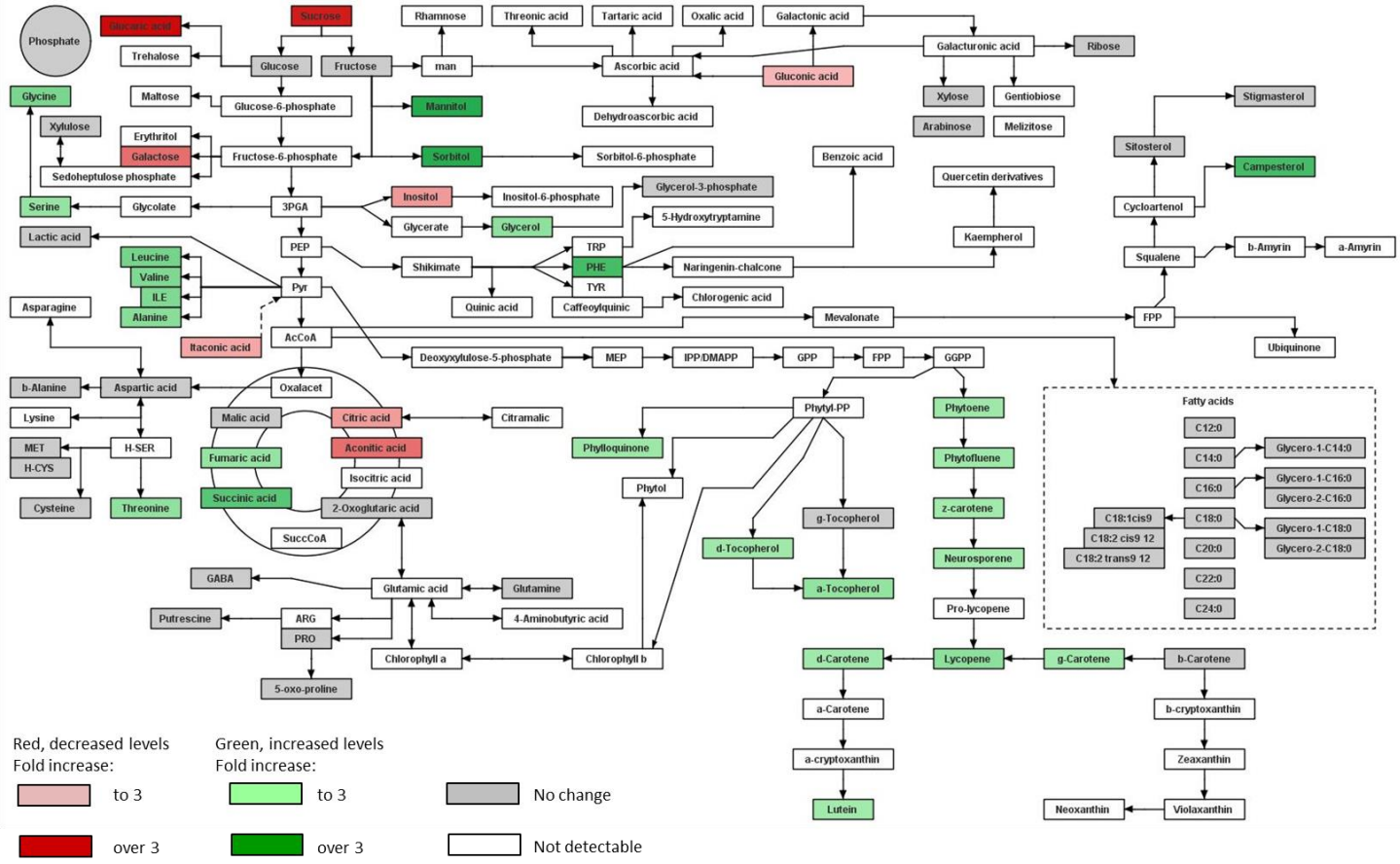
Phosphate
Glucaric acid
Sucrose
Rhamnose
Threonic acid
Tartaric acid
Oxalic acid
Galactonic acid
Galacturonic acid
Ribose
Trehalose
Glucose
Fructose
man
Ascorbic acid
Gluconic acid
Glycine
Maltose
Glucose-6-phosphate
Mannitol
Dehydroascorbic acid
Xylose
Gentiobiose
Arabinose
Melizitose
Xylulose
Erythritol
Galactose
Fructose-6-phosphate
Sorbitol
Sorbitol-6-phosphate
Sedoheptulose phosphate
Benzoic acid
Quercetin derivatives
Kaempherol
Stigmasterol
Sitosterol
Campesterol
Cycloartenol
Squalene
b-Amyrin
a-Amyrin
Serine
Glycolate
3PGA
Inositol
Inositol-6-phosphate
Glycerol-3-phosphate
Glycerate
Glycerol
5-Hydroxytryptamine
Lactic acid
PEP
TRP
PHE
TYR
Shikimate
Naringenin-chalcone
Leucine
Valine
ILE
Alanine
Pyr
Quinic acid
Caffeoylquinic
Chlorogenic acid
Asparagine
Itaconic acid
AcCoA
Mevalonate
FPP
Ubiquinone
Deoxyxylulose-5-phosphate
MEP
IPP/DMAPP
GPP
FPP
GGPP
b-Alanine
Aspartic acid
Oxalacet
Lysine
Malic acid
Citric acid
Citramalic
Phytyl-PP
Phytoene
Fatty acids
C12:0
C14:0
Glycero-1-C14:0
MET
H-CYS
H-SER
Fumaric acid
Aconitic acid
Phylloquinone
Phytofluene
C16:0
Glycero-1-C16:0
Glycero-2-C16:0
Isocitric acid
Phytol
z-carotene
C18:1cis9
C18:2 cis9 12
C18:2 trans9 12
C18:0
Glycero-1-C18:0
Glycero-2-C18:0
Succinic acid
2-Oxoglutaric acid
g-Tocopherol
d-Tocopherol
C20:0
C22:0
C24:0
Cysteine
Threonine
SuccCoA
Neurosporene
GABA
Glutamic acid
Glutamine
a-Tocopherol
Pro-lycopene
Putrescine
ARG
PRO
4-Aminobutyric acid
Chlorophyll a
Chlorophyll b
Lycopene
g-Carotene
b-Carotene
d-Carotene
5-oxo-proline
a-Carotene
b-cryptoxanthin
a-cryptoxanthin
Zeaxanthin
Lutein
Neoxanthin
Violaxanthin
Red, decreased levels
Fold increase:
to 3
over 3
Green, increased levels
Fold increase:
to 3
over 3
No change
Not detectable

b

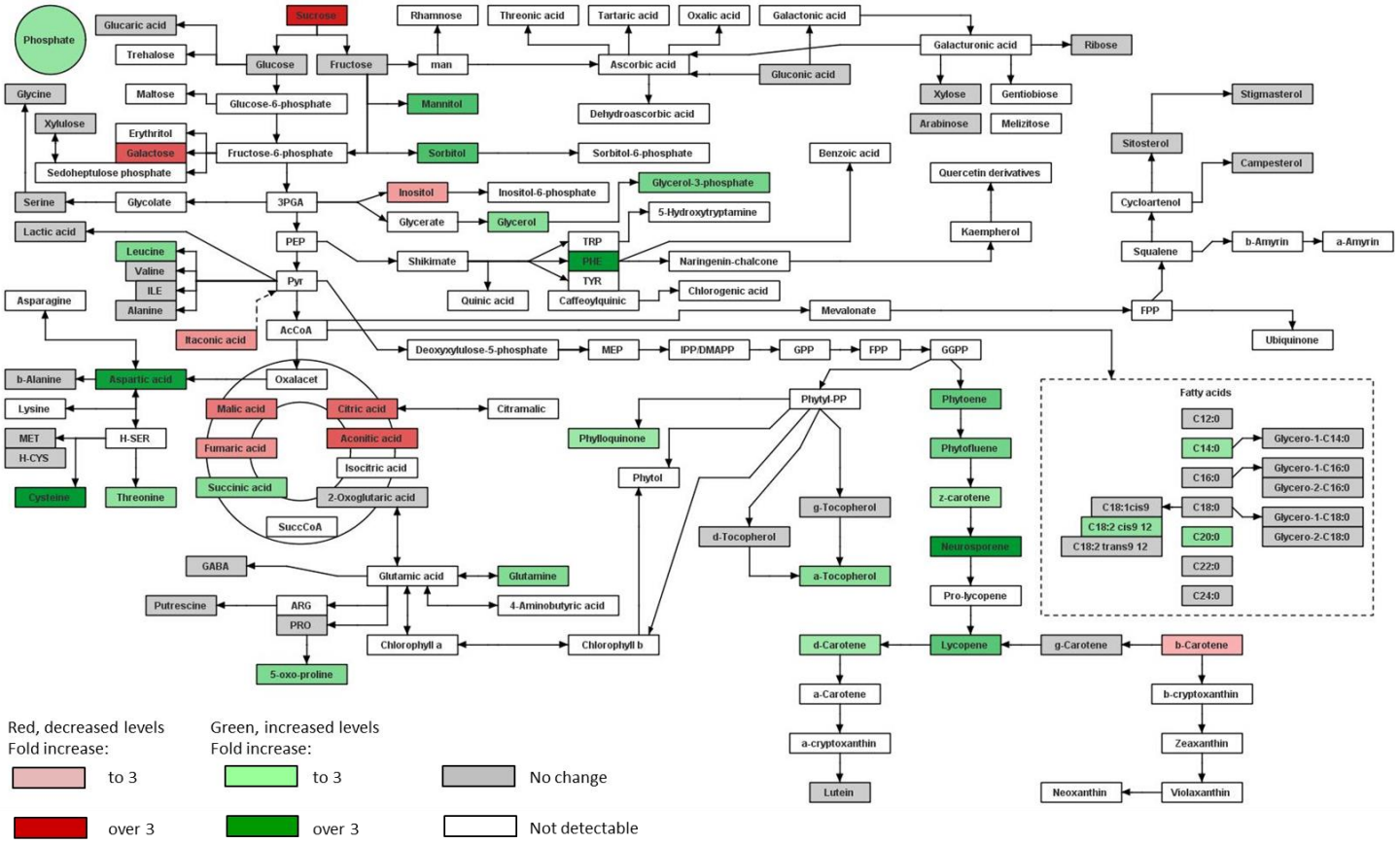

Figure 3-20 Metabolite changes in ripe tomato fruit as a result of *ZFPIDD2* down-regulation.

Figure 3-20 Metabolite changes in ripe tomato fruit as a result of *ZFPIDD2* down-regulation.

The metabolomics data acquired by GC-MS and UPLC chromatographic systems are displayed quantitatively over schematic representations of biochemical pathways produced using BioSynLab software (www.biosynlab.com). False colour scale is used to display the quantity of each metabolite in down-regulated transgenic lines relative to azygous controls (a) and AC controls (b). Green indicates significant increases. Pale green represents small fold changes up to 3-fold whilst darker green indicates >3-fold. Red colouration has been used to represent decreased metabolite levels; dark red is over 3-fold, light red is to 3-fold. Grey indicates no significant change. White represents metabolites that were not detected in the samples analysed, because they was not present in samples or could not be detected using the analytical platforms available.3PGA, glyceraldehyde-3-phosphate; Ac- CoA, acetyl-coenzyme A; ARG, arginine; DMAPP, dimethylallyl pyrophosphate; FPP, farnesyl diphosphate; GGPP, geranylgeranyl-pyrophosphate; GPP, geranyl diphosphate; H-CYS, homo cysteine; H-SER, homo serine; IPP, isopentenyl pyrophosphate; ILE, isoleucine; man; mannose, MEP, 2-C-methyl-D-erythritol 4-phosphate; MET, methionine; PEP, phosphoenolpyruvate; PHE, phenylalanine; Phytyl-PP, Phytyl diphosphate; PRO, proline; PS/PC, phosphatidylserine/phosphatidylcholine; Pyr, pyruvate; SuccCoA, succinyl-coenzyme A; TRP, tryptophan; TYR, tyrosine.

3.2.3.5 Altered post-harvest ripening-related fruit quality of down-regulated lines

Previous generations demonstrated the potential of transgenic lines to shorten ripening-related colour transition, and reduce the rate of fruit softening. Both parameters were studied on fruit that ripened on the plant. Therefore, it was important to establish whether these improved quality traits were maintained post-harvest when fruits ripened off the plant. Fruits were harvested at breaker stage, sterilised and stored at room temperature, following common commercial practices (as described in section 2.1.5). This ensured fruits were harvested at the same time point during development and kept at optimal ripening conditions, limiting potential variation. The main objective of the experiment was to test whether reduced rate of fruit softening, and increased ripening-associated colour development could be attributed to *ZFPIDD2* down-regulation.

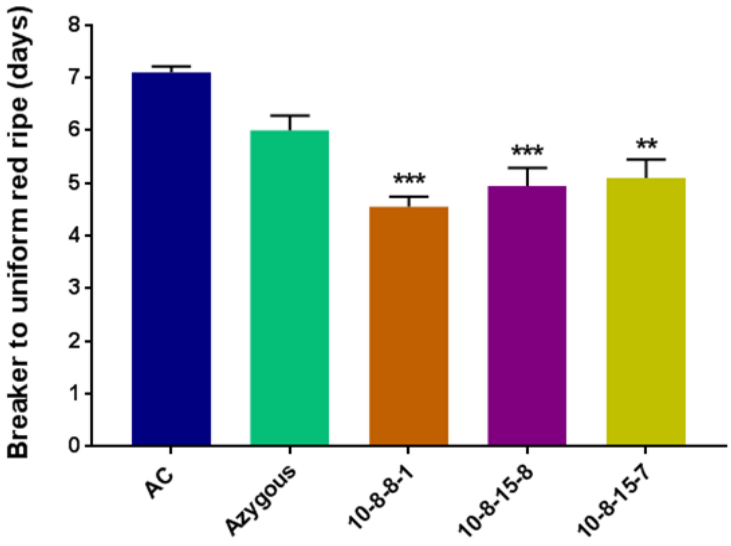

Figure 3-21 Comparison of the rapidity of postharvest fruit ripening determined by the presence of a uniform red colouration.

Representative fruit were harvested at breaker, sterilised and stored separately at room temperature. The rapidity of ripening was compared for down-regulated transgenic lines, and both non-transgenic (azygous) and wild type (AC) controls. Fruits were judged to be ripe upon visual determination of the presence of a uniform red colouration. Five fruits per plant were analysed, four individual plants were studied for each line. This ensured the study included a minimum of five technical replicates and four biological replicates. Methods are described in section 2.1.5. Statistical determinations are shown as mean ± SD values, Dunnett's analysis illustrates statistically significant (denoted $P < 0.05$, $^{**}P < 0.01$, and $^{***}P < 0.001$) from the non-transgenic controls.

The time fruits took to ripen post-harvest was studied by visual determination of a uniform red colouration (Figure 3-21). Transgenic lines exhibited increased colour transition to ripe, on average taking 4.9 days compared to 6.0 and 7.1 days for azygous and AC controls, respectively. 10-8-8-1 lines took just 4.6 days to reach red ripe from breaker, displaying 1.4 to 2.6 day reduction compared to both controls. Colour development was assessed at multiple time points throughout ripening using a colourimeter. A colourimeter defines colour related to human perception, where all conceivable colours can be located within the colour CIELAB sphere, and are defined by three perpendicular axes: L* (from white to black), a* (green to red) and b* (blue to yellow). The same system has been used previously to determine colour changes throughout tomato ripening, displaying significant changes to L*, a* and b* values

(López Camelo and Gómez, 2004). Colourimeter colour assessment is utilised by industry, including collaborators within the project. Therefore, this provided a quantitative approach to identify ripening-related colour changes between different genotypes, while determining whether transgenic fruits post-harvest had an altered time to reach uniform red from breaker (Figure 3-22).

The L* score quantified the relative darkness or lightness of fruits, with higher values indicating elevated brightness. L* scores were shown to steadily decrease throughout ripening, as detailed in previous literature, this was associated to lycopene accumulation (Figure 3-22a). Transgenic lines had reduced L* scores across all time points studied compared to both controls, although consistent statistically significant differences were only obtained when comparing to AC lines. The results indicated that transgenic fruits were on average 15% darker to AC fruits from B+3 onwards. Comparison with azygous lines only revealed a statistically significant difference at B+3 to 10-8-8-1 lines.

The A* score determined the changes along the green-red axis, with negative and positive values representing green and red colouration, respectively. As expected A* scores increased throughout ripening, this can mostly be attributed to lycopene accumulation (Figure 3-22b). More rapid colour transition from green to red were seen in transgenic fruits, indicated by sharper rise to A* scores. The largest differences were seen at B+3 where transgenic fruits exhibited a 4.7-fold increase to A* values compared to azygous controls, this rose to 10-fold when compared to AC lines. From B+3 onwards a consistent 1.5- and 2.0-fold increase was detected for both azygous and AC controls, respectively. The fold changes exhibited at the later stages of ripening are similar to the carotenoid differences seen in down-regulated lines, indicating that elevated isoprenoids are contributing to the elevated A* score. Therefore, increased rate of carotenoid biosynthesis is expected to contribute to the sharp rise in colour development at B+3, and end point levels of pigments. The accuracy of visual determination of ripening-related colour transition measured across the different generations was confirmed by the colourimeter. Using the different visually determined ripening times for transgenic and control lines, and the A* curves, prediction of an A* value indicating ripe fruit was calculated. The y axis intercept values between all lines displayed a small variation; indicating that visual determination of colour associated ripening time was consistent. The results confirmed the visual phenotype of a reduced time to reach red ripe from breaker, and that fruits from down-regulated lines appear darker red.

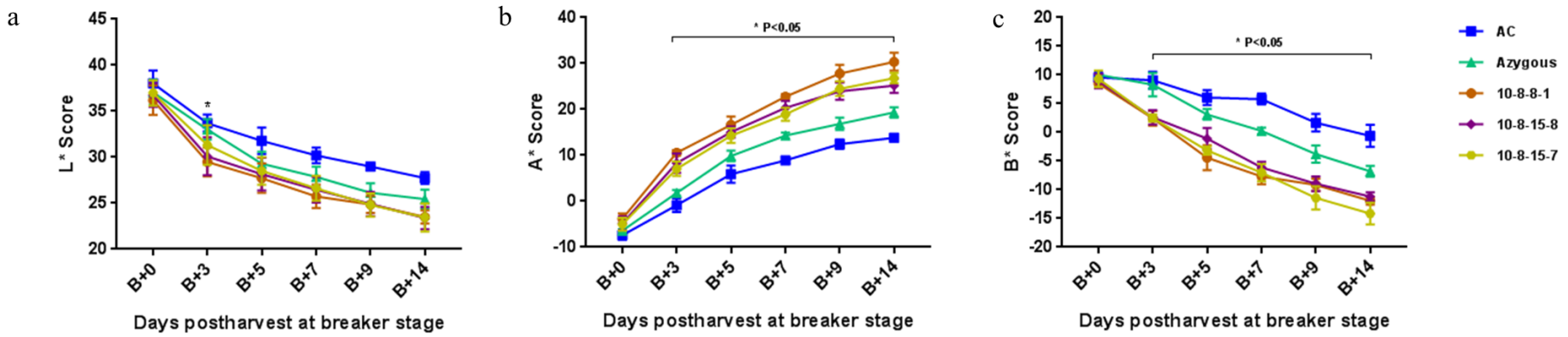

Figure 3-22 Study of post-harvest ripening-related colour development using a colourimeter.

Representative fruit were harvested at breaker, sterilised and stored separately at room temperature. A colourimeter monitored colour transition for down-regulated transgenic lines and both non-transgenic (azygous) and wild type (AC) controls. The colourimeter used the CIELAB colour sphere to monitor fruit ripening-related colour development across six specific time points throughout ripening, from breaker (B+0) to breaker plus fourteen days (B+14). Each panel indicates the numerical expression of colour along three separate axes: L*, A* and B* (from white to black; green to red and blue to yellow, respectively). Four colourimeter measurements were taken per fruit, per time point, with five fruits analysed per plant. Four individual plants were studied for each line. This ensured the study included a minimum of five technical replicates and four biological replicates. Methods are described in section 2.1.5. Statistical determinations are shown as mean ± SD values, Dunnett's analysis illustrates statistically significant differences (denoted $P < 0.05$) between all transgenic lines and the non-transgenic controls azygous controls.

Similarly, the B* scores displayed significant differences throughout ripening (Figure 3-22c). B* values were significantly reduced in transgenic lines, indicating increased transition from yellow to blue. This can be explained by the reduced time from breaker to ripe, the accumulation of red pigments and reduction in abundance ratio of yellow/orange carotenoids (López Camelo and Gómez, 2004). This can further explain why down-regulated fruits appear a darker red in comparison to both controls. Also, this result could indicate changes to flavonoid content.

While the colourimeter experiment was ongoing, the rate of fruit softening was monitored throughout ripening until fruits reached overripe. Transgenic fruits remained firmer from 1 dpb onwards, demonstrating a reduced rate of fruit softening (Figure 3-23a). The most dramatic changes to fruit firmness were seen in the down-regulated 10-8-8-1 lines, displaying a 16% (1.3-fold) increase in firmness compared to azygous controls that extends to 23% (1.4-fold) compared to AC lines at 7 dpb. These differences were maintained at 14 dpb with azygous fruits being 15% (1.4-fold) softer and AC displaying a 26% (1.8-fold) reduction to firmness. By 21 dpb, transgenic fruits are 13% (1.6-fold) and 20% (2.4-fold) firmer compared to azygous and AC controls, respectively. Reduced softening was also identified in both 10-8-15-7 and 10-8-15-8 lines, with fruits averaging an increase to firmness of 10% (1.3-fold) to azygous controls and 18% (1.7-fold) to AC controls from 7 to 14 dpb. Generally, fruits are required to reach red ripe before being sold to consumers, reaching the acceptable quality demands required from an industry, supplier and consumer prospective. Therefore, Figure 3-23b compares the firmness from red ripe onwards, accounting for the altered ripening times between transgenic and control varieties. In this study acceptable firmness-related quality was defined as being above 50%, providing a threshold value to determine any potential extensions to shelf-life. AC controls dropped below this threshold 1 day post ripe, azygous controls took 4.5 days, while transgenic fruit took between 9 and 12 days for firmness to fall below 50%. The delayed softening and maintained integrity for an extended period highlights the potential for transgenic lines to double the shelf-life of ripe fruit in comparison to azygous controls, while providing an extension up to 11 days compared to AC controls. Therefore, the enhanced colour formation and reduced softening phenotypes demonstrates the significant potential to improve key commercial quality traits.

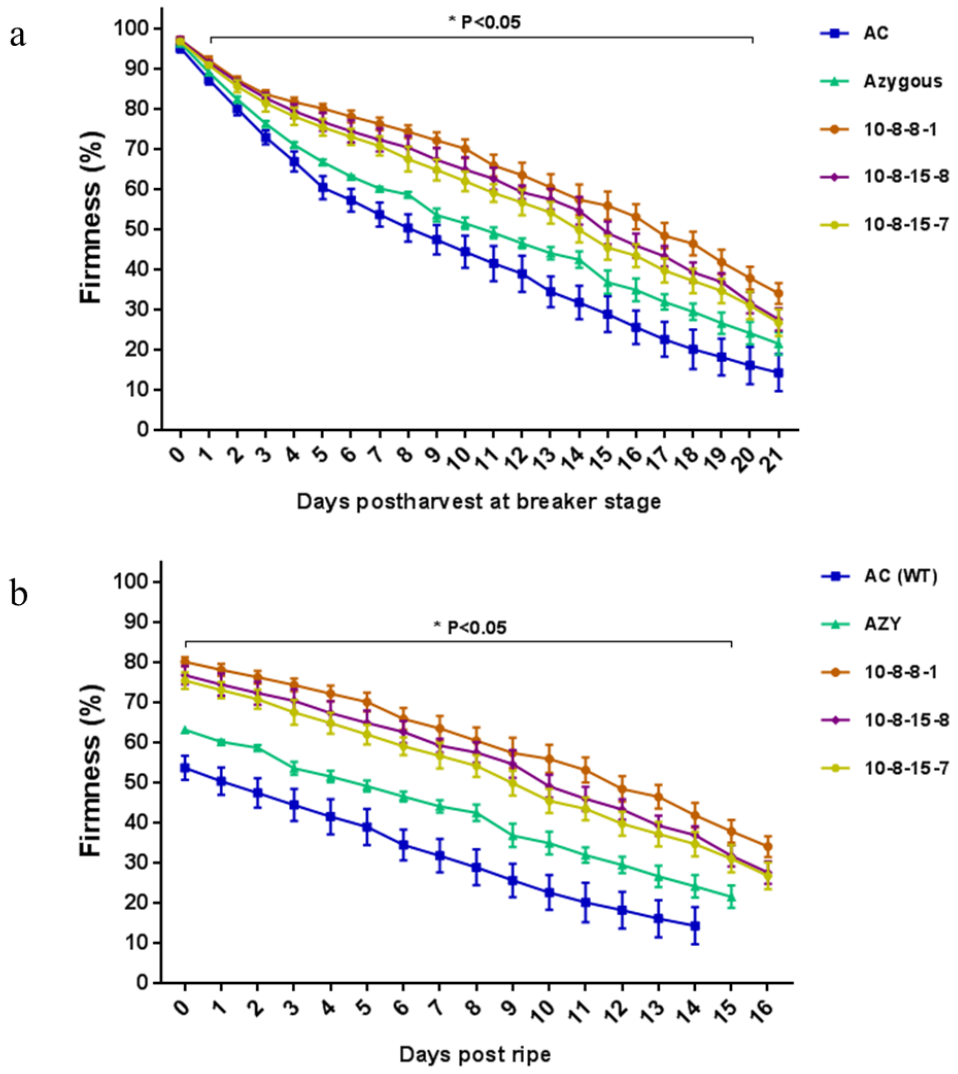

Figure 3-23 Effect of *ZFPIDD2* down-regulation on the rate of postharvest fruit softening.

Representative fruit were harvested at breaker, sterilised and stored separately at room temperature. Softening was monitored throughout ripening between transgenic lines and both azygous and AC controls. Firmness values given represent the percentage firmness remaining as measured by a fruit firmness meter. Firmness was compared at breaker (a) or post ripe (b) in line with retailer and consumer quality assessment, accounting for altered ripening times for each genotype. Four random points were recorded per time point, five fruits analysed per plant and a minimum of four individual plants from each line were combined for the analyses. This ensured the study included a minimum of five technical replicates and four biological replicates. Methods are described in section 2.1.5. Statistical determinations are shown as mean ± SD values, Dunnett's analysis illustrates statistically significant differences (denoted $P < 0.05$) between all transgenic lines and the non-transgenic controls azygous controls.

Overall, both colour accumulation and altered fruit softening display dose dependency for the zinc finger protein down-regulation. 10-8-8-1 displayed the largest reduction to zinc finger protein transcript abundance, increased rate of colour development, highest end point levels of pigments, coupled with most significantly reduced fruit softening. Again the results demonstrated the partial uncoupling of ripening-related processes, as seen in previous generations.

3.2.3.6 Confirming developmental and yield-related phenotypes in *ZFPIDD2* down-regulated fruits

Fruit development and plant morphology phenotypes were compared for transgenic lines displaying reduced *ZFPIDD2* transcript levels, with both azygous and AC controls. A darker leaf phenotype was identified in transgenic lines compared with both controls (not shown), in addition to reduced internode length and total plant height (Figure 3-24a and Figure 3-24b). Compared to azygous controls, the average internode length was 1.2 cm shorter, and plant height was reduced by 15 cm. Similar comparisons with AC controls, revealed that transgenic lines had shorter internodes by 2.0 cm, while height was reduced by 51 cm. Differences to non-vegetative biomass could also be identified (Figure 3-24c), transgenic lines exhibited a 36% and 20% increase compared to azygous and AC controls, respectively. This phenotype is mostly attributed to increased leaf nodes resulting in elevated leaf biomass (not shown).

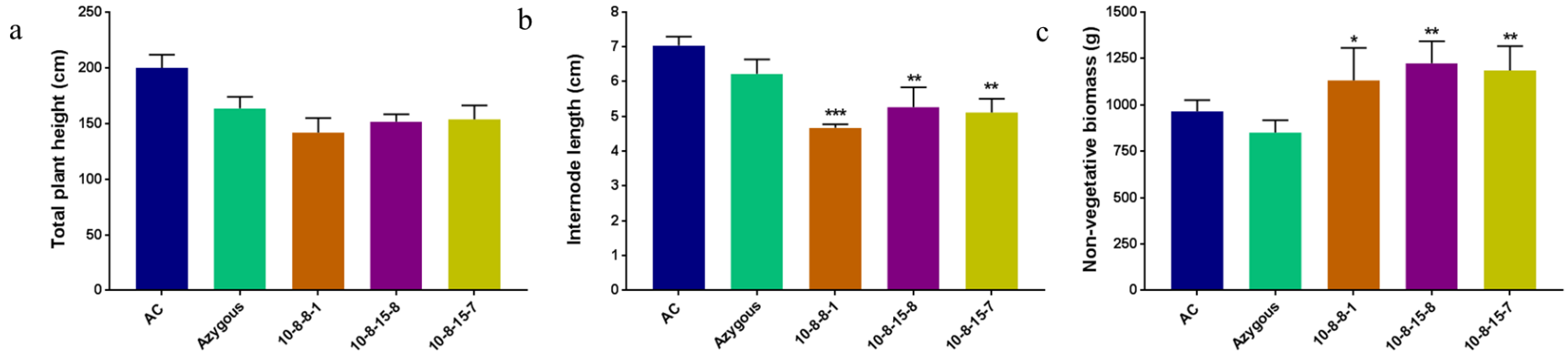

Figure 3-24 Using plant height, internode length and non-vegetative biomass to determine differences in plant morphology during development.

Differences to plant morphology were determined by analysis of plant height (a), internode length (b) and non-fruiting biomass (c) for down-regulated transgenic lines, compared with non-transgenic (azygous) and wild type (AC) controls. The plant developmental parameters were measured once the wild type background had formed five trusses with fruit set. Total plant height was measured from soil to last node; twelve random internodes were measured from base of the plant to the last node. Non-fruiting biomass combined the tallying of shoot cuttings during development prior to senescing, and the remaining total leaf and stem weights post harvesting of all fruits. Four plants per genotype ensured that four separate biological replicates were used for the analysis. Statistical determinations are shown as mean ± SD values, Dunnett's test analysis illustrates statistically significant differences (denoted $P < 0.05$, $^{**}P < 0.01$, and $^{***}P < 0.001$) from the non-transgenic controls.

Fruit yield-related phenotypes were also studied (Figure 3-25), to ascertain whether potential yield increases observed in previous generations could be seen in down-regulated zinc finger protein lines. Firstly, transgenic lines yielded more fruit in comparison to both controls (Figure 3-25a), producing 12 more fruits compared to azygous and 7 more to AC controls. Despite this, only 10-8-15-7 individually yielded significantly more fruits compared to AC controls. Fruit size was positively improved (Figure 3-25b), with transgenic fruits displaying on average an 11 g (38%) and 9 g (29%) increase compared to azygous and AC controls, respectively. Elevated fruit number and size in transgenic lines resulted in higher total fruit yield (Figure 3-25c), resulting in a 72% increase to total fruit biomass to azygous controls, likewise the difference to AC controls was 48%. On average transgenic lines exhibited an increased harvest index (crop production efficiency) when compared to azygous (1.3-fold) and AC (1.2-fold) controls, although both comparisons proved not to be significant.

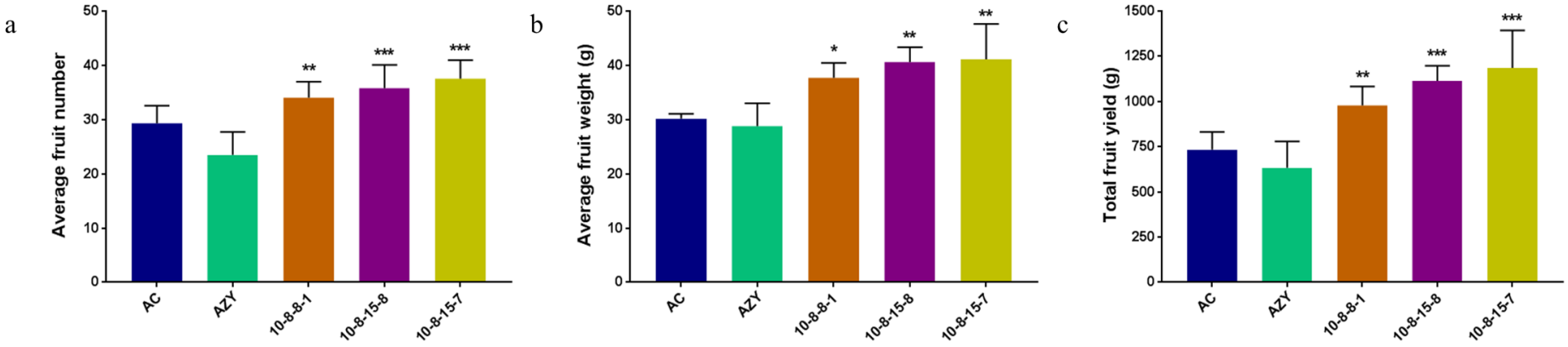

Figure 3-25 Using total fruit number, average fruit weight and total fruit yield as markers for altered fruit set and development.

Total fruit number (a), average fruit weight (b) and total fruit yield (c) phenotypes were recorded to test whether zinc finger protein down-regulation altered the fruit set efficiency, and fruit growth against both non-transgenic (azygous) and wild type (AC) controls. All parameters were measured once the wild type background had formed five trusses with fruit set. All fruit weights were recorded individually postharvest and combined to determine total fruit yield. Four plants per genotype ensured that four separate biological replicates were used for the analysis. Statistical determinations are shown as mean ± SD values, Dunnett's test analysis illustrates statistically significant differences (denoted $P < 0.05$, $^{**}P < 0.01$, and $^{***}P < 0.001$) from the non-transgenic controls.

Fruit development was monitored across several intervals during development, which started once AC lines yielded the first ripe fruit (Figure 3-26). During early development, slower transgenic fruit set was demonstrated by the reductions to fruit number at time point one, with 10-8-15-8 lines significantly yielding four less fruit. On average transgenic lines have five and seven less fruit at the first time point compared to azygous and AC controls, respectively. Elevated fruit production throughout the subsequent time points was exhibited by transgenic lines. This resulted in 10-8-15-7 having significantly more fruit by time point three, and all transgenic lines significantly yielding more fruit upon harvesting.

The percentage of ripe fruit on each plant was recorded (Figure 3-26b), with transgenic lines demonstrating a delay to the onset fruit ripening. At the second time point, almost all transgenic fruit were still developing, while 13% and 22% of fruits has surpassed breaker stage in both azygous and AC controls, respectively. The differences were extended into the third time point, between 24-39% of transgenic fruit had reached breaker stage, significantly less than the 56% of azygous and 52% of AC control fruits that had reached ripening. However, as shown in Figure 3-26a transgenic lines exhibited an accelerated rate of fruit production, thus compared to azygous controls the number of ripe fruits proved not to be significant. Despite this, significantly more ripe fruit were recorded for AC controls at this time point. Fewer significant differences were observed at the final time point, as increased fruit number resulted in transgenic lines yielding significantly more ripe fruit compared to azygous lines, but similar numbers to AC controls. The result supports the extended development time required by transgenic fruit to reach breaker, shown in the T_1 generation (Figure 3-2a), while showing the potential to improve ripe fruit output during the latter stages of development.

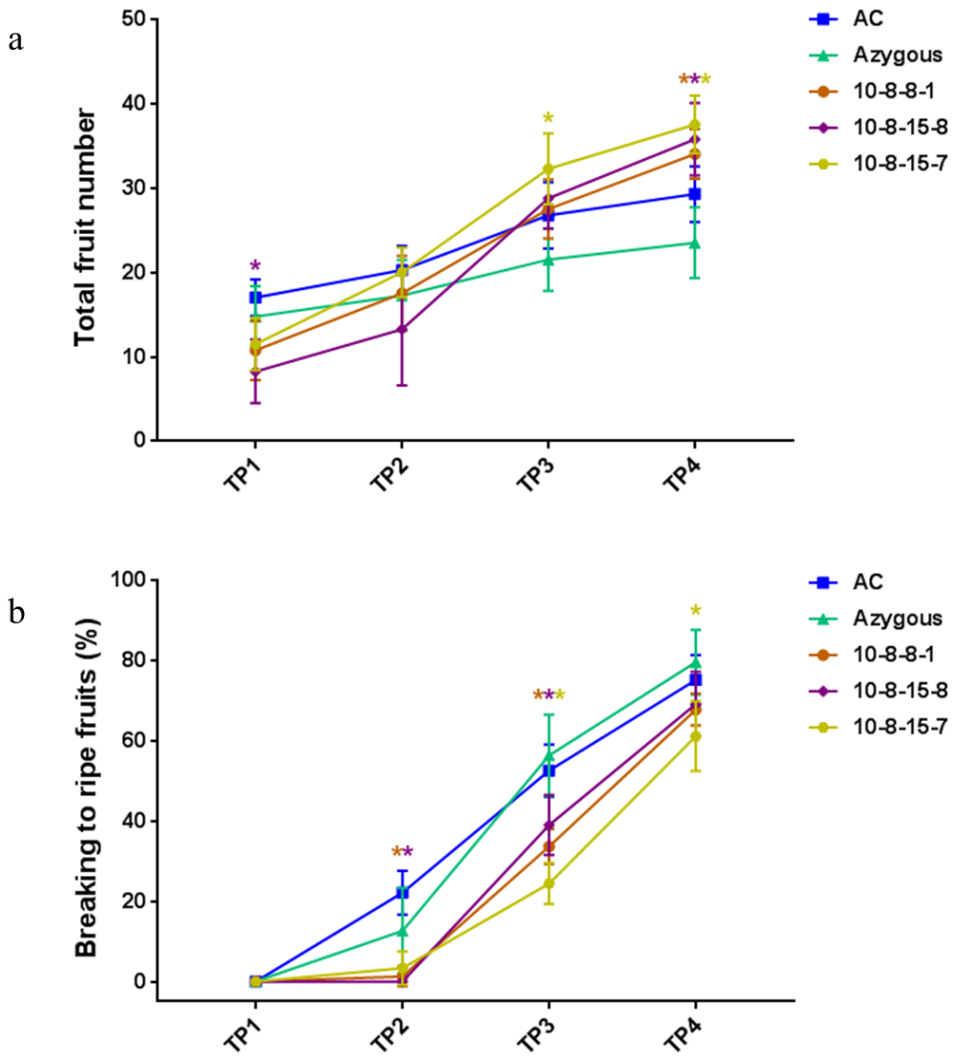

Figure 3-26 Monitoring fruit development and ripening through several time points.

Both the total fruit number (a) and percentage that had reached or surpassed breaker stage (b) were recorded at several time points during development. The time point one (TP1) represents when the first AC line yielded a ripe fruit. Fourteen days separate each subsequent time point until the final time point (TP4), which was recorded once the majority of fruit were red ripe. Four plants per genotype ensured that four separate biological replicates were used for the analysis. Statistical determinations are shown as mean ± SD values, Dunnett's test analysis illustrates statistically significant differences (denoted $P < 0.05$) from the non-transgenic controls.

3.3 Discussion

The zinc finger protein was predicted to be *INDETERMINATE DOMAIN 2* (*IDD2*), where IDD proteins have been demonstrated to have roles in gibberellin signalling. Feurtado et al., (2011) was first to demonstrate that an IDD protein, AtIDD1, could interact with DELLA proteins, a key negative regulator of GA signalling, repressing the expression of GA biosynthesis and signalling genes. Later it was proposed that DELLA acts as a transcriptional coactivator through the IDD proteins (Yoshida et al., 2014). IDD family proteins were shown to serve as transcriptional scaffolds, enabling DELLA that lacks a DNA-binding domain, to mediate between DELLAs and the promoter sequence of the downstream genes and regulate gene expression. Through a co-regulator exchange system: DELLA/IDD promotes the expression of the GA-positive regulator *SCARECROW-LIKE 3* (*SCL3*), whilst SLC3 could supress its own expression by the formation of SCL3/IDD inhibiting gibberellin signalling. Various members of IDD proteins have been shown to control flowering time, including acting as a master switch from vegetative to floral development in rice (Colasanti et al., 1998; Wu et al., 2008; Seo et al., 2011a; Deng et al., 2017). Other functions include leaf development, organ morphogenesis, gravitropism, root development and patterning, sucrose metabolism as well as responses to cold stimulus, most established in *Arabidopsis* (Cui et al., 2013; Wu et al., 2013; Dou et al., 2016; Jost et al., 2016). More specifically, IDD2 in rice was shown to control secondary cell wall formation (Huang et al., 2017). Therefore, it was important to determine whether altered gibberellin synthesis or signalling, and the delicate interplay between plant phytohormones were disrupted by the *ZINC FINGER PROTEIN INDETERMINATE DOMAIN 2* (*ZFPIDD2*) down-regulation. As this could explain the broad nonspecific effects exhibited in transgenic lines.

3.3.1 Altered gibberellin and abscisic acid content in developing fruits provides a potential mechanism for fruit size and yield improvements

Potential increases to both fruit size and total fruit yield were seen across all generations studied. The identification of azygous lines revealed further improvement, with a 72% increase in fruit yield, contributed by elevated fruit size up to 29%. Importantly, the same phenotype was recorded in down-regulated lines (Figure 3-25). Selection of the

most improved lines, whereby yield was a key parameter studied, resulted in more consistent yield increases as shown in the T_3 generation (Figure 3-10 & 3-25). Potentially yield phenotypes could display dose dependency, whereby less significantly down-regulated lines, 10-8-15-7 and 10-8-15-8, produce larger fruits and provide a greater total fruit output compared to 10-8-8-1, the most down-regulated line. This could explain why some transgenic lines within the T_1 and T_2 generation had a reduction to fruit yield, and through selection this trait was removed from the population.

Fruit yield has proven to be the most important breeding trait in tomato, significantly the importance of phytohormone control to both fruit set and size through the delicate regulation of genes has been demonstrated (Ariizumi et al., 2013). Gibberellins (GAs) have been shown to be the key hormones that control fruit set and growth (Groot et al., 1987; Serrani et al., 2007b; de Jong et al., 2009a; Ariizumi et al., 2013; Chen et al., 2016). Their accumulation peaks coincide with both cell division and cell expansion phases in tomato, further highlighting roles in early development (Srivastava and Handa, 2005). From the many forms of GA present, only GA_1, GA_4, GA_3 and GA_7 are biologically active, with GA_1 and GA_4 acting as the predominant bioactive forms in various plant species including tomato.

The phytohormone LC-MS analysis enabled the quantification of multiple GA forms, including the bioactive GA_1 and GA_4, and some precursors. GA biosynthesis is a well elucidated pathway (Figure 3-27), that stems from the formation of trans-geranylgeranyl diphosphate (GGPP). GGPP is converted to *ent*-kaurene by the action of two cyclases: ENT-DIPHOSPHATE SYNTHASE (CPS) and ENT-KAURENE SYNTHASE (KS). Then *ent*- kaurene is then metabolised by the action of P450-dependent monooxygenases to GA_{12} and/or GA_{53}. These precursors are then converted via several intermediate forms to the bioactive GA_1 and GA_4 by GA20-oxidases and GA3-oxidases, acting consecutively through two parallel pathways: the non-13-hydroxylation pathway (leading to GA_4) and the early-13-hydroxylation pathway (leading to GA_1). The analysis was able to identify GA_4 and GA_9 from the non-13-hydroxylation pathway. The precursors GA_{19} and GA_{20}, in addition to the bioactive GA_1 were quantified from the early-13-hydroxylation pathway. Active GAs and their precursors can be inactivated by GA2-oxidases, introducing a hydroxyl at the 2β position; none of these forms were identified or quantified in the phytohormone screen.

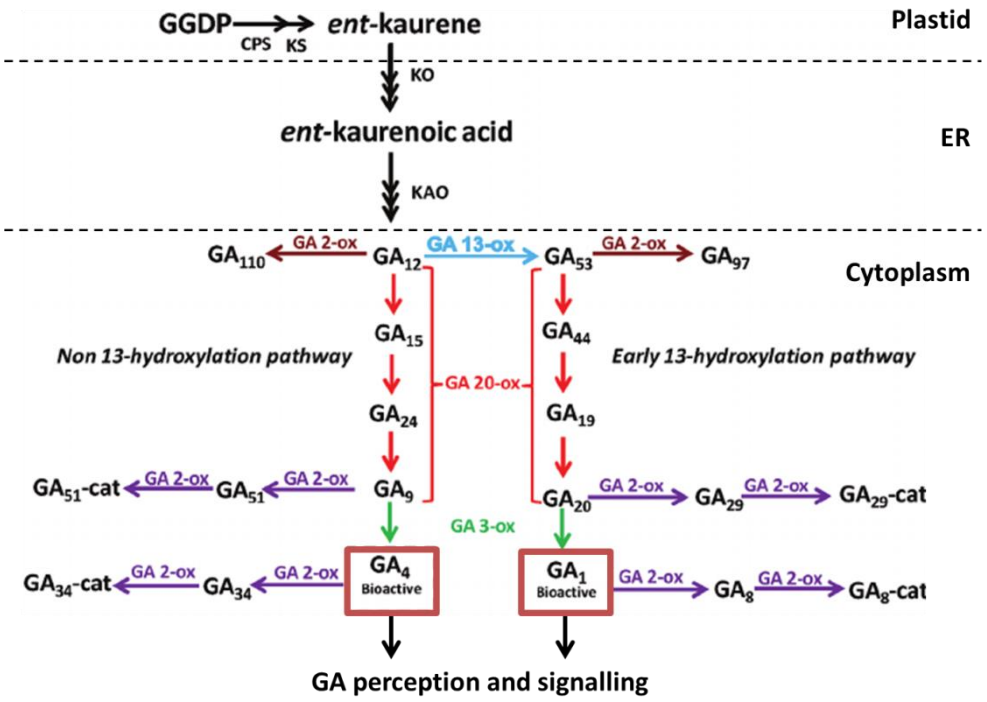

Figure 3-27 Gibberellin biosynthesis pathway resulting in the formation of the bioactive GA forms in tomato. Adapted from Martínez-Bello et al., (2015).

Gibberellin biosynthesis pathway, including both GA activation and inactivation. GGDP, geranylgeranyl diphosphate; CPS, ENT-COPALYL DIPHOSPHATE SYNTHASE; KS, ENT-KAURENE SYNTHASE; KO, ENT-KAURENE OXIDASE; KAO, ENT-KAURENOIC ACID OXIDASE; GA13ox, GA 13-oxidase; GA20ox, GA 20-oxidase; GA3ox, GA 3-oxidase; GA2ox, GA 2-oxidase; GA-cat, GA-catabolite. Adapted from Martínez-Bello et al., (2015).

Interestingly, GA_1 could only be detected in transgenic lines, and was shown previously by inhibitor studies to be the active GA form for tomato fruit growth (Serrani et al., 2007b; Zhang et al., 2007). The LAB 198999 GA inhibitor was used, an acylcyclohexanedione derivative that inhibits 2-oxoglutarate-dependent dioxygenases (Santes and Garcia-Martinez, 1995; Serrani et al., 2007b). The inhibitor reduced both fruit growth and GA_1 content by 50%, whilst accumulating GA_1 precursors: GA_{53}, GA_{44}, GA_{19}, and GA_{20}. These and later results proved GA_1 was the main active GA in developing fruits, and that its precursors only become active upon conversion to GA_1 (Chen et al., 2016). GA_1 was below the level of quantification for both azygous and AC controls (Table 3-2), consequently the fruit size increases seen cannot be directly correlated to GA_1 as seen in Serrani et al., 2007. Nevertheless, the increased GA_1 content remains an important candidate for the larger fruit produced by *ZFPIDD2* down-

regulated lines. Interestingly, the quantified levels in this study were similar to *PSY-1* antisense lines (Fraser et al., 1995), which redirects GGPP from the carotenoid to gibberellin biosynthesis pathway (Fray et al., 1995).

The other bioactive form, GA_4, was demonstrated to be involved in tomato seed germination and fruit development (Serrani et al., 2007b; Nakaune et al., 2012). However, the 13-hydroxylation pathway has been shown to be the primary GA pathway in the growing ovary of developing fruits, demonstrated by relatively low levels of metabolites of the GA_4 biosynthetic pathway in these tissues, suggesting that GA_4 may have a less prominent role in fruit growth post pollination compared to GA_1 (Bohner et al., 1988; Koshioka et al., 1994; Fos et al., 2000; de Jong et al., 2009a). Despite this, potential fruit development functions were shown through treating unpollinated ovaries with GA_4, increasing fruit weight (Serrani et al., 2007b). Furthermore, GA_4 was shown to influence fruit yield through increasing the number of fruits produced, without affecting fruit weight (Garcia-Hurtado et al., 2012). Therefore, GA_4 seems to uncouple the normal mechanism whereby increased fruit number is accompanied by a reduction to average fruit size. The yield-related phenotypes matched the differences seen in the phytohormone screen (Table 3-2). Transgenic lines had both increased number of fruits and a higher GA_4 content (above limit of quantification) compared to the azygous controls. While no consistent differences between transgenic and AC control lines for fruit number and GA_4 levels could be identified. The results, like Garcia-Hurtado et al., (2012), suggest that elevated GA_4 content can increase fruit set and improve total fruit output and yield, without compensating for fruit size. Furthermore, Garcia-Hurtado et al., (2012) identified the above phenotypes in *GA20ox* overexpressing lines, which led to a greater relative flux through the non-13-hydroxylation pathway. This was correlated to improved sink strength, through the enhancement of leaf photosynthetic capacity resulting in greater sugar flux to the reproductive tissues, that was previously demonstrated in citrus fruits (Huerta et al., 2008; Garcia-Hurtado et al., 2012).

Fruit set appears to be trigged by auxin which enhances GA biosynthesis and limits GA inactivation (Serrani et al., 2008; de Jong et al., 2009a). GA's control of tomato fruit set has been shown through GA application and inhibitor studies, along with quantification of GA and transcript abundance of GA biosynthesis genes. GA content increases in the ovary upon pollination and in parthenocarpic mutants, which has been correlated with the upregulation of multiple *SlGA20ox* genes, but not with *SlGA3ox* and *SlGA2ox*. Exogenous treatment with GAs reversed this effect, in addition to improving fruit set

(Serrani et al., 2007b).The intracellular concentrations of the active GA forms are controlled by the transcription alteration of GA biosynthesis (GA20ox and/or GA3ox) and inactivation enzymes (GA2ox, GA epoxidases, and GA methyltransferases). Therefore, the quantification of GAs upstream of the bioactive GAs was important to determine the potential mechanisms involved in the GA_1 and GA_4 increases. Consistent with literature, the reductions to GA_{19} and GA_{20} levels identified in *ZFPIDD2* transgenic lines were similar to untreated LAB 198999 GA inhibitor fruits, while the elevated levels of these GAs in control genotypes were similar to treated fruits with the GA inhibitor (Serrani et al., 2007b). Multiple decreases to GA_1 precursor levels suggested transgenic lines exhibit increased flux through the early-13-hydroxylation pathway, especially as GA20ox is considered to be the rate limiting step for GA_1 biosynthesis (Serrani et al., 2007b). Compared to azygous lines and despite not being significant, a 1.6-fold reduction to the average GA_{19} levels was seen. This pointed towards elevated GA20ox activity, increasing the rate of conversion to GA_{20}. Undetected reduced flux further upstream of GA20ox could also be another possibility resulting in the observed decrease to GA_{19}. However, with GA20ox suggested to be the rate limiting step for increased GA_1, this seems unlikely. Increased GA20ox activity was demonstrated by unchanged GA_{20} levels, whereby less GA_{19} yields the same amount of GA_{20}. Flux increases continue, suggesting elevated GA3ox activity with the rise in GA_1 content.

Meanwhile, more consistent differences could be detected between AC and transgenic lines, with both GA_{19} and GA_{20} being reduced 2.7- and 2.0-fold, respectively, with the latter proving to be significant. The results again suggest increased flux through the GA20ox and GA3ox-mediated sections of the early-13-hydroxylation pathway. The consistent fold change reductions to GA_{19} and GA_{20} content in transgenic lines, could imply that GA20ox activity remains comparable to controls downstream of GA_{19}, until elevated GA3ox activity results in significantly greater GA_1 content. Therefore, GA3ox appears to be the bottleneck for GA_1 biosynthesis in AC controls. Literature provides further evidence for this mechanism, whereby *GA20ox* overexpression can divert GA metabolism from the early-13-hydroxylation pathway more to the non-13-hydroxylation pathway, leading to enhanced GA_4 synthesis (Garcia-Hurtado et al., 2012). Therefore, the unchanged *GA20ox* expression predicted, can explain why no change to GA_4 content could be identified between transgenic and wild type varieties.

Overall, it can be predicted that transgenic lines exhibit elevated GA20ox and GA3ox in comparison to azygous controls, explaining the increased GA_1 content. This is

demonstrated by consistent flux increases throughout the pathway as there is less GA_{19} in transgenic fruits, similar GA_{20} and elevated GA_1. Furthermore, Garcia-Hurtado et al., (2012) positively correlated increased *GA20ox* expression with increased GA_4 content and fruit number. Thus, the predicted increase to *GA20ox* expression in transgenic lines can explain the elevated GA_4 content and the number of fruits produced, when compared to azygous lines. Furthermore, increased flux through GA3ox, indicate that increased GA3ox activity is catalysing the elevated GA_1 content in transgenic fruits. Whereas, GA3ox alone is predicted to be main candidate for elevated GA_1 content in transgenic lines compared to AC controls. AC fruits contain more GA_{19} and GA_{20} but less GA_1, indicating a bottleneck at GA3ox rather than GA20ox. Without changes to *GA20ox* expression, there would be no diversion to/from the early-13-hydroxylation pathway to the non-13-hydroxylation pathway. This can explain why no significant differences to GA_4 content and fruit number were identified in transgenic lines compared to AC controls.

Lastly, the rise to both GA_1 and GA_4 could also be due in part to reduced *GA2ox* expression resulting in less inactivation. Previous literature has demonstrated that increased expression of the fruit specific *GA2ox*, with highest expression in immature fruits, is correlated to reduced bioactive GA and fruit weight (Chen et al., 2016). The LC-MS analysis could not identify GA_8 or other hormones further downstream, thus potential differences concerning the inactivating role of GA2ox in transgenic lines needs further investigation.

Interestingly, ABA was significantly reduced in transgenic lines, 1.3- and 1.2-fold to azygous and AC controls, respectively. Similar to GA, the levels of ABA were in accordance with Fraser et al., (1995). Through inhibition studies utilising the *notabilis*, *flacca* mutants, and the combined *notabilis*/*flacca* (*not/flc*) double mutant, ABA was shown to correlate to fruit weight (Nitsch et al., 2012). ABA deficient mutants yielded significantly smaller fruits, all parts of mature fruits were reduced including the pericarp, locule and placenta. The smaller fruits were associated to a reduced cell expansion in pericarp tissues and not cell division. The result was consistent with previous findings, where a rise in ABA can be detected at the beginning of the cell expansion phase, peaking around the middle (Sjut and Bangerth, 1982). The reduction to fruit size in ABA-deficient mutants is hypothesised to be due to water loss, through elevated transpiration (Ariizumi et al., 2013). Other studies have suggested that ABA stimulates phloem unloading in placenta tissues, thus increasing sink activity in both pericarp and

locule during the high growth rate phase of tomato development (Kojima, 2005; Nitsch et al., 2012). The ABA-deficient double mutant also exhibited higher steady state ethylene emissions in tomato tissues, demonstrating an antagonistic relationship between ABA and ethylene. Furthermore, the increases to ethylene emissions in developing fruit from mutant lines, suggest that ABA has an ethylene-independent effect on growth or ethylene sensitivity (Nitsch et al., 2012). Also, no change to auxin was observed, which has been shown to be a key regulator for fruit set and cell expansion in tomato (Ariizumi et al., 2013).

With all evidence pointing towards ABA promoting cell expansion and tomato growth, reduced ABA in *ZFPIDD2* down-regulated lines contradicts the larger fruit phenotype witnessed. The results suggest that reduced ABA is not the dominant factor for the differences in fruit weight. One explanation is the dose dependent effects of ABA-deficiency, whereby the reduction in ABA needs to surpass a threshold level before expected characteristics are displayed. This was demonstrated by Nitsch et al., 2012, where the single *not* mutant had reduced ABA, but no change to fruit weight was recorded. Only the double mutant with a more severe ABA-deficiency had a reduction to fruit size. Another explanation for the reduced ABA in transgenic lines could be delayed synthesis. Where normal or potentially elevated ABA levels, which peak later, result in no reduction to cell expansion and fruit weight.

Finally, another zinc finger protein, *SlZFP2*, was shown to regulate both ABA and tomato ripening (Weng et al., 2015a; Weng et al., 2015b). *SlZFP2* has been characterised as a negative regulator of ABA biosynthesis. Altered *SlZFP2* expression resulted in an extended development time to the onset of ripening, between 5-7 days. Interestingly, silencing accelerated ripening but this was not governed by altered ABA biosynthesis. With the zinc finger protein from our study (*ZFPIDD2*) displaying similar phenotypes, it highlights the importance of zinc finger proteins in the phytohormonal control of both development and the onset of ripening, while showing the potential to accelerate colour development.

The phytohormone screen predicts that *ZFPIDD2* is a negative regulator of GA synthesis and signalling, thus down-regulation promotes GA responses. The increased GA_4 can explain the improved fruit number and set of transgenic lines compared to non-transgenic controls. While the elevated GA_1 and reduced ABA in transgenic lines suggest that the fruit growth phases have been extended. The phytohormone profile of transgenic lines compared to both controls suggests that fruits were harvested at an

earlier time point of development, despite being harvested at the same time point post anthesis (Figure 3-28 and Table 3-2). Either increased GA levels or a prolonged GA phase result in greater bioactive GA exposure, promoting increased cell division or expansion. This is demonstrated by increased GA_1, that is likely to confer increased fruit size in down-regulated lines, contributing to improved fruit biomass output. Due to the antagonistic relationship between GA and ABA, the extension to the GA phase is expected to delay the onset of ABA production, explaining the reduction to ABA levels in transgenic fruit (Sun and Gubler, 2004; Zhang et al., 2007; Martin-Rodriguez et al., 2016). The positive correlation between ABA levels and fruit weight detailed in literature, and the opposite being true in transgenic lines, provide further evidence that ABA is more likely to be delayed rather than decreased. The postponement to ABA synthesis and signalling is predicted to delay the onset of ethylene production and ripening, as demonstrated by the extended developmental time to ripening in transgenic lines (Figure3-2a and Figure 3-26). Microscopy based approaches could be used to determine whether altered cell number or size are contributing to the yield improvements.

Previous work comparing two Late-maturing Japanese pear cultivars identified a similar mechanism that altered fruit size (Zhang et al., 2007). The Atago cultivar yielded fruits up to four times the weight of Shinkou. Atago produced fruit had an extended period of rapid cell division, resulting in increased cell numbers. Increases to bioactive GA_1, GA_3 and GA_4 were associated with the rapid cell division phenotype of the larger Atago fruits. Whereas, increases to GA_3 and GA_4 were linked with increased sink strength and carbon partitioning influencing cell expansion between the two cultivars. While a higher ABA level during the early period of fruit growth was correlated to reduced cell division in the Shinkou cultivar, suggesting ABA exerts antagonistic effects on GA-regulated processes. With both GA and ABA sharing the common precursor, GGPP, altered flux downstream controls the shift between both GA and ABA. Therefore, the growth differences between the different pear cultivars, as well as *ZFPIDD2* down-regulated lines with both controls in this project, can be explained by a switch in the flux downstream of GGPP. The mechanisms described by Zhang et al., 2007, are very similar to the proposed hypothesis predicting why *ZFPIDD2* down-regulated tomato lines have improved fruit size. Both centre on combined increases to GA_1 and altered ABA in fruit growth phases that promotes cell division for an extended period.

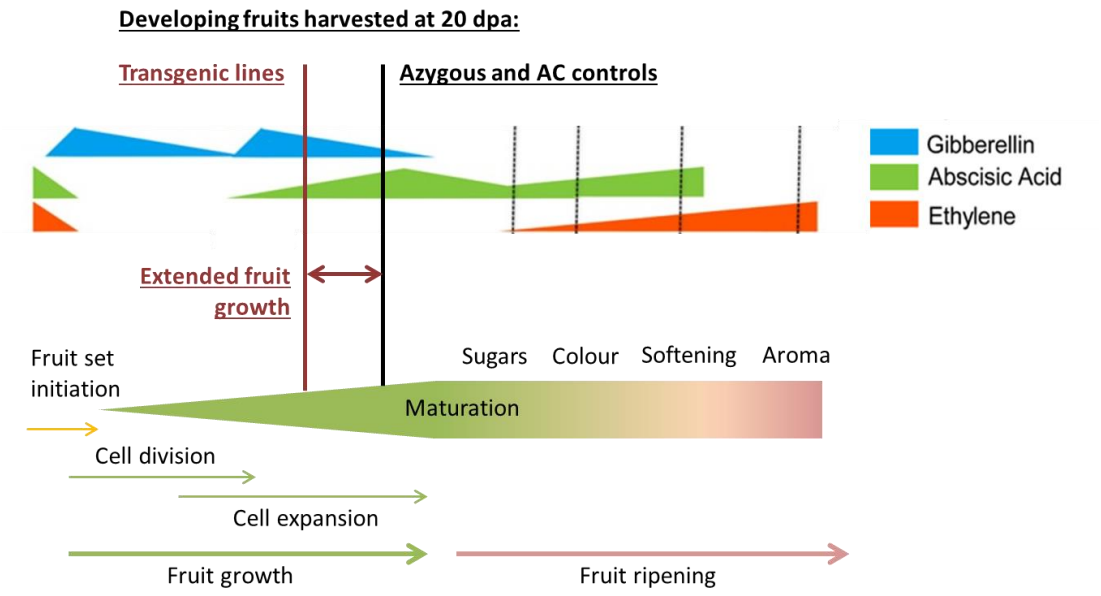

Figure 3-28 Altered phytohormone profiles underlying the yield improvements of transgenic lines.

The proposed mechanism for the improved fruit yield of transgenic lines involves elevated gibberellin exposure combined with a delayed peak of abscisic acid content, determined by LC-MS analysis described in section 2.3.6. The phytohormone profiles of transgenic lines indicated an extended fruit growth phase and that fruits were harvested earlier in development, despite being collected at the same time point (20 days post anthesis) as both azygous and AC controls. Prolonged growth phase can explain increased fruit size and extended developmental time, potentially due to delayed onset of ethylene production. Adapted from McAtee et al., (2013).

3.3.2 Increased auxin and cis-zeatin riboside are partly responsible for altered ripening-related phenotypes of down-regulated lines

Turning fruits harvested at four days post breaker were analysed in the phytohormone screen, to ascertain whether any changes to ripening-related hormones, with the exception of ethylene, were potentially affecting the altered ripening pattern of fruits from transgenic lines. Indoleacetic acid (IAA) was elevated 1.4- and 1.5-fold in transgenic lines compared to azygous and AC controls, respectively. Further increases were identified to cis-zeatin riboside (c-ZR) and ABA compared to AC controls. The levels of these hormones in turning fruits were in accordance with literature (Buta and Spaulding, 1994; Fraser et al., 1995; Pattison and Catalá, 2012; Breitel et al., 2016; Kumar et al., 2017; Sravankumar et al., 2018).

IAA has been demonstrated to modulate tomato fruit ripening, but the mechanism to achieve this is not well established (Srivastava and Handa, 2005; Seymour et al., 2013a; Seymour et al., 2013b). Treatment studies indicate that IAA application delays fruit ripening (Vendrell, 1985; Cohen, 1996; Giovannoni, 2007; Su et al., 2015; Li et al., 2016b). Fruits treated with IAA were shown to transition from green to red slower, with delayed and reduced ethylene synthesis and have a slower rate of fruit softening (Su et al., 2015; Li et al., 2016b). Transcriptome analysis from Li et al., (2016) confirmed significant crosstalk between auxin and ethylene during tomato ripening, that also has been demonstrated in other climacteric fruits (Trainotti et al., 2007). Auxin was shown to maintain system 1 ethylene synthesis; whilst numerous genes predicted to play important roles in the transition to system 2, and the ethylene synthesis and signalling genes associated to the system 2 are suppressed (Li et al., 2016b). Thus, the transition from the auto-inhibitory system 1 in non-ripening fruits, to the autocatalytic system 2 associated with the burst of ethylene in ripening fruits, being significantly delayed (Li et al., 2016b).

Recently, it has been demonstrated that IAA delayed fruit colour transition by reducing both lycopene accumulation and the decrease of chlorophyll *a*, whilst displaying elevated β-xanthophyll biosynthesis (Su et al., 2015). Expression analysis revealed significant changes to genes involved in carotenoid metabolism, where the majority of genes upstream of lycopene were down-regulated by auxin (Su et al., 2015; Li et al., 2016b). The most significant of which being *PHYTOENE SYNTHASE 1* (*PSY-1*), the rate-limiting enzyme for carotenoid biosynthesis (Fraser et al., 2002). Furthermore, two genes encoding *LYCOPENE β-CYCLASE* (*LYC-β*) and single genes encoding *ZEAXANTHIN EPOXIDASE* (*ZEP-1*) and *ABA4* were upregulated, promoting the elevated β-carotene, neoxanthin and violaxanthin synthesis (Su et al., 2015; Li et al., 2016b). Observation of carotenoid analysis from *ZFPIDD2* down-regulation shows the opposite trend, with significant increases to phytoene, phytofluene, ζ-carotene, neurosporene and lycopene. Whereas, the differences in carotenoid levels post lycopene display only modest fold changes. Therefore, the biosynthesis genes upstream of lycopene are expected to be upregulated in transgenic lines, with decreases expected downstream. The results imply that the elevated auxin observed can only be restraining the increases to carotenoid content, or the increases to auxin are not high enough to induce an effect. Su et al., (2015) also studied the application effects of an ethylene precursor (ACC, 1-aminocyclopropane-1-carboxylic acid), combined IAA and ACC, and an auxin antagonist (PCIB). Comparison between Su et al., (2015) and our carotenoid

analysis showed that *ZFPIDD2* down-regulated lines exhibit a similar carotenoid profile to both ACC and PCIB treated fruits. Consequently, the results predict increased ethylene in down-regulated lines, with ethylene taking the predominant role in pigment accumulation over the increased auxin seen.

The exact mechanism controlling the transition from system 1 to system 2 ethylene upon the onset of ripening remains unknown (Barry and Giovannoni, 2007; Cara and Giovannoni, 2008). Evidence for system 1 involvement in the transition phase is supported by the observation that ethylene treatment only shortens the time until system 2, but does not immediately induce autocatalytic ethylene production. This implies that a threshold of ethylene content, or increased ethylene sensitivity, is required to induce system 2 and ripening (Barry et al., 2000; Klee, 2004). Therefore, it could be speculated that the increased auxin present, which originates from elevated auxin in mature green fruits, provides a stronger autocatalytic system 2 response. This could explain the elevated ethylene response expected in transgenic fruits, conferring increased fruit ripening-related pigmentation that shares similarities with ACC treatment.

Both auxin and multiple AUXIN RESPONSE FACTORS (ARFs) involved in auxin signalling have been reported to alter fruit softening in tomato (Jones et al., 2002; Guillon et al., 2008; Breitel et al., 2016; Li et al., 2016b; Sravankumar et al., 2018). Specifically, Li et al., (2016) proved that the application of auxin was shown to down-regulate multiple genes involved in cell wall degradation, delaying the softening process in tomato. Multiple *POLYGALACTURONASE* (*PG*), *PECTINESTERASE* (*PME*), *β-XYLOSIDASE, PECTATE LYASE* (*PL*) and *EXPANSIN* (*EXP*) genes have been shown to play crucial roles in cell wall degradation and were down-regulated. Additionally, auxin treatment seemed to induce a greater softening response, with larger fold reductions to softening-related gene expression compared to carotenoid biosynthesis genes. This could help explain why elevated auxin in *ZFPIDD2* down-regulated lines failed to inhibit carotenoid synthesis, but delayed softening. Therefore, auxin is expected to play an important role in the partially uncoupled ripening phenotypes of transgenic fruits. The levels of IAA in transgenic lines (Table 3-2) were similar to those reported in Sravankumar et al., (2018); who correlated increased auxin levels found in the IAA-amido synthetase *GRETCHEN-HAGEN 3-2* (*SlGH3-2*) RNAi lines to reduced fruit softening and extended shelf-life. Also, Li et al., (2016b) revealed that *ZFPIDD2* expression was suppressed by auxin, with a significant reduction to transcript levels seven days post treatment. Combined with our findings, an antagonistic relationship

between the *ZFPIDD2* and auxin can be predicted, explaining why increased auxin was seen in down-regulated lines.

The phytohormone screen can also help explain the ripening-related differences between azygous and AC controls. Phenotypic differences were unexpected; especially as *ZFPIDD2* transcript levels were unchanged between both controls, whilst regular PCR was able confirm no insertion of the transgene. Interestingly, transgenic and azygous lines had significantly more ABA in comparison with AC controls. ABA has been shown to trigger and accelerate climacteric fruit ripening (Zhang et al., 2009a; Zhang et al., 2009b; Sun et al., 2012c; Zaharah et al., 2013; Mou et al., 2016). Separately treating fruits with ABA and an ABA inhibitor (NDGA; Nordihydroguaiaretic acid) prior to the onset of ripening was able to identify ABA's specific role in tomato ripening (Mou et al., 2016). ABA was shown to facilitate ethylene production through the regulation of multiple ripening-related transcription factors, *MADS-RIN*, *TAGL1*, *CNR* and *NOR*, all previously shown to control ethylene action. For transgenic and azygous lines, the phytohormone screen (Table 3-2) showed that ABA was increased on average 2.2-fold in comparison to AC controls, whilst lycopene and total carotenoid contents were increased 2.7- and 1.9-fold, respectively. Furthermore, the colourimeter analysis demonstrated that transgenic and azygous lines transitioned quicker from green to red compared to AC controls. Thus, the altered ripening-associated colour development can be attributed to the changes to ABA content, in accordance with literature (Wang et al., 2007; Zhang et al., 2009b; Sun et al., 2012b; Barickman et al., 2014).

Additionally, ABA can alter fruit softening by directly participating in cell wall catabolism through regulation of gene expression (Zhang et al., 2009b; Sun et al., 2012a). ABA treatment and inhibitor studies revealed that reduced ABA levels delayed softening. Transgenic lines displayed a reduced rate of softening compared to both controls, despite only AC lines having a significant difference to ABA content in turning fruits. The results suggest that other phytohormones and/or altered softening-related gene expression is the predominant mechanism for the reduced fruit softening of down-regulated lines. Transgenic fruits harvested for the hormone analysis proved to be firmer in comparison to AC controls, supporting the conclusion that ABA accumulation in turning fruits is not closely related to softening.

Overall, transcriptome analysis of fruit with ABA and NDGA treatments found only a small change in *ZFPIDD2* expression (Mou et al., 2016). Likewise, ABA levels in down-regulated lines remained unchanged when compared to the true, non-transgenic

azygous controls. Taken together, both results imply that the *ZFPIDD2* does not play an important role in ABA synthesis, and most likely differences between azygous and transgenic lines are due to another phytohormonal or transcriptional mechanism. However, ABA can explain the increased carotenoid accumulation of both azygous and transgenic lines compared to AC controls.

3.3.3 Elevated cytokinin content in both leaf and fruit tissues in down-regulated lines could provide improved sink strength and sugar accumulation potential

Cytokinins (CKs) have been shown to be important regulators for multiple aspects plant growth and development that include: lateral root formation, apical dominance, cell division, stress tolerance, nutritional signalling and leaf senescence (Sakakibara, 2006; Argueso et al., 2009; Shani et al., 2010; Ghanem et al., 2011; Matsuo et al., 2012; Gupta et al., 2013; Schafer et al., 2015). Recently, the involvement of phytohormones including CKs in controlling sink strength has been revealed. Source–sink balance regulates carbon status in plants by controlling carbohydrate content (Osorio et al., 2014). It defines the sugar production and export from photosynthesising leaves to non-photosynthetic tissues, which is intimately connected to plant growth, providing energy for metabolism and maintenance of biomass. The combined increases to fruit yield and non-vegetative biomass, as well as elevated carbon flux through metabolism resulting in increased isoprenoid biosynthesis, suggest that transgenic lines have improved to sink strength during development and ripening.

The phytohormone screen identified differences to auxin and CK levels in source and sink tissues, specifically in leaf and turning fruits. The levels identified in ripening fruits were consistent with those reported in literature (Breitel et al., 2016). Both phytohormones have been shown to regulate carbohydrate metabolism and sink activity (Roitsch and Gonzalez, 2004; Sagar et al., 2013; Albacete et al., 2014; Bianchetti et al., 2017). Specifically, CKs have been positively associated with elevated sink strength by promoting invertase activity and sugar accumulation (Albacete et al., 2014; Bianchetti et al., 2017). While, sucrose-cleaving enzymes were promoted by auxin treatment (Tang et al., 2015). In developing fruits both hormones were demonstrated to induce the carbohydrate metabolism-related enzymes: CELL-WALL INVERTASES (LINs), SUCROSE TRANSPORT PROTEINS (SUTs) and ADP-GLUCOSE

PYROPHOSPHORYLASES (AGPases). These contribute to sink activity and fruit growth rates (Baxter et al., 2005; Zanor et al., 2009; Albacete et al., 2014; Bianchetti et al., 2017). Moreover, both hormones have functions in chloroplast biogenesis and differentiation in vegetative and reproductive tissues (Sagar et al., 2013; Cortleven and Schmulling, 2015; Bianchetti et al., 2017). A reduction in activity of both hormones was correlated with reduced chloroplast number and chlorophyll (Bianchetti et al., 2017). The same study demonstrated that inhibition to both auxin and CK induced a reduction to photosynthesis and sugar import, reducing sink strength and starch accumulation (Bianchetti et al., 2017). A consequence was the delay to the onset of ripening, ethylene synthesis and carotenoid accumulation. The ethylene precursor ACC and ethylene emissions were delayed, while both ACC OXIDASE (ACO) and ethylene signalling were delayed and reduced.

If both auxin and CKs have similar functions on photosynthetic tissues from leaves, as they do with fruit, the elevation to these phytohormones in down-regulated lines may be contributing to the darker leaf phenotype, by inducing plastid biogenesis and chlorophyll levels. It has been established that CK application can mimic the *det* mutant phenotype, while cytokinin-hypersensitive gene responses have been correlated to elevated cell proliferation and chloroplast development, yielding increases to chlorophyll levels (Fletcher and McCullagh, 1971; Mustilli et al., 1999; Kubo and Kakimoto, 2000; Zubo et al., 2008). Thus, establishing a link between CKs and photomorphogenic signal transduction that controls plastid compartment size (Cookson et al., 2003). Combined vegetative biomass and chlorophyll increases would confer a greater photosynthetic potential, enabling increased starch biosynthesis. This could be enhanced by the upregulation of AGPase enzymes, that represents a limiting step for starch biosynthesis, that are both positively correlated to auxin and CK levels (Petreikov et al., 2009). CKs have been shown to delay leaf senescence that could be the cause of the larger vegetative biomass of transgenic lines, potentially improving carbon assimilation (Ori et al., 1999; Balibrea Lara et al., 2004). Achieving delayed senescence is a strategy adopted by breeders to increase yield (Rossi et al., 2015). Increased CK levels have proven to improve fruit set by enhancing the ovary fruit sink strength resulting in higher total solids in fruits (Martineau et al., 1995; Srivastava and Handa, 2005). Furthermore, cytokinin-overproducing lines display similar developmental related phenotypes to *ZFPIDD2* down-regulated transgenic lines. Increased CKs are associated with short, more branched plant morphology with elevated flower numbers (Li et al., 1992; Sun et al., 2004).

Together both hormones may improve the availability of more sugar for export to fruit, the main sinks in tomato. Improved source to sink ratio can be associated with elevated fruit number and size, thus contributing to the increase in fruit biomass of *ZFPIDD2* down-regulated lines (Ho, 1996; Bertin et al., 2002; Albacete et al., 2014; Osorio et al., 2014). This has been shown across a variety of species, where fruit development and composition largely relies on the size of the photosynthate pool available in leaves, in addition to the sink strength of the fruit. Combined quantitative trait locus (QTL), network, and molecular biology analyses indicated that the major QTLs for both fruit size and sugar composition are genes associated with cell division/number, auxin signalling during development and invertase activity with the ability to convert the imported glucose and sucrose sugars (Frary et al., 2000; Fridman et al., 2004; Cong et al., 2008; Cocaliadis et al., 2014). Furthermore, elevation of leaf photosynthesis has been shown to provide a proportional increase to fruit yield. These results indicate that elevated sink strength combined with improved leaf photosynthesis is likely to play a prominent role in the yield increases, and both auxin and CKs are likely candidates initiating these phenotypes. Elevation to these hormones levels can explain the increased source supply and activity necessary to meet the developmental sink demands. Furthermore, both CKs and GAs are known to be regulated by KNOTTED-LIKE HOMEOBOX (KNOX) proteins, which directly repress transcription of genes encoding GA 20-oxidases (Ori et al., 1999). This could provide a link between the altered GA synthesis and signalling, and CK content during development.

Differences to both auxin and CKs (c-ZR and t-ZR) were also recorded in turning fruits. Like auxin, zeatin-ribosides have been linked with the inhibition of tomato fruit ripening, especially as CK levels were shown to decrease during ripening (Varga and Bruinsma, 1974; Davey and Van Staden, 1978; Desai and W. Chism, 2006). Recently, c-ZR and other CK members were suspected to be a target of ethylene, auxin and the ABA responsive AUXIN RESPONSE FACTOR 2A (ARF2A), which was shown to positively regulate ripening (Breitel et al., 2016). The c-ZR levels correlated with ARF2A antisense and overexpression lines, suggesting c-ZR has a positive ripening effect, which could be involved in different colour development and softening phenotypes associated with altered ARF2A expression (Breitel et al., 2016). The elevated c-ZR levels were detected in red sections of ripening fruit upon the overexpression of ARF2A; these were in accordance with the levels identified in the phytohromone screen (Table 3-2). This potentially could explain the improved pigmentation of transgenic lines with higher c-ZR levels compared to AC controls. Combined treatment of auxin and CKs were able to

influence the onset of ripening, potentially increasing ethylene activity, again implying a positive role in ripening (Bianchetti et al., 2017). CK was also shown to stimulate ethylene production in *Arabidopsis* seedlings (Cary et al., 1995). Carotenoid and GC-MS profiles of down-regulated ripe fruit revealed a reduction to sugar content, while isoprenoid and the majority of amino acids were increased. The results indicate elevated carbon flux through metabolism and the citric acid cycle. To achieve this transgenic fruits were expected to display elevated source to sink strength. As mentioned earlier, altered phytohormone content, elevated vegetative biomass and the darker leaf phenotype with potentially increased chlorophyll levels were expected to contribute to elevated sugar accumulation. This would enable increased sugar export and phloem unloading into sink tissues. Additionally, both auxin and CKs have been shown to induce greater sink strength by upregulating LINs, SUTs and AGPases, reducing the sugars highlighted by the GC-MS analysis. Together these changes could facilitate increased carbon flux to support the elevated plant metabolism.

Both auxin and CKs are important for both source and sink activity. Fruits are regarded as photosynthate sinks, relying on imported carbon from leaves throughout development and ripening (Lytovchenko et al., 2011; Osorio et al., 2014). With the combined increases to fruit yield, carotenoid, tocopherol and phylloquinone biosynthesis in transgenic lines, an improvement to sink strength during development and ripening is likely. Elevated vegetative biomass of down-regulated lines and darker leaf phenotypes suggest improved photosynthetic potential, which could provide the source supply and activity necessary to meet the developmental sink demands.

Taken together, the elevated CKs in leaves could be contributing to their darker leaf phenotype observed in transgenic lines, by inducing plastid biogenesis and chlorophyll biosynthesis. The potentially elevated photosynthetic potential and upregulation of starch biosynthesis could provide an improvement to the source strength. Also, CKs have been shown to delay leaf senescence that could be the cause of the larger vegetative biomass of transgenic lines, resulting in improved sugar biosynthesis and source strength. Thus the availability of more sugar for export can improve sink strength associated with elevated fruit number and size, contributing to the increased fruit biomass of *ZFPIDD2* down-regulated lines.

3.3.4 Broad metabolism changes influencing the altered ripening in tomato fruits

Fruit ripening is characterised by the accumulation of carbohydrates, which provide the energy required for fruit development and contribute to nutritional quality and flavour. Due to their importance, the main sugars fructose, glucose and sucrose were quantified in an absolute manner. Sucrose is imported into fruits and degradation results in hexose (glucose and fructose) production. Large reductions to sucrose contents were identified in *ZFPIDD2* down-regulated lines, 6.6- and 7.1-fold to azygous and AC controls, respectively. While fructose and glucose remained unchanged. Significant increases to many amino acids and isoprenoids, in addition to total fatty acid content, and no change to fructose and glucose all indicated increased sucrose metabolism in transgenic lines. Sucrose turnover is governed by SUCROSE SYNTHASE (SS) and INVERTASE, the latter catalyses the hydrolysis of sucrose into glucose and fructose, in an irreversible reaction. Interestingly, CKs were elevated in turning fruits, which have been associated with elevated sink strength by upregulating invertase activity. Both metabolite profiling and phytohormone screening predict the upregulation of invertase enzymes, potentially a cytokinin-mediated response, resulting in the significant reduction to sucrose seen. Furthermore, invertase mediated sucrose metabolism, and the resulting hexose accumulation at the point of unloading, can increase the gradient of translocation of sugars from source-to-sink. Consequently, this increases the flux of sucrose from phloem into sink tissues, elevating sugar import (Ho, 1996; Fridman et al., 2004; Koch, 2004; Osorio et al., 2014).

The regulatory role of sugars on photosynthetic activity and plant metabolism has long been established. However, less is known of how sugars affect fruit quality traits and regulate ripening. Large reductions to sucrose are associated to elevated sucrose metabolism rather than reduced sugar import, as lower sucrose content was one of the pivotal factors that resulted in the late-ripening process of a mutant sweet orange (Zhang et al., 2015). Furthermore, sucrose treatment accelerated ripening and enhanced ethylene synthesis in tomato (Li et al., 2016a). Several invertases have been classified into different groups: CELL WALL INVERTASE (CWI), VACUOLAR INVERTASE (VI), and CYTOPLASMIC INVERTASE (CI) or NEUTRAL INVERTASE (NI) forms. CWI activity is tightly linked with fruit sugar levels. VI modulates the sucrose/hexose ratio in fruits, where suppression resulted in sucrose accumulation and hexose reduction, significantly reducing fruit growth (Klann et al., 1996). This highlights the potential

invertase roles contributing to elevated fruit size in *ZFPIDD2* transgenic lines. Recently, RIN was shown to regulate the expression of genes involved in sucrose metabolism, including eleven *INVERTASE* genes, a single *INVERTASE INHIBITOR* gene, six *SUCROSE SYNTHASE* genes, four *SUCROSE PHOSPHATE* genes and six *HEXOKINASE* genes (Qin et al., 2016). Furthermore, RIN binding sites were identified in *VI*, *VIF*, *LIN7*, *LIN8*, *CIF1*, *NI2*, and *NI4* by the presence of CArG-box motifs, implying RIN can directly control sucrose metabolism. The study also demonstrated the involvement of sucrose metabolism genes in ripening, whereby repressing the *VACUOLAR INVERTASE INHIBITOR* (*VIF*) delayed ripening, overexpression accelerated ripening, both by altering lycopene production and ethylene biosynthesis. The results highlight the role of sucrose in promoting fruit ripening and quality, potentially through RIN-mediated ripening regulatory mechanisms. In relation to *ZFPIDD2* down-regulation, the results indicate the elevated sucrose metabolism exhibited in transgenic lines can accelerate tomato ripening. Furthermore, invertase activity was positively associated with fruit size.

Additionally, sugars also function as signalling molecules in many developmental processes. Sugar signalling has been demonstrated to interact with plant hormones including abscisic acid, jasmonate, gibberellins and auxin, the main phytohormones altered in transgenic lines (Heil et al., 2012; Bolouri Moghaddam and Van den Ende, 2013; Liu et al., 2013). Recently, sucrose treatment accelerated ripening, highlighting both its role in ripening and as a signalling molecule (Li et al., 2016a). Interestingly, sucrose treatment resulted in no consistent change to sucrose or hexose degradation products. A contributing factor to this was the differential expression of multiple sucrose biosynthesis and degradation genes. Post treatment, sucrose levels increased in fruits, but were counteracted by significant reductions at the next time point studied, before levelling out. Glucose and fructose levels remained constant throughout. The reduction to sucrose content was correlated to the upregulation of multiple sucrose degradation enzymes. This highlights the probability of increased sucrose degradation enzyme expression in *ZFPIDD2* transgenic lines. Furthermore, it was predicted that sucrose was being used as a signalling molecule, independent of hexose-derived systems. This provides another explanation for the reduced sucrose post treatment, and in *ZFPIDD2* transgenic lines. Li et al., (2016) also supported previous studies that outlined the detrimental developmental effects of sugar limitation (Boyer and McLaughlin, 2006; Liu et al., 2013); while suggesting that sucrose metabolism accelerates ripening by its effects on the expedition of metabolic carbohydrate fluxes, which was shown to be important

for secondary metabolism (Li et al., 2016a). This is in agreement with our hypothesis for *ZFPIDD2* down-regulation, whereby elevated metabolic carbon fluxes enable elevated carotenoid, tocopherol and phylloquinone content. This is further supported by the overexpression of *SUCROSE INVERTASE CWIN1* (*LIN5*), which induced elevated carbohydrate and carbon flux, yielding increases to organic acids, amino acids, shikmate and phenolics (Albacete et al., 2015). Lastly, the sucrose treatment induced ethylene production, via the upregulation of genes involved in the auto-catalytic system of ethylene biosynthesis. This resulted in increased ripening-related colour transition. Multiple ethylene signalling genes were also upregulated. The results from our study suggest a similar mechanism, whereby increased sucrose metabolism could facilitate elevated ethylene biosynthesis, contributing to the increased colour transition and carotenoid content in *ZFPIDD2* down-regulated lines.

Overall, isoprenoid levels were increased in ripe fruit from *ZFPIDD2* down-regulated lines, exhibiting elevated total carotenoid, tocopherol and phylloquinone content (Table 3-3). *ZFPIDD2* down-regulation resulted in significant elevation to carotenoids found upstream of lycopene. Phytoene represents the first committed step in carotenoid biosynthesis, and significant increases were witnessed across the generations studied. Similarly, phytofluene content was improved in transgenic lines when compared to both controls. Relatively minor increases in comparison were detected for ζ-carotene and neurosporene. The most dramatic increases throughout was to lycopene content, with down-regulated lines exhibiting a 50 and 165% increases compared to azygous and AC controls, respectively (Table 3-3). The results display increased flux upstream of lycopene, with PSY-1 being the main candidate. Elevated *PSY-1* would explain the increases to phytoene, as it has been demonstrated to be the main rate-limiting step in the carotenoid pathway (Fraser et al., 2002). *PSY-1* overexpression displayed elevation to carotenoids upstream of lycopene, with significant improvements to phytoene and phytofluene content (Fraser et al., 2007). Differences decreased with ζ-carotene, displaying a nonsignificant increase and lycopene levels remained unchanged. *ZFPIDD2* down-regulated lines displayed similar phenotypes, with much smaller increases seen to ζ-carotene and neurosporene, suggesting *PSY-1* upregulation is likely contributing to elevated carotenoid content upstream of lycopene. Increased phytofluene indicates that *PHYTOENE DESATURASE* (*PDS*) could also be potentially upregulated, or elevated substrate availability for PDS results in increased desaturation, resulting in more phytofluene. The latter seems more likely, as PDS also catalyses the desaturation of phytofluene to ζ-carotene, thus upregulation would likely maintain the fold increases

through to ζ-carotene. However, this is not seen in down-regulated lines and increases to ζ-carotene are relatively small in comparison to phytofluene. Similar phenotypes are displayed when comparing to AC controls, but with larger fold increases to phytoene and phytofluene. The only difference is that neurosporene could only be detected in transgenic lines, and not in AC controls, suggesting upregulation of *ζ-CAROTENE ISOMERASE* (*ZDS*).

Neurosporene production and conversion to pro-lycopene is catalysed ZDS, then CAROTENE ISOMERASE (CRTISO) produces lycopene via an isomerisation reaction. With only small differences to neurosporene, and pro-lycopene remaining undetected, *CRTISO* upregulation can be expected to facilitate the significant elevation to lycopene content, when compared to both controls. Post cyclisation of lycopene, fold increases fall dramatically, indicating lycopene cyclases either are down-regulated or remain unchanged. This bottleneck can explain the reduced ABA seen in AC controls, while no differences were detected between transgenic and azygous lines. Comparison between transgenic and AC lines reveal that the down-regulation of *ZFPIDD2* results in the reduction to β-carotene. The β-pathway, that includes β-carotene, leads to the production of ABA via several intermediates (Liu et al., 2015a). The reduced β-carotene in transgenic lines compared to AC controls suggest increased flux through the β-pathway, resulting in elevated levels of ABA. While no differences to β-carotene or ABA was observed between transgenic and azygous lines, supporting this hypothesis.

As mentioned earlier, rate-limiting steps for carotenoid and lycopene production are catalysed by PSY-1, PDS, ZDS, Z-ISO and CRTISO (Giuliano et al., 1993; Fraser et al., 1994; Fantini et al., 2013). RIN has been shown to directly regulate the expression of *PSY-1*, *Z-ISO*, *CRTISO* (Martel et al., 2011; Fujisawa et al., 2013). Su et al., (2015) studied the application effects of an ethylene precursor (ACC), combined IAA and ACC, and an auxin antagonist (PCIB) on carotenoid biosynthesis enzymes expression and carotenoid content. The most striking difference was ACC and PCIB treated fruits producing significantly more phytoene, phytofluene and lycopene, in addition to δ-, α- and β-carotene. Just *PSY-1* and *ABA4* were upregulated by ACC alone, while *LYC-β1*, *CRTR-β2* and *NCED* were down-regulated. The results imply that increased ethylene could be inducing the expected upregulation of *PSY-1* in *ZFPIDD2* transgenic lines, resulting in elevated phytoene content. Ethylene also upregulated ABA biosynthesis through increased *ABA4* expression, explaining the elevated ABA in both *ZFPIDD2* transgenic and azygous lines compared to AC controls. Furthermore, the reduced

expression of *LYC-β1*, *CRTR-β2* and *NCED* resulted in elevated δ-, α- and β-carotene, and can explain small increases to δ-carotene in our analysis. Overall, the carotenoid profiles of down-regulated *ZFPIDD2* lines indicate elevated ethylene in ripe fruit, as they share many similarities with ACC treatment, most significantly increased phytoene, phytofluene and lycopene content (Su et al., 2015). Interestingly, many of the genes expected to be upregulated in transgenic lines directly correlate to RIN, providing further evidence of ethylene involvement (Su et al., 2015). The increased ethylene could then enhance RIN expression in a positive feedback loop (Fujisawa and Ito, 2013), upregulating the RIN regulated *PSY-1* and *CRTISO* resulting in phytoene and lycopene accumulation.

Interestingly, multiple studies have associated sugars and pigment accumulation in fleshy fruits. In tomato, sucrose limitation was demonstrated to inhibit phytoene and lycopene accumulation, with sucrose sugars being associated with the upregulation of *PSY-1* and potentially *DXS* (Télef et al., 2006). *PSY-1*-overexpression resulted in the reduction to sucrose (Fraser et al., 2007). Elevated phytoene and lycopene in *ZFPIDD2* down-regulated lines suggest that increased *PSY-1* is likely causing the reduction to sucrose. Furthermore, sucrose was predicted to improve carbon flux, channelling efficiency from pyruvate and GA3P into the citric acid cycle (Télef et al., 2006). Sucrose was also demonstrated to enhance ethylene synthesis, through the upregulation of *ACS4* and *ACS2* (Télef et al., 2006). Additionally, sucrose supplementation was shown to induce ripening-related colour changes in citrus (*Citrus unshiu*) fruit epicarp (Iglesias et al., 2001). The results from these studies suggest elevated carotenoid content in transgenic lines can be associated with increases to sugar metabolism.

Elevated vitamin E content was exhibited by *ZFPIDD2* down-regulated lines compared to both controls, with significant increases to δ-and α-tocopherol. Tocopherols are non-enzymatic lipid-soluble antioxidants that inhibit lipid peroxidation and protect photosystem II (PSII) from oxidative damage, through scavenging lipid peroxyl radicals and singlet oxygen (Munné-Bosch and Alegre, 2002; Krieger-Liszkay and Trebst, 2006; Falk and Munne-Bosch, 2010; Takahashi and Badger, 2011; Loyola et al., 2012). Tocopherol accumulation in ripening fruits was previously attributed to elevated CHORISMATE SYNTHASE (CS) and CHORISMATE MUTASE (CM) expression from the shikimate pathway (SK), as well as AROGENATE DEHYDROGENASE (TYRA), TYROSINE AMINOTRANSFERASE (TAT) and 4-HYDROXYPHENYLPYRUVATE DIOXYGENASE (HPPD) particularly in ripening

fruits (Quadrana et al., 2013). The same study indicated that increased tocopherol content could also be due to the upregulation of the methylerythritol phosphate (MEP) pathway at late ripening stages, through increased expression of: *1-DEOXY-D-XYLULOSE-5-P SYNTHASE* (*DXS*), *2-C-METHYL-D-ERYTHRITOL 4-PHOSPHATE SYNTHASE* (*DXR*), *2-C-METHYL-D-ERYTHRITOL 4-PHOSPHATE CYTIDYLYLTRANSFERASE* (*CMS*), *4-(CYTIDINE 5'-DIPHOSPHO)-2-C-METHYL-D-ERYTHRITOL KINASE* (*ISPE*), *4-HYDROXY-3-METHYLBUT-2-ENYL-DIPHOSPHATE REDUCTASE* (*HDR*), *ISOPENTENYL DIPHOSPHATE D–ISOMERASE* (*IPI*), *GERANYL PYROPHOSPHATE SYNTHASE* (*GPPS),* and *GERANYLGERANYL PYROPHOSPHATE SYNTHASE* (*GGPS*). The sets of genes listed have been demonstrated to elevate metabolic flux, potentially resulting in increased tocopherol content. Evidence for strengthened flux through the SK pathway in *ZFPIDD2* transgenic lines is shown by the elevated 3.3- and 11.0-fold phenylalanine increases compared to azygous and AC controls, respectively. Increased MEP pathway expression could also be an important factor, explaining the elevated carotenoid profiles. Both tocopherol and carotenoid biosynthesis compete for intermediates, and GGDR appears as a limiting step for tocopherol precursor availability (Quadrana et al., 2013). Thus, elevated tocopherol and carotenoid content suggests that precursor pathway's bottlenecks have been reduced. Mutations conferring or predicting altered flux through SK and MEP pathways have been shown to alter tocopherol content (Enfissi et al., 2010; Dal Cin et al., 2011).Taken together upregulation to either of these pathways could explain the elevated isoprenoids, enabling the increased tocopherol and phylloquinone witnessed.

Increased tocopherol content could also be due to alterations to the tocopherol-core pathway. The first committed steps are catalysed by HPPD and then HOMOGENTISATE PHYTYL TRANSFERASE (VTE2). Combined action of 2-METHYL-6-PHYTYL-1,4-BENZOQUINOL METHYLTRANSFERASE (VTE3) and TOCOPHEROL CYCLASE (VTE1) results in the formation of γ-tocopherol, while TOCOPHEROL CYCLASE (VTE1) alone catalyses δ-tocopherol. γ-TOCOPHEROL METHYL TRANSFERASE (VTE4) converts γ-tocopherol to α-tocopherol, and δ-tocopherol to β-tocopherol. With elevated δ-and α-tocopherol in *ZFPIDD2* transgenic lines compared with azygous lines, and just α-tocopherol compared to AC lines, increased HPPD, VTE2, VTE3 and VTE4 activities could be predicted. Furthermore, VTE5 catalyses the conversion of chlorophyll degradation-derived phytyl-diphosphate into tocopherol biosynthesis (Ischebeck et al., 2006; Valentin et al., 2006; Quadrana et

al., 2013). The importance of VTE5 was demonstrated through suppression, reducing tocopherol content in ripe fruits in addition to quinones and carotenoid content (Almeida et al., 2016). Interestingly, silenced fruits exhibited 30% less phytoene, phytofluene, ζ-carotene and lycopene. These results imply that increased VTE5 could be displayed by *ZFPIDD2* transgenic lines, contributing to elevated isoprenoid levels.

Tocopherol contents have been demonstrated to increase upon ripening in climacteric fruits, with the function of limiting oxidation (Singh et al., 2011). Intense respiration and ethylene production are associated with an oxidative phenomenon with increased hydrogen peroxide content, lipid peroxidation, and protein oxidation, resulting from of senescence (Jimenez et al., 2002). Therefore, activation of the tocopherol biosynthetic pathway is clearly advantageous to limit the oxidative environment (Quadrana et al., 2013). With α-tocopherol playing a significant role in developmental signalling, increased tocopherol content could be in response to increased ethylene by *ZFPIDD2* transgenic lines (Traber and Atkinson, 2007).

The GC-MS profiling of *ZFPIDD2* down-regulated lines revealed elevated sucrose metabolism enabling increased carbon flux through metabolism. Another important observation was that many metabolite differences between down-regulated lines with both controls correlate with further ripening progression. For example, *SUCROSE INVERTASES* were demonstrated to be RIN regulated, catalysing sucrose metabolism resulting in hexose accumulation. Sucrose was significantly reduced in transgenic lines, indicating further progression through ripening. Ripening was also associated with accumulation of cell wall components, aromatic amino acids as well as aspartate, lysine, methionine, and cysteine, in addition to isoprenoids (Carrari and Fernie, 2006). Furthermore, ripe fruits displayed reduced TCA intermediates, hexose phosphates and sugar alcohols. Correlating the metabolite differences between *ZFPIDD2* down-regulated fruit and both controls, with literature, can help understand why the uncoupled ripening-related phenotypes are seen in transgenic lines.

Numerous metabolites in *ZFPIDD2* down-regulated fruits were significantly altered, correlating with ripening progression. This indicates that increased rapidity of ripening was due to broad changes to metabolism. Additionally, it enabled the prediction of metabolites and pathways that were contributing to the increased rapidity of ripening. Earlier during development, alanine, asparagine, arginine, GABA, glutamine, valine and proline were found as the predominant amino acids. However, during ripening their concentrations decline, while aspartate, cysteine, glutamate, lysine, methionine,

phenylalanine, putrescine and tryptophan increase (Carrari and Fernie, 2006; Carrari et al., 2007; Osorio et al., 2011a). Transgenic fruits exhibited increases to the multiple amino acids compared to both controls, including phenylalanine in accordance with fruit ripening. This could indicate elevated aromatic amino acid content, as shown by ripe fruits. Compared to AC controls more increases to ripening-related amino acids were identified, with elevated aspartate and cysteine. While pyruvate and 3PGA derived amino acids displayed fewer differences compared to AC than to azygous controls. Throughout lysine, phenylalanine and threonine were elevated in transgenic lines compared to both controls. Importantly, increased lysine, phenylalanine were associated with ripening, potentially highlighting their importance to control ripening rapidity. Additionally, amino acids associated with early development generally remained unchanged. Phenylalanine is an important precursor for the phenylpropanoid pathway that has been demonstrated to be important in fruit ripening, influencing colour, flavour/aroma, pathogen resistance and softening (Singh et al., 2010; Zhang et al., 2013). Interestingly, phenylalanine pool size was predicted to be a key limiting step for phenylpropanoid regulation (Ozeki et al., 1990; Bate et al., 1994).

Similarly, decreased organic acid content is associated with fruit pericarp ripening (Carrari et al., 2006; Osorio et al., 2011a). *ZFPIDD2* transgenic lines exhibited reductions to the majority of organic acids, resulting in a significant 1.3- and 1.8-fold reduction to total organic acid content compared to azygous and AC lines, respectively. Most TCA intermediates decrease in red fruits (Carrari and Fernie, 2006). Transgenic lines displayed consistent decreases to citric and aconitic acid from the TCA cycle, compared to both controls. Compared to AC controls, further reductions to fumaric acid and malic acid were observed. All organic acids displaying reductions in transgenic lines, were shown to decrease with ripening progression (Carrari and Fernie, 2006; Osorio et al., 2011a). Glucaric acid displayed the largest fold reductions: 20.3- and 7.8-fold compared with azygous and AC controls, respectively. Gluconic acid (gluconate) was also decreased compared to azygous lines. Increased gluconic acid was associated with elevated fruit softening and reduction to carotenoid content (Kwon et al., 2014). Interestingly, multiple studies have demonstrated that organic acids strongly correlate with genes linked to ethylene and cell wall metabolism-associated pathways, highlighting their importance to fruit ripening (Carrari et al., 2006; Centeno et al., 2011; Osorio et al., 2011a). The levels of all organic acids, particularly the TCA cycle intermediates, were strongly affected across ripening in several ripening mutants (Osorio et al., 2011a). The largest alterations to organic acid content was identified in *nor*, a

mutation with severely affected ethylene biosynthesis and signalling (Osorio et al., 2011a). The results demonstrate the importance of ethylene for organic acid content. This provides further evidence for altered ethylene biosynthesis and signalling in *ZFPIDD2* transgenic lines, which is expected to be conferring the alterations to ripening-related metabolism compared to both controls.

Ripening is associated with the decline of sugar alcohols (Carrari and Fernie, 2006). Inositol was the most abundant polyol quantified by the GC-MS analysis, and its content was reduced 1.3-fold in *ZFPIDD2* transgenic lines compared to both controls. However, total polyol content remained unchanged between transgenic lines and both controls studied.

The fruit metabolism study revealed that many metabolites displaying significant differences to control lines were positively correlated to ripening. However, multiple metabolites displayed the opposite trend, correlating more to green unripe fruits. These were expected to contribute to the uncoupled ripening phenotype in transgenic fruits by delaying softening. From the amino acids, the higher glutamine, glycine, leucine, serine and valine levels correlated to unripe fruit. Likewise, the levels of sugar alcohols, glycerol and sorbitol/mannitol; organic acids, gluconic acid, fumaric acid and succinic acid; as well as the sugar galactose proved to negatively correlate to ripening.

An important difference highlighted above was the 1.8- and 2.9-fold reduction to galactose content in *ZFPIDD2* transgenic lines compared to both azygous and AC controls, respectively. Tomato ripening is associated with the decline to polymeric galactose in cell walls and the rise in free galactose (Wallner and Bloom, 1977; Gross and Wallner, 1979; Kim et al., 1991), in addition to the reduction in intercellular adhesion, solubilisation of pectins, and depolymerisation of hemicelluloses. Ripening-related differences to galactose content were mainly observed in pectic fractions, the increase to free galactose was mostly associated with pectin depolymerisation and the loss of cell wall galactose side chains from rhamnogalacturonan I (Gross, 1984; Seymour et al., 1990). Galactose is mostly present in type I (1→4)β-D-galactan chains that were shown to be degraded during ripening (Seymour et al., 1990). Multiple ripening inhibitor and reduced softening tomato mutants display reduced free galactose (Gross and Wallner, 1979; Gross, 1983, 1984; Kim et al., 1991; Smith et al., 2002). Small changes were also observed in matrix glycan and cellulose fractions. Also, the side chains of glucomannan have single units of terminal galactose forms, while xyloglucan also has galactose forms in their side chains.

Previous studies, demonstrated that β-GALACTOSIDASE (TBG) II, β-GALACTOSIDASE/EXO-GALACTANASE, is active against a (1→4)β-D-galactan-rich polymer prepared from tomato cell walls. A total of seven TBG genes expressed during fruit development and maturation have been identified in tomato (Smith and Gross, 2000). Six were expressed during ripening and five were localised to the cell wall. Exo-galactanase activity increased up to 5-fold during ripening and was correlated with the rise in free galactose (Pressey, 1983; Kim et al., 1991; Carey et al., 1995). Suppression studies revealed that reduced TBG1 mRNA produced no observable differences to exo-galactanase activity, cell wall composition or fruit texture (Carey et al., 2001). Antisense suppression of *TBG3* did display reduced exo-galactanase activity and an increase in wall galactosyl content, but firmness remained unaltered. However, *TBG3* antisense fruits exhibited slower deterioration in storage, while elevated viscosity and insoluble solids were identified after processing into a paste. Unlike other β-GALACTOSIDASES, *TBG4* expression and exo-galactanase activity were markedly reduced in *rin* and *nor* ripening-mutants relative to the wild-type controls (Smith et al., 2002). Furthermore, antisense lines yielded red-ripe fruits that were up to 40% firmer, displaying reduced exo-galactanase levels and high wall galactosyl content. Elevated firmness was associated with reduced loss and thus increased content of pectic galactan side-chains, shown to induce mechanical strength in the cell wall of pea cotyledons (McCartney et al., 2000). Decreases to: wall porosity, access of cell wall hydrolases to wall components, and depolymerisation of structural polysaccharides are predicted to be the mechanism for improved fruit firmness (Redgwell et al., 1997a; Brummell and Harpster, 2001; Smith et al., 2002). *TBG6* suppression increased fruit cracking, reduced locular space, and doubled the thickness of the fruit cuticle. These phenotypes were also attributed to reduced exo-galactanase activity (Moctezuma et al., 2003).

Overall, TBG activity has been associated with softening across multiple fruit species; with reduced galactose content being linked to reduced softening (Nakamura et al., 2003; Brummell et al., 2004; Mwaniki et al., 2005; Ogasawara et al., 2007; Paniagua et al., 2016). Therefore, the reduced free galactose in *ZFPIDD2* down-regulated lines is indicative of a ripening mutation with reduced TBG expression, which could be contributing to a slower rate of fruit softening. TBG is just one class of enzyme involved with pectin remodelling; sequential, and synergistic action of other pectin-degrading enzymes is expected to contribute to pectin-related softening. These include POLYGALACTURONASE, EXO-POLYGALACTURONASE, PECTIN

METHYLESTERASE, PECTIN LYASE and EXPANSIN in tomato (Brummell and Harpster, 2001; Goulao and Oliveira, 2008; Wang et al., 2018).

3.4 Conclusion of chapter

The aim of the project was to identify a novel ripening-related transcription factor that controls fruit quality. Affymetrix GeneChip transcriptomic data and artificial neural network (ANN) inference analysis from Pan et al., (2013), identified several potential ripening-regulators that were believed to be fruit specific, and were shown to have expression patterns that mirrored RIN. The predicted C2H2-type *ZINC FINGER PROTEIN INDETERMINATE DOMAIN 2* (*ZFPIDD2*) transcription factor was identified and demonstrated to have a ripening-related expression profile. Its expression was reduced in both *rin* and *nor* ripening mutant lines. Also, the transcription factor was demonstrated to be a direct RIN target (Fujisawa et al., 2012b), therefore it was predicted to be acting further down the cascade of transcription factors and global ripening-regulators involved in fruit ripening. The project aimed to manipulate the expression of *ZFPIDD2* to provide specific tomato improvement, avoiding the global ripening-related effects of other tomato mutations. It was hoped that the reduced softening benefits of the *rin* mutation would be maintained without reducing other important fruit quality traits.

Through the insertion of a knock-down 35S::RNAi construct under constitutive control, functional characterisation was performed. *ZFPIDD2* was demonstrated to have global effects to plant and fruit development, whilst a ripening-related function was confirmed. The broad non-specific effects of the transcription factor can be attributed to multiple differences to several major classes of phytohormones across different tissues. Altered phytohormones were expected, as the zinc finger protein was predicted to be an INDETERMINATE DOMAIN 2 (IDD2) protein. IDD proteins have been associated with being both a repressor and co-activator of DELLA-mediated gibberellin signalling.

Altered phythormones including gibberellin, auxin and cytokinins are predicted to contribute to the increased source-to-sink strength of fruit, and elevated non-vegetative biomass caused by reduced leaf senescence. Phytohormone differences combined with altered sink strength is predicted to promote increased fruit set and growth, displaying a potential to double fruit yield. Specifically, altered GA and ABA contents suggested an

extension to cell division or expansion phases of fruit growth, subsequently delaying the onset of ripening. Down-regulated fruits exhibit a partial uncoupling of ripening, whereby fruits reach red ripe quicker but fruit softening is delayed, owing to elevated outer pericarp firmness. Altered IAA and CK content are predicted to contribute to ripening changes; differences to ethylene can also be expected. Overall, the disruption of the delicate interplay between phytohormones is likely the key factor influencing the many developmental and ripening-related differences observed.

Down-regulated lines display elevated phytoene, phytofluene and lycopene in ripe fruit pericarp and jelly tissues. Therefore, upregulation of the RIN-induced carotenoid biosynthesis enzymes: *PSY-1*, *CRTISO* and *PDS* were expected. Ethylene treatment has been demonstrated to induce the expression of these enzymes, producing similar carotenoid profiles, suggesting increased ethylene could be associated with the carotenoid increases upstream of lycopene cyclisation. Compared to non-transgenic controls, total carotenoid content was improved 27% and 20% in pericarp and jelly tissues, respectively. Increases between 91% and 118% were seen in the same tissues when compared to AC controls. Improved carotenoid content can explain the qualitative differences to fruit colour both internally and externally. Total tocopherol and phyllquinone contents were also increased. The result highlights the elevated antioxidant and vitamin E potential of transgenic fruits.

ZFPIDD2 down-regulation had broad effects to metabolism, with many metabolites associated with ripening, including isoprenoids, showing significant fold changes when compared to both controls. This supports the observation of increased rapidity of ripening in transgenic fruits. The large reductions to sucrose, in addition to multiple TCA cycle intermediates indicate elevated carbon flux through metabolism, which is required to facilitate the extended progression into ripening. RIN has been shown to regulate sucrose metabolism, again highlighting the potential for elevated ethylene in ripening transgenic fruits. Total sugar levels including fructose, the main sugar conferring sweetness, and fruit pH levels remain unchanged, thus no major changes to the sweetness or acidity is expected.

Additionally, fruits had delayed softening both on the vine and post-harvest, the latter demonstrated a potential 5 to 11 day extension to shelf-life. The reduction to free galactose provides evidence for this mechanism, indicating that pectin depolymerisation and the loss of cell wall galactose side chains from rhamnogalacturonan I is reduced. Therefore, reduced TBG activity is an important candidate that is expected to be

contributing to the reduced fruit softening observed in transgenic fruits. The potential extension to shelf-life could improve fruit quality and profitability by reducing wastage, infection by post-harvest pathogens, frequency of harvest, while extending fruit transportation and storage opportunities. Therefore, the decline of fruit spoilage has great commercial importance for both retail of fresh fruit and processed tomatoes. The reduced softening and potential improvement to shelf-life would benefit both local and global supply chains, particularly markets with longer transportation distances such as the United States of America and Asia. Harvesting at breaker had no effect on the improved colour development and softening-related phenotypes. Further post-harvest phenotypic and metabolic assessment of quality would be necessary to confirm an improved shelf-life: including ethylene quantification and both texture and flavour volatile analysis.

Overall, the project succeeded in identifying a ripening-related transcription factor that could improve fruit quality. However, transcription factor manipulation may not be the best approach to deliver targeted tomato improvement. Manipulations of structural genes or enzymes, demonstrated by later studies, provide a more targeted improvement to quality. Despite this, the targeting of the *ZFPIDD2* transcription factor has been shown to improve multiple areas of quality. Down-regulated lines uncouple colour development and softening whilst improving fruit yield, demonstrating that transcription factor manipulation can result in broad effects to quality which can contribute to the understanding of tomato development and ripening. Consequently, the project proved successful, demonstrating that *ZFPIDD2* can provide significant improvement on the *rin* mutation currently commercially utilised. As down-regulated fruits maintain the reduced fruit softening phenotype, but improve other key quality traits, with elevated ripening-related colour and isoprenoid accumulation associated with increased nutritional potential, without affecting the main metabolites linked with sweetness or acidity. Future studies should involve the quantification of ethylene and analysis of samples sent for RNA sequencing. Both would provide further elucidation of the mechanisms facilitating fruit yield improvements, and the partial uncoupling of fruit ripening displayed by down-regulated lines. To date, very few studies have been able to improve multiple aspects of fruit quality, specifically by promoting colour formation and inhibiting softening.

Chapter IV: Functional characterisation of the ZINC-FINGER PROTEIN ZPR1

4.1 Introduction

The ZINC-FINGER PROTEIN ZPR1 in animal cells has been shown to participate in cell cycle, growth and proliferation through the interaction with other proteins including growth factors (Galcheva-Gargova et al., 1998; Gangwani, 2006). Despite this, current knowledge regarding plant ZPR1 proteins remains scarce. Recently, a novel ZPR1 in *Solanum tuberosum* was identified as a clock-associated protein, necessary for the accurate rhythmic expression of specific circadian-regulated genes (Kiełbowicz-Matuk et al., 2017). Additionally, a *ZINC-FINGER PROTEIN ZPR1* (Solyc02g069120) gene was identified in tomato, and was shown to accumulate in apical meristems in response to ABA (abscisic acid) treatment and heat stress (Li et al., 2013). The same study identified ZPR1 as a transcriptional activator, with ability to bind to ABRE (ABA-responsive elements), which are positive regulators of ABA signalling. The results indicated that the transcription factor was involved in the ABA signalling network, potentially playing an important role in plant cell development and abiotic stress responses (Li et al., 2013).

The ripening-related expression profile, reduced expression in *cnr*, *nor* and *rin* tomato mutants, combined with altered carotenoid profiles in the T_0 generation indicated an important ripening-related function for the *ZINC-FINGER PROTEIN ZPR1*. Detailed phenotypic characterisation and metabolic profiling was performed, enabling the assessment of how manipulation affected development, fruit ripening and fruit quality traits.

4.2 Results

4.2.1 Phenotypic and genotypic screening of the T_1 generation to identify potential functions of *ZPR1*

4.2.1.1 Screening for altered plant morphology, fruit development, and ripening-related quality traits associated with transgenic lines

Potential ripening-related functions for the transcription factor were demonstrated by elevated pigmentation in *ZPR1* transgenic lines, with the insertion of the knock-down 35S::RNAi construct. Carotenoid screening of the T_0 generation revealed that transgenic lines accumulated more phytoene, phytofluene and lycopene, while β-carotene was reduced compared to wild type controls. Similar to section 3.2, lines with altered carotenoid contents were selected for further characterisation. These individuals were propagated and broad phenotyping was conducted to characterise the transcription factor, providing an assessment of quality and to reduce the number of individuals and genotypes present. The T_1 generation included 68 *ZPR1* transgenic lines, up to 20 lines per insertional event, in addition to 20 representative Alisa Craig (AC) wild type controls. Without knowing the insert number, zygosity and potential segregation within each insertion event, all transgenic lines were analysed separately.

Transgenic lines were shown to have altered plant morphology (Figure 4-1). In total 83% of transgenic lines exhibited reduced internode lengths compared with AC controls, with several proving to be statistically significant. On average, internode lengths were reduced by 1.6 cm. Similarly, 77% of transgenic lines had a reduced plant height, on average being 12.2 cm shorter compared to AC controls. Furthermore, ten transgenic lines displayed a more severely perturbed development, whereby the height and average internode lengths were below 100 and 5 cm, respectively. The results demonstrated that transgenic lines exhibited a more condensed plant architecture compared with AC controls.

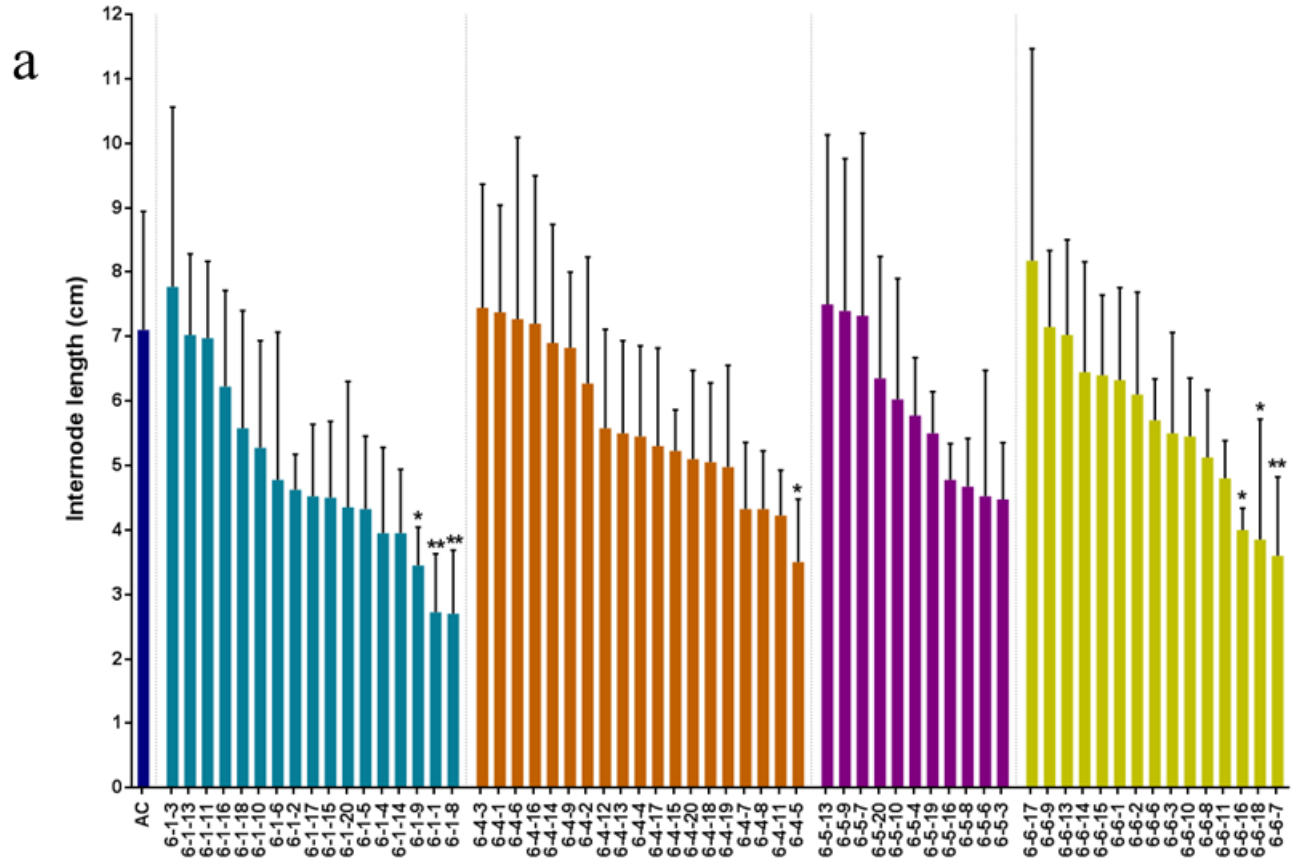
a
Internode length (cm)
0
1
2
3
4
5
6
7
8
9
10
11
12
AC
6-1-3
6-1-13
6-1-11
6-1-16
6-1-18
6-1-10
6-1-6
6-1-2
6-1-17
6-1-15
6-1-20
6-1-5
6-1-4
6-1-14
6-1-9
6-1-1
6-1-8
6-4-3
6-4-1
6-4-6
6-4-16
6-4-14
6-4-9
6-4-2
6-4-12
6-4-13
6-4-4
6-4-17
6-4-15
6-4-20
6-4-18
6-4-19
6-4-7
6-4-8
6-4-11
6-4-5
6-5-13
6-5-9
6-5-7
6-5-20
6-5-10
6-5-4
6-5-19
6-5-16
6-5-8
6-5-6
6-5-3
6-6-17
6-6-9
6-6-13
6-6-14
6-6-15
6-6-1
6-6-2
6-6-5
6-6-3
6-6-10
6-6-8
6-6-11
6-6-16
6-6-18
6-6-7

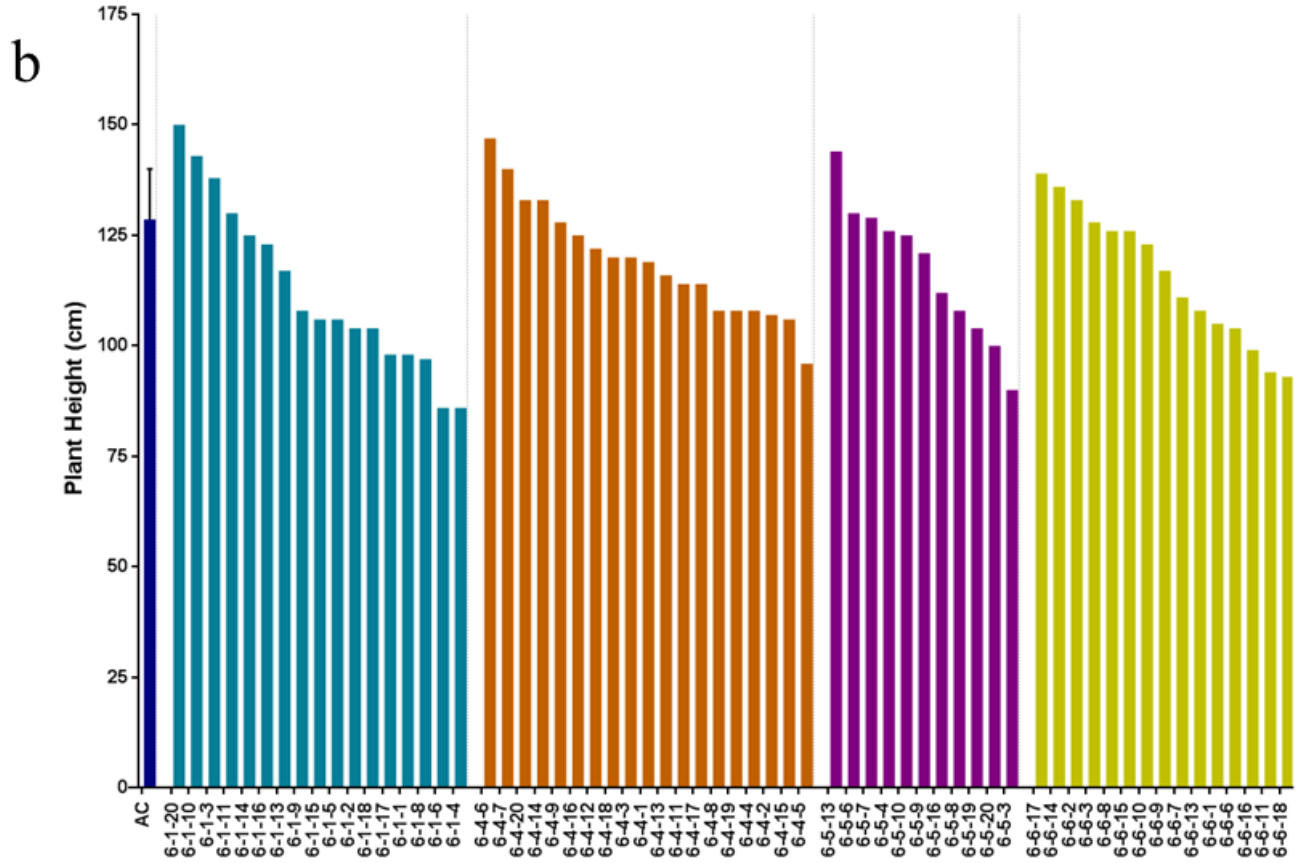

Figure 4-1 Assessment of altered plant morphology by screening stem internode lengths and plant height.

Figure 4-1 Assessment of altered plant morphology by screening stem internode lengths and plant height.

Stem internode length (a) and total plant height (b) were used to identify differences to plant development between Ailsa Craig (AC) and transgenic lines. Plant parameters were measured once the AC wild type background had three trusses with fruit set. Total plant height was measured from the soil to last node; four random internodes were measured from the base of the plant to the last node. Each transgenic individual is represented by a single column, for AC a total of nineteen lines were averaged ensuring enough wild type biological replicates were spread throughout the population. Statistical determinations are shown as mean ± SD, Dunnett's test analysis illustrates statistically significant differences between wild type background (AC) and the transgenic varieties, $P < 0.05$, $^{**}P < 0.01$, and $^{***}P < 0.001$ are designated by *, **, and ***, respectively.

Following the identification of altered plant morphology, fruit development time was evaluated as described in section 2.1.4, which refers to time taken for fruits to reach breaker stage from anthesis. *ZPR1* transgenic lines took on average 50.9 days compared to just 45.1 days for the AC controls (Figure 4-2a). Several transgenic lines exhibited elevated fruit size and total fruit yield (Figure 4-2b and c). Fruit size proved more consistent, as an average of all transgenic lines revealed that fruit size was increased by 28% compared to AC controls, while total fruit yield remained unchanged. A total of five transgenic individuals had an increase in yield of over 50%, rising up to 334% for the highest yielding line. Most transgenic lines yielded larger fruits, with fourteen individuals on average producing fruits that were 25% larger than AC controls. The results indicated that the transcription factor may have important roles in fruit set and development, and could be manipulated to improve crop productivity. Further crops were required to confirm the phenotypes identified, as unfavourable conditions of a winter crop resulted in low fruit yields and variation.

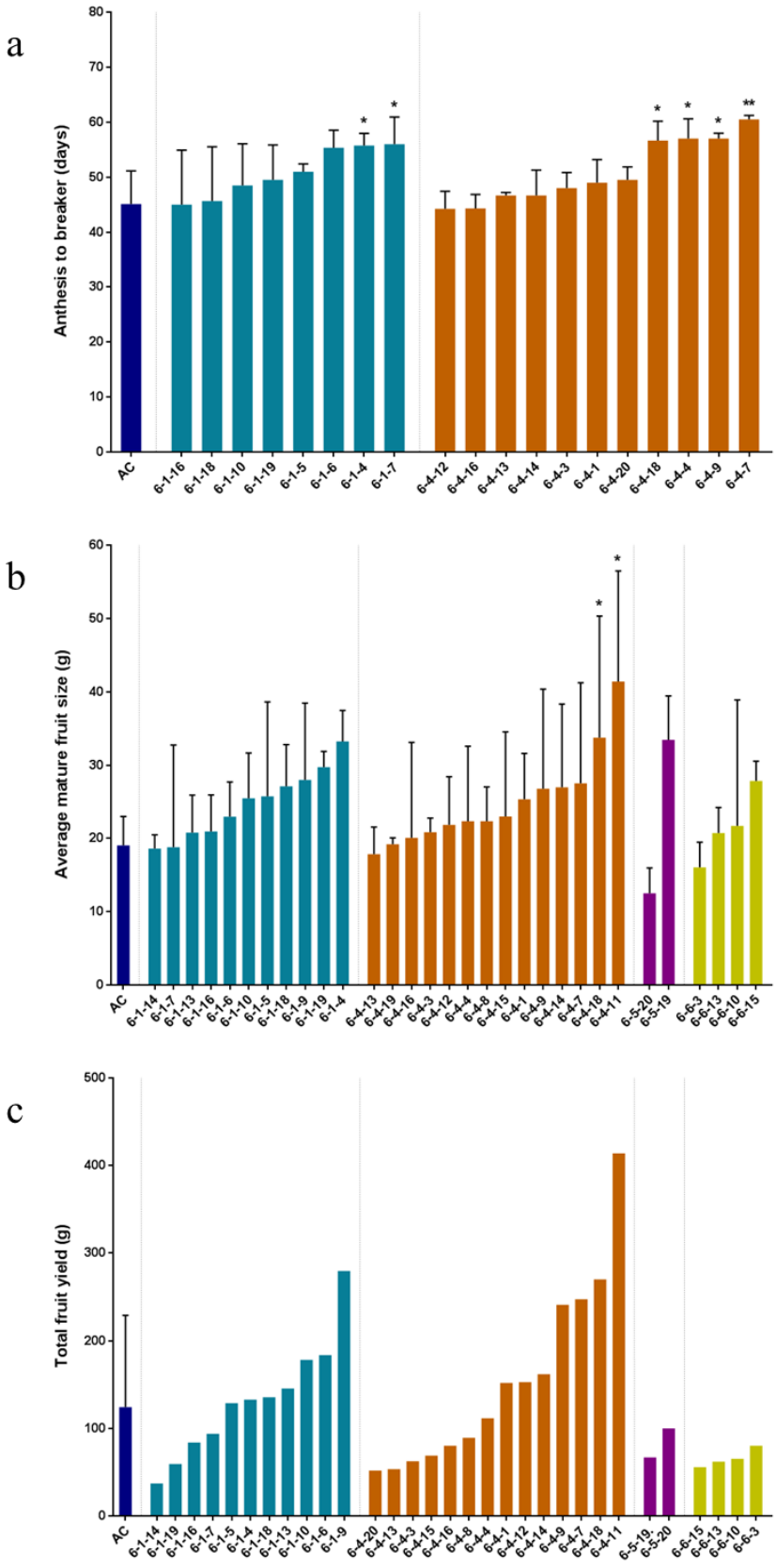

Figure 4-2 Evaluating fruit set and development by screening the time from anthesis to breaker, average fruit weight and total fruit yield.

Figure 4-2 Evaluating fruit set and development by screening the time from anthesis to breaker, average fruit weight and total fruit yield.

The maturity time from anthesis to breaker (a), average fruit weight (b) and total fruit yield (c) were recorded, to test whether transgenic lines exhibited altered fruit set and developmental phenotypes. Flowers were tagged at anthesis and the time taken to reach the onset of ripening at breaker stage was recorded. Fruit weights were determined individually postharvest and combined to determine total fruit yield. Fruit parameters were measured once the wild type AC background had formed five trusses. Each transgenic individual is represented by a single column, for AC up to twelve lines were averaged, ensuring enough wild type biological replicates were spread throughout the population. Between two and ten fruit measurements were recorded for each plant for either fruit maturity time or average fruit weight. Statistical determinations are shown as mean ± SD, Dunnett's test analysis illustrates statistically significant differences between wild type background (AC) and the transgenic varieties, $P < 0.05$, $^{**}P < 0.01$, and $^{***}P < 0.001$ are designated by *, **, and ***, respectively.

A ripening-related function was predicted with the elevated *ZPR1* expression upon the onset of ripening. Therefore, it was important to establish whether the insertion of the knockdown construct altered ripening-related fruit quality. Fruit firmness was measured using a fruit firmness meter at 14 days post breaker, when fruit were expected to be approaching overripe (Figure 4-3a). At this time point a total of 78% of transgenic lines exhibited increases to fruit firmness compared with wild type AC controls, although only three lines proved statistically significant. On average, transgenic fruits were 14% firmer in comparison to AC controls, indicating a reduced rate of softening. Then the rapidity of ripening-associated colour development was visually assessed (Figure 4-3b). Most transgenic fruits displayed a reduced time to transition from breaker to uniform red ripe, taking on average 1.6 less days compared to AC controls. At its extreme, the ripening time was reduced by 3.8 days. In total 89% of transgenic lines exhibited a reduced time to reach red ripe, with multiple lines from the 6-4 insertion event proving to be significant, indicating increased rate of ripening-related colour development.

To confirm elevated colour development in transgenic lines, spectrophotometric quantification of the end point levels of carotenoids were performed (Figure 4-4). This assessed whether the altered ripening times and darker fruit phenotypes observed in transgenic lines, were due to an increase in pigment accumulation during ripening. Carotenoid extraction of freeze dried fruit material harvested at seven and fourteen days post breaker (7 dpb and 14 dpb, respectively) was performed (section 2.3.1). The

extraction and spectrophotometer method performed is described in section 2.3.2. The wavelength of 470nm was used to quantify the levels of carotenoids, specifically lycopene, the predominant carotenoid in ripe tomato.

The majority of transgenic lines exhibited increased carotenoid content at 7 dpb compared to AC controls (Figure 4-4a). The lines displaying large reductions to ripening time exhibit significant improvements to ripening-related carotenoid content at 7 dpb. The correlation between phenotypes (R^2=0.83) validates the visually determined ripening times. On average the transgenic lines 6-4-1 and 6-4-14 exhibit a significant 1.8-fold reduction to ripening time, whilst demonstrating a 1.3-fold increase to carotenoid content at 470nm. The results indicate that the elevated ripening-related carotenoids are contributing to the visually determined reduced ripening time. Significant carotenoid improvements were also identified for 6-4-11 and 6-1-10, exhibiting 1.3-fold increases to carotenoid content.

Similarly, most transgenic lines (72%) exhibited increased pigmentation at 14 dpb, with lines from the 6-4 insertion event proving to be most consistent for this trend (Figure 4-4b). Only 6-4 lines yielded significant carotenoid increases, averaging a 1.3-fold elevation to pigmentation compared to AC controls. Interestingly, the 6-4 lines with the highest carotenoid content at 7 dpb also showed amplified pigmentation at 14 dpb. This indicated a sustained increased rate of carotenoid accumulation throughout the ripe stages of fruit ripening.

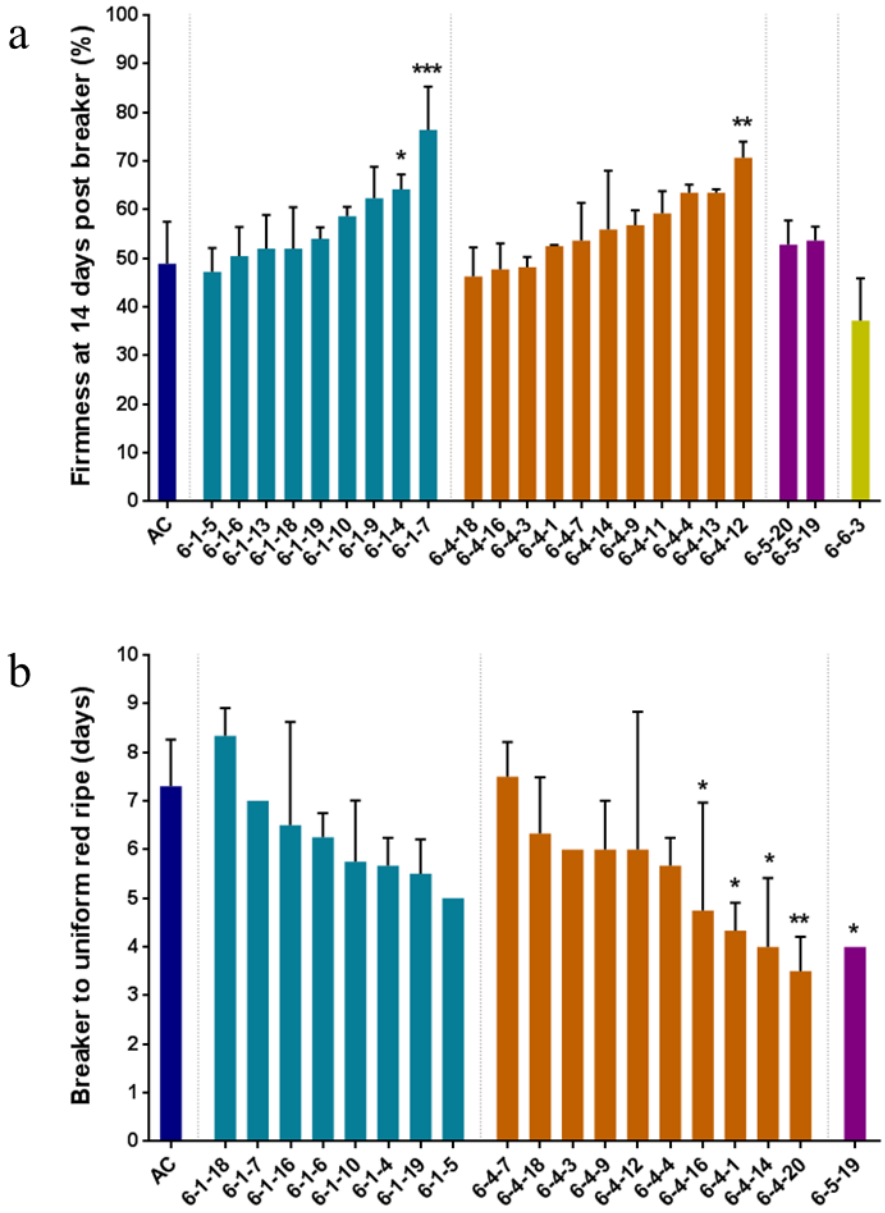

Figure 4-3 Assessment of ripening-associated fruit quality by screening colour development and fruit softening.

Colour related rapidity of ripening represents visual determination of the time taken for fruits to transition from breaker to uniform red (a). Fruit softening was measured in fruits at fourteen days post breaker using a fruit firmness meter; three measurements were taken per fruit (b). For both analyses between two and four fruits were studied. Each transgenic individual is represented by a single column, for AC a total of up to seven lines were averaged, ensuring enough wild type biological replicates were spread throughout the population. Statistical determinations are shown as mean ± SD, Dunnett's test analysis illustrates statistically significant differences between wild type background (AC) and the transgenic varieties, $P < 0.05$, $^{**}P < 0.01$, and $^{***}P < 0.001$ are designated by *, **, and ***, respectively.

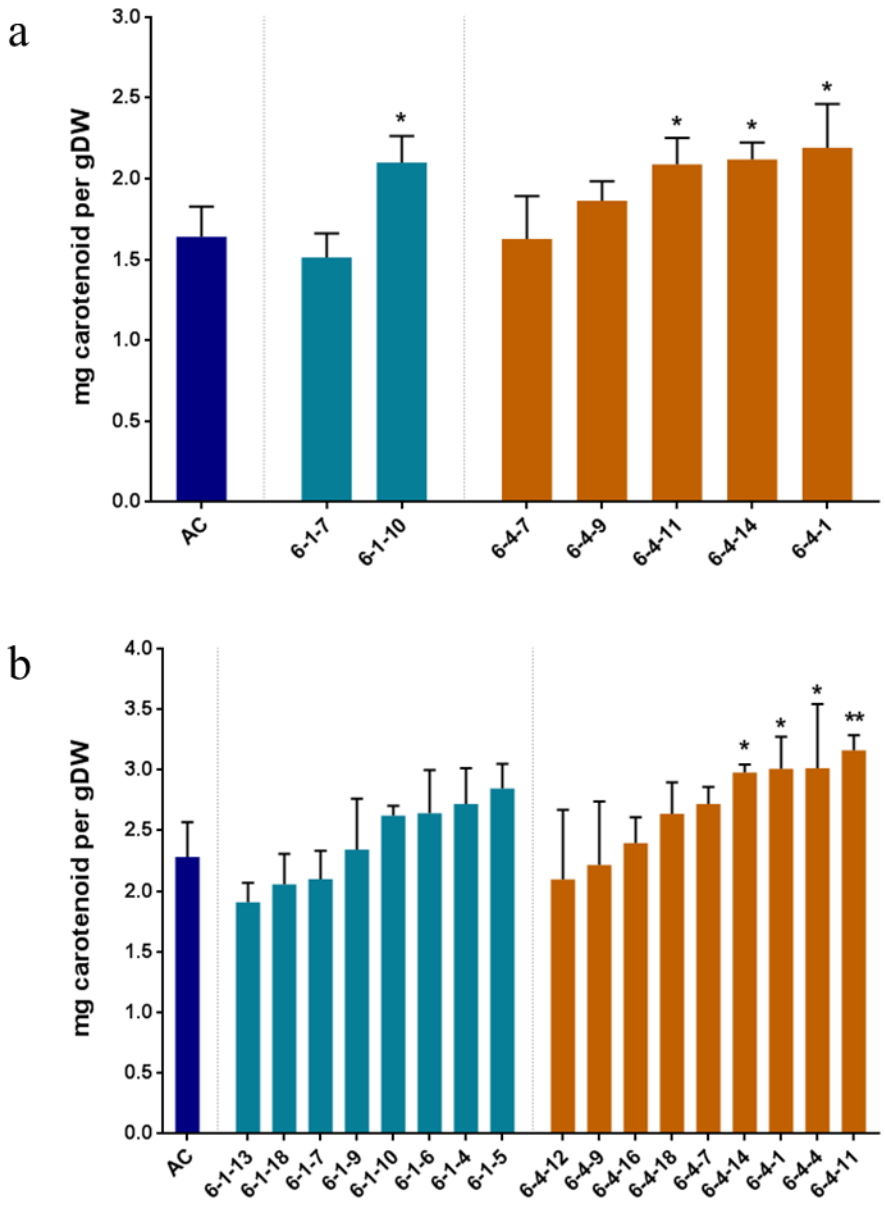

Figure 4-4 Spectrophotometer quantification of carotenoid content in ripe fruits.

Carotenoid content of two ripe fruit stages, seven (a) and fourteen days (b) post breaker, were quantified by spectrophotometer at 470 nm. Between two and four representative fruits were pooled per individual, then three technical and analytical determinations were made. Methods used for these determinations are described in section 2.3. Each transgenic individual is represented by a single column, for AC a total of up to seven lines were averaged, ensuring enough wild type biological replicates were spread throughout the population. Statistical determinations are shown as mean ± SD, Dunnett's test analysis illustrates statistically significant differences between wild type background (AC) and the transgenic varieties, $P < 0.05$, $^{**}P < 0.01$, and $^{***}P < 0.001$ are designated by *, **, and ***, respectively.

4.2.1.2 Molecular characterisation of transgenic lines by PCR, and Southern blotting to determine insert number

Combined phenotypic and spectrophotometer screening enabled the selection of lines with the most positively improved quality traits for genotyping. The next objective was to identify individuals with the insertion of the knockout construct. DNA was extracted from previously harvested leaf material from young tomato plants. Insertion of the transgene was verified by PCR, using specific primers to amplify the *NEOMYCIN PHOSPHOTRANSFERASE II* (*NPTII*) gene (section 2.2.3.2 and primers are described in appendix Table 1). On the resultant gel, transgenic lines were determined by the presence of the *NPTII* amplicon (ran alongside other constructs, similar to Figure 3-5). The PCR confirmed that the most improved lines were transgenic. Despite this, no azygous lines were identified by a negative signal identical to AC controls. Real-time PCR was performed on several lines to confirm the number of inserts and potential zygosity (method is described in section 2.2.5.6). The relative quantification ratios of *PHYTOENE DESATURASE* (endogenous single-copy gene) to the *NPTII* gene, suggested that all lines tested were homozygous with two inserts.

Lines from the 6-4 insertion event displayed the most consistent phenotypic improvements. Therefore, the objective was use Southern blotting to determine the insert number of various lines from this insertion event. However, Southern blotting was only conducted on 6-4-4 (section 2.2.5.7), which was used as a marker for the 6-4 insertion event, as combined PCR and phenotypic screening enabled rapid selection of lines for the next generation. First, the probe was created and tested, and then the Southern blot was performed using the DNA cut by the SacI restriction enzyme. The number of bands corresponded to the number of transgene inserts in the transgenic line. Interestingly, the Southern blot revealed the presence of just one band with a strong signal, indicating the presence of a singular insert (Figure 4-5).

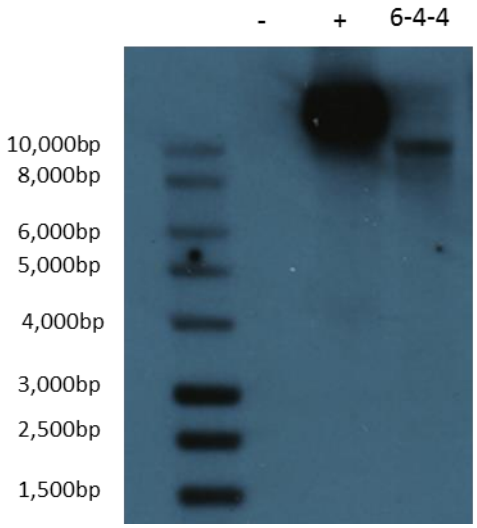

Figure 4-5 Autoradiogram of Southern blot used to determine the insert number of the 6-4-4 transgenic line against a representative control.

The Southern blot used DNA from 6-4-4 against pooled DNA from multiple AC lines. Digest was achieved using the SacI restriction enzyme and hybridisation was carried out using a specific probe to identify the transgene. The numbers correspond to the different plants tested. -, a negative control (DNA from the AC control) and +, positive control (DNA from the plasmid).

4.2.1.3 Combining results from the genotypic and phenotypic screen to select lines for further characterisation in the next generation

The results from previous expression profiling and carotenoid screening, combined with the phenotypic characterisation of the T_1 generation, indicated possible ripening-related functions for the ZPR1 transcription factor. Importantly, the majority of transgenic lines displayed increased carotenoid and ripening associated colour development, combined with reduced rate of softening. The partial uncoupling of ripening-related processes showed potential to provide significant improvement to the *rin* mutation currently utilised. Additionally, fruit and plant development roles were also predicted for the transcription factor with most lines exhibiting reduced internode lengths and height, combined with larger fruits influencing potential increases to total fruit yield. The condensed plant architecture could indicate increased diversion of photosynthates from source tissues to fruit development and ripening, rather than plant growth. Ranking these traits enabled the selection of the most improved individuals, whereby lines from the 6-4 insertion event proved to be more consistent. The line 6-4-4 was chosen for reaching a

uniform red 1.6 days quicker with a 1.3-fold increase to carotenoid content and 30% reduction to fruit softening at fourteen days post breaker, while fruit size and total fruit yield remained unchanged relative to AC controls. Importantly, Southern blotting revealed that this line had a singular insert, providing greater evidence that the specific single insertion of the transgene is conferring the multiple phenotypes witnessed. Similarly, 6-4-11 was chosen for increased carotenoid content (1.4-fold) and firmness (1.2-fold) at fourteen days post breaker. Additionally, 6-4-11 exhibited a significant 2.2-fold increase to fruit size and a 3.3-fold increase to total fruit yield.

4.2.2 Detailed characterisation of the T_2 generation and identification of azygous non-transgenic controls

Suitable propagation of the most improved individuals from the T_1 generation followed, with aim of improving quality-related traits through selection, in addition to promoting segregation within the population for the identification of azygous controls. Two populations of twenty transgenic individuals and ten AC wild type lines were grown: one was used for more detailed phenotypic and metabolic characterisation; the other was grown at the University of Nottingham to determine potential altered yield and fruit firmness traits at separate locations.

4.2.2.1 Genotypic screening to identify non-transgenic azygous individuals in the T_2 generation

Young leaf material was harvested from individuals grown at Royal Holloway. The presence of the transgene was confirmed using PCR and specific primers to amplify the *NPTII* gene (section 2.2.3.2 and primers are described in appendix Table 1). Azygous lines were verified by the absence of *NPTII* amplicon (Figure 4-6). In total two azygous lines were identified by the absence of PCR product, yielding a negative signal on the resulting gel identical to both AC and non template controls. With real-time PCR and Southern blotting across all three constructs not being feasible to determine insert number and zygosity, and the transgenic lines clearly still segregating, all lines that were verified to be positive for the transgene were kept separate in the subsequent analyses.

Azygous lines are considered the non-transgenic true control as they have been through transformation and tissue culture.

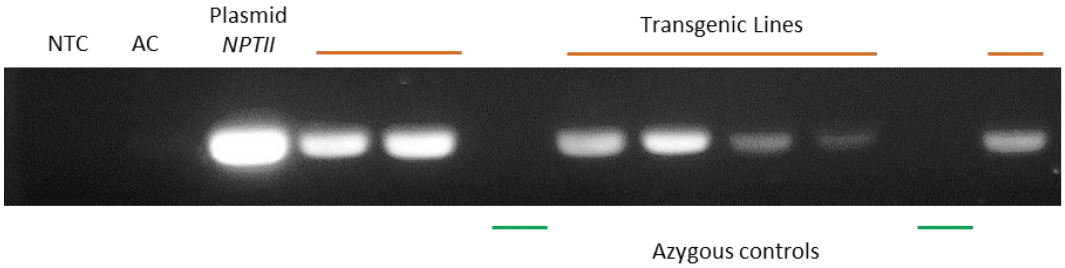

Figure 4-6 PCR confirmation to determine the presence of the knockout transgene in the transgenic lines and identification of azygous non-transgenic controls.
Amplification of the *NPTII* gene was performed by PCR on the majority of transgenic lines and visualised under UV light. Transgenic lines from the T_1 generation that yielded a negative signal identical to AC lines were identified as non-transgenic azygous controls (orange markers). DNA was extracted from a pool of 3 representative leaves of each plant. NTC: non template control**.**

4.2.2.2 Using altered ripening-related and developmental traits to select most improved individuals for detailed phenotypic characterisation

The T_1 generation identified altered colour development, fruit firmness, fruit yield and internode length phenotypes in transgenic lines. These traits were used as markers to identify and select the best lines for more detailed characterisation. Due to identification of just two azygous lines within the population and considerable variation between these individuals, statistical comparisons were made between transgenic lines and AC controls. This comparison revealed similar phenotypic differences to the T_1 generation, which were maintained into the T_2 generation. Firstly, reduced internode lengths were identified in transgenic lines, indicating altered plant morphology. On average internode lengths of transgenic lines were 2.5 cm shorter in comparison to AC controls (Figure 4-7a). Importantly, transgenic fruit transitioned from green to red ripe on average 1.5 days earlier (Figure 4-8a), while fruits approaching overripe at fourteen days post breaker were 10% firmer on average compared to AC lines (Figure 4-8b). Mature fruit yield proved to be variable, but several transgenic lines exhibited large improvements compared to AC controls (Figure 4-7b). Overall, fewer differences were identified between transgenic lines when compared to azygous controls than to AC controls.

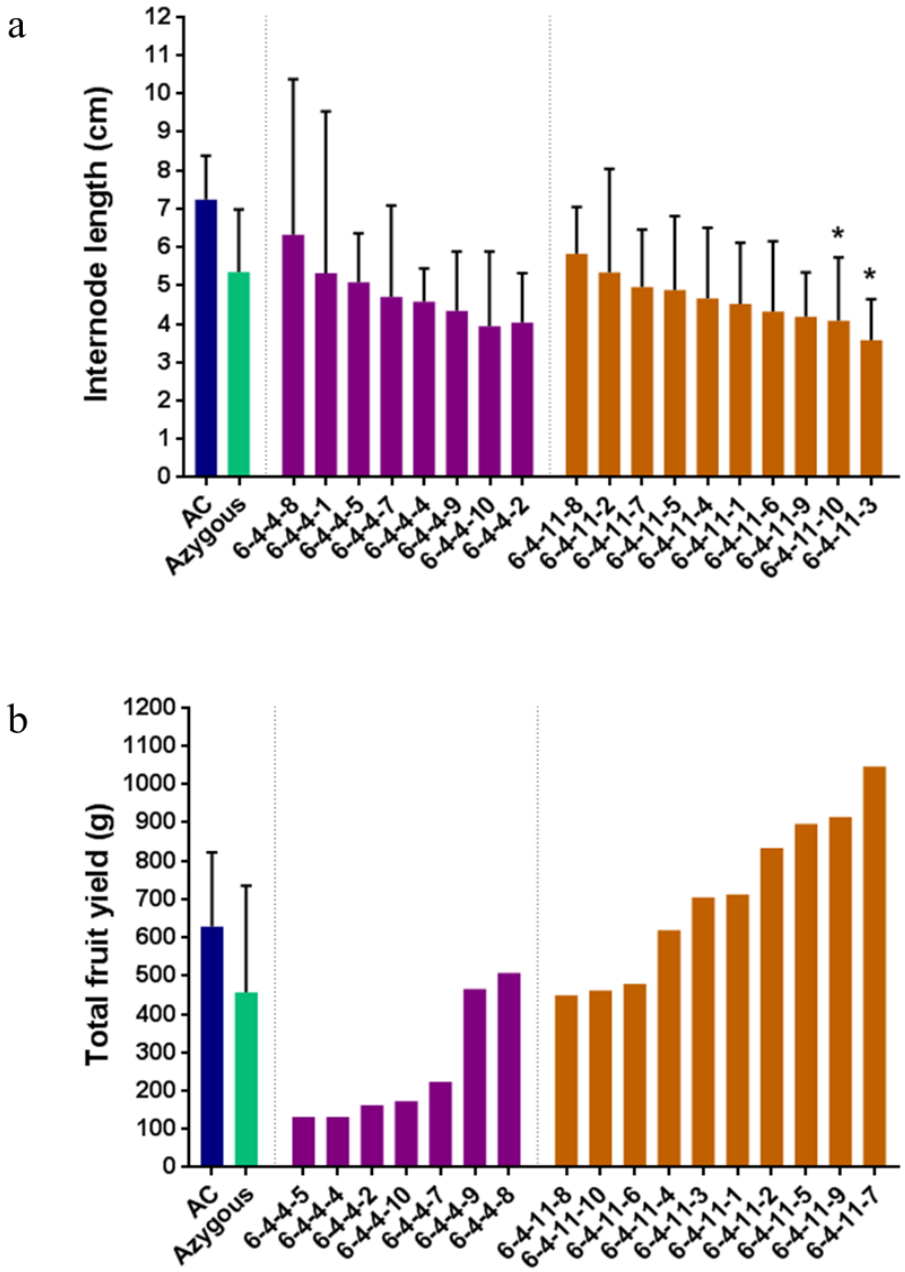

Figure 4-7 Internode length and total fruit yield screening of the T_2 population.

Internode lengths (a) and total fruit yield (b) of the T_2 population enabled a screen for altered development. Phenotypic screening enabled the selection of extremes with the most positively altered phenotypes, and correlated with similar experiments conducted on the T_1 generation. Five random internodes were measured from the base of the plant to the last node. Fruit were weighed individually postharvest and combined to determine total fruit yield. Each transgenic individual is represented by a single column. A total of two and nine individuals were combined for azygous and AC controls, respectively. Statistical determinations are shown as mean ± SD, Dunnett's test analysis illustrates statistically significant differences between wild type AC controls and the transgenic varieties, $P < 0.05$, $^{**}P < 0.01$, and $^{***}P < 0.001$ are designated by *, **, and ***, respectively.

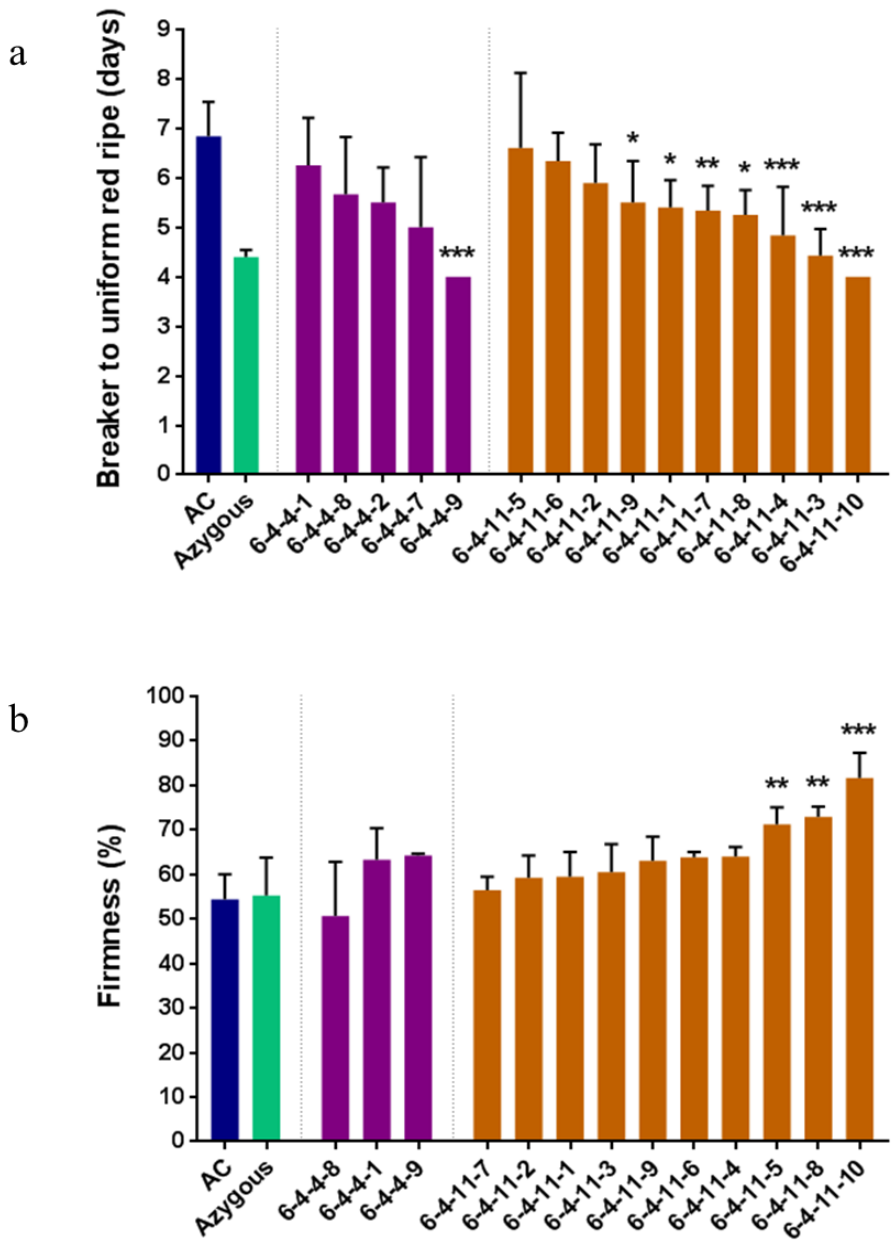

Figure 4-8 Ripening-related colour development and fruit firmness screening of the T_2 population.

Assessment of ripening-associated colour development (a) and fruit firmness (b) enabled the selection of the most improved lines, in addition to confirming the results obtained for the T_1 generation. Colour-related rapidity of ripening represents visual determination of the time taken for fruits to transition from breaker to uniform red. Fruit softening was measured at fourteen days post breaker using a fruit firmness meter; four measurements were taken per fruit. For both analyses between two and nine representative fruit were studied. Each transgenic individual is represented by a single column. A total of two and nine individuals were combined for azygous and AC controls, respectively. Statistical determinations are shown as mean ± SD, Dunnett's test analysis illustrates statistically significant differences between AC controls and the transgenic varieties, $P < 0.05$, $^{**}P < 0.01$, and $^{***}P < 0.001$ are designated by *, **, and ***, respectively.

4.2.2.3 Detailed developmental-related phenotypic characterisation of the most improved individuals

Figure 4-7 and 4-8 were used to select the most consistently improved phenotypes, focusing on positively altered fruit quality and yield. More detailed characterisation was then conducted to explain the altered phenotypes observed. Firstly, yield-related traits were studied and demonstrated no consistent trend to either fruit size or total fruit yield (Figure 4-9a). Although, three transgenic lines exhibited a 43-66% yield increase relative to AC controls, while a larger 96-129% elevation to yield was observed when compared to azygous lines. The same three lines demonstrated a significant 25- 42% increase to fruit size compared to both controls (student's t-test). Larger fruits were also identified for 6-4-4-9, 6-4-11-4 and 6-4-11-3 indicating that increased fruit size was more consistent in comparison to altered total fruit yield. Fruit set phenotypes were also assessed (Figure 4-9b). Interestingly, transgenic lines on average produced 11.0 and 13.4 fewer flowers compared to both AC and azygous controls, respectively. Compared to AC, the majority of transgenic lines yielded less fruit; however no consistent trend could be identified. Conversely, transgenic lines produced 7.4 more fruit on average compared to azygous controls. The result reveals that transgenic lines have the highest fruit set (41%) compared to both AC (36%) and azygous (19%) controls. Figure 4-9 demonstrates that the potential yield increases compared to azygous controls are due to improved fruit set and the production of larger fruits, while only the latter seems to be influencing the yield improvements when compared to AC controls.

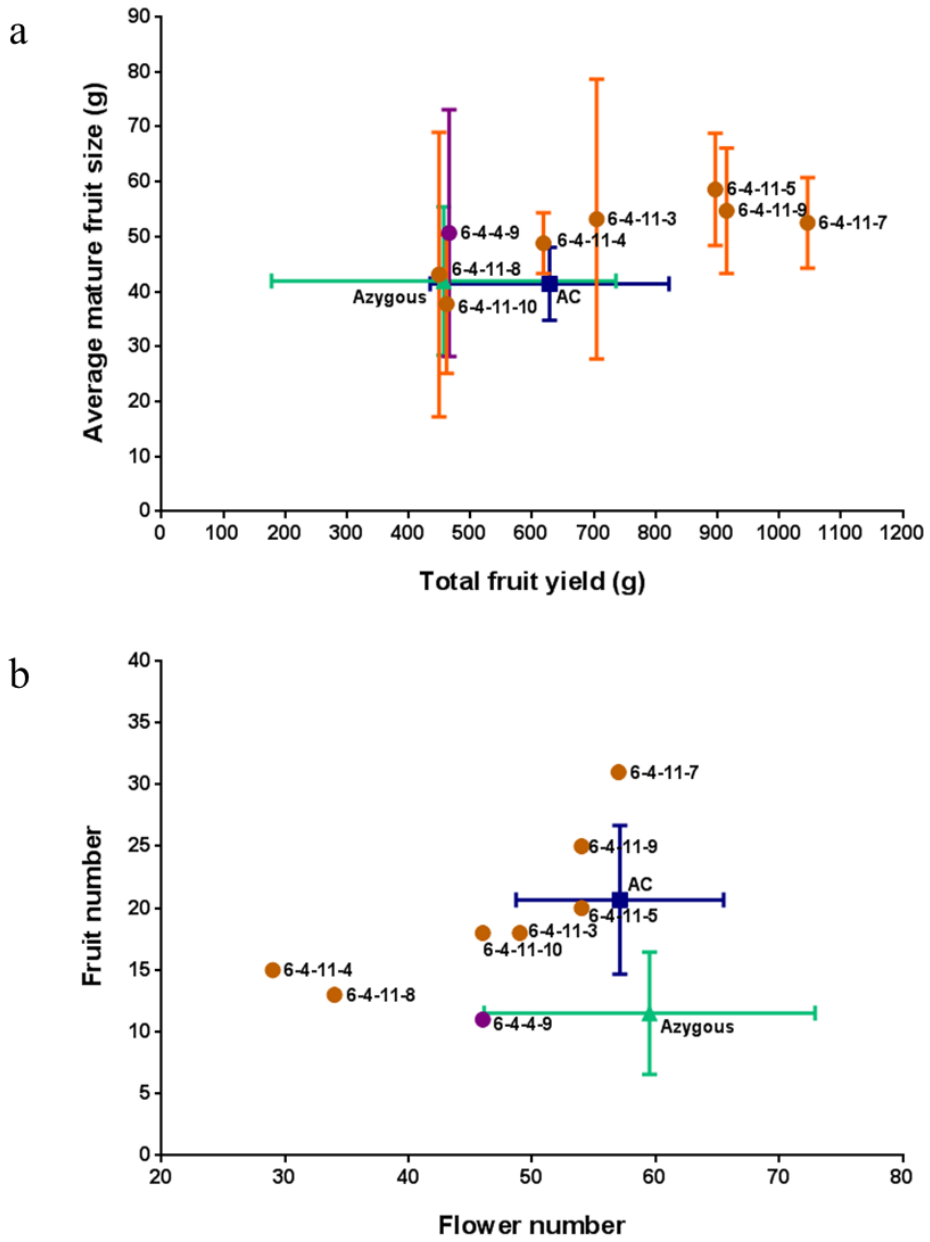

Figure 4-9 Assessment of fruit yield, size and set phenotypes for the most improved *ZPR1* transgenic lines.

Total fruit yield and average ripe fruit size were correlated (a) to assess the fruit yield-related phenotypes. Fruit set was evaluated by determination of flower and fruit number (b). Only selected transgenic lines with the most improved yield and quality traits are shown. Ten representative fruits weights were combined for this analysis. Fruit weights were determined individually postharvest and combined to determine total fruit yield. Fruit parameters were measured once the wild type AC background had formed five trusses. Each transgenic individual is represented by a single point. A total of two and nine individuals were combined for azygous and AC controls, respectively. Statistical determinations are shown as mean ± SD.

Truss morphology was studied to investigate whether altered flowers per truss and truss forking phenotypes were contributing to the reduction to flower numbers, identified in transgenic lines. Figure 4-10a demonstrates that transgenic lines on average produce fewer flowers per truss when compared to azygous controls, while no consistent differences were identified relative to AC controls. The result prompted the assessment of truss forking (Figure 4-10b), which is defined by a singular truss axis that splits into multiple axes capable of yielding more flowers. Transgenic lines trusses' split on average 1.7 times compared to 1.3 and 2.3 for AC and azygous controls, respectively. The results from Figure 4-10 indicate that transgenic lines and AC controls share similar truss morphology. However, increased forking likely contributes to elevated flower number in azygous controls, potentially negatively impacting fruit set. The transgenic line 6-4-11-3 yields the most flower numbers per truss and average truss split score of any line. However, this did not result in increased fruit yield as fruit set remains fairly low in comparison to other transgenic lines standing at 36%. Therefore, it is predicted that 6-4-11-3 exhibits a similar trend to azygous lines, whereby elevation of flower number through alteration of truss morphology fails to enhance yield or fruit set.

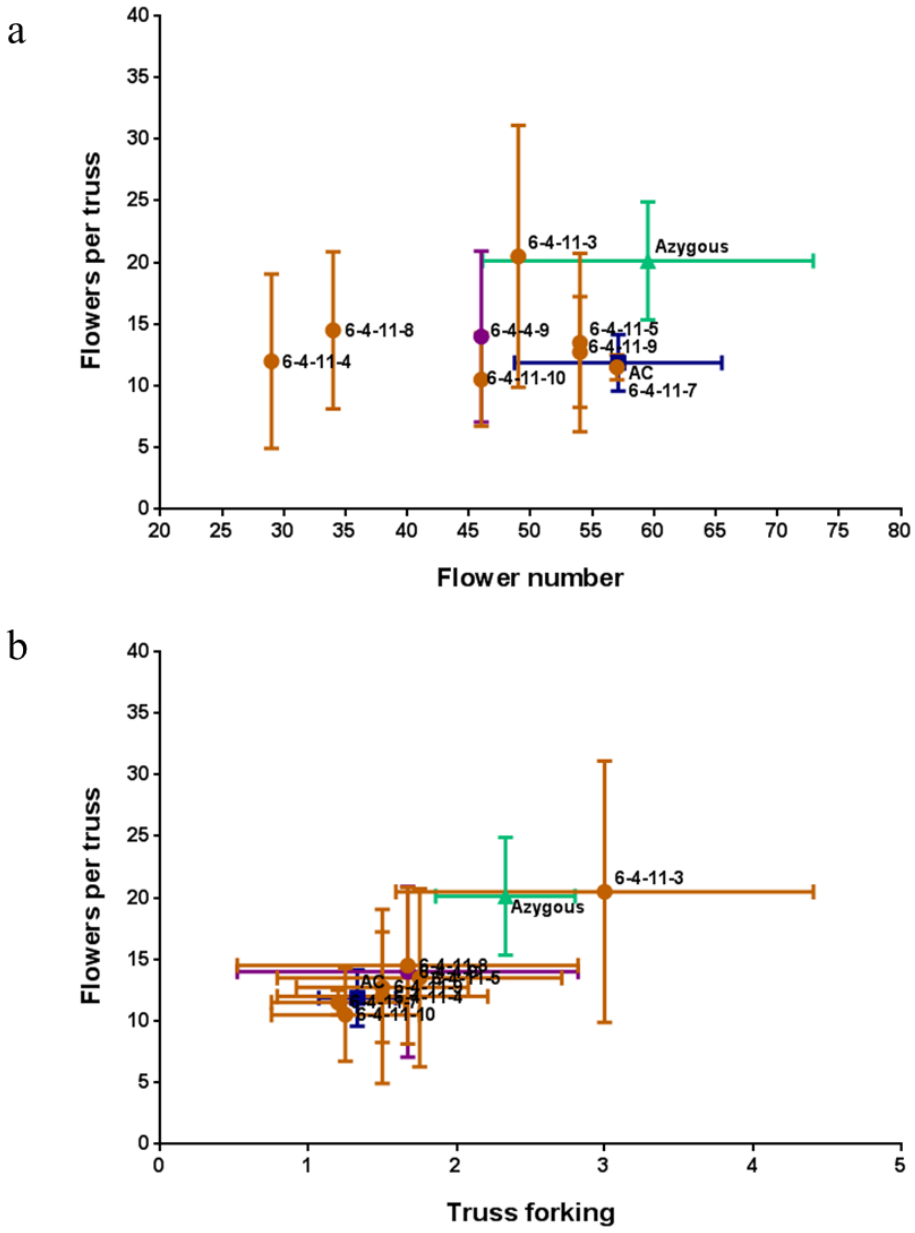

Figure 4-10 Phenotypic assessment of truss morphology for the most improved *ZPR1* transgenic lines.

The number of flowers per truss and total flower number were correlated (a), and then flowers per truss and truss forking were compared (b). These phenotypic traits were used as markers for evaluating altered flower development in relation to truss architecture. Truss forking is defined by a singular truss axis that splits into multiple axes capable of yielding flowers. A minimum of four trusses were combined for both analyses. Fruit parameters were measured once the wild type AC background had formed five trusses. Each transgenic individual is represented by a single point. A total of two and nine individuals were combined for azygous and AC controls, respectively. Statistical determinations are shown as mean ± SD.

Transgenic lines exhibited a more condensed plant morphology in comparison with AC controls. This is demonstrated by the clear separation of transgenic lines away from AC controls (Figure 4-11). On average transgenic lines had a reduced internode length of 2.7 cm and a plant height of 42.8 cm when compared to AC controls. Comparisons with azygous controls reveal no consistent changes to either plant internode length or total plant height.

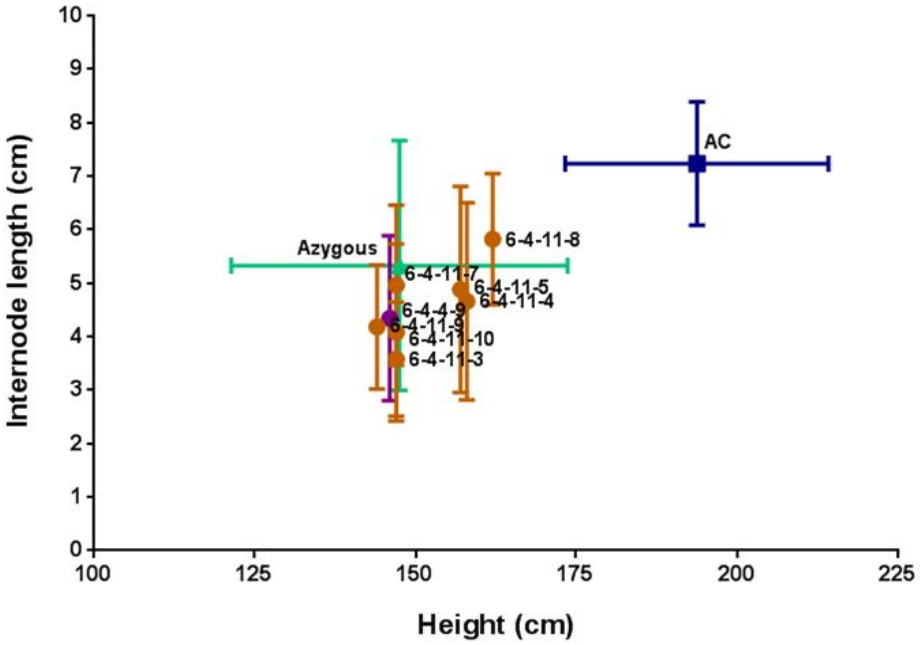

Figure 4-11 Phenotypic assessment of plant height and internode length for the most improved *ZPR1* transgenic lines.

Both plant height and internode lengths were recorded once the wild type AC background had formed five trusses. Five random internodes were measured from the base of the plant to the last node. Each transgenic individual is represented by a single point. A total of two and nine individuals were combined for azygous and AC controls, respectively. Statistical determinations are shown as mean ± SD.

4.2.2.4 Detailed ripening-related phenotypic characterisation of the most improved individuals

As demonstrated previously, transgenic lines exhibited increased ripening-related colour transition, combined with the potential to delay fruit softening. Fruits from selected transgenic lines took on average 1.8 days less compared to AC controls to appear ripe, shown by the presence of a uniform red colouration (Figure 4-12a). Despite this, no observable difference was detected when comparing to azygous controls. Assessment of transgenic fruit firmness (Figure 4-12b) revealed only small changes at both mature green and breaker stages. However, more dramatic increases to fruit firmness were recorded post breaker compared to both controls, as transgenic fruit exhibited a reduced rate of fruit softening during ripening. At seven days post breaker transgenic fruits were 9% (1.1-fold) firmer compared to AC controls, and 7% (1.1-fold) to azygous lines. The differences are extended as fruits progress to 14 dpb, where fruits from transgenic lines are 12% (1.2-fold) and 10% (1.2-fold) firmer compared to AC and azygous lines, respectively.

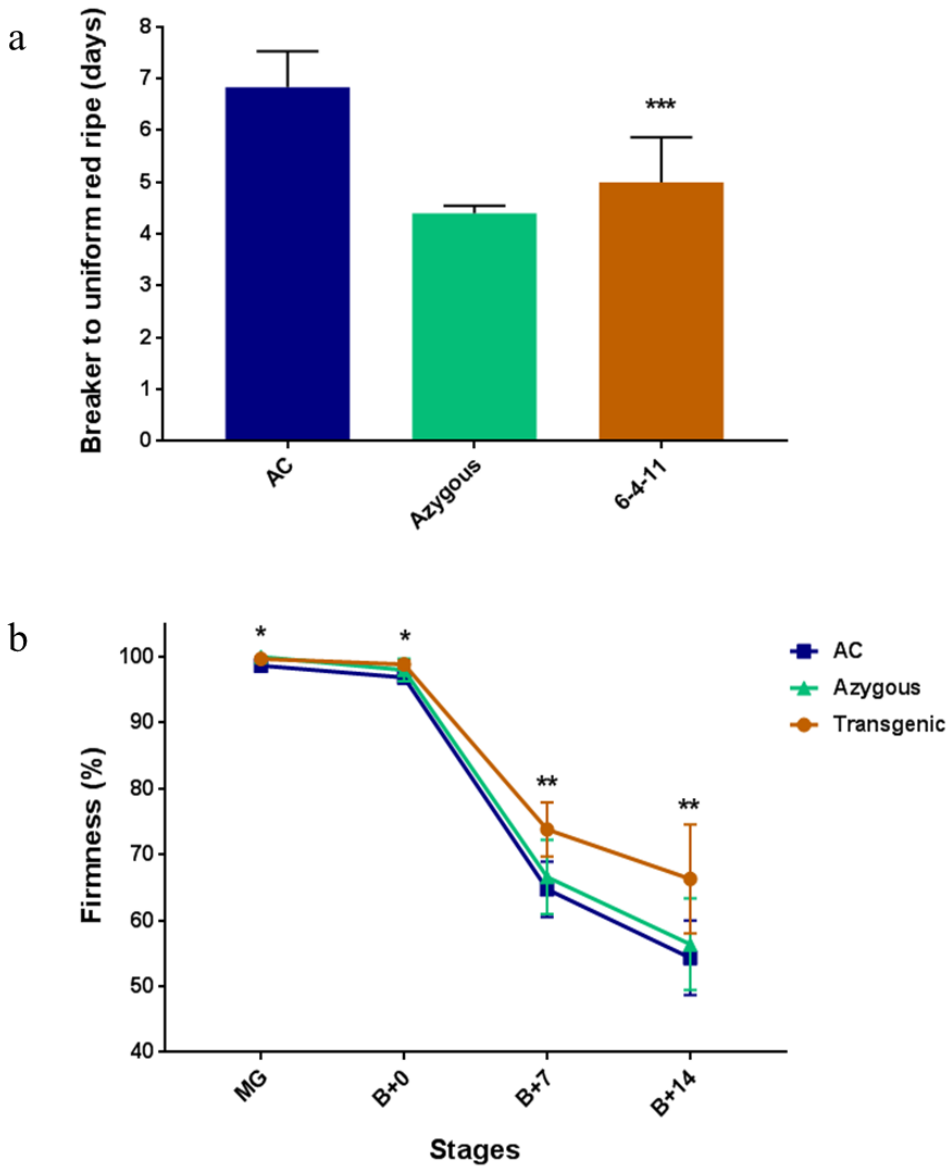

Figure 4-12 Combined ripening-related colour development and fruit firmness of most improved *ZPR1* individuals.

Ripening-associated colour development (a) and fruit firmness (b) quality traits of the most phenotypically improved individuals. Colour-related rapidity of ripening represents visual determination of the time taken for fruits to transition from breaker to uniform red. Fruit softening was measured at multiple stages post breaker using a fruit firmness meter; four measurements were taken per fruit. For both analyses between two and nine representative fruit were studied. Transgenic values incorporate the most improved eight individuals. A total of two and nine individuals were combined for azygous and AC controls, respectively. Statistical determinations are shown as mean ± SD, Dunnett's test analysis illustrates statistically significant differences between AC controls and the transgenic varieties, $P < 0.05$, **$P < 0.01$, and ***$P < 0.001$ are designated by *, **, and ***, respectively.

4.2.2.5 Parallel experiment to determine potential yield improvements and probe penetration tests to establish differences to inner and outer pericarp firmness

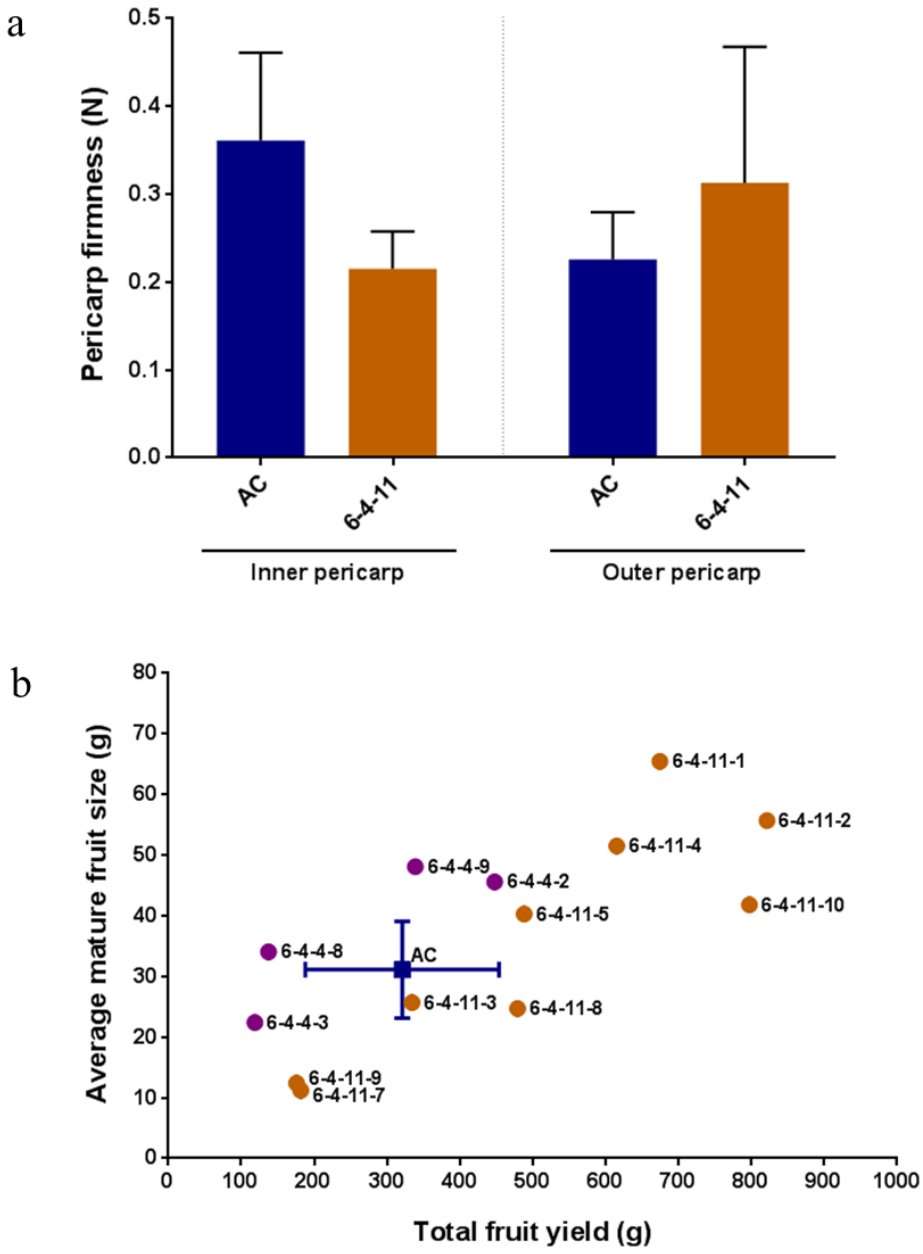

Figure 4-13 Assessment of fruit yield phenotypes and probe penetrations tests to determine firmness of ripe pericarp tissues.

Probe penetration tests were conducted to assess the firmness of the outer and inner pericarp tissues (a), while total fruit yield and average ripe fruit weight were recorded to evaluate yield-related phenotypes (b). Both were conducted at the University of Nottingham. For the probe penetration tests a minimum of three representative fruit were harvested per line. A 6-mm transverse section was cut from each fruit, probe penetration tests recorded the maximum load

required to penetrate the pericarp tissue at 10 mm min−1. Measurements were taken separately from the outer and inner pericarp in duplicate. Outer pericarp tissues were defined as being below the skin but before the vascular boundary. Inner pericarp represents the cells between the vascular boundary and the endodermis. Probe penetration method is described in section 2.1.6. For yield-related phenotypes, each transgenic individual is represented by a single point. A total of nine individuals were combined AC controls. Statistical determinations are shown as mean ± SD values. A *t test* analysis illustrates statistically significant differences (denoted $P < 0.05$) from the AC controls.

Preliminary probe penetration tests were conducted by myself at Nottingham University to ascertain whether there were any differences to the firmness of the outer or inner pericarp tissues from ripe fruit. A Lloyd Instrument LF calculated the maximum load required to penetrate the pericarp tissues at 10 mm min^{-1}. Tests detected a 1.7-fold reduction to inner pericarp firmness and a 1.4-fold increase to outer pericarp firmness in transgenic lines, although both proved nonsignificant to AC controls (Figure 4-13a).

The parallel yield experiment conducted at University of Nottingham (Figure 4-13b) provided similar results to that recorded at Royal Holloway (Figure 4-7). Overall, 70% of transgenic lines displayed increases to fruit yield. A total of 23% of transgenic lines had over double the fruit biomass output of AC controls, highlighting the potential to provide significant improvements to fruit yield. Furthermore, increased fruit size was again shown by the majority of transgenic lines, contributing to yield increases. Importantly, the consistency between the results obtained at different locations provides further evidence for the improvement of both fruit yield and size in transgenic lines.

4.2.2.6 Selection of lines with most improved fruit yield and ripening-related quality traits

Potential developmental and ripening-related functions were demonstrated by the genotypic and phenotypic screening conducted, supporting the results obtained in the previous generation. The identification of azygous controls and subsequent propagation in the next generation will enable comparisons with true controls, potentially providing more accurate characterisation of the transcription factor. The results demonstrated improvements to ripening-related colour development, combined with the potential to

delay fruit softening. Therefore, *ZPR1* transcription factor manipulation could maintain *rin* associated quality of reduced softening, in addition to improving ripening-related colour transition. Furthermore, the results confirmed that selection of the best lines was successful, providing more consistent ripening-related improvements. The lines 6-4-11-7 and 6-4-11-9 were selected for the next generation as they provided the most consistent improvements to colour development, fruit firmness and yield.

4.2.3 Metabolite profiling combined with phenotypic evaluation of plant morphology, fruit development and post-harvest quality of the T_3 generation

4.2.3.1 The effect of the insertion of the *ZPR1* transgene on isoprenoid content in ripe fruit

Ripe fruit carotenoid profiles from ZPR1 transgenic lines (Table 4-1) display several similarities with ZFPIDD2 down-regulation (Table 3-3), exhibiting increases to carotenoids upstream of lycopene cyclisation. These increases contribute to the significantly elevated total carotenoid content compared to both azygous and AC controls, 1.1- and 1.3-fold, respectively. Consistent significant increases were identified for phytoene (1.1-fold) and phytofluene (1.1-fold) compared with azygous controls, while larger increases to lycopene (1.3-fold) were observed. Likewise, elevated phytoene (1.8-fold), phytofluene (1.4-fold) and lycopene (1.8-fold) were identified in comparison to AC controls. While β-carotene content was significantly reduced in transgenic lines (1.2-fold) compared with AC controls. All other carotenoids, tocopherols and phylloquinone identified by UPLC remained unchanged.

Line	AC	Azygous	6-4-11-7	6-4-11-9
Lutein	531.1 ± 9.5	523.1 ± 8.6	522.4 ± 13.4	521.8 ± 14.0
Lycopene	1822.4 ± 161.6	2531.7 ± 649.7	**3258.2 ± 366.2*** **	**3225.7 ± 520.2** **
γ-carotene	728.6 ± 13.1	718.1 ± 12.1	724.0 ± 18.2	719.9 ± 17.6
β-carotene	873.5 ± 29.4	764.4 ± 13.6	759.8 ± 20.5	757.8 ± 20.0
ζ-carotene	720.6 ± 13.4	717.7 ± 12.0	724.6 ± 17.7	722.1 ± 16.7
Phytofluene	319.4 ± 7.4	392.9 ± 31.1	**421.8 ± 19.5***	**445.6 ± 25.6*** **
Phytoene	185.8 ± 8.4	308.8 ± 41.7	317.4 ± 28.6	**368.1 ± 36.5** **
Total CAR	5181.6 ± 165.8	5956.7 ± 725.4	**6728.3 ± 404.6** **	**6761.0 ± 521.1** **
α-Tocopherol	388.4 ± 32.8	409.7 ± 38.4	405.1 ± 15.1	405.5 ± 17.6
δ-tocopherol	262.0 ± 9.5	255.8 ± 19.3	251.5 ± 8.6	254.9 ± 8.9
Total TOCO	650.4 ± 41.4	665.5 ± 57.2	656.6 ± 20.2	660.4 ± 24.1
Phylloquinone	194.3 ± 27.7	197.9 ± 23.1	205.5 ± 20.1	211.7 ± 13.5

Table 4-1 Carotenoid, tocopherol and phylloquinone composition of *ZPR1* transgenic ripe fruit compared to both controls.

Carotenoid, tocopherol and phylloquinone contents are presented as μg/g DW. A minimum of five representative fruits from a minimum of three plants were used. Fruits were pooled and three determinations were made, ensuring a minimum of three biological and three technical replicates. Methods used for these determinations are described in section 2.3. The mean data are presented ± SD, with n=9. Dunnett's test analysis illustrates statistically significant differences between non-transgenic azygous controls and the transgenic varieties, $P < 0.05$, $^{**}P < 0.01$, and $^{***}P < 0.001$ are designated by *, **, and ***, respectively.

4.2.3.2 Post-harvest assessment of ripening-associated fruit quality of transgenic lines

In previous generations, transgenic lines exhibited accelerated ripening-related colour transition and reduced fruit softening phenotypes when compared to AC controls. Therefore, it was important to establish whether these improved quality traits were maintained post-harvest, when fruits ripened off the plant. In order to limit variation, fruits were harvested at the same time point during ripening, at breaker stage, before being stored following common commercial practices outlined in section 2.1.5.

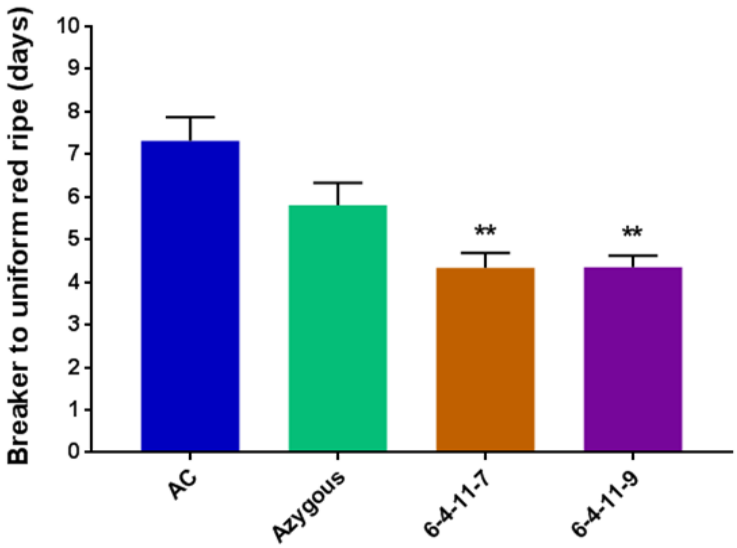

Figure 4-14 Comparison of the rapidity of post-harvest fruit ripening determined by the presence of a uniform red colouration.

Representative fruit were harvested at breaker, sterilised and stored separately at room temperature. The rapidity of ripening was compared for transgenic lines, and both non-transgenic (azygous) and wild type (AC) controls. Fruits were judged to be ripe upon visual determination of the presence of a uniform red colouration. Five fruits per plant were analysed, a minimum of three individual plants were studied for each line. This ensured the study included a minimum of five technical replicates and three biological replicates. Methods are described in section 2.1.5. Statistical determinations are shown as mean ± SD values, Dunnett's analysis illustrates statistically significant differences (denoted $P < 0.05$, $^{**}P < 0.01$, and $^{***}P < 0.001$) from the non-transgenic controls.

The time fruits took to ripen post-harvest was studied by visual determination of a uniform red colouration (Figure 4-14). Transgenic lines displayed more rapid colour transition from breaker to red ripe, taking on average just 4.3 days in comparison to 5.8 and 7.3 days for both azygous and AC controls, respectively. Thus, colour-related ripening time from breaker was reduced by 1.5 days compared to azygous and 2.0 days to AC controls. Post-harvest ripening-related colour development of the fruit harvested at breaker was monitored in more detail using a colourimeter, utilising the CIELAB sphere, defining colour along three perpendicular axes: L* (from white to black), a* (green to red) and b* (blue to yellow). The L* score quantified the relative darkness or lightness of fruits, with higher values indicating elevated brightness. L* scores decreased with progression through ripening (Figure 4-15a), in accordance with literature. No consistent significant differences were identified between transgenic and azygous fruits. However, transgenic fruits exhibited significant reductions at B+5 (1.1-fold) and B+7 (1.1-fold) when compared to AC controls.

This quantitative approach identified that A* contributed most to the altered ripening time exhibited by transgenic lines (Figure 4-15). The A* score determined the changes along the green-red axis, with negative and positive values representing green and red colouration, respectively. More rapid colour transition from green to red were seen in transgenic fruits, indicated by a sharper rise to A* scores (Figure 4-15b). Compared to azygous controls, transgenic lines exhibited significant increases to A* scores at all stages post B+0; the largest difference was a 2.2-fold increase at B+3. Increased A* scores were also identified at B+5 (2.0-fold), B+7 (1.7-fold), B+9 (1.6-fold) and B+14 (1.3-fold). A large 35-fold increase to A* score at B+3 was identified in transgenic fruits compared to AC controls. From B+3 onwards, elevated A* scores were observed at B+5 (2.3-fold), B+7 (2.2-fold), B+9 (1.8-fold) and B+14 (1.7-fold). The fold changes to A* scores at the later stages of ripening mirror the lycopene differences identified in transgenic lines. Therefore, increased lycopene biosynthesis is expected to contribute to sharp rise to A* scores at B+3, and the darker red colouration of ripe fruits post ripening. Additionally, the A* scores confirmed the accuracy of the visually assessed ripening times for transgenic and control lines. Using the different visually assessed ripening times for transgenic and control lines, and the A* curves, prediction of an A* value indicating ripe fruit was calculated. The y axis intercept values between all lines displayed a small variation; indicating that visual determination of colour associated ripening time was consistent. Overall, the results confirmed reduced ripening time and darker fruit phenotype of transgenic lines.

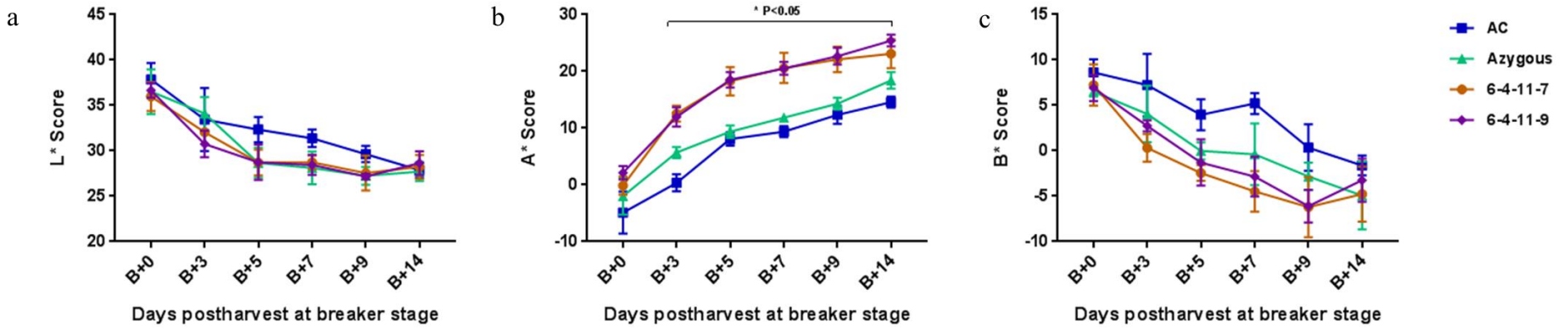

Figure 4-15 Study of post-harvest ripening-related colour development using a colourimeter.

Representative fruit were harvested at breaker, sterilised and stored separately at room temperature. A colourimeter monitored colour transition for down-regulated transgenic lines and both non-transgenic (azygous) and wild type (AC) controls. The colourimeter used the CIELAB colour sphere to monitor fruit ripening-related colour development across six specific time points throughout ripening, from breaker (B+0) to breaker plus fourteen days (B+14). Each panel indicates the numerical expression of colour along three separate axes: L*, A* and B* (from white to black; green to red and blue to yellow, respectively). Four colourimeter measurements were taken per fruit, per time point, with five fruits analysed per plant. A minimum of three individual plants were studied for each line. This ensured the study included a minimum of five technical replicates and three biological replicates. Methods are described in section 2.1.5. Statistical determinations are shown as mean ± SD values, Dunnett's analysis illustrates statistically significant differences (denoted $P < 0.05$) between all transgenic lines and the non-transgenic controls azygous controls.

The B* scores decreased throughout ripening, indicating that fruits transitioned from yellow to a more blue coloration (Figure 4-15c). Transgenic fruits generally exhibited reduced B* scores compared to both controls (Figure 4-15c), although comparison with azygous controls revealed no statistically significant differences. However, consistent significant reductions were identified at B+5 (2.1-fold), B+7 (1.4-fold) and B+9 (17.5-fold) when compared to AC controls.

While colour development was studied using a colourimeter, fruit firmness was monitored throughout ripening until overripe stages (Figure 4-16). Both 6-4-11-7 and 6-4-11-9 transgenic lines exhibited a reduced rate of fruit softening compared to both controls (Figure 4-16a). Compared with azygous lines, transgenic fruits were significantly firmer from 0 dpb until 10 dpb, along with fruits at 12 dpb. Transgenic fruits at breaker stage were on average 4% (1.1-fold) firmer compared to azygous controls, the differences extended to 13% (1.2-fold) and 16% (1.3-fold) at 4 and 7 dpb, respectively. The largest fold change was identified at 8 dpb, with transgenic fruit being on average 17% (1.4-fold) firmer. By 10 dpb transgenic fruits displayed a 12% (1.3-fold) increase in firmness, falling to 6% (1.2-fold) by 14 dpb when compared to azygous controls. The differences between transgenic and azygous fruits then remained consistent, around 1.3-fold, until 21 dpb. Similar differences were observed between both transgenic lines and AC controls.

As mentioned previously, fruits are generally required to reach red ripe before being sold to consumers, reaching the acceptable quality demands required from an industry, supplier and consumer prospective. Therefore, Figure 4-16b accounts for the altered ripening time required for fruits to reach a uniform red colouration between transgenic and control varieties. In this study acceptable firmness-related quality was defined as being above 50%, providing a threshold value to determine any potential extensions to shelf-life. Both AC and azygous controls dropped below this threshold 1 day post ripe, while transgenic fruit took on average 7 days for firmness to fall below 50%. Therefore, more dramatic firmness differences were identified through comparisons of post ripe fruits rather than those at breaker stage, with transgenic fruit displaying reduced softening when compared to both controls, with a potential 6 day extension to shelf-life. Also, fruit weights were monitored daily to identify potential changes to water loss contributing to increased firmness, however, no observable changes were detected between transgenic and controls lines (not shown).

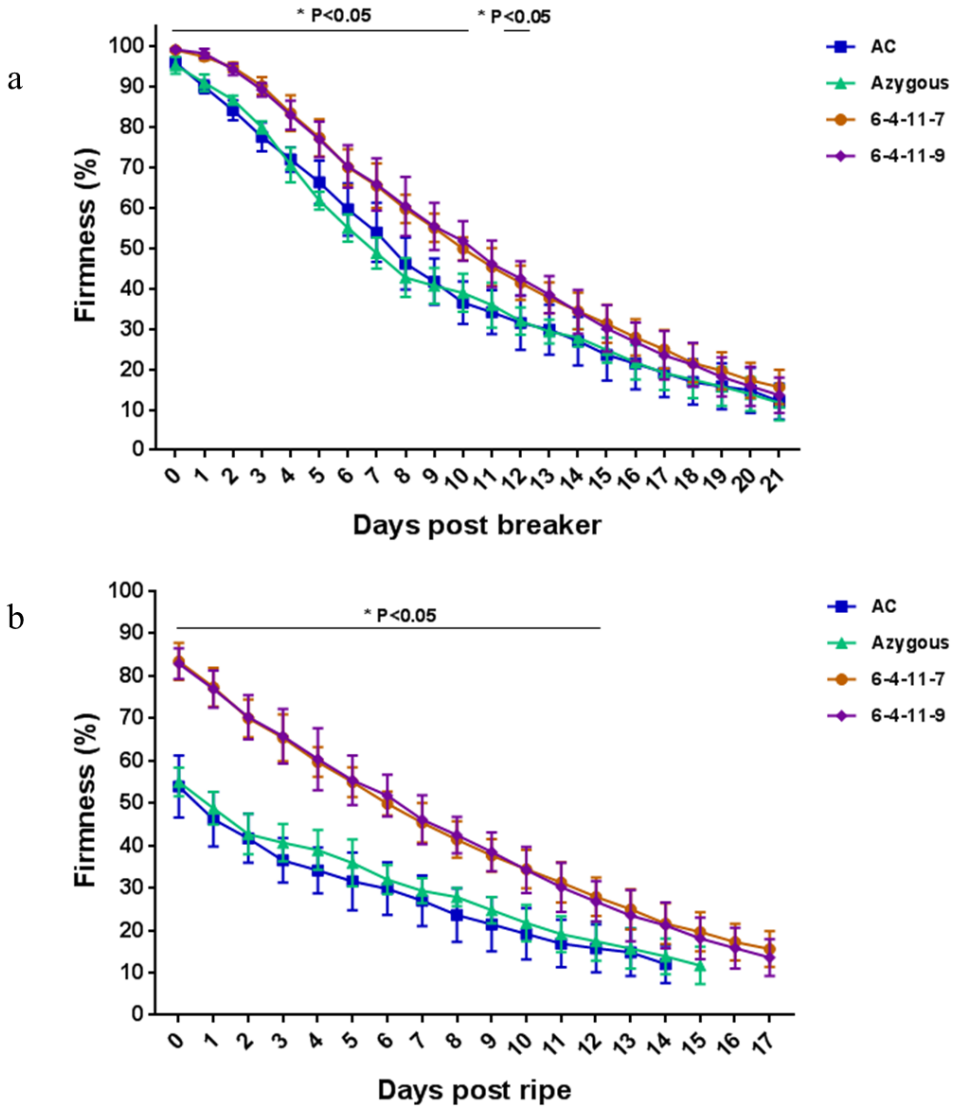

Figure 4-16 Altered rate of postharvest fruit softening.

Representative fruit were harvested at breaker, sterilised and stored separately at room temperature. Softening was monitored throughout ripening between transgenic lines and both azygous and AC controls. Firmness values given represent the percentage firmness remaining as measured by a fruit firmness meter. Firmness was compared at breaker (a) or post ripe (b) in line with retailer and consumer quality assessment, accounting for altered ripening times for each genotype. Four random points were recorded per time point, five fruits analysed per plant and a minimum of three individual plants from each line were combined for the analyses. This ensured the study included a minimum of five technical replicates and three biological replicates. Methods are described in section 2.1.5. Statistical determinations are shown as mean ± SD values, Dunnett's analysis illustrates statistically significant differences (denoted $P < 0.05$) between all transgenic lines and the non-transgenic controls azygous controls.

Fruit development and plant morphology phenotypes were compared for transgenic lines with both azygous and AC controls (Figure 4-17 and Figure 4-18). Small reductions to plant height were observed in transgenic lines, on average 6-4-11-9 lines were significantly shorter by 27.5 cm compared to azygous lines (Figure 4-17a). Larger reductions to internode lengths were exhibited in transgenic lines, on average internodes were reduced by 1.8 cm and 2.0 cm compared to azygous and AC controls, respectively (Figure 4-17b). Despite a more compact plant architecture, non-vegetative biomass remained unchanged compared to both controls (Figure 4-17c). Fruit development phenotypes were also studied (Figure 4-18), to determine whether transgenic lines had any changes to fruit yield. No consistent differences were detected for average total fruit number, fruit weight or total fruit yield compared to both azygous and AC controls. The only significant difference identified was to 6-4-11-7, which significantly yielded 27 more fruit compared to AC controls. However, this failed to improve fruit yield as these lines on average had a reduced average fruit biomass. Harvest index remained unchanged, when compared to both azygous and AC controls.

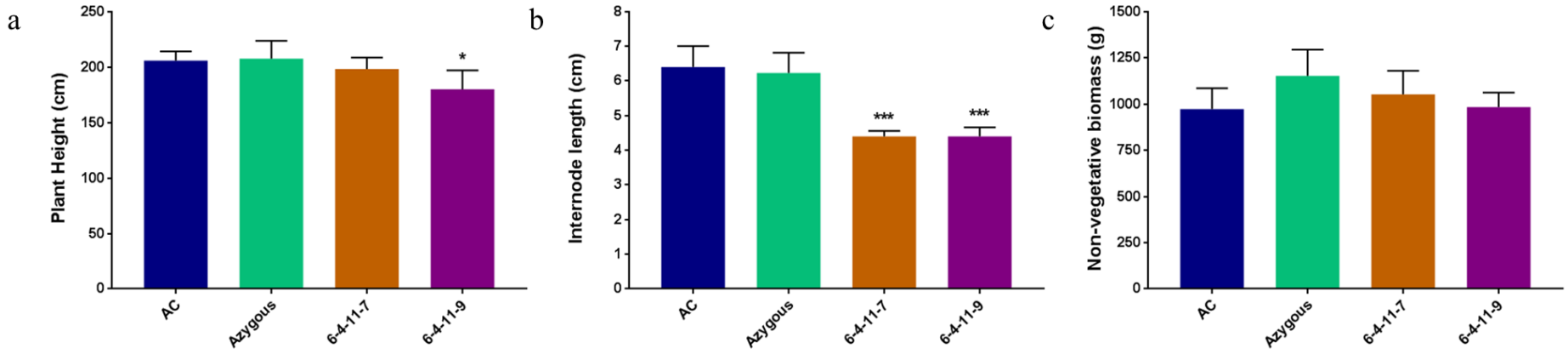

Figure 4-17 Plant morphology phenotypes during development.

Differences to plant morphology were determined by analysis of plant height (a), internode length (b) and non-fruiting biomass (c) for transgenic lines, compared with non-transgenic (azygous) and wild type (AC) controls. The plant developmental parameters were measured once the wild type background had formed five trusses with fruit set. Total plant height was measured from the soil to last node; twelve random internodes were measured from base of the plant to the last node. Non-fruiting biomass combined the tallying of shoot cuttings during development prior to senescing, and the remaining total leaf and stem weights post harvesting of all fruits. A minimum of three plants per genotype ensured that three separate biological replicates were used for the analysis. Statistical determinations are shown as mean ± SD values, Dunnett's test analysis illustrates statistically significant differences (denoted $P < 0.05$, $^{**}P < 0.01$, and $^{***}P < 0.001$) from the non-transgenic controls.

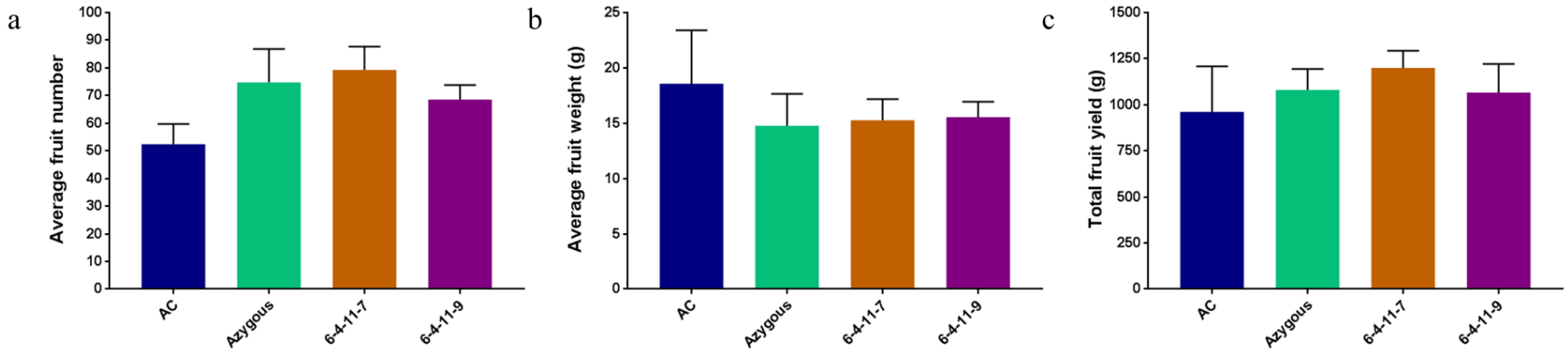

Figure 4-18 Using total fruit number, average fruit weight and total fruit yield as markers for altered fruit set and development.

Total fruit number (a), average fruit weight (b) and total fruit yield (c) phenotypes were recorded to test whether transgenic lines had altered fruit set and fruit growth compared to both non-transgenic (azygous) and wild type (AC) controls. All parameters were measured once the wild type background had formed five trusses with fruit set. All fruit weights were recorded individually postharvest and combined to determine total fruit yield. A minimum of three plants per genotype ensured that three separate biological replicates were used for the analysis. Statistical determinations are shown as mean ± SD values, Dunnett's test analysis illustrates statistically significant differences (denoted $P < 0.05$, $^{**}P < 0.01$, and $^{***}P < 0.001$) from the non-transgenic controls.

4.2.3.3 Broader metabolism differences arising from the insertion of the *ZPR1* transgene

The post-harvest experiments revealed a partial uncoupling of ripening, thus metabolite perturbations beyond the isoprenoid pathway were expected. The UPLC platform was used to determine differences to the phenolic content of ripe fruits. While the Gas Chromatography-Mass Spectrometry (GC-MS) platform was utilised to generate a metabolite profile of ripe fruits, screening the broader effects to metabolism in transgenic lines. Therefore, a combination of analytical platforms and methods, with different phase extractions, coupled with different loadings enabled identification and quantification in a relative or absolute manner of over 95 metabolites. Metabolome comparisons were made between transgenic lines and both non-transgenic azygous and wild type (AC) controls (as described in section 2.3). Statistical determinations were made to assess the differences between genotypes (as described in section 2.4). Significant (p-value <0.05) changes to metabolite levels were identified in most classes of compounds analysed (Table 4-2). The altered isoprenoid levels in different tissues of ripe fruits have been described in section 4.2.3.1. Transgenic fruit exhibited increases to the majority of amino acids, resulting in a nonsignificant 1.1-fold and a significant 1.3-fold increase compared to azygous and AC controls, respectively. Significant increases to 5-oxo-proline, alanine, aspartic acid, glutamic acid and serine were observed in transgenic fruit compared with both controls, contributing to the rise in amino acids. Compared with azygous lines, further increases to isoleucine and proline were identified. Furthermore, methionine levels were elevated 1.9-fold and 5.0-fold compared to both azygous and AC controls, respectively, with the latter proving significant.

Total amyrin content was significantly elevated 1.6-fold in transgenic lines compared with azygous controls, although only a nonsignificant 1.2-fold increase was observed when compared to AC controls. Elevated α-amyrin and β-amyrin contributed to the increases observed in transgenic lines, however the only significant alteration was a 1.6-fold rise to α-amyrin compared to azygous controls.

Total fatty acid content remained unchanged, despite significant reductions to several forms compared to both controls. C16:0, C17:0 and C24:0 were significantly reduced in transgenic lines compared with azygous controls, similarly, significantly less C18:2 trans9,12, C24:0 content was identified when compared to AC controls. Total organic acid content was reduced 1.1- and 1.8-fold compared with both azygous and AC

controls, respectively. Both malic and succinic acid levels were significantly lower compared to both controls, the latter displaying between 25.5- and 30.8-fold reductions. Comparisons between transgenic and AC lines revealed further significant reductions to aconitic acid, citric acid, gluconic acid, gucuronic acid and itaconic acid.

Significant differences to both glucose-6-phosphate and glycerol-3-phosphate were identified in both controls. Despite several differences to both controls total sugar content remained unchanged in transgenic lines. Compared to azygous controls, transgenic lines exhibited significant increases to stigmasterol, inositol, galactose and sucrose, in addition to multiple reductions including putrescine and ribose. Similarly, comparisons with AC revealed significant increases to nonacosane, pentose, trehalose and xylulose, and reductions to gamma-aminobutyric acid (GABA), inositol-6-phosphate and sitosterol.

The UPLC platform was also used to screen the phenolic content of ripe fruits (Table 4-2), relative to an internal standard. Multiple significant differences were identified in transgenic lines compared to both controls, although total phenolic content remained unchanged. Interestingly, n-chlorogenic was the most abundant form of chlorogenic acid in both controls; however, it was not detected in in transgenic lines. Therefore, large fold decreases to n-chlorogenic is predicted. Similarly, transgenic lines exhibited significant 1.8- and 2.6-fold reductions to cryptochlorogenic acid when compared to azygous and AC controls, respectively. Conversely, neochlorogenic acid was the least abundant chlorogenic acid form, and transgenic lines displayed significant increases between 1.62- and 3.8-fold compared to both controls. Overall, total chlorogenic acid content was significantly reduced in transgenic lines compared to azygous (3.2-fold) and AC (3.4-fold) controls.

Differences to multiple forms of flavonoids were identified. Compared to both controls, transgenic lines displayed nonsignificant reductions to naringenin content (1.5- to 2.1-fold). Comparisons with azygous controls revealed a significant reduction to kaempferol (2.3-fold), combined with small nonsignificant increases to quercitrin (1.1-fold), rutin (1.1-fold) and kaempferol-3-O-rutinoside (1.3-fold). More differences were observed when comparing transgenic and AC lines, with significant increases to both quercitrin (2.4-fold) and rutin (1.4-fold). Consistent with the comparison to azygous lines, transgenic lines exhibited significantly reduced kaempferol (2.9-fold) and a nonsignificant increase to kaempferol-3-O-rutinoside (2.1-fold) when compared to AC controls.

	Ratio	
Metabolite	Transgenic to Azy	Transgenic to AC
Amino acid		
5-oxo-proline	**1.38 ± 0.32**	**1.54 ± 0.36**
Alanine	**2.32 ± 0.47**	**1.52 ± 0.31**
Asparagine	1.15 ± 0.57	0.87 ± 0.43
Aspartic acid	**1.58 ± 0.41**	**2.69 ± 0.71**
b-Alanine	1.02 ± 0.12	1.02 ± 0.12
Cysteine	1.01 ± 0.41	0.83 ± 0.34
Glutamic acid	**1.40 ± 0.32**	**1.55 ± 0.36**
Glutamine	1.04 ± 0.68	0.87 ± 0.56
Glycine	1.26 ± 0.46	0.94 ± 0.34
Homocysteine	1.03 ± 0.15	1.20 ± 0.18
Isoleucine	**1.45 ± 0.34**	1.02 ± 0.24
Leucine	1.26 ± 0.29	0.90 ± 0.21
Lysine	1.12 ± 0.41	1.12 ± 0.41
Methionine	1.85 ± 1.86	**5.04 ± 5.07**
Proline	**1.68 ± 0.47**	0.99 ± 0.28
Serine	**1.91 ± 0.34**	**1.38 ± 0.24**
Threonine	1.34 ± 0.29	1.11 ± 0.24
Valine	1.32 ± 0.24	0.85 ± 0.16
Amyrin		
a-Amyrin	**1.61 ± 0.38**	1.32 ± 0.31
b-Amyrin	1.49 ± 0.53	1.07 ± 0.38
Fatty acid		
C14:0	1.00 ± 0.13	1.03 ± 0.14
C16:0	**0.84 ± 0.09**	0.91 ± 0.10
C17:0	**0.59 ± 0.27**	1.96 ± 0.88
C18:0	1.00 ± 0.11	1.02 ± 0.11
C18:2 cis9,12	0.83 ± 0.11	0.98 ± 0.12
C18:2 trans9,12	0.98 ± 0.40	**0.68 ± 0.28**
C20:0	0.93 ± 0.19	0.87 ± 0.18
C22:0	0.92 ± 0.18	1.06 ± 0.21
C24:0	**0.66 ± 0.21**	**0.60 ± 0.19**
Glycero-1-C14:0	0.96 ± 0.17	1.00 ± 0.18
Glycero-1-C16:0	0.98 ± 0.11	1.03 ± 0.12
Glycero-1-C18:0	0.97 ± 0.11	1.03 ± 0.11
Glycero-1-C18:2 cis9,12	1.14 ± 0.62	0.93 ± 0.50
Glycero-2-C16:0	0.97 ± 0.16	0.98 ± 0.16
Glycero-2-C18:0	0.99 ± 0.12	1.09 ± 0.13
Hydrocarbon		
Nonacosane	1.33 ± 1.17	**11.64 ± 10.25**
Hentriacontane	1.06 ± 0.47	0.90 ± 0.40
Isoprenoid		
β-Carotene	**0.99 ± 0.01**	**0.86 ± 0.01**
γ-Carotene	1.00 ± 0.01	**0.98 ± 0.01**

Lutein	**0.99 ± 0.01**	**0.97 ± 0.01**
Lycopene	**1.35 ± 0.11**	**1.87 ± 0.15**
Phytoene	**1.12 ± 0.12**	**1.87 ± 0.20**
Phytofluene	**1.11 ± 0.06**	**1.37 ± 0.08**
ζ-carotene	1.00 ± 0.01	1.00 ± 0.01
α-Tocopherol	1.00 ± 0.04	1.05 ± 0.04
δ-Tocopherol	0.98 ± 0.03	**0.96 ± 0.03**
γ-Tocopherol	**0.43 ± 0.08**	**0.22 ± 0.04**
Phylloquinone	**1.06 ± 0.04**	**1.08 ± 0.04**
Lipid		
GABA	1.10 ± 0.34	**0.62 ± 0.19**
Non amino acid N-Containing compound		
Putrescine	**0.44 ± 0.17**	0.73 ± 0.28
Organic acids		
2-oxoglutaric acid	0.81 ± 0.11	0.88 ± 0.12
Aconitic acid	0.99 ± 0.37	**0.56 ± 0.21**
Benzoic acid	0.59 **±** 0.46	0.78 **±** 0.61
Citraconic acid	1.11 ± 0.19	1.07 ± 0.18
Citric acid	0.90 ± 0.16	**0.47 ± 0.08**
Glucaric acid	0.63 ± 0.22	1.14 ± 0.40
Gluconic acid	0.96 ± 0.10	**0.80 ± 0.09**
Glucuronic acid	0.96 ± 0.12	**0.75 ± 0.09**
Itaconic acid	1.03 ± 0.14	**0.82 ± 0.11**
Lactic acid	0.96 ± 0.22	1.07 ± 0.24
Malic acid	**0.65 ± 0.12**	**0.51 ± 0.09**
Succinic acid	**0.03 ± 0.02**	**0.04 ± 0.03**
Phenolics		
n-Chlorogenic acid	**0.01***	**0.01***
Cryptochlorogenic acid	**0.55 ± 0.35**	**0.39 ± 0.25**
Kaempferol	**0.42 ± 0.17**	**0.34 ± 0.13**
Kaempferol-3-O-rutinoside	1.32 ± 0.79	2.09 ± 1.24
Naringenin	0.68 ± 0.95	0.47 ± 0.66
Neochlorogenic acid	**1.62 ± 0.54**	**3.82 ± 1.28**
Quercitrin	1.11 **±** 0.29	**2.43 ± 0.64**
Rutin	1.08 **±** 0.45	**1.41 ± 0.58**
Phosphate		
Glucose-6-phosphate	**1.16 ± 0.18**	**0.45 ± 0.07**
Glycerol-3-phosphate	**1.41 ± 0.14**	**1.48 ± 0.15**
Inositol-6-phosphate	1.17 ± 0.21	**0.63 ± 0.11**
Phosphate	0.98 ± 0.06	0.90 ± 0.05
Phytosterol		
Campesterol	0.25 ± 0.62	**0.11 ± 0.27**
Stigmasterol	**1.16 ± 0.20**	1.08 ± 0.19
Sitosterol	0.77 ± 0.24	**0.65 ± 0.20**
Polyol		

Glycerol	1.02 ± 0.25	1.90 ± 0.47
Inositol	**1.30 ± 0.14**	0.92 ± 0.10
Mannitol	0.96 ± 1.27	4.77 ± 6.29
Sorbitol	0.96 ± 1.27	4.77 ± 6.29
Pyrimidone		
Dihydrouracil	1.20 0.45	1.09 0.41
Sugar		
Arabinose	1.02 ± 0.08	1.05 ± 0.08
Erythrose	0.86 ± 0.28	1.00 ± 0.32
Fructose	0.95 ± 0.07	0.97 ± 0.07
Galactose	**1.45 ± 0.56**	0.88 ± 0.34
Glucose	1.00 ± 0.05	0.95 ± 0.05
Maltose	1.03 ± 0.35	0.73 ± 0.25
Pentose	1.08 ± 0.10	**1.08 ± 0.10**
Me-Galactose	**0***	**0.01***
Ribose	**0.61 ± 0.15**	0.82 ± 0.20
Sucrose	**2.13 ± 0.71**	1.27 ± 0.42
Trehalose	1.29 ± 0.26	**1.79 ± 0.36**
Xylose	1.02 ± 0.08	1.05 ± 0.08
Xylulose	1.44 ± 0.45	**10.22 ± 3.19**

Table 4-2 Differences to metabolites occurring in *ZPR1* transgenic ripe fruit compared to both azygous and AC controls.

Data has been compiled from multiple analytical platforms. Metabolites were quantified, then ratios were calculated and presented as mean ± SD. Student's t-test was performed, significant changes are represented in bold (p-value < 0.05). 10*, indicates the theoretical value when a metabolite is unique to transgenic at the concentration used, thus was not detected in control samples. 0.01*, indicates theoretical value when a metabolite is unique to the controls at the sample concentration used. GABA, gamma-aminobutyric acid, 5-oxo-proline, pyroglutamic acid.

Multivariate principal component analysis (PCA) enabled assessment of the overall variance in chemical composition of ripe fruits from transgenic, azygous and AC lines, whilst identifying the contributions of each metabolite to the overall variance. The score values for the PCA are represented in a score scatter plot (Figure 4-19), displaying the separation between genotypes indicating statistically significant differences between the clusters. The largest difference in chemical composition was revealed to be between both transgenic lines and AC controls, as shown by large separation between clusters. Azygous controls were demonstrated to be an intermediate between both AC and

transgenic lines. Interestingly, multivariate PCA of just azygous and transgenic lines produced two statistically different clusters, with the separation confirming a significant difference between the genotypes (Figure 4-20). Loading scatter plots displays the numerous metabolites that have significant weightings (Figure 4-19), indicating that cluster separation was due to multiple metabolites from various metabolite classes. As expected multiple isoprenoids including phylloquinone, phytoene, phytofluene and lycopene had the highest loading in transgenic fruit, as well as the sugars arabinose, pentose, xylose and xylulose. Also, two phenolic compounds, neochlorogenic acid and quercitrin, and the amino acids aspartic acid and homocysteine had the highest loadings in transgenic fruit. The same metabolites had the highest loadings when comparing just transgenic and azygous fruits, with the exception of quercitrin. Additional compounds including 5-oxo-proline, alanine, proline, isoleucine, serine, threonine, α-amyrin, citraconic acid, glucose-6-phosphate, glycerol-3-phosphate, stigmasterol, inositol, glucose, sucrose and trehalose had the highest loadings in transgenic fruits, driving the separation from the azygous controls (Figure 4-20).

For both controls the isoprenoids β-carotene, γ-carotene, lutein, γ-tocopherol and δ-tocopherol had the highest loadings (Figure 4-19). Similarly multiple organic acids including aconitic acid, citric acid, gluconic acid, glucuronic acid, malic acid, succinic acid, in addition to C24:0, glucose-6-phosphate, inositol-6-phosphate, campesterol, sitosterol, n-chlorogenic acid, cryptochlorogenic acid had the highest loadings driving separation from transgenic fruits. Removing AC enabled identification of compounds with highest loadings in azygous fruits, which caused the separation from transgenic tissues (Figure 4-20). Multiple fatty acids including C16:0, C17:0, C18:2 cis9,12 and C24:0 had the highest loading for azygous lines, in addition to the phenolics n-chlorogenic acid, cryptochlorogenic acid kaempferol. Moreover, citric acid, malic acid, succinic acid, lutein, putrescine, sitosterol and ribose contribute to the separation.

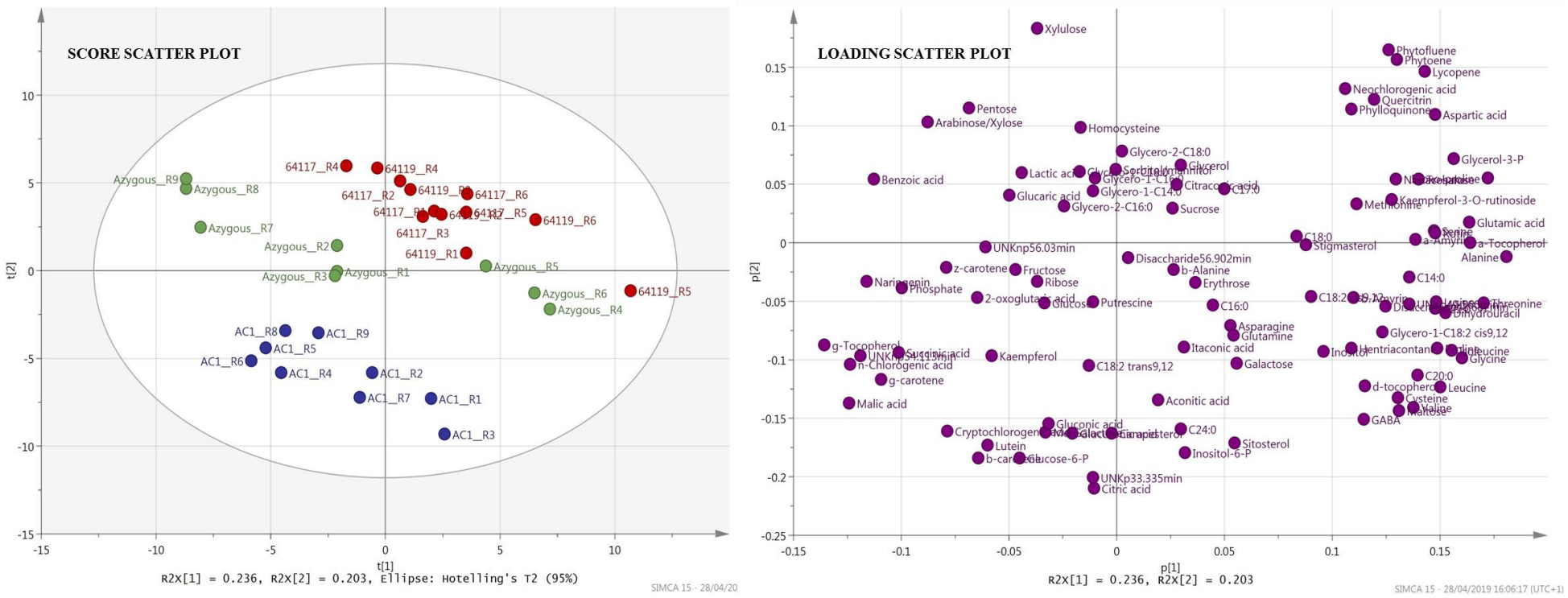

Figure 4-19 Principle component analysis of ripe fruit metabolism for *ZPR1* transgenic lines with both azygous and AC controls.

Between three and five biological and two to three technical replicates were analysed for each experiment. Metabolite levels from the GC-MS and UPLC analytical platforms were combined. The UPLC method used to analyse isoprenoids and phenolics, the GC-MS method to assess broader metabolism effects, and the treatment and processing of data are described in section 2.3.3, 2.3.5 and 2.4, respectively.

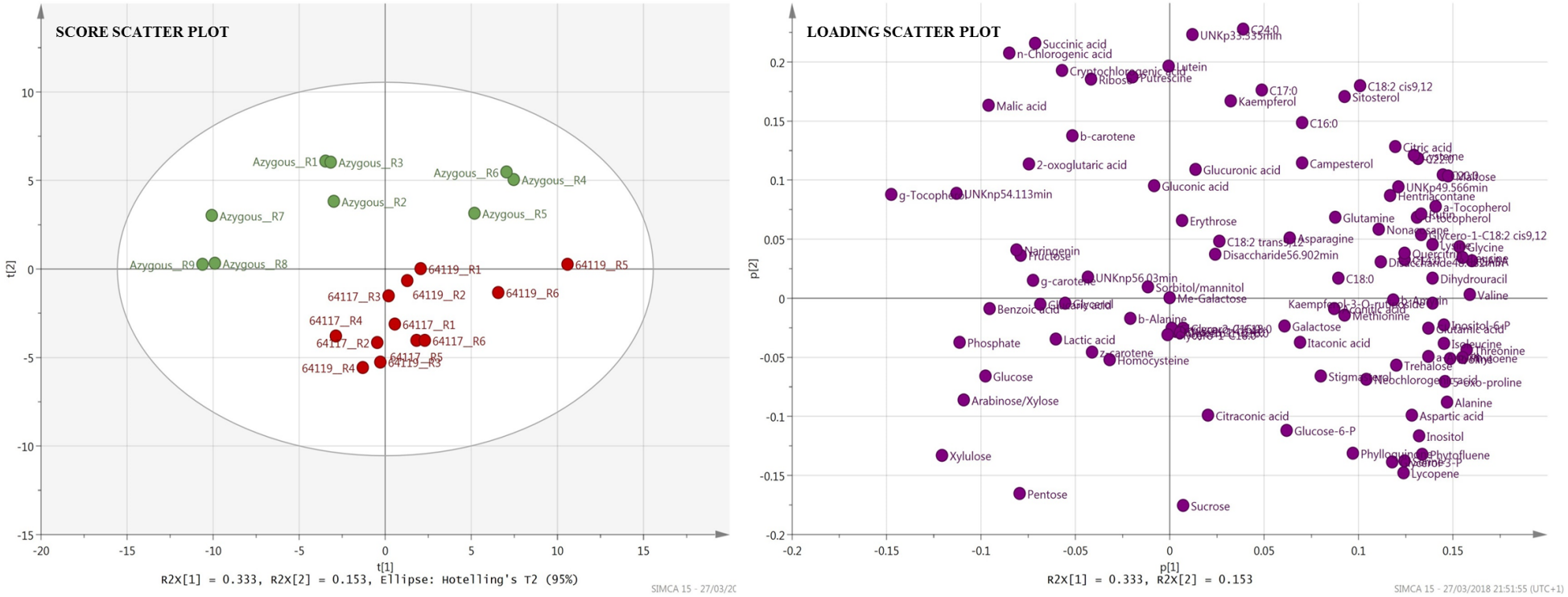

Figure 4-20 Principle component analysis of ripe fruit metabolism for *ZPR1* transgenic lines with azygous controls.

Between three and five biological and two to three technical replicates were analysed for each experiment. Metabolite levels from the GC-MS and UPLC analytical platforms were combined. The UPLC method used to analyse isoprenoids and phenolics, the GC-MS method to assess broader metabolism effects, and the treatment and processing of data are described in section 2.3.3, 2.3.5 and 2.4, respectively.

a

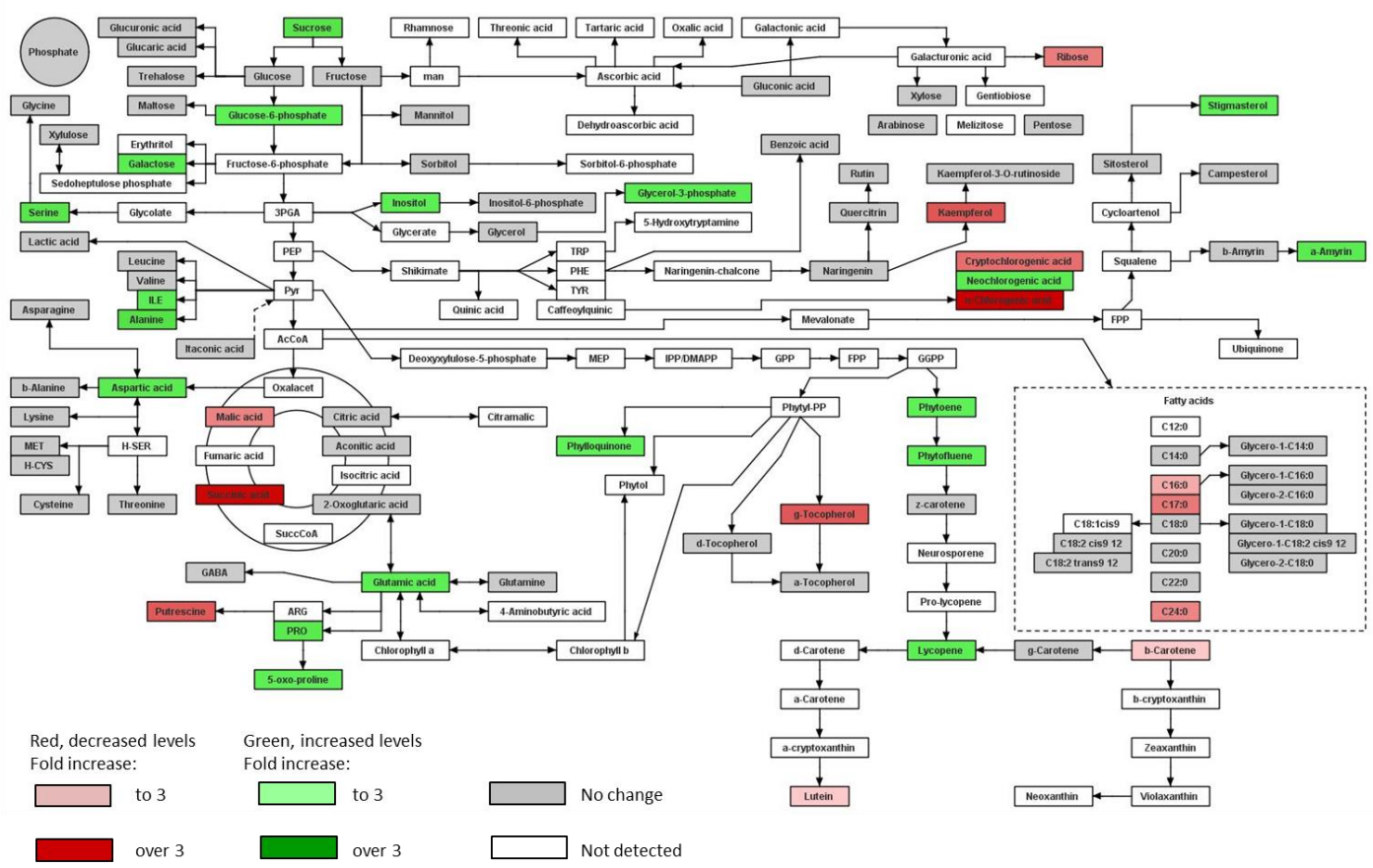
Phosphate
Glucuronic acid
Glucaric acid
Sucrose
Rhamnose
Threonic acid
Tartaric acid
Oxalic acid
Galactonic acid
Galacturonic acid
Ribose
Trehalose
Glucose
Fructose
man
Ascorbic acid
Gluconic acid
Xylose
Gentiobiose
Glycine
Maltose
Glucose-6-phosphate
Mannitol
Dehydroascorbic acid
Arabinose
Melizitose
Pentose
Stigmasterol
Xylulose
Erythritol
Galactose
Fructose-6-phosphate
Sorbitol
Sorbitol-6-phosphate
Benzoic acid
Sitosterol
Campesterol
Sedoheptulose phosphate
Rutin
Kaempferol-3-O-rutinoside
Serine
Glycolate
3PGA
Inositol
Inositol-6-phosphate
Glycerol-3-phosphate
Quercitrin
Kaempferol
Cycloartenol
Lactic acid
Glycerate
Glycerol
5-Hydroxytryptamine
Leucine
Valine
ILE
Alanine
PEP
Pyr
TRP
PHE
TYR
Shikimate
Quinic acid
Caffeoylquinic
Naringenin-chalcone
Naringenin
Cryptochlorogenic acid
Neochlorogenic acid
Squalene
b-Amyrin
a-Amyrin
Asparagine
Itaconic acid
AcCoA
Mevalonate
FPP
Ubiquinone
Deoxyxylulose-5-phosphate
MEP
IPP/DMAPP
GPP
FPP
GGPP
b-Alanine
Aspartic acid
Oxalacet
Lysine
Malic acid
Citric acid
Citramalic
Phytyl-PP
Phytoene
Fatty acids
C12:0
MET
H-SER
Fumaric acid
Aconitic acid
Phylloquinone
Phytofluene
C14:0
Glycero-1-C14:0
H-CYS
Isocitric acid
Phytol
C16:0
Glycero-1-C16:0
Cysteine
Threonine
Succinic acid
2-Oxoglutaric acid
g-Tocopherol
z-carotene
C17:0
Glycero-2-C16:0
C18:1cis9
C18:0
Glycero-1-C18:0
SuccCoA
d-Tocopherol
Neurosporene
C18:2 cis9 12
C20:0
Glycero-1-C18:2 cis9 12
C18:2 trans9 12
Glycero-2-C18:0
GABA
Glutamic acid
Glutamine
a-Tocopherol
C22:0
Putrescine
ARG
4-Aminobutyric acid
Pro-lycopene
C24:0
PRO
Chlorophyll a
Chlorophyll b
d-Carotene
Lycopene
g-Carotene
b-Carotene
5-oxo-proline
a-Carotene
b-cryptoxanthin
a-cryptoxanthin
Zeaxanthin
Lutein
Neoxanthin
Violaxanthin
Red, decreased levels
Fold increase:
to 3
over 3
Green, increased levels
Fold increase:
to 3
over 3
No change
Not detected

b

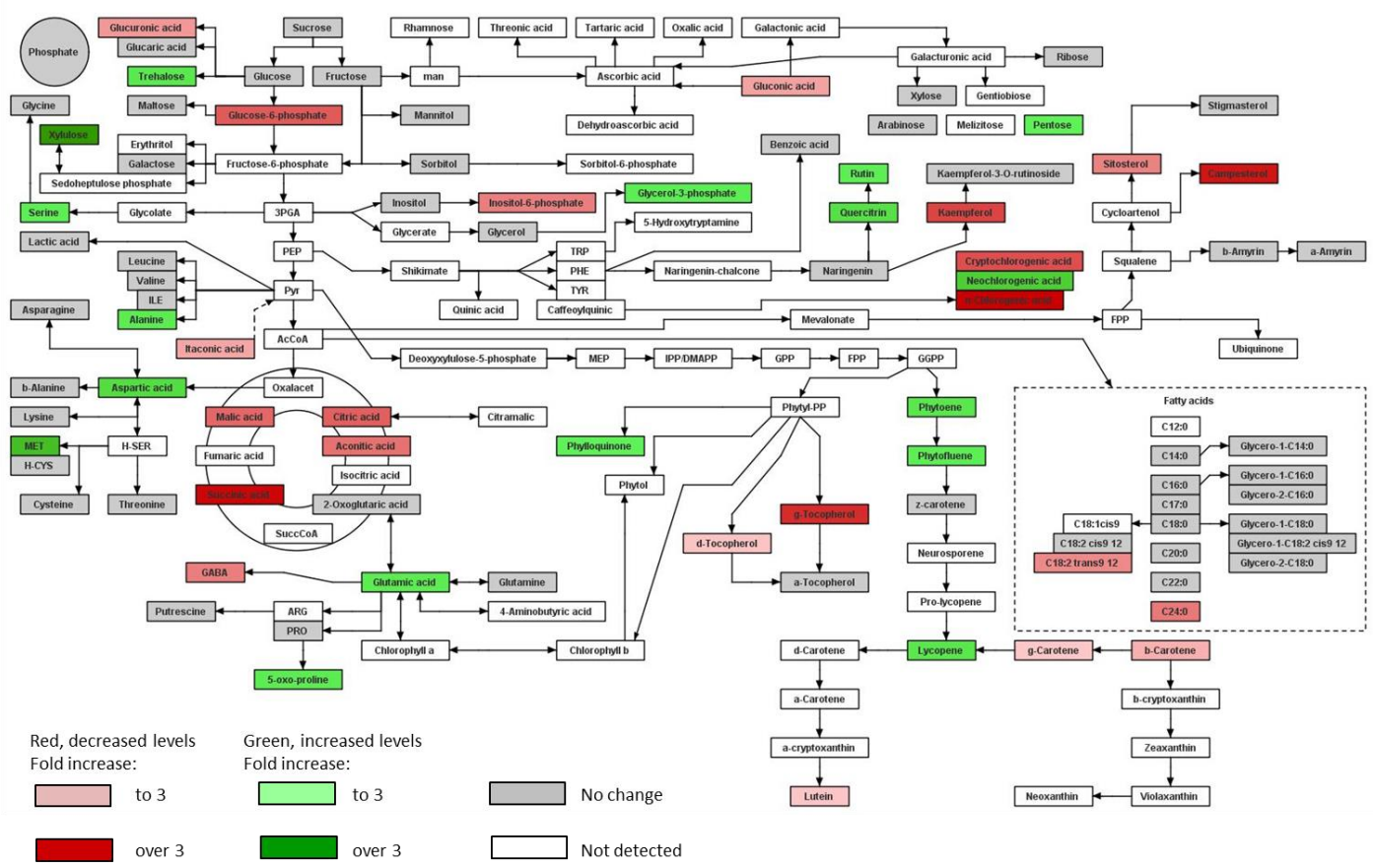

Figure 4-21 Metabolite changes in ripe tomato fruit as a result of the insertion of the *ZPR1* transgene.

Figure 4-21 Metabolite changes in ripe tomato fruit as a result of the insertion of the *ZPR1* transgene.

The metabolomics data acquired by GC-MS and UPLC chromatographic systems are displayed quantitatively over schematic representations of biochemical pathways produced using BioSynLab software (www.biosynlab.com). False colour scale is used to display the quantity of each metabolite in transgenic lines relative to azygous controls (a) and AC controls (b). Green indicates significant increases. Pale green represents small fold changes up to 3-fold whilst darker green indicates >3-fold. Red colouration has been used to represent decreased metabolite levels; dark red is over 3-fold, light red is to 3-fold. Grey indicates no significant change. White represents metabolites that were not detected in the samples analysed, because they was not present in samples or could not be detected using the analytical platforms available.3PGA, glyceraldehyde-3-phosphate; Ac- CoA, acetyl-coenzyme A; ARG, arginine; DMAPP, dimethylallyl pyrophosphate; FPP, farnesyl diphosphate; GGPP, geranylgeranyl-pyrophosphate; GPP, geranyl diphosphate; H-CYS, homo cysteine; H-SER, homo serine; IPP, isopentenyl pyrophosphate; ILE, isoleucine; man; mannose, MEP, 2-C-methyl-D-erythritol 4-phosphate; MET, methionine; PE, phosphatidylethanolamine; PEP, phosphoenolpyruvate; PHE, phenylalanine; Phytyl-PP, Phytyl diphosphate; PRO, proline; PS/PC, phosphatidylserine/phosphatidylcholine; Pyr, pyruvate; SuccCoA, succinyl-coenzyme A; TRP, tryptophan; TYR, tyrosine.

4.3 Discussion

The main sugars fructose, glucose and sucrose were quantified in an absolute manner due to their central roles in metabolism, and their accumulation in ripe fruits that contribute to nutritional quality and flavour (Table 4-2). Transgenic lines displayed a significant 2.1-fold increase to sucrose compared to azygous controls, and a nonsignificant 1.3-fold elevation to AC controls. Both glucose and fructose remained unchanged. The sugar profiles combined with increases to multiple metabolism pathways indicate increased sink strength and sucrose metabolism, potentially through elevated sucrose import and invertase activity (Osorio et al., 2014). Both increased sucrose synthase and reduced invertase activity were not expected to induce the changes to sucrose content, as both glucose and fructose remained unchanged. Greater sugar expedition is required by the diverse metabolic pathways used to activate ripening, including secondary metabolism. Therefore, the elevated sucrose import is contributing to increased sink strength and carbon flux through metabolism, both enable the

acceleration of fruit ripening in transgenic lines. The *SUCROSE TRANSPORTER* family (*SUT/SUC*) consist of three sucrose transporter genes. From these genes the main candidate is *LeSUT2*, as it is expressed predominantly in sink organs, and could facilitate the increases to sucrose witnessed (Barker et al., 2000; Osorio et al., 2014). Also, *SWEET* sucrose effluxers recently reported in *Arabidospis* and rice could also mediate the elevated sucrose import (Chen et al., 2012).

Sucrose has been shown to be an important signalling molecule involved in fruit ripening (Jia et al., 2016; Li et al., 2016a). This was demonstrated by exogenous sucrose treatment, which accelerated ripening (Li et al., 2016a). Sucrose treatment induced more rapid ripening-related colour transition that correlated with greater ethylene production, consistent with results and predictions for transgenic lines. Hexose degradation products remained unchanged, which is consistent with *ZPR1* transgenic fruit sugar profiles with elevated sucrose levels. Elevated sucrose degradation genes counteracted the sucrose increases, which facilitates the increased nutrients and ethylene fluxes (Li et al., 2016a). Therefore, a similar mechanism involving elevated sucrose could explain the improved carotenoid contents in *ZPR1* transgenic fruits. Further studies provide evidence for this mechanism, whereby sugars have been associated with pigment accumulation in fleshy fruits. In tomato, sucrose was associated with the upregulation of *PSY-1* and potentially *DXS*, while sucrose limitation was demonstrated to inhibit lycopene and phytoene accumulation (Télef et al., 2006). Furthermore, sucrose was predicted to improve carbon flux, channelling efficiency from pyruvate and GA3P into the citric acid cycle. Again, sucrose was demonstrated to enhance ethylene synthesis, through the upregulation of *ACS4* and *ACS2* (Télef et al., 2006).

Increased ethylene biosynthesis and signalling are key components that can explain the accelerated colour-associated ripening of the transgenic lines. Ethylene is formed from methionine via S-adenosyl-L-methionine (AdoMet) and the cyclic non-protein amino acid 1-aminocyclopropane-1-carboxylic acid (ACC). Transgenic fruits display elevated methionine content, with a nonsignificant 1.9-fold increase to azygous controls, and a significant 5.0-fold compared to AC controls (Table 4-2). The increased methionine potentially indicates elevated flux into the ethylene biosynthesis pathway, providing a larger precursor pool for the production of AdoMet, whose levels directly correlate with ethylene production (Van de Poel et al., 2013). The elevated AdoMet is predicted to provide more substrate for ACC SYNTHASE (ACS) to convert more AdoMet to ACC; enabling the release of more ethylene through the degradation of ACC by ACC

OXIDASE (ACO). Interestingly, the levels of soluble methionine was first shown to limit ethylene production in apple (Lieberman et al., 1966), prior to the identification of similar effects in maturing tomato fruit (Katz et al., 2006). Additionally, the same study demonstrated that the application of exogenous methionine to pericarp tissue resulted in the higher rates of ethylene evolution. Therefore, it was predicted that soluble methionine could be a rate limiting metabolite for ethylene synthesis.

Another indicator of elevated ethylene in transgenic lines was the reduction to putrescine when compared to both controls, although only proving to be significant when compared with azygous lines (Table 4-2). Putrescine along with other polyamines was shown to be increased upon treatment with the ethylene inhibitor 1-MCP (Van de Poel et al., 2013). Additionally, citric acid, malic acid, and succinic acid content was reduced upon ethylene treatment (Lim et al., 2017), consistent with transgenic lines (Table 4-2).

Isoprenoid levels were increased in ripe fruit from transgenic lines, contributed by elevated carotenoid and phylloquinone content (Table 4-1). Insertion of the ZPR1 transgene resulted in the significant elevation to carotenoids found upstream of lycopene. The formation of phytoene represents the first committed step in the carotenoid pathway. Overall, significant increases to phytoene were observed in transgenic lines compared to both controls, which proved to be most consistent in the 6-4-11-9 lines. Phytofluene content was significantly improved in transgenic lines when compared to both controls. The most dramatic consistent increases were observed for lycopene content, with transgenic lines exhibiting a 23 and 78% increase compared to azygous and AC controls, respectively (Table 4-1). Interestingly, colour-related ripening time from breaker was reduced by 1.5 days (1.4-fold) compared to azygous and 2.0 days (2.0-fold) to AC controls (Figure 4-14). An important observation was that both the fold changes associated with lycopene accumulation, and colour transition from breaker to red ripe were very similar. The results indicate that the elevated lycopene accumulation is conferring the reduced visually determined colour accumulation during ripening.

The carotenoid profiles of the ZPR1 transgenic lines (Table 4-1) shares multiple similarities with *ZINC FINGER PROTEIN INDETERMINATE DOMAIN 2* down-regulation (Table 3-3). Transgenic lines display increased flux upstream of lycopene, with elevated *PSY-1* expression being the main candidate. Especially as PSY-1 has been demonstrated to be the main rate-limiting step in the carotenoid pathway, and enhanced *PSY-1* expression would facilitate the increased formation of phytoene and phytofluene witnessed (Fraser et al., 2002; Fraser et al., 2007). The elevated phytofluene could also

indicate the upregulation of *PHYTOENE DESATURASE* (*PDS*), or could be attributed to increased substrate availability for PDS, enabling more phytoene destaturation and the formation of phytofluene. The latter seems more likely, as PDS also catalyses the desaturation of phytofluene to ζ-carotene. Therefore, *PDS* upregulation would likely maintain the fold increases through to ζ-carotene, which remains unchanged when compared to both controls. Overall, transgenic lines exhibit larger increases when compared to AC controls, as opposed to azygous lines, thus *PSY-1* expression is expected to be lowest in AC controls.

Post ζ-carotene, PDS catalyses the production of neurosporene, conversion to pro-lycopene is catalysed by ZDS, and then CAROTENE ISOMERASE (CRTISO) produces lycopene via an isomerisation reaction. With both neurosporene and pro-lycopene remaining undetected, CRTISO upregulation can be expected to facilitate the significant elevation to lycopene content when compared to both controls, especially when neurosporene was detected in previous analysis (Table 3-3). Post cyclisation of lycopene, fold increases fall dramatically into small fold decreases to γ-carotene, β-carotene and lutein. Therefore, a bottleneck was identified within the pathway, likely due to down-regulation of lycopene cyclases.

As mentioned earlier, the rate-limiting steps for carotenoid and lycopene production are catalysed by PSY-1, PDS, ZDS, Z-ISO and CRTISO (Giuliano et al., 1993; Fraser et al., 1994; Fantini et al., 2013). RIN has been shown to directly regulate the expression of *PSY-1*, *Z-ISO*, *CRTISO* (Martel et al., 2011; Fujisawa et al., 2013). Both *PSY-1* and *CRTISO* were expected to upregulated in transgenic fruits, thus a mechanism involving RIN can be expected. Furthermore, the carotenoid profiles of transgenic lines shared multiple similarities with ethylene treatment. Su et al., 2015 studied the application effects of an ethylene precursor (ACC), which resulted in fruits producing significantly more phytoene, phytofluene and lycopene comparable with transgenic lines, in addition to elevating δ-, α- and β-carotene contents. Increased carotenoids upstream of and including lycopene were correlated with the upregulation *PSY-1* and *ABA4*, and the reduced expression of *LYB-β1*, *CRTR-β2* and *NCED* (Su et al., 2015).

The results demonstrate that elevated ethylene biosynthesis is the main candidate for the reduced time from breaker to uniform red, by promoting carotenoid accumulation. The upregulation of *PSY-1* can explain the increased flux upstream of lycopene, resulting in elevated phytoene, phytofluene and lycopene. While reduced expression of *LYC-β1*, *CRTR-β2* and *NCED* can explain the bottleneck post lycopene, resulting in reduced γ-

carotene, β-carotene and lutein. Ethylene treatment increases chlorophyll degradation, likely contributing to the reduction of time to reach red ripe and the increased A* scores in transgenic lines (Figure 4-14 and Figure 4-15b). Interestingly, many genes expected to be upregulated in transgenic lines directly correlate to RIN, providing further evidence of ethylene involvement (Su et al., 2015). The increased ethylene could then enhance RIN expression in a positive feedback loop (Fujisawa and Ito, 2013), upregulating RIN regulated *PSY-1* and *CRTISO* resulting in phytoene and lycopene accumulation.

Multiple chlorogenic acid forms were identified in the phenolic screen (Table 4-2). The most abundant forms were n-chlorogenic acid and cryptochlorogenic acid, found in significantly larger quantities compared to neochlorogenic acid. Both n-chlorogenic acid and cryptochlorogenic acid exhibited significant reductions in both transgenic lines. n-Chlorogenic acid could not be identified in transgenic lines, while 1.6- to 2.2-fold reductions to cryptochlorogenic acid were observed. Interestingly, chlorogenic acid levels were shown to peak at breaker and decline during fruit ripening (Buta and Spaulding, 1997). The accumulation pattern of chlorogenic acid during growth and maturation paralleled the changes in IAA levels (Buta and Spaulding, 1997). Chlorogenic acid is predicted to be an inhibitor of IAA oxidation, thus the decline during ripening progression would result in less protection of endogenous IAA. With IAA shown to negatively influence ripening (Vendrell, 1985; Cohen, 1996; Giovannoni, 2007; Su et al., 2015; Li et al., 2016b), chlorogenic acid was expected to be part of the metabolic control of the ripening process in tomato fruits (Buta and Spaulding, 1997). IAA has been shown to inhibit carotenoid accumulation resulting in a slower transition from green to red, by inhibiting *PSY-1*, *PDS*, *Z-ISO* and *CRTISO* from the carotenoid pathway (Su et al., 2015). Auxin also delayed and reduced ethylene synthesis. The reductions to chlorogenic acid further demonstrate that transgenic lines have progressed further into ripening, whilst the potential reductions to IAA could explain the elevated ethylene predicted and increased carotenoid accumulation.

The phenolic screen also identified multiple differences to flavonoids that stem from the general phenylpropanoid pathway (Table 4-2). Naringenin was the first flavonoid identified in the flavonol biosynthesis pathway, transgenic lines exhibited nonsignficant 1.5- and 2.1-fold reductions compared to azygous and AC controls, respectively. Naringenin is then hydroxylated by FLAVANONE-3-HYDROXYLASE (F3H) at position C-3 to form the dihydroflavonol dihydrokeampferol, which can be further hydroxylated to dihydroquercetin by FLAVONOID-3′-HYDROSYLASE (F3’H), both

were not identified by the chromatographic screen. FLAVONOL SYNTHASE (FLS) converts dihydrokeampferol to kaempferol and dihydroquercetin to quercitrin. Finally, kaempferol and quercitrin are substrates for FLAVONOL-3-GLUCOSYLTRANSFERASE (GT) and FLAVONOL-3-GLUCOSIDE-RHAMNOSYLTRANSFERASE (RT). Kaempferol is converted to kaempferol-3-O-rutinoside, while quercitrin is converted to rutin. Transgenic lines exhibited significant reductions to kaempferol and nonsignificant increases to kaempferol-3-O-rutinoside. Furthermore, elevated quercitrin and rutin was identified in transgenic lines, although only comparisons with AC controls proved significant. In accordance with literature rutin was the predominant flavonoid identified.

The flavonoid profiles of transgenic fruit suggest increased flux through the flavonol pathway. The decreases to naringenin are predicted to be due to increased *F3H* expression. While elevated *F3'H* expression can explain the elevated quercitrin and rutin through diverting greater flux through this section of the pathway. Despite the increased quercitrin, the expression of *FLS* is expected to remain unchanged or reduced, as kaempferol is reduced and the elevated quercitrin is likely due to flux increases through *F3'H* upregulation. Increased *GT* and *RT* expression can also explain the reduction to kaempferol, in addition to the increases to kaempferol-3-O-rutinoside and rutin. The reduction to kaempferol, a major yellow flavonoid in tomato fruit peel, as well as naringenin could contribute to the reduced B* score of transgenic lines that were screened by colourimeter (Figure 4-15c).

Based on colour, transgenic lines have accelerated ripening. Transgenic lines display the largest differences when compared with AC controls, with azygous controls being a midpoint between extremes. GC-MS profiling of broader metabolism revealed a similar trend, with numerous metabolite differences in transgenic lines also correlating with further ripening progression (Table 4-2). Significant changes to metabolite levels were identified for most classes of compounds analysed. Overall, comparisons between transgenic and AC lines revealed double the number of compounds that were significantly different, whose levels correlated with ripening progression, when comparing with the same comparison with azygous controls. Also, the fold changes associated with these compounds were largest when compared to AC controls. An example is aspartic acid that normally accumulates during ripening; transgenic lines exhibited the largest aspartic acid content, with AC having the lowest. This provides more evidence for the accelerated ripening in transgenic lines. Other metabolites

demonstrated the same trend when compared to both controls, including many organic acids. Reduced organic acid content is associated with fruit pericarp ripening (Carrari et al., 2006; Osorio et al., 2011a), and transgenic lines display a significant 1.1-fold and 1.8-fold reduction compared to azygous and AC controls, respectively. Compared to both controls, decreased levels of malic acid and succinic acid from the TCA cycle were observed. Malic acid reduction has been shown to be an important fruit ripening indicator and is commonly measured to determine the maturity status of fruits (Dalal et al., 2017). Interestingly, multiple studies have demonstrated that organic acids strongly correlate with genes linked with ethylene and cell wall metabolism-associated pathways, highlighting their importance to fruit ripening (Carrari et al., 2006; Centeno et al., 2011; Osorio et al., 2011a). The levels of all organic acids, particularly the TCA cycle intermediates, were strongly affected across ripening in several ripening mutants (Osorio et al., 2011a). The largest alterations to organic acid content was identified in *nor*, a mutation with severely affected ethylene biosynthesis and signalling (Osorio et al., 2011a). The results demonstrate the importance of ethylene for organic acid content, providing further evidence for altered ethylene biosynthesis and signalling, which is expected to be conferring the alterations to ripening-related metabolism compared to both controls. Furthermore, aconitic acid, citric acid and glucuronic acid were reduced in transgenic lines compared with AC controls. In addition to aspartic acid, the amino acid glutamic acid was also increased in accordance with ripening (Boggio et al., 2000; Carrari and Fernie, 2006; Mounet et al., 2007; Akihiro et al., 2008; Osorio et al., 2011a; Koike et al., 2013). Glutamate is associated with umami flavour, thus savoury flavour could be enhanced in transgenic lines. The isoprenoids phytoene, phytofluene and lycopene indicated increased ripening progression in transgenic lines. Compared to AC controls, transgenic lines also exhibit reductions to glucose-6-phosophate and inositol-6-phosphate and increased methionine and trehalose.

The fruit metabolism study revealed that many metabolites displaying significant differences to control lines were positively correlated to ripening. However, multiple metabolites displayed the opposite trend, correlating more to green fruits (Table 4-2). These were expected to contribute to the uncoupled ripening phenotype in transgenic fruits by delaying softening. The differences include serine and glycerol-3-phosphate when compared to both controls. Compared to azygous controls, proline, glucose-6-phosphate, inositiol and putrescine levels associate more with green fruits (Carrari and Fernie, 2006; Osorio et al., 2011a).

Across multiple generations, transgenic lines exhibited greater ripe fruit firmness. The results demonstrate reduced rates of fruit softening, which could potentially correspond to extended post-harvest shelf-life up to 6 days (Figure 4-16). Probe penetration test revealed nonsignificant increases to outer pericarp firmness, potentially contributing to the reduced fruit softening of transgenic lines. Of particular interest was the observation that transgenic fruits may have thicker pericarp, which could provide elevated mechanical firmness (not shown), although further investigation is required. Pericarp thickness and development have been shown to be controlled by two cyclin-dependent kinases, *CDKB* and *CDKA1* (Czerednik et al., 2012). *CDKB* overexpression resulted in reduced pericarp thickness and firmness, potentially involving jasmonate and cytokinin synthesis and signalling pathways (Andersen et al., 2008). Additional studies involving SlNAC1 and the tomato AGAMOUS-LIKE1 transcription factors, highlight that reduced pericarp size can affect fruit turgor, a major determinant of tomato fruit firmness (Saladié et al., 2007; Ma et al., 2014). Ripening-related fruit softening is associated with the decline to polymeric galactose in cell walls and the rise in free galactose (Wallner and Bloom, 1977; Gross and Wallner, 1979; Kim et al., 1991). No consistent change to galactose was identified in transgenic lines compared to both controls. This provides evidence for another mechanism, including the observation of increased pericarp thickness that may be the cause of the reduced fruit softening phenotype. Therefore, no change to β-GALACTOSIDASE induced pectin depolymerisation is expected, which catalyses the loss of cell wall galactose side chains from rhamnogalacturonan I.

4.4 Conclusion to chapter

Pan et al., (2013) identified several potential fruit specific ripening-regulators that were shown to have expression patterns that mirrored RIN. The ripening-related expression profile of ZINC-FINGER PROTEIN ZPR1 and its reduced expression in *rin*, *cnr* and *nor* ripening mutant lines, suggested an important role in fruit ripening. The insertion of a knock-down 35S::RNAi construct under constitutive control, was used characterise the function of the transcription factor.

The ZPR1 was demonstrated to have global effects to plant and fruit development, whilst a ripening-related function was confirmed. Transgenic lines were shown to increase ripening-related colour development, with fruits reaching red ripe significantly faster than both controls. Transgenic lines exhibited elevated phytoene, phytofluene and

lycopene content in ripe fruits. Carotenoid profiling predicted the upregulation of RIN-induced carotenoid biosynthesis enzymes *PSY-1*, *CRTISO* as well as *PDS*. Ethylene treatment has been demonstrated to induce the expression of these enzymes, yielding similar carotenoid profiles, suggesting increased ethylene could be associated with the carotenoid increases upstream of lycopene cyclisation.

Transgenic lines demonstrated broad changes to metabolism, with many metabolites associated with ripening, including isoprenoids and organic acids, showing significant fold changes when compared to both controls. The majority of compound alterations support the hypothesis of increased rapidity of ripening in transgenic fruits. The sugar profiles, reduction to TCA cycle intermediates combined with increases to multiple metabolism pathways, indicate increased carbon flux through metabolism. Improved sink strength was predicted, through elevated sucrose import and metabolism, facilitating the increased ripening progression of transgenic lines. Elevated aspartic acid and methionine suggest elevated flux into the ethylene biosynthesis pathway, providing a large precursor pool for the production of AdoMet, whose levels directly correlate with ethylene production (Van de Poel et al., 2013). The result provides further evidence for a rise in ethylene levels, which is predicted to induce the increased rapidity of colour-associated ripening, especially as methionine limits ethylene production in maturing tomato fruit. Overall, total sugar content remained unchanged, thus no change to sweetness was expected. Although, flavour could be affected with the reduction to total organic acid content and the increased glutamic acid, potentially decreasing acidity and intensifying umami flavour. Lastly, transgenic lines consistently exhibited elevated ripe fruit firmness. Reduced outer pericarp softening, or increased pericarp thickness and subsequent maintenance of turgor pressure are the predicted mechanisms associated with the firmness increases.

Overall, the project succeeded in identifying another ripening-related transcription factor, with manipulation improving multiple areas of quality. Interestingly, the *ZINC-FINGER PROTEIN ZPR1* functionally shared many similarities with the *ZINC-FINGER PROTEIN IDD2* (chapter III), potentially indicating they are part of the same ripening cascade of transcription factors. *ZPR1* transgenic lines uncouple colour development and softening, providing a significant improvement on the *rin* mutation currently commercially utilised. Transgenic fruits maintain fruit firmness but also improve other key quality traits: with elevated ripening-related colour and isoprenoid accumulation associated with increased nutritional potential.

Chapter V: Functional characterisation of the HEAT SHOCK TRANSCRIPTION FACTOR A3

5.1 Introduction

In tomato the *HEAT SHOCK TRANSCRIPTION FACTOR A3* (Solyc08g062960; *HSFA2*, previously denoted *HSP30*) was shown to be upregulated upon heat stress (Frank et al., 2009; Yang et al., 2016; Keller et al., 2017). Expression increased by 150 times compared with controls at one hour post heat stress (HS) treatment, indicating that the transcription factor is a very sensitive response acceptor that responds strongly (von Koskull-Doring et al., 2007; Yang et al., 2016). Therefore, *HSFA2* has been shown to be the major heat shock factor gene in thermotolerant cells (Frank et al., 2009). HS induced expression of *HSFA2* is regulated by the constitutively expressed *HSFA1*, considered to be the master regulator of the HS responses in tomato (Frank et al., 2009). In *Arabidopsis*, expression of *HSFA2* proved to be strictly HS-dependent, with similar regulatory networks and functions as tomato, including the extension of acquired thermotolerance (Schramm et al., 2006; Charng et al., 2007; Li et al., 2017b).

In tomato, a ripening-related expression profile was identified for *HSFA2*, while expression was reduced in *cnr*, *nor* and *rin* mutants. Furthermore, altered carotenoid profiles were identified in transgenic lines from the T_0 generation, with the insertion of the knock-down 35S::RNAi construct. Together these results suggested an important ripening-related function for the transcription factor. Therefore, detailed phenotypic characterisation and metabolic profiling was performed, enabling the evaluation of how manipulation affected development, fruit ripening and fruit quality traits.

5.2 Results

5.2.1 Phenotypic and genotypic screening of the T_1 generation to identify potential functions of the *HSFA2*

5.2.1.1 Screening for altered plant morphology, fruit development, and ripening-related quality traits associated with *HSFA2* transgenic lines

Carotenoid screening of the T_0 generation demonstrated potential ripening and quality-associated roles for the *HSFA2* transcription factor. Transgenic lines containing the knock-down 35S::RNAi construct exhibited increased phytoene, phytofluene and lycopene levels, combined with reductions to β-carotene and chlorophyll. As a result, the insertion events (4-1, 4-2, 4-5 and 4-6) with increased carotenoid content were selected and propagated. A total of 60 *HSFA2* transgenic individuals were studied, including up to 19 lines per insertional event, with 20 representative Alisa Craig (AC) wild type controls. Similar to sections 3-2-1 and 4-2-1, rapid and broad phenotyping was conducted to further characterise the function of the transcription factor, provide an assessment of quality and through selection reduce the number of individuals and genotypes. Transgenic lines were analysed separately, as the insert number, zygosity and potential segregation within each insertion event was unknown.

Similar to the other constructs analysed (Figure 3-1 and Figure 4-1), *HSFA2* transgenic lines exhibited a more condensed plant architecture (short and bushy). In total 75% of transgenic lines displayed reduced internode length, which were on average 1.2 cm shorter than AC controls (Figure 5-1a). Similarly, 73% of transgenic lines exhibited reduced plant height, on average the length from soil to the last node was reduced 12.4 cm compared with AC controls (Figure 5-1b). Overall, eight different transgenic lines displayed a more severely perturbed development, whereby the height and average internode lengths were below 100 and 5 cm, respectively. The altered plant morphology highlights potential plant growth and developmental roles for the *HSFA2*.

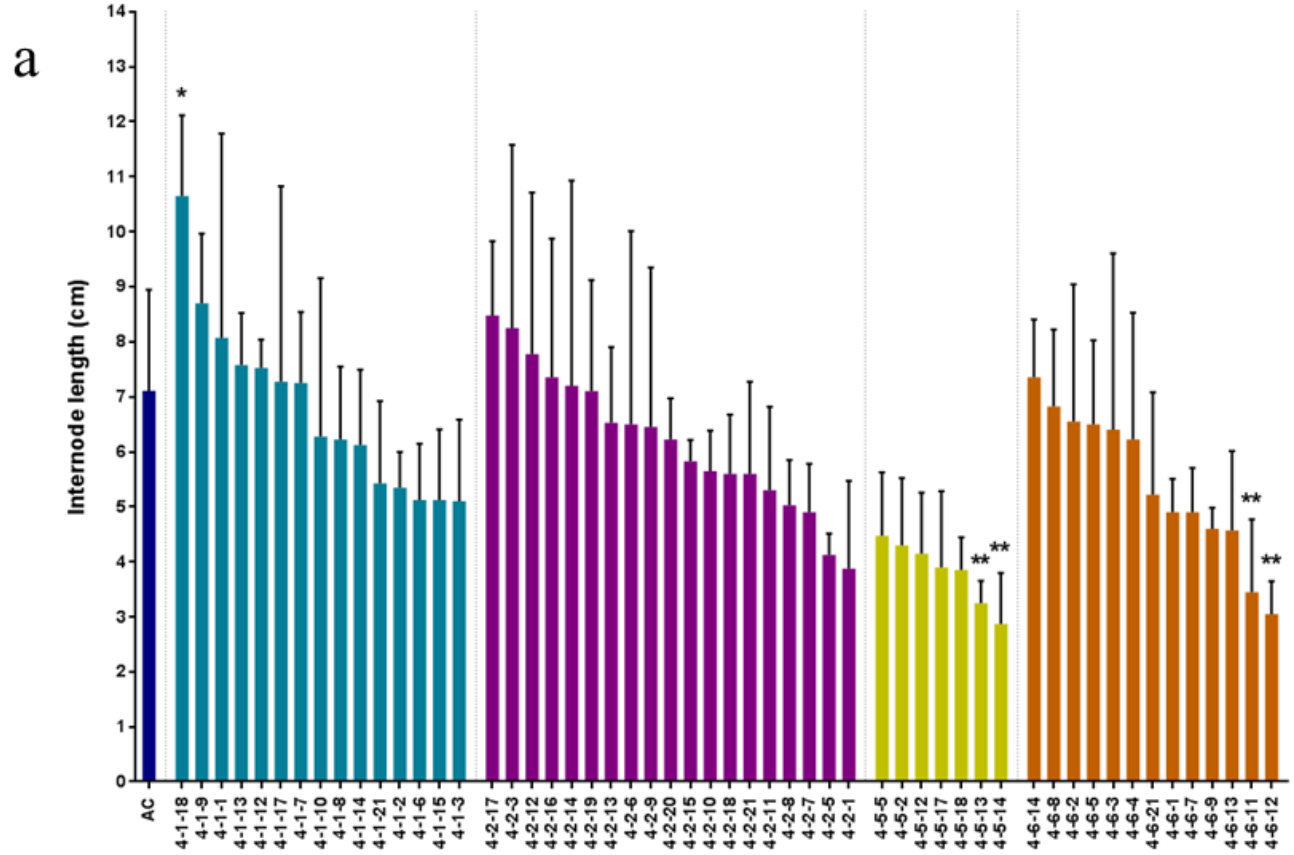
a
Internode length (cm)
0
1
2
3
4
5
6
7
8
9
10
11
12
13
14
*
**
**
**
**
AC
4-1-18
4-1-9
4-1-1
4-1-13
4-1-12
4-1-17
4-1-7
4-1-10
4-1-8
4-1-14
4-1-21
4-1-2
4-1-6
4-1-15
4-1-3
4-2-17
4-2-3
4-2-12
4-2-16
4-2-14
4-2-19
4-2-13
4-2-6
4-2-9
4-2-20
4-2-15
4-2-10
4-2-18
4-2-21
4-2-11
4-2-8
4-2-7
4-2-5
4-2-1
4-5-5
4-5-2
4-5-12
4-5-17
4-5-18
4-5-13
4-5-14
4-6-14
4-6-8
4-6-2
4-6-5
4-6-3
4-6-4
4-6-21
4-6-1
4-6-7
4-6-9
4-6-13
4-6-11
4-6-12

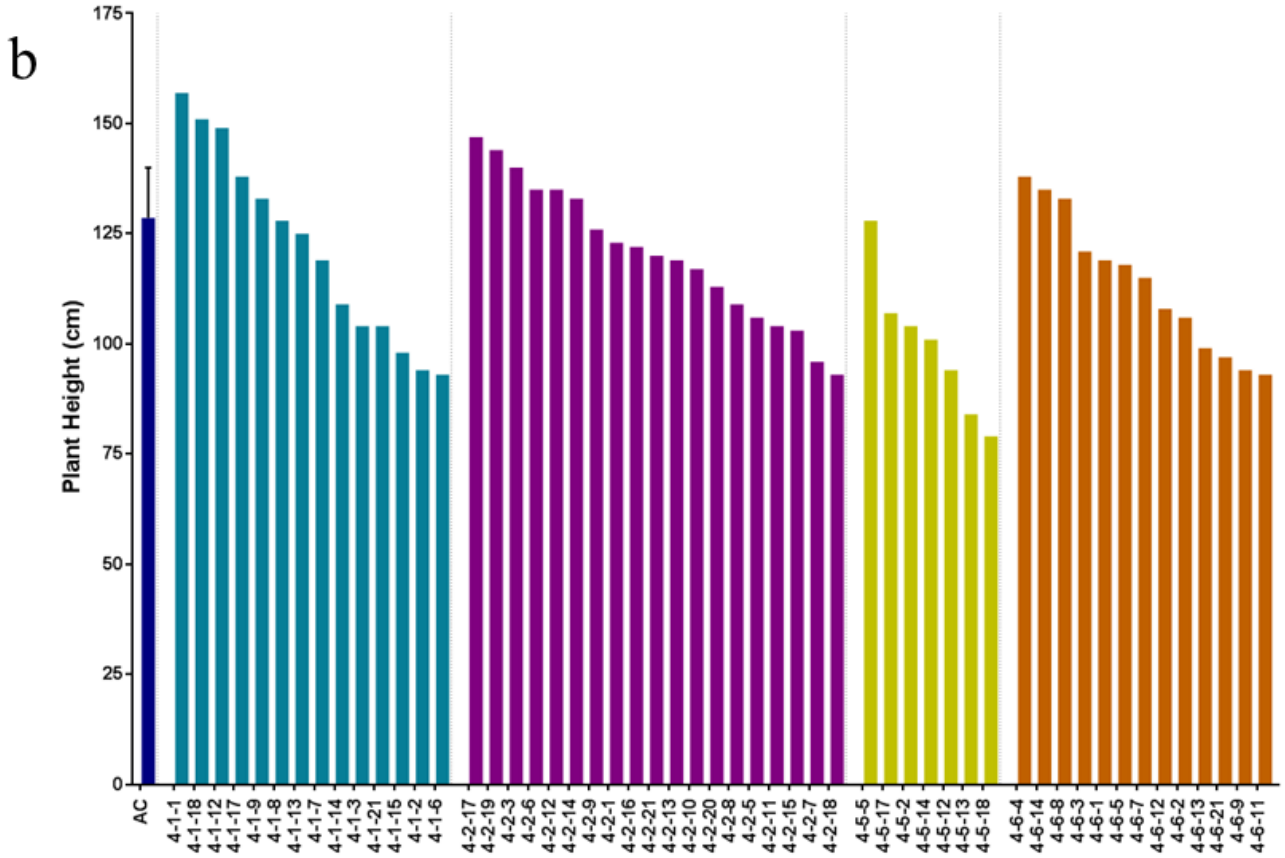

Figure 5-1 Assessment of altered plant morphology by screening stem internode lengths and plant height.

Figure 5-1 Assessment of altered plant morphology by screening stem internode lengths and plant height.

Stem internode length (a) and total plant height (b) were used to identify differences to plant development between Ailsa Craig (AC) and transgenic lines. Plant parameters were measured once the AC wild type background had three trusses with fruit set. Total plant height was measured from the soil to last node; four random internodes were measured from the base of the plant to the last node. Each transgenic individual is represented by a single column, for AC a total of nineteen lines were averaged ensuring enough wild type biological replicates were spread throughout the population. Statistical determinations are shown as mean ± SD, Dunnett's test analysis illustrates statistically significant differences between wild type background (AC) and the transgenic varieties, $P < 0.05$, $^{**}P < 0.01$, and $^{***}P < 0.001$ are designated by *, **, and ***, respectively.

Fruit development time was assessed, by tagging flowers at anthesis and determining the time fruits took to set, develop and reach breaker stage of ripening. Fruit set refers to the transition of a flower or a flower bud into a fruit. Similar to the previous constructs studied, transgenic lines displayed an extended time to reach breaker, with fruits taking on average 49.6 days compared to just 45.1 days for the AC controls (Figure 5-2a). However, the differences to AC were smaller than identified in previous constructs. Interestingly, few significant differences were identified to both fruit size (Figure 5-2b) and total fruit yield (Figure 5-2c), which on average remained unchanged. Both 4-6-9 and 4-6-12 produced significantly larger fruit that were 57% and 85% heavier compared to AC controls, respectively. Additionally, large increases to total fruit yield was identified in 4-6-1 (50%), 4-6-9 (160%), 4-6-2 (200%) and 4-6-12 (313%). The results suggested that the transcription factor may be involved in fruit set and development, although further crops were necessary to confirm the above phenotypes.

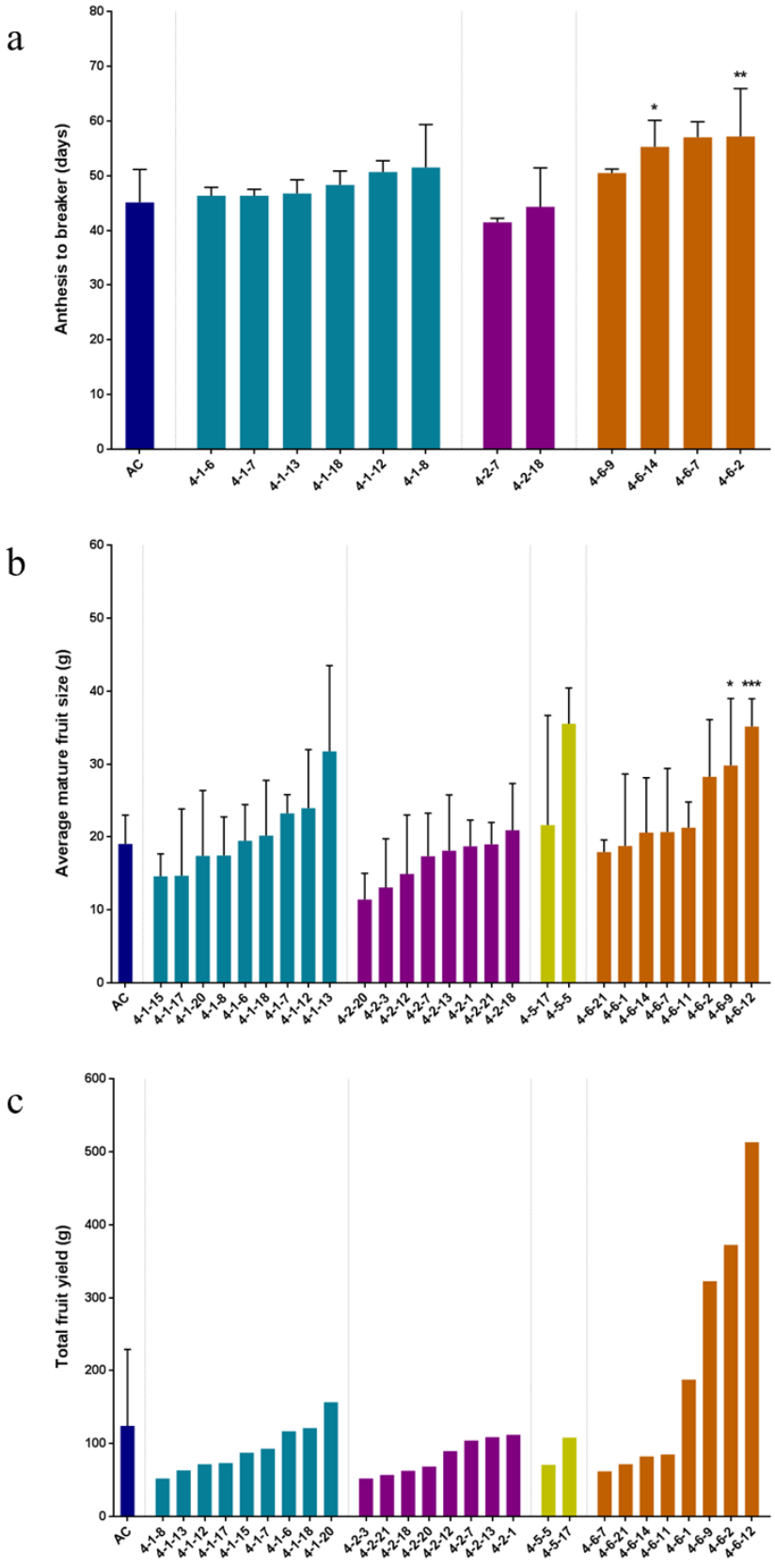

Figure 5-2 Evaluating fruit set and development by screening the time from anthesis to breaker, average fruit weight and total fruit yield.

Figure 5-2 Evaluating fruit set and development by screening the time from anthesis to breaker, average fruit weight and total fruit yield.

The maturity time from anthesis to breaker (a), average fruit weight (b) and total fruit yield (c) were recorded, to test whether transgenic lines exhibited altered fruit set and developmental phenotypes. Flowers were tagged at anthesis and the time taken to reach the onset of ripening at breaker stage was recorded. Fruit weights were determined individually postharvest and combined to determine total fruit yield. Fruit parameters were measured once the wild type AC background had formed five trusses. Each transgenic individual is represented by a single column, for AC up to twelve lines were averaged, ensuring enough wild type biological replicates were spread throughout the population. Between two and ten fruit measurements were recorded for each plant for either fruit maturity time or average fruit weight. Statistical determinations are shown as mean ± SD, Dunnett's test analysis illustrates statistically significant differences between wild type background (AC) and the transgenic varieties, $P < 0.05$, $^{**}P < 0.01$, and $^{***}P < 0.001$ are designated by *, **, and ***, respectively.

To confirm the role of *HSFA2* in ripening, previously predicted based upon its expression profile; ripening-related fruit quality was assessed. A fruit firmness meter was used to determine the firmness of fruit at fourteen days post breaker, when fruits were expected to be approaching overripe stages (Figure 5-3a). Compared to AC controls, a total of 66% of transgenic lines exhibited elevated fruit firmness. On average transgenic lines were 10% firmer, which could indicate reduced fruit softening, although only one line proved significant. More significant changes were identified to the rapidity of ripening-associated colour development (Figure 5-3b). Fruits from all transgenic individuals displayed a reduced time to transition from breaker to uniform red ripe, taking on average 2.0 less days compared to AC controls. Several lines proved significant, including five that on average reached red ripe two days quicker than AC controls, indicating an increased rate of ripening-related colour development.

Similar to the other constructs studied, spectrophotometric quantification of the end point levels of carotenoids was performed (as described in section 2.3.2), to confirm the altered ripening times and darker fruit phenotypes observed. The wavelength of 470 nm was used to quantify carotenoids, specifically lycopene, the predominant carotenoid in ripe tomato. For fruit at 7 dpb, all transgenic lines exhibited elevated carotenoid contents compared to AC controls (Figure 5-4a). Carotenoid content was significantly increased 1.3-fold for both 4-6-2 and 4-6-9 lines, whilst ripening times were decreased 1.3 and 1.5-fold, respectively. The results indicated that elevated carotenoid content was influencing

the reduced time for fruits to transition from breaker to red ripe. Lines from the 4-6 insertion event displayed the largest increases to carotenoid content, averaging an elevation of 1.3-fold. Similarly, most transgenic lines (81%) exhibited increased pigmentation at 14 dpb (Figure 5-4b). Compared to AC controls a significant 1.4-fold increase was identified to 4-2-7, while carotenoid levels were improved 1.3-fold in the lines 4-6-1, 4-6-2 and 4-6-9. The results from Figure 5-4 indicated that transgenic lines sustain an increased rate of carotenoid accumulation throughout the red ripe stages of fruit ripening.

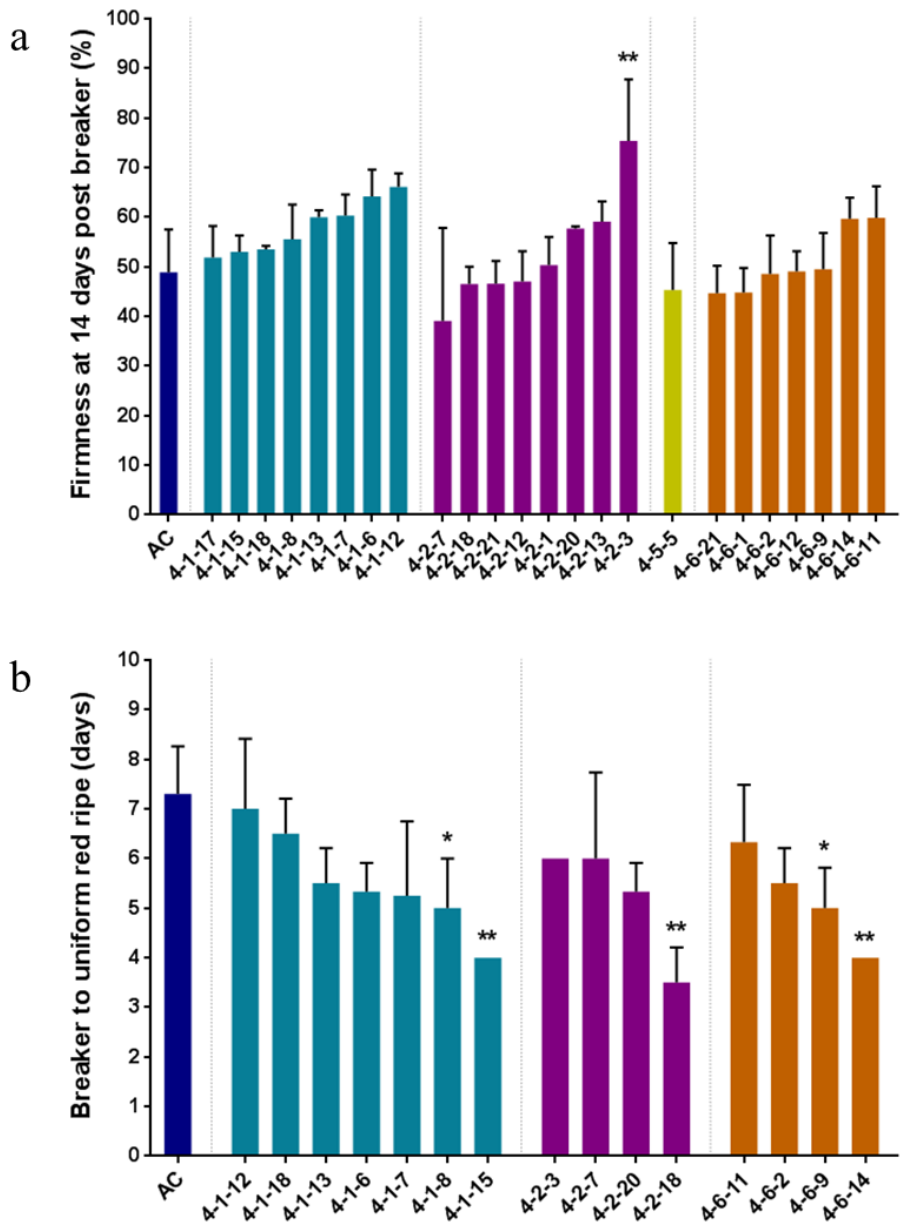

Figure 5-3 Assessment of ripening-associated fruit quality by screening colour development and fruit softening.

Colour related rapidity of ripening represents visual determination of the time taken for fruits to transition from breaker to uniform red (a). Fruit softening was measured in fruits at fourteen days post breaker using a fruit firmness meter; three measurements were taken per fruit (b). For both analyses between two and seven fruits were studied. Each transgenic individual is represented by a single column, for AC a total of up to seven lines were averaged, ensuring enough wild type biological replicates were spread throughout the population. Statistical determinations are shown as mean ± SD, Dunnett's test analysis illustrates statistically significant differences between wild type background (AC) and the transgenic varieties, $P < 0.05$, $^{**}P < 0.01$, and $^{***}P < 0.001$ are designated by *, **, and ***, respectively.

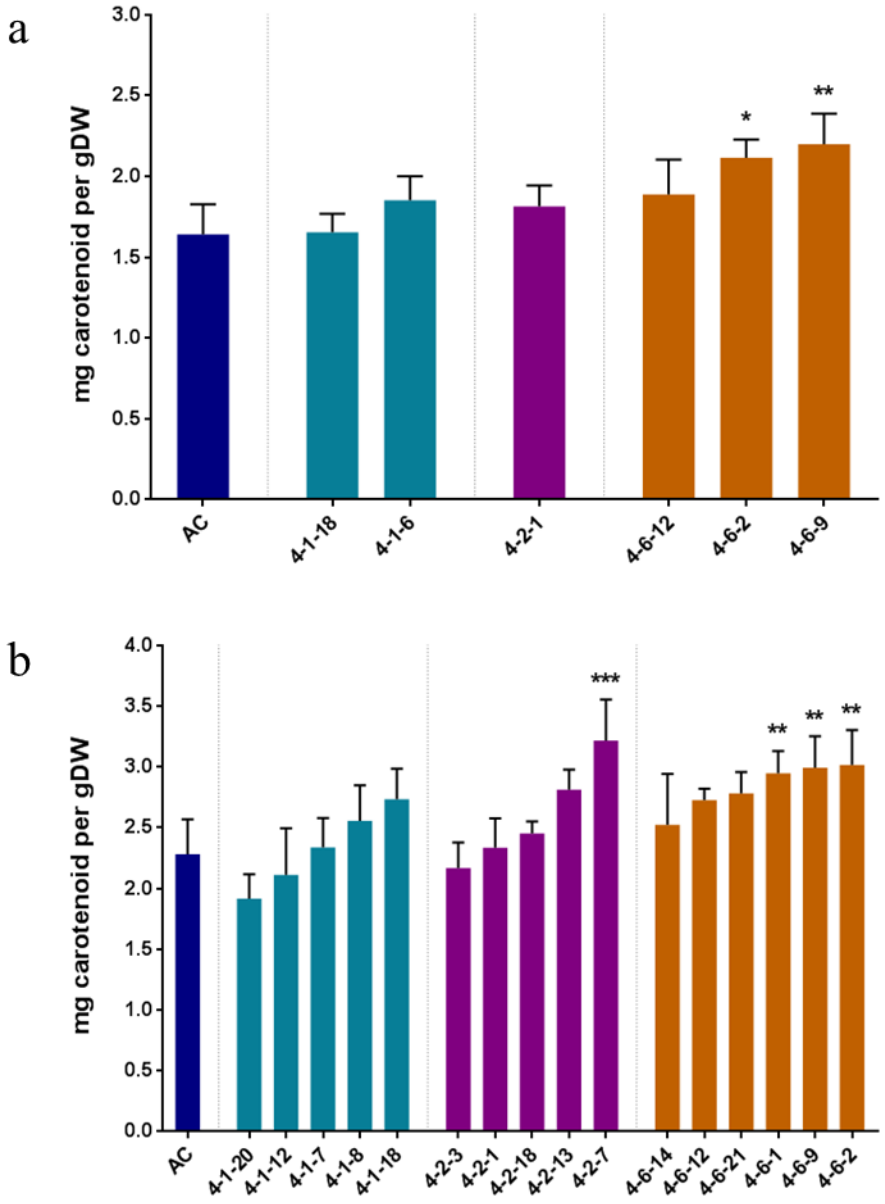

Figure 5-4 Spectrophotometer quantification of carotenoid content in ripe fruits.

Carotenoid content of two ripe fruit stages, seven (a) and fourteen days (b) post breaker, were quantified by spectrophotometer at 470 nm. Between two and five representative fruits were pooled per individual, then three technical and analytical determinations were made. Methods used for these determinations are described in section 2.3. Each transgenic individual is represented by a single column, for AC a total of up to seven lines were averaged, ensuring enough wild type biological replicates were spread throughout the population. Statistical determinations are shown as mean ± SD, Dunnett's test analysis illustrates statistically significant differences between wild type background (AC) and the transgenic varieties, $P < 0.05$, $^{**}P < 0.01$, and $^{***}P < 0.001$ are designated by *, **, and ***, respectively.

5.2.1.2 Genotypic screening of transgenic lines by PCR

Combined phenotypic and spectrophotometer screening enabled the selection of lines with the most positively improved quality traits for genotyping. The next objective was to genotype individuals, through the identification of lines with or without the insertion of the knockout construct. DNA extraction was performed (as described in section 2.2.1) and the insertion of the transgene was verified by PCR, using specific primers to amplify the *NEOMYCIN PHOSPHOTRANSFERASE II* (*NPTII*) gene (section 2.2.3.2 and primers are described in appendix Table 1). The presence of the *NPTII* amplicon on the resultant gel confirmed that the most improved individuals were transgenic and contained the transgene (ran alongside other constructs, similar to Figure 3-5). Despite this, no azygous lines were identified by a negative signal (absence of *NPTII* amplicon) identical to AC and no template controls.

5.2.1.3 Combining results from the genotypic and phenotypic screen to select lines for further characterisation in the next generation

The genotypic, phenotypic and carotenoid screening performed on the T_1 generation enabled the ranking of fruit quality traits, to select lines with the most significant improvements to commercial and consumer quality traits. Lines from the 4-6 insertion event demonstrated the most consistent improvements. The individuals 4-6-2 and 4-6-9 were selected as they reached a uniform red colouration 1.8-2.3 days quicker relative to controls, combined with a 1.3-fold elevation to carotenoid content at both ripe fruit stages. Both lines displayed large increases to total fruit yield (2.6- and 3.0-fold) and fruit size (1.6- and 1.9-fold), while firmness remained unchanged when compared to AC controls. Furthermore, 4-2-7 was selected as it exhibited the largest carotenoid increases (1.4-fold) at fourteen days post breaker, while other traits generally remained unchanged. Characterisation indicated that the *HSFA2* transcription factor has both developmental and ripening-related functions, with the potential to control pigmentation in accordance with previous carotenoid profiling.

5.2.2 Identification of azygous individuals combined with more detailed characterisation in the T_2 generation

Propagation of the most improved individuals: 4-2-7, 4-6-2 and 4-6-9 followed, to generate azygous lines through segregation (similar to sections 3.2.2 and 4.2.2). Further characterisation of the *HSFA2* transcription factor was performed on the progeny through comparisons with AC controls, utilising genotypic approaches to confirm the presence of the knockdown construct, followed by more detailed phenotypic and metabolic characterisation. Furthermore, a parallel crop was grown at the University of Nottingham to establish any changes to yield- and softening-related phenotypes across two separate locations.

5.2.2.1 Genotypic screening to identify non-transgenic azygous individuals in the T_2 generation

Transgenic lines were genotyped using PCR, which amplified the *NPTII* gene using specific primers (section 2.2.3.2 and primers are described in appendix Table 1). Visualisation of the resultant gel enabled the identification of ten azygous individuals, verified by a negative signal that was identical to both AC and no template controls (Figure 5-5). Azygous lines are considered to be the non-transgenic true control, as they have been through transformation and tissue culture and regular PCR was able to determine the absence of the transgene. Due to continued segregation, transgenic lines verified to be positive for the transgene were kept separate in the following analyses.

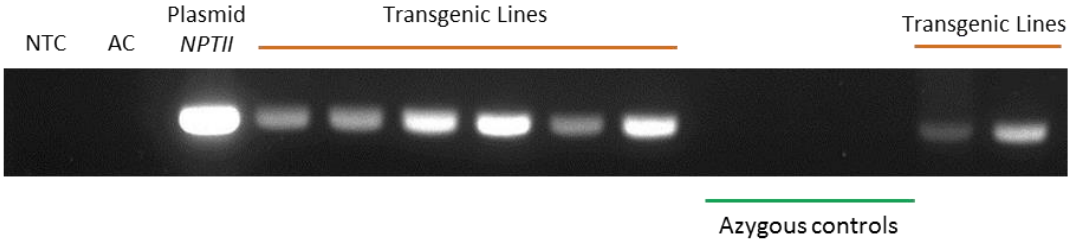

Figure 5-5 PCR confirmation to determine the presence of the knockout transgene in the transgenic lines and identification of azygous non-transgenic controls.

Amplification of the *NPTII* gene was performed by PCR on the majority of transgenic lines and visualised under UV light. Transgenic lines from the T_1 generation that yielded a negative signal identical to AC lines were identified as non-transgenic azygous controls (orange markers). DNA was extracted from a pool of 3 representative leaves of each plant. NTC: non template control.

5.2.2.2 Using altered ripening-related and developmental traits to select most improved individuals for detailed phenotypic characterisation

The T_1 generation identified altered fruit colour development and reduced internode length, combined with large fold changes to fruit yield. These traits, along with fruit firmness, were used as markers to identify and select the best lines for more detailed characterisation. Comparisons between the transgenic and AC lines demonstrate that these phenotypic differences are maintained into the T_2 generation. Transgenic lines display a consistent reduction to internode length, indicating altered plant morphology. Despite no individual line proving significant, on average internode lengths of transgenic lines were 1.2 cm shorter than both AC and azygous controls (Figure 5-6a). Importantly, the majority (69%) of transgenic lines exhibited a reduced time to transition from breaker to uniform red ripe (Figure 5-7a), taking on average 0.4 and 0.6 days less compared to azygous and AC controls, respectively. No consistent trend to fruit firmness could be identified for transgenic lines 14 dpb, due to large differences between azygous and AC controls (Figure 5-7b). The majority of transgenic lines (79%) displayed reduced fruit firmness at 14 dpb compared to azygous controls (Figure 5-7b). Conversely, all but one transgenic line exhibited elevated fruit firmness at 14 dpb when compared with AC controls. Mature fruit yield proved variable (Figure 5-6b), but several transgenic lines demonstrated considerable improvements to both azygous and AC controls. Interestingly, all lines originating from the 4-2 insertion event displayed reduced yield to both controls, while the majority 4-6 lines exhibited yield improvements.

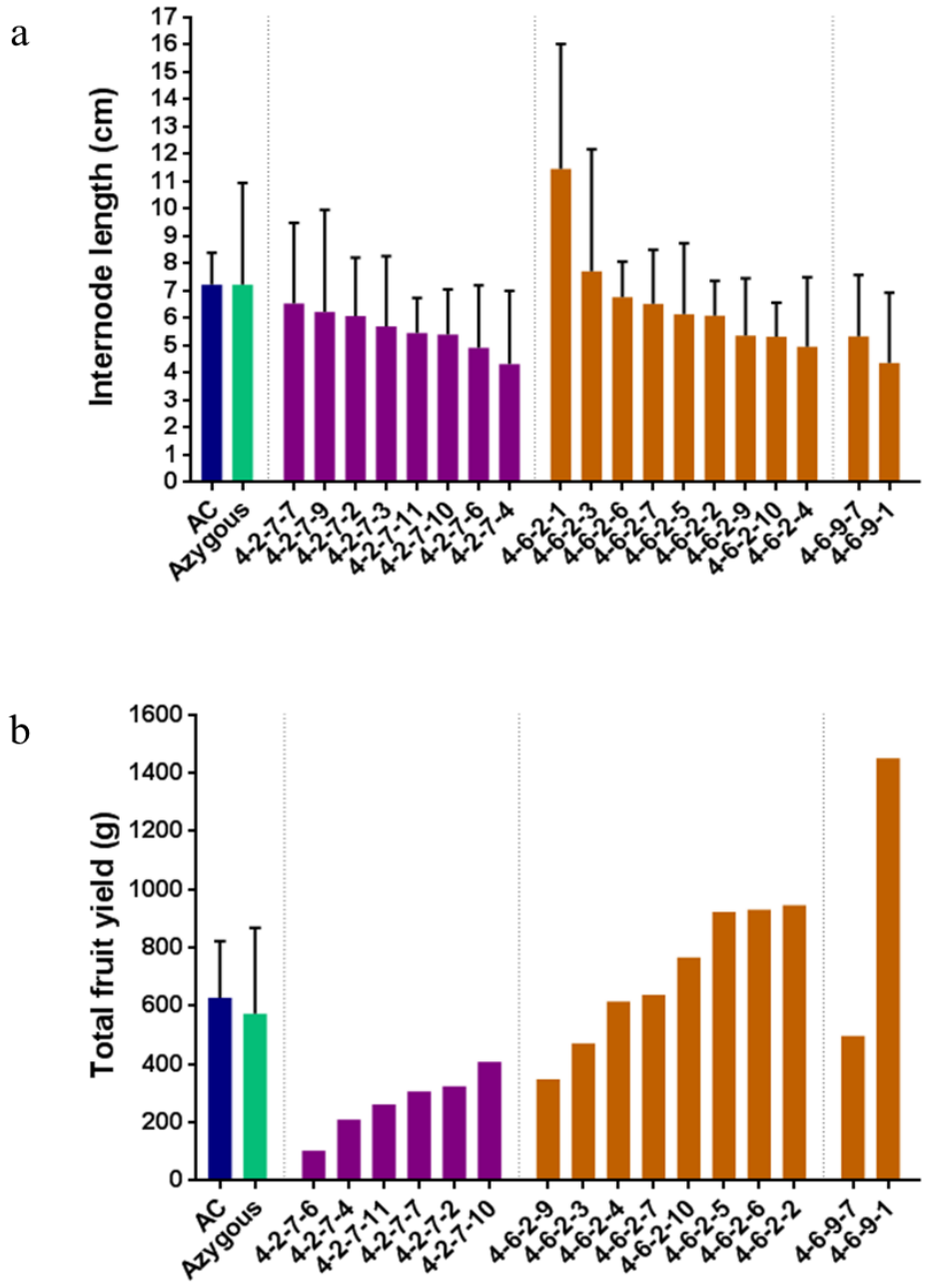

Figure 5-6 Internode length and total fruit yield screening of the T_2 population.

Internode lengths (a) and total fruit yield (b) of the T_2 population enabled a screen for altered development. Phenotypic screening enabled the selection of extremes with the most positively altered phenotypes, and correlated with similar experiments conducted on the T_1 generation. Five random internodes were measured from the base of the plant to the last node. Fruit were weighed individually postharvest and combined to determine total fruit yield. Each transgenic individual is represented by a single column. A total of up to seven and nine individuals were combined for azygous and AC controls, respectively. Statistical determinations are shown as mean ± SD, Dunnett's test analysis illustrates statistically significant differences between non-transgenic azygous controls and the transgenic varieties, $P < 0.05$, $^{**}P < 0.01$, and $^{***}P < 0.001$ are designated by *, **, and ***, respectively.

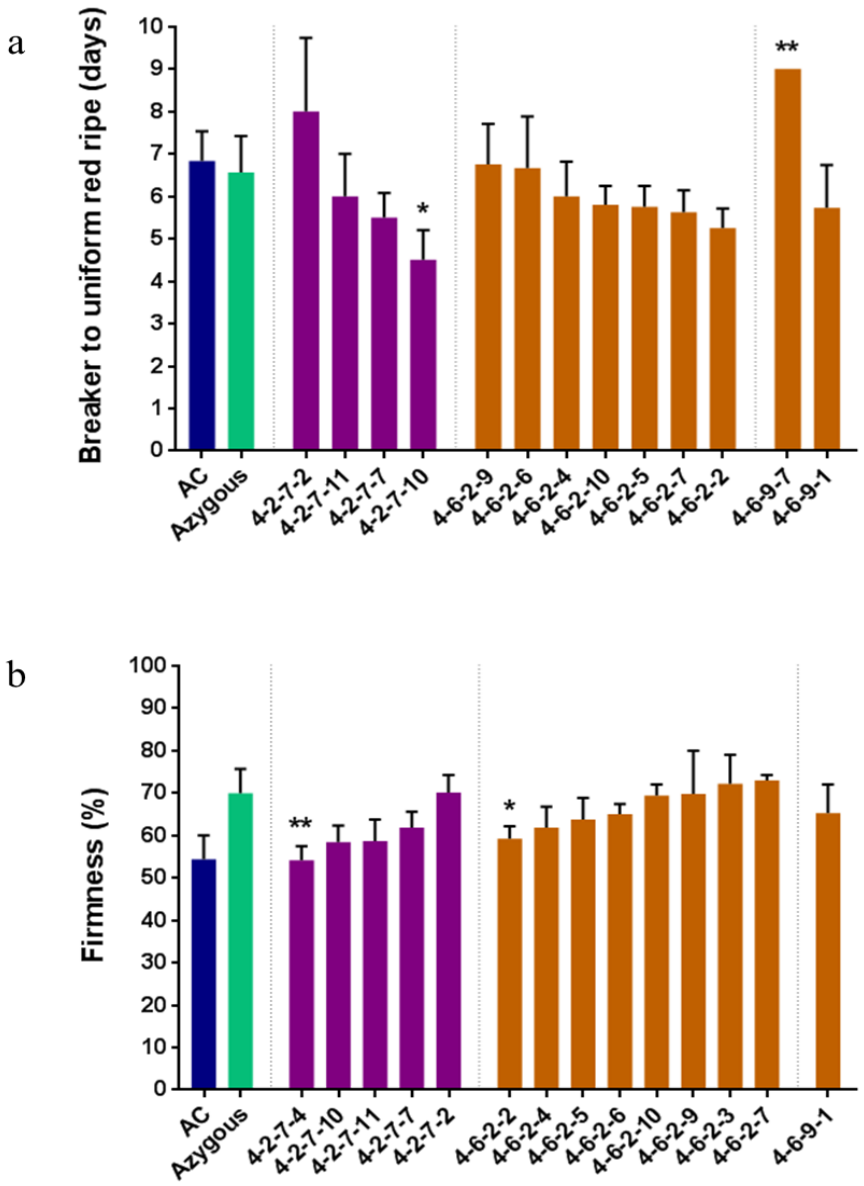

Figure 5-7 Ripening-related colour development and fruit firmness screening of the T_2 population.

Assessment of ripening-associated colour development (a) and fruit firmness (b) enabled the selection of the most improved lines, in addition to confirming the results obtained for the T_1 generation. Colour-related rapidity of ripening represents visual determination of the time taken for fruits to transition from breaker to uniform red. Fruit softening was measured at fourteen days post breaker using a fruit firmness meter; four measurements were taken per fruit. For both analyses between two and nine representative fruit were studied. Each transgenic individual is represented by a single column. A total of up to five and nine individuals were combined for azygous and AC controls, respectively. Statistical determinations are shown as mean ± SD, Dunnett's test analysis illustrates statistically significant differences between non-transgenic azygous and the transgenic varieties, $P < 0.05$, $^{**}P < 0.01$, and $^{***}P < 0.001$ are designated by *, **, and ***, respectively.

5.2.2.3 Detailed developmental-related phenotypic characterisation of the most improved *HSFA2* individuals

Figures 5-6 and 5-7 were used to select the most consistently improved phenotypes, focusing on positively altered fruit quality and yield. More detailed characterisation was then conducted to explain the altered phenotypes observed. Firstly, yield-related traits were studied. The majority of the selected *HSFA2* transgenic lines had improved total fruit yield and fruit size compared to both azygous and AC controls (Figure 5-8a). Increases to total fruit yield ranged from 11-253% and 2-231% to azygous and AC controls, respectively. The five transgenic lines with the highest yield exhibited greater fruit size by 19-36% to azygous controls, with 4-6-2-6 proving to be significant. Larger increases to average fruit size were identified to AC controls (34-53%), with all five lines proving to be significant. A positive correlation (R^2=0.68) between yield and average mature fruit weight was identified. This suggests that the increase to average fruit size was the main contributor to improved fruit yield.

Fruit set phenotypes were also studied (Figure 5-8b), where it was determined that on average transgenic lines produced 7.3 and 11.2 more flowers compared to azygous and AC controls, respectively. On average transgenic lines were also shown to produce 7.0 more fruit compared with azygous controls, with lines from the 4-6 insertion event yielding significantly more fruit. No change to average fruit number was identified when compared to AC controls. The result reveals that AC controls have the highest fruit set (36%), compared to transgenic lines (34%) and azygous controls (23%). Figure 5-8 demonstrates the potential yield improvements of the lines from the 6-4 insertion event, due to elevated fruit size compared to AC controls, and a combination of fruit size and number compared to azygous controls.

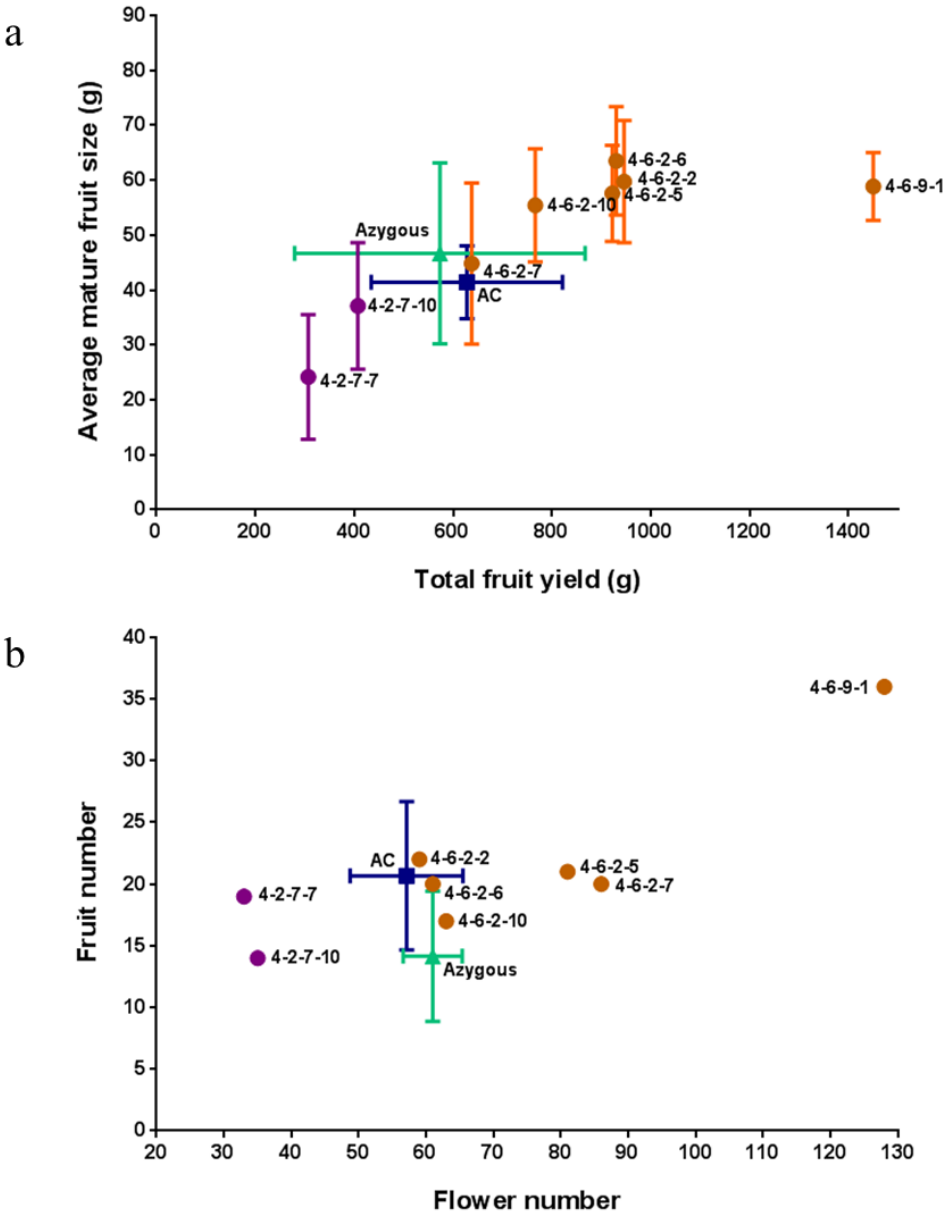

Figure 5-8 Assessment of fruit yield, size and set phenotypes for the most improved *HSFA2* transgenic lines.

Total fruit yield and average ripe fruit size were correlated (a) to assess the fruit yield-related phenotypes. Fruit set was evaluated by determination of flower and fruit number (b). Only selected transgenic lines with the most improved yield and quality traits are shown. Ten representative fruits weights were combined for this analysis. Fruit weights were determined individually postharvest and combined to determine total fruit yield. Fruit parameters were measured once the wild type AC background had formed five trusses. Each transgenic individual is represented by a single point. A total of up to seven and nine individuals were combined for azygous and AC controls, respectively. Statistical determinations are shown as mean ± SD.

Truss morphology was also investigated to determine whether altered flowers per truss and truss forking phenotypes were contributing to the altered fruit set and yield traits identified. Figure 5-9a demonstrates that the majority of transgenic lines produce more flowers per truss when compared to both controls. On average transgenic lines yield 3.6 (29%) and 4.2 (35%) more flower per individual truss compared to azygous and AC controls, respectively. This result prompted the assessment of truss forking (Figure 5-9b), which is defined by a singular truss axis that splits into multiple axes capable of yielding more flowers. It was calculated that on average transgenic lines trusses' split on average 1.7 times compared to 1.5 (1.1-fold) and 1.3 (1.3-fold) for both azygous and AC controls, respectively. Due to similar increases, it can be predicted that elevated truss forking is contributing to the increases to the number of flowers per truss in transgenic lines when compared to AC controls. While a more similar truss morphology is shared between transgenic and azygous lines, suggesting that transgenic lines just yield more flowers per truss, without the alteration of truss structure. Interestingly, 4-6-9-1 displays the highest truss forking value (2.5), flowers per truss (24.4), fruit number (36) and yield (1450 g), while fruit size remains consistent with other transgenic lines from the 4-6 insertion event. The results enabled the prediction that altered truss morphology contributed to elevated flowers per truss and in total, which did not alter fruit set phenotypes, enabling the production of more fruit. The combination of elevated fruit size and number contributed to significant yield improvements.

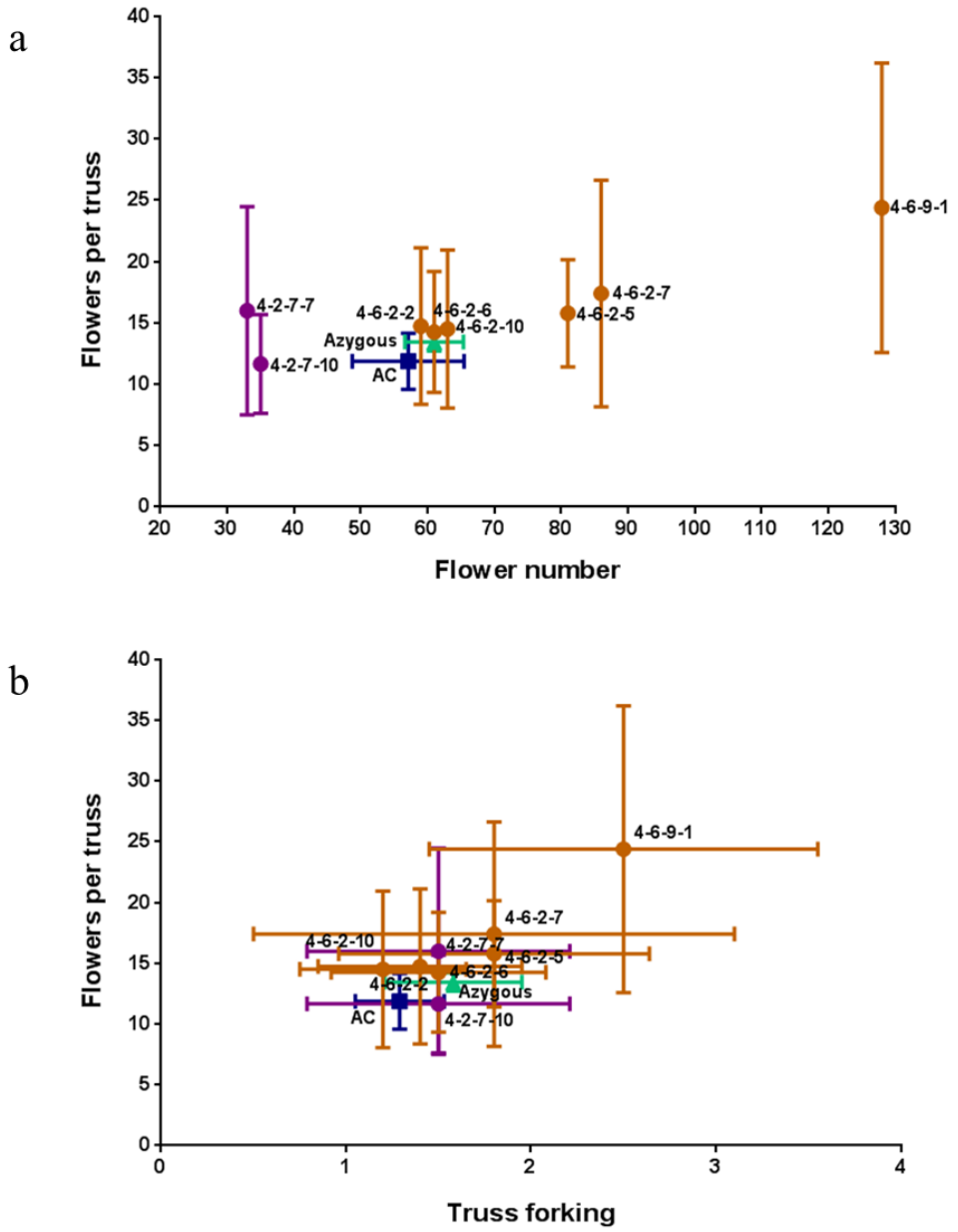

Figure 5-9 Phenotypic assessment of truss morphology for the most improved *HSFA2* transgenic lines.

The number of flowers per truss and total flower number were correlated (a), and then flowers per truss and truss forking were compared (b). These phenotypic traits were used as markers for evaluating altered flower development in relation to truss architecture. Truss forking is defined by a singular truss axis that splits into multiple axes capable of yielding flowers. A minimum of four trusses were combined for both analyses. Fruit parameters were measured once the wild type AC background had formed five trusses. Each transgenic individual is represented by a single point. A total of up to seven and nine individuals were combined for azygous and AC controls, respectively. Statistical determinations are shown as mean ± SD.

A more condensed plant morphology (short and bushy) was exhibited by transgenic lines compared with AC controls. This is shown by the clear separation of transgenic lines away from AC controls (Figure 5-10). On average the selected transgenic lines exhibited a reduced internode length of 1.3 cm and a plant height of 33.9 cm, when compared to AC controls. Interestingly, transgenic lines also displayed shorter internode lengths by 1.3 cm to azygous controls, although no consistent changes to plant height were identified.

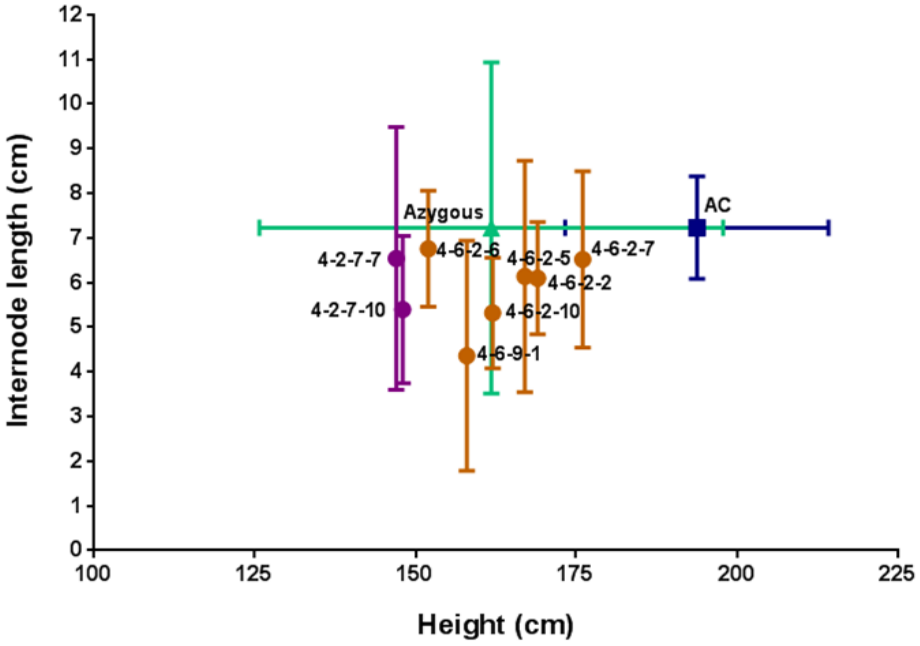

Figure 5-10 Phenotypic assessment of plant height and internode length for the most improved *HSFA2* transgenic lines.

Both plant height and internode lengths were recorded once the wild type AC background had formed five trusses. Five random internodes were measured from the base of the plant to the last node. Each transgenic individual is represented by a single point. A total of up to ten and nine individuals were combined for azygous and AC controls, respectively. Statistical determinations are shown as mean ± SD.

5.2.2.4 Detailed ripening-related phenotypic characterisation of most improved *HSFA2* individuals

As demonstrated previously, *HSFA2* transgenic lines exhibited increased ripening-related colour transition, combined with the potential to alter fruit softening. Fruits from selected transgenic lines ripened significantly quicker in terms of colour development when compared to both controls (Figure 5-11a). Transgenic lines took on average 1.0 days less to appear red ripe than azygous controls, and 1.2 days less to AC controls. Fruit firmness was monitored prior to ripening at the mature green stage, upon the onset of ripening at breaker, in addition to the ripe stages seven and fourteen days post breaker (Figure 5-11b). Compared to both controls, firmness at both mature green and breaker stages remained unchanged in selected transgenic lines. However, several firmness differences were identified in ripe fruit compared to both control genotypes. Selected transgenic lines demonstrate elevated fruit softening compared with azygous controls. At 7 dpb, transgenic lines displayed a significant 11.8% (1.2-fold) reduction to fruit firmness. Transgenic lines also exhibited a nonsignifcant 5.4% (1.1-fold) reduction to firmness at 14 dpb, suggesting that transgenic lines are softening at reduced rate during the overripe stages. Interestingly, fruit firmness was significantly elevated by 9.8% (1.2-fold) at 7 dpb, and 10.2% (1.2-fold) at 14 dpb compared to AC controls, indicating reduced fruit softening.

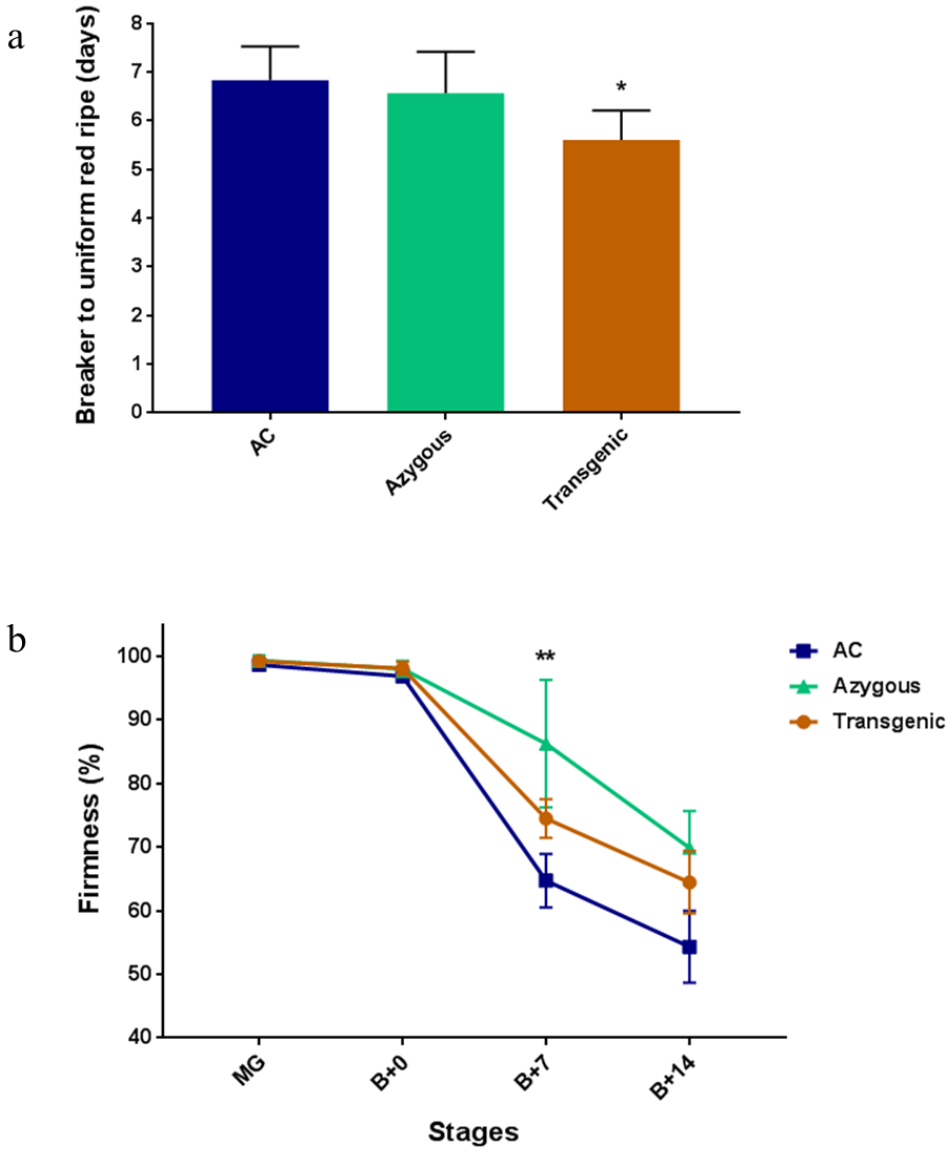

Figure 5-11 Combined ripening-related colour development and fruit firmness of most improved *HSFA2* individuals.

Ripening-associated colour development (a) and fruit firmness (b) quality traits of the most phenotypically improved individuals. Colour-related rapidity of ripening represents visual determination of the time taken for fruits to transition from breaker to uniform red. Fruit softening was measured at multiple stages post breaker using a fruit firmness meter; four measurements were taken per fruit. For both analyses between two and nine representative fruit were studied. Transgenic values incorporate the most improved eight individuals. A total of up to five and nine individuals were combined for azygous and AC controls, respectively. Statistical determinations are shown as mean ± SD, Dunnett's test analysis illustrates statistically significant differences between non-transgenic azygous and the transgenic varieties, $P < 0.05$, $^{**}P < 0.01$, and $^{***}P < 0.001$ are designated by *, **, and ***, respectively.

5.2.2.5 The effect of the insertion of the *HSFA2* transgene to isoprenoid content in ripe fruit

The altered times from breaker to uniform red ripe indicated changes to the rate of colour accumulation, therefore the carotenoid content of ripe fruits were assessed (Table 5-1 and Table 5-2). Two separate time points were chosen for the analysis, seven and fourteen days post breaker, when fruits were expected to have reached ripe and overripe, respectively. The total carotenoid content remained unchanged for the majority of transgenic lines at 7 dpb to the azygous controls (Table 5-1). While several transgenic lines displayed significant increases to carotenoid content when compared to AC controls. An average of all transgenic lines revealed a small significant 1.1-fold increase to the total carotenoid content compared to AC controls. On average, these increases were due to significantly elevated lycopene (1.3-fold) content, counteracted by reductions to β-carotene (1.1-fold). Similar to carotenoid content, the total tocopherol level was unchanged to azygous controls, but was significantly increased (1.1-fold) compared to AC controls. Transgenic lines on average exhibited a significant 1.1-fold increase to α-tocopherol to AC controls, while no consistent differences to δ-tocopherol were identified.

More differences were identified in fruit harvested at 14 dpb (Table 5-2). Compared to azygous controls, multiple transgenic lines displayed significant reductions to phytoene and phytofluene, combined with nonsignificant reductions to lycopene. This culminated in a decreased total carotenoid content in most transgenic lines, although few proved to be significant. Combining all transgenic lines revealed significant reductions to phytoene (1.2-fold), phyotfluene (1.1-fold) and total carotenoid content (1.1-fold), in addition to a nonsignificant 1.1-fold reduction to lycopene. Interestingly, comparisons between transgenic and azygous lines revealed a significant 1.1-fold increase to α-tocopherol in transgenic lines, although both δ-tocopherol and total tocopherol content remained unchanged.

Similar to 7 dpb, multiple transgenic lines exhibited significant increases to several isoprenoids at 14 dpb (Table 5-2), resulting in elevated total carotenoid (1.1-fold) compared to AC controls. On average transgenic lines displayed significant increases to phytoene (1.3-fold), phytofluene (1.1-fold) and lycopene (1.3-fold), while β-carotene was significantly reduced 1.1-fold. Small significant increases to α-tocopherol (1.1-fold) were recorded although δ-tocopherol and total tocopherol content remained unchanged.

Line	AC	Azygous	4-6-2-2	4-6-2-5	4-6-2-6	4-6-2-10	4-6-9-1
Lutein	530.7 ± 15.0	529.4 ± 17.3	540.8 ± 11.2	524.6 ± 7.8	**558.4 ± 13.9***	529.8 ± 20.1	517.8 ± 7.6
Neurosporene	736.8 ± 21.2	734.4 ± 24.1	743.7 ± 14.8	732.0 ± 10.6	769.2 ± 16.9	735.5 ± 30.0	716.7 ± 11.6
δ-Carotene	745.2 ± 21.3	746.4 ± 24.2	755.0 ± 13.9	745.9 ± 10.4	782.6 ± 16.9	746.6 ± 29.7	727.0 ± 12.2
Lycopene	1169.1 ± 236.6	1696.4 ± 58.5	1495.4 ± 17.5	1891.5 ± 109.8	1640.2 ± 198.1	1549.7 ± 45.6	**1199.0 ± 95.9*** **
γ-Carotene	742.4 ± 20.8	731.4 ± 26.1	740.0 ± 14.4	731.6 ± 10.1	767.6 ± 15.9	734.3 ± 28.9	715.9 ± 10.1
β-Carotene	868.4 ± 19.7	794.2 ± 30.6	815.2 ± 14.8	803.2 ± 7.2	833.7 ± 26.7	795.1 ± 31.4	761.9 ± 13.4
ζ-Carotene	733.8 ± 21.5	729.7 ± 24.3	740.4 ± 14.6	728.4 ± 10.5	765.0 ± 17.0	733.3 ± 28.9	714.2 ± 10.8
Phytofluene	316.6 ± 25.2	335.1 ± 18.3	316.6 ± 5.8	343.2 ± 2.5	331.4 ± 13.6	334.4 ± 10.5	315.6 ± 7.6
Phytoene	184.8 ± 37.8	209.1 ± 20.4	174.2 ± 4.7	223.1 ± 8.4	196.5 ± 18.0	215.4 ± 6.9	196.6 ± 7.2
Total CAR	6027.8 ± 300.8	6506.1 ± 188.0	6321.2 ± 75.0	6723.6 ± 64.3	6644.5 ± 332.8	6374.1 ± 155.2	**5864.7 ± 158.5****
α-Tocopherol	329.8 ± 17.3	360.7 ± 33.4	401.2 ± 7.1	369.2 ± 12.8	379.2 ± 48.5	385.8 ± 13.6	352.8 ± 13.8
δ-Tocopherol	209.1 ± 8.3	213.1 ± 12.6	206.2 ± 4.0	201.9 ± 10.8	210.6 ± 9.5	207.5 ± 4.0	200.5 ± 1.0
Total TOCO	538.9 ± 21.1	573.8 ± 29.8	607.4 ± 3.7	571.1 ± 16.7	589.8 ± 56.4	593.2 ± 17.6	553.3 ± 13.7

Table 5-1 Carotenoid and tocopherol composition of *HSFA2* transgenic ripe fruit at seven days post breaker compared to both controls.

Carotenoid and tocopherol contents of ripe fruits at seven days post breaker are presented as μg/g DW. Each transgenic line is kept separate, while three and five individuals were combined for azygous and AC controls, respectively. A minimum of five representative fruits per individual were pooled and three determinations were made. This ensured a minimum of three biological and three technical replicates for control lines. Methods used for these determinations are described in section 2.3. The mean data are presented ± SD. Dunnett's test analysis illustrates statistically significant differences between non-transgenic azygous controls and the transgenic varieties, $P < 0.05$, $^{**}P < 0.01$, and $^{***}P < 0.001$ are designated by *, **, and ***, respectively.

Line	AC	Azygous	4-6-2-2	4-6-2-5	4-6-2-6	4-6-2-7	4-6-2-10	4-6-9-1
Lutein	532.0 ± 17.6	533.7 ± 15.0	534.9 ± 23.9	511.6 ± 7.4	522.9 ± 21.7	550.2 ± 6.4	537.6 ± 19.6	535.9 ± 17.9
Neurosporene	744.5 ± 24.8	752.9 ± 20.9	747.9 ± 34.6	721.9 ± 9.6	730.7 ± 31.8	774.3 ± 9.6	761.1 ± 28.2	752.2 ± 25.5
δ-Carotene	762.3 ± 24.8	779.1 ± 21.1	775.0 ± 36.5	747.9 ± 10.1	754.9 ± 32.9	798.5 ± 10.6	790.1 ± 28.3	774.9 ± 28.7
Lycopene	1955.6 ± 343.0	2843.2 ± 368.3	2640.1 ± 287.7	2997.8 ± 86.8	**2224.1 ± 113.4***	2420.8 ± 62.1	2900.1 ± 168.7	2369.9 ± 265.6
γ-Carotene	749.5 ± 24.1	749.5 ± 20.4	743.7 ± 33.5	720.3 ± 10.8	730.2 ± 31.2	770.6 ± 9.3	757.2 ± 27.4	750.3 ± 26.0
β-Carotene	879.8 ± 46.1	804.5 ± 21.4	794.2 ± 36.7	800.3 ± 12.7	786.2 ± 30.6	836.5 ± 12.7	808.2 ± 32.5	810.4 ± 26.5
ζ-Carotene	740.3 ± 25.4	752.7 ± 21.0	745.3 ± 33.4	714.4 ± 10.0	731.8 ± 31.1	773.0 ± 9.2	759.6 ± 27.4	751.7 ± 26.4
Phytofluene	349.2 ± 28.9	449.6 ± 48.3	**385.0 ± 21.3***	**350.1 ± 5.7*****	**389.4 ± 9.9***	408.6 ± 4.1	449.5 ± 36.3	408.5 ± 20.9
Phytoene	215.4 ± 36.3	356.0 ± 68.4	**271.9 ± 11.8***	**222.7 ± 4.4*****	287.2 ± 6.0	289.1 ± 6.7	353.7 ± 33.0	297.5 ± 22.2
Total CAR	6928.6 ± 415.0	8021.1 ± 461.2	7638.1 ± 492.9	7787.1 ± 145.2	**7157.3 ± 188.0***	7621.5 ± 122.2	8116.9 ± 383.3	7451.2 ± 445.1
α-Tocopherol	337.0 ± 19.1	334.7 ± 21.4	345.3 ± 27.5	362.7 ± 9.5	352.6 ± 6.6	**378.6 ± 15.9****	333.2 ± 12.3	352.6 ± 13.5
δ-Tocopherol	213.4 ± 9.9	215.5 ± 11.3	214.0 ± 9.2	198.6 ± 16.9	200.0 ± 14.0	209.9 ± 3.8	227.9 ± 3.3	209.1 ± 9.5
Total TOCO	550.4 ± 19.3	550.2 ± 25.0	559.3 ± 36.7	561.3 ± 25.2	552.6 ± 15.7	588.5 ± 15.1	561.1 ± 14.6	561.7 ± 10.2

Table 5-2 Carotenoid and tocopherol composition of *HSFA2* transgenic ripe fruit at fourteen days post breaker compared to both controls.

Carotenoid and tocopherol contents of ripe fruits at fourteen days post breaker are presented as μg/g DW. Each transgenic line is kept separate, while three and five individuals were combined for azygous and AC controls, respectively. A minimum of five representative fruits per individual were pooled and three determinations were made. This ensured a minimum of three biological and three technical replicates for control lines. Methods used for these determinations are described in section 2.3. The mean data are presented ± SD. Dunnett's test analysis illustrates statistically significant differences between non-transgenic azygous controls and the transgenic varieties, $P < 0.05$, $^{**}P < 0.01$, and $^{***}P < 0.001$ are designated by *, **, and ***, respectively.

5.2.2.6 Broader metabolism differences arising from the insertion of the *HSFA2* transgene

The broader effects to metabolism were screened using Gas Chromatography-Mass Spectrometry (GC-MS), generating a metabolite profile of two ripe fruit stages. A combination of analytical platforms, with different phase extractions, coupled with different loadings enabled identification and quantification in a relative or absolute manner of over 75 metabolites. Metabolome comparisons were made between *HSFA2* transgenic lines and both non-transgenic (azygous) and wild type (AC) controls at 7 and 14 dpb (as described in section 2.3). Statistical determinations were made to assess the differences between genotypes (as described in section 2.4). Significant (p-value <0.05) changes to metabolite levels were identified in most classes of compounds analysed (Table 5-3). The altered isoprenoid levels in ripe fruit tissues have been described in section 5.2.2.5. Compared to both controls, total amino acid content remained unchanged at both time points studied. Compared to AC controls at 7 dpb, reduced alanine (4.5-fold) and increased aspartic acid (2.0-fold) were the only significant changes identified in transgenic lines. More significant alterations to different amino acids were identified at 14 dpb. Significant differences to cysteine, serine and valine content were identified when compared to both controls. Furthermore, reduced phenylalanine and elevated alanine, isoleucine and threonine were identified when compared to azygous controls. While reduced leucine and proline, and increased aspartic acid were observed in transgenic lines compared with AC controls.

Total amyrin content was significantly reduced 1.6-fold in transgenic lines compared with AC controls at both time points studied, due to significantly less α-amyrin and β-amyrin contents. Differences proved less consistent when compared to azygous controls, where transgenic lines exhibited a nonsignificant 1.1-fold increase and 1.2-fold decrease at 7 and 14 dpb, respectively.

Multiple fatty acids were altered in transgenic lines compared to both controls. At 7 dpb, consistent reductions to glycero-1-C14:0, glycero-1-C16:0 and glycero-2-C16:0 were identified in transgenic lines. Less C16:0 was also observed when compared to azygous controls, while significant increases to C22:0 and C24:0 contents were identified in transgenic lines when compared to AC controls. Despite numerous differences, total fatty acid content remained unchanged at 7 dpb. More differences were observed at 14 dpb, with reductions to the majority of fatty acids identified. This resulted in consistent

1.2-fold reductions to total fatty acid content compared to both controls, although comparisons with AC lines only proved significant. Fruits from transgenic lines contained significantly less C16:0 and C18:0, in addition to all monoglyceride and diglyceride forms identified. The reductions to the majority of fatty acid forms were counteracted with large increases to C18:1cis9 in transgenic lines, displaying an 8.2-fold increase to azygous controls, while it could not be detected in AC controls.

At 7 dpb, transgenic lines exhibited a nonsignificant 1.2-fold elevation to organic acid content compared with azygous lines, and a significant 1.8-fold increase to AC controls. Significantly elevated gluconic acid (1.6-fold) compared to azygous controls and increased lactic acid (1.4-fold) and succinic acid (40.7-fold) compared to AC controls, contribute to the increased total organic acid content in transgenic lines. Again, more significant differences were identified at 14 dpb, with transgenic lines exhibiting elevated gluconic acid (1.1-1.2-fold) compared to both controls. Comparison with azygous lines revealed elevated itaconic acid (1.3-fold), while increased 2-oxoglutaric acid (1.3-fold) and reduced aconitic acid (1.6-fold), citraconic acid (1.2-fold), citric acid (1.3-fold), fumaric acid (12.2-fold) and malic acid (2.0-fold) were identified when compared to AC controls.

Compared to azygous controls total phosphate content was significantly reduced 1.2-fold in transgenic lines at 14 dpb. Significant reductions were also identified to inositol-6-phosphate and free phosphate compared with AC controls, although total phosphate levels remained unchanged. Similarly, total phytosterol content was significantly reduced in transgenic lines at 14 dpb when compared to azygous lines, due to less campesterol and stigmasterol, although only the former proved significant. While significantly increased phytosterol content was observed at 7 dpb compared with AC controls, due to significantly elevated sitosterol (1.9-fold) combined with nonsignificant increases to campesterol (1.8-fold). Campesterol was also increased 1.2-fold at 14 dpb compared with AC lines. Despite consistent reductions to inositol at both stages compared with AC controls, total polyol content remained unchanged. GABA at both stages and hentriacontane content at 7 dpb were also increased in AC controls.

Finally, despite no change to the total sugar contents at both ripe stages, significant differences were identified to multiple sugar forms. At 7 dpb, significant increases to fructose (1.1 to 1.2-fold) and glucose (1.1-fold) were identified in transgenic lines compared with both controls. Galactose was increased 1.3-fold when compared to AC lines, while arabinose, ribose and xylose were increased 1.5-fold to azygous controls.

Transgenic lines exhibited elevated xylulose at 14 dpb compared to azygous controls, while increased arabinose, ribose, trehalose and xylose, combined with lower galactose, maltose and sucrose contents were detected in comparison to AC controls.

	Ratio			
Stage	7 days post breaker		14 days post breaker	
Metabolite	Tr: Azy	Tr: AC	Tr: Azy	Tr: AC
Amino acid				
5-oxo-proline	0.92 ± 0.49	1.38 ± 0.73	0.82 ± 0.28	1.29 ± 0.44
Alanine	1.05 ± 0.78	**0.22 ± 0.17**	**1.60 ± 0.32**	0.74 ± 0.15
b-Alanine	1.16 ± 0.06	1.22 ± 0.06	0.95 ± 0.15	0.87 ± 0.14
Aspartic acid	0.93 ± 0.46	**1.98 ± 0.97**	0.91 ± 0.31	**1.67 ± 0.56**
Cysteine	-	-	**10***	**0.34 ± 0.29**
Glutamine	-	-	0.79 ± 0.60	0.93 ± 0.70
Homocysteine	1.07 ± 0.10	0.96 ± 0.09	1.02 ± 0.34	1.05 ± 0.35
Isoleucine	0.60 ± 0.79	0.48 ± 0.64	**1.21 ± 0.36**	0.77 ± 0.23
Leucine	-	-	0.52 ± 0.59	**0.21 ± 0.24**
Phenylalanine	-	-	**0.45 ± 0.24**	0.88 ± 0.47
Proline	-	-	3.06 ± 3.61	**0.21 ± 0.24**
Serine	0.93 ± 0.42	0.72 ± 0.33	**1.29 ± 0.33**	**0.74 ± 0.19**
Threonine	0.90 ± 0.55	0.94 ± 0.58	**1.23 ± 0.29**	0.82 ± 0.20
Valine	-	-	**1.55 ± 0.62**	**0.55 ± 0.22**
Amyrin				
α-Amyrin	1.11 ± 0.22	**0.72 ± 0.14**	0.84 ± 0.19	**0.61 ± 0.13**
β-Amyrin	1.13 ± 0.35	**0.56 ± 0.17**	0.88 ± 0.27	**0.63 ± 0.19**
Fatty acid				
C14:0	0.94 ± 0.09	1.08 ± 0.10	0.85 ± 0.22	1.02 ± 0.27
C16:0	**0.88 ± 0.11**	1.01 ± 0.13	**0.80 ± 0.19**	**0.86 ± 0.21**
C18:0	0.92 ± 0.13	1.06 ± 0.15	**0.67 ± 0.32**	**0.68 ± 0.33**
C18:1cis9	-	-	**8.15 ± 4.97**	**10***
C18:2 cis9,12	0.94 ± 0.30	0.91 ± 0.30	0.96 ± 0.08	1.14 ± 0.09
C18:2 trans9,12	1.36 ± 0.51	1.08 ± 0.41	-	-
C20:0	0.99 ± 0.13	0.87 ± 0.12	1.00 ± 0.12	0.75 ± 0.09
C22:0	1.18 ± 0.23	**1.45 ± 0.28**	0.97 ± 0.19	0.93 ± 0.19
C24:0	1.08 ± 0.22	**1.22 ± 0.25**	1.02 ± 0.53	1.13 ± 0.59
Glycero-1-C14:0	**0.76 ± 0.03**	**0.79 ± 0.03**	**0.35 ± 0.37**	**0.32 ± 0.34**
Glycero-1-C16:0	**0.78 ± 0.02**	**0.79 ± 0.02**	**0.43 ± 0.29**	**0.37 ± 0.25**
Glycero-1-C18:0	0.82 ± 0.11	0.77 ± 0.11	**0.40 ± 0.27**	**0.33 ± 0.22**
Glycero-2-C16:0	**0.58 ± 0.17**	**0.60 ± 0.17**	**0.38 ± 0.41**	**0.31 ± 0.34**
Glycero-2-C18:0	0.78 ± 0.24	0.79 ± 0.24	**0.37 ± 0.43**	**0.23 ± 0.27**

Hydrocarbon				
Hentriacontane	1.12 ± 0.30	**0.65 ± 0.17**	0.94 ± 0.50	0.67 ± 0.36
Isoprenoid				
β-Carotene	1.01 ± 0.03	**0.92 ± 0.03**	1.00 ± 0.02	**0.92 ± 0.02**
δ-Carotene	1.01 ± 0.03	1.01 ± 0.03	0.99 ± 0.03	1.01 ± 0.03
γ-Carotene	1.01 ± 0.03	0.99 ± 0.03	0.99 ± 0.02	0.99 ± 0.02
ζ-Carotene	1.01 ± 0.03	1.00 ± 0.03	0.99 ± 0.03	1.00 ± 0.03
Lutein	1.01 ± 0.03	1.01 ± 0.03	1.00 ± 0.02	0.99 ± 0.02
Lycopene	**0.92 ± 0.15**	**1.41 ± 0.23**	**0.91 ± 0.11**	**1.48 ± 0.18**
Neurosporene	1.01 ± 0.03	1.00 ± 0.03	0.99 ± 0.03	1.00 ± 0.03
Phytoene	0.96 ± 0.09	1.08 ± 0.10	**0.81 ± 0.12**	**1.40 ± 0.21**
Phytofluene	0.98 ± 0.04	1.04 ± 0.04	**0.89 ± 0.07**	**1.16 ± 0.10**
α-Tocopherol	1.05 ± 0.05	**1.15 ± 0.05**	**1.06 ± 0.05**	**1.07 ± 0.05**
δ-Tocopherol	**0.96 ± 0.02**	0.98 ± 0.02	0.97 ± 0.05	**0.96 ± 0.05**
g-Tocopherol	1.07 ± 0.35	0.81 ± 0.26	0.65 ± 0.13	**0.47 ± 0.10**
Lipid				
GABA	1.07 ± 0.77	**0.43 ± 0.31**	1.21 ± 0.65	**0.39 ± 0.21**
Organic acids				
2-oxoglutaric acid	1.06 ± 0.22	1.18 ± 0.25	1.05 ± 0.25	**1.26 ± 0.30**
Aconitic acid	-	-	1.05 ± 0.69	**0.62 ± 0.41**
Citraconic acid	-	-	1.50 ± 0.50	**0.81 ± 0.27**
Citric acid	1.09 ± 0.17	**0.74 ± 0.12**	0.95 ± 0.11	**0.78 ± 0.09**
Fumaric acid	-	-	2.59 ± 4.01	**0.08 ± 0.13**
Glucaric acid	0.63 ± 0.48	1.70 ± 1.30	0.82 ± 0.29	1.19 ± 0.41
Gluconic acid	**1.58 ± 0.72**	1.25 ± 0.57	**1.18 ± 0.11**	**1.09 ± 0.11**
Glucuronic acid	1.19 ± 0.43	1.39 ± 0.51	1.11 ± 0.24	1.11 ± 0.25
Itaconic acid	-	-	**1.30 ± 0.41**	0.89 ± 0.28
Lactic acid	1.21 ± 0.24	**1.42 ± 0.29**	1.06 ± 0.29	1.39 ± 0.38
Malic acid	0.82 ± 0.20	**0.54 ± 0.13**	1.02 ± 0.27	**0.49 ± 0.13**
Succinic acid	1.63 ± 1.49	**40.72 ± 37.08**	1.31 ± 0.83	1.53 ± 0.97
Phosphate				
Glucose-6-phosphate	1.57 ± 1.03	1.34 ± 0.88	1.04 ± 0.26	0.85 ± 0.21
Glycerol-3-phosphate	0.64 ± 0.28	0.64 ± 0.28	0.78 ± 0.22	1.05 ± 0.30
Inositol-6-phosphate	-	-	0.84 ± 0.46	**0.40 ± 0.22**
Phosphate	0.99 ± 0.07	**0.90 ± 0.07**	0.93 ± 0.04	**0.92 ± 0.04**
Phytosterol				
Campesterol	0.91 ± 0.93	1.75 ± 1.79	**0.73 ± 0.17**	1.16 ± 0.27
Sitosterol	1.21 ± 0.19	**1.86 ± 0.29**	-	-
Stigmasterol	0.95 ± 0.25	1.09 ± 0.29	0.89 ± 0.08	1.03 ± 0.10
Polyol				
Glycerol	0.64 ± 0.32	1.64 ± 0.82	0.90 ± 0.29	0.93 ± 0.30
Inositol	0.97 ± 0.17	**0.54 ± 0.10**	0.98 ± 0.14	**0.53 ± 0.08**
Pyrimidone				
Dihydrouracil	0.81 ± 0.59	1.17 ± 0.86	0.77 ± 0.26	1.07 ± 0.36

Sugar				
Arabinose	1.02 ± 0.22	**1.49 ± 0.33**	1.17 ± 0.14	**1.21 ± 0.15**
Erythrose	1.08 ± 0.35	1.15 ± 0.37	1.37 ± 0.57	0.93 ± 0.39
Fructose	**1.09 ± 0.10**	**1.17 ± 0.10**	1.06 ± 0.05	1.03 ± 0.05
Galactose	**1.32 ± 0.31**	0.84 ± 0.20	0.98 ± 0.10	**0.82 ± 0.09**
Glucose	**1.09 ± 0.09**	**1.07 ± 0.08**	1.05 ± 0.06	0.96 ± 0.05
Maltose	3.65 ± 8.16	7.28 ± 16.29	0.74 ± 0.52	**0.29 ± 0.20**
Pentose	1.02 ± 0.06	1.05 ± 0.06	1.12 ± 0.06	0.96 ± 0.05
Ribose	1.02 ± 0.22	**1.49 ± 0.33**	1.17 ± 0.14	**1.21 ± 0.15**
Sedoheptulose	0.88 ± 0.96	0.98 ± 1.06	0.90 ± 0.29	1.34 ± 0.43
Sucrose	1.13 ± 0.84	0.97 ± 0.72	0.87 ± 0.46	**0.37 ± 0.19**
Trehalose	-	-	1.06 ± 0.48	**1.70 ± 0.77**
Xylose	1.02 ± 0.22	**1.49 ± 0.33**	1.17 ± 0.14	**1.21 ± 0.15**
Xylulose	0.90 ± 0.22	1.17 ± 0.28	**1.27 ± 0.24**	0.98 ± 0.19

Table 5-3 Differences to metabolites occurring in *HSFA2* transgenic ripe fruit compared to both azygous and AC controls.

Data has been compiled from multiple analytical platforms. Metabolites were quantified, then ratios were calculated and presented as mean ± SD. Student's t-test was performed, significant changes are represented in bold (p-value < 0.05). 10*, indicates the theoretical value when a metabolite is unique to transgenic at the concentration used, thus was not detected in control samples. 0.01*, indicates theoretical value when a metabolite is unique to the controls at the sample concentration used. GABA, gamma-aminobutyric acid, 5-oxo-proline, pyroglutamic acid.

Multivariate principal component analysis (PCA) enabled assessment of the overall variance in chemical composition of ripe fruits at both time points from transgenic, azygous and AC lines, whilst identifying the contributions of each metabolite to the overall variance. The score values of ripe fruits at 7 dpb for the PCA are represented in a score scatter plot (Figure 5-12a). Transgenic and azygous genotypes fail to separate, but both cluster away from AC controls, indicating statistically significant differences between the two clusters. A PCA of just transgenic lines with azygous controls confirmed no statistically significant differences between these genotypes (not shown). The loading scatter plot displays the numerous metabolites that have significant weightings at 7 dpb (Figure 5-12a), indicating that cluster separation was due to multiple metabolites from various metabolite classes. Multiple isoprenoids had the highest loadings in transgenic and azygous fruits, including δ-carotene, ζ-carotene, lutein,

lycopene, neurosporene, phytoene, phytofluene, and α-tocopherol. Multiple sugars including arabinose, erythrose, glucose, fructose, ribose, sedoheptulose and xylose, as well as the organic acids glucaric acid, lactic acid and succinic acid had the highest loadings in azygous and transgenic tissues. Glycerol, campesterol, sitosterol, C22:0 and the amino acids aspartic acid and 5-oxo-proline also had the highest loadings in azygous and transgenic tissues at 7dpb. For AC controls, the organic acids malic acid and citric acid, the amino acids alanine and serine, the isoprenoids β-carotene and γ-tocopherol, both α-amyrin and β-amyrin, multiple glycerides, in addition to hentriacontane, GABA, inositiol and phosphate had the highest loadings at 7 dpb.

Similar results were obtained at 14 dpb (Figure 5-12b), with no separation between transgenic and azygous lines, although these tissues are statistically significantly different to AC controls. Azygous and transgenic tissues failed to separate on a separate PCA, again indicating no significant differences between these genotypes (not shown). Most of the compounds with highest loadings for each genotype at 7 dpb are consistent with tissues at 14 dpb. For azygous and transgenic lines the isoprenoids δ-carotene, lycopene, phytoene phyotfluene, α-tocopherol had the highest loadings. In addition to the amino acids aspartic acid and 5-oxo-proline, the organic acids 2-oxoglutaric acid, glucaric acid and lactic acid, as well as trehalose, campesterol and C18:2 cis9,12 had the highest loadings. While multiple amino acids including alanine, cysteine, isoleucine, leucine, proline, serine, threonine and valine, the organic acids fumaric acid and malic acid, in addition to β-carotene, GABA, inositol-6-phosphate, inositol, maltose and sucrose had the highest loadings at 14 dpb.

a

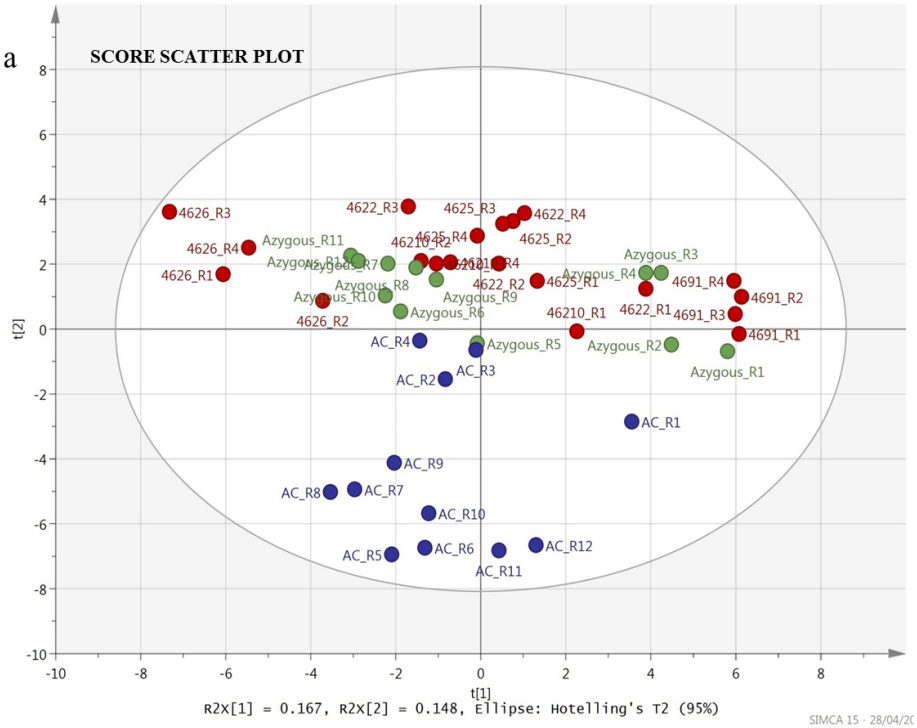
SCORE SCATTER PLOT
t[1]
t[2]
4626_R3
4622_R3
4625_R3
4622_R4
4626_R4
Azygous_R11
4625_R4
4625_R2
4626_R1
Azygous_R3
Azygous_R8
Azygous_R10
Azygous_R9
4622_R2
4625_R1
Azygous_R4
4691_R4
4691_R2
Azygous_R6
46210_R1
4622_R1
4691_R3
4626_R2
4691_R1
AC_R4
Azygous_R5
Azygous_R2
Azygous_R1
AC_R2
AC_R3
AC_R1
AC_R9
AC_R8
AC_R7
AC_R10
AC_R5
AC_R6
AC_R12
AC_R11
R2X[1] = 0.167, R2X[2] = 0.148, Ellipse: Hotelling's T2 (95%)
SIMCA 15 - 28/04/2(

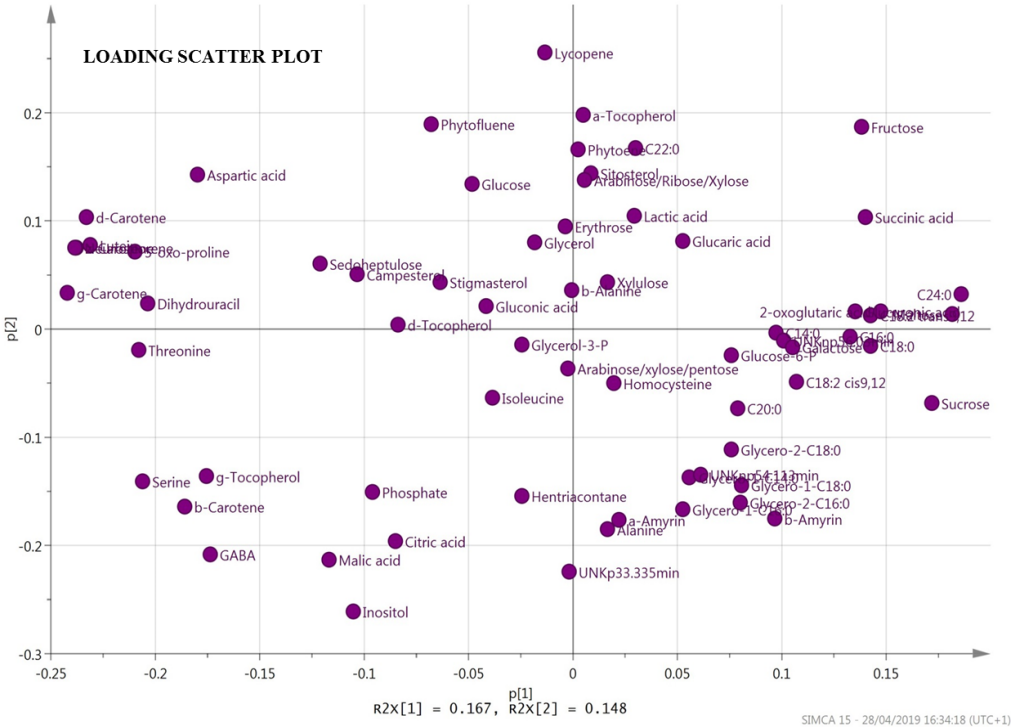
LOADING SCATTER PLOT
p[1]
p[2]
Lycopene
Phytofluene
a-Tocopherol
Fructose
Phytoene
C22:0
Aspartic acid
Sitosterol
Glucose
Arabinose/Ribose/Xylose
d-Carotene
Lactic acid
Succinic acid
Erythrose
Glycerol
Glucaric acid
5-oxo-proline
Sedoheptulose
Campesterol
Stigmasterol
Xylulose
b-Alanine
g-Carotene
Dihydrouracil
Gluconic acid
C24:0
d-Tocopherol
Threonine
Glycerol-3-P
C18:0
Glucose-6-P
Arabinose/xylose/pentose
Homocysteine
C18:2 cis9,12
Isoleucine
C20:0
Sucrose
Glycero-2-C18:0
Serine
g-Tocopherol
Glycero-1-C18:0
Phosphate
Hentriacontane
b-Carotene
Glycero-2-C16:0
a-Amyrin
Alanine
b-Amyrin
Citric acid
GABA
Malic acid
UNKp33.335min
Inositol
R2X[1] = 0.167, R2X[2] = 0.148
SIMCA 15 - 28/04/2019 16:34:18 (UTC+1)

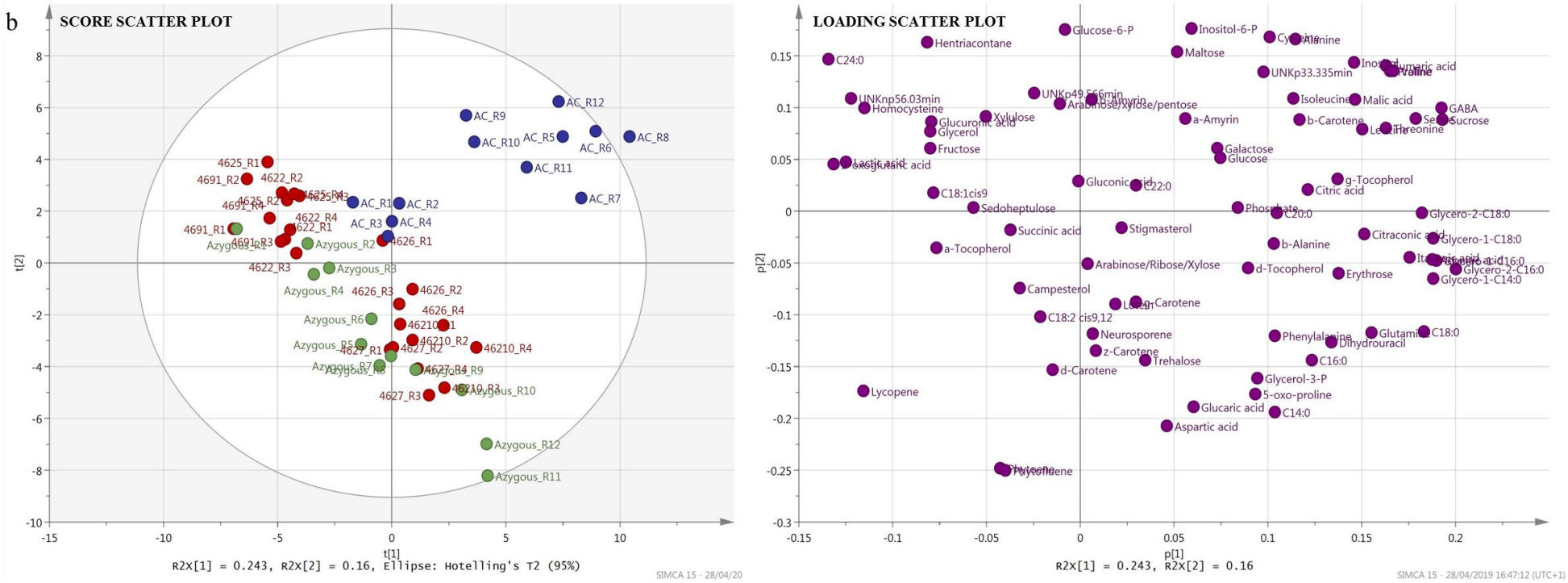

Figure 5-12 Principle component analysis of ripe fruit metabolism for *HSFA2* transgenic lines with both azygous and AC controls.

Score and loading scatter plots of fruits at seven (a) and fourteen days post breaker (b). Between three and five biological and two to three technical replicates were analysed for each experiment. Metabolite levels from the GC-MS and UPLC analytical platforms were combined. The UPLC method used to analyse isoprenoids, the GC-MS method to assess broader metabolism effects, and the treatment and processing of data are described in section 2.3.3, 2.3.5 and 2.4, respectively.

a

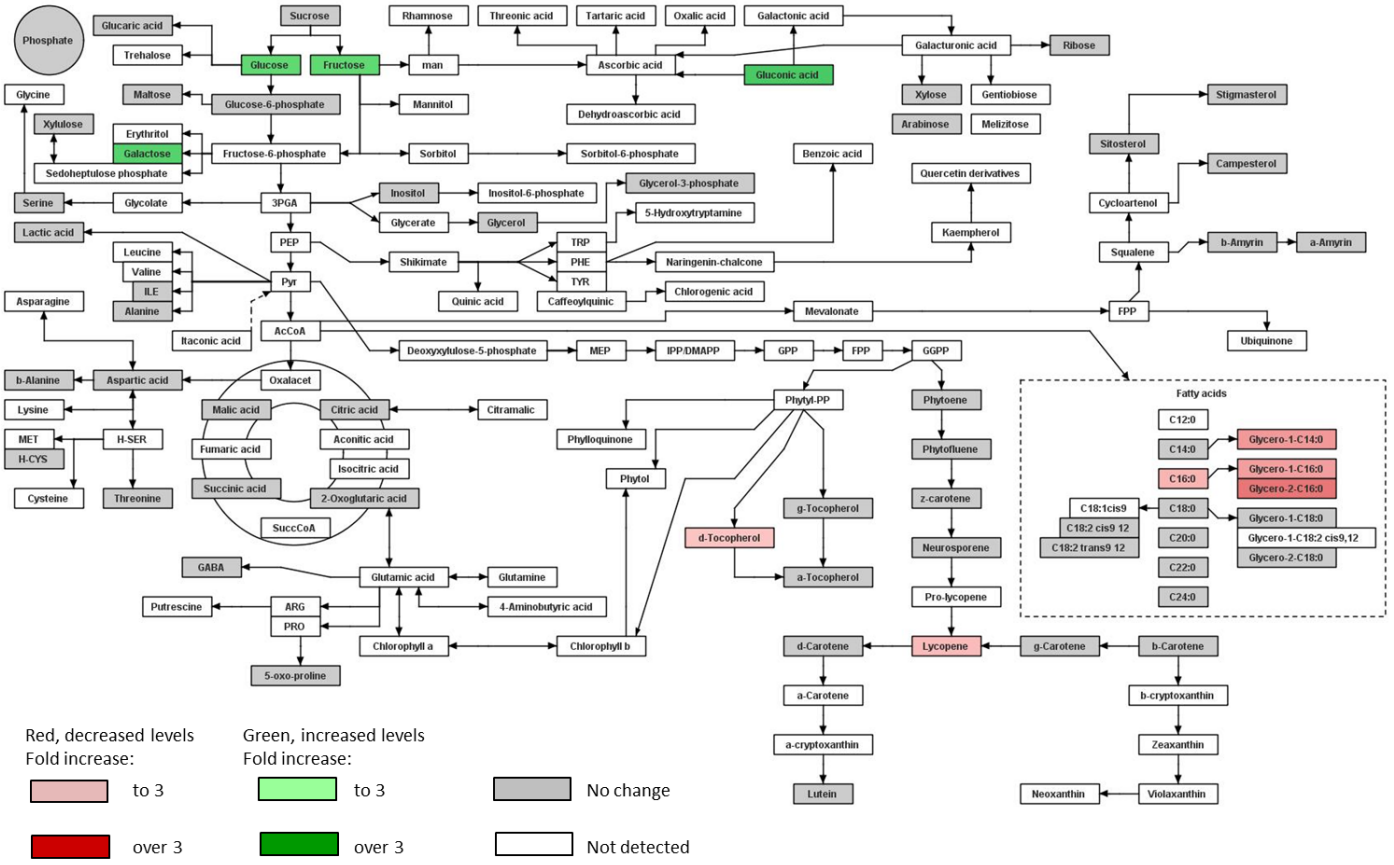
Phosphate
Glucaric acid
Trehalose
Glycine
Maltose
Xylulose
Erythritol
Galactose
Sedoheptulose phosphate
Serine
Glycolate
Lactic acid
Leucine
Valine
ILE
Alanine
Asparagine
Itaconic acid
b-Alanine
Aspartic acid
Lysine
MET
H-SER
H-CYS
Cysteine
Threonine
Sucrose
Glucose
Fructose
Glucose-6-phosphate
Fructose-6-phosphate
3PGA
PEP
Pyr
AcCoA
Oxalacet
Malic acid
Citric acid
Fumaric acid
Aconitic acid
Isocitric acid
Succinic acid
2-Oxoglutaric acid
SuccCoA
Citramalic
GABA
Glutamic acid
Glutamine
Putrescine
ARG
PRO
4-Aminobutyric acid
5-oxo-proline
Chlorophyll a
Chlorophyll b
Rhamnose
man
Mannitol
Sorbitol
Threonic acid
Tartaric acid
Oxalic acid
Galactonic acid
Ascorbic acid
Gluconic acid
Dehydroascorbic acid
Sorbitol-6-phosphate
Inositol
Inositol-6-phosphate
Glycerate
Glycerol
Glycerol-3-phosphate
5-Hydroxytryptamine
Shikimate
TRP
PHE
TYR
Quinic acid
Caffeoylquinic
Chlorogenic acid
Naringenin-chalcone
Benzoic acid
Quercetin derivatives
Kaempherol
Mevalonate
Deoxyxylulose-5-phosphate
MEP
IPP/DMAPP
GPP
FPP
GGPP
Phytyl-PP
Phylloquinone
Phytol
d-Tocopherol
g-Tocopherol
a-Tocopherol
Phytoene
Phytofluene
z-carotene
Neurosporene
Pro-lycopene
Lycopene
d-Carotene
g-Carotene
b-Carotene
a-Carotene
a-cryptoxanthin
Lutein
b-cryptoxanthin
Zeaxanthin
Neoxanthin
Violaxanthin
Galacturonic acid
Ribose
Xylose
Gentiobiose
Arabinose
Melizitose
Sitosterol
Stigmasterol
Campesterol
Cycloartenol
Squalene
b-Amyrin
a-Amyrin
FPP
Ubiquinone
Fatty acids
C12:0
C14:0
C16:0
C18:0
C20:0
C22:0
C24:0
C18:1cis9
C18:2 cis9 12
C18:2 trans9 12
Glycero-1-C14:0
Glycero-1-C16:0
Glycero-2-C16:0
Glycero-1-C18:0
Glycero-1-C18:2 cis9,12
Glycero-2-C18:0
Red, decreased levels
Fold increase:
to 3
over 3
Green, increased levels
Fold increase:
to 3
over 3
No change
Not detected

b

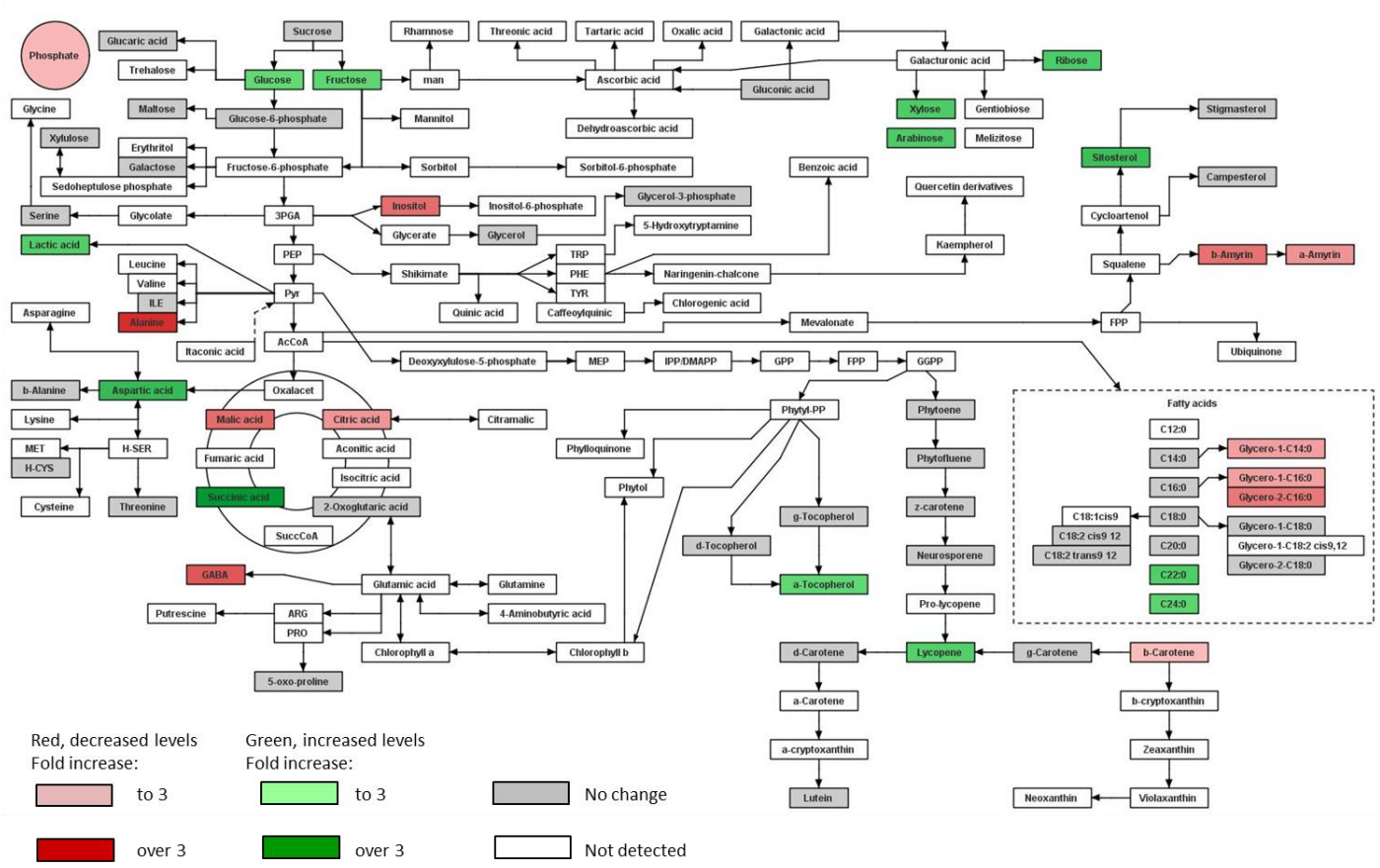
Phosphate
Glucaric acid
Sucrose
Rhamnose
Threonic acid
Tartaric acid
Oxalic acid
Galactonic acid
Galacturonic acid
Ribose
Trehalose
Glucose
Fructose
man
Ascorbic acid
Gluconic acid
Glycine
Maltose
Glucose-6-phosphate
Mannitol
Dehydroascorbic acid
Xylose
Gentiobiose
Xylulose
Arabinose
Melizitose
Erythritol
Galactose
Fructose-6-phosphate
Sorbitol
Sorbitol-6-phosphate
Sedoheptulose phosphate
Benzoic acid
Quercetin derivatives
Serine
Glycolate
3PGA
Inositol
Inositol-6-phosphate
Glycerol-3-phosphate
Glycerate
Glycerol
5-Hydroxytryptamine
Kaempherol
Lactic acid
PEP
TRP
Leucine
Shikimate
PHE
Naringenin-chalcone
Valine
TYR
ILE
Pyr
Quinic acid
Caffeoylquinic
Chlorogenic acid
Asparagine
Alanine
Mevalonate
FPP
Itaconic acid
AcCoA
Ubiquinone
Deoxyxylulose-5-phosphate
MEP
IPP/DMAPP
GPP
FPP
GGPP
b-Alanine
Aspartic acid
Oxalacet
Phytyl-PP
Phytoene
Lysine
Malic acid
Citric acid
Citramalic
Phylloquinone
Phytofluene
MET
H-SER
Fumaric acid
Aconitic acid
Phytol
z-carotene
H-CYS
Isocitric acid
g-Tocopherol
Succinic acid
2-Oxoglutaric acid
Cysteine
Threonine
d-Tocopherol
Neurosporene
SuccCoA
a-Tocopherol
Pro-lycopene
GABA
Glutamic acid
Glutamine
Putrescine
ARG
4-Aminobutyric acid
PRO
Chlorophyll a
Chlorophyll b
d-Carotene
Lycopene
g-Carotene
b-Carotene
5-oxo-proline
a-Carotene
b-cryptoxanthin
a-cryptoxanthin
Zeaxanthin
Lutein
Neoxanthin
Violaxanthin
Fatty acids
C12:0
C14:0
C16:0
C18:0
C20:0
C22:0
C24:0
C18:1cis9
C18:2 cis9 12
C18:2 trans9 12
Glycero-1-C14:0
Glycero-1-C16:0
Glycero-2-C16:0
Glycero-1-C18:0
Glycero-1-C18:2 cis9,12
Glycero-2-C18:0
Sitosterol
Stigmasterol
Campesterol
Cycloartenol
Squalene
b-Amyrin
a-Amyrin
Red, decreased levels
Fold increase:
to 3
over 3
Green, increased levels
Fold increase:
to 3
over 3
No change
Not detected

c

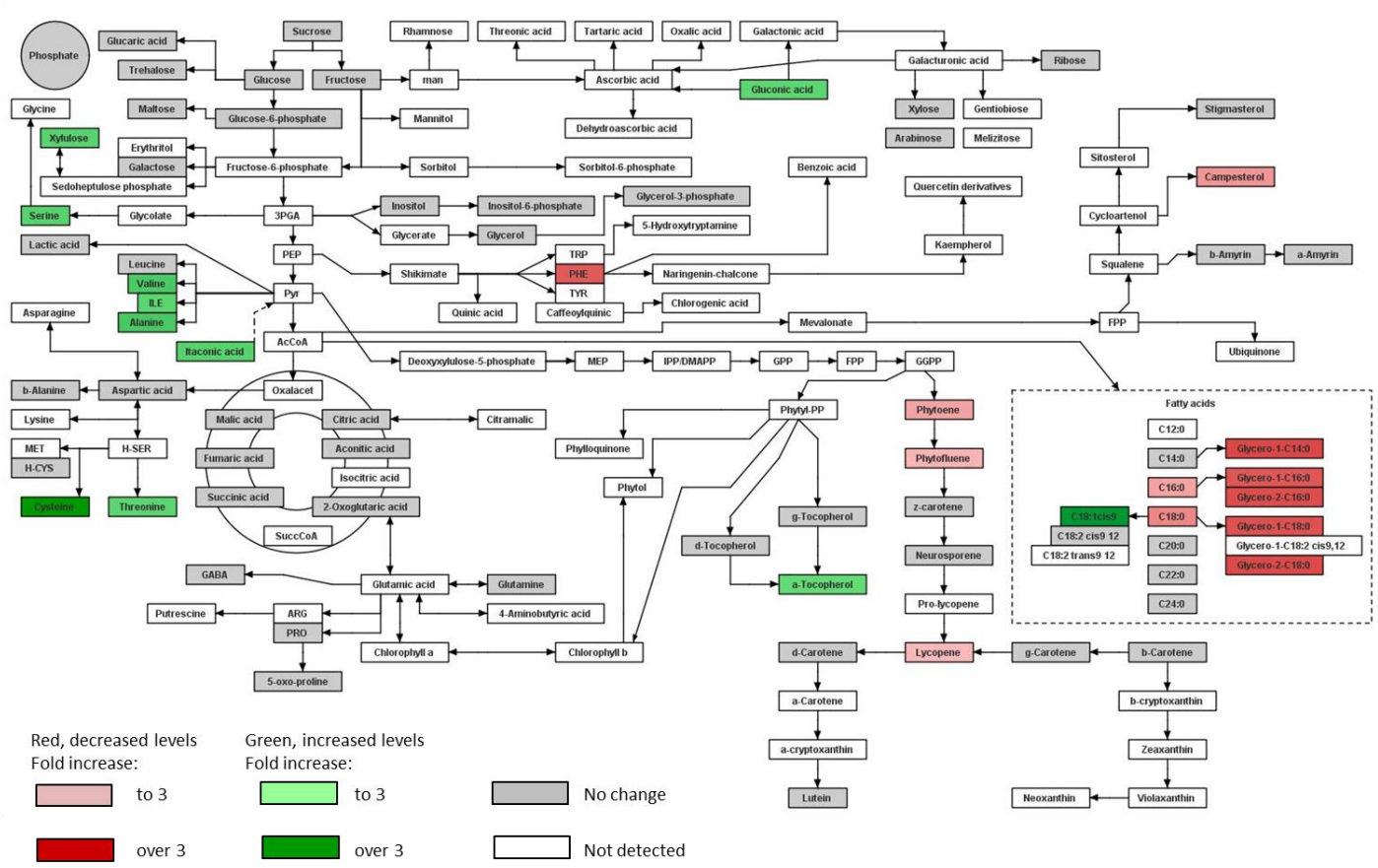
Phosphate
Glucaric acid
Trehalose
Glycine
Xylulose
Erythritol
Galactose
Sedoheptulose phosphate
Serine
Lactic acid
Leucine
Valine
ILE
Alanine
Asparagine
Itaconic acid
b-Alanine
Aspartic acid
Lysine
MET
H-CYS
H-SER
Cysteine
Threonine
Sucrose
Glucose
Fructose
Maltose
Glucose-6-phosphate
Fructose-6-phosphate
Glycolate
3PGA
PEP
Pyr
AcCoA
Oxalacet
Malic acid
Citric acid
Fumaric acid
Aconitic acid
Isocitric acid
Succinic acid
2-Oxoglutaric acid
SuccCoA
Citramalic
GABA
Glutamic acid
Glutamine
Putrescine
ARG
PRO
4-Aminobutyric acid
5-oxo-proline
Rhamnose
man
Mannitol
Sorbitol
Sorbitol-6-phosphate
Inositol
Inositol-6-phosphate
Glycerate
Glycerol
Shikimate
Quinic acid
Threonic acid
Tartaric acid
Oxalic acid
Galactonic acid
Ascorbic acid
Gluconic acid
Dehydroascorbic acid
Galacturonic acid
Ribose
Xylose
Gentiobiose
Arabinose
Melizitose
Glycerol-3-phosphate
5-Hydroxytryptamine
TRP
PHE
TYR
Naringenin-chalcone
Caffeoylquinic
Chlorogenic acid
Benzoic acid
Quercetin derivatives
Kaempherol
Mevalonate
Deoxyxylulose-5-phosphate
MEP
IPP/DMAPP
GPP
FPP
GGPP
FPP
Ubiquinone
Sitosterol
Stigmasterol
Campesterol
Cycloartenol
Squalene
b-Amyrin
a-Amyrin
Phytyl-PP
Phylloquinone
Phytol
d-Tocopherol
g-Tocopherol
a-Tocopherol
Phytoene
Phytofluene
z-carotene
Neurosporene
Pro-lycopene
Lycopene
d-Carotene
a-Carotene
a-cryptoxanthin
Lutein
g-Carotene
b-Carotene
b-cryptoxanthin
Zeaxanthin
Violaxanthin
Neoxanthin
Chlorophyll a
Chlorophyll b
Fatty acids
C12:0
C14:0
C16:0
C18:0
C20:0
C22:0
C24:0
C18:1cis9
C18:2 cis9 12
C18:2 trans9 12
Glycero-1-C14:0
Glycero-1-C16:0
Glycero-2-C16:0
Glycero-1-C18:0
Glycero-1-C18:2 cis9,12
Glycero-2-C18:0
Red, decreased levels
Fold increase:
to 3
over 3
Green, increased levels
Fold increase:
to 3
over 3
No change
Not detected

d

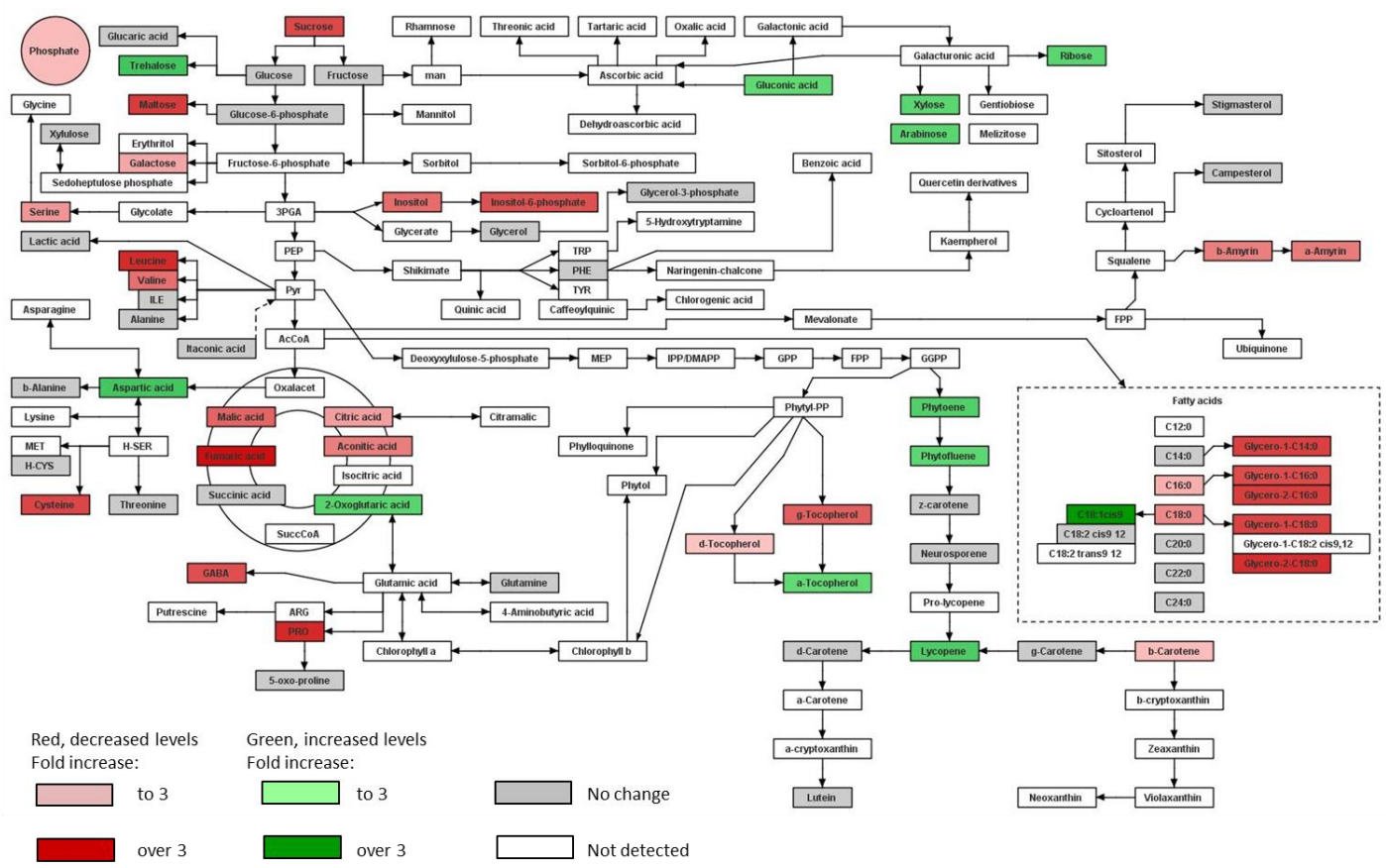

Figure 5-13 Metabolite changes in ripe fruit resulting from the insertion of the *HSFA2* transgene.

Figure 5-13 Metabolite changes in ripe fruit resulting from the insertion of the *HSFA2* transgene.

The metabolomics data acquired by GC-MS and UPLC chromatographic systems are displayed quantitatively over schematic representations of biochemical pathways produced using BioSynLab software (www.biosynlab.com). False colour scale is used to display the quantity of each metabolite in transgenic lines relative to azygous controls (a) and AC controls (b) at seven days post breaker. Similar comparisons to azygous (c) and AC (d) controls are made at fourteen days post breaker, representing fruits approaching overripe. Green indicates significant increases. Pale green represents small fold changes up to 3-fold whilst darker green indicates >3-fold. Red colouration has been used to represent decreased metabolite levels; dark red is over 3-fold, light red is to 3-fold. Grey indicates no significant change. White represents metabolites that were not detected in the samples analysed, because they was not present in samples or could not be detected using the analytical platforms available.3PGA, glyceraldehyde-3-phosphate; Ac- CoA, acetyl-coenzyme A; ARG, arginine; DMAPP, dimethylallyl pyrophosphate; FPP, farnesyl diphosphate; GGPP, geranylgeranyl-pyrophosphate; GPP, geranyl diphosphate; H-CYS, homo cysteine; H-SER, homo serine; IPP, isopentenyl pyrophosphate; ILE, isoleucine; man; mannose, MEP, 2-C-methyl-D-erythritol 4-phosphate; MET, methionine; PE, phosphatidylethanolamine; PEP, phosphoenolpyruvate; PHE, phenylalanine; Phytyl-PP, Phytyl diphosphate; PRO, proline; PS/PC, phosphatidylserine/phosphatidylcholine; Pyr, pyruvate; SuccCoA, succinyl-coenzyme A; TRP, tryptophan; TYR, tyrosine.

5.2.2.7 Selection of lines with most improved yield and quality traits

Genotypic screening enabled more accurate characterisation of the *HSFA2* transcription factor: by the identification and subsequent comparison of the most improved individuals that contained the transgene, with azygous controls with the absence of the *NPTII* amplicon that have been through transformation and tissue culture. A reduction to the visually assessed ripening-times was demonstrated in transgenic lines, reaching red ripe quicker compared to both controls. Carotenoid screening supported this observation, providing an explanation for the significant improvement to colour development in transgenic lines compared with AC controls. Despite this, small reductions to total carotenoid content were identified when compared to azygous controls. Potential ripening-related functions were supported through the screening of broad metabolism, whereby significant changes to metabolite levels were identified in most classes of compounds analysed at two ripe fruit stages. The genotypic, phenotypic and metabolic

screening of the T_2 generation confirmed the phenotypes witnessed in previous generations, while improved quality traits indicated that the selection and propagation of the best lines was successful. Ranking of quality associated traits resulted in the transgenic lines 4-6-2-5 and 4-6-9-1 being selected for the next generation, especially as both lines demonstrated an improved fruit yield compared to both controls.

5.2.2.8 Parallel experiment to confirm yield improvements and probe penetration tests to establish differences to inner and outer pericarp firmness

Potential differences to the firmness of outer and inner pericarp tissues from ripe fruit were determined by preliminary probe penetration tests, performed at Nottingham University by myself. (Figure 5-14a). A Lloyd Instrument LF calculated the maximum load required to penetrate the pericarp tissues at 10 mm min^{-1}. Tests revealed that *HSFA2* transgenic fruits displayed a 2.1-fold elevation to inner pericarp firmness; however it was not significant due to large variation (Figure 5-14a). While the outer pericarp firmness was significantly increased 3.6-fold relative to AC controls (Figure 5-14a).

The parallel yield experiment conducted at University of Nottingham (Figure 5-14b) provided similar results to that recorded at Royal Holloway (Figure 5-8). Overall, the majority of transgenic lines demonstrated increased fruit yield (71%) and average ripe fruit size (83%) compared to AC controls. Similar to Figure 5-6b, transgenic lines from the 4-2 insertion event proved to be lower yielding compared with lines from the 4-6 insertion event. A total of 21% of transgenic lines had over double the total fruit biomass output of AC controls, while 17% of transgenic lines displayed a doubling of fruit size. Combined both fruit size and total fruit yield was significantly elevated in transgenic lines to AC controls. The consistency between the results obtained at different locations, provides further evidence for the potential improvements to both fruit yield and size in transgenic lines.

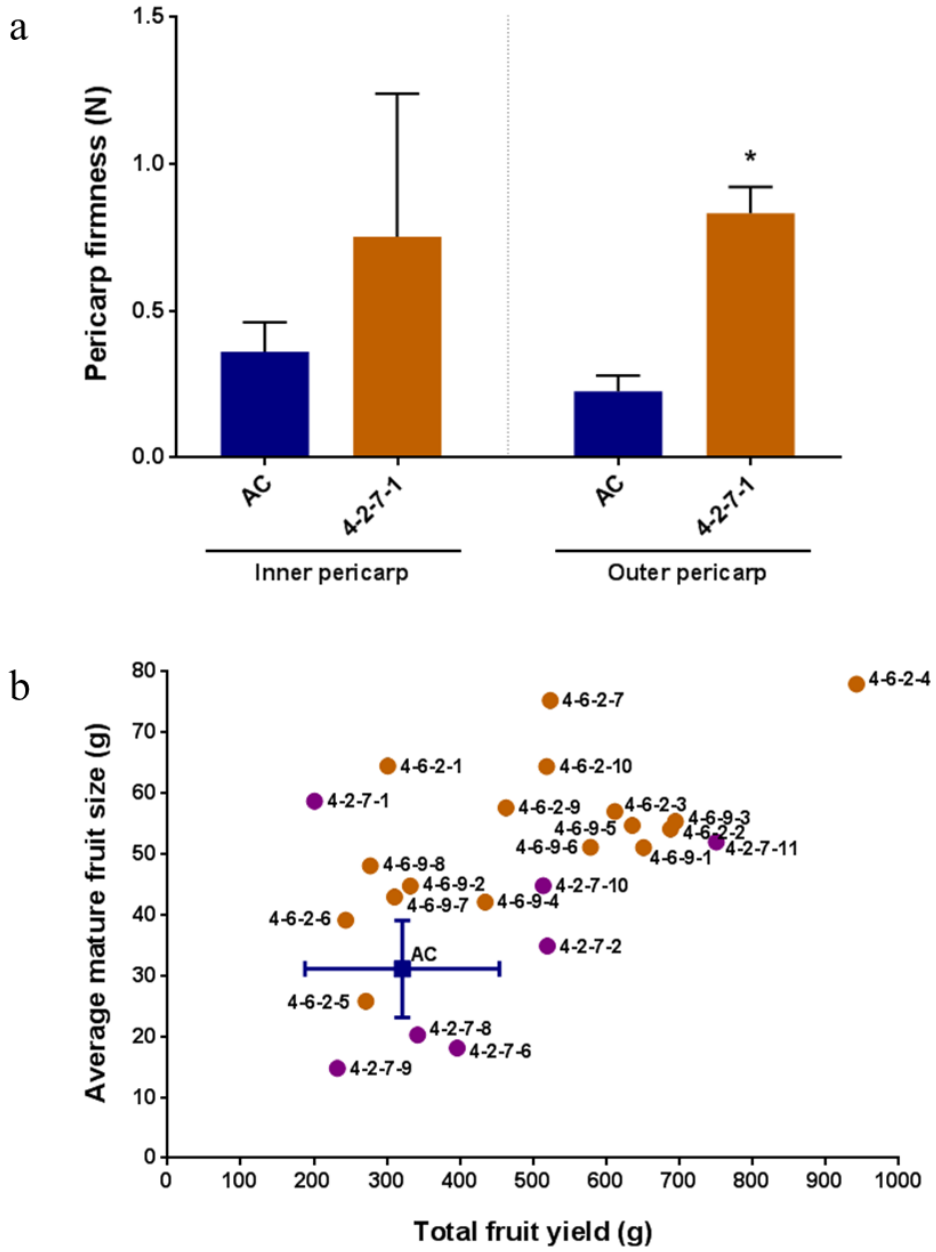

Figure 5-14 Assessment of fruit yield phenotypes and probe penetrations tests to determine firmness of ripe pericarp tissues.

Probe penetration tests were conducted to assess the firmness of the outer and inner pericarp tissues (a), while total fruit yield and average ripe fruit weight were recorded to evaluate yield-related phenotypes (b). Both were conducted at the University of Nottingham. For the probe penetration tests a minimum of three representative fruit were harvested per line. A 6-mm transverse section was cut from each fruit, probe penetration tests recorded the maximum load required to penetrate the pericarp tissue at 10 mm min−1. Measurements were taken separately from the outer and inner pericarp in duplicate. Outer pericarp tissues were defined as being below the skin but before the vascular boundary. Inner pericarp represents the cells between the vascular boundary and the endodermis. Probe penetration method is described in section 2.1.6.

For yield-related phenotypes, each transgenic individual is represented by a single point. A total of nine individuals were combined AC controls. Statistical determinations are shown as mean ± SD values. A *t test* analysis illustrates statistically significant differences (denoted $P < 0.05$) from the AC controls.

5.2.3 Evaluation of plant morphology and fruit development phenotypes of the T_3 generation with assessment of post-harvest fruit quality

5.2.3.1 Post-harvest assessment of ripening-associated fruit quality of *HSFA2* transgenic lines

Previous generations demonstrated the potential of *HSFA2* transgenic lines to shorten ripening-related colour transition and to affect fruit softening. Both parameters were studied on fruit that ripened on the plant. Therefore, fruits were harvested at breaker and stored following common commercial practices (as described in section 2.1.5).The main objective of the experiment was to determine whether there were any differences to the rate of ripening-related fruit softening and colour development post-harvest in transgenic lines. Post-harvest ripening time was assessed by the visual determination of a uniform red colouration (Figure 5-15). Elevated colour development was demonstrated by *HSFA2* transgenic lines, taking on average 4.8-5.4 days to transition from breaker to red ripe, compared with 5.8 and 6.8 days for azygous and AC controls, respectively. Thus, colour-related ripening time was reduced on average by 0.7 days compared to azygous lines and 1.7 days to AC controls.

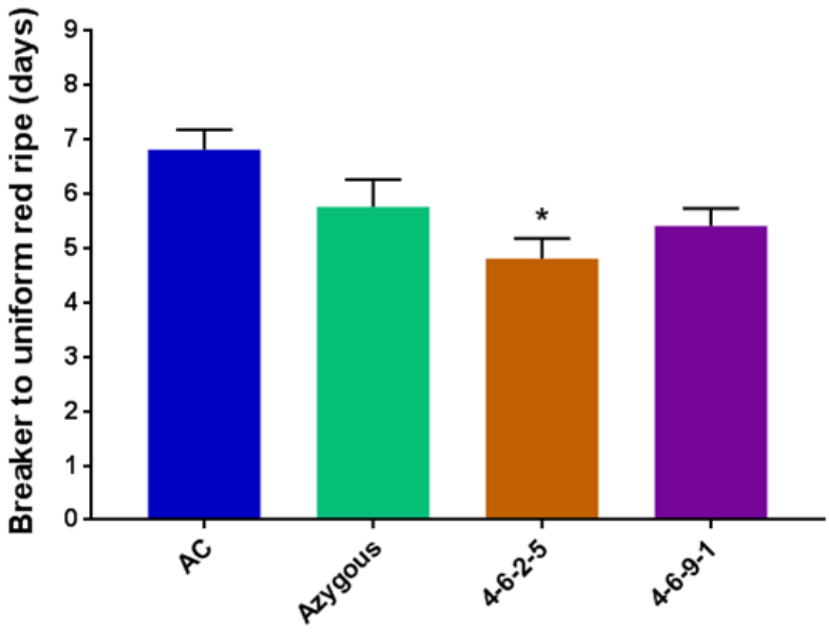

Figure 5-15 Comparison of the rapidity of post-harvest fruit ripening determined by the presence of a uniform red colouration.

Representative fruit were harvested at breaker, sterilised and stored separately at room temperature. The rapidity of ripening was compared for transgenic lines, and both non-transgenic (azygous) and wild type (AC) controls. Fruits were judged to be ripe upon visual determination of the presence of a uniform red colouration. Five fruits per plant were analysed, a minimum of four individual plants were studied for each line. This ensured the study included a minimum of five technical replicates and four biological replicates. Methods are described in section 2.1.5. Statistical determinations are shown as mean ± SD values, Dunnett's analysis illustrates statistically significant differences (denoted $P < 0.05$, $^{**}P < 0.01$, and $^{***}P < 0.001$) from the non-transgenic controls.

The rate of post-harvest fruit softening was monitored by recording fruit firmness throughout ripening until overripe (Figure 5-16a). The rate of softening of *HSFA2* transgenic fruits remained unchanged to azygous controls, shown by similar firmness scores during the latter fruit ripening and overripe stages. Despite this, azygous lines do appear to exhibit reduced softening during early ripening stages, on average displaying significant 1.1-fold increases between 5-8 dpb. The increases to firmness were then counteracted by elevated softening once fruits had reached red ripe, therefore no significant changes could be identified from 9 dpb onwards. Compared with AC controls, both transgenic and azygous lines demonstrated increased fruit firmness

throughout. Significant increases to transgenic fruit firmness were identified at 4 dpb, on average being 5% (1.1-fold) firmer. The differences extended to 6% (1.1-fold) at 7 dpb, 9% (1.2-fold) at 10 dpb and 10% (1.4-fold) at 14 dpb. After 15 dpb, only nonsignificant increases to fruit firmness were identified in transgenic lines compared with AC controls, ranging from 6-9% (1.4- to 1.5-fold).

Fruits are generally required to reach red ripe before being sold to consumers, reaching the acceptable quality demands required from an industry, supplier and consumer prospective. Therefore, Figure 5-16b accounts for the altered ripening times required for fruits to reach a uniform red colouration between transgenic and control varieties. Transgenic fruit firmness remained consistent with azygous controls, while dramatic increases 12-18% (1.2- to 2.0-fold) to firmness were identified when compared with AC controls. In this study acceptable firmness-related quality was defined as being above 50%, providing a threshold value to determine any potential extensions to shelf-life. Both transgenic and azygous lines dropped below this threshold at 7 days post ripe, while AC fruit took on average 2 days for firmness to fall below 50%. Comparisons at post ripe revealed more dramatic firmness differences, with transgenic fruit exhibiting reduced softening when compared to AC controls.

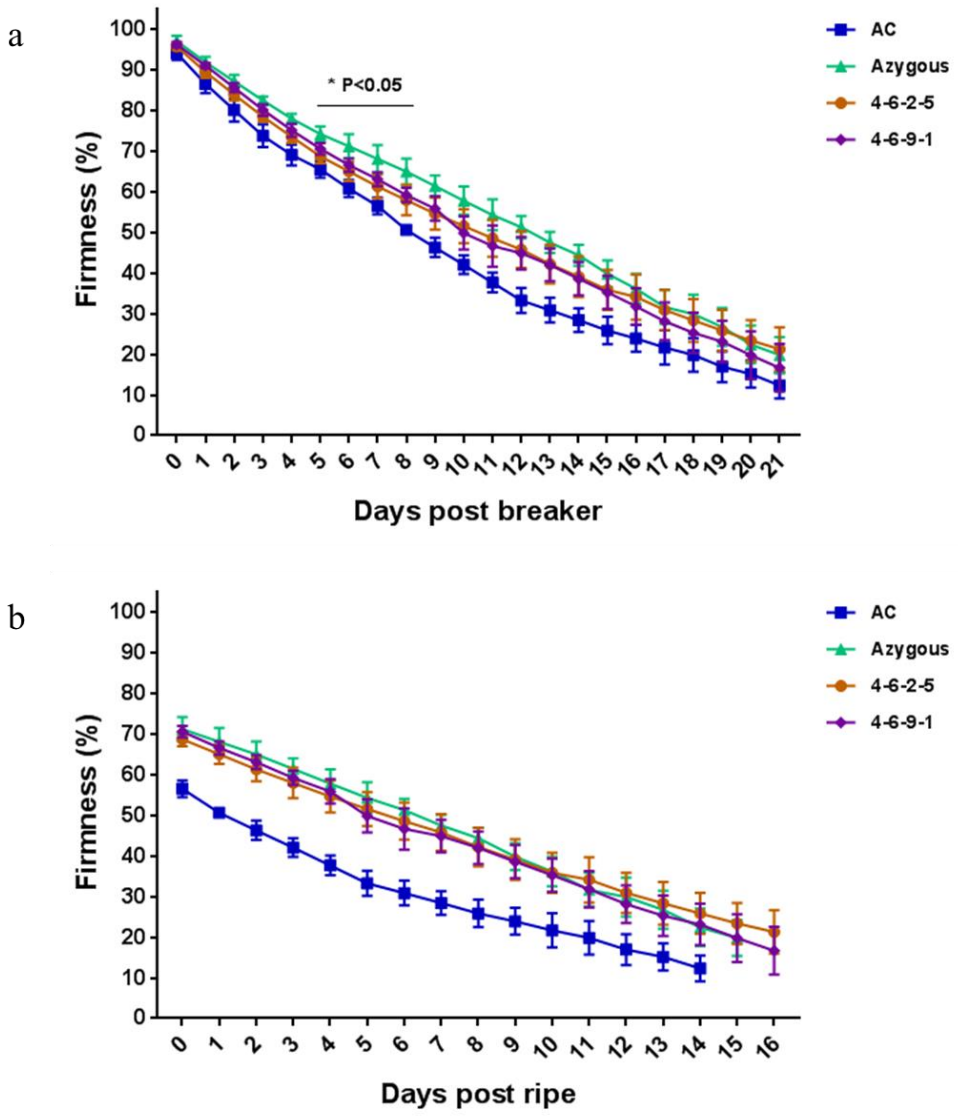

Figure 5-16 Altered rate of postharvest fruit softening.

Representative fruit were harvested at breaker, sterilised and stored separately at room temperature. Softening was monitored throughout ripening between transgenic lines and both azygous and AC controls. Firmness values given represent the percentage firmness remaining as measured by a fruit firmness meter. Firmness was compared at breaker (a) or post ripe (b) in line with retailer and consumer quality assessment, accounting for altered ripening times for each genotype. Four random points were recorded per time point, five fruits analysed per plant, and a minimum of four individual plants from each line were combined for the analyses. This ensured the study included a minimum of five technical replicates and four biological replicates. Methods are described in section 2.1.5. Statistical determinations are shown as mean ± SD values, Dunnett's analysis illustrates statistically significant differences (denoted $P < 0.05$) between all transgenic lines and the non-transgenic controls azygous controls.

Early shoot and leaf phenotypes were assessed (Figure 5-17 and 5-18). The first qualitative differences identified in *HSFA2* transgenic lines were elevated stem growth, in addition to reduced cotyledon and early leaf pigmentation (Figure 5-17). On average the shoots from transgenic lines were 4.5 cm (1.7-fold) and 5.2 cm (1.9-fold) longer compared with azygous and AC controls, respectively. These phenotypic differences identified in young tomato plants, provide early selectable markers for the rapid detection of transgenic lines. Consistent with the cotyledons, the true leaves of transgenic lines exhibited reduced pigmentation compared to both azygous and AC controls, in addition to altered leaf margins (Figure 5-18).

Then final plant morphology phenotypes were assessed for transgenic lines with both azygous and AC controls (Figure 5-19). Reductions to plant height were identified in transgenic lines compared to both controls (Figure 5-19a), on average being 10.5 cm and 32.4 cm shorter than azygous and AC controls, respectively. Only height comparisons between transgenic lines and AC controls proved to be significant. Larger significant reductions to internode lengths were exhibited in transgenic lines to both controls (Figure 5-19b). On average transgenic internode lengths proved to be 1.4 cm shorter than azygous controls and 1.9 cm smaller to AC controls. Consistent with a more compact plant architecture, significantly elevated non-vegetative biomass (40%) was detected in 4-6-9-1 transgenic lines compared with azygous controls (Figure 5-19c). Although increases in transgenic lines compared to AC controls proved not to be significant.

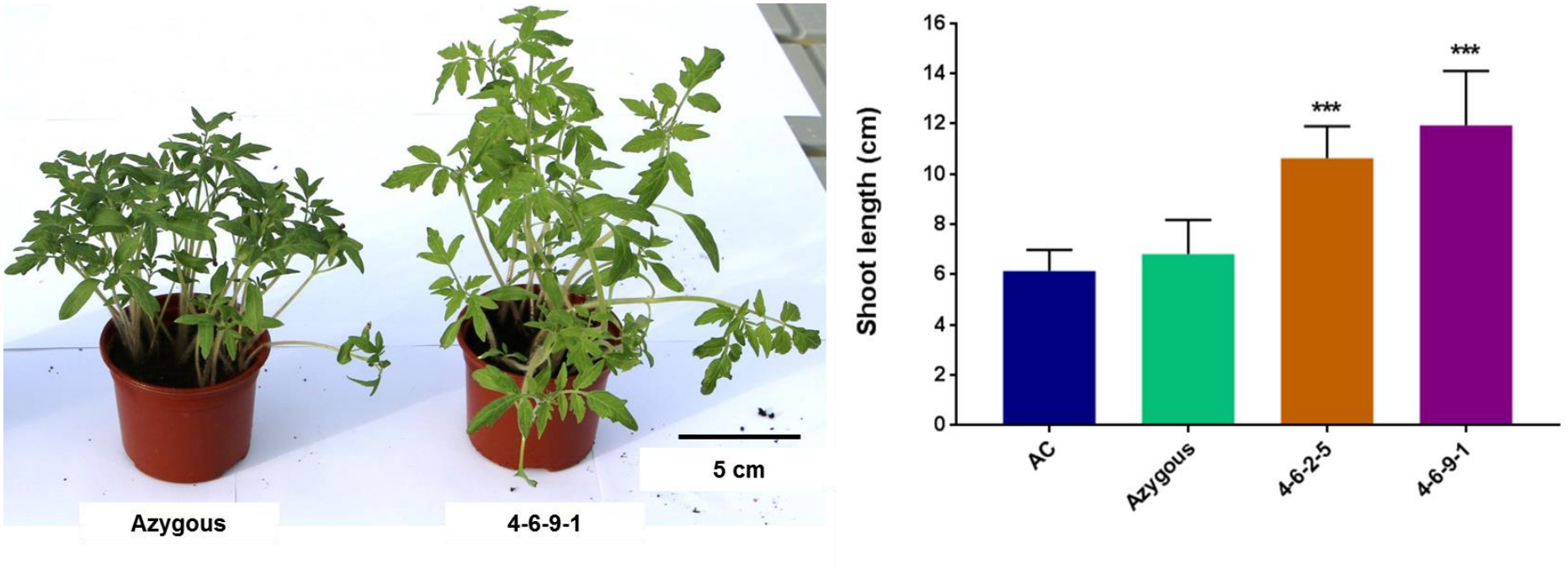

Figure 5-17 Altered early developmental shoot and leaf phenotypes.

Shoot length (a) and leaf pigmentation (b) of young tomato plants were recorded. Total shoot length was measured from the soil to the top of the plant, a total of eight representative individuals were combined for this analysis. Statistical determinations are shown as mean ± SD values, Dunnett's test analysis illustrates statistically significant differences (denoted $P < 0.05$, $^{**}P < 0.01$, and $^{***}P < 0.001$) from the non-transgenic controls.

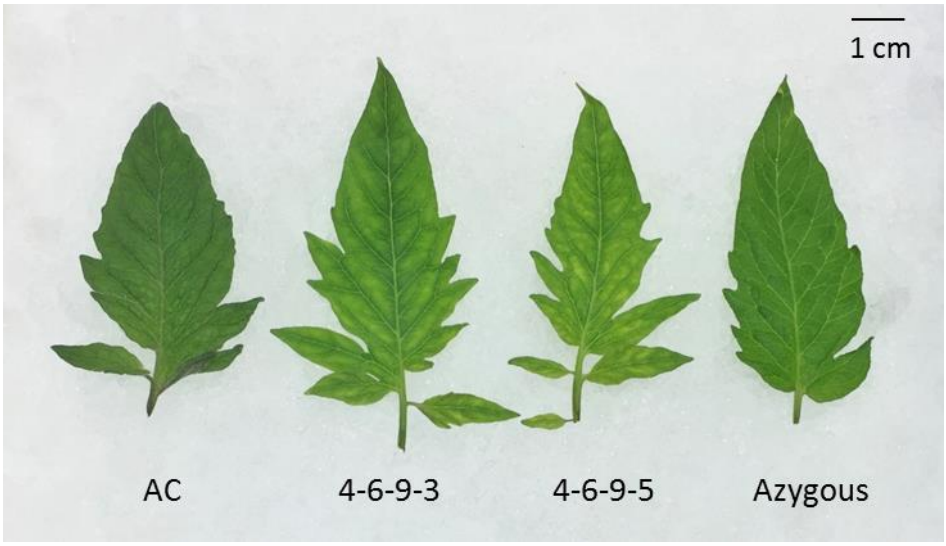

Figure 5-18 Altered leaf phenotypes.

Representative leaves were harvested and the leaf phenotypic differences were compared between transgenic lines and both azygous and AC controls. The scale bar indicates 1 cm.

Fruit development phenotypes were also studied (Figure 5-20), to confirm whether potential yield increases observed in previous generations were consistent within the current crop. Small increases to fruit number were identified in transgenic lines (Figure 5-20a), although comparisons with both controls proved not to be significant. The 4-6-9-1 transgenic lines produced significantly larger fruits compared with azygous controls, while fruit size was significantly improved in both 4-6-2-5 and 4-6-9-1 to AC controls (Figure 5-20b). Likewise, both 4-6-2-5 and 4-6-9-1 transgenic lines displayed elevated total fruit yield compared with azygous controls, while just 4-6-9-1 proved significant to AC controls (Figure 5-20c). Overall, when combining all transgenic lines and subsequent t-test comparisons with both controls, elevated fruit size and yield in transgenic lines was confirmed (not shown). Therefore, increased fruit size was shown to be the main contributor to total fruit yield. Harvest index remained unchanged, when compared to both azygous and AC controls.

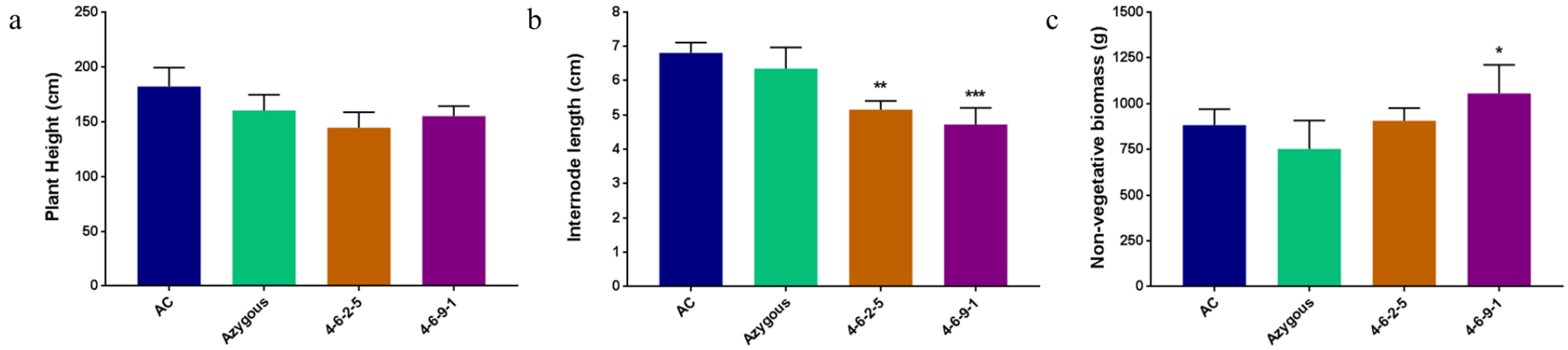

Figure 5-19 Plant morphology phenotypes during development.

Mature plant morphology differences were determined by analysis of plant height (a), internode length (b) and non-fruiting biomass (c) for transgenic lines, compared with non-transgenic (azygous) and wild type (AC) controls. The plant developmental parameters were measured once the wild type background had formed five trusses with fruit set. Total plant height was measured from the soil to last node; twelve random internodes were measured from base of the plant to the last node. Non-fruiting biomass combined the tallying of shoot cuttings during development prior to senescing, and the remaining total leaf and stem weights post harvesting of all fruits. A minimum of four plants per genotype ensured that four separate biological replicates were used for the analysis. Statistical determinations are shown as mean ± SD values, Dunnett's test analysis illustrates statistically significant differences (denoted $P < 0.05$, $^{**}P < 0.01$, and $^{***}P < 0.001$) from the non-transgenic controls.

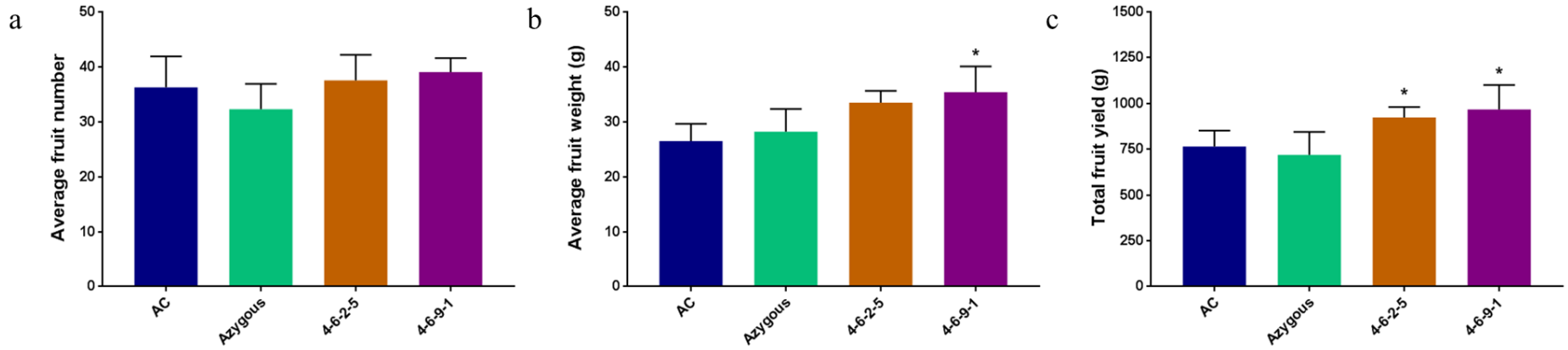

Figure 5-20 Using total fruit number, average fruit weight and total fruit yield as markers for altered fruit set and development.

Total fruit number (a), average fruit weight (b) and total fruit yield (c) phenotypes were recorded to test whether transgenic lines had altered fruit set and fruit growth compared to both non-transgenic (azygous) and wild type (AC) controls. All parameters were measured once the wild type background had formed five trusses with fruit set. All fruit weights were recorded individually postharvest and combined to determine total fruit yield. A minimum of four plants per genotype ensured that four separate biological replicates were used for the analysis. Statistical determinations are shown as mean ± SD values, Dunnett's test analysis illustrates statistically significant differences (denoted $P < 0.05$, $^{**}P < 0.01$, and $^{***}P < 0.001$) from the non-transgenic controls.

5.3 Discussion

Many of the significant differences in *HEAT SHOCK TRANSCRIPTION FACTOR A3* (*HSFA2*) transgenic lines were to plant and fruit developmental traits, including early extended shoot growth in young plants and reduced leaf pigmentation throughout development. Additionally, final plant morphology was affected, whereby transgenic lines yielded a more condensed final plant architecture, through smaller internode lengths and plant height resulting in increases to non-vegetative biomass. Interestingly, many of the phenotypes identified proved to be consistent with the down-regulation of *ELONGATED HYPOCOTYL5* (*HY5*). *HY5* is a basic leucine zipper (bZIP) transcription factor that acts downstream of multiple photoreceptors in the light signal transduction pathway, linking various pathways including light and phytohormone signalling (Cluis et al., 2004; Jiao et al., 2007; Lau and Deng, 2010; Gangappa and Botto, 2016). *HY5* has been demonstrated to play a central role in seedling development, in addition to regulating fundamental developmental processes such as cell elongation, cell proliferation, chloroplast development, pigment accumulation, and nutrient assimilation (Jiao et al., 2007; Heijde and Ulm, 2012; Lau and Deng, 2012; Gangappa and Botto, 2014; Gangappa and Botto, 2016).

HSFA2 transgenic seedlings exhibited elongated hypocotyls, while both true leaves and cotyledons appeared a lighter green (Figure 5-17 and Figure 5-18). The identification of these traits provides both early and simple selectable markers for the identification of individuals with the insertion of the transgene. Interestingly, both phenotypes were consistent with *hy5* mutants. Down-regulation of *HY5* showed a significant increase in hypocotyl growth in tomato (Liu et al., 2004), consistent with *hy5* loss-of-function mutants in *Arabidopsis* (Oyama et al., 1997). Additionally, it was reported that both leaves were paler than controls under both greenhouse and field conditions, due to a 30% reduction to leaf chlorophyll content (Liu et al., 2004). Silencing *HY5* by RNAi also resulted in less chlorophyll accumulation in immature fruits (Liu et al., 2004), which can explain the paler immature fruit phenotypes observed in multiple *HSFA2* transgenic lines (not shown).

Another important observation was the reduction to carotenoid content in ripe fruit at both 7 and 14 dpb in transgenic lines, when compared to azygous controls (Table 5-1 and Table 5-2). Again this proved to be consistent with reduced *HY5* expression, which exhibited decreased total carotenoid levels (12-32%) compared with normal controls

(Liu et al., 2004). The results from Liu et al., 2004, confirmed that the modification of the light signal transduction machinery can alter fruit carotenoid content and associated nutritional quality, potentially explaining the reduced carotenoid profiles of transgenic lines.

The same study correlated the reduction to chlorophyll and carotenoid contents to abnormalities in both organization and abundance of thylakoids. In *Arabidopsis*, *HY5* is required for transcription of the *CHLOROPHYLL A/B-BINDING PROTEIN* (*CAB*) gene, whose product is necessary for thylakoid organization (Chattopadhyay et al., 1998; Maxwell et al., 2003), providing a potential mechanism for altered thylakoid and chlorophyll phenotypes. Later studies revealed HY5 regulates the expression of the carotenoid biosynthetic gene *PHYTOENE SYNTHASE* (*PSY*), and a subset of chlorophyll biosynthesis genes such as *LIGHT-HARVESTING COMPLEX 4* (*LHCA4*), *PROTOCHLOROPHYLLIDE OXIDOREDUCTASE C* (*PORC*), and *GENOMES UNCOUPLED 5* (*GUN5*) by directly binding on their promoters (Toledo-Ortiz et al., 2014). Additionally, HY5 was shown to be involved in chloroplast biogenesis through the promotion of *DIGALACTOSYLDIACYLGLYCEROL SYNTHASE 1* (*DGD1*). *DGD1* is involved in the synthesis of the galactolipid digalactosyldiacylglycerol (DGDG) that is required for the biogenesis of thylakoids (Kobayashi et al., 2014; Afitlhile et al., 2015; Gangappa and Botto, 2016). Potentially similar mechanisms through altered *HY5* expression, could explain the reduced chlorophyll and carotenoid contents in *HSFA2* transgenic fruits.

The HY5 transcription factor has been shown to be important for promoting flavonoid accumulation by the activation of MYBs and key structural genes of the flavonoid pathway (Oyama et al., 1997; Holm et al., 2002; Stracke et al., 2010; Peng et al., 2013; Shin et al., 2013; Zoratti et al., 2014; Gangappa and Botto, 2016). It has been demonstrated that HY5 directly binds to either the G-box or ACE-box of MYB transcription factors, such as *PRODUCTION OF FLAVONOL GLYCOSIDES* (*MYB12/PFG1* and *MYB111/PGF3*), *PRODUCTION OF ANTHOCYANIN PIGMENT1*, (*MYB75/PAP1*), and *MYB-LIKE DOMAIN* (*MYBD*) to promote their expression (Stracke et al., 2010; Zhang et al., 2011a). The MYB transcription factors can then bind to the promoters of several flavonoid biosynthetic genes including *CHALCONE SYNTHASE* (*CHS*), *CHALCONE ISOMERASE* (*CHI*), *FLAVANONE 3-HYDROXYLASE* (*F3H*), *DIHYDROFLAVONOL-4-REDUCTASE* (*DFR*), *LEUCOANTHOCYANIDIN DIOXYGENASE* (*LDOX*), and *FLAVONOID 3-O-GLUCOSYLTRANSFERASE* (*UF3GT*)

(Dare et al., 2008; Stracke et al., 2010; Shin et al., 2013). Furthermore, the cooperative function of PIF3 with HY5 has been demonstrated to stimulate anthocyanin accumulation (Shin et al., 2007). With the important role that *HY5* plays in inducing both flavonoid and anthocyanin synthesis, and its potential altered expression predicted in transgenic lines, these could explain the differences to the visually determined ripening times compared to both controls. Therefore, potential reductions to chlorophyll and flavonoids due to possible altered *HY5* expression, could explain the increased ripening-related colour transition of transgenic fruits compared to both controls.

As mentioned previously, potentially reduced *HY5* expression could be influencing the reduced carotenoid content of ripe fruit from transgenic lines compared to azygous controls, potentially by altering *PSY-1* expression. HY5 directly binds to the promoter of the *PSY-1* (Toledo-Ortiz et al., 2014; Llorente et al., 2015), the rate limiting enzyme in the carotenoid pathway, whereby *PSY-1* expression positively correlates to levels of phytoene and phytofluene (Fraser et al., 2002; Fraser et al., 2007). On average, transgenic lines produced significantly less phytoene and phytofluene at fourteen days post breaker, consistent with reduced *PSY-1* expression. The largest reduction was to phytoene, indicating that the insertion of the transgene has the strongest negative effect to *PSY-1* expression. Differences to phytofluene were smaller in comparison. The expected reduction to *PSY-1* expression could facilitate the decreased phytoene content, which could result in less substrate availability for PDS, explaining the reduction to phytofluene rather than altered *PDS* expression. Lastly, silencing *HY5* was correlated with reduced lycopene content, again proving consistent with *HSFA2* transgenic lines (Liu et al., 2004). Overall, the carotenoid profiles exhibited by *HSFA2* transgenic lines proved to be similar to *hy5* mutants, providing further evidence for reduced *HY5* expression, which is expected to be contributing to the phenotypes witnessed.

Interestingly, both azygous and transgenic lines that have been through transformation and tissue culture, displayed elevated carotenoid content compared with AC controls at 7 and 14 dpb (Table 5-1 and Table 5-2). Significant increases to phytoene, phytofluene and lycopene were identified, combined with small reductions to β-carotene. More numerous and larger fold increases were identified at 14 dpb compared to 7 dpb. The results shared multiple similarities with ethylene treatment. Su et al., 2015 studied the application effects of an ethylene precursor (ACC), which resulted in fruits producing significantly more phytoene, phytofluene and lycopene, comparable with both transgenic and azygous lines compared with AC controls. Ethylene treatment induced the upregulation of *PSY-1*,

resulting in increased flux upstream of lycopene. Similar flux increases are witnessed in transgenic and azygous lines, thus a similar mechanism is predicted. While reduced expression of *LYC-β1*, *CRTR-β2* and *NCED* upon ethylene treatment can explain the bottleneck post lycopene, resulting in reduced β-carotene. Chlorophyll degradation rate was also increased with ethylene treatment, again contributing to reduced ripening time from breaker. Additionally, RIN has been shown to directly regulate the expression of *PSY-1* combined with *Z-ISO* and *CRTISO* (Martel et al., 2011; Fujisawa et al., 2013). These enzymes are involved in the formation of phytoene and lycopene, which displayed the largest differences in transgenic and azygous lines. Therefore, a mechanism involving RIN can also be expected. Overall, elevated ethylene biosynthesis is the main candidate for the increased carotenoid accumulation, of azygous and transgenic lines compared with AC controls. The upregulation of *PSY-1* is expected to facilitate the elevated flux upstream of lycopene. Combined increases to lycopene and reduced β-carotene are likely contributing to the reduced colour-associated ripening times. With only relatively small changes to lycopene and its precursors between transgenic lines and azygous controls, fewer significant differences to ethylene levels are expected between these genotypes.

Similar to the ripening related-colour development, transgenic lines demonstrated more numerous and larger differences to broader metabolism when compared to AC lines, than to azygous controls (Table 5-3). Significant changes to metabolite levels were identified in most classes of compounds analysed, more differences between genotypes were identified at 14 dpb than 7 dpb. Importantly, many of the significant differences identified in transgenic lines through GC-MS profiling, correlated with ripening progression when compared with AC controls. While more metabolites remained unchanged or displayed the opposite trend when compared to azygous controls, correlating more to similar or reduced ripening progression. These results support the carotenoid screen, whereby transgenic lines were a midpoint between AC and azygous controls. An example is valine that normally declines during ripening; azygous controls exhibited the lowest valine content, with AC having the highest.

Other metabolites demonstrated a similar trend, including multiple organic acids. Reduced organic acid content is associated with fruit pericarp ripening (Carrari and Fernie, 2006; Osorio et al., 2011a). Transgenic lines displayed a significant 1.3-fold reduction to AC controls at 14 dpb, while levels remained unchanged to azygous controls. Compared to AC controls, decreased levels of aconitic acid, citric acid, fumaric

acid, malic acid from the TCA cycle were observed. Additionally, reductions to citric acid and malic acid were identified at 7 dpb. Malic acid has been shown to be an important fruit ripening indicator, commonly measured to determine maturity status of the fruits (Dalal et al., 2017). Interestingly, multiple studies have demonstrated that organic acids strongly correlate with genes linked with ethylene and cell wall metabolism-associated pathways, highlighting their importance to fruit ripening (Carrari et al., 2006; Centeno et al., 2011; Osorio et al., 2011a). The levels of all organic acids, particularly the TCA cycle intermediates, were strongly affected across ripening in several ripening mutants (Osorio et al., 2011a). The largest alterations to organic acid content was identified in *nor*, a mutation with severely affected ethylene biosynthesis and signalling (Osorio et al., 2011a). The results demonstrate the importance of ethylene for organic acid content, providing further evidence for altered ethylene biosynthesis and signalling, which is expected to be conferring the alterations to ripening-related metabolism compared to AC controls.

Ripening is associated with numerous changes to amino acids, including the accumulation of aspartic acid and the decline of leucine, proline, serine and valine (Boggio et al., 2000; Carrari and Fernie, 2006; Mounet et al., 2007; Osorio et al., 2011a; Koike et al., 2013). The levels of these amino acids in transgenic lines were in accordance with further ripening progression when compared to AC controls at 14 dpb (Table 5-3). While the opposite trend or no significant differences were identified when compared to azygous controls. At 7 dpb, transgenic lines displayed elevated aspartic acid compared with AC controls, whereas comparisons with azygous controls revealed no significant differences. Furthermore, the levels of the isoprenoids phytoene, phytofluene and lycopene, the lipid GABA, the polyols inositol and inositol-6-phosphate exhibit the same trend. Thus indicating that transgenic fruit correlates with increased ripening progression to AC controls, while generally remaining unchanged to azygous controls (Carrari and Fernie, 2006; Osorio et al., 2011a; Takayama and Ezura, 2015).

Differences to multiple sugar forms were identified at both ripening stages studied. The main sugars fructose, glucose and sucrose were quantified in an absolute manner due to their central roles in metabolism, and their accumulation in ripe fruits that contribute to nutritional quality and flavour (Table 5-3). At 7 dpb, elevated fructose and glucose content were observed in transgenic lines compared with both controls, while sucrose content remained unchanged. The sugar profiles combined with increases to multiple metabolism pathways, suggest there is not a bottleneck at the hexose sugars, but

potentially improved sink strength through elevated sucrose import and invertase activity (Osorio et al., 2014). Invertase activity catalyses the hydrolysis of sucrose into glucose and fructose in an irreversible reaction, upregulation could explain the increases to fructose and glucose observed. The sugar profiles of transgenic lines at 14 dpb differ from 7 dpb, fructose and glucose are now unchanged to both controls. Furthermore, large reductions to sucrose were detected in transgenic lines compared to AC controls, while no differences were observed to azygous controls. The results indicated elevated HEXOKINASE (HK) and FRUCTOKINASE (FK) mediated phosphorylation of fructose and glucose, these enzymes have been shown to be important in hexose metabolism, sensing, and signalling (Eveland and Jackson, 2012). Therefore, it can be predicted that hexose accumulation at 7 dpb, has induced the expression of *HK* and *FK* enzymes, consequently promoting multiple metabolism pathways. Further elevated SUCROSE INVERTASE activity can also be expected in transgenic lines compared with AC controls, which can explain the large 2.7-fold reduction to sucrose at 14 dpb. A fall in sucrose content has been correlated to ripening progression (Carrari and Fernie, 2006; Osorio et al., 2011a), providing further evidence of increased rapidity of ripening in transgenic lines. The predicted upregulation of *SUCROSE INVERTASES* combined with *HKs* and *FKs* in transgenic lines would promote greater sugar expedition, required by the diverse metabolic pathways used to activate ripening. This includes secondary metabolism that can explain the acceleration of colour-related fruit ripening in transgenic lines. Increased sugar metabolism shown by the reduction to sucrose and the decline in hexose content, at 14 dpb in transgenic lines compared to AC controls, could explain why larger and more numerous differences to carotenoid and broader metabolism profiles are detected when compared with 7 dpb.

Sucrose has been shown to be an important signalling molecule involved in fruit ripening (Jia et al., 2016; Li et al., 2016a); and can provide an explanation for altered metabolism and elevated colour development in transgenic lines. Sucrose treatment accelerated ripening through inducing more rapid ripening-related colour transition, which correlated with greater system 2 ethylene production and the upregulation of ethylene signalling genes (Li et al., 2016a), consistent with results and predictions for transgenic lines compared to AC controls. Application of exogenous sucrose resulted in the upregulation of sucrose degradation genes, which counteracted the sucrose increases, facilitating increased nutrient and ethylene fluxes (Li et al., 2016a). Furthermore, hexose sugar content remained unchanged, consistent with transgenic lines, despite elevated sucrose metabolism. Therefore, elevated sucrose metabolism and sugar expedition is

expected to be driving the increased carotenoid content and rapidity of ripening of transgenic lines compared with AC controls. Also, the reductions to sucrose is not expected to be due to limitations of sugar import, as lower sucrose content was one of the pivotal factors that resulted in the late-ripening process of a mutant sweet orange (Zhang et al., 2015).

Multiple changes to galactose content were identified in the GC-MS profiling of metabolism. Tomato ripening is associated with the decline to polymeric galactose in cell walls and the rise in free galactose (Wallner and Bloom, 1977; Gross and Wallner, 1979; Kim et al., 1991). Generally, the levels of free galactose (Table 5-3) in transgenic lines mirrored differences to fruit firmness between genotypes (Figure 5-16). At 7dpb, transgenic lines exhibited elevated galactose, consistent with increased fruit softening when compared with azygous controls. Conversely, nonsignificant reductions to free galactose were identified to AC controls, potentially explaining the reduced softening of transgenic lines. At 14 dpb, galactose content remained consistent between transgenic and azygous lines, while a significant reduction was identified to AC controls. Again, this proved to be similar to fruit softening, as transgenic fruit were firmer in comparison to AC controls, while remaining unchanged to azygous controls.

The changes in galactose content in transgenic lines could due to altered β-GALACTOSIDASE (TBG) expression, which hydrolyse cell wall β-(1,4)-galactans (Eda et al., 2016). TBG activity has been associated with softening across multiple fruit species, while reduced softening is linked with lower galactose content (Nakamura et al., 2003; Brummell et al., 2004; Mwaniki et al., 2005; Ogasawara et al., 2007; Paniagua et al., 2016). The increased exo-galactanase activity during tomato ripening is correlated to the loss of cell wall galactose side chains from rhamnogalacturonan I and the rise in free galactose (Pressey, 1983; Kim et al., 1991; Carey et al., 1995). TBG enzymes play important roles in cell wall expansion and degradation, as well as turnover of signalling molecules during ripening (Eda et al., 2016). Multiple TBG forms have been identified in tomato; several could be candidates for the reduced softening phenotypes and galactose content identified in *HSFA2* transgenic lines in comparison to both controls. In particular, altered expression of *TBG4* delayed fruit softening, which was correlated to reduced exo-galactanase levels and high cell wall galactosyl content (Smith et al., 2002). Furthermore, suppression of *TBG4* decreased wall porosity and obstructed the access of cell wall hydrolases to wall components, preventing the depolymerisation of structural polysaccharides that maintains firmness (Redgwell et al., 1997a; Brummell and

Harpster, 2001; Smith et al., 2002). While reduced *TBG3* expression resulted in reduced exo-galactanase activity and increased cell wall galactosyl content, resulting in slower fruit deterioration in storage (Carey et al., 2001).

Finally, alterations to the content of many fatty acid forms were observed at both ripening time points studied (Table 5-3). At 14 dpb when compared to both controls, transgenic lines consistently displayed significant reductions to C16:0 and C18:0, in addition to all monoglyceride and diglyceride forms identified, while significant increases to C18:1cis9 were detected. Total fatty acid content was reduced in transgenic lines (1.2-fold), although only comparisons with AC controls proved significant. At 7 dpb, transgenic lines also exhibited reduced glycero-1-C14:0, glycero-1-C16:0 and glycero-2-C16:0 compared to both controls. Therefore, total glyceride content was reduced compared to both controls at 7 and 14 dpb. Tomato ripening has been associated with an increase to the ratio of polyunsaturated fatty acids to saturated fatty acids, through increases to polyunsaturated fatty acid forms (Saini et al., 2017). In transgenic lines total unsaturated fatty acid content was significantly increased (1.8 to 2.4-fold) at 14 dpb compared to both controls, while nonsignificant decreases were identified to saturated fatty acid forms (1.1-fold). Therefore, transgenic lines demonstrated a significantly increased ratio of polyunsaturated fatty acids to saturated fatty acids compared to azygous (2.2) and AC controls (2.9). The fatty acid profiles provided further evidence of increased ripening progression in transgenic lines, consistent with the visually assessed ripening times. Additionally, the elevated ratio of unsaturated fatty acid to saturated fatty acid in transgenic lines could suggest an improved nutritional value compared to both controls.

5.4 Conclusion to chapter

The *HEAT SHOCK TRANSCRIPTION FACTOR A3* (*HSFA2*) was identified through affymetrix GeneChip transcriptomic data and artificial neural network (ANN) inference analysis from Pan et al., (2013). This resulted in the identification of several potential ripening-regulators that were believed to be fruit specific, and were shown to have expression patterns that mirrored RIN. The ripening-related expression profile and the reduced *HSFA2* expression in *rin*, *cnr* and *nor* ripening mutant lines, suggested an important role in fruit ripening. The insertion of a knock-down 35S::RNAi construct

under constitutive control, was used to characterise the function of the transcription factor.

Interestingly, multiple phenotypic differences identified were to plant and fruit developmental traits. Many proved to be consistent with the down-regulation of *ELONGATED HYPOCOTYL5* (*HY5*), including extended shoot growth and reduced leaf pigmentation during early development (Oyama et al., 1997; Liu et al., 2004). The identification of these traits provides both early and simple selectable markers for the identification of individuals with the insertion of the transgene. Similarly, transgenic lines yielded paler immature fruits, while reductions to carotenoid content including lycopene was identified when compared with the true (azygous) controls (Liu et al., 2004). The carotenoid profiles suggested reduced *PSY-1* expression, combined with potentially altered *PDS*, *Z-ISO* and *CRTISO* expression. HY5 was shown to directly bind to the promoter and induce expression the *PSY-1* (Toledo-Ortiz et al., 2014; Llorente et al., 2015) positively regulating carotenoid accumulation. Therefore, reduced *HY5* expression expected in transgenic lines could explain the carotenoid decreases compared to azygous controls. Lastly, HY5 has been demonstrated to be important for promoting chlorophyll, anthocyanin and flavonoid accumulation. Potential reductions to chlorophyll, combined with altered anthocyanin and flavonoid content, could be contributing to the consistent reduction to colour-associated ripening-times. This can explain why transgenic fruits appear to reach uniform red ripe quicker than azygous controls, despite small reductions to carotenoid content. The results suggest that the *HSFA2* could lie upstream and potentially influence the expression of *HY5*. Consequently, altered expression of *HY5* through the insertion of the *HSFA2* knock-down 35S::RNAi construct is expected to contribute to the phenotypes witnessed in transgenic lines. Additional developmental traits were identified, including consistent reductions to both final plant height and internode length. Potential improvements to fruit size, total fruit yield and non-vegetative biomass were identified but proved to be less conclusive.

Transgenic lines demonstrated broad changes to metabolism, with many metabolite changes correlating to further ripening progression in transgenic lines. The numerous differences to fatty acids were consistent with this trend. Particularly with the increased ratio of unsaturated fatty acid to saturated fatty acid, through increases to polyunsaturated fatty acid forms and decreases to multiple saturated forms. Similarly, differences to multiple amino acid contents combined with the reduction to total organic

acid levels, including multiple forms from the TCA cycle, indicated elevated ripening progression, particularly compared with AC controls. Transgenic lines' metabolite profiles indicated altered ethylene biosynthesis and signalling when compared to AC controls, due to reductions to organic acid levels, combined with increased sucrose metabolism and isoprenoid content. Transgenic lines displayed elevated phytoene, phytofluene, lycopene and reductions to β-carotene, consistent with ethylene treatments, which could explain the increases to the rapidity of colour-associated ripening to AC controls. Overall, larger and more numerous differences to metabolism were identified at 14 dpb compared with 7 dpb, suggesting that the *HSFA2* has a greater influence during the latter stages of fruit ripening.

Despite relatively small reductions to fruit firmness during the early ripening stages, the rate of transgenic fruit softening remained unchanged when compared to azygous controls. Conversely, significant improvements to fruit firmness across multiple generations demonstrated reduced rates of softening when compared to AC controls. Probe penetration tests revealed large increases to outer pericarp firmness compared to AC controls. Alterations to galactose content in transgenic lines relative to both controls correlated to differences in fruit firmness. Ripening-related increases to free galactose have been associated with pectin depolymerisation and the loss of cell wall galactose side chains from rhamnogalacturonan I. Therefore, altered TBG activity and the maintenance of cell wall galactosyl content is a main candidate for the altered softening rates identified in transgenic lines.

Overall, the study succeeded in identifying another transcription factor with important ripening-related and developmental roles. Manipulation demonstrates the potential to improve visually assessed ripening time and fruit yield-related traits compared to both controls.

Chapter VI: General discussion

6.1 Summary and general conclusions

6.1.1 Aim and objectives of the project and PhD study

The overarching aim of the project was to identify transcription factors, which compared to RIN were down-stream in the ripening cascade and other global ripening-regulators. In this way future modulation of their activity could facilitate a more targeted approach for improvement compared with the heterozygous *rin* mutation currently utilised, by maintaining the extended shelf-life of the *rin* mutation without the adverse effects to sensory quality. Three uncharacterised ripening-related transcription factors downstream of RIN were identified and transformed within the program. *ZINC FINGER PROTEIN INDETERMINATE DOMAIN 2* (*ZFPIDD2*) has been shown to be a direct RIN target, while *ZINC FINGER PROTEIN ZPR1* (*ZPR1*) and *HEAT STRESS TRANSCRIPTION FACTOR A3* (*HSFA2*) were suspected to be indirect downstream targets of RIN (Fujisawa et al., 2012b; Fujisawa et al., 2013). The objective of the PhD study was to characterise the function of these transcription factors. Detailed phenotypic analysis was used to confirm altered plant morphology, fruit development and ripening-related fruit quality. Metabolite profiling utilising several extraction methods and analytical platforms enabled the identification of differences in fruit metabolism. Broad changes to numerous classes of compounds supported the altered quality traits identified. Both strategies provided an insight into the functions of the transcription factors and how they influence fruit quality.

Omic technology and integrative biology approaches were combined to construct a regulatory network called FruitNet. The transcriptomic and correlation network analysis from FruitNet was then used to identify candidate genes linked to each transcription factor. Altered expression or activity of these candidate genes could then explain the altered phenotypes observed, providing a mechanism of action for each transcription factor. The transcriptomic analysis conducted by project collaborators measured the expression profiles of 2,000 genes, at 13 different time points during tomato fruit development and ripening. Pearson's correlation coefficient was then calculated to determine links between genes (Hodgman et al., unpublished). The large-scale transcriptome profiling provided by FruitNet could also be used as a functional genomics tool, with the potential to identify novel developmental and ripening-related genes. The well characterised *RIN* and *PSY-1* genes were used to validate the network, to determine the reliability of the outputs provided.

6.1.2 Validation of FruitNet

The *RIN* transcription factor was chosen due to its central role in fruit ripening (Vrebalov et al., 2002). Additionally, previous microarray analysis and then chromatin immunoprecipitation coupled with DNA microarray analysis (ChIP-chip), identified both direct and indirect RIN targets which could be compared to the outputs from FruitNet to validate the network (Martel et al., 2011; Fujisawa et al., 2012b; Fujisawa et al., 2013). RIN has been shown to be involved in the transcriptional control network involved in carotenoid accumulation. The rate limiting enzyme in the carotenoid pathway, *PHYTOENE SYNTHASE* (*PSY-1*), in addition to *Z-CAROTENE ISOMERASE* (*Z-ISO*) and *CAROTENOID ISOMERASE* (*CRTISO*) were demonstrated to be direct RIN targets, consistent with predicted RIN targets identified by FruitNet (Martel et al., 2011; Fujisawa et al., 2012b; Fujisawa et al., 2013). Similarly, *4-DIPHOSPHOCYTIDYL-2-C-METHYL-D-ERYTHRITOL KINASE* (*ISPE*) from the 2-C-methyl-D-erythritol 4-phosphate/1-deoxy-Dxylulose 5-phosphate (MEP/DOXP) pathway was a direct RIN target in accordance with both literature and FruitNet (Fujisawa et al., 2013). *ISPE* is involved in terpenoid backbone biosynthesis pathways, considered to be the main route for plastidic carotenoid production. Furthermore, *GERANYLGERANYL PYROPHOSPHATE SYNTHASE 2* (*GGPS2*) and *PHYTOENE DESATURASE* (*PDS*) were linked to RIN on FruitNet, while in literature they were shown to be regulated by an indirect effect of RIN (Martel et al., 2011; Fujisawa et al., 2012b; Fujisawa et al., 2013).

Multiple genes involved in ethylene synthesis and signalling that are direct or indirect targets of RIN were identified by FruitNet, including*: 1-AMINOCYCLOPROPANE-1-CARBOXYLATE OXIDASE 1* (*ACO1*), ethylene receptor *NEVER RIPE* (*NR*) and the *ETHYLENE RESPONSE FACTOR 6* (*ERF6*) (Lee et al., 2011; Martel et al., 2011). Additionally, RIN was shown to directly bind to the MADS box FRUITFULL homologs *FUL1* and *FUL2* to regulate ripening (Shima et al., 2013; Fujisawa et al., 2014; Shima et al., 2014). The *FUL1* homolog was shown to be a target of RIN on FruitNet. Other RIN targets consistent with FruitNet include the cell wall–modifying enzyme *POLYGALACTURONASE 2A* (*PG2A*), *SENESCENCE-INDUCIBLE CHLOROPLAST STAY-GREEN PROTEIN 1* (*SGR1*), also the ethylene and ripening-regulated GRAS family (*SCL32-like*) and the BZIP (*ABZ1*) transcription factors (Fujisawa et al., 2013).

The carotenoid biosynthesis gene *PSY-1* was also used to validate the outputs of FruitNet. Genes encoding enzymes upstream of *PSY-1* from the MEP/DOXP pathway including *ISPE*, *GERANYL PYROPHOSPHATE SYNTHASE* (*GPS*) and *GGPS2* were linked to *PSY-1* on FruitNet; in addition to *PDS* downstream of *PSY-1*. Tomato ripening is correlated with a burst of ethylene, which has been shown to induce *PSY-1* expression (Su et al., 2015). Several ethylene biosynthesis genes link to *PSY-1* on FruitNet, including *1-AMINOCYCLOPROPANE-1-CARBOXYLIC ACID SYNTHASE-2* (*ACC2*) and *ACO1*. *ACO1* has been identified as one of the main *ACO* genes supporting ripening-associated ethylene production, converting ACC into ethylene, whereby silencing resulted in reduced carotenoid biosynthesis (Steve et al., 1993; Nakatsuka et al., 1998; Liu et al., 2015b). Suppression of *ACO1* also resulted in an extension to shelf-life in tomato fruits (Behboodian et al., 2012). Similarly, several ethylene signalling genes link to *PSY-1* on FruitNet including *NR* and *ERF6*. Antisense inhibition of *NR* resulted in reduced *PSY-1* expression (Hackett et al., 2000), while *ERF6* influences carotenoid and ethylene biosynthesis pathways (Lee et al., 2011). *PSY-1* also directly links to *RIN* and *FUL1* on FruitNet, both have been shown to bind to the promoter and induce expression of *PSY-1* (Martel et al., 2011; Fujisawa et al., 2013; Shima et al., 2013). Finally, *DAMAGED DNA BINDING PROTEIN 1* (*DDB1*) was shown inhibit *PSY-1*, as a mutation to *DDB1* (also known as *HP-1*) resulted in elevated *PSY-1* activity (Cookson et al., 2003; Kilambi et al., 2013). A link between *PSY-1* and *DDB1* was demonstrated by FruitNet.

The results above validate the outputs provided by FruitNet. Therefore, FruitNet can be an important tool to predict the functions of novel genes, and used to identify their associated genes.

6.1.3 Discussion on the role of the *ZINC FINGER PROTEIN INDETERMINATE DOMAIN 2*

ZFPIDD2 down-regulation was characterised by broad phenotypic changes. Several can be attributed to differences to multiple classes of phytohormones identified through metabolite profiling. Elevated levels of the bioactive gibberellin form GA_1, combined with reduced ABA and increased fruit development time, indicated an extension to cell division or expansion phases of fruit growth, subsequently delaying the onset of ripening

contributing to improved fruit size (Table 3-2, Figure 3-2a Figure 3-26b). Increased GA_4 can be expected to contribute to improved fruit yield through increasing the number of fruits produced, without affecting fruit weight (Table 3-2). Imbalances to gibberellin, auxin and cytokinin levels are predicted to result in increased source-to-sink strength of fruit, contributing to the yield increases, in addition to the elevated non-vegetative biomass caused by reduced leaf senescence.

The *ZFPIDD2* was identified as an INDETERMINATE DOMAIN (IDD) protein, which previously has been demonstrated to be involved in gibberellin signalling (Feurtado et al., 2011; Yoshida et al., 2014). IDD proteins have been shown to bind to DELLA and SCARECROW-LIKE 3 (SCL3) via their C-terminal GRAS domains, to mediate gibberellin signalling (Yoshida et al., 2014; Yoshida and Ueguchi-Tanaka, 2014). A *SCARECROW-LIKE 1* (*GRAS9*) transcription factor was linked to *ZFPIDD2* on FruitNet. It was shown to be involved in gibberellin mediated signalling and is down-regulated upon gibberellin (GA_3) treatment and fruit set (Tang et al., 2015). Therefore, altered *GRAS9* expression could result in the altered bioactive GA forms and fruit yield phenotypes of *ZFPIDD2* down-regulated lines. Another FruitNet candidate is *GPS*, which is required for the biosynthesis of GAs (van schie et al., 2007). Also, *1-DEOXY-D-XYLULOSE 5-PHOSPHATE SYNTHASE 3* (*DXS3*) and *HOMEOBOX 2 PROTEIN* (*KNOX2*) are linked to *ZFPIDD2* on FruitNet, both genes or their gene family are suspected to be involved in gibberellin synthesis and signalling. *DXS* levels positively correlate to active GA content (Estevez et al., 2001; Cordoba et al., 2011), while *KNOX* genes have been shown to directly regulate GA content by altering expression of GA biosynthesis enzymes (Sakamoto et al., 2001; Hay et al., 2002; Yan et al., 2015). The results confirmed that *ZFPIDD2* has roles in gibberellin synthesis and signalling, consistent with other IDD proteins from other species. While FruitNet provides several candidates that with altered expression could explain the elevated bioactive GA forms identified.

Phytohormones are also are predicted to contribute to the ripening-related changes, altered IAA and cytokinin content were detected, while differences to ethylene can be expected (Table 3-2). Increased expression of *ZFPIDD2* during ripening, combined with reduced expression in *rin* and *nor* ripening mutants suggested a ripening-related function. *ZFPIDD2* was shown to be positively-regulated directly by RIN, FUL1 and FUL2, indicating that it is regulated by the tetramer model of MADS-box proteins along with TAGL1 (Fujisawa et al., 2012b; Fujisawa et al., 2013; Fujisawa et al., 2014; Ito,

2016). *ZFPIDD2* down-regulation resulted in a partial uncoupling of ripening, with significant reductions to fruit softening and elevated ripening associated colour development (Figure 3-22 and Figure 3-24). The latter was supported by carotenoid profiling, with elevated total carotenoid contents in both pericarp and jelly tissues (Table 3-3). Large increases to phytoene, phytofluene, neurosporene and lycopene demonstrated elevated flux upstream of lycopene in the carotenoid pathway. Increases to lycopene can explain the elevated A* scores within the CIELAB colour sphere (Figure 3-23). Carotenoid profiles suggested potential upregulation of *PSY-1*, *PDS*, *ZDS*, *Z-ISO* and *CRTISO*. Several of these structural genes along with the carotenoids they synthesise were linked to *ZFPIDD2* previously (Ye et al., 2015), although none correlated on FruitNet. Interestingly, the carotenoid profiles were consistent with the application of the ethylene precursor ACC (Su et al., 2015), therefore elevated ethylene biosynthesis is expected in *ZFPIDD2* transgenic lines. The results potentially indicate that *ZFPIDD2* indirectly inhibits carotenoid accumulation by fine-tuning ethylene levels, which can explain why no carotenoid structural genes were linked to *ZFPIDD2* on FruitNet.

From the terpenoid biosynthesis pathway only *GPS* and *DXS* were linked to *ZFPIDD2* on FruitNet. *DXS* was shown to be a rate limiting enzyme for carotenoid biosynthesis and enhanced transcription can facilitate increased lycopene (Lois et al., 2000; Rodríguez-Concepción et al., 2001; Rodríguez-Concepción et al., 2003). Vitamin E potential was also increased in transgenic lines with elevated tocopherol contents (Table 3-3). FruitNet did not correlate any tocopherol biosynthesis genes to *ZFPIDD2*. The results could indicate that *ZFPIDD2* negatively influences the MEP/DOXP pathway flux upstream of isoprenoids, thus suppression of *ZFPIDD2* results in elevated carotenoid and tocopherol contents. Also, reduced sucrose contents indicated elevated sucrose metabolism (Table 3-4), which previously was shown to increase phytoene and lycopene accumulation through upregulation of *PSY-1* (Telef et al., 2006). This can also explain the carotenoid increases observed in *ZFPIDD2* transgenic lines.

Broad differences to metabolism provide further evidence of accelerated ripening and elevated ethylene (Table 3-4), with reductions to sucrose (Li et al., 2016b), total organic acid and polyol contents with alterations to several amino acids (Carrari and Fernie, 2006; Osorio et al., 2011a; Li et al., 2016b). An example is the increases to phenylalanine in transgenic lines, which has been demonstrated to be important for fruit ripening, influencing colour, flavour/aroma and softening (Singh et al., 2010; Zhang et al., 2013). Interestingly a negative correlation between fruit size and sugar content was

previously identified (Tieman et al., 2017), *ZFPIDD2* down-regulation appears to uncouple this by improving yield without significantly altering total sugar content.

FruitNet also correlated the *PROTEIN PHOSPHATASE 2C* and *ETHYLENE RESPONSIVE TRANSCRIPTION FACTOR C4* (*ERFC4*) to *ZFPIDD2*. Suppression of a group A type *2C PROTEIN PHOSPHATASE* accelerated ripening through elevated colour accumulation and fruit softening, and increased levels of ethylene and ABA (Zhang et al., 2018b). *ZFPIDD2* down-regulation also resulted in the altered ABA during development, increased ripening-related colour development and predicted differences to ethylene, suggesting that *PROTEIN PHOSPHATASE 2C* could prove to be a candidate for the accelerated ripening phenotypes. The *ERFC4* was shown to be regulated by auxin, while conflicting roles in ripening are reported in literature (Pirrello et al., 2012; Li et al., 2016b). Whether *ERFC4* promotes or inhibits ripening, it remains a candidate for the altered ripening-related phenotypes.

Reduced fruit softening, delayed loss of fruit integrity and potential extension to shelf-life were detected with *ZFPIDD2* down-regulation (Figure 3-24). Less gluconic acid in transgenic lines provide evidence for the uncoupled ripening phenotype (Table 3-4), correlating to reduced fruit softening and elevated carotenoid content (Kwon et al., 2014). Additionally, less free galactose was detected (Table 3-4), consistent with multiple ripening inhibitor and reduced softening tomato mutants (Gross and Wallner, 1979; Gross, 1983, 1984; Kim et al., 1991; Smith et al., 2002). The results indicate that *ZFPIDD2* promotes fruit softening; more softening-related enzymes were correlated to *ZFPIDD2* on FruitNet when compared to genes involved in colour development. FruitNet links include *POLYGALACTURONASE A* (*PG2A*), *EXPANSIN1* (*EXP1*) and a *XYLOGLUCAN ENDOTRANSGLUCOSYLASE* (*XTH5*). *PG2A* is an enzyme involved in pectin depolymerisation and is highly up-regulated in close association with fruit ripening in tomato (DellaPenna et al., 1989). *EXP1* directly influences fruit softening, potentially through promoting cell wall loosening enabling hemicellulose depolymerisation (McQueen-Mason and Cosgrove, 1995; Brummell et al., 1999; Minoia et al., 2016). *XTH5* is expressed abundantly during ripening, acting as a cell wall remodelling enzyme with transglucosylase activity, catalysing the transfer of a xyloglucan molecule fragment to another xyloglucan molecule (Saladie et al., 2006; Miedes and Lorences, 2009; Miedes et al., 2010). It is involved in the maintenance of xyloglucan and the cell wall structure rather than cell wall loosening agents (Saladie et al., 2006). Altered transglucosylase activity was shown to alter fruit firmness in tomato

by decreasing the depolymerisation of xyloglucan (Miedes and Lorences, 2009; Miedes et al., 2010). Reduced expression of *EXP1* could limit access for softening-related enzymes including β-galactosidases from promoting pectin depolymerisation, and the loss of β-galactosyl during ripening. While both reduced *PG2A* and altered *XTH* expression would limit depolymerisation of hemicelluloses and pectins, with potential changes to cell wall integrity. Together these could be contributing to the slower rate of softening, explaining the reduced galactose levels and the potential extended shelf-life of transgenic lines.

Interestingly, elevated IAA was detected in transgenic fruits (Table 3-4), and has been shown to delay ripening (Vendrell, 1985; Cohen, 1996; Giovannoni, 2007; Su et al., 2015; Li et al., 2016b). IAA was shown to inhibit fruit softening by suppressing multiple genes involved in cell wall degradation including: *PG*, *PECTINESTERASE* (*PME*), *β-XYLOSIDASE*, *PECTATE LYASE* (*PL*) and *EXPANSIN* (*EXP*) (Li et al., 2016b), both *EXP* and *PG* being linked to *ZFPIDD2* on FruitNet. Li et al., 2016 demonstrated that IAA had a greater impact on softening than colour development, therefore is expected to contribute to the reduced softening-related phenotypes without severely impacting colour.

FruitNet also correlated *ZFPIDD2* with the ethylene-regulated *LIPOXYGENASE B* (*LOXB*), which is expressed upon ripening and was shown to influence postharvest shelf-life (Griffiths et al., 1999; Leon-Garcia et al., 2017). Suppression resulted in a reduced rate of softening, maintaining fruit integrity and texture for forty days compared to just six for representative controls. Unlike other LOX members, *LOXB* is not shown to be directly involved in generating the C5 flavour volatiles and C6 aldehyde and alcohol flavour compounds (Chen et al., 2004b; Mariutto et al., 2011; Shen et al., 2014). Delayed membrane leakage, maintenance of turgor and reduced softening was correlated with changes to linoleic acid (Leon-Garcia et al., 2017), which is a main fatty acid in ripe fruits and LOX substrates in tomato (Todd et al., 1990; Chen et al., 2004b; Baysal and Demirdöven, 2007; Ties and Barringer, 2012). Consistent with *LOXB* suppression, significant reductions to softening, increased fruit integrity and texture, combined with elevated linoleic acid content were identified in *ZFPIDD2* transgenic lines (Table 3-4). The results indicate that reduced LOXB activity could be contributing to the reduced softening phenotypes and uncoupling of ripening, especially as mature fruits showed normal appearance, with typical size, shape and red colour (Leon-Garcia et al., 2017).

Other softening-relating candidates linked to *ZFPIDD2* identified by FruitNet are the *N*-glycan processing enzymes α-MANNOSIDASE (α-MAN) and β-D-N-ACETYLHEXOSAMINIDASE (β-HEX). Free *N*-glycans accumulate in pericarp tissues during ripening as precursors of N-glycosylation, or as a result of N-glycoprotein degradation, which stimulates ripening by inducing ethylene biosynthesis and signalling (Priem and Gross, 1992; Priem et al., 1993; Nakamura et al., 2008). Ripening is associated with increased *α-MAN* and *β-HEX* expression and activity in various fruits. Individual suppression of *α-MAN* and *β-HEX* reduced fruit softening and considerably extended shelf-life in climacteric tomato and non-climacteric capsicum (*Capsicum annuum*); while excessive fruit softening was identified in overexpression lines (Meli et al., 2010; Ghosh et al., 2011). Both *α-MAN* and *β-HEX* RNAi fruits exhibited less trimming of *N*-glycans attached to cell wall glycoproteins, demonstrating to be an important regulatory mechanism controlling the fruit softening process (Meli et al., 2010). The cell walls of *α-MAN* RNAi fruits were much more compact with more polysaccharide deposition, while reduced cell separation was observed in *β-HEX* RNAi fruits (Meli et al., 2010). Numerous genes encoding cell wall-degrading proteins were down-regulated in both *α-MAN* and *β-HEX* RNAi fruits, including *EXPANSIN 1*, *PECTINACETYLESTERASE* and *PG2A*, which are candidates linked to *ZFPIDD2* on FruitNet. *PECTIN METHYL ESTERASE*, *GLUCAN ENDO1,3-β-D-GLUCOSIDASE*, *β 1,3 GLUCANSE*, *ENDO-XYLOGLUCAN TRANSFERASE*, *PECTIN ESTERASE*, α-*GALACTOSIDASE*, *PL* and *(1-4)-β-MANNAN ENDOHYDROLASE* were also down-regulated (Meli et al., 2010). Therefore, suppression of *α-MAN* and *β-HEX* not only inhibited *N*-glycoprotein degradation, but also cellulose, hemicellulose, and pectin degradation. The same study demonstrated that ethylene biosynthesis genes (*ACC SYNTHASE*, and *ACC OXIDASE*) were down-regulated with α-*MAN*-suppression. While reduced ETHYLENE RESPONSE FACTOR (ERF) family expression was identified in both *α-MAN* and *β-HEX* RNAi fruits. RIN and ethylene positively regulates *α-MAN* and *β-HEX*, and RIN has been shown to directly bind to the promoter of both enzymes (Irfan et al., 2014; Irfan et al., 2016). Furthermore, expression of both *α-MAN* and *β-HEX* were reduced in the *rin* and *nr* ripening-impaired mutants, which are deficient in ripening-associated ethylene biosynthesis or ethylene perception (Meli et al., 2010). Consistent with peach softening (Cao et al., 2014), these softening-relating enzymes are predicted to be part of a positive feed-back regulation of fruit ripening (Meli et al., 2010). Significantly, in tomato vegetative growth, fruit development, days to maturity, yield, climacteric ripening-related colour development remained unchanged with RNAi

mediated suppression (Meli et al., 2010). This study suggests that reduced *α-MAN* and *β-HEX* could be contributing to the reduced fruit softening and uncoupling of normal ripening in *ZFPIDD2* transgenic lines.

FruitNet also links *GALACTURONOSYLTRANSFERASE 5* (*GAUT5*), whose family have been shown to be involved in pectin biosynthesis (Sterling et al., 2006; Caffall et al., 2009; Kong et al., 2011). In tomato, GAUTs can influence carbon metabolism, partitioning and allocation, in addition to influencing plant growth and fruit yield in tomato (de Godoy et al., 2013). Therefore, it could be a candidate for both altered softening and non-vegetative or fruiting biomass phenotypes of *ZFPIDD2* transgenic lines.

The uncoupling of colour development and softening demonstrated by *ZFPIDD2* down-regulation remains an important objective. To date few examples have been able to achieve this, especially with strategies targeting single genes. However, suppression of *NAC1* in tomato produced a similar phenotype to *ZFPIDD2* down-regulation, through improved colour development and carotenoid content, with reduced fruit softening (Meng et al., 2016). Other similarities include an extended time from anthesis to breaker by several days with *NAC1* suppression. Also, elevated *PSY-1* expression was expected to confer the increased flux through the carotenoid pathway, resulting in greater accumulation of lycopene and total carotenoid content during late stages of ripening. Carotenoid profiles and increases to *PSY-1* transcripts were consistent with elevated ethylene production; that was delayed, but occurred to a higher extent than that of wild type fruits. Softening of antisense fruits was slower than that of wild type fruits, with reduced expression to the cell wall metabolism genes: *PG2A*, *EXP1*, *ENDO-1,4-β-CELLULOSE 1* (*CEL1*), and *ACID INVERTASE 1* (*WIV1*). Interestingly, *PG2A* and *EXP1* were correlated to *ZFPIDD2* on FruitNet. Softening phenotypes were also correlated to thicker pericarp (also shown in *ZFPIDD2* transgenic lines) and lower ABA contents in antisense fruits. Overexpression lines exhibited the opposite phenotype, with reduced carotenoids and ethylene biosynthesis combined with elevated softening (Ma et al., 2014).

The numerous phenotypic similarities between *ZFPIDD2* and *NAC1* suppression, combined with the rarity of such combination of ripening-related phenotypes suggested they could be part of the same ripening cascade. FruitNet linked *ZFPIDD2* to a *E3 UBIQUITIN-PROTEIN LIGASE* (*SINA*), which has been demonstrated to ubiquitinate the transcriptional factor *NAC1* in tomato, resulting in its degradation (Miao et al.,

2016). The link was established due to the involvement of *NAC1* in defence and stress-related functions (Selth et al., 2005; Ma et al., 2013), and shown to be fine-tuned at both transcriptional and post-translational levels (Huang et al., 2013). Therefore, *SINA* was suspected to play a negative role in defence signalling (Miao et al., 2016). The results potentially indicate that *ZFPIDD2* negatively regulates *SINA*, which would explain the several ripening-related similarities with *NAC1* suppression, as upregulation of *SINA* would result in greater ubiquitination of *NAC1*. *ZFPIDD2* down-regulation exhibited a stronger ripening-related phenotype compared to *NAC1* suppression, combined with additional plant and fruit development roles, while being directly correlated to *SINA*, suggesting that *ZFPIDD2* potentially lies upstream of *NAC1*.

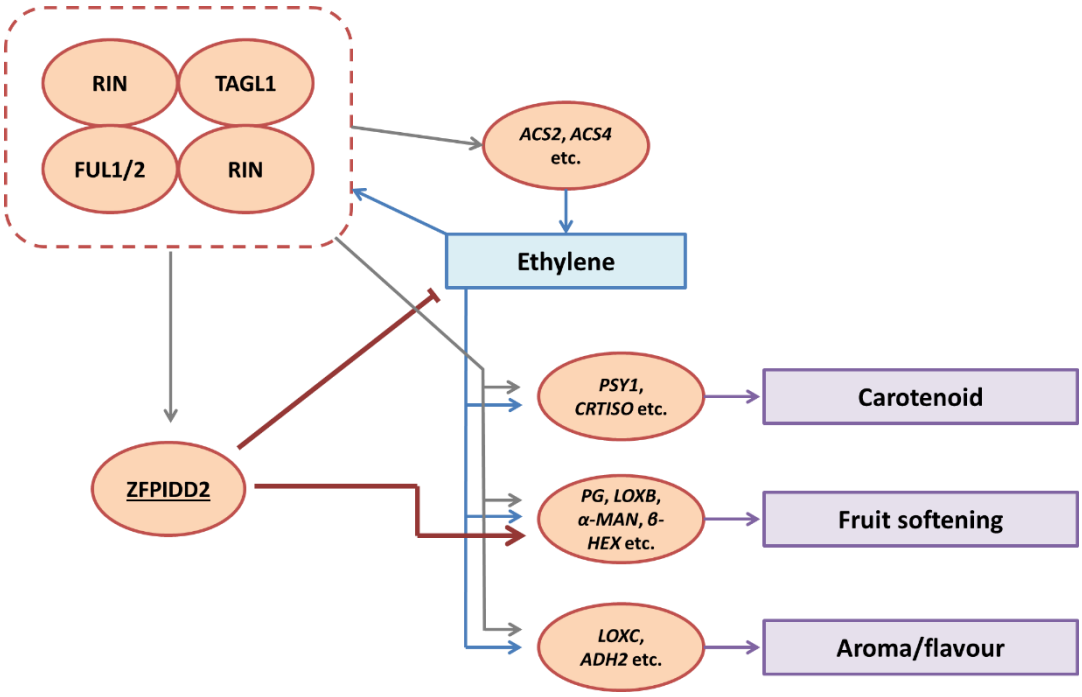

Figure 6-1 Proposed mechanism for the role of *ZFPIDD2* in tomato fruit ripening.
RIN, RIPENING INHIBITOR; TAGL1, TOMATO AGAMOUS-LIKE 1; FUL1/2, FRUITFULL homologs 1 or 2; ZFPIDD2, ZINC FINGER PROTEIN INDETERMINATE DOMAIN 2; ACS2, 1-AMINOCYCLOPROPANE-1-CARBOXYLATE SYNTHASE 2; ACS4, 1-AMINOCYCLOPROPANE-1-CARBOXYLATE SYNTHASE 4; PSY-1, PHYTOENE SYNTHASE 1; CRTISO, CAROTENOID ISOMERASE; PG, POLYGALACTURONASE; LOXB, LIPOXYGENASE B; α-MAN, α-MANNOSIDASE; β-HEX, β-D-N-ACETYLHEXOSAMINIDASE; LOXC, LIPOXYGENASE C; ADH2, ALCOHOL DEHYDROGENASE 2.

6.1.4 Discussion on the role of the *ZINC FINGER PROTEIN ZPR1*

Characterisation of the *ZINC-FINGER PROTEIN ZPR1* also proved successful. Multiple similarities with *ZFPIDD2* suppression were identified. Interestingly, FruitNet linked *ZPR1* to the GA receptor *GIBBERELLIN INSENSITIVE DWARF1* (*GID1*). The binding of GA to *GID1* triggers interaction with DELLA proteins (Ueguchi-Tanaka et al., 2005; Griffiths et al., 2006; Nakajima et al., 2006), stimulating interaction with the F box protein SLEEPY1/GID2, and then into an SCF E3 ubiquitin ligase complex. The SCF complex polyubiquitinates the DELLA proteins, targeting them for destruction by the 26S proteasome (Griffiths et al., 2006). Mutation to *GID1* was shown to induce dwarfism (Ueguchi-Tanaka et al., 2005), potentially explaining the reduction to plant height and internode lengths of *ZPR1* transgenic lines. Furthermore, *ZPR1* was linked to the gibberellin biosynthesis enzyme GA20ox3, which is expressed mostly in roots, thus is expected to be involved in root development (Xiao et al., 2006). Despite redundant functions compared with GA20ox1 and -2, root growth, internode elongation, and flowering were impacted with loss of GA20ox2 and -3, due to large enough reductions to GA (Plackett et al., 2012). Potentially alterations to GA biosynthesis or signalling could lead to changes to bioactive GA levels, which could potentially explain the developmental and ripening-related similarities with *ZFPIDD2* suppression.

The ripening-related expression profile of the *ZINC-FINGER PROTEIN ZPR1* combined with reduced expression in *rin, cnr* and *nor* ripening mutant lines, indicated an important role in ripening. This was confirmed where *ZPR1* transgenic lines exhibited an uncoupled ripening phenotype, with elevated colour development and reduced softening (Figure 4-14 to Figure 4-16). Like *ZFPIDD2*, *ZPR1* was a positively-regulated direct FUL1 target (Fujisawa et al., 2014), potentially explaining the ripening-related similarities with *ZFPIDD2*. The carotenoid profiles indicated increased flux upstream of lycopene (Table 4-1). Multiple enzymes that catalyse this section of the carotenoid pathway were linked to *ZPR1* on FruitNet, including: *PSY-1*, *PDS* and *Z-ISO* combined with *ISPE* from the MEP pathway. Carotenoid profiles were consistent with ethylene treatment (Su et al., 2015), with greater amounts of phytoene, phytofluene and lycopene combined with reduced β-carotene. Ethylene treatment induced elevated *PSY-1* expression, the rate limiting step for carotenoid production (Fraser et al., 2007), and was linked to *ZPR1* on FruitNet. The results indicate that *ZPR1* fine-tunes ethylene biosynthesis, limiting carotenoid accumulation.

DNA DAMAGE-BINDING PROTEIN1 (*DDB1*, the *HP-1* allele), acts as a negative regulator of fruit pigmentation and was linked to *ZPR1* on FruitNet. Suppression of *DDB1* increased plastid number without altering typical thylakoid structure and grana stacking, resulting in elevated lycopene and total carotenoid content in tomato fruits (Liu et al., 2004; Wang et al., 2008). Interestingly, the activity of the *PSY-1* enzyme was upregulated 2-fold in the *hp-1* (*ddb1*) mutant lines, with no corresponding increase in the transcripts levels. Thus, enzymes upstream of lycopene are predicted to be regulated at the posttranscriptional level by *DDB1* (Cookson et al., 2003; Kilambi et al., 2013). Therefore, altered *DDB1* expression is a candidate for the darker fruit phenotypes and elevated carotenoid contents of *ZPR1* transgenic lines. The direct RIN target *GRAS38* was also correlated to *ZPR1* (Fujisawa et al., 2012b; Fujisawa et al., 2013). Suppression of *GRAS38* resulted in reduced lycopene and ethylene biosynthesis (Shinozaki et al., 2018b). Therefore, *GRAS38* was shown to be a component of the regulatory cascade downstream of RIN, coordinating ripening processes associated with carotenoid and ethylene metabolism. Altered expression could also explain further ripening progression of *ZPR1* transgenic lines, including elevated lycopene and total carotenoid contents.

Elevated levels of the ethylene precursor methionine in *ZPR1* transgenic lines (Table 4-2), provides further evidence for increased ethylene biosynthesis. Previously, methionine content has been demonstrated to directly correlate with ethylene production, with increases providing a larger precursor pool for the production of S-adenosyl-L-methionine (AdoMet), 1-aminocyclopropane-1-carboxylic acid (ACC) and then ethylene (Van de Poel et al., 2013). The levels of soluble methionine limits ethylene production in maturing tomato fruit, while application of exogenous methionine resulted in the higher rates of ethylene evolution (Katz et al., 2006). Further metabolism differences were consistent with ethylene treatment (Table 4-2), including reduced putrescine, citric acid, malic acid, and succinic acid (Van de Poel et al., 2013; Lim et al., 2017).

Interestingly, multiple enzymes involved in synthesis of ethylene from methionine were correlated to *ZPR1* on FruitNet. This included *1-AMINOCYCLOPROPANE-1-CARBOXYLATE OXIDASE* (*ACO1*), the predominant *ACO* isoform that catalyses the last step in ethylene biosynthesis pathway (Barry et al., 1996; Anjanasree et al., 2005; Jafari et al., 2013). Large increases to *ACO1* expression are witnessed during ripening-related system 2 of ethylene biosynthesis (Barry et al., 1996; Nakatsuka et al., 1998; Van de Poel et al., 2013). Jafari et al., 2013 stated that *ACO1* expression could be used as a marker for the rate of ripening. The *ZPR1* was also correlated to an unknown *ACO*

member and the *ACO-LIKE E8 PROTEIN HOMOLOG* (*E86*), predicted to be involved in ethylene biosynthesis (Yuan et al., 2016).

Additionally, multiple genes involved in ethylene signalling were linked to *ZPR1* on FruitNet, including the well characterised ethylene receptor *NEVER RIPE* (*NR*) (Wilkinson et al., 1995; Payton et al., 1996). The *NR* gene is involved in ethylene perception. Ethylene insensitivity was demonstrated in the *nr* mutant, whereby fruits failed to ripen normally (Lanahan et al., 1994). Another target is the *RIPENING REGULATED PROTEIN* (*DDTFR5*) that has been shown to interact with *NR* and *ETR1*, modulating ethylene and auxin responses and development (Lin et al., 2008a). FruitNet also correlates the *ETHYLENE RECEPTOR 2* (*ETR2*) to *ZPR1*, which is constitutively expressed in all tomato tissues and is associated with broad growth, development and ripening functions (Lashbrook et al., 1998; Wang et al., 2006). *ETR2* suppression increased fruit weight and altered fruit shape, elevated fruit softening and reduced shelf-life, and increased ripening-related colour development (Bao et al., 2007). *ETR2* could be associated with several phenotypic differences in *ZPR1* transgenic lines. Another FruitNet link is the *ETHYLENE-RESPONSIVE HEAT SHOCK PROTEIN COGNATE 70* (*ER21*), which is expressed in tomato ripening (Zegzouti et al., 1999). *ER21* is predicted to be involved in the transition from of chloroplasts to chromoplasts, to obtain maximal lycopene accumulation (Neta-Sharir et al., 2005). Therefore, *ER21* could contribute to the elevated lycopene and colour development of *ZPR1* transgenic lines.

Sucrose levels were also increased in *ZPR1* transgenic lines (Table 4-2). Elevated sucrose accelerated ripening, inducing more rapid ripening-related colour transition through the upregulation of *PSY-1* and potentially *DXS* (Télef et al., 2006; Li et al., 2016a). Also, sucrose induced greater ethylene production through promoting genes involved in the auto-catalytic system of ethylene biosynthesis, combined with multiple ethylene signalling genes (Télef et al., 2006; Li et al., 2016a). Sucrose was predicted to improve carbon flux, channelling efficiency from pyruvate and GA3P into the citric acid cycle. Increases to sucrose and carotenoid content, combined with predicted elevation to ethylene biosynthesis in *ZPR1* transgenic lines, indicate that altered sucrose levels could be influencing the phenotypes recorded. The *SUCROSE ACCUMULATOR* (*SUCR*) was shown to control fruit sucrose contents and was correlated to *ZPR1* using FruitNet (Chetelat et al., 1995), potentially explaining the increased sucrose contents in transgenic fruits.

Differences to phenolic and flavonoid contents were also identified (Table 4-2). Reduced total chlorogenic acid was detected in transgenic lines, consistent with further ripening progression. Chlorogenic acid levels decline during fruit ripening and is predicted to inhibit IAA oxidation, promoting ripening as IAA delays fruit maturation (Buta and Spaulding, 1997; Li et al., 2016b). Consistent reduction to kaempferol was also identified. Kaempferol is a major yellow flavonoid, and could contribute to the reduced B* score of transgenic lines screened by colourimeter. The reduced total organic acid, several sugar phosphates, combined with increases to aspartic acid, glutamic acid and trehalose indicated further ripening progression (Carrari et al., 2006; Centeno et al., 2011; Osorio et al., 2011a). Glutamate is associated with umami flavour, thus increases suggest that savoury flavour could be enhanced in transgenic lines.

FruitNet also correlates *LIPOXYGENASE C* (*LOXC*) to *ZPR1*. *LOXC* is an essential enzyme for the generation of fruit C5 and C6 volatiles (Chen et al., 2004b; Shen et al., 2014); *LOXC* suppression reduced flavour volatile levels. Therefore, altered expression would likely impact fruit flavour. Similar to *ZFPIDD2*, FruitNet also links *ZPR1* to *LOXB*. As mentioned earlier *LOXB* influences postharvest shelf-life, as it is involved in fruit softening and the maintenance of fruit integrity and texture (Griffiths et al., 1999; Leon-Garcia et al., 2017). Therefore, *LOXB* is an important candidate for the reduced softening phenotypes exhibited by both *ZPR1* and *ZFPIDD2* transgenic lines. Altered *LOXB* expression in *ZPR1* could explain the delay to fruit softening without impacting size, shape or red colour of fruits (Leon-Garcia et al., 2017). Further softening related enzymes are linked to *ZPR1* on FruitNet, including the pectin depolymerising enzyme PG2A, and β-D-XYLOSIDASE 1 which participates in the breakdown of *N-g*lycans in cell walls (Yokouchi et al., 2013; Buanafina et al., 2015). *β-D-XYLOSIDASE 1* is expressed strongly during the final stages of fruit ripening, particularly in over-ripe fruit (Itai et al., 2003), and has been shown to be suppressed in multiple tomato mutants with reduced softening (Zhang et al., 2018a). Both *PG2A* and *β-D-XYLOSIDASE 1* could be contributing to the uncoupling of ripening by reducing softening, without impacting colour development.

6.1.5 Discussion on the role of the *HEAT STRESS TRANSCRIPTION FACTOR A3* (*HSFA2*)

Broad developmental and ripening-related differences were identified in *HEAT STRESS TRANSCRIPTION FACTOR A3* (*HSFA2*) transgenic lines. Several phenotypes consistent with reduced *ELONGATED HYPOCOTYL 5* (*HY5*) expression, including extended shoot growth during early development, reduced leaf pigmentation, paler immature fruit, with reductions to carotenoid content including lycopene at ripe fruit stages (Liu et al., 2004) (Table 5-2 and Figure 5-17). Importantly, *HY5* was linked to the *HSFA2*, demonstrating the strongest Pearson correlation coefficient of any transcription factor on FruitNet. Therefore, reduced *HY5* expression in transgenic lines is expected to be contributing to the altered developmental and ripening related phenotypes identified.

Unlike the other transcription factors characterised, colour development was the only ripening-related quality trait altered in transgenic lines (Figure 5-17). Metabolite profiles confirmed a reduction to phytoene and lycopene when compared to non-transgenic controls (Table 5-2). This provides further evidence for the *HY5* suppression phenotype, as HY5 has been shown to bind to the promoter of *PSY-1* and promote lycopene accumulation (Liu et al., 2004; Toledo-Ortiz et al., 2014). The results suggest that *HSFA2* is either upstream of *HY5* and induces its expression, or is downstream of *HY5* and involved its signalling processes. Fewer genes were correlated to *HSFA2* compared with *HY5* on FruitNet, potentially indicating that *HSFA2* lies upstream of *HY5* with the ability to regulate its expression.

HSFA2 is a heat shock factor, which binds to the heat shock elements of the heat shock proteins (HSP) genes, inducing their expression (Zhang et al., 2011b). FruitNet also correlates multiple HSPs to *HSFA2*, including *TSW12* (*HSP4*) which was expressed during seed germination and stress, mainly in stems (Torres-Schumann et al., 1992). This further validates FruitNet, while altered *TSW12* expression could explain the early extended shoot growth (Figure 5-17). Another FruitNet link is *HSP110*, which is an *ATP-DEPENDENT CASEIN LYTIC PROTEINASE* (*CLPB*). The *CLPB* family have been shown to be involved in chloroplast development, in *Arabidopsis CLPB-p* knockouts failed to accumulate chlorophyll or properly develop chloroplasts (Lee et al., 2007). CLP PROTEASES have been shown to degrades the DXS enzyme or CLPB3 promotes their solubility and hence enzymatic activity (Perello et al., 2016; Pulido et al., 2016; Llamas et al., 2017). In tomato, suppression of a *CLP PROTEASE* altered

carotenoid content, upregulated *DXS* and *PSY-1* and displayed aberrant chromoplasts (D'Andrea et al., 2018). The CLP PROTEASE contributes to the differentiation of chloroplasts into chromoplasts during tomato fruit ripening and prevents carotenoid degradation by co-ordination with specific chaperones (D'Andrea et al., 2018). In tomato the *HSP110* were localised to the chloroplast contributing to acquired thermotolerance, and the plastid with predicted roles in chromoplast differentiation (Yang et al., 2006; Barsan et al., 2012; Keller et al., 2017). Similarly, a heat shock protein *CHAPERONE PROTEIN DNAJ 49* was linked to the *HSFA2* on FruitNet, most members of the DNAJ family demonstrate stress-related functions. Further roles in chromoplast differentiation with chlorophyll and carotenoid accumulation have been established (Li and Van Eck, 2007; Kong et al., 2014; Zhou et al., 2015; Park et al., 2016; Chayut et al., 2017).

ER21 (*HSP70*) was expressed under heat stress and normal conditions during fruit maturation (Zegzouti et al., 1999; Neta-Sharir et al., 2005; Albert et al., 2016). *ER21* was linked to *HSFA2*, and is predicted to be involved in transition from of chloroplasts to chromoplasts, obtaining maximal lycopene accumulation (Neta-Sharir et al., 2005). Reductions to carotenoid and lycopene content were detected in transgenic lines (Table 5-2). *ER21* is an important candidate for the altered carotenoid profiles identified. Interestingly, *ER21* was identified under antagonist and drought-specific QTLs for fructose and malic acid content (Albert et al., 2016), significant differences to both metabolites were identified in *HSFA2* transgenic lines. Previous studies have shown that *HSP70* and *DNAJ* were shown to interact as predicted by FruitNet (King et al., 1999), further validating the outputs provided.

Deficiencies in both the organization and abundance of thylakoids were identified in *Arabidopsis hy5* mutants. These abnormalities were consistent with the fact that HY5 is required for transcription of the *CAB* gene, whose product is necessary for thylakoid organization (Chattopadhyay et al., 1998; Maxwell et al., 2003). The considerable reduction of thylakoid organization is suspected to result in the reduced capacity for carotenoid accumulation. *CLPB* (*HSP110*), *CHAPERONE PROTEIN DNAJ 49* and *ER21* (*HSP70*) have been correlated to chloroplast and chromoplast development or differentiation. Therefore, these could be involved in the reduced pigmentation phenotypes of *HSFA2* transgenic lines, potentially due to reduced organization and abundance of thylakoids consistent with *hy5* mutants, especially as *CLPB* and *ER21* also links to *HY5* on FruitNet.

6.2 Relevance to current understanding

Manipulation of two zinc finger proteins yielded nonspecific changes to tomato development and ripening. *ZPR1* has been shown to accumulate in tomato apical meristems in response to ABA treatment and heat stress, acting as a transcriptional activator with the ability to bind to ABRE (ABA-responsive element). Therefore, it was predicted to be involved in the ABA signalling network, with potential roles in plant cell development and abiotic stress response (Li et al., 2013). *ZFPIDD2* has been identified as a C2H2-type zinc finger protein; members are involved in the transcriptional regulation of diverse biological processes (Englbrecht et al., 2004). The C2H2 family have mainly been correlated to plant development regulation or involved in various types of stress responses (Gupta et al., 2012). Developmental roles include flowering time and floral organ formation, in addition to trichome development by acting on the GA pathway (Gan et al., 2006; Gan et al., 2007; Zhou et al., 2013). INDETERMINATE DOMAIN1 (IDD1)/ENHYDROUS (ENY) protein was shown to interact with DELLA, mediating GA effects to balance ABA-promoted maturation during late seed development (Feurtado et al., 2011). Interestingly, there is growing evidence supporting their involvement in fruit ripening, especially through phytohormonal control (Weng et al., 2015b; Han et al., 2016; Wu et al., 2016). *ZFPIDD2* has been shown to be positively-regulated directly by RIN, FUL1 and FUL2, while FUL1 directly induces *ZPR1* expression (Fujisawa et al., 2013; Fujisawa et al., 2014), indicating that both ZFPs are involved in ripening and can potentially explain the phenotypic similarities.

Consistent with *ZFPIDD2*, the C2H2 transcription factor *SlZFP2* was shown be involved in various plant development and fruit ripening roles (Weng et al., 2015a; Weng et al., 2015b). *SlZFP2* overexpression resulted in multiple phenotypic changes, including more branches, early flowering, delayed fruit ripening, lighter seeds, and faster seed germination. Down-regulation caused problematic fruit set, accelerated ripening, and inhibited seed germination. *SlZFP2* is mainly expressed during fruit development and is activated by ABA, but it represses ABA biosynthesis during fruit development by directly suppressing the ABA biosynthetic genes *NOTABILIS*, *SITIENS*, *FLACCA* and the *ALDEHYDE OXIDASE* (*SlAO1*) (Weng et al., 2015a; Weng et al., 2015b). The result indicated that *SlZFP2* mainly fine-tunes ABA biosynthesis during vegetative growth and fruit development. *SlZFP2* was demonstrated to regulate fruit ripening through transcriptional suppression of the ripening regulator *COLOURLESS NON-RIPENING*

(*CNR*), independent of *RIN*. Similar mechanisms were reported consistent with *ZFPIDD2*, including roles involved with the fine-tuning of phytohormones, and how imbalances to auxin, gibberellin and ABA impacted fruit set. Also, *SlZFP2* was shown to negatively regulate fruit ripening, through delaying colour development and ripening time, consistent with both *ZFPIDD2* and *ZPR1* transgenic lines. Despite this, an uncoupling of ripening with altered fruit firmness was not reported. The results from Weng et al., 2015b confirms the broad functions of ZFPs, validating the dual functions of *ZFPIDD2* and *ZPR1* transcription factors in both tomato development and ripening, in addition to the altered phenotypes obtained through manipulation. Additionally, two other ripening-induced C2H2 zinc finger proteins were shown act as transcriptional repressors of ripening, fine-tuning the regulation of ethylene production during banana fruit ripening, possibly via supressing ethylene biosynthetic genes (Han et al., 2016). The results further supported our hypotheses outlined.

To date few examples have been able to achieve the uncoupling of colour development and fruit softening during ripening, especially with strategies targeting single genes. Although, suppression of *NAC1* improved colour development and carotenoid content, combined with reducing fruit softening providing and an extension to shelf-life (Meng et al., 2016). Several phenotypic similarities were shared by *NAC1*, *ZFPIDD2* and *ZPR1* transgenic lines. Both *NAC1* and *ZFPIDD2* exhibited similar levels of suppression, although larger more consistent increases to total carotenoid and lycopene content throughout ripening were identified in *ZFPIDD2* transgenic lines. Additionally, *ZFPIDD2* suppression resulted in larger reductions to the rate of fruit softening that may provide a greater shelf-life potential, combined with an extended fruit development time from anthesis to breaker. Also, improved vitamin E potential and fruit yield were identified in *ZFPIDD2* transgenic lines, changes to these traits were not reported in Meng et al., 2016. The results combined with FruitNet led to hypothesis that both *NAC1* and *ZFPIDD2* are part of the same ripening cascade, potentially *ZFPIDD2* indirectly promoting *NAC1* through regulation of *SINA*. Similar improvements were identified to *ZPR1* transgenic lines when compared to *NAC1* suppression, with more consistent increases to carotenoid content and comparable improvements to fruit softening. Overall, both *ZFPIDD2* and *ZPR1* manipulation provide greater commercial potential, particularly *ZFPIDD2* which is an important target to exploit for improved ripening-related fruit quality and yield.

The accelerated ripening-related colour development and carotenoid accumulation ensured fruit reach red ripe quicker; thus more rapidly meeting the acceptable quality demands required from an industry, supplier and consumer prospective for retail and consumption. Darker red tomatoes are proving more popular, particularly with their association with improved health benefits. Carotenoids have been shown to be beneficial to human health, due to their antioxidant, anti-inflammatory, hypolipidemic, and anticarcinogenic activities. Lycopene has been shown to be a potent antioxidant compared to alpha-tocopherol (ten times more potent) or beta-carotene (twice as potent) (Kim et al., 2010b; Kong et al., 2010). Lycopene consumption has been associated with decreased risk of chronic diseases such as cardiovascular disease, and several different types of cancer, including prostate, lung and stomach (Fraser and Bramley, 2004; Story et al., 2010; Viuda-Martos et al., 2014; Mozos et al., 2018). The improvements to total carotenoid and lycopene content highlighted in our study are comparable with increases reported in several tomato fruit metabolic engineering studies (Fraser et al., 2002; Enfissi et al., 2005; Galpaz et al., 2008; Sun et al., 2012b; Nogueira et al., 2013; Meng et al., 2016). Therefore, manipulation of *ZFPIDD2* and *ZPR1* have resulted in the production of biofortified tomato plants with enhanced antioxidant contents. Lycopene confers the attractive colour and economical quality to the fruit; thus the enhanced lycopene accumulation in *ZFPIDD2* transgenic fruit would improve both the visual and functional properties of tomato (Li et al., 2018).

Elevated vitamin E (VTE) contents were observed in *ZFPIDD2* transgenic lines. Importantly, significant improvements to alpha-tocopherol were detected, as it has been shown to have the highest biological activity compared to the other VTE forms. Selective retention of alpha-tocopherol is mediated by the HEPATIC α-TOCOPHEROL TRANSFER PROTEIN (α-TTP), the major VTE regulator in humans. Similar to carotenoids, high VTE intakes are linked to a reduced risk of cardiovascular diseases, while also possessing anti-cancer properties, due to its antioxidant ability (Rizvi et al., 2014; Raiola et al., 2015). Other evidence demonstrated that VTE could decrease the risk of type-2 diabetes, cataracts, Alzheimer's disease in older patients, while stimulating the immune system and anaemia prevention (Sano et al., 1997; Li et al., 1999; Mangialasche et al., 2010; Rizvi et al., 2014). The increases to alpha-tocopherol in pericarp tissues compared between *ZFPIDD2* down-regulation and AC controls, were comparable to those reported with the overexpression of *HOMOGENTISATE PHYTYLTRANSFERASE* (*HPT*), an important enzyme in the biosynthesis of tocopherols (vitamin E) (Seo et al.,

2011b). The results provide further evidence of improved nutritional content in *ZFPIDD2* transgenic fruit.

Significant improvements to fruit softening were also identified in both *ZFPIDD2* and *ZPR1* transgenic lines. The reduced rate of softening is comparable to strategies aimed at targeting genes involved in cell wall integrity (Lu et al., 2001; Smith et al., 2002; Minoia et al., 2016) and other ripening-related transcription factors (Meng et al., 2016). Outer pericarp firmness increases were comparable with *PL* suppression (Uluisik et al., 2016). The reduced softening phenotype demonstrates the potential to provide significant extension to shelf-life and fruit integrity. Both would improve quality from a commercial perspective: as fruits would be able to withstand handling and transportation, limiting damage and disease and have a longer marketable shelf-life. As a result losses would be limited, expanding both delivery and storage opportunities, while reducing costs as fewer harvests would be necessary. Improvements to these traits would benefit both local and global tomato distribution, particularly the supply chains which require extensive transportation of fruits such as the United States of America or Asia. The delayed softening would enable producers to harvest later to maximise nutritional potential, or harvest at mature green stage as *ZFPIDD2* and *ZPR1* transgenic fruits provide improved isoprenoid potential while extending shelf-life. Furthermore, consumer related quality would be improved as the increases to fruit firmness are expected to contribute to maintenance of fruit texture for longer. Texture is the principal fruit quality attribute and an important driver of consumer preferences for tomato fruits (Goulao and Oliveira, 2008).Genetic studies have identified several quantitative trait loci (QTLs) associated with fruit mass and yield in tomato (Grandillo et al., 1999; Frary et al., 2000; van der Knaap and Tanksley, 2003; Chakrabarti et al., 2013). However, functional analyses are required to understand the mechanism behind their respective regulatory properties. A mechanism for *ZFPIDD2* was identified, as it was shown to inhibit GA_1 biosynthesis (Table 3-2), previously demonstrated to influence fruit size (Serrani et al., 2007b). The results contribute to the understanding of transcription factors that limit the formation of bioactive GAs. Similar fruit number and yield increases were also reported with altered gibberellin metabolism, due to overexpression of GA 20-oxidase (Garcia-Hurtado et al., 2012). The same study also identified an extension in time from anthesis to breaker, consistent with *ZFPIDD2* suppression. Fruit size and yield improvements were also comparable with shikimic acid treatment, along with lycopene and total carotenoid increases (Al-Amri, 2013). Down-regulation of

ZFPIDD2 demonstrated elevated fruit number, size and total yield, which could potentially improve both land use efficiency and crop profitably.

Previous studies revealed that the *HSFA2* is involved in acquired thermotolerance, and was shown to be a very sensitive response acceptor that responds strongly to heat stress (von Koskull-Doring et al., 2007; Frank et al., 2009; Yang et al., 2016; Keller et al., 2017). Manipulation of *HSFA2* yielded a phenotype consistent with reduced *HY5* expression (Chapter V), thus it is predicted that *HSFA2* is likely upstream of *HY5* and induces its expression. In *Arabidopsis*, heat shock treatment was shown to stabilise and induce *HY5* by reducing the nuclear abundance of CONSTITUTIVE PHOTOMORPHOGENIC1 (COP1), which directly interacts and targets *HY5* for degradation in the 26S proteasome (Osterlund et al., 2000; Karayekov et al., 2013; Song et al., 2017). Therefore, large induction of *HSFA2* upon heat shock (up to 150 times) suggests it is likely an integral part of heat stress signalling, involved in reduction of *COP1* and the increase to *HY5*. Manipulation likely results in elevated COP1-mediated degradation of *HY5*, explaining the phenotypes observed in transgenic lines.

Overall, characterisation of all three transcription factors revealed broad non-specific development and ripening-related functions. The results indicate that manipulation of a structural gene or enzyme, rather than a transcription factor, would more likely facilitate a more targeted improvement to quality, as demonstrated by other studies. *PECTATE LYASE* (*PL*) suppression exclusively reduced softening (Uluisik et al., 2016), or elevated colour and nutritional content with *DE-ETIOLATED1* (*DET1*) down-regulation (Enfissi et al., 2010).

6.3 Future directions and recommendations

Further experiments could be performed to advance our understanding of how each transcription factor influences fruit ripening.

ZINC FINGER PROTEIN INDETERMINATE DOMAIN 2 (*ZFPIDD2*) transgenic lines (Chapter III)

It would be interesting to continue RNA sequencing analysis. Ripe fruits were harvested, pooled and RNA was extracted for down-regulated *ZFPIDD2* transgenic lines with both azygous and AC controls. Samples were sent for analysis, however time constraints prevented analysis of the outputs provided. The results from the RNA sequencing could provide an insight into uncoupled ripening phenotype.

Carotenoid profiles and numerous broader metabolite changes were consistent with ethylene treatment and more rapid ripening progression. RNA sequencing would be able to detect transcript levels of genes involved ethylene biosynthesis and signalling, in particular *ACS* (*1-AMINOCYCLOPROPANE-1-CARBOXYLATE SYNTHASE*) and *ACO* (*1-AMINOCYCLOPROPANE-1-CARBOXYLATE OXIDASE*) the main rate-limiting steps in autocatalytic system 2 ethylene production. Candidates include *ACS2*, *ACS4* and *ACO1*, which are highly expressed upon ripening, direct RIN targets, and involved with activation of system 2 (Nakatsuka et al., 1998; Barry et al., 2000; Van de Poel et al., 2012; Fujisawa et al., 2013). Gas chromatography with flame ionisation detector (GC-FID) was set up to quantify to levels of ethylene produced by ripe fruit. However, all columns tested proved unsuccessful for the separation of compounds and ethylene could not be quantified. Separation therefore required a CP-PoraPLOT Q column (Fraser et al., 2007), but due to time limitations ethylene screening could not be performed.

The RNA sequencing analysis would also confirm whether the elevated flux upstream of lycopene was due to the upregulation of *PSY-1*, the rate-limiting enzyme involved in carotenoid biosynthesis (Fraser et al., 2007). Additionally, the expression of *PDS*, *ZDS*, *Z-ISO* and *CRTISO* upstream of lycopene, combined with lycopene cyclases would improve the understanding of how *ZFPIDD2* controls colour development. Furthermore, it would be interesting to look at the transcript levels of genes involved in the MEP pathway, such as *DXS*, *ISPE* and *GGPS*, to see whether these genes are influencing the

changes to the carotenoid and tocopherol pathway and profiles. All three MEP pathway genes were demonstrated to have ripening-related expression profiles, are regulated by RIN, while being shown to influence isoprenoid content during ripening (Rodríguez-Concepción et al., 2001; Fujisawa et al., 2013; Quadrana et al., 2013; Liu et al., 2015a).

Further biochemical characterisation through determination of flux control coefficients would also be valuable addition to the work presented and RNA sequencing analysis, to ascertain how the overall flux is controlled through several pathways. *In vitro* assays would provide information about the enzyme activities and the flux control of the ethylene and carotenoid biosynthesis pathway. Labelling studies would quantitatively determine dynamic alterations to intermediary and secondary metabolism, correlating to metabolite and phenotypic changes detailed in this study. For instance the results could confirm that elevated *PSY-1* expression and activity is most influential for elevated lycopene and total carotenoid increases, consistent with literature (Fraser et al., 2002; Fraser et al., 2007).

Large reductions to sucrose were identified, this could be explained analysing the transcript levels of *SUCROSE INVERTASE* genes. Increases to invertase activity and sucrose degradation accelerated ripening, inducing more rapid ripening-related colour transition that correlated with greater ethylene production (Li et al., 2016a). RNA sequencing analysis would also identify changes to softening related genes, including those linked to *ZFPIDD2* on FruitNet. Alteration to transcript levels would provide candidates for the elevated fruit firmness and reductions to free galactose, correlated with reduced softening. This would highlight the transcriptional control of *ZFPIDD2* that promotes fruit softening, potentially identifying multiple targets, as numerous genes are expected to be acting in concert in the softening process (Saladié et al., 2007).

As mentioned previously, *NAC1* suppression demonstrated numerous ripening-related similarities with *ZFPIDD2* down-regulation, thus was expected to part of the same ripening cascade. FruitNet correlated *SINA* to *ZFPIDD2*, which has been demonstrated to ubiquitinate the transcriptional factor *NAC1* in tomato, resulting in its degradation. Therefore, *ZFPIDD2* was expected to negatively regulate *SINA*, positively regulating *NAC1*. Studying the expression of these genes would provide further evidence of this mechanism, which can explain the uncoupled ripening phenotype observed with *ZFPIDD2* down-regulation.

Flavour and aroma are essential parameters of quality in tomatoes. The pleasant sweet-sour taste of tomatoes is mainly influenced by the sugar and organic acids, that have already been quantified, but taste can also be influenced by aroma volatiles. Therefore, solid-phase microextraction (SPME) coupled with gas chromatography (GC–MS) could be utilised to determine any differences to the volatiles that could impact flavour in fresh tissue. Over 400 volatiles have been detected in tomato (Buttery and Ling, 1993), analysis should focus on the 15–20 that are produced in sufficient quantities to have an impact on human perception (Baldwin et al., 2000). Carotenoid content has been shown to influence taste perception and volatile composition, with the ability to impact consumer liking (Vogel et al., 2010). The amounts of apocarotenoid volatiles are proportional to their carotenoid precursor contents in fruits (Lewinsohn et al., 2005; Vogel et al., 2010). Phytoene, phytofluene, ζ-carotene, and neurosporene are precursors for geranylacetone, while lycopene content is directly proportional to 6-methyl-5-hepten-2-one (Tieman et al., 2017). Therefore, the numerous metabolism changes and elevation to isoprenoids in *ZFPIDD2* transgenic lines could point towards altered flavour. The *rin* mutation negatively impacts both fruit aroma and flavour, and is impaired in the synthesis of a subset of flavour volatiles (Baldwin et al., 2000). Therefore, it is important to determine whether there are any flavour changes in *ZFPIDD2* transgenic lines, to fully determine its potential impact on the improvement of ripening-related quality compared to commercial varieties.

Fluorescence microscopy and the resulting captured micrographs could be used to study histological cross-sections of tomatoes, to determine whether differences to number of cell division and/or cell expansion are contributing to the yield improvements identified (Liu et al., 2018b). Pericarp thickness should also be determined for transgenic and control genotypes, to verify if it responsible for the increases in fruit weight. Microscopy could also be used to study pericarp tissue for altered polysaccharide deposition and cell separation that has been shown to influence softening (Meli et al., 2010). It would be interesting to use atomic force microscopy (AFM) that has previously been used to examine the nanostructural conformation (height, length, branching, polymer aggregation) of its isolated cell wall polysaccharides, combined with the nanotexture of fruits enabling to probe plant tissue mechanics at cellular level (Round et al., 2010; Posé et al., 2018). AFM enables study of cell wall structure at high magnification in a more natural context with minimum sample preparation. The platform could identify changes

to the cell wall disassembly process associated with texture changes and fruit softening of transgenic lines with increased firmness.

Finally, it would be important to confirm whether transgenic lines can deliver improved shelf-life that both consumers and industry demand (Causse et al., 2010; Meli et al., 2010; Zhang et al., 2018a). To achieve this, many of the analyses performed in this study and the future directions outlined above, should be conducted on fruits post-harvest following commercial practises. UPLC analysis should be used to confirm the elevated isoprenoid content in transgenic lines post-harvest. GC-MS analysis can then be used to determine broad metabolism changes, in addition to the quantification of total sugar and acid content which are essential metabolites contributing to tomato flavour. SPME based GC-MS approaches could then determine any differences to flavour volatiles linked to tomato olfaction. GC-MS approaches can also be used to quantify ethylene and respiration levels of fruits post-harvest, which should be monitored at defined ripening stages.

ZINC FINGER PROTEIN ZPR1 transgenic lines (Chapter IV)

Firstly, an important experiment would be to confirm *ZPR1* down-regulation in transgenic lines when compared to both azygous and AC controls, using real time quantitative PCR (RT-qPCR). Then, transcript levels of candidate genes identified by FruitNet could then be carried out. Expression of *PSY-1*, *PDS* and *Z-ISO* could explain the altered carotenoid profiles and improved total carotenoid content. Similar to *ZFPIDD2*, carotenoid profiles of *ZPR1* transgenic lines were consistent with ethylene treatment. Further evidence of increased ethylene was the increased methionine content, which has been demonstrated to directly correlate with ethylene production (Van de Poel et al., 2013). The levels of ethylene could then be quantified using the GC-FID platform, and combined with expression analysis, demonstrating if or how *ZPR1* fine-tunes ethylene biosynthesis during ripening. FruitNet correlated *ZPR1* to *ACO1*, which catalyses the last step in ethylene biosynthesis pathway and its expression can be used as a marker for the rate of ripening (Jafari et al., 2013). *ACS2* and *ACS4* expression should also be quantified due to their importance in ethylene biosynthesis, as they are the rate-limiting steps within the pathway. Quantification of other phytohormones could also be analysed in order to reveal the mechanism behind the uncoupled ripening-phenotype.

It would be interesting to study the expression of fruit softening-related genes, including *PG2A* that was linked to *ZPR1* on FruitNet, which has been used previously as a marker for altered softening. Transcript levels of other FruitNet targets could be carried out, including *LOXB* and *β-D-XYLOSIDASE 1*. *LOXB* influences postharvest shelf-life, as it is involved in fruit softening and the maintenance of fruit integrity and texture (Griffiths et al., 1999; Leon-Garcia et al., 2017). *PG2A* and *β-D-XYLOSIDASE 1* participates in the breakdown of *N-g*lycans in cell walls (Yokouchi et al., 2013; Buanafina et al., 2015).

Due to the delayed softening phenotype of *ZPR1* transgenic lines, it would be important to utilise biochemical and phenotypic approaches to confirm the potential improvements to shelf-life post-harvest identified in this study. Similar to the future directions for *ZFPIDD2* transgenic lines, isoprenoids levels should be quantified using the UPLC platform, while GC-MS based approaches can be used to determine broad metabolism differences as well as quantification of key flavour volatile, ethylene and respiration levels.

HEAT STRESS TRANSCRIPTION FACTOR A3 (*HSFA2*) transgenic lines (Chapter V)

A RT-qPCR experiment is required to confirm the down-regulation of the *HSFA2* in transgenic lines, compared to both azygous and AC controls. *HSFA2* transgenic lines exhibit multiple similarities with *HY5* down-regulation. Quantification of transcript levels by RT-qPCR and protein levels by Western-blot would verify whether *HY5* is down-regulated in transgenic lines. The results would determine whether reduced *HY5* expression should be considered the main candidate for the altered phenotypes observed. If *HY5* is down-regulated in transgenic lines, chromatin immunoprecipitation coupled with DNA microarray analysis (ChIP-chip) would be able to determine whether *HSFA2* directly binds to the promoter of *HY5*, regulating its expression. HY5 has been shown to bind to the promoter of *PSY-1* and promote lycopene accumulation (Liu et al., 2004; Toledo-Ortiz et al., 2014). With the reductions to phytoene and lycopene in transgenic lines it would be important to determine the transcript levels of *PSY-1*, to provide further evidence for *HY5* down-regulation and reduced carotenoid contents.

HY5 down-regulation is also characterised by reduced chlorophyll levels in both leaf and fruit. Reductions to both chorophyll and carotenoid contents were predicted to be due to abnormalities in both organization and abundance of thylakoids (Liu et al., 2004).

Chlorophyll contents of both leaf and mature green fruits should be quantified using the UPLC platform, and combined with transmission electron microscopy of chloroplasts. The results would determine whether differences to chloroplast structure could be influencing potential changes to chlorophyll contents, providing further evidence that *HSFA2* promotes *HY5* expression. Additionally, *HY5* has been shown to promote flavonoid accumulation by the activation of MYBs and key structural genes of the flavonoid pathway (Oyama et al., 1997; Holm et al., 2002; Stracke et al., 2010; Peng et al., 2013; Shin et al., 2013; Zoratti et al., 2014; Gangappa and Botto, 2016). Especially, as *HSFA2* was shown to positively interact with a MYB transcription factor (Pan et al., 2013). Differences to flavonoid contents could be achieved using the UPLC method described in section 2.3.3. This could provide further evidence for reduced *HY5*, provide details potentially how *HSFA2* directly controls flavonoid biosynthesis, and generally improve the understanding of *HSFA2* involvement in colour development.

In conclusion, the project utilised a System Biology approach, with transcriptomic and virus-induced gene silencing (VIGS) strategies to select uncharacterised transcription factors with suspected ripening-related functions. Transcriptomic and correlation network analysis have previously identified a putative regulator of pigment accumulation in tomato (Pan et al., 2013), in addition to several genes in the calcium signalling cascade that are expected to be regulated by SUN that impacts fruit shape (Clevenger et al., 2015). An RNAi approach was used to down-regulate the gene expression of three transcription factors, which was confirmed in *ZFPIDD2* transgenic lines. Detailed phenotypic and metabolic analysis conducted, combined with the outputs from the transcriptional and correlation analysis from FruitNet, provided broad coverage ensuring that characterisation proved successful. The results confirmed that the project successfully identified ripening-related transcription factors, which can improve fruit quality compared to the heterozygous *rin* mutation currently utilised. *ZFPIDD2* and *ZPR1* manipulation uncoupled regulatory mechanisms controlling colour development and softening, therefore understanding the mechanism should be a priority to provide significant improvements to commercial quality traits. Fruits retained the delayed softening and potentially the shelf-life benefits of the *rin* mutation to extend delivery and storage opportunities, but by elevating isoprenoid accumulation the compromised sensory quality associated with *rin* was reversed. As a consequence, fruits more rapidly reach acceptable colour-related quality for retail and consumption, potentially limiting

losses to damage and disease, combined with improved nutritional content. *ZFPIDD2* increases fruit yield without impacting sugar content, likely through altered interplay between GA and ABA, which should be investigated further to improve fruit number, size and yield to maximise crop potential. The substantial improvements to each individual trait identified (isoprenoid content, fruit firmness, and fruit yield) are comparable with previously reported tomato engineering studies, aimed at targeting a specific quality trait.

These transcription factors were shown to be important targets for breeding. Modulating expression using natural variation or TILLING (Targeting Induced Local Lesions In Genomes) would be more advantageous to achieve a phenotype by down-regulation, due to improved consumer perception as these strategies are more acceptable than genetic modification. Similarly, transcription factors can also be targeted using gene editing approaches such as CRISPR/cas9 (Ito et al., 2015). The emerging field of gene editing provides simplicity, precision, and a quicker and more powerful approach for crop improvement, without the incorporation of foreign transgenes. Gene editing enabled the enrichment of lycopene, improvements to shelf-life and fruit yield in tomato (Lin et al., 2016; Yu et al., 2017; Li et al., 2018), further applications of gene editing include yield and nutritional enhancement, with abiotic and biotic stress management in several other important food crops (Jaganathan et al., 2018). Despite being subject to genetic modification laws in the European Union, the ruling could be reversed if gene-editing techniques are approved as being as safe as mutagenesis methods already exempt from the law. Although, the generation of knock out lines using this technology could be introduced for instance in the United States, Canada and China, due to fewer restrictions as the technology is regarded as an equivalent to traditional breeding.

Commercially, manipulation of transcription factors can provide significant improvement, but often impacts other traits (e.g. *RIPENING INHIBITOR*, *RIN*; *NON-RIPENING*, *NOR*; *APETALA2A*, *AP2A*; *TOMATO AGAMOUS-LIKE1*, *AGAMOUS*; *ZINC FINGER PROTEIN 2*, *ZFP2*; NAC *DOMAIN* 4/9, *NAC4/9*). Whereas, approaches for targeted improvement strategies should focus on structural genes or enzymes, due to specific functions that are easier to predict (e.g. *PECTATE LYASE*, *PL*; *DE-ETIOLATED 1*, *DET1*). However, from a fundamental point of view transcription factors can contribute to the elucidation of the complex transcriptional control that governs fruit ripening and quality.

Appendices

Appendix 1

Gene ID	Primers sequences	
	Forward	Reverse
Primers used for real-time qPCR* and RT real-time qPCR		
ZFPIDD2	AGATGTGATTGTGGAACCCTTT	AGTTGAAGAATTTGGTGGTGGGA
PDS	AAGGCGCTGTCTTATCAGGA	ACTGCTGACACCCAGTGAGA
ACTIN	AGGTATTGTGTTGGACTCTGGTGA	ACGGAGAATGGCATGTGGAA
NPTII	ATACGGATCGTCCTGCAGTC	GAGGAGCATCGTGGAAAAAG
Primers used for PCR		
NPTII	GCAAGCCTTGAATCGTCCATAC	GGCAGGTCTCATCAAGACGAT

Table A1- 1 Sequences of primers used in (RT) real-time qPCR and PCR analyses.

Line	AC	Azy	10-8-8-1	10-8-15-7	10-8-15-8
Firmness at B+4	78.6 ± 2.5	83.1 ± 2.1	**96.7 ± 2.3*** **	**95.7 ± 2.8*** **	**95.4 ± 1.7*** **

Table A1-2 Firmness of *ZFPIDD2* turning fruits harvested for transcript level quantification.

The firmness of turning fruits were recorded and used as a marker to determine whether breaker plus four days was a suitable time point for *ZFPIDD2* transcript level quantification, based upon a reduced softening phenotype previously identified in transgenic lines across multiple generations. Firmness was assessed on four random points on each fruit, a minimum of three fruits were analysed per plant and three individual plants from each line were combined for the analyses. This ensured the study included a minimum of three technical replicates and three biological replicates. Statistical determinations are shown as mean ± SD values, Dunnett's test analysis illustrates statistically significant differences (denoted $P < 0.05$, $**P < 0.01$, and $***P < 0.001$) from the non-transgenic controls.

Appendix 2

a

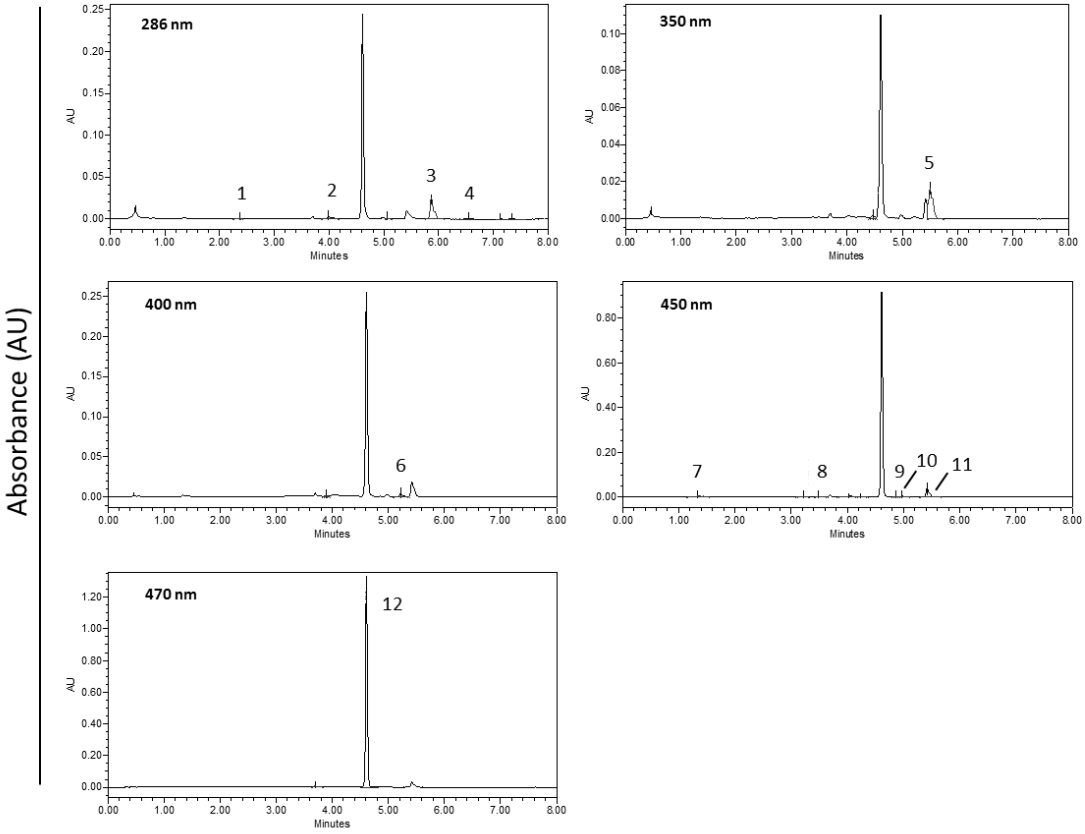
Absorbance (AU)
286 nm
350 nm
400 nm
450 nm
470 nm
AU
Minutes
1
2
3
4
5
6
7
8
9
10
11
12

b

Names	Peak number	Retention time (min)	Spectra λmax (nm)	Dose response curve
Phylloquinone	1	2.4	274.0	y=261388x-4244.7
α-Tocopherol	2	4.0	293.4	y=261388x-4244.7
Phytoene	3	5.9	286.2	y=4000000x-24989
δ-tocopherol	4	6.5	297.0	y=261388x-4244.7
Phytofluene	5	5.5	349.0, 368.3	y=3000000x- 68968
ζ-Carotene	6	5.2	400.8, 425.0	y=10000000x-731324
Lutein	7	1.3	448.0, 476.0	y=9000000x-462175
δ-Carotene	8	3.5	433.0, 459.0, 490.0	y=10000000x-731324
Neurosporene	9	4.9	415.0, 440.5, 467.4	y=10000000x-731324
γ-Carotene	10	5.0	462.6, 493.0	y=10000000x-731324
β-Carotene	11	5.4	454.1, 479.6	y=10000000x-731324
Lycopene	12	4.6	472.3, 502.7	y=6000000x-101170

Figure A 0-1 Chromatographic profiles, spectral characteristics and dose response curves of isoprenoids identified.

Chromatographic profiles of isoprenoids identified (a) with the chromatographic annotations and spectral characteristics recorded from 250 to 600 nm (b) obtained using the UPLC platform.

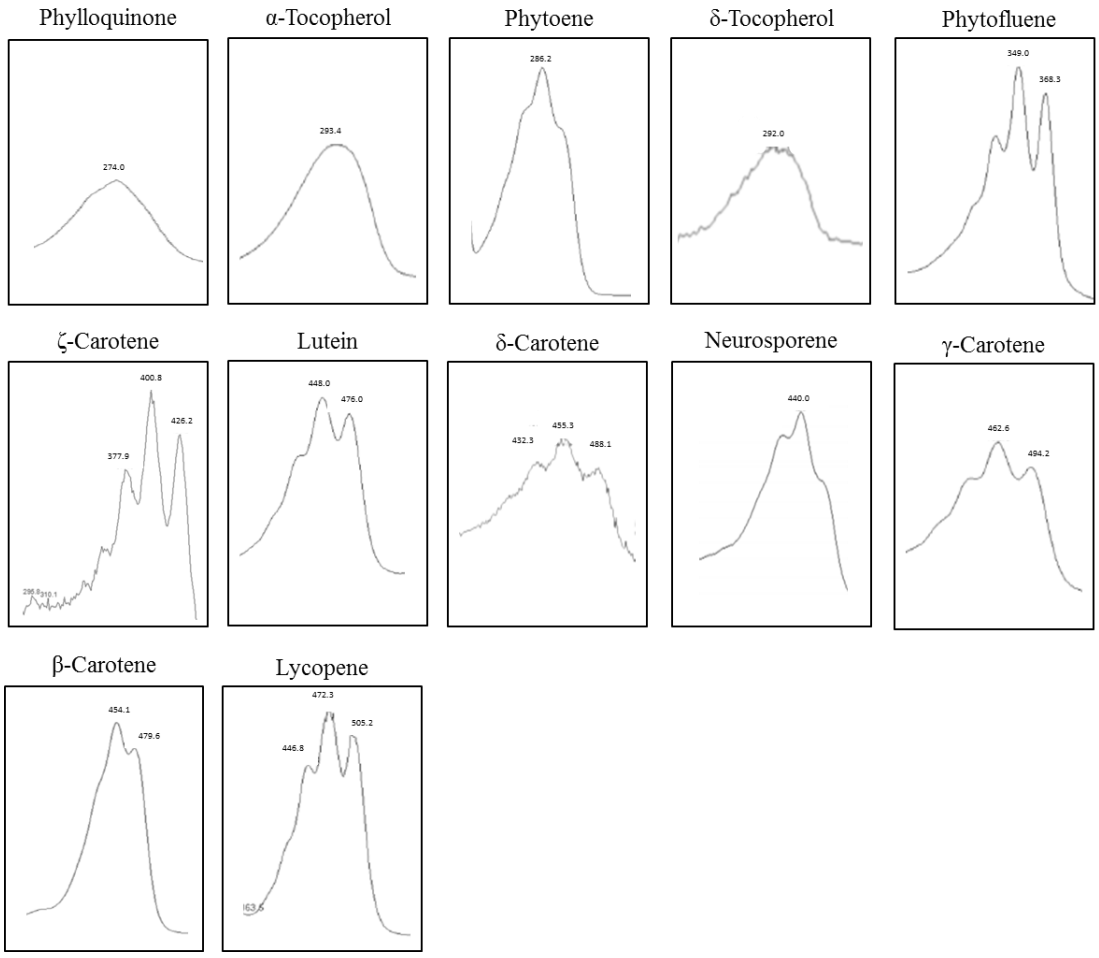

Figure A 0-2 Spectra of isoprenoids identified.

References

Afitlhile, M., Fry, M., and Workman, S. (2015). The TOC159 mutant of *Arabidopsis thaliana* accumulates altered levels of saturated and polyunsaturated fatty acids. Plant Physiology and Biochemistry **87**, 61-72.

Akihiro, T., Koike, S., Tani, R., Tominaga, T., Watanabe, S., Iijima, Y., Aoki, K., Shibata, D., Ashihara, H., Matsukura, C., Akama, K., Fujimura, T., and Ezura, H. (2008). Biochemical mechanism on GABA accumulation during fruit development in tomato. Plant and Cell Physiology **49**, 1378-1389.

Al-Amri, S.M. (2013). Improved growth, productivity and quality of tomato (*Solanum lycopersicum L.*) plants through application of shikimic acid. Saudi Journal of Biological Sciences **20**, 339-345.

Alba, R., Payton, P., Fei, Z., McQuinn, R., Debbie, P., Martin, G.B., Tanksley, S.D., and Giovannoni, J.J. (2005). Transcriptome and selected metabolite analyses reveal multiple points of ethylene control during tomato fruit development. Plant Cell **17**, 2954-2965.

Albacete, A., Cantero-Navarro, E., Balibrea, M.E., Grosskinsky, D.K., de la Cruz Gonzalez, M., Martinez-Andujar, C., Smigocki, A.C., Roitsch, T., and Perez-Alfocea, F. (2014). Hormonal and metabolic regulation of tomato fruit sink activity and yield under salinity. Journal of Experimental Botany **65**, 6081-6095.

Albacete, A., Cantero-Navarro, E., Großkinsky, D.K., Arias, C.L., Balibrea, M.E., Bru, R., Fragner, L., Ghanem, M.E., González, M.d.l.C., Hernández, J.A., Martínez-Andújar, C., van der Graaff, E., Weckwerth, W., Zellnig, G., Pérez-Alfocea, F., and Roitsch, T. (2015). Ectopic overexpression of the cell wall invertase gene CIN1 leads to dehydration avoidance in tomato. Journal of Experimental Botany **66**, 863-878.

Albert, E., Segura, V., Gricourt, J., Bonnefoi, J., Derivot, L., and Causse, M. (2016). Association mapping reveals the genetic architecture of tomato response to water deficit: focus on major fruit quality traits. Journal of Experimental Botany **67**, 6413-6430.

Almeida, J., Azevedo, M.d.S., Spicher, L., Glauser, G., vom Dorp, K., Guyer, L., del Valle Carranza, A., Asis, R., de Souza, A.P., Buckeridge, M., Demarco, D., Bres, C., Rothan, C., Peres, L.E.P., Hörtensteiner, S., Kessler, F., Dörmann, P., Carrari, F., and Rossi, M. (2016). Down-regulation of tomato PHYTOL KINASE strongly impairs tocopherol biosynthesis and affects prenyllipid metabolism in an organ-specific manner. Journal of Experimental Botany **67**, 919-934.

Alonso, J.M., Hirayama, T., Roman, G., Nourizadeh, S., and Ecker, J.R. (1999). EIN2, a bifunctional transducer of ethylene and stress responses in *Arabidopsis*. Science **284**, 2148-2152.

Andersen, S.U., Buechel, S., Zhao, Z., Ljung, K., Novák, O., Busch, W., Schuster, C., and Lohmann, J.U. (2008). Requirement of B2-type cyclin-dependent kinases for meristem integrity in *Arabidopsis thaliana*. The Plant Cell **20**, 88-100.

Anjanasree, K.N., Verma, P.K., and Bansal, K.C. (2005). Differential expression of tomato ACC oxidase gene family in relation to fruit ripening. Current Science **89**, 1394-1399.

Arah, I.K., Amaglo, H., Kumah, E.K., and Ofori, H. (2015). Preharvest and postharvest factors affecting the quality and shelf life of harvested tomatoes: a mini review. International Journal of Agronomy, 1-6.

Argueso, C.T., Ferreira, F.J., and Kieber, J.J. (2009). Environmental perception avenues: the interaction of cytokinin and environmental response pathways. Plant Cell and Environment **32**, 1147-1160.

Ariizumi, T., Shinozaki, Y., and Ezura, H. (2013). Genes that influence yield in tomato. Breeding Science **63**, 3-13.

Aruoma, O.I. (1994). Nutrition and health aspects of free radicals and antioxidants. Food and Chemical Toxicology **32**, 671-683.

B. Seymour, G., Lasslett, Y., and A. Tucker, G. (1987). Differential effects of pectolytic enzymes on tomato polyuronides in vivo and in vitro. Phytochemistry **26**, 3137-3139.

Baldwin, E.A., Scott, J., K. Shewmaker, C., and Schuch, W. (2000). Flavor trivia and tomato aroma: Biochemistry and possible mechanisms for control of important aroma components. HortScience **35**, 1013-1022.

Balibrea Lara, M.E., Gonzalez Garcia, M.-C., Fatima, T., Ehneß, R., Lee, T.K., Proels, R., Tanner, W., and Roitsch, T. (2004). Extracellular invertase is an essential component of cytokinin-mediated delay of senescence. Plant Cell **16**, 1276-1287.

Bao, B., Ke, L., Jiang, J., and Ying, T. (2007). Fruit quality of transgenic tomatoes with suppressed expression of LeETR1 and LeETR2 genes. Asia Pacific Journal of Clinical Nutrition **16 Suppl 1**, 122-126.

Bapat, V.A., Trivedi, P.K., Ghosh, A., Sane, V.A., Ganapathi, T.R., and Nath, P. (2010). Ripening of fleshy fruit: molecular insight and the role of ethylene. Biotechnology Advances **28**, 94-107.

Bar-Peled, M., Urbanowicz, B.R., and O'Neill, M.A. (2012). The synthesis and origin of the pectic polysaccharide rhamnogalacturonan II – insights from nucleotide sugar formation and diversity. Frontiers in Plant Science **3**, 1-12.

Barickman, T.C., Kopsell, D.A., and Sams, C.E. (2014). Abscisic acid increases carotenoid and chlorophyll concentrations in leaves and fruit of two tomato genotypes. Journal of the American Society for Horticultural Science **139**, 261-266.

Barker, L., Kühn, C., Weise, A., Schulz, A., Gebhardt, C., Hirner, B., Hellmann, H., Schulze, W., Ward, J.M., and Frommer, W.B. (2000). SUT2, a putative sucrose sensor in sieve elements. The Plant Cell **12**, 1153-1164.

Baron, M., Davies, S., Alexander, L., Snellgrove, D., and Sloman, K.A. (2008). The effect of dietary pigments on the coloration and behaviour of flame-red dwarf gourami, *Colisa lalia*. Animal Behaviour **75**, 1041-1051.

Barrangou, R., Fremaux, C., Deveau, H., Richards, M., Boyaval, P., Moineau, S., Romero, D.A., and Horvath, P. (2007). CRISPR provides acquired resistance against viruses in prokaryotes. Science **315**, 1709-1712.

Barry, C.S., Blume, B., Bouzayen, M., Cooper, W., Hamilton, A.J., and Grierson, D. (1996). Differential expression of the 1-aminocyclopropane-1-carboxylate oxidase gene family of tomato. Plant Journal **9**, 525-535.

Barry, C.S., and Giovannoni, J.J. (2006). Ripening in the tomato Green-ripe mutant is inhibited by ectopic expression of a protein that disrupts ethylene signaling. Proceedings of the National Academy of Sciences USA **103**, 7923-7928.

Barry, C.S., and Giovannoni, J.J. (2007). Ethylene and fruit ripening. Journal of Plant Growth Regulation **26**, 143–159.

Barry, C.S., Llop-Tous, M.I., and Grierson, D. (2000). The regulation of 1-aminocyclopropane-1-carboxylic acid synthase gene expression during the transition from system-1 to system-2 ethylene synthesis in tomato. Plant Physiology **123**, 979-986.

Barsan, C., Zouine, M., Maza, E., Bian, W., Egea, I., Rossignol, M., Bouyssie, D., Pichereaux, C., Purgatto, E., Bouzayen, M., Latche, A., and Pech, J.C. (2012). Proteomic analysis of chloroplast-to-chromoplast transition in tomato reveals metabolic shifts coupled with disrupted thylakoid biogenesis machinery and elevated energy-production components. Plant Physiology **160**, 708-725.

Bate, N.J., Orr, J., Ni, W., Meromi, A., Nadler-Hassar, T., Doerner, P.W., Dixon, R.A., Lamb, C.J., and Elkind, Y. (1994). Quantitative relationship between phenylalanine ammonia-lyase levels and phenylpropanoid accumulation in transgenic tobacco identifies a rate-determining step in natural product synthesis. Proceedings of the National Academy of Sciences USA **91**, 7608-7612.

Baxter, C.J., Carrari, F., Bauke, A., Overy, S., Hill, S.A., Quick, P.W., Fernie, A.R., and Sweetlove, L.J. (2005). Fruit carbohydrate metabolism in an introgression line of tomato with increased fruit soluble solids. Plant and Cell Physiology **46**, 425-437.

Baysal, T., and Demirdöven, a. (2007). Lipoxygenase in fruits and vegetables: A review. Enzyme and Microbial Technology **40**, 491-496.

Behboodian, B., Mohd Ali, Z., Ismail, I., and Zainal, Z. (2012). Postharvest analysis of lowland transgenic tomato fruits harboring hpRNAi-ACO1 construct. TheScientificWorldJournal **2012**, 439870-439870.

Bemer, M., Karlova, R., Ballester, A.R., Tikunov, Y.M., Bovy, A.G., Wolters-Arts, M., Rossetto Pde, B., Angenent, G.C., and de Maagd, R.A. (2012). The tomato FRUITFULL homologs TDR4/FUL1 and MBP7/FUL2 regulate ethylene-independent aspects of fruit ripening. Plant Cell **24**, 4437-4451.

Bensen, R.J., and Zeevaart, J.A.D. (1990). Comparison of ent-kaurene synthetase A and B activities in cell-free extracts from young tomato fruits of wild-type and *gib-1*, *gib-2*, and *gib-3* tomato plants. Journal of Plant Growth Regulation **9**, 237-242.

Bertin, N., Gautier, H., and Roche, C. (2002). Number of cells in tomato fruit depending on fruit position and source-sink balance during plant development. Plant Growth Regulation **36**, 105-112.

Beyer, P., Al-Babili, S., Ye, X., Lucca, P., Schaub, P., Welsch, R., and Potrykus, I. (2002). Golden Rice: introducing the β-carotene biosynthesis pathway into rice endosperm by genetic engineering to defeat vitamin A deficiency. The Journal of Nutrition **132**, 506-510.

Bianchetti, R.E., Cruz, A.B., Oliveira, B.S., Demarco, D., Purgatto, E., Peres, L.E.P., Rossi, M., and Freschi, L. (2017). Phytochromobilin deficiency impairs sugar metabolism through the regulation of cytokinin and auxin signaling in tomato fruits. Scientific Reports **7**, 1-15.

Bick, J.A., and Lange, B.M. (2003). Metabolic cross talk between cytosolic and plastidial pathways of isoprenoid biosynthesis: unidirectional transport of intermediates across the chloroplast envelope membrane. Archives of Biochemistry and Biophysics **415**, 146-154.

Boggio, S.B., Palatnik, J.F., Heldt, H.W., and Valle, E.M. (2000). Changes in amino acid composition and nitrogen metabolizing enzymes in ripening fruits of *Lycopersicon esculentum* Mill. Plant Science **159**, 125-133.

Bohner, J., and Bangerth, F. (1988). Effects of fruit set sequence and defoliation on cell number, cell size and hormone levels of tomato fruits (*Lycopersicon esculentum Mill.*) within a truss. Plant Growth Regulation **7**, 141-155.

Bohner, J., Hedden, P., Bora-Haber, E., and Bangerth, F. (1988). Identification and quantitation of gibberellins in fruits of *Lycopersicon esculentum*, and their relationship to fruit size in *L. esculentum* and *L. pimpinellfolium*. Physiologia Plantarum **73**, 348-353.

Bolouri Moghaddam, M.R., and Van den Ende, W. (2013). Sweet immunity in the plant circadian regulatory network. Journal of Experimental Botany **64**, 1439-1449.

Bombarely, A., Menda, N., Tecle, I.Y., Buels, R.M., Strickler, S., Fischer-York, T., Pujar, A., Leto, J., Gosselin, J., and Mueller, L.A. (2011). The Sol Genomics Network (solgenomics.net): growing tomatoes using Perl. Nucleic Acids Research **39**, 1149-1155.

Bottcher, C., Boss, P.K., and Davies, C. (2011). Acyl substrate preferences of an IAA-amido synthetase account for variations in grape (*Vitis vinifera L.*) berry ripening caused by different auxinic compounds indicating the importance of auxin conjugation in plant development. Journal of Experimental Botany **62**, 4267-4280.

Bottcher, C., Keyzers, R.A., Boss, P.K., and Davies, C. (2010). Sequestration of auxin by the indole-3-acetic acid-amido synthetase GH3-1 in grape berry (*Vitis vinifera L.*) and the proposed role of auxin conjugation during ripening. Journal of Experimental Botany **61**, 3615-3625.

Boyer, J.S., and McLaughlin, J.E. (2006). Functional reversion to identify controlling genes in multigenic responses: analysis of floral abortion. Journal of Experimental Botany **58**, 267-277.

Breitel, D.A., Chappell-Maor, L., Meir, S., Panizel, I., Puig, C.P., Hao, Y., Yifhar, T., Yasuor, H., Zouine, M., Bouzayen, M., Granell Richart, A., Rogachev, I., and Aharoni, A. (2016). AUXIN RESPONSE FACTOR 2 intersects hormonal signals in the regulation of tomato fruit ripening. PLoS Genet **12**, 1-34.

Britton, G. (1995). Structure and properties of carotenoids in relation to function. The FASEB Journal **9**, 1551-1558.

Britton, G. (2009). Vitamin A and Vitamin A Deficiency. In Carotenoids: volume 5: Nutrition and health, G. Britton, H. Pfander, and S. Liaaen-Jensen, eds. (Basel: Birkhäuser Basel), pp. 173-190.

Broxterman, S.E., and Schols, H.A. (2018). Characterisation of pectin-xylan complexes in tomato primary plant cell walls. Carbohydrate Polymers **197**, 269-276.

Brummell, D.A. (2006). Cell wall disassembly in ripening fruit. Functional Plant Biology **33**, 103-119.

Brummell, D.A., Dal Cin, V., Crisosto, C.H., and Labavitch, J.M. (2004). Cell wall metabolism during maturation, ripening and senescence of peach fruit. Journal of Experimental Botany **55**, 2029-2039.

Brummell, D.A., and Harpster, M.H. (2001). Cell wall metabolism in fruit softening and quality and its manipulation in transgenic plants. Plant Molecular Biology **47**, 311-340.

Brummell, D.A., Harpster, M.H., Civello, P.M., Palys, J.M., Bennett, A.B., and Dunsmuir, P. (1999). Modification of expansin protein abundance in tomato fruit alters softening and cell wall polymer metabolism during ripening. Plant Cell **11**, 2203-2216.

Brummell, D.A., Lashbrook, C.C., and Bennett, A.B. (1994). Plant Endo-1,4-β-D-glucanases. In Enzymatic conversion of biomass for fuels production (American Chemical Society), pp. 100-129.

Buanafina, M.M., Dalton, S., Langdon, T., Timms-Taravella, E., Shearer, E.A., and Morris, P. (2015). Functional co-expression of a fungal ferulic acid esterase and a beta-1,4 endoxylanase in *Festuca arundinacea* (tall fescue) modifies post-harvest cell wall deconstruction. Planta **242**, 97-111.

Bünger-Kibler, S., and Bangerth, F. (1982). Relationship between cell number, cell size and fruit size of seeded fruits of tomato (*Lycopersicon esculentum Mill.*), and those induced parthenocarpically by the application of plant growth regulators. Plant Growth Regulation **1**, 143-154.

Buta, J.G., and Spaulding, D.W. (1994). Changes in indole-3-acetic acid and abscisic acid levels during tomato (*Lycopersicon esculentum* Mill.) fruit development and ripening. Journal of Plant Growth Regulation **13**, 163-166.

Buta, J.G., and Spaulding, D.W. (1997). Endogenous levels of phenolics in tomato fruit during growth and maturation. Journal of Plant Growth Regulation **16**, 43-46.

Buttery, R.G., and Ling, L.C. (1993). Volatile components of tomato fruit and plant parts. In Bioactive volatile compounds from plants (American Chemical Society), pp. 23-34.

Buttery, R.G., Teranishi, R., Flath, R.A., and Ling, L.C. (1989). Fresh tomato volatiles. In Flavor chemistry (American Chemical Society), pp. 213-222.

Caffall, K.H., Pattathil, S., Phillips, S.E., Hahn, M.G., and Mohnen, D. (2009). *Arabidopsis thaliana* T-DNA mutants implicate GAUT genes in the biosynthesis of pectin and xylan in cell walls and seed testa. Molecular Plant **2**, 1000-1014.

Cao, L., Zhao, C., Su, S., Luo, C., and Han, M. (2014). The role of β-hexosaminidase in peach (*Prunus persica*) fruit softening. Scientia Horticulturae **169**, 226-233.

Cara, B., and Giovannoni, J.J. (2008). Molecular biology of ethylene during tomato fruit development and maturation. Plant Science **175**, 106-113.

Carey, A.T., Holt, K., Picard, S., Wilde, R., Tucker, G.A., Bird, C.R., Schuch, W., and Seymour, G.B. (1995). Tomato exo-(1-->4)-beta-D-galactanase. Isolation, changes during ripening in normal and mutant tomato fruit, and characterization of a related cDNA clone. Plant Physiology **108**, 1099-1107.

Carey, A.T., Smith, D.L., Harrison, E., Bird, C.R., Gross, K.C., Seymour, G.B., and Tucker, G.A. (2001). Down-regulation of a ripening-related beta-galactosidase gene (TBG1) in transgenic tomato fruits. Journal of Experimental Botany **52**, 663-668.

Carrari, F., Asis, R., oacute, and Fernie, A.R. (2007). The metabolic shifts underlying tomato fruit development. Plant Biotechnology **24**, 45-55.

Carrari, F., Baxter, C., Usadel, B., Urbanczyk-Wochniak, E., Zanor, M.-I., Nunes-Nesi, A., Nikiforova, V., Centero, D., Ratzka, A., Pauly, M., Sweetlove, L.J., and Fernie, A.R. (2006). Integrated analysis of metabolite and transcript levels reveals the metabolic shifts that underlie tomato fruit development and highlight regulatory aspects of metabolic network behavior. Plant Physiology **142**, 1380-1396.

Carrari, F., and Fernie, A.R. (2006). Metabolic regulation underlying tomato fruit development. Journal of Experimental Botany **57**, 1883-1897.

Carrera, E., Ruiz-Rivero, O., Peres, L.E.P., Atares, A., and Garcia-Martinez, J.L. (2012). Characterization of the *procera* tomato mutant shows novel functions of the SlDELLA protein in the control of flower morphology, cell division and expansion, and the auxin-signaling pathway during fruit-set and development. Plant Physiology **160**, 1581-1596.

Cary, A.J., Liu, W., and Howell, S.H. (1995). Cytokinin action is coupled to ethylene in its effects on the inhibition of root and hypocotyl elongation in *Arabidopsis thaliana* seedlings. Plant Physiology **107**, 1075-1082.

Causse, M., Friguet, C., Coiret, C., Lépicier, M., Navez, B., Lee, M., Holthuysen, N., Sinesio, F., Moneta, E., and Grandillo, S. (2010). Consumer preferences for fresh tomato at the European scale: a common segmentation on taste and firmness. Journal of Food Science **75**, 531-541.

Cazzonelli, C.I. (2011). Carotenoids in nature: insights from plants and beyond. Functional Plant Biology **38**, 833-847.

Cazzonelli, C.I., and Pogson, B.J. (2010). Source to sink: regulation of carotenoid biosynthesis in plants. Trends in Plant Science **15**, 266-274.

Centeno, D.C., Osorio, S., Nunes-Nesi, A., Bertolo, A.L.F., Carneiro, R.T., Araújo, W.L., Steinhauser, M.-C., Michalska, J., Rohrmann, J., Geigenberger, P., Oliver, S.N., Stitt, M., Carrari, F., Rose, J.K.C., and Fernie, A.R. (2011). Malate plays a crucial role in starch metabolism, ripening, and soluble solid content of tomato fruit and affects postharvest softening. The Plant Cell **23**, 162-184.

Chakrabarti, M., Zhang, N., Sauvage, C., Munos, S., Blanca, J., Canizares, J., Diez, M.J., Schneider, R., Mazourek, M., McClead, J., Causse, M., and van der Knaap, E. (2013). A cytochrome P450 regulates a domestication trait in cultivated tomato. Proceedings of the National Academy of Sciences USA **110**, 17125-17130.

Chapman, N.H., Bonnet, J., Grivet, L., Lynn, J., Graham, N., Smith, R., Sun, G., Walley, P.G., Poole, M., Causse, M., King, G.J., Baxter, C., and Seymour, G.B. (2012). High-resolution mapping of a fruit firmness-related quantitative trait locus in tomato reveals epistatic interactions associated with a complex combinatorial locus. Plant Physiology **159**, 1644-1657.

Charng, Y.-y., Liu, H.-c., Liu, N.-y., Chi, W.-t., Wang, C.-n., Chang, S.-h., and Wang, T.-t. (2007). A heat-inducible transcription factor, HsfA2, is required for extension of acquired thermotolerance in *Arabidopsis*. Plant Physiology **143**, 251-262.

Chattopadhyay, S., Ang, L.-H., Puente, P., Deng, X.-W., and Wei, N. (1998). *Arabidopsis* bZIP protein HY5 directly interacts with light-responsive promoters in mediating light control of gene expression. The Plant Cell **10**, 673-683.

Chayut, N., Yuan, H., Ohali, S., Meir, A., Sa'ar, U., Tzuri, G., Zheng, Y., Mazourek, M., Gepstein, S., Zhou, X., Portnoy, V., Lewinsohn, E., Schaffer, A.A., Katzir, N., Fei, Z., Welsch, R., Li, L., Burger, J., and Tadmor, Y. (2017). Distinct mechanisms of the ORANGE protein in controlling carotenoid flux. Plant Physiology **173**, 376-389.

Chen, G., Alexander, L., and Grierson, D. (2004a). Constitutive expression of EIL-like transcription factor partially restores ripening in the ethylene-insensitive *Nr* tomato mutant. Journal of Experimental Botany **55**, 1491-1497.

Chen, G., Hackett, R., Walker, D., Taylor, A., Lin, Z., and Grierson, D. (2004b). Identification of a specific isoform of tomato lipoxygenase (TomloxC) involved in the generation of fatty acid-derived flavor compounds. Plant Physiology **136**, 2641-2651.

Chen, L.-Q., Qu, X.-Q., Hou, B.-H., Sosso, D., Osorio, S., Fernie, A.R., and Frommer, W.B. (2012). Sucrose efflux mediated by SWEET proteins as a key step for phloem transport. Science **335**, 207-211.

Chen, S., Wang, X., Zhang, L., Lin, S., Liu, D., Wang, Q., Cai, S., El-Tanbouly, R., Gan, L., Wu, H., and Li, Y. (2016). Identification and characterization of tomato gibberellin 2-oxidases (GA2oxs) and effects of fruit-specific SlGA2ox1 overexpression on fruit and seed growth and development. Horticulture Research **3**, 16059.

Chen, Y., Li, F., and Wurtzel, E.T. (2010). Isolation and characterization of the Z-ISO gene encoding a missing component of carotenoid biosynthesis in plants. Plant Physiology **153**, 66-79.

Chetelat, R.T., DeVerna, J.W., and Bennett, A.B. (1995). Introgression into tomato (*Lycopersicon esculentum*) of the *L. chmielewskii* sucrose accumulator gene (sucr) controlling fruit sugar composition. Theoretical and Applied Genetics **91**, 327-333.

Chinnusamy, V., Gong, Z., and Zhu, J.K. (2008). Abscisic acid-mediated epigenetic processes in plant development and stress responses. Journal of Integrative Plant Biology **50**, 1187-1195.

Chung, M.-Y., Vrebalov, J., Alba, R., Lee, J., McQuinn, R., Chung, J.-D., Klein, P., and Giovannoni, J. (2010). A tomato (*Solanum lycopersicum*) APETALA2/ERF gene, SlAP2a, is a negative regulator of fruit ripening. Plant Journal **64**, 936-947.

Clevenger, J.P., Van Houten, J., Blackwood, M., Rodríguez, G.R., Jikumaru, Y., Kamiya, Y., Kusano, M., Saito, K., Visa, S., and van der Knaap, E. (2015). Network analyses reveal shifts in transcript profiles and metabolites that accompany the expression of SUN and an elongated tomato fruit. Plant Physiology **168**, 1164-1178.

Cliff, M., Lok, S., Lu, C., and Toivonen, P.M. (2009). Effect of 1-methylcyclopropene on the sensory, visual, and analytical quality of greenhouse tomatoes. Postharvest biology and technology **53**, 11-15.

Cluis, C.P., Mouchel, C.F., and Hardtke, C.S. (2004). The *Arabidopsis* transcription factor HY5 integrates light and hormone signaling pathways. Plant Journal **38**, 332-347.

Cocaliadis, M.F., Fernández-Muñoz, R., Pons, C., Orzaez, D., and Granell, A. (2014). Increasing tomato fruit quality by enhancing fruit chloroplast function. A double-edged sword? Journal of Experimental Botany **65**, 4589-4598.

Coenen, C., Christian, M., Luthen, H., and Lomax, T.L. (2003). Cytokinin inhibits a subset of diageotropica-dependent primary auxin responses in tomato. Plant Physiology **131**, 1692-1704.

Cohen, J.D. (1996). In vitro tomato fruit cultures demonstrate a role for indole-3-acetic acid in regulating fruit ripening. Journal of the American Society for Horticultural Science **121**, 520-524.

Colasanti, J., Yuan, Z., and Sundaresan, V. (1998). The indeterminate gene encodes a zinc finger protein and regulates a leaf-generated signal required for the transition to flowering in maize. Cell **93**, 593-603.

Cong, B., Barrero, L.S., and Tanksley, S.D. (2008). Regulatory change in YABBY-like transcription factor led to evolution of extreme fruit size during tomato domestication. Nature Genetics **40**, 800-804.

Cookson, P.J., Kiano, J.W., Shipton, C.A., Fraser, P.D., Romer, S., Schuch, W., Bramley, P.M., and Pyke, K.A. (2003). Increases in cell elongation, plastid

compartment size and phytoene synthase activity underlie the phenotype of the high pigment-1 mutant of tomato. Planta **217**, 896-903.

Cordoba, E., Porta, H., Arroyo, A., San Roman, C., Medina, L., Rodriguez-Concepcion, M., and Leon, P. (2011). Functional characterization of the three genes encoding 1-deoxy-D-xylulose 5-phosphate synthase in maize. Journal of Experimental Botany **62**, 2023-2038.

Cortleven, A., and Schmulling, T. (2015). Regulation of chloroplast development and function by cytokinin. Journal of Experimental Botany **66**, 4999-5013.

Cosgrove, D.J. (2000). Loosening of plant cell walls by expansins. Nature **407**, 321-326.

Cosgrove, D.J. (2005). Growth of the plant cell wall. Nature Reviews Molecular Cell Biology **6**, 850-861.

Cosgrove, D.J. (2014). Re-constructing our models of cellulose and primary cell wall assembly. Current Opinion in Plant Biology **22**, 122-131.

Crane, J.C. (1964). Growth substances in fruit setting and development. Annual Review of Plant Physiology **15**, 303-326.

Csukasi, F., Osorio, S., Gutierrez, J.R., Kitamura, J., Giavalisco, P., Nakajima, M., Fernie, A.R., Rathjen, J.P., Botella, M.A., Valpuesta, V., and Medina-Escobar, N. (2011). Gibberellin biosynthesis and signalling during development of the strawberry receptacle. New Phytologist **191**, 376-390.

Cui, D., Zhao, J., Jing, Y., Fan, M., Liu, J., Wang, Z., Xin, W., and Hu, Y. (2013). The *Arabidopsis* IDD14, IDD15, and IDD16 cooperatively regulate lateral organ morphogenesis and gravitropism by promoting auxin biosynthesis and transport. PLoS Genet **9**, 1-15.

Czerednik, A., Busscher, M., Bielen, B.A.M., Wolters-Arts, M., de Maagd, R.A., and Angenent, G.C. (2012). Regulation of tomato fruit pericarp development by an interplay between CDKB and CDKA1 cell cycle genes. Journal of Experimental Botany **63**, 2605-2617.

D'Andrea, L., Simon-Moya, M., Llorente, B., Llamas, E., Marro, M., Loza-Alvarez, P., Li, L., and Rodriguez-Concepcion, M. (2018). Interference with Clp protease impairs carotenoid accumulation during tomato fruit ripening. Journal of Experimental Botany **69**, 1557-1568.

Dal Cin, V., Tieman, D.M., Tohge, T., McQuinn, R., de Vos, R.C., Osorio, S., Schmelz, E.A., Taylor, M.G., Smits-Kroon, M.T., Schuurink, R.C., Haring, M.A., Giovannoni, J., Fernie, A.R., and Klee, H.J. (2011). Identification of genes in the phenylalanine metabolic pathway by ectopic expression of a MYB transcription factor in tomato fruit. Plant Cell **23**, 2738-2753.

Dalal, A., Rana, J.S., and Kumar, A. (2017). Ultrasensitive nanosensor for detection of malic acid in tomato as fruit ripening indicator. Food Analytical Methods **10**, 3680-3686.

Dare, A.P., Schaffer, R.J., Lin-Wang, K., Allan, A.C., and Hellens, R.P. (2008). Identification of a cis-regulatory element by transient analysis of co-ordinately regulated genes. Plant Methods **4**, 17-27.

Davey, J.E., and Van Staden, J. (1978). Endogenous cytokinins in the fruits of ripening and non-ripening tomatoes. Plant Science Letters **11**, 359-364.

Davis, J.M., and Gardner, R.G. (1994). Harvest maturity affects fruit yield, size, and grade of fresh-market tomato cultivars. HortScience **29**, 613-615.

Davuluri, G.R., van Tuinen, A., Fraser, P.D., Manfredonia, A., Newman, R., Burgess, D., Brummell, D.A., King, S.R., Palys, J., Uhlig, J., Bramley, P.M., Pennings, H.M., and Bowler, C. (2005). Fruit-specific RNAi-mediated suppression of DET1 enhances carotenoid and flavonoid content in tomatoes. Nature Biotechnology **23**, 890-895.

de Godoy, F., Bermudez, L., Lira, B.S., de Souza, A.P., Elbl, P., Demarco, D., Alseekh, S., Insani, M., Buckeridge, M., Almeida, J., Grigioni, G., Fernie, A.R., Carrari, F., and Rossi, M. (2013). Galacturonosyltransferase 4 silencing alters pectin

composition and carbon partitioning in tomato. Journal of Experimental Botany **64**, 2449-2466.

de Jong, M., Mariani, C., and Vriezen, W.H. (2009a). The role of auxin and gibberellin in tomato fruit set. Journal of Experimental Botany **60**, 1523-1532.

de Jong, M., Wolters-Arts, M., Feron, R., Mariani, C., and Vriezen, W.H. (2009b). The *Solanum lycopersicum* auxin response factor 7 (SlARF7) regulates auxin signaling during tomato fruit set and development. Plant Journal **57**, 160-170.

de Jong, M., Wolters-Arts, M., García-Martínez, J.L., Mariani, C., and Vriezen, W.H. (2011). The *Solanum lycopersicum* AUXIN RESPONSE FACTOR 7 (SlARF7) mediates cross-talk between auxin and gibberellin signalling during tomato fruit set and development. Journal of Experimental Botany **62**, 617-626.

DellaPenna, D., Alexander, D.C., and Bennett, A.B. (1986). Molecular cloning of tomato fruit polygalacturonase: Analysis of polygalacturonase mRNA levels during ripening. Proceedings of the National Academy of Sciences USA **83**, 6420-6424.

DellaPenna, D., Kates, D.S., and Bennett, A.B. (1987). Polygalacturonase Gene Expression in Rutgers, *rin*, *nor*, and *Nr* tomato fruits. Plant Physiology **85**, 502-507.

DellaPenna, D., Lincoln, J.E., Fischer, R.L., and Bennett, A.B. (1989). Transcriptional analysis of polygalacturonase and other ripening associated genes in Rutgers, *rin*, *nor*, and *Nr* tomato fruit. Plant Physiology **90**, 1372-1377.

Demmig-Adams, B., and Adams, W.W. (1996). Xanthophyll cycle and light stress in nature: uniform response to excess direct sunlight among higher plant species. Planta **198**, 460-470.

Deng, L., Li, L., Zhang, S., Shen, J., Li, S., Hu, S., Peng, Q., Xiao, J., and Wu, C. (2017). Suppressor of rid1 (SID1) shares common targets with RID1 on florigen genes to initiate floral transition in rice. PLoS Genet **13**, 1-24.

Desai, N., and W. Chism, G. (2006). Changes in cytokinin activity in the ripening tomato fruit. Journal of Food Science **43**, 1324-1326.

Devoghalaere, F., Doucen, T., Guitton, B., Keeling, J., Payne, W., Ling, T.J., Ross, J.J., Hallett, I.C., Gunaseelan, K., Dayatilake, G.A., Diak, R., Breen, K.C., Tustin, D.S., Costes, E., Chagne, D., Schaffer, R.J., and David, K.M. (2012). A genomics approach to understanding the role of auxin in apple (*Malus x domestica*) fruit size control. BMC Plant Biology **12**, 1-15.

Dong, T., Hu, Z., Deng, L., Wang, Y., Zhu, M., Zhang, J., and Chen, G. (2013). A tomato MADS-box transcription factor, SlMADS1, acts as a negative regulator of fruit ripening. Plant Physiology **163**, 1026-1036.

Dou, M., Cheng, S., Zhao, B., Xuan, Y., and Shao, M. (2016). The indeterminate domain protein ROC1 regulates chilling tolerance via activation of DREB1B/CBF1 in rice. International Journal of Molecular Sciences **17**, 233-247.

Eda, M., Matsumoto, T., Ishimaru, M., and Tada, T. (2016). Structural and functional analysis of tomato beta-galactosidase 4: insight into the substrate specificity of the fruit softening-related enzyme. Plant Journal **86**, 300-307.

Edan, Y., Pasternak, H., Shmulevich, I., Rachmani, D., Guedalia, D., Grinberg, S., and Fallik, E. (1997). Color and firmness classification of fresh market tomatoes. Journal of Food Science **62**, 793-796.

Egea, I., Barsan, C., Bian, W., Purgatto, E., Latché, A., Chervin, C., Bouzayen, M., and Pech, J.-C. (2010). Chromoplast differentiation: current status and perspectives. Plant and Cell Physiology **51**, 1601-1611.

Eggersdorfer, M., and Wyss, A. (2018). Carotenoids in human nutrition and health. Archives of Biochemistry and Biophysics **652**, 18-26.

Elitzur, T., Vrebalov, J., Giovannoni, J.J., Goldschmidt, E.E., and Friedman, H. (2010). The regulation of MADS-box gene expression during ripening of banana and their regulatory interaction with ethylene. Journal of Experimental Botany **61**, 1523-1535.

Enfissi, E.M., Barneche, F., Ahmed, I., Lichtle, C., Gerrish, C., McQuinn, R.P., Giovannoni, J.J., Lopez-Juez, E., Bowler, C., Bramley, P.M., and Fraser, P.D.

(2010). Integrative transcript and metabolite analysis of nutritionally enhanced DE-ETIOLATED1 downregulated tomato fruit. Plant Cell **22**, 1190-1215.

Enfissi, E.M.A., Fraser, P.D., Lois, L.-M., Boronat, A., Schuch, W., and Bramley, P.M. (2005). Metabolic engineering of the mevalonate and non-mevalonate isopentenyl diphosphate-forming pathways for the production of health-promoting isoprenoids in tomato. Plant Biotechnology Journal **3**, 17-27.

Englbrecht, C.C., Schoof, H., and Bohm, S. (2004). Conservation, diversification and expansion of C2H2 zinc finger proteins in the *Arabidopsis thaliana* genome. BMC Genomics **5**, 39-56.

Estevez, J.M., Cantero, A., Reindl, A., Reichler, S., and Leon, P. (2001). 1-Deoxy-D-xylulose-5-phosphate synthase, a limiting enzyme for plastidic isoprenoid biosynthesis in plants. Journal of Biological Chemistry **276**, 22901-22909.

Eveland, A.L., and Jackson, D.P. (2012). Sugars, signalling, and plant development. Journal of Experimental Botany **63**, 3367-3377.

Falk, J., and Munne-Bosch, S. (2010). Tocochromanol functions in plants: antioxidation and beyond. Journal of Experimental Botany **61**, 1549-1566.

Fantini, E., Falcone, G., Frusciante, S., Giliberto, L., and Giuliano, G. (2013). Dissection of Tomato Lycopene Biosynthesis through Virus-Induced Gene Silencing. Plant Physiology **163**, 986-998.

Fei, Z., Tang, X., Alba, R., and Giovannoni, J. (2006). Tomato Expression Database (TED): a suite of data presentation and analysis tools. Nucleic Acids Research **34**, D766-770.

Feurtado, J.A., Huang, D., Wicki-Stordeur, L., Hemstock, L.E., Potentier, M.S., Tsang, E.W., and Cutler, A.J. (2011). The *Arabidopsis* C2H2 zinc finger INDETERMINATE DOMAIN1/ENHYDROUS promotes the transition to germination by regulating light and hormonal signaling during seed maturation. Plant Cell **23**, 1772-1794.

Fleishon, S., Shani, E., Ori, N., and Weiss, D. (2011). Negative reciprocal interactions between gibberellin and cytokinin in tomato. New Phytologist **190**, 609-617.

Fletcher, R.A., and McCullagh, D. (1971). Cytokinin-induced chlorophyll formation in cucumber cotyledons. Planta **101**, 88-90.

Fos, M., Nuez, F., and Garcia-Martinez, J.L. (2000). The gene pat-2, which induces natural parthenocarpy, alters the gibberellin content in unpollinated tomato ovaries. Plant Physiology **122**, 471-480.

Frank, G., Pressman, E., Ophir, R., Althan, L., Shaked, R., Freedman, M., Shen, S., and Firon, N. (2009). Transcriptional profiling of maturing tomato (*Solanum lycopersicum L.*) microspores reveals the involvement of heat shock proteins, ROS scavengers, hormones, and sugars in the heat stress response. Journal of Experimental Botany **60**, 3891-3908.

Frary, A., Nesbitt, T.C., Grandillo, S., Knaap, E., Cong, B., Liu, J., Meller, J., Elber, R., Alpert, K.B., and Tanksley, S.D. (2000). fw2.2: a quantitative trait locus key to the evolution of tomato fruit size. Science **289**, 85-88.

Fraser, P.D., Bramley, P., and Seymour, G.B. (2001). Effect of the *Cnr* mutation on carotenoid formation during tomato fruit ripening. Phytochemistry **58**, 75-79.

Fraser, P.D., and Bramley, P.M. (2004). The biosynthesis and nutritional uses of carotenoids. Progress in Lipid Research **43**, 228-265.

Fraser, P.D., Enfissi, E.M., Halket, J.M., Truesdale, M.R., Yu, D., Gerrish, C., and Bramley, P.M. (2007). Manipulation of phytoene levels in tomato fruit: effects on isoprenoids, plastids, and intermediary metabolism. Plant Cell **19**, 3194-3211.

Fraser, P.D., Hedden, P., Cooke, D.T., Bird, C.R., Schuch, W., and Bramley, P.M. (1995). The effect of reduced activity of phytoene synthase on isoprenoid levels in tomato pericarp during fruit development and ripening. Planta **196**, 321-326.

Fraser, P.D., Kiano, J.W., Truesdale, M.R., Schuch, W., and Bramley, P.M. (1999). Phytoene synthase-2 enzyme activity in tomato does not contribute to carotenoid synthesis in ripening fruit. Plant Molecular Biology **40**, 687-698.

Fraser, P.D., Miura, Y., and Misawa, N. (1997). In vitro characterization of astaxanthin biosynthetic enzymes. Journal of Biological Chemistry **272**, 6128-6135.

Fraser, P.D., Romer, S., Shipton, C.A., Mills, P.B., Kiano, J.W., Misawa, N., Drake, R.G., Schuch, W., and Bramley, P.M. (2002). Evaluation of transgenic tomato plants expressing an additional phytoene synthase in a fruit-specific manner. Proceedings of the National Academy of Sciences USA **99**, 1092-1097.

Fraser, P.D., Schuch, W., and Bramley, P.M. (2000). Phytoene synthase from tomato (*Lycopersicon esculentum*) chloroplasts-partial purification and biochemical properties. Planta **211**, 361-369.

Fraser, P.D., Shimada, H., and Misawa, N. (1998). Enzymic confirmation of reactions involved in routes to astaxanthin formation, elucidated using a direct substrate in vitro assay. European Journal of Biochemistry **252**, 229-236.

Fraser, P.D., Truesdale, M.R., Bird, C.R., Schuch, W., and Bramley, P.M. (1994). Carotenoid biosynthesis during tomato fruit development (evidence for tissue-specific gene expression). Plant Physiology **105**, 405-413.

Fray, R.G., Wallace, A., Fraser, P.D., Valero, D., Hedden, P., Bramley, P.M., and Grierson, D. (1995). Constitutive expression of a fruit phytoene synthase gene in transgenic tomatoes causes dwarfism by redirecting metabolites from the gibberellin pathway. Plant Journal **8**, 693-701.

Fridman, E., Carrari, F., Liu, Y.-S., Fernie, A.R., and Zamir, D. (2004). Zooming in on a quantitative trait for tomato yield using interspecific introgressions. Science **305**, 1786-1789.

Fry, S.C. (1989). The structure and functions of xyloglucan. Journal of Experimental Botany **40**, 1-11.

Fry, S.C. (2004). Primary cell wall metabolism: tracking the careers of wall polymers in living plant cells. New Phytologist **161**, 641-675.

Fu, D.-Q., Zhu, B.-Z., Zhu, H.-L., Jiang, W.-B., and Luo, Y.-B. (2005). Virus-induced gene silencing in tomato fruit. Plant Journal **43**, 299-308.

Fujisawa, M., and Ito, Y. (2013). The regulatory mechanism of fruit ripening revealed by analyses of direct targets of the tomato MADS-box transcription factor RIPENING INHIBITOR. Plant Signaling & Behavior **8**, 1-3.

Fujisawa, M., Nakano, T., and Ito, Y. (2011). Identification of potential target genes for the tomato fruit-ripening regulator RIN by chromatin immunoprecipitation. BMC Plant Biology **11**, 26-40.

Fujisawa, M., Nakano, T., Shima, Y., and Ito, Y. (2013). A large-scale identification of direct targets of the tomato MADS box transcription factor RIPENING INHIBITOR reveals the regulation of fruit ripening. Plant Cell **25**, 371-386.

Fujisawa, M., Shima, Y., Higuchi, N., Nakano, T., Koyama, Y., Kasumi, T., and Ito, Y. (2012a). Direct targets of the tomato-ripening regulator RIN identified by transcriptome and chromatin immunoprecipitation analyses. Planta **235**, 1107-1122.

Fujisawa, M., Shima, Y., Higuchi, N., Nakano, T., Koyama, Y., Kasumi, T., and Ito, Y. (2012b). Direct targets of the tomato-ripening regulator RIN identified by transcriptome and chromatin immunoprecipitation analyses. Planta **235**, 1107-1122.

Fujisawa, M., Shima, Y., Nakagawa, H., Kitagawa, M., Kimbara, J., Nakano, T., Kasumi, T., and Ito, Y. (2014). Transcriptional regulation of fruit ripening by tomato FRUITFULL homologs and associated MADS box proteins. Plant Cell **26**, 89-101.

Fukazawa, J., Teramura, H., Murakoshi, S., Nasuno, K., Nishida, N., Ito, T., Yoshida, M., Kamiya, Y., Yamaguchi, S., and Takahashi, Y. (2014). DELLAs function as coactivators of GAI-ASSOCIATED FACTOR1 in regulation of gibberellin homeostasis and signaling in *Arabidopsis*. Plant Cell **26**, 2920-2938.

Gady, A.L., Vriezen, W.H., Van de Wal, M.H., Huang, P., Bovy, A.G., Visser, R.G., and Bachem, C.W. (2012). Induced point mutations in the phytoene synthase 1 gene cause differences in carotenoid content during tomato fruit ripening. Molecular Breeding **29**, 801-812.

Galcheva-Gargova, Z., Gangwani, L., Konstantinov, K.N., Mikrut, M., Theroux, S.J., Enoch, T., and Davis, R.J. (1998). The cytoplasmic zinc finger protein ZPR1 accumulates in the nucleolus of proliferating cells. Molecular Biology of the Cell **9**, 2963-2971.

Galpaz, N., Wang, Q., Menda, N., Zamir, D., and Hirschberg, J. (2008). Abscisic acid deficiency in the tomato mutant high-pigment 3 leading to increased plastid number and higher fruit lycopene content. Plant Journal **53**, 717-730.

Gamboa, G., Mingorría, S., Di Masso, M., and Giampietro, M. (2017). Local, mixed and global organic tomato supply chains: some learned lessons from a real-world case study. In, pp. 291-318.

Gan, Y., Kumimoto, R., Liu, C., Ratcliffe, O., Yu, H., and Broun, P. (2006). GLABROUS INFLORESCENCE STEMS modulates the regulation by gibberellins of epidermal differentiation and shoot maturation in *Arabidopsis*. Plant Cell **18**, 1383-1395.

Gan, Y., Liu, C., Yu, H., and Broun, P. (2007). Integration of cytokinin and gibberellin signalling by *Arabidopsis* transcription factors GIS, ZFP8 and GIS2 in the regulation of epidermal cell fate. Development **134**, 2073-2081.

Gangappa, S.N., and Botto, J.F. (2014). The BBX family of plant transcription factors. Trends in Plant Science **19**, 460-470.

Gangappa, Sreeramaiah N., and Botto, Javier F. (2016). The multifaceted roles of HY5 in plant growth and development. Molecular Plant **9**, 1353-1365.

Gangwani, L. (2006). Deficiency of the zinc finger protein ZPR1 causes defects in transcription and cell cycle progression. Journal of Biological Chemistry **281**, 40330-40340.

Garcia-Hurtado, N., Carrera, E., Ruiz-Rivero, O., Lopez-Gresa, M.P., Hedden, P., Gong, F., and Garcia-Martinez, J.L. (2012). The characterization of transgenic tomato overexpressing gibberellin 20-oxidase reveals induction of parthenocarpic fruit growth, higher yield, and alteration of the gibberellin biosynthetic pathway. Journal of Experimental Botany **63**, 5803-5813.

Ghanem, M.E., Albacete, A., Smigocki, A.C., Frebort, I., Pospisilova, H., Martinez-Andujar, C., Acosta, M., Sanchez-Bravo, J., Lutts, S., Dodd, I.C., and Perez-Alfocea, F. (2011). Root-synthesized cytokinins improve shoot growth and fruit yield in salinized tomato (*Solanum lycopersicum L.*) plants. Journal of Experimental Botany **62**, 125-140.

Ghosh, S., Meli, V.S., Kumar, A., Thakur, A., Chakraborty, N., Chakraborty, S., and Datta, A. (2011). The N-glycan processing enzymes alpha-mannosidase and beta-D-N-acetylhexosaminidase are involved in ripening-associated softening in the non-climacteric fruits of capsicum. Journal of Experimental Botany **62**, 571-582.

Gillaspy, G., Ben-David, H., and Gruissem, W. (1993). Fruits: a developmental perspective. Plant Cell **5**, 1439-1451.

Giménez, E., Pineda, B., Capel, J., Antón, M.T., Atarés, A., Pérez-Martín, F., García-Sogo, B., Angosto, T., Moreno, V., and Lozano, R. (2010). Functional analysis of the *arlequin* mutant corroborates the essential role of the ARLEQUIN/TAGL1 gene during reproductive development of tomato. PLoS One **5**, 1-16.

Giovannoni, J.J. (2004). Genetic regulation of fruit development and ripening. Plant Cell **16 Suppl**, S170-180.

Giovannoni, J.J. (2007). Fruit ripening mutants yield insights into ripening control. Current Opinion in Plant Biology **10**, 283-289.

Giuliano, G., Bartley, G.E., and Scolnik, P.A. (1993). Regulation of carotenoid biosynthesis during tomato development. Plant Cell **5**, 379-387.

Goff, S.A., and Klee, H.J. (2006). Plant volatile compounds: sensory cues for health and nutritional value? Science **311**, 815-819.

Goulao, L.F., and Oliveira, C.M. (2008). Cell wall modifications during fruit ripening: when a fruit is not the fruit. Trends in Food Science & Technology **19**, 4-25.

Gould, S.B., Waller, R.F., and McFadden, G.I. (2008). Plastid evolution. Annual Review of Plant Biology **59**, 491-517.

Grandillo, S., Ku, H.M., and Tanksley, S.D. (1999). Identifying the loci responsible for natural variation in fruit size and shape in tomato. Theoretical and Applied Genetics **99**, 978-987.

Grierson, D., and Tucker, G.A. (1983). Timing of ethylene and polygalacturonase synthesis in relation to the control of tomato fruit ripening. Planta **157**, 174-179.

Griffiths, A., Barry, C., Alpuche-Solis, A.G., and Grierson, D. (1999). Ethylene and developmental signals regulate expression of lipoxygenase genes during tomato fruit ripening. Journal of Experimental Botany **50**, 793-798.

Griffiths, J., Murase, K., Rieu, I., Zentella, R., Zhang, Z.L., Powers, S.J., Gong, F., Phillips, A.L., Hedden, P., Sun, T.P., and Thomas, S.G. (2006). Genetic characterization and functional analysis of the GID1 gibberellin receptors in *Arabidopsis*. Plant Cell **18**, 3399-3414.

Grilli Caiola, M., and Canini, A. (2004). Ultrastructure of chromoplasts and other plastids in *Crocus sativus L.* (Iridaceae). Plant Biosystems - An International Journal Dealing with all Aspects of Plant Biology **138**, 43-52.

Groot, S.P.C., Bruinsma, J., and Karssen, C.M. (1987). The role of endogenous gibberellin in seed and fruit development of tomato: Studies with a gibberellin-deficient mutant. Physiologia Plantarum **71**, 184-190.

Gross, K.C. (1983). Changes in free galactose, myo-inositol and other monosaccharides in normal and non-ripening mutant tomatoes. Phytochemistry **22**, 1137-1139.

Gross, K.C. (1984). Fractionation and partial characterization of cell walls from normal and non-ripening mutant tomato fruit. Physiologia Plantarum **62**, 25-32.

Gross, K.C., and Wallner, S.J. (1979). Degradation of cell wall polysaccharides during tomato fruit ripening. Plant Physiology **63**, 117-120.

Grune, T., Lietz, G., Palou, A., Ross, A.C., Stahl, W., Tang, G., Thurnham, D., Yin, S.-a., and Biesalski, H.K. (2010). β-Carotene is an important vitamin A source for humans. The Journal of Nutrition **140**, 2268S-2285S.

Guillon, F., Philippe, S., Bouchet, B., Devaux, M.F., Frasse, P., Jones, B., Bouzayen, M., and Lahaye, M. (2008). Down-regulation of an Auxin Response Factor in the tomato induces modification of fine pectin structure and tissue architecture. Journal of Experimental Botany **59**, 273-288.

Gülçin, İ. (2012). Antioxidant activity of food constituents: an overview. Archives of Toxicology **86**, 345-391.

Guo, H., and Ecker, J.R. (2003). Plant responses to ethylene gas are mediated by SCFEBF1/EBF2-dependent proteolysis of EIN3 transcription factor. Cell **115**, 667-677.

Gupta, S., Shi, X., Lindquist, I.E., Devitt, N., Mudge, J., and Rashotte, A.M. (2013). Transcriptome profiling of cytokinin and auxin regulation in tomato root. Journal of Experimental Botany **64**, 695-704.

Gupta, S.K., Rai, A.K., Kanwar, S.S., and Sharma, T.R. (2012). Comparative analysis of zinc finger proteins involved in plant disease resistance. PLoS One **7**, 1-15.

Hackett, R.M., Ho, C.W., Lin, Z., Foote, H.C., Fray, R.G., and Grierson, D. (2000). Antisense inhibition of the Nr gene restores normal ripening to the tomato *Never-ripe* mutant, consistent with the ethylene receptor-inhibition model. Plant Physiology **124**, 1079-1086.

Hamamura, Y., Nagahara, S., and Higashiyama, T. (2012). Double fertilization on the move. Current Opinion in Plant Biology **15**, 70-77.

Hamilton, A.J., and Baulcombe, D.C. (1999). A species of small antisense RNA in posttranscriptional gene silencing in plants. Science **286**, 950-952.

Han, Y.-c., Fu, C.-c., Kuang, J.-f., Chen, J.-y., and Lu, W.-j. (2016). Two banana fruit ripening-related C2H2 zinc finger proteins are transcriptional repressors of ethylene biosynthetic genes. Postharvest Biology and Technology **116**, 8-15.

Handelman, G.J., Nightingale, Z.D., Lichtenstein, A.H., Schaefer, E.J., and Blumberg, J.B. (1999). Lutein and zeaxanthin concentrations in plasma after dietary supplementation with egg yolk. The American Journal of Clinical Nutrition **70**, 247-251.

Harberd, N.P., Belfield, E., and Yasumura, Y. (2009). The angiosperm gibberellin-GID1-DELLA growth regulatory mechanism: how an "inhibitor of an inhibitor" enables flexible response to fluctuating environments. Plant Cell **21**, 1328-1339.

Harriman, R.W., Tieman, D.M., and Handa, A.K. (1991). Molecular cloning of tomato pectin methylesterase gene and its expression in Rutgers, *ripening inhibitor*, *nonripening*, and *never ripe* tomato fruits. Plant Physiology **97**, 80-87.

Harris, W.M., and Spurr, A.R. (1969). Chromoplasts of tomato fruits. II. the red tomato. American Journal of Botany **56**, 380-389.

Hay, A., Kaur, H., Phillips, A., Hedden, P., Hake, S., and Tsiantis, M. (2002). The gibberellin pathway mediates KNOTTED1-type homeobox function in plants with different body plans. Current Biology **12**, 1557-1565.

Heijde, M., and Ulm, R. (2012). UV-B photoreceptor-mediated signalling in plants. Trends in Plant Science **17**, 230-237.

Heil, M., Ibarra-Laclette, E., Adame-Álvarez, R.M., Martínez, O., Ramirez-Chávez, E., Molina-Torres, J., and Herrera-Estrella, L. (2012). How plants sense wounds: damaged-self recognition is based on plant-derived elicitors and induces octadecanoid signaling. PLoS One **7**, 1-9.

Hiwasa, K., Nakano, R., Hashimoto, A., Matsuzaki, M., Murayama, H., Inaba, A., and Kubo, Y. (2004). European, Chinese and Japanese pear fruits exhibit differential softening characteristics during ripening. Journal of Experimental Botany **55**, 2281-2290.

Ho, L.C. (1996). The mechanism of assimilate partitioning and carbohydrate compartmentation in fruit in relation to the quality and yield of tomato. Journal of Experimental Botany **47**, 1239-1243.

Hobson, G.E. (1964). Polygalacturonase in normal and abnormal tomato fruit. Biochemical Journal **92**, 324-332.

Holm, M., Ma, L., Qu, L.-J., and Deng, X.-W. (2002). Two interacting bZIP proteins are direct targets of COP1-mediated control of light-dependent gene expression in *Arabidopsis*. Genes and Development **16**, 1247-1259.

Hu, Z.L., Deng, L., Chen, X.Q., Wang, P.Q., and Chen, G.P. (2010). Co-suppression of the EIN2-homology gene LeEIN2 inhibits fruit ripening and reduces ethylene sensitivity in tomato. Russian Journal of Plant Physiology **57**, 554-559.

Huang, P., Yoshida, H., Yano, K., Kinoshita, S., Kawai, K., Koketsu, E., Hattori, M., Takehara, S., Huang, J., Hirano, K., Ordonio, R.L., Matsuoka, M., and Ueguchi-Tanaka, M. (2017). OsIDD2, a zinc finger and INDETERMINATE DOMAIN protein, regulates secondary cell wall formation. Journal of Integrative Plant Biology, 130-143.

Huang, W., Miao, M., Kud, J., Niu, X., Ouyang, B., Zhang, J., Ye, Z., Kuhl, J.C., Liu, Y., and Xiao, F. (2013). SlNAC1, a stress-related transcription factor, is fine-tuned on both the transcriptional and the post-translational level. New Phytologist **197**, 1214-1224.

Huerta, L., Forment, J., Gadea, J., Fagoaga, C., Pena, L., Perez-Amador, M.A., and Garcia-Martinez, J.L. (2008). Gene expression analysis in citrus reveals the role of gibberellins on photosynthesis and stress. Plant Cell and Environment **31**, 1620-1633.

Iglesias, D.J., Tadeo, F.R., Legaz, F., Primo-Millo, E., and Talon, M. (2001). In vivo sucrose stimulation of colour change in citrus fruit epicarps: Interactions between nutritional and hormonal signals. Physiologia Plantarum **112**, 244-250.

Ireland, H.S., Yao, J.L., Tomes, S., Sutherland, P.W., Nieuwenhuizen, N., Gunaseelan, K., Winz, R.A., David, K.M., and Schaffer, R.J. (2013). Apple SEPALLATA1/2-like genes control fruit flesh development and ripening. Plant Journal **73**, 1044-1056.

Irfan, M., Ghosh, S., Kumar, V., Chakraborty, N., Chakraborty, S., and Datta, A. (2014). Insights into transcriptional regulation of β-D-N-acetylhexosaminidase, an N-glycan-processing enzyme involved in ripening-associated fruit softening. Journal of Experimental Botany **65**, 5835-5848.

Irfan, M., Ghosh, S., Meli, V.S., Kumar, A., Kumar, V., Chakraborty, N., Chakraborty, S., and Datta, A. (2016). Fruit ripening regulation of α-mannosidase expression by the MADS box transcription factor RIPENING INHIBITOR and ethylene. Frontiers in Plant Science **7**, 10-22.

Isaacson, T., Ohad, I., Beyer, P., and Hirschberg, J. (2004). Analysis in vitro of the enzyme CRTISO establishes a poly-cis-carotenoid biosynthesis pathway in plants. Plant Physiology **136**, 4246-4255.

Isaacson, T., Ronen, G., Zamir, D., and Hirschberg, J. (2002). Cloning of *tangerine* from tomato reveals a carotenoid isomerase essential for the production of beta-carotene and xanthophylls in plants. Plant Cell **14**, 333-342.

Ischebeck, T., Zbierzak, A.M., Kanwischer, M., and Dormann, P. (2006). A salvage pathway for phytol metabolism in *Arabidopsis*. Journal of Biological Chemistry **281**, 2470-2477.

Itai, A., Ishihara, K., and Bewley, J.D. (2003). Characterization of expression, and cloning, of beta-D-xylosidase and alpha-L-arabinofuranosidase in developing and ripening tomato (*Lycopersicon esculentum Mill*.) fruit. Journal of Experimental Botany **54**, 2615-2622.

Itkin, M., Seybold, H., Breitel, D., Rogachev, I., Meir, S., and Aharoni, A. (2009). TOMATO AGAMOUS-LIKE 1 is a component of the fruit ripening regulatory network. Plant Journal **60**, 1081-1095.

Ito, Y. (2016). Regulation of tomato fruit ripening by MADS-box transcription factors. Japan Agricultural Research Quarterly: JARQ **50**, 33-38.

Ito, Y., Nishizawa-Yokoi, A., Endo, M., Mikami, M., Shima, Y., Nakamura, N., Kotake-Nara, E., Kawasaki, S., and Toki, S. (2017). Re-evaluation of the *rin* mutation and the role of RIN in the induction of tomato ripening. Nature Plants **3**, 866-874.

Ito, Y., Nishizawa-Yokoi, A., Endo, M., Mikami, M., and Toki, S. (2015). CRISPR/Cas9-mediated mutagenesis of the RIN locus that regulates tomato fruit ripening. Biochemical and Biophysical Research Communications **467**, 76-82.

Jafari, Z., Haddad, R., Hosseini, R., and Garoosi, G. (2013). Cloning, identification and expression analysis of ACC oxidase gene involved in ethylene production pathway. Molecular Biology Reports **40**, 1341-1350.

Jaganathan, D., Ramasamy, K., Sellamuthu, G., Jayabalan, S., and Venkataraman, G. (2018). CRISPR for crop improvement: an update review. Frontiers in Plant Science **9**, 1-17.

Jahns, P., and Holzwarth, A.R. (2012). The role of the xanthophyll cycle and of lutein in photoprotection of photosystem II. Biochim Biophys Acta **1817**, 182-193.

Jahns, P., Latowski, D., and Strzalka, K. (2009). Mechanism and regulation of the violaxanthin cycle: the role of antenna proteins and membrane lipids. Biochim Biophys Acta **1787**, 3-14.

Jia, H., Jiu, S., Zhang, C., Wang, C., Tariq, P., Liu, Z., Wang, B., Cui, L., and Fang, J. (2016). Abscisic acid and sucrose regulate tomato and strawberry fruit ripening through the abscisic acid-stress-ripening transcription factor. Plant Biotechnology Journal **14**, 2045-2065.

Jiao, Y., Lau, O.S., and Deng, X.W. (2007). Light-regulated transcriptional networks in higher plants. Nature Reviews Genetics **8**, 217-230.

Jimenez, A., Creissen, G., Kular, B., Firmin, J., Robinson, S., Verhoeyen, M., and Mullineaux, P. (2002). Changes in oxidative processes and components of the antioxidant system during tomato fruit ripening. Planta **214**, 751-758.

Johnson, E.A., and Lewis, M.J. (1979). Astaxanthin formation by the yeast *Phaffia rhodozyma*. Microbiology **115**, 173-183.

Johnson, E.J., McDonald, K., Caldarella, S.M., Chung, H.-y., Troen, A.M., and Snodderly, D.M. (2008). Cognitive findings of an exploratory trial of docosahexaenoic acid and lutein supplementation in older women. Nutritional Neuroscience **11**, 75-83.

Jones, B., Frasse, P., Olmos, E., Zegzouti, H., Li, Z.G., Latche, A., Pech, J.C., and Bouzayen, M. (2002). Down-regulation of DR12, an auxin-response-factor homolog, in the tomato results in a pleiotropic phenotype including dark green and blotchy ripening fruit. Plant Journal **32**, 603-613.

Jones, M.O., Piron-Prunier, F., Marcel, F., Piednoir-Barbeau, E., Alsadon, A.A., Wahb-Allah, M.A., Al-Doss, A.A., Bowler, C., Bramley, P.M., Fraser, P.D., and Bendahmane, A. (2012). Characterisation of alleles of tomato light signalling genes generated by TILLING. Phytochemistry **79**, 78-86.

Jost, M., Hensel, G., Kappel, C., Druka, A., Sicard, A., Hohmann, U., Beier, S., Himmelbach, A., Waugh, R., Kumlehn, J., Stein, N., and Lenhard, M. (2016). The INDETERMINATE DOMAIN protein BROAD LEAF1 limits barley leaf width by restricting lateral proliferation. Current Biology **26**, 903-909.

Karadas, F., Grammenidis, E., Surai, P.F., Acamovic, T., and Sparks, N.H.C. (2006). Effects of carotenoids from lucerne, marigold and tomato on egg yolk pigmentation and carotenoid composition. British Poultry Science **47**, 561-566.

Karayekov, E., Sellaro, R., Legris, M., Yanovsky, M.J., and Casal, J.J. (2013). Heat shock–induced fluctuations in clock and light signaling enhance phytochrome B–mediated *Arabidopsis* deetiolation. Plant Cell **25**, 2892-2906.

Karlova, R., Chapman, N., David, K., Angenent, G.C., Seymour, G.B., and de Maagd, R.A. (2014). Transcriptional control of fleshy fruit development and ripening. Journal of Experimental Botany **65**, 4527-4541.

Karlova, R., Rosin, F.M., Busscher-Lange, J., Parapunova, V., Do, P.T., Fernie, A.R., Fraser, P.D., Baxter, C., Angenent, G.C., and de Maagd, R.A. (2011). Transcriptome and metabolite profiling show that APETALA2a is a major regulator of tomato fruit ripening. Plant Cell **23**, 923-941.

Katz, Y.S., Galili, G., and Amir, R. (2006). Regulatory role of cystathionine-γ-synthase and de novo synthesis of methionine in ethylene production during tomato fruit ripening. Plant Molecular Biology **61**, 255-268.

Keller, M., Hu, Y., Mesihovic, A., Fragkostefanakis, S., Schleiff, E., and Simm, S. (2017). Alternative splicing in tomato pollen in response to heat stress. DNA Research **24**, 205-217.

Kevany, B.M., Tieman, D.M., Taylor, M.G., Cin, V.D., and Klee, H.J. (2007). Ethylene receptor degradation controls the timing of ripening in tomato fruit. Plant Journal **51**, 458-467.

Kiełbowicz-Matuk, A., Czarnecka, J., Banachowicz, E., Rey, P., and Rorat, T. (2017). Solanum tuberosum ZPR1 encodes a light-regulated nuclear DNA-binding protein adjusting the circadian expression of StBBX24 to light cycle. Plant, Cell & Environment **40**, 424-440.

Kilambi, H.V., Kumar, R., Sharma, R., and Sreelakshmi, Y. (2013). Chromoplast-specific carotenoid-associated protein appears to be important for enhanced accumulation of carotenoids in *hp1* tomato fruits. Plant Physiology **161**, 2085-2101.

Kim, J., and DellaPenna, D. (2006). Defining the primary route for lutein synthesis in plants: the role of *Arabidopsis* carotenoid beta-ring hydroxylase CYP97A3. Proceedings of the National Academy of Sciences USA **103**, 3474-3479.

Kim, J., Gross, K.C., and Solomos, T. (1991). Galactose metabolism and ethylene production during development and ripening of tomato fruit. Postharvest Biology and Technology **1**, 67-80.

Kim, J.E., Rensing, K.H., Douglas, C.J., and Cheng, K.M. (2010a). Chromoplasts ultrastructure and estimated carotene content in root secondary phloem of different carrot varieties. Planta **231**, 549-558.

Kim, O.Y., Yoe, H.Y., Kim, H.J., Park, J.Y., Kim, J.Y., Lee, S.-H., Lee, J.H., Lee, K.P., Jang, Y., and Lee, J.H. (2010b). Independent inverse relationship between serum lycopene concentration and arterial stiffness. Atherosclerosis **208**, 581-586.

King, C., Eisenberg, E., and Greene, L.E. (1999). Interaction between Hsc70 and DnaJ homologues: relationship between Hsc70 polymerization and ATPase activity. Biochemistry **38**, 12452-12459.

Klann, E.M., Hall, B., and Bennett, A.B. (1996). Antisense acid invertase (TIV1) gene alters soluble sugar composition and size in transgenic tomato fruit. Plant Physiology **112**, 1321-1330.

Klee, H.J. (2004). Ethylene signal transduction. Moving beyond *Arabidopsis*. Plant Physiology **135**, 660-667.

Klee, H.J., and Giovannoni, J.J. (2011). Genetics and control of tomato fruit ripening and quality attributes. Annual Review of Genetics **45**, 41-59.

Kobayashi, K., Fujii, S., Sasaki, D., Baba, S., Ohta, H., Masuda, T., and Wada, H. (2014). Transcriptional regulation of thylakoid galactolipid biosynthesis coordinated with chlorophyll biosynthesis during the development of chloroplasts in *Arabidopsis*. Frontiers in Plant Science **5**, 272-283.

Koch, J.L., and Nevins, D.J. (1989). Tomato fruit cell wall : I. use of purified tomato polygalacturonase and pectinmethylesterase to identify developmental changes in pectins. Plant Physiology **91**, 816-822.

Koch, K. (2004). Sucrose metabolism: regulatory mechanisms and pivotal roles in sugar sensing and plant development. Current Opinion in Plant Biology **7**, 235-246.

Koike, S., Matsukura, C., Takayama, M., Asamizu, E., and Ezura, H. (2013). Suppression of γ-aminobutyric acid (GABA) transaminases induces prominent GABA accumulation, dwarfism and infertility in the tomato (*Solanum lycopersicum L.*). Plant and Cell Physiology **54**, 793-807.

Kojima, K. (2005). Phytohormones in shoots and fruits of tomato; apoplast solution and seedless fruit. Japan Agricultural Research Quarterly: JARQ **39**, 77-81.

Kong, F., Deng, Y., Zhou, B., Wang, G., Wang, Y., and Meng, Q. (2014). A chloroplast-targeted DnaJ protein contributes to maintenance of photosystem II under chilling stress. Journal of Experimental Botany **65**, 143-158.

Kong, K.W., Khoo, H.E., Prasad, K.N., Ismail, A., Tan, C.P., and Rajab, N.F. (2010). Revealing the power of the natural red pigment lycopene. Molecules **15**, 959-987.

Kong, Y., Zhou, G., Yin, Y., Xu, Y., Pattathil, S., and Hahn, M.G. (2011). Molecular analysis of a family of *Arabidopsis* genes related to galacturonosyltransferases. Plant Physiology **155**, 1791-1805.

Koshioka, M., Nishijima, T., Yamazaki, H., Liu, Y., Nonaka, M., and Mander, L.N. (1994). Analysis of gibberellins in growing fruits of *Lycopersicon esculentum* after pollination or treatment with 4-chlorophenoxyacetic acid. Journal of Horticultural Science **69**, 171-179.

Kostecka-Gugała, A., Latowski, D., and Strzałka, K. (2003). Thermotropic phase behaviour of α-dipalmitoylphosphatidylcholine multibilayers is influenced to various extents by carotenoids containing different structural features- evidence from differential scanning calorimetry. Biochimica et Biophysica Acta (BBA) - Biomembranes **1609**, 193-202.

Kramer, M., Sanders, R., Bolkan, H., Waters, C., Sheeny, R.E., and Hiatt, W.R. (1992). Postharvest evaluation of transgenic tomatoes with reduced levels of polygalacturonase: processing, firmness and disease resistance. Postharvest Biology and Technology **1**, 241-255.

Krieger-Liszkay, A., and Trebst, A. (2006). Tocopherol is the scavenger of singlet oxygen produced by the triplet states of chlorophyll in the PSII reaction centre. Journal of Experimental Botany **57**, 1677-1684.

Kubo, M., and Kakimoto, T. (2000). The Cytokinin-hypersensitive genes of *Arabidopsis* negatively regulate the cytokinin-signaling pathway for cell division and chloroplast development. Plant Journal **23**, 385-394.

Kumar, R., Agarwal, P., Tyagi, A.K., and Sharma, A.K. (2012). Genome-wide investigation and expression analysis suggest diverse roles of auxin-responsive GH3 genes during development and response to different stimuli in tomato (*Solanum lycopersicum*). Molecular Genetics and Genomics **287**, 221-235.

Kumar, R., Khurana, A., and Sharma, A.K. (2014). Role of plant hormones and their interplay in development and ripening of fleshy fruits. Journal of Experimental Botany **65**, 4561-4575.

Kumar, R., Tamboli, V., Sharma, R., and Sreelakshmi, Y. (2017). NAC-NOR mutations in tomato Penjar accessions attenuate multiple metabolic processes and prolong the fruit shelf life. Food Chemistry **259**, 234-244.

Kumar, R., Tyagi, A.K., and Sharma, A.K. (2011). Genome-wide analysis of auxin response factor (ARF) gene family from tomato and analysis of their role in flower and fruit development. Molecular Genetics and Genomics **285**, 245-260.

Kwon, S.-J., Lee, G.-J., Roy, S., Cho, K.-Y., Moon, Y.-J., Cho, J.-W., Woo, S.-H., and Kim, H.-H. (2014). Effects of Ca-gluconate on fruit firmness and softening enzyme activities in tomato using hydroponics systems. Korean Society of Crop Science **59**, 539-546.

LaBorde, J.A., and Spurr, A.R. (1973). Chromoplast ultrastructure as affected by genes controlling grana retention and carotenoids in fruits of *Capsicum annuum*. American Journal of Botany **60**, 736-744.

Lanahan, M.B., Yen, H.C., Giovannoni, J.J., and Klee, H.J. (1994). The *never ripe* mutation blocks ethylene perception in tomato. Plant Cell **6**, 521-530.

Langley, K.R., Martin, A., Stenning, R., Murray, A.J., Hobson, G.E., Schuch, W.W., and Bird, C.R. (1994). Mechanical and optical assessment of the ripening of tomato fruit with reduced polygalacturonase activity. Journal of the Science of Food and Agriculture **66**, 547-554.

Lashbrook, C.C., Tieman, D.M., and Klee, H.J. (1998). Differential regulation of the tomato ETR gene family throughout plant development. Plant Journal **15**, 243-252.

Lau, O.S., and Deng, X.W. (2010). Plant hormone signaling lightens up: integrators of light and hormones. Current Opinion in Plant Biology **13**, 571-577.

Lau, O.S., and Deng, X.W. (2012). The photomorphogenic repressors COP1 and DET1: 20 years later. Trends in Plant Science **17**, 584-593.

Lee, J., Je-Gun Joung, J.G., McQuinn, R., Chung, M.-Y., Fei, Z., Tieman, D., Klee, H., and Giovannoni, J. (2011). Combined transcriptome genetic diversity and metabolite profiling in tomato fruit reveals that the ethylene response factor SIERF6 plays an important role in ripening and carotenoid accumulation. Plant Journal **70**, 191-204.

Lee, U., Rioflorido, I., Hong, S.W., Larkindale, J., Waters, E.R., and Vierling, E. (2007). The *Arabidopsis* ClpB/Hsp100 family of proteins: chaperones for stress and chloroplast development. Plant Journal **49**, 115-127.

Leng, P., Yuan, B., and Guo, Y. (2014). The role of abscisic acid in fruit ripening and responses to abiotic stress. Journal of Experimental Botany **65**, 4577-4588.

Leon-Garcia, E., Vela-Gutierrez, G., Del Angel-Coronel, O.A., Torres-Palacios, C., La Cruz-Medina, J., Gomez-Lim, M.A., and Garcia, H.S. (2017). Increased Postharvest Life of TomLox B Silenced Mutants of Tomato (*Solanum lycopersicum*) Var. TA234. Plant Foods for Human Nutrition **72**, 380-387.

Leseberg, C.H., Eissler, C.L., Wang, X., Johns, M.A., Duvall, M.R., and Mao, L. (2008). Interaction study of MADS-domain proteins in tomato. Journal of Experimental Botany **59**, 2253-2265.

Lewinsohn, E., Sitrit, Y., Bar, E., Azulay, Y., Meir, A., Zamir, D., and Tadmor, Y. (2005). Carotenoid pigmentation affects the volatile composition of tomato and watermelon fruits, as revealed by comparative genetic analyses. Journal of Agricultural and Food Chemistry **53**, 3142-3148.

Li, D., Mou, W., Wang, Y., Li, L., Mao, L., Ying, T., and Luo, Z. (2016a). Exogenous sucrose treatment accelerates postharvest tomato fruit ripening through the influence

on its metabolism and enhancing ethylene biosynthesis and signaling. Acta Physiologiae Plantarum **38**, 225-237.

Li, D., Saldeen, T., Romeo, F., and Mehta, J.L. (1999). Relative effects of alpha- and gamma-tocopherol on low-density lipoprotein oxidation and superoxide dismutase and nitric oxide synthase activity and protein expression in rats. Journal of Cardiovascular Pharmacology and Therapeutics **4**, 219-226.

Li, J., Sima, W., Ouyang, B., Luo, Z., Yang, C., Ye, Z., and Li, H. (2013). Identification and expression pattern of a ZPR1 gene in wild tomato (*Solanum Pennellii*). Plant Molecular Biology Reporter **31**, 409-417.

Li, J., Tao, X., Li, L., Mao, L., Luo, Z., Khan, Z.U., and Ying, T. (2016b). Comprehensive RNA-Seq analysis on the regulation of tomato ripening by exogenous auxin. PLoS One **11**, 1-22.

Li, L., Paolillo, D.J., Parthasarathy, M.V., DiMuzio, E.M., and Garvin, D.F. (2001). A novel gene mutation that confers abnormal patterns of β-carotene accumulation in cauliflower (*Brassica oleracea var. botrytis*). Plant Journal **26**, 59-67.

Li, L., and Van Eck, J. (2007). Metabolic engineering of carotenoid accumulation by creating a metabolic sink. Transgenic Research **16**, 581-585.

Li, S., Xu, H., Ju, Z., Cao, D., Zhu, H., Fu, D., Grierson, D., Qin, G., Luo, Y., and Zhu, B. (2017a). The RIN-MC fusion of MADS-box transcription factors has transcriptional activity. Plant Physiology **176**, 891–909.

Li, X.-d., Wang, X.-l., Cai, Y.-M., Wu, J.-h., Mo, B.-t., and Yu, E.-r. (2017b). *Arabidopsis* heat stress transcription factors A2 (HSFA2) and A3 (HSFA3) function in the same heat regulation pathway. Acta Physiologiae Plantarum **39**, 67-76.

Li, X., Wang, Y., Chen, S., Tian, H., Fu, D., Zhu, B., Luo, Y., and Zhu, H. (2018). Lycopene is enriched in tomato fruit by CRISPR/Cas9-mediated multiplex genome editing. Frontiers in Plant Science **9**, 559-571.

Li, Y., Hagen, G., and Guilfoyle, T.J. (1992). Altered morphology in transgenic tobacco plants that overproduce cytokinins in specific tissues and organs. Developmental Biology **153**, 386-395.

Li, Z., Wakao, S., Fischer, B.B., and Niyogi, K.K. (2009). Sensing and responding to excess light. Annual Review of Plant Biology **60**, 239-260.

Lieberman, M., Alice, K., Mapson, L.W., and Wardale, D.A. (1966). Stimulation of ethylene production in apple tissue slices by methionine. Plant Physiology **41**, 376-382.

Lim, C.W., Baek, W., Jung, J., Kim, J.-H., and Lee, S.C. (2015). Function of ABA in stomatal defense against biotic and drought stresses. International Journal of Molecular Sciences **16**, 15251-15270.

Lim, S., Lee, J.G., and Lee, E.J. (2017). Comparison of fruit quality and GC–MS-based metabolite profiling of kiwifruit 'Jecy green': Natural and exogenous ethylene-induced ripening. Food Chemistry **234**, 81-92.

Lin, D., Xiang, Y., Xian, Z., and Li, Z. (2016). Ectopic expression of SlAGO7 alters leaf pattern and inflorescence architecture and increases fruit yield in tomato. Physiologia Plantarum **157**, 490-506.

Lin, Z., Arciga-Reyes, L., Zhong, S., Alexander, L., Hackett, R., Wilson, I., and Grierson, D. (2008a). SlTPR1, a tomato tetratricopeptide repeat protein, interacts with the ethylene receptors NR and LeETR1, modulating ethylene and auxin responses and development. Journal of Experimental Botany **59**, 4271-4287.

Lin, Z., Hong, Y., Yin, M., Li, C., Zhang, K., and Grierson, D. (2008b). A tomato HD-Zip homeobox protein, LeHB-1, plays an important role in floral organogenesis and ripening. Plant Journal **55**, 301-310.

Liu, D.D., Zhou, L.J., Fang, M.J., Dong, Q.L., An, X.H., You, C.X., and Hao, Y.J. (2016a). Polycomb-group protein SlMSI1 represses the expression of fruit-ripening genes to prolong shelf life in tomato. Scientific Reports **6**, 1-9.

Liu, K., Kang, B.-C., Jiang, H., Moore, S.L., Li, H., Watkins, C.B., Setter, T.L., and Jahn, M.M. (2005). A GH3-like gene, CcGH3, isolated from *Capsicum chinense L.* fruit is regulated by auxin and ethylene*. Plant Molecular Biology **58**, 447-464.

Liu, L., Shao, Z., Zhang, M., and Wang, Q. (2015a). Regulation of carotenoid metabolism in tomato. Molecular Plant **8**, 28-39.

Liu, M., Chen, Y., Chen, Y., Shin, J.-H., Mila, I., Audran, C., Zouine, M., Pirrello, J., and Bouzayen, M. (2018a). The tomato ethylene response factor Sl-ERF.B3 integrates ethylene and auxin signaling via direct regulation of Sl-Aux/IAA27. New Phytologist **219**, 631-640.

Liu, M., Gomes, B.L., Mila, I., Purgatto, E., Peres, L.E.P., Frasse, P., Maza, E., Zouine, M., Roustan, J.-P., Bouzayen, M., and Pirrello, J. (2016b). Comprehensive profiling of ethylene response factor expression identifies ripening-associated ERF genes and their link to key regulators of fruit ripening in tomato. Plant Physiology **170**, 1732-1744.

Liu, M., Pirrello, J., Chervin, C., Roustan, J.P., and Bouzayen, M. (2015b). Ethylene control of fruit ripening: revisiting the complex network of transcriptional regulation. Plant Physiology **169**, 2380-2390.

Liu, R., How-Kit, A., Stammitti, L., Teyssier, E., Rolin, D., Mortain-Bertrand, A., Halle, S., Liu, M., Kong, J., Wu, C., Degraeve-Guibault, C., Chapman, N.H., Maucourt, M., Hodgman, T.C., Tost, J., Bouzayen, M., Hong, Y., Seymour, G.B., Giovannoni, J.J., and Gallusci, P. (2015c). A DEMETER-like DNA demethylase governs tomato fruit ripening. Proceedings of the National Academy of Sciences USA **112**, 10804-10809.

Liu, S., Zhang, Y., Feng, Q., Qin, L., Pan, C., Lamin-Samu, A.T., and Lu, G. (2018b). Tomato AUXIN RESPONSE FACTOR 5 regulates fruit set and development via the mediation of auxin and gibberellin signaling. Scientific Reports **8**, 1-16.

Liu, Y.-H., Offler, C.E., and Ruan, Y.-L. (2013). Regulation of fruit and seed response to heat and drought by sugars as nutrients and signals. Frontiers in Plant Science **4**, 282-294.

Liu, Y., Roof, S., Ye, Z., Barry, C., van Tuinen, A., Vrebalov, J., Bowler, C., and Giovannoni, J. (2004). Manipulation of light signal transduction as a means of modifying fruit nutritional quality in tomato. Proceedings of the National Academy of Sciences USA **101**, 9897-9902.

Llamas, E., Pulido, P., and Rodriguez-Concepcion, M. (2017). Interference with plastome gene expression and Clp protease activity in *Arabidopsis* triggers a chloroplast unfolded protein response to restore protein homeostasis. PLoS Genetics **13**, 1-27.

Llorente, B., D'Andrea, L., Ruiz-Sola, M.Á., Botterweg, E., Pulido, P., Andilla, J., Loza-Alvarez, P., and Rodríguez-Concepción, M. (2015). Tomato fruit carotenoid biosynthesis is adjusted to actual ripening progression by a light-dependent mechanism. Plant Journal **85**, 107-119.

Lois, L.M., Rodríguez-Concepción, M., Gallego, F., Campos, N., and Boronat, A. (2000). Carotenoid biosynthesis during tomato fruit development: regulatory role of 1-deoxy-D-xylulose 5-phosphate synthase. Plant Journal **22**, 503-513.

Loix, C., Huybrechts, M., Vangronsveld, J., Gielen, M., Keunen, E., and Cuypers, A. (2017). Reciprocal interactions between cadmium-induced cell wall responses and oxidative stress in plants. Frontiers in Plant Science **8**, 1-19.

Lopez, A.B., Van Eck, J., Conlin, B.J., Paolillo, D.J., O'Neill, J., and Li, L. (2008). Effect of the cauliflower Or transgene on carotenoid accumulation and chromoplast formation in transgenic potato tubers. Journal of Experimental Botany **59**, 213-223.

López Camelo, A.F., and Gómez, P.A. (2004). Comparison of color indexes for tomato ripening. Horticultura Brasileira **22**, 534-537.

Loyola, J., Verdugo, I., Gonzalez, E., Casaretto, J.A., and Ruiz-Lara, S. (2012). Plastidic isoprenoid biosynthesis in tomato: physiological and molecular analysis in genotypes resistant and sensitive to drought stress. Plant Biology **14**, 149-156.

Lu, C., Zainal, Z., Tucker, G.A., and Lycett, G.W. (2001). Developmental abnormalities and reduced fruit softening in tomato plants expressing an antisense Rab11 GTPase gene. Plant Cell **13**, 1819-1833.

Lu, S., Van Eck, J., Zhou, X., Lopez, A.B., O'Halloran, D.M., Cosman, K.M., Conlin, B.J., Paolillo, D.J., Garvin, D.F., Vrebalov, J., Kochian, L.V., Küpper, H., Earle, E.D., Cao, J., and Li, L. (2006). The cauliflower Or gene encodes a DnaJ cysteine-rich domain-containing protein that mediates high levels of β-carotene accumulation. Plant Cell **18**, 3594-3605.

Lunn, D., Phan, T.D., Tucker, G.A., and Lycett, G.W. (2013). Cell wall composition of tomato fruit changes during development and inhibition of vesicle trafficking is associated with reduced pectin levels and reduced softening. Plant Physiology and Biochemistry **66**, 91-97.

Lytovchenko, A., Eickmeier, I., Pons, C., Osorio, S., Szecowka, M., Lehmberg, K., Arrivault, S., Tohge, T., Pineda, B., Anton, M.T., Hedtke, B., Lu, Y., Fisahn, J., Bock, R., Stitt, M., Grimm, B., Granell, A., and Fernie, A.R. (2011). Tomato fruit photosynthesis is seemingly unimportant in primary metabolism and ripening but plays a considerable role in seed development. Plant Physiology **157**, 1650-1663.

Ma, N.-N., Zuo, Y.-Q., Liang, X.-Q., Yin, B., Wang, G.-D., and Meng, Q.-W. (2013). The multiple stress-responsive transcription factor SlNAC1 improves the chilling tolerance of tomato. Physiologia Plantarum **149**, 474-486.

Ma, N., Feng, H., Meng, X., Li, D., Yang, D., Wu, C., and Meng, Q. (2014). Overexpression of tomato SlNAC1 transcription factor alters fruit pigmentation and softening. BMC Plant Biology **14**, 351-365.

Malzahn, A., Lowder, L., and Qi, Y. (2017). Plant genome editing with TALEN and CRISPR. Cell & Bioscience **7**, 21-39.

Mangialasche, F., Kivipelto, M., Mecocci, P., Rizzuto, D., Palmer, K., Winblad, B., and Fratiglioni, L. (2010). High plasma levels of vitamin E forms and reduced Alzheimer's disease risk in advanced age. Journal of Alzheimer's Disease **20**, 1029-1037.

Manning, K. (1994). Changes in gene expression during strawberry fruit ripening and their regulation by auxin. Planta **194**, 62-68.

Manning, K., Tor, M., Poole, M., Hong, Y., Thompson, A.J., King, G.J., Giovannoni, J.J., and Seymour, G.B. (2006). A naturally occurring epigenetic mutation in a gene encoding an SBP-box transcription factor inhibits tomato fruit ripening. Nature Genetics **38**, 948-952.

Mariotti, L., Picciarelli, P., Lombardi, L., and Ceccarelli, N. (2011). Fruit-set and early fruit growth in tomato are associated with increases in indoleacetic acid, cytokinin, and bioactive gibberellin contents. Journal of Plant Growth Regulation **30**, 405–415.

Mariutto, M., Duby, F., Adam, A., Bureau, C., Fauconnier, M.L., Ongena, M., Thonart, P., and Dommes, J. (2011). The elicitation of a systemic resistance by *Pseudomonas putida* BTP1 in tomato involves the stimulation of two lipoxygenase isoforms. BMC Plant Biology **11**, 29-44.

Marraffini, L.A., and Sontheimer, E.J. (2008). CRISPR interference limits horizontal gene transfer in staphylococci by targeting DNA. Science **322**, 1843-1845.

Marsch-Martinez, N., Ramos-Cruz, D., Irepan Reyes-Olalde, J., Lozano-Sotomayor, P., Zuniga-Mayo, V.M., and de Folter, S. (2012). The role of cytokinin during *Arabidopsis* gynoecia and fruit morphogenesis and patterning. Plant Journal **72**, 222-234.

Martel, C., Vrebalov, J., Tafelmeyer, P., and Giovannoni, J.J. (2011). The tomato MADS-box transcription factor RIPENING INHIBITOR interacts with promoters involved in numerous ripening processes in a COLORLESS NONRIPENING-dependent manner. Plant Physiology **157**, 1568-1579.

Marti, C., Orzaez, D., Ellul, P., Moreno, V., Carbonell, J., and Granell, A. (2007). Silencing of DELLA induces facultative parthenocarpy in tomato fruits. Plant Journal **52**, 865-876.

Martin-Rodriguez, J.A., Huertas, R., Ho-Plagaro, T., Ocampo, J.A., Tureckova, V., Tarkowska, D., Ludwig-Muller, J., and Garcia-Garrido, J.M. (2016). Gibberellin-abscisic acid balances during arbuscular mycorrhiza formation in tomato. Frontiers in Plant Science **7**, 1273-1287.

Martineau, B., R. Summerfelt, K., F. Adams, D., and W. DeVerna, J. (1995). Production of high solids tomatoes through molecular modification of Levels of the plant growth regulator cytokinin. Nature Biotechnology **13**, 250-254.

Martínez-Bello, L., Moritz, T., and López-Díaz, I. (2015). Silencing C(19)-GA 2-oxidases induces parthenocarpic development and inhibits lateral branching in tomato plants. Journal of Experimental Botany **66**, 5897-5910.

Masamoto, K., Misawa, N., Kaneko, T., Kikuno, R., and Toh, H. (1998). Beta-carotene hydroxylase gene from the cyanobacterium *Synechocystis* sp. PCC6803. Plant and Cell Physiology **39**, 560-564.

Mata-Gómez, L.C., Montañez, J.C., Méndez-Zavala, A., and Aguilar, C.N. (2014). Biotechnological production of carotenoids by yeasts: an overview. Microbial Cell Factories **13**, 12-12.

Matsuo, S., Kikuchi, K., Fukuda, M., Honda, I., and Imanishi, S. (2012). Roles and regulation of cytokinins in tomato fruit development. Journal of Experimental Botany **63**, 5569-5579.

Maxwell, B.B., Andersson, C.R., Poole, D.S., Kay, S.A., and Chory, J. (2003). HY5, Circadian Clock-Associated 1, and a cis-element, DET1 dark response element, mediate DET1 regulation of chlorophyll a/b-binding protein 2 expression. Plant Physiology **133**, 1565-1577.

McAtee, P., Karim, S., Schaffer, R., and David, K. (2013). A dynamic interplay between phytohormones is required for fruit development, maturation, and ripening. Frontiers in Plant Science **4**, 79-86.

McCartney, L., Ormerod, A.P., Gidley, M.J., and Knox, J.P. (2000). Temporal and spatial regulation of pectic (1→4)-β-D-galactan in cell walls of developing pea cotyledons: implications for mechanical properties. Plant Journal **22**, 105-113.

McGraw, K.J., Crino, O.L., Medina-Jerez, W., and Nolan, P.M. (2006). Effect of dietary carotenoid supplementation on food intake and immune function in a songbird with no carotenoid coloration. Ethology **112**, 1209-1216.

McGraw, K.J., and Klasing, K.C. (2006). Carotenoids, immunity, and integumentary coloration in Red Junglefowl (*Gallus gallus*) The Auk **123**, 1161-1171.

McQueen-Mason, S.J., and Cosgrove, D.J. (1995). Expansin mode of action on cell walls. Analysis of wall hydrolysis, stress relaxation, and binding. Plant Physiology **107**, 87-100.

Meli, V.S., Ghosh, S., Prabha, T.N., Chakraborty, N., Chakraborty, S., and Datta, A. (2010). Enhancement of fruit shelf life by suppressing N-glycan processing enzymes. Proceedings of the National Academy of Sciences USA **107**, 2413-2418.

Meng, C., Yang, D., Ma, X., Zhao, W., Liang, X., Ma, N., and Meng, Q. (2016). Suppression of tomato SlNAC1 transcription factor delays fruit ripening. Plant Physiology **193**, 88-96.

Mezzomo, N., and Ferreira, S.R.S. (2016). Carotenoids functionality, sources, and processing by supercritical technology: a review. Journal of Chemistry **2016**, 1-16.

Miao, M., Niu, X., Kud, J., Du, X., Avila, J., Devarenne, T.P., Kuhl, J.C., Liu, Y., and Xiao, F. (2016). The ubiquitin ligase SEVEN IN ABSENTIA (SINA) ubiquitinates a defense-related NAC transcription factor and is involved in defense signaling. New Phytologist **211**, 138-148.

Micheli, F. (2001). Pectin methylesterases: cell wall enzymes with important roles in plant physiology. Trends in Plant Science **6**, 414-419.

Miedes, E., Herbers, K., Sonnewald, U., and Lorences, E.P. (2010). Overexpression of a cell wall enzyme reduces xyloglucan depolymerization and softening of transgenic tomato fruits. Journal of Agricultural and Food Chemistry **58**, 5708-5713.

Miedes, E., and Lorences, E.P. (2009). Xyloglucan endotransglucosylase/hydrolases (XTHs) during tomato fruit growth and ripening. Plant Physiology **166**, 489-498.

Mínguez-Alarcón, L., Mendiola, J., López-Espín, J.J., Sarabia-Cos, L., Vivero-Salmerón, G., Vioque, J., Navarrete-Muñoz, E.M., and Torres-Cantero, A.M. (2012). Dietary intake of antioxidant nutrients is associated with semen quality in young university students. Human Reproduction **27**, 2807-2814.

Minoia, S., Boualem, A., Marcel, F., Troadec, C., Quemener, B., Cellini, F., Petrozza, A., Vigouroux, J., Lahaye, M., Carriero, F., and Bendahmane, A. (2016). Induced mutations in tomato SlExp1 alter cell wall metabolism and delay fruit softening. Plant Science **242**, 195-202.

Minoia, S., Petrozza, A., D'Onofrio, O., Piron, F., Mosca, G., Sozio, G., Cellini, F., Bendahmane, A., and Carriero, F. (2010). A new mutant genetic resource for tomato crop improvement by TILLING technology. BMC Research Notes **3**, 69-77.

Misawa, N. (2009). Pathway engineering of plants toward astaxanthin production. Plant Biotechnology **26**, 93-99.

Misawa, N., Kajiwara, S., Kondo, K., Yokoyama, A., Satomi, Y., Saito, T., Miki, W., and Ohtani, T. (1995a). Canthaxanthin biosynthesis by the conversion of methylene to keto groups in a hydrocarbon beta-carotene by a single gene. Biochem Biophys Res Commun **209**, 867-876.

Misawa, N., Nakagawa, M., Kobayashi, K., Yamano, S., Izawa, Y., Nakamura, K., and Harashima, K. (1990). Elucidation of the *Erwinia uredovora* carotenoid biosynthetic pathway by functional analysis of gene products expressed in *Escherichia coli*. Journal of Bacteriology **172**, 6704-6712.

Misawa, N., Satomi, Y., Kondo, K., Yokoyama, A., Kajiwara, S., Saito, T., Ohtani, T., and Miki, W. (1995b). Structure and functional analysis of a marine bacterial carotenoid biosynthesis gene cluster and astaxanthin biosynthetic pathway proposed at the gene level. Journal of Bacteriology **177**, 6575-6584.

Misawa, N., and Shimada, H. (1998). Metabolic engineering for the production of carotenoids in non-carotenogenic bacteria and yeasts. Journal of Biotechnology **59**, 169-181.

Moctezuma, E., Smith, D.L., and Gross, K.C. (2003). Antisense suppression of a β-galactosidase gene (TB G6) in tomato increases fruit cracking. Journal of Experimental Botany **54**, 2025-2033.

Moneruzzaman, K., Hossain, A., Sani, W., Saifuddin, M., and Alenazi, M. (2009). Effect of harvesting and storage conditions on the post harvest quality of tomato (*Lycopersicon esculentum Mill*) cv. Roma VF. Australian Journal of Crop Science **3**, 113-121.

Monti, L. (1979). The breeding of tomatoes for peeling. Paper presented at: Symposium on Production of Tomatoes for Processing 100.

Moran, N.A., and Jarvik, T. (2010). Lateral transfer of genes from fungi underlies carotenoid production in aphids. Science **328**, 624-627.

Mou, W., Li, D., Bu, J., Jiang, Y., Khan, Z.U., Luo, Z., Mao, L., and Ying, T. (2016). Comprehensive analysis of ABA effects on ethylene biosynthesis and signaling during tomato fruit ripening. PLoS One **11**, 1-30.

Mounet, F., Lemaire-Chamley, M., Maucourt, M., Cabasson, C., Giraudel, J.-L., Deborde, C., Lessire, R., Gallusci, P., Bertrand, A., Gaudillère, M., Rothan, C., Rolin, D., and Moing, A. (2007). Quantitative metabolic profiles of tomato flesh and seeds during fruit development: complementary analysis with ANN and PCA. Metabolomics **3**, 273-288.

Mozos, I., Stoian, D., Caraba, A., Malainer, C., Horbanczuk, J.O., and Atanasov, A.G. (2018). Lycopene and vascular health. Frontiers in Pharmacology **9**, 1-16.

Mueller, L.A., Solow, T.H., Taylor, N., Skwarecki, B., Buels, R., Binns, J., Lin, C., Wright, M.H., Ahrens, R., Wang, Y., Herbst, E.V., Keyder, E.R., Menda, N., Zamir, D., and Tanksley, S.D. (2005). The SOL Genomics Network: a comparative resource for Solanaceae biology and beyond. Plant Physiology **138**, 1310-1317.

Munné-Bosch, S., and Alegre, L. (2002). The function of tocopherols and tocotrienols in plants. Critical Reviews in Plant Sciences **21**, 31-57.

Murray, J.A., Jones, A., Godin, C., and Traas, J. (2012). Systems analysis of shoot apical meristem growth and development: integrating hormonal and mechanical signaling. Plant Cell **24**, 3907-3919.

Mustilli, A.C., Fenzi, F., Ciliento, R., Alfano, F., and Bowler, C. (1999). Phenotype of the tomato high pigment-2 mutant is caused by a mutation in the tomato homolog of DEETIOLATED1. Plant Cell **11**, 145-157.

Mwaniki, M.W., Mathooko, F.M., Matsuzaki, M., Hiwasa, K., Tateishi, A., Ushijima, K., Nakano, R., Inaba, A., and Kubo, Y. (2005). Expression characteristics of seven members of the β-galactosidase gene family in 'La France' pear (*Pyrus communis* L.) fruit during growth and their regulation by 1-methylcyclopropene during postharvest ripening. Postharvest Biology and Technology **36**, 253-263.

Nakajima, M., Shimada, A., Takashi, Y., Kim, Y.C., Park, S.H., Ueguchi-Tanaka, M., Suzuki, H., Katoh, E., Iuchi, S., Kobayashi, M., Maeda, T., Matsuoka, M., and Yamaguchi, I. (2006). Identification and characterization of *Arabidopsis* gibberellin receptors. Plant Journal **46**, 880-889.

Nakamura, A., Maeda, H., Mizuno, M., Koshi, Y., and Nagamatsu, Y. (2003). β-Galactosidase and its significance in ripening of "*Saijyo*" *Japanese Persimmon* fruit. Bioscience, Biotechnology, and Biochemistry **67**, 68-76.

Nakamura, K., Inoue, M., Yoshiie, T., Hosoi, K., and Kimura, Y. (2008). Changes in structural features of free N-glycan and endoglycosidase activity during tomato fruit ripening. Bioscience, Biotechnology, and Biochemistry **72**, 2936-2945.

Nakatsuka, A., Murachi, S., Okunishi, H., Shiomi, S., Nakano, R., Kubo, Y., and Inaba, A. (1998). Differential expression and internal feedback regulation of 1-aminocyclopropane-1-carboxylate synthase, 1-aminocyclopropane-1-carboxylate oxidase, and ethylene receptor genes in tomato fruit during development and ripening. Plant Physiology **118**, 1295-1305.

Nakaune, M., Hanada, A., Yin, Y.-G., Matsukura, C., Yamaguchi, S., and Ezura, H. (2012). Molecular and physiological dissection of enhanced seed germination using short-term low-concentration salt seed priming in tomato. Plant Physiology and Biochemistry **52**, 28-37.

Nekrasov, V., Wang, C., Win, J., Lanz, C., Weigel, D., and Kamoun, S. (2017). Rapid generation of a transgene-free powdery mildew resistant tomato by genome deletion. Scientific Reports **7**, 1-6.

Neta-Sharir, I., Isaacson, T., Lurie, S., and Weiss, D. (2005). Dual role for tomato heat shock protein 21: protecting photosystem II from oxidative stress and promoting color changes during fruit maturation. Plant Cell **17**, 1829-1838.

Nisar, N., Li, L., Lu, S., Khin, N.C., and Pogson, B.J. (2015). Carotenoid metabolism in plants. Molecular Plant **8**, 68-82.

Nishitani, K. (1997). The role of endoxyloglucan transferase in the organization of plant cell walls. International Review of Cytology **173**, 157-206.

Nishiyama, K., Guis, M., Rose, J.K., Kubo, Y., Bennett, K.A., Wangjin, L., Kato, K., Ushijima, K., Nakano, R., Inaba, A., Bouzayen, M., Latche, A., Pech, J.C., and Bennett, A.B. (2007). Ethylene regulation of fruit softening and cell wall disassembly in Charentais melon. Journal of Experimental Botany **58**, 1281-1290.

Nitsch, J.P. (1952). Plant hormones in the development of fruits. The Quarterly Review of Biology **27**, 33-57.

Nitsch, L., Kohlen, W., Oplaat, C., Charnikhova, T., Cristescu, S., Michieli, P., Wolters-Arts, M., Bouwmeester, H., Mariani, C., Vriezen, W.H., and Rieu, I. (2012). ABA-deficiency results in reduced plant and fruit size in tomato. Plant Physiology **169**, 878-883.

Nogueira, M., Enfissi, E.M.A., Martínez Valenzuela, M.E., Menard, G.N., Driller, R.L., Eastmond, P.J., Schuch, W., Sandmann, G., and Fraser, P.D. (2017). Engineering of tomato for the sustainable production of ketocarotenoids and its

evaluation in aquaculture feed. Proceedings of the National Academy of Sciences USA, 10876-10881.

Nogueira, M., Mora, L., Enfissi, E.M., Bramley, P.M., and Fraser, P.D. (2013). Subchromoplast sequestration of carotenoids affects regulatory mechanisms in tomato lines expressing different carotenoid gene combinations. Plant Cell **25**, 4560-4579.

Nour, V., Panaite, T.D., Ropota, M., Turcu, R., Trandafir, I., and Corbu, A.R. (2018). Nutritional and bioactive compounds in dried tomato processing waste. CyTA - Journal of Food **16**, 222-229.

Oeller, P.W., Lu, M.W., Taylor, L.P., Pike, D.A., and Theologis, A. (1991). Reversible inhibition of tomato fruit senescence by antisense RNA. Science **254**, 437-439.

Ogasawara, S., Abe, K., and Nakajima, T. (2007). Pepper β-galactosidase 1 (PBG1) plays a significant role in fruit ripening in bell pepper (*Capsicum annuum*). Bioscience, Biotechnology, and Biochemistry **71**, 309-322.

Okabe, Y., Asamizu, E., Saito, T., Matsukura, C., Ariizumi, T., Bres, C., Rothan, C., Mizoguchi, T., and Ezura, H. (2011). Tomato TILLING technology: development of a reverse genetics tool for the efficient isolation of mutants from Micro-Tom mutant libraries. Plant and Cell Physiology **52**, 1994-2005.

Olimpieri, I., Siligato, F., Caccia, R., Mariotti, L., Ceccarelli, N., Soressi, G.P., and Mazzucato, A. (2007). Tomato fruit set driven by pollination or by the parthenocarpic fruit allele are mediated by transcriptionally regulated gibberellin biosynthesis. Planta **226**, 877-888.

Ori, N., Juarez, M.T., Jackson, D., Yamaguchi, J., Banowetz, G.M., and Hake, S. (1999). Leaf senescence is delayed in tobacco plants expressing the maize homeobox gene knotted1 under the control of a senescence-activated promoter. Plant Cell **11**, 1073-1080.

Osorio, S., Alba, R., Damasceno, C.M.B., Lopez-Casado, G., Lohse, M., Zanor, M.I., Tohge, T., Usadel, B., Rose, J.K.C., Fei, Z., Giovannoni, J.J., and Fernie, A.R. (2011a). Systems biology of tomato fruit development: combined transcript, protein, and metabolite analysis of tomato transcription factor (*nor*, *rin*) and ethylene receptor (*Nr*) mutants reveals novel regulatory interactions. Plant Physiology **157**, 405-425.

Osorio, S., Alba, R., Damasceno, C.M.B., Lopez-Casado, G., Lohse, M., Zanor, M.I., Tohge, T., Usadel, B., Rose, J.K.C., Fei, Z., Giovannoni, J.J., and Fernie, A.R. (2011b). Systems biology of tomato fruit development: combined transcript, protein, and metabolite analysis of tomato transcription factor (*nor*, *rin*) and ethylene receptor (*Nr*) mutants reveals novelregulatory interactions. Plant Physiology **157**, 405-425.

Osorio, S., Alba, R., Nikoloski, Z., Kochevenko, A., Fernie, A.R., and Giovannoni, J.J. (2012). Integrative comparative analyses of transcript and metabolite profiles from pepper and tomato ripening and development stages uncovers species-specific patterns of network regulatory behavior. Plant Physiology **159**, 1713-1729.

Osorio, S., Ruan, Y.L., and Fernie, A.R. (2014). An update on source-to-sink carbon partitioning in tomato. Frontiers in Plant Science **5**, 516-527.

Osterlund, M.T., Hardtke, C.S., Wei, N., and Deng, X.W. (2000). Targeted destabilization of HY5 during light-regulated development of *Arabidopsis*. Nature **405**, 462-466.

Oyama, T., Shimura, Y., and Okada, K. (1997). The *Arabidopsis* HY5 gene encodes a bZIP protein that regulates stimulus-induced development of root and hypocotyl. Genes and Development **11**, 2983-2995.

Ozeki, Y., Komamine, A., and Tanaka, Y. (1990). Induction and repression of phenylalanine ammonia-lyase and chalcone synthase enzyme proteins and mRNAs in carrot cell suspension cultures regulated by 2,4-D. Physiologia Plantarum **78**, 400-408.

Paine, J.A., Shipton, C.A., Chaggar, S., Howells, R.M., Kennedy, M.J., Vernon, G., Wright, S.Y., Hinchliffe, E., Adams, J.L., Silverstone, A.L., and Drake, R. (2005). Improving the nutritional value of Golden Rice through increased pro-vitamin A content. Nature Biotechnology **23**, 482-487.

Pan, Y., Bradley, G., Pyke, K., Ball, G., Lu, C., Fray, R., Marshall, A., Jayasuta, S., Baxter, C., van Wijk, R., Boyden, L., Cade, R., Chapman, N.H., Fraser, P.D., Hodgman, C., and Seymour, G.B. (2013). Network inference analysis identifies an APRR2-like gene linked to pigment accumulation in tomato and pepper fruits. Plant Physiology **161**, 1476-1485.

Paniagua, C., Blanco-Portales, R., Barceló-Muñoz, M., García-Gago, J.A., Waldron, K.W., Quesada, M.A., Muñoz-Blanco, J., and Mercado, J.A. (2016). Antisense down-regulation of the strawberry β-galactosidase gene FaβGal4 increases cell wall galactose levels and reduces fruit softening. Journal of Experimental Botany **67**, 619-631.

Paniagua, C., Pose, S., Morris, V.J., Kirby, A.R., Quesada, M.A., and Mercado, J.A. (2014). Fruit softening and pectin disassembly: an overview of nanostructural pectin modifications assessed by atomic force microscopy. Annals of Botany **114**, 1375-1383.

Park, S., Kim, H.S., Jung, Y.J., Kim, S.H., Ji, C.Y., Wang, Z., Jeong, J.C., Lee, H.-S., Lee, S.Y., and Kwak, S.-S. (2016). Orange protein has a role in phytoene synthase stabilization in sweetpotato. Scientific Reports **6**, 1-12.

Pascual, L., Blanca, J.M., Canizares, J., and Nuez, F. (2009). Transcriptomic analysis of tomato carpel development reveals alterations in ethylene and gibberellin synthesis during pat3/pat4 parthenocarpic fruit set. BMC Plant Biology **9**, 67-85.

Pattison, R.J., and Catalá, C. (2012). Evaluating auxin distribution in tomato (*Solanum lycopersicum*) through an analysis of the PIN and AUX/LAX gene families. Plant Journal **70**, 585-598.

Payton, S., Fray, R.G., Brown, S., and Grierson, D. (1996). Ethylene receptor expression is regulated during fruit ripening, flower senescence and abscission. Plant Molecular Biology **31**, 1227-1231.

Peng, T., Saito, T., Honda, C., Ban, Y., Kondo, S., Liu, J.H., Hatsuyama, Y., and Moriguchi, T. (2013). Screening of UV-B-induced genes from apple peels by SSH: possible involvement of MdCOP1-mediated signaling cascade genes in anthocyanin accumulation. Physiologia Plantarum **148**, 432-444.

Perello, C., Llamas, E., Burlat, V., Ortiz-Alcaide, M., Phillips, M.A., Pulido, P., and Rodriguez-Concepcion, M. (2016). Differential subplastidial localization and turnover of enzymes involved in isoprenoid biosynthesis in chloroplasts. PLoS One **11**, 1-17.

Petreikov, M., Yeselson, L., Shen, S., Levin, I., Schaffer, A.A., Efrati, A., and Bar, M. (2009). Carbohydrate balance and accumulation during development of near-isogenic tomato lines differing in the AGPase-L1 allele. Journal of the American Society for Horticultural Science **134**, 134-140.

Pike, T.W., Blount, J.D., Bjerkeng, B., Lindstrom, J., and Metcalfe, N.B. (2007). Carotenoids, oxidative stress and female mating preference for longer lived males. Proceedings of the Royal Society B: Biological Sciences **274**, 1591-1596.

Pirrello, J., Prasad, B.C., Zhang, W., Chen, K., Mila, I., Zouine, M., Latche, A., Pech, J.C., Ohme-Takagi, M., Regad, F., and Bouzayen, M. (2012). Functional analysis and binding affinity of tomato ethylene response factors provide insight on the molecular bases of plant differential responses to ethylene. BMC Plant Biology **12**, 190-205.

Plackett, A.R.G., Powers, S.J., Fernandez-Garcia, N., Urbanova, T., Takebayashi, Y., Seo, M., Jikumaru, Y., Benlloch, R., Nilsson, O., Ruiz-Rivero, O., Phillips, A.L., Wilson, Z.A., Thomas, S.G., and Hedden, P. (2012). Analysis of the developmental roles of the *Arabidopsis* gibberellin 20-oxidases demonstrates that GA20ox1, -2, and -3 are the dominant paralogs. Plant Cell **24**, 941-960.

Polivka, T., and Frank, H.A. (2010). Molecular factors controlling photosynthetic light harvesting by carotenoids. Accounts of Chemical Research **43**, 1125-1134.

Posé, S., Paniagua, C., Matas, A.J., Gunning, A.P., Morris, V.J., Quesada, M.A., and Mercado, J.A. (2018). A nanostructural view of the cell wall disassembly process during fruit ripening and postharvest storage by atomic force microscopy. Trends in Food Science & Technology, 47-58.

Pressey, R. (1983). beta-Galactosidases in ripening tomatoes. Plant Physiology **71**, 132-135.

Priem, B., Gitti, R., Bush, C.A., and Gross, K.C. (1993). Structure of ten free N-glycans in ripening tomato fruit (arabinose is a constituent of a plant N-glycan). Plant Physiology **102**, 445-458.

Priem, B., and Gross, K.C. (1992). Mannosyl- and xylosyl-containing glycans promote tomato (*Lycopersicon esculentum Mill.*) fruit ripening. Plant Physiology **98**, 399-401.

Pulido, P., Llamas, E., Llorente, B., Ventura, S., Wright, L.P., and Rodríguez-Concepción, M. (2016). Specific hsp100 chaperones determine the fate of the first enzyme of the plastidial isoprenoid pathway for either refolding or degradation by the stromal clp protease in *Arabidopsis*. PLoS Genetics **12**, 1-19.

Qin, G., Zhu, Z., Wang, W., Cai, J., Chen, Y., Li, L., and Tian, S. (2016). A tomato vacuolar invertase inhibitor mediates sucrose metabolism and influences fruit ripening. Plant Physiology **172**, 1596-1611.

Quadrana, L., Almeida, J., Otaiza, S.N., Duffy, T., Corrêa da Silva, J.V., de Godoy, F., Asís, R., Bermúdez, L., Fernie, A.R., Carrari, F., and Rossi, M. (2013). Transcriptional regulation of tocopherol biosynthesis in tomato. Plant Molecular Biology **81**, 309-325.

Raghavan, V. (2003). Some reflections on double fertilization, from its discovery to the present. New Phytologist **159**, 565-583.

Raiola, A., Rigano, M.M., Calafiore, R., Frusciante, L., and Barone, A. (2014). Enhancing the health-promoting effects of tomato fruit for biofortified food. Mediators of Inflammation **2014**, 1-16.

Raiola, A., Tenore, G.C., Barone, A., Frusciante, L., and Rigano, M.M. (2015). Vitamin E content and composition in tomato fruits: beneficial roles and bio-fortification. International Journal of Molecular Sciences **16**, 29250-29264.

Ralet, M.C., Crepeau, M.J., Vigouroux, J., Tran, J., Berger, A., Salle, C., Granier, F., Botran, L., and North, H.M. (2016). Xylans provide the structural driving force for mucilage adhesion to the *Arabidopsis* seed coat. Plant Physiology **171**, 165-178.

Rama, M.V., and Narasimham, P. (2003). Potatoes and related crops | Fruits of the solanaceae. In Encyclopedia of food sciences and nutrition (second edition), B. Caballero, ed. (Oxford: Academic Press), pp. 4666-4674.

Redgwell, R.J., Fischer, M., Kendal, E., and MacRae, E.A. (1997a). Galactose loss and fruit ripening: high-molecular-weight arabinogalactans in the pectic polysaccharides of fruit cell walls. Planta **203**, 174-181.

Redgwell, R.J., MacRae, E., Hallett, I., Fischer, M., Perry, J., and Harker, R. (1997b). In vivo and in vitro swelling of cell walls during fruit ripening. Planta **203**, 162-173.

Rizvi, S., Raza, S.T., Ahmed, F., Ahmad, A., Abbas, S., and Mahdi, F. (2014). The role of vitamin E in human health and some diseases. Sultan Qaboos University Medical Journal **14**, 157-165.

Rodríguez-Concepción, M., Ahumada, I., Diez-Juez, E., Sauret-Güeto, S., Lois, L.M., Gallego, F., Carretero-Paulet, L., Campos, N., and Boronat, A. (2001). 1-Deoxy-d-xylulose 5-phosphate reductoisomerase and plastid isoprenoid biosynthesis during tomato fruit ripening. Plant Journal **27**, 213-222.

Rodríguez-Concepción, M., Querol, J., Lois, L.M., Imperial, S., and Boronat, A. (2003). Bioinformatic and molecular analysis of hydroxymethylbutenyl diphosphate synthase (GCPE) gene expression during carotenoid accumulation in ripening tomato fruit. Planta **217**, 476-482.

Roitsch, T., and Gonzalez, M.C. (2004). Function and regulation of plant invertases: sweet sensations. Trends in Plant Science **9**, 606-613.

Rose, J.K., Braam, J., Fry, S.C., and Nishitani, K. (2002). The XTH family of enzymes involved in xyloglucan endotransglucosylation and endohydrolysis: current perspectives and a new unifying nomenclature. Plant and Cell Physiology **43**, 1421-1435.

Rossi, M., Bermudez, L., and Carrari, F. (2015). Crop yield: challenges from a metabolic perspective. Current Opinion in Plant Biology **25**, 79-89.

Round, A.N., Rigby, N.M., MacDougall, A.J., and Morris, V.J. (2010). A new view of pectin structure revealed by acid hydrolysis and atomic force microscopy. Carbohydrate Research **345**, 487-497.

Ruan, Y.L., Patrick, J.W., Bouzayen, M., Osorio, S., and Fernie, A.R. (2012). Molecular regulation of seed and fruit set. Trends in Plant Science **17**, 656-665.

Ruiz-Sola, M.Á., and Rodríguez-Concepción, M. (2012). Carotenoid biosynthesis in *Arabidopsis*: a colorful pathway. The Arabidopsis Book, 1-28.

Sagar, M., Chervin, C., Mila, I., Hao, Y., Roustan, J.P., Benichou, M., Gibon, Y., Biais, B., Maury, P., Latche, A., Pech, J.C., Bouzayen, M., and Zouine, M. (2013). SlARF4, an auxin response factor involved in the control of sugar metabolism during tomato fruit development. Plant Physiology **161**, 1362-1374.

Saini, R.K., Zamany, A.J., and Keum, Y.S. (2017). Ripening improves the content of carotenoid, alpha-tocopherol, and polyunsaturated fatty acids in tomato (*Solanum lycopersicum* L.) fruits. 3 Biotech **7**, 43-50.

Sakakibara, H. (2006). Cytokinins: activity, biosynthesis, and translocation. Annual Review of Plant Biology **57**, 431-449.

Sakamoto, T., Kamiya, N., Ueguchi-Tanaka, M., Iwahori, S., and Matsuoka, M. (2001). KNOX homeodomain protein directly suppresses the expression of a gibberellin biosynthetic gene in the tobacco shoot apical meristem. Genes and Development **15**, 581-590.

Saladié, M., Matas, A.J., Isaacson, T., Jenks, M.A., Goodwin, S.M., Niklas, K.J., Xiaolin, R., Labavitch, J.M., Shackel, K.A., Fernie, A.R., Lytovchenko, A., O'Neill, M.A., Watkins, C.B., and Rose, J.K.C. (2007). A reevaluation of the key factors that influence tomato fruit softening and integrity. Plant Physiology **144**, 1012-1028.

Saladie, M., Rose, J.K., Cosgrove, D.J., and Catala, C. (2006). Characterization of a new xyloglucan endotransglucosylase/hydrolase (XTH) from ripening tomato fruit and implications for the diverse modes of enzymic action. Plant Journal **47**, 282-295.

Sampedro, J., and Cosgrove, D.J. (2005). The expansin superfamily. Genome Biology **6**, 242-253.

Sander, J.D., and Joung, J.K. (2014). CRISPR-Cas systems for genome editing, regulation and targeting. Nature Biotechnology **32**, 347-355.

Sano, M., Ernesto, C., Thomas, R.G., Klauber, M.R., Schafer, K., Grundman, M., Woodbury, P., Growdon, J., Cotman, C.W., Pfeiffer, E., Schneider, L.S., and Thal, L.J. (1997). A controlled trial of selegiline, alpha-Tocopherol, or both as treatment for Alzheimer's Disease. New England Journal of Medicine **336**, 1216-1222.

Santes, C.M., and Garcia-Martinez, J.L. (1995). Effect of the growth retardant 3,5-dioxo-4-butyryl-cyclohexane carboxylic acid ethyl ester, an acylcyclohexanedione compound, on fruit growth and gibberellin content of pollinated and unpollinated ovaries in pea. Plant physiology **108**, 517-523.

Sattler, M.C., Carvalho, C.R., and Clarindo, W.R. (2016). The polyploidy and its key role in plant breeding. Planta **243**, 281-296.

Schafer, M., Brutting, C., Meza-Canales, I.D., Grosskinsky, D.K., Vankova, R., Baldwin, I.T., and Meldau, S. (2015). The role of cis-zeatin-type cytokinins in plant growth regulation and mediating responses to environmental interactions. Journal of Experimental Botany **66**, 4873-4884.

Schaffer, R.J., Ireland, H.S., Ross, J.J., Ling, T.J., and David, K.M. (2013). SEPALLATA1/2-suppressed mature apples have low ethylene, high auxin and reduced transcription of ripening-related genes. AoB Plants **5**, 47-57.

Scheller, H.V., and Ulvskov, P. (2010). Hemicelluloses. Annual Review of Plant Biology **61**, 263-289.

Schramm, F., Ganguli, A., Kiehlmann, E., Englich, G., Walch, D., and von Koskull-Döring, P. (2006). The heat stress transcription factor HsfA2 serves as a regulatory amplifier of a subset of genes in the heat stress response in *Arabidopsis*. Plant Molecular Biology **60**, 759-772.

Schweigert, F.J., Klingner, J., Hurtienne, A., and Zunft, H.J. (2003). Vitamin A, carotenoid and vitamin E plasma concentrations in children from Laos in relation to sex and growth failure. Nutrition Journal **2**, 17-17.

Selth, L.A., Dogra, S.C., Rasheed, M.S., Healy, H., Randles, J.W., and Rezaian, M.A. (2005). A NAC domain protein interacts with tomato leaf curl virus replication accessory protein and enhances viral replication. Plant Cell **17**, 311-325.

Seo, P.J., Kim, M.J., Ryu, J.Y., Jeong, E.Y., and Park, C.M. (2011a). Two splice variants of the IDD14 transcription factor competitively form nonfunctional heterodimers which may regulate starch metabolism. Nature Communications **2**, 303-311.

Seo, Y.S., Kim, S.J., Harn, C.H., and Kim, W.T. (2011b). Ectopic expression of apple fruit homogentisate phytyltransferase gene (MdHPT1) increases tocopherol in transgenic tomato (*Solanum lycopersicum* cv. Micro-Tom) leaves and fruits. Phytochemistry **72**, 321-329.

Serrani, J.C., Fos, M., Atarés, A., and García-Martínez, J.L. (2007a). Effect of gibberellin and auxin on parthenocarpic fruit growth induction in the cv Micro-Tom of tomato. Journal of Plant Growth Regulation **26**, 211-221.

Serrani, J.C., Ruiz-Rivero, O., Fos, M., and García-Martínez, J.L. (2008). Auxin-induced fruit-set in tomato is mediated in part by gibberellins. Plant Journal **56**, 922-934.

Serrani, J.C., Sanjuan, R., Ruiz-Rivero, O., Fos, M., and Garcia-Martinez, J.L. (2007b). Gibberellin regulation of fruit set and growth in tomato. Plant Physiology **145**, 246-257.

Seymour, G.B., Chapman, N.H., Chew, B.L., and Rose, J.K. (2013a). Regulation of ripening and opportunities for control in tomato and other fruits. Plant Biotechnology Journal **11**, 269-278.

Seymour, G.B., Colquhoun, I.J., Dupont, M.S., Parsley, K.R., and R. Selvendran, R. (1990). Composition and structural features of cell wall polysaccharides from tomato fruits. Phytochemistry **29**, 725-731.

Seymour, G.B., Ostergaard, L., Chapman, N.H., Knapp, S., and Martin, C. (2013b). Fruit development and ripening. Annual Review of Plant Biology **64**, 219-241.

Seymour, G.B., Ryder, C.D., Cevik, V., Hammond, J.P., Popovich, A., King, G.J., Vrebalov, J., Giovannoni, J.J., and Manning, K. (2011). A SEPALLATA gene is involved in the development and ripening of strawberry (*Fragaria×ananassa Duch.*) fruit, a non-climacteric tissue*. Journal of Experimental Botany **62**, 1179-1188.

Shani, E., Ben-Gera, H., Shleizer-Burko, S., Burko, Y., Weiss, D., and Ori, N. (2010). Cytokinin regulates compound leaf development in tomato. Plant Cell **22**, 3206-3217.

Sheehy, R.E., Kramer, M., and Hiatt, W.R. (1988). Reduction of polygalacturonase activity in tomato fruit by antisense RNA. Proceedings of the National Academy of Sciences USA **85**, 8805-8809.

Shen, J., Tieman, D., Jones, J.B., Taylor, M.G., Schmelz, E., Huffaker, A., Bies, D., Chen, K., and Klee, H.J. (2014). A 13-lipoxygenase, TomloxC, is essential for synthesis of C5 flavour volatiles in tomato. Journal of Experimental Botany **65**, 419-428.

Shima, Y., Fujisawa, M., Kitagawa, M., Nakano, T., Kimbara, J., Nakamura, N., Shiina, T., Sugiyama, J., Nakamura, T., Kasumi, T., and Ito, Y. (2014). Tomato

FRUITFULL homologs regulate fruit ripening via ethylene biosynthesis. Bioscience, Biotechnology, and Biochemistry **78**, 231-237.

Shima, Y., Kitagawa, M., Fujisawa, M., Nakano, T., Kato, H., Kimbara, J., Kasumi, T., and Ito, Y. (2013). Tomato FRUITFULL homologues act in fruit ripening via forming MADS-box transcription factor complexes with RIN. Plant Molecular Biology **82**, 427-438.

Shin, D.H., Choi, M., Kim, K., Bang, G., Cho, M., Choi, S.B., Choi, G., and Park, Y.I. (2013). HY5 regulates anthocyanin biosynthesis by inducing the transcriptional activation of the MYB75/PAP1 transcription factor in *Arabidopsis*. FEBS Letters **587**, 1543-1547.

Shin, J., Park, E., and Choi, G. (2007). PIF3 regulates anthocyanin biosynthesis in an HY5-dependent manner with both factors directly binding anthocyanin biosynthetic gene promoters in *Arabidopsis*. Plant Journal **49**, 981-994.

Shinozaki, Y., Ezura, H., and Ariizumi, T. (2018a). The role of ethylene in the regulation of ovary senescence and fruit set in tomato (*Solanum lycopersicum*). Plant Signaling & Behavior **13**, 1-4.

Shinozaki, Y., Hao, S., Kojima, M., Sakakibara, H., Ozeki-Iida, Y., Zheng, Y., Fei, Z., Zhong, S., Giovannoni, J.J., Rose, J.K.C., Okabe, Y., Heta, Y., Ezura, H., and Ariizumi, T. (2015). Ethylene suppresses tomato (*Solanum lycopersicum*) fruit set through modification of gibberellin metabolism. Plant Journal **83**, 237-251.

Shinozaki, Y., Nicolas, P., Fernandez-Pozo, N., Ma, Q., Evanich, D.J., Shi, Y., Xu, Y., Zheng, Y., Snyder, S.I., Martin, L.B.B., Ruiz-May, E., Thannhauser, T.W., Chen, K., Domozych, D.S., Catala, C., Fei, Z., Mueller, L.A., Giovannoni, J.J., and Rose, J.K.C. (2018b). High-resolution spatiotemporal transcriptome mapping of tomato fruit development and ripening. Nature Communications **9**, 364-377.

Silletti, M.F., Petrozza, A., Stigliani, A.L., Giorio, G., Cellini, F., D'Ambrosio, C., and Carriero, F. (2013). An increase of lycopene content in tomato fruit is associated with a novel Cyc-B allele isolated through TILLING technology. Molecular Breeding **31**, 665-674.

Simkin, A.J., Gaffé, J., Alcaraz, J.-P., Carde, J.-P., Bramley, P.M., Fraser, P.D., and Kuntz, M. (2007). Fibrillin influence on plastid ultrastructure and pigment content in tomato fruit. Phytochemistry **68**, 1545-1556.

Simkin, A.J., Schwartz, S.H., Auldridge, M., Taylor, M.G., and Klee, H.J. (2004). The tomato carotenoid cleavage dioxygenase 1 genes contribute to the formation of the flavor volatiles beta-ionone, pseudoionone, and geranylacetone. Plant Journal **40**, 882-892.

Singh, R., Rastogi, S., and Dwivedi, U.N. (2010). Phenylpropanoid metabolism in ripening fruits. Comprehensive reviews in food science and food safety **9**, 398-416.

Singh, R.K., Ali, S.A., Nath, P., and Sane, V.A. (2011). Activation of ethylene-responsive p-hydroxyphenylpyruvate dioxygenase leads to increased tocopherol levels during ripening in mango. Journal of Experimental Botany **62**, 3375-3385.

Sjut, V., and Bangerth, F. (1982). Induced parthenocarpy—a way of changing the levels of endogenous hormones in tomato fruits (*Lycopersicon esculentum* Mill.) 1. Extractable hormones. Plant Growth Regulation **1**, 243-251.

Smith, C.J., Watson, C.F., Morris, P.C., Bird, C.R., Seymour, G.B., Gray, J.E., Arnold, C., Tucker, G.A., Schuch, W., Harding, S., and et al. (1990). Inheritance and effect on ripening of antisense polygalacturonase genes in transgenic tomatoes. Plant Molecular Biology **14**, 369-379.

Smith, C.J.S., Watson, C.F., Ray, J., Bird, C.R., Morris, P.C., Schuch, W., and Grierson, D. (1988). Antisense RNA inhibition of polygalacturonase gene expression in transgenic tomatoes. Nature **334**, 724–726

Smith, D.L., Abbott, J.A., and Gross, K.C. (2002). Down-regulation of tomato beta-galactosidase 4 results in decreased fruit softening. Plant Physiology **129**, 1755-1762.

Smith, D.L., and Gross, K.C. (2000). A family of at least seven β-galactosidase genes is expressed during tmato fruit development. Plant Physiology **123**, 1173-1184.

Somerville, C. (2006). Cellulose synthesis in higher plants. Annual Review of Cell and Developmental Biology **22**, 53-78.

Song, J., Liu, Q., Hu, B., and Wu, W. (2017). Photoreceptor PhyB involved in *Arabidopsis* temperature perception and heat-tolerance formation. International Journal of Molecular Sciences **18**, 1194-1207.

Sravankumar, T., Akash, Naik, N., and Kumar, R. (2018). A ripening-induced SlGH3-2 gene regulates fruit ripening via adjusting auxin-ethylene levels in tomato (*Solanum lycopersicum* L.). Plant Molecular Biology **98**, 455-469.

Srivastava, A., and Handa, A.K. (2005). Hormonal regulation of tomato fruit development: a molecular perspective. Journal of Plant Growth Regulation **24**, 67-82.

Sterling, J.D., Atmodjo, M.A., Inwood, S.E., Kumar Kolli, V.S., Quigley, H.F., Hahn, M.G., and Mohnen, D. (2006). Functional identification of an *Arabidopsis* pectin biosynthetic homogalacturonan galacturonosyltransferase. Proceedings of the National Academy of Sciences USA **103**, 5236-5241.

Steve, P., Louise, B.S., Mondher, B., John, H.A., and Don, G. (1993). Altered fruit ripening and leaf senescence in tomatoes expressing an antisense ethylene-forming enzyme transgene. Plant Journal **3**, 469-481.

Story, E.N., Kopec, R.E., Schwartz, S.J., and Harris, G.K. (2010). An update on the health effects of tomato lycopene. Annual Review of Food Science and Technology **1**, 189-210.

Stracke, R., Favory, J.J., Gruber, H., Bartelniewoehner, L., Bartels, S., Binkert, M., Funk, M., Weisshaar, B., and Ulm, R. (2010). The *Arabidopsis* bZIP transcription factor HY5 regulates expression of the PFG1/MYB12 gene in response to light and ultraviolet-B radiation. Plant Cell and Environment **33**, 88-103.

Su, L., Diretto, G., Purgatto, E., Danoun, S., Zouine, M., Li, Z., Roustan, J.-P., Bouzayen, M., Giuliano, G., and Chervin, C. (2015). Carotenoid accumulation during tomato fruit ripening is modulated by the auxin-ethylene balance. BMC Plant Biology **15**, 114-126.

Sun, L., Sun, Y., Zhang, M., Wang, L., Ren, J., Cui, M., Wang, Y., Ji, K., Li, P., Li, Q., Chen, P., Dai, S., Duan, C., Wu, Y., and Leng, P. (2012a). Suppression of 9-cis-epoxycarotenoid dioxygenase, which encodes a key enzyme in abscisic acid biosynthesis, alters fruit texture in transgenic tomato. Plant Physiology **158**, 283-298.

Sun, L., Yuan, B., Zhang, M., Wang, L., Cui, M., Wang, Q., and Leng, P. (2012b). Fruit-specific RNAi-mediated suppression of SlNCED1 increases both lycopene and β-carotene contents in tomato fruit. Journal of Experimental Botany **63**, 3097-3108.

Sun, T.-p., and Gubler, F. (2004). Molecular mechanism of gibberellin signaling in plants. Annual Review of Plant Biology **55**, 197-223.

Sun, W., Kieliszewski, M.J., and Showalter, A.M. (2004). Overexpression of tomato LeAGP-1 arabinogalactan-protein promotes lateral branching and hampers reproductive development. Plant Journal **40**, 870-881.

Sun, Y., Chen, P., Duan, C., Tao, P., Wang, Y., Ji, K., Hu, Y., Li, Q., Dai, S., Wu, Y., Luo, H., Sun, L., and Leng, P. (2012c). Transcriptional regulation of genes encoding key enzymes of abscisic acid metabolism during melon (*Cucumis melo* L.) fruit development and ripening. Plant Growth Regulation **32**, 233–244.

Sun, Z., Gantt, E., and Cunningham, F.X., Jr. (1996). Cloning and functional analysis of the beta-carotene hydroxylase of *Arabidopsis thaliana*. Journal of Biological Chemistry **271**, 24349-24352.

Takahashi, S., and Badger, M.R. (2011). Photoprotection in plants: a new light on photosystem II damage. Trends in Plant Science **16**, 53-60.

Takaichi, S. (2011). Carotenoids in algae: distributions, biosyntheses and functions. Marine Drugs **9**, 1101-1118.

Takayama, M., and Ezura, H. (2015). How and why does tomato accumulate a large amount of GABA in the fruit? Frontiers in Plant Science **6**, 612.

Tan, L., Eberhard, S., Pattathil, S., Warder, C., Glushka, J., Yuan, C., Hao, Z., Zhu, X., Avci, U., Miller, J.S., Baldwin, D., Pham, C., Orlando, R., Darvill, A., Hahn, M.G., Kieliszewski, M.J., and Mohnen, D. (2013). An *Arabidopsis* cell wall proteoglycan consists of pectin and arabinoxylan covalently linked to an arabinogalactan protein. Plant Cell **25**, 270-287.

Tang, G., and Russell, R.M. (2009). Carotenoids as provitamin A. In Carotenoids: Volume 5: Nutrition and Health, G. Britton, H. Pfander, and S. Liaaen-Jensen, eds. (Basel: Birkhäuser Basel), pp. 149-172.

Tang, N., Deng, W., Hu, G., Hu, N., and Li, Z. (2015). Transcriptome Profiling Reveals the Regulatory Mechanism Underlying Pollination Dependent and Parthenocarpic Fruit Set Mainly Mediated by Auxin and Gibberellin. PLoS One **10**, 1-22.

Telef, N., Stammitti-Bert, L., Mortain-Bertrand, A., Maucourt, M., Carde, J.P., Rolin, D., and Gallusci, P. (2006). Sucrose deficiency delays lycopene accumulation in tomato fruit pericarp discs. Plant Molecular Biology **62**, 453-469.

Télef, N., Stammitti-Bert, L., Mortain-Bertrand, A., Maucourt, M., Carde, J.P., Rolin, D., and Gallusci, P. (2006). Sucrose deficiency delays lycopene accumulation in tomato fruit pericarp discs. Plant Molecular Biology **62**, 453-469.

Thakur, B., Singh, R., and Handa, A. (1996). Effect of an antisense pectin methylesterase gene on the chemistry of pectin in tomato (*Lycopersicon esculentum*) juice. Journal of Agricultural and Food Chemistry **44**, 628–630.

The Age-Related Eye Disease Study 2 Research, G. (2013). Lutein + zeaxanthin and omega-3 fatty acids for age-related macular degeneration: The age-related eye disease study 2 (areds2) randomized clinical trial. JAMA **309**, 2005-2015.

The Tomato Genome, C. (2012). The tomato genome sequence provides insights into fleshy fruit evolution. Nature **485**, 635-641.

Theologis, A., Zarembinski, T.I., Oeller, P.W., Liang, X., and Abel, S. (1992). Modification of fruit ripening by suppressing gene expression. Plant Physiology **100**, 549-551.

Thomas, T.R., Shackel, K.A., and Matthews, M.A. (2008). Mesocarp cell turgor in *Vitis vinifera* L. berries throughout development and its relation to firmness, growth, and the onset of ripening. Planta **228**, 1067-1076.

Tian, L., and DellaPenna, D. (2001). Characterization of a second carotenoid beta-hydroxylase gene from *Arabidopsis* and its relationship to the LUT1 locus. Plant Molecular Biology **47**, 379-388.

Tian, L., Magallanes-Lundback, M., Musetti, V., and DellaPenna, D. (2003). Functional analysis of beta- and epsilon-ring carotenoid hydroxylases in *Arabidopsis*. Plant Cell **15**, 1320-1332.

Tian, L., Musetti, V., Kim, J., Magallanes-Lundback, M., and DellaPenna, D. (2004). The *Arabidopsis* LUT1 locus encodes a member of the cytochrome P450 family that is required for carotenoid ε-ring hydroxylation activity. Proceedings of the National Academy of Sciences USA **101**, 402-407.

Tieman, D., Bliss, P., McIntyre, L.M., Blandon-Ubeda, A., Bies, D., Odabasi, A.Z., Rodriguez, G.R., van der Knaap, E., Taylor, M.G., Goulet, C., Mageroy, M.H., Snyder, D.J., Colquhoun, T., Moskowitz, H., Clark, D.G., Sims, C., Bartoshuk, L., and Klee, H.J. (2012). The chemical interactions underlying tomato flavor preferences. Current Biology **22**, 1035-1039.

Tieman, D., Zhu, G., Resende, M.F., Jr., Lin, T., Nguyen, C., Bies, D., Rambla, J.L., Beltran, K.S., Taylor, M., Zhang, B., Ikeda, H., Liu, Z., Fisher, J., Zemach, I., Monforte, A., Zamir, D., Granell, A., Kirst, M., Huang, S., and Klee, H. (2017). A chemical genetic roadmap to improved tomato flavor. Science **355**, 391-394.

Tieman, D.M., Harriman, R.W., Ramamohan, G., and Handa, A.K. (1992). An antisense pectin methylesterase gene alters pectin chemistry and soluble solids in tomato fruit. Plant Cell **4**, 667-679.

Tieman, D.M., Taylor, M.G., Ciardi, J.A., and Klee, H.J. (2000). The tomato ethylene receptors NR and LeETR4 are negative regulators of ethylene response and exhibit functional compensation within a multigene family. Proceedings of the National Academy of Sciences USA **97**, 5663-5668.

Ties, P., and Barringer, S. (2012). Influence of lipid content and lipoxygenase on flavor volatiles in the tomato peel and flesh. Journal of Food Science **77**, C830-837.

Todd, J.F., Paliyath, G., and Thompson, J.E. (1990). Characteristics of a membrane-associated lipoxygenase in tomato fruit. Plant Physiology **94**, 1225-1232.

Toledo-Ortiz, G., Johansson, H., Lee, K.P., Bou-Torrent, J., Stewart, K., Steel, G., Rodríguez-Concepción, M., and Halliday, K.J. (2014). The HY5-PIF regulatory module coordinates light and temperature control of photosynthetic gene transcription. PLoS Genetics **10**, 1-14.

Torres-Schumann, S., Godoy, J.A., and Pintor-Toro, J.A. (1992). A probable lipid transfer protein gene is induced by NaCl in stems of tomato plants. Plant Molecular Biology **18**, 749-757.

Traber, M.G., and Atkinson, J. (2007). Vitamin E, antioxidant and nothing more. Free Radical Biology and Medicine **43**, 4-15.

Trainotti, L., Tadiello, A., and Casadoro, G. (2007). The involvement of auxin in the ripening of climacteric fruits comes of age: the hormone plays a role of its own and has an intense interplay with ethylene in ripening peaches. Journal of Experimental Botany **58**, 3299-3308.

Tucker, G., Yin, X., Zhang, A., Wang, M., Zhu, Q., Liu, X., Xie, X., Chen, K., and Grierson, D. (2017). Ethylene† and fruit softening. Food Quality and Safety **1**, 253-267.

Tucker, G.A., Robertson, N.G., and Grierson, D. (1982). Purification and changes in activities of tomato pectinesterase isoenzymes. Journal of the Science of Food and Agriculture **33**, 396-400.

Ueguchi-Tanaka, M., Ashikari, M., Nakajima, M., Itoh, H., Katoh, E., Kobayashi, M., Chow, T.Y., Hsing, Y.I., Kitano, H., Yamaguchi, I., and Matsuoka, M. (2005). Gibberellin insensitive dwarf1 encodes a soluble receptor for gibberellin. Nature **437**, 693-698.

Uluisik, S., Chapman, N.H., Smith, R., Poole, M., Adams, G., Gillis, R.B., Besong, T.M., Sheldon, J., Stiegelmeyer, S., Perez, L., Samsulrizal, N., Wang, D., Fisk, I.D., Yang, N., Baxter, C., Rickett, D., Fray, R., Blanco-Ulate, B., Powell, A.L., Harding, S.E., Craigon, J., Rose, J.K., Fich, E.A., Sun, L., Domozych, D.S., Fraser, P.D., Tucker, G.A., Grierson, D., and Seymour, G.B. (2016). Genetic improvement of tomato by targeted control of fruit softening. Nature Biotechnology **34**, 950-952.

Urbanowicz, B.R., Bennett, A.B., del Campillo, E., Catalá, C., Hayashi, T., Henrissat, B., Höfte, H., McQueen-Mason, S.J., Patterson, S.E., Shoseyov, O., Teeri, T.T., and Rose, J.K.C. (2007). Structural organization and a standardized nomenclature for plant endo-1,4-β-glucanases (cellulases) of glycosyl hydrolase family 9. Plant Physiology **144**, 1693-1696.

Valentin, H.E., Lincoln, K., Moshiri, F., Jensen, P.K., Qi, Q., Venkatesh, T.V., Karunanandaa, B., Baszis, S.R., Norris, S.R., Savidge, B., Gruys, K.J., and Last, R.L. (2006). The *Arabidopsis* vitamin E pathway gene5-1 mutant reveals a critical role for phytol kinase in seed tocopherol biosynthesis. Plant Cell **18**, 212-224.

Van de Poel, B., Bulens, I., Markoula, A., Hertog, M.L., Dreesen, R., Wirtz, M., Vandoninck, S., Oppermann, Y., Keulemans, J., Hell, R., Waelkens, E., De Proft, M.P., Sauter, M., Nicolai, B.M., and Geeraerd, A.H. (2012). Targeted systems biology profiling of tomato fruit reveals coordination of the Yang cycle and a distinct regulation of ethylene biosynthesis during postclimacteric ripening. Plant Physiology **160**, 1498-1514.

Van de Poel, B., Bulens, I., Oppermann, Y., Hertog, M.L., Nicolai, B.M., Sauter, M., and Geeraerd, A.H. (2013). S-adenosyl-L-methionine usage during climacteric ripening of tomato in relation to ethylene and polyamine biosynthesis and transmethylation capacity. Physiologia Plantarum **148**, 176-188.

van der Knaap, E., and Tanksley, S.D. (2003). The making of a bell pepper-shaped tomato fruit: identification of loci controlling fruit morphology in Yellow Stuffer tomato. Theoretical and Applied Genetics **107**, 139-147.

van schie, C., Ament, K., Schmidt, A., Lange, T., A Haring, M., and C Schuurink, R. (2007). Geranyl diphosphate synthase is required for biosynthesis of gibberellins. Plant Journal **52**, 752-762.

Varga, A., and Bruinsma, J. (1974). The growth and ripening of tomato fruits at different levels of endogenous cytokinins. Journal of Horticultural Science **49**, 135-142.

Vasquez-Caicedo, A.L., Heller, A., Neidhart, S., and Carle, R. (2006). Chromoplast morphology and beta-carotene accumulation during postharvest ripening of Mango Cv. 'Tommy Atkins'. Journal of Agricultural and Food Chemistry **54**, 5769-5776.

Vendrell, M. (1985). Dual effect of 2, 4-D on ethylene production and ripening of tomato fruit tissue. Physiologia Plantarum **64**, 559-563.

Vishnevetsky, M., Ovadis, M., and Vainstein, A. (1999). Carotenoid sequestration in plants: the role of carotenoid-associated proteins. Trends in Plant Science **4**, 232-235.

Viuda-Martos, M., Sanchez-Zapata, E., Sayas-Barbera, E., Sendra, E., Perez-Alvarez, J.A., and Fernandez-Lopez, J. (2014). Tomato and tomato byproducts. Human health benefits of lycopene and its application to meat products: a review. Critical Reviews in Food Science and Nutrition **54**, 1032-1049.

Vivian-Smith, A., and Koltunow, A.M. (1999). Genetic analysis of growth-regulator-induced parthenocarpy in *Arabidopsis*. Plant Physiology **121**, 437-451.

Vogel, J.T., Tieman, D.M., Sims, C.A., Odabasi, A.Z., Clark, D.G., and Klee, H.J. (2010). Carotenoid content impacts flavor acceptability in tomato (*Solanum lycopersicum*). Journal of the Science of Food and Agriculture **90**, 2233-2240.

von Koskull-Doring, P., Scharf, K.D., and Nover, L. (2007). The diversity of plant heat stress transcription factors. Trends in Plant Science **12**, 452-457.

Vrebalov, J., Pan, I.L., Arroyo, A.J., McQuinn, R., Chung, M., Poole, M., Rose, J., Seymour, G., Grandillo, S., Giovannoni, J., and Irish, V.F. (2009). Fleshy fruit expansion and ripening are regulated by the Tomato SHATTERPROOF gene TAGL1. Plant Cell **21**, 3041-3062.

Vrebalov, J., Ruezinsky, D., Padmanabhan, V., White, R., Medrano, D., Drake, R., Schuch, W., and Giovannoni, J. (2002). A MADS-box gene necessary for fruit ripening at the tomato ripening-inhibitor (*rin*) locus. Science **296**, 343-346.

Vriezen, W.H., Feron, R., Maretto, F., Keijman, J., and Mariani, C. (2008). Changes in tomato ovary transcriptome demonstrate complex hormonal regulation of fruit set. New Phytologist **177**, 60-76.

Wada, H., Matthews, M.A., and Shackel, K.A. (2009). Seasonal pattern of apoplastic solute accumulation and loss of cell turgor during ripening of *Vitis vinifera* fruit under field conditions. Journal of Experimental Botany **60**, 1773-1781.

Wallner, S.J., and Bloom, H.L. (1977). Characteristics of tomato cell wall degradation in vitro: implications for the study of fruit-softening enzymes. Plant Physiology **60**, 207-210.

Walter, M.H., Floss, D.S., and Strack, D. (2010). Apocarotenoids: hormones, mycorrhizal metabolites and aroma volatiles. Planta **232**, 1-17.

Wang, D., and Seymour, G.B. (2017). Tomato flavor: lost and found? Molecular Plant **10**, 782-784.

Wang, D., Yeats, T.H., Uluisik, S., Rose, J.K.C., and Seymour, G.B. (2018). Fruit softening: revisiting the role of pectin. Trends in Plant Science **23**, 302-310.

Wang, H.-C., Huang, H., and Huang, X. (2007). Differential effects of abscisic acid and ethylene on the fruit maturation of *Litchi chinensis* Sonn. Plant Growth Regulation **52**, 189-198.

Wang, S., Liu, J., Feng, Y., Niu, X., Giovannoni, J., and Liu, Y. (2008). Altered plastid levels and potential for improved fruit nutrient content by downregulation of the tomato DDB1-interacting protein CUL4. Plant Journal **55**, 89-103.

Wang, S., Lu, G., Hou, Z., Luo, Z., Wang, T., Li, H., Zhang, J., and Ye, Z. (2014). Members of the tomato FRUITFULL MADS-box family regulate style abscission and fruit ripening. Journal of Experimental Botany **65**, 3005-3014.

Wang, Z.F., Ying, T.J., Zhang, Y., Bao, B.L., and Huang, X.D. (2006). Characteristics of transgenic tomatoes antisensed for the ethylene receptor genes LeETR1 and LeETR2. Journal of Zhejiang University Science B **7**, 591-595.

Weiss, D., and Ori, N. (2007). Mechanisms of cross talk between gibberellin and other hormones. Plant Physiology **144**, 1240-1246.

Wellburn, A.R. (1994). The spectral determination of chlorophylls a and b, as well as total carotenoids, using various solvents with spectrophotometers of different resolution. Plant Physiology **144**, 307-313.

Weng, L., Zhao, F., Li, R., and Xiao, H. (2015a). Cross-talk modulation between ABA and ethylene by transcription factor SlZFP2 during fruit development and ripening in tomato. Plant Signaling & Behavior **10**, 1-4.

Weng, L., Zhao, F., Li, R., Xu, C., Chen, K., and Xiao, H. (2015b). The zinc finger transcription factor SlZFP2 negatively regulates abscisic acid biosynthesis and fruit ripening in tomato. Plant Physiology **167**, 931-949.

Werner, T., Motyka, V., Laucou, V., Smets, R., Van Onckelen, H., and Schmülling, T. (2003). Cytokinin-deficient transgenic *Arabidopsis* plants show multiple developmental alterations indicating opposite functions of cytokinins in the regulation of shoot and root meristem activity. The Plant Cell **15**, 2532-2550.

Wiedenheft, B., Sternberg, S.H., and Doudna, J.A. (2012). RNA-guided genetic silencing systems in bacteria and archaea. Nature **482**, 331-338.

Wilkinson, J.Q., Lanahan, M.B., Yen, H.C., Giovannoni, J.J., and Klee, H.J. (1995). An ethylene-inducible component of signal transduction encoded by never-ripe. Science **270**, 1807-1809.

Willats, W.G., McCartney, L., Mackie, W., and Knox, J.P. (2001a). Pectin: cell biology and prospects for functional analysis. Plant Molecular Biology **47**, 9-27.

Willats, W.G., Orfila, C., Limberg, G., Buchholt, H.C., van Alebeek, G.J., Voragen, A.G., Marcus, S.E., Christensen, T.M., Mikkelsen, J.D., Murray, B.S., and Knox, J.P. (2001b). Modulation of the degree and pattern of methyl-esterification of pectic homogalacturonan in plant cell walls. Implications for pectin methyl esterase action, matrix properties, and cell adhesion. Journal of Biological Chemistry **276**, 19404-19413.

Wills, R.B.H., and Ku, V.V.V. (2002). Use of 1-MCP to extend the time to ripen of green tomatoes and postharvest life of ripe tomatoes. Postharvest Biology and Technology **26**, 85-90.

Wu, C., You, C., Li, C., Long, T., Chen, G., Byrne, M.E., and Zhang, Q. (2008). RID1, encoding a Cys2/His2-type zinc finger transcription factor, acts as a master switch from vegetative to floral development in rice. Proceedings of the National Academy of Sciences USA **105**, 12915-12920.

Wu, J., Fu, L., and Yi, H. (2016). Genome-wide identification of the transcription factors involved in citrus fruit ripening from the transcriptomes of a late-ripening sweet orange mutant and its wild type. PLoS One **11**, 1-22.

Wu, X., Tang, D., Li, M., Wang, K., and Cheng, Z. (2013). Loose Plant Architecture1, an INDETERMINATE DOMAIN protein involved in shoot gravitropism, regulates plant architecture in rice. Plant Physiology **161**, 317-329.

Wuddineh, W.A., Mazarei, M., Zhang, J., Poovaiah, C.R., Mann, D.G., Ziebell, A., Sykes, R.W., Davis, M.F., Udvardi, M.K., and Stewart, C.N., Jr. (2015).

Identification and overexpression of gibberellin 2-oxidase (GA2ox) in switchgrass (*Panicum virgatum* L.) for improved plant architecture and reduced biomass recalcitrance. Plant Biotechnology Journal **13**, 636-647.

Xiao, J., Li, H., Zhang, J., Chen, R., Zhang, Y., Ouyang, B., Wang, T., and Ye, Z. (2006). Dissection of GA 20-oxidase members affecting tomato morphology by RNAi-mediated silencing. Plant Growth Regulation **50**, 179-189.

Yan, F., Hu, G., Ren, Z., Deng, W., and Li, Z. (2015). Ectopic expression a tomato KNOX Gene Tkn4 affects the formation and the differentiation of meristems and vasculature. Plant Molecular Biology **89**, 589-605.

Yang, J.Y., Sun, Y., Sun, A.Q., Yi, S.Y., Qin, J., Li, M.H., and Liu, J. (2006). The involvement of chloroplast HSP100/ClpB in the acquired thermotolerance in tomato. Plant Molecular Biology **62**, 385-395.

Yang, X., Zhu, W., Zhang, H., Liu, N., and Tian, S. (2016). Heat shock factors in tomatoes: genome-wide identification, phylogenetic analysis and expression profiling under development and heat stress. PeerJ **4**, 1-16.

Ye, J., Hu, T., Yang, C., Li, H., Yang, M., Ijaz, R., Ye, Z., and Zhang, Y. (2015). Transcriptome profiling of tomato fruit development reveals transcription factors associated with ascorbic acid, carotenoid and flavonoid biosynthesis. PLoS One **10**, 1-25.

Ye, X., Al-Babili, S., Klöti, A., Zhang, J., Lucca, P., Beyer, P., and Potrykus, I. (2000). Engineering the Provitamin A (β-Carotene) Biosynthetic Pathway into (Carotenoid-Free) Rice Endosperm. Science **287**, 303-305.

Yen, H.C., Lee, S., Tanksley, S.D., Lanahan, M.B., Klee, H.J., and Giovannoni, J.J. (1995). The tomato Never-ripe locus regulates ethylene-inducible gene expression and is linked to a homolog of the *Arabidopsis* ETR1 gene. Plant Physiology **107**, 1343-1353.

Yokouchi, D., Ono, N., Nakamura, K., Maeda, M., and Kimura, Y. (2013). Purification and characterization of β-xylosidase that is active for plant complex type N-glycans from tomato (*Solanum lycopersicum*): removal of core α1-3 mannosyl residue is prerequisite for hydrolysis of β1-2 xylosyl residue. Glycoconjugate Journal **30**, 463-472.

Yoshida, H., Hirano, K., Sato, T., Mitsuda, N., Nomoto, M., Maeo, K., Koketsu, E., Mitani, R., Kawamura, M., Ishiguro, S., Tada, Y., Ohme-Takagi, M., Matsuoka, M., and Ueguchi-Tanaka, M. (2014). DELLA protein functions as a transcriptional activator through the DNA binding of the INDETERMINATE DOMAIN family proteins. Proceedings of the National Academy of Sciences USA **111**, 7861-7866.

Yoshida, H., and Ueguchi-Tanaka, M. (2014). DELLA and SCL3 balance gibberellin feedback regulation by utilizing INDETERMINATE DOMAIN proteins as transcriptional scaffolds. Plant Signaling & Behavior **9**, 1-3.

Younis, A., Siddique, M.I., Kim, C.K., and Lim, K.B. (2014). RNA interference (RNAi) induced gene silencing: a promising approach of hi-tech plant breeding. International Journal of Biological Sciences **10**, 1150-1158.

Yu, Q.H., Wang, B., Li, N., Tang, Y., Yang, S., Yang, T., Xu, J., Guo, C., Yan, P., Wang, Q., and Asmutola, P. (2017). CRISPR/Cas9-induced targeted mutagenesis and gene replacement to generate long-shelf life tomato lines. Scientific Reports **7**, 1-9.

Yuan, J.S., Galbraith, D.W., Dai, S.Y., Griffin, P., and Stewart, C.N., Jr. (2008). Plant systems biology comes of age. Trends in Plant Science **13**, 165-171.

Yuan, X.-Y., Wang, R.-H., Zhao, X.-D., Luo, Y.-B., and Fu, D.-Q. (2016). Role of the tomato non-ripening mutation in regulating fruit quality elucidated using iTRAQ protein profile analysis. PLoS One **11**, 1-21.

Zaharah, S.S., Singh, Z., Symons, G.M., and Reid, J.B. (2012). Role of brassinosteroids, ethylene, abscisic acid, and indole-3-acetic acid in mango fruit ripening. Journal of Plant Growth Regulation **31**, 363-372.

Zaharah, S.S., Singh, Z., Symons, G.M., and Reid, J.B. (2013). Mode of action of abscisic acid in triggering ethylene biosynthesis and softening during ripening in mango fruit. Postharvest Biology and Technology **75**, 37-44.

Zanor, M.I., Osorio, S., Nunes-Nesi, A., Carrari, F., Lohse, M., Usadel, B., Kuhn, C., Bleiss, W., Giavalisco, P., Willmitzer, L., Sulpice, R., Zhou, Y.H., and Fernie, A.R. (2009). RNA interference of LIN5 in tomato confirms its role in controlling Brix content, uncovers the influence of sugars on the levels of fruit hormones, and demonstrates the importance of sucrose cleavage for normal fruit development and fertility. Plant Physiology **150**, 1204-1218.

Zegzouti, H., Jones, B., Frasse, P., Marty, C., Maitre, B., Latch, A., Pech, J.C., and Bouzayen, M. (1999). Ethylene-regulated gene expression in tomato fruit: characterization of novel ethylene-responsive and ripening-related genes isolated by differential display. Plant Journal **18**, 589-600.

Zhang, C., Tanabe, K., Tani, H., Nakajima, H., Mori, M., and Sakuno, E. (2007). Biologically active gibberellins and abscisic acid in fruit of two late-maturing Japanese pear cultivars with contrasting fruit size. Journal of the American Society for Horticultural Science **132**, 452-458.

Zhang, H., He, H., Wang, X., Wang, X., Yang, X., Li, L., and W Deng, X. (2011a). Genome-wide mapping of the HY5-mediated genenetworks in *Arabidopsis* that involve both transcriptional and post-transcriptional regulation. Plant Journal **65**, 346-358.

Zhang, L., Zhu, M., Ren, L., Li, A., Chen, G., and Hu, Z. (2018a). The SlFSR gene controls fruit shelf-life in tomato. Journal of Experimental Botany **69**, 2897-2909.

Zhang, M., Leng, P., Zhang, G., and Li, X. (2009a). Cloning and functional analysis of 9-cis-epoxycarotenoid dioxygenase (NCED) genes encoding a key enzyme during abscisic acid biosynthesis from peach and grape fruits. Plant Physiology **166**, 1241-1252.

Zhang, M., Yuan, B., and Leng, P. (2009b). The role of ABA in triggering ethylene biosynthesis and ripening of tomato fruit. Journal of Experimental Botany **60**, 1579-1588.

Zhang, Y.-J., Wang, X.-J., Wu, J.-X., Chen, S.-Y., Chen, H., Chai, L.-J., and Yi, H.-L. (2015). Comparative transcriptome analyses between a spontaneous late-ripening sweet orange mutant and its wild type suggest the functions of ABA, sucrose and JA during citrus fruit ripening. PLoS One **9**, 1-27.

Zhang, Y., Butelli, E., De Stefano, R., Schoonbeek, H.-j., Magusin, A., Pagliarani, C., Wellner, N., Hill, L., Orzaez, D., Granell, A., Jones, Jonathan D., and Martin, C. (2013). Anthocyanins double the shelf life of tomatoes by delaying overripening and reducing susceptibility to gray mold. Current Biology **23**, 1094-1100.

Zhang, Y., Chou, S.D., Murshid, A., Prince, T.L., Schreiner, S., Stevenson, M.A., and Calderwood, S.K. (2011b). The role of heat shock factors in stress-induced transcription. Methods in Molecular Biology **787**, 21-32.

Zhang, Y., Li, Q., Jiang, L., Kai, W., Liang, B., Wang, J., Du, Y., Zhai, X., Wang, J., Zhang, Y., Sun, Y., Zhang, L., and Leng, P. (2018b). Suppressing type 2C protein phosphatases alters fruit ripening and the stress response in tomato. Plant and Cell Physiology **59**, 142-154.

Zhao, X., Yuan, X., Chen, S., Meng, L., and Fu, D. (2018). Role of the tomato TAGL1 gene in regulating fruit metabolites elucidated using RNA sequence and metabolomics analyses. PLoS One **13**, 1-14.

Zhong, S., Lin, Z., and Grierson, D. (2008). Tomato ethylene receptor–CTR interactions: visualization of NEVER-RIPE interactions with multiple CTRs at the endoplasmic reticulum. Journal of Experimental Botany **59**, 965-972.

Zhou, X., Welsch, R., Yang, Y., Alvarez, D., Riediger, M., Yuan, H., Fish, T., Liu, J., Thannhauser, T.W., and Li, L. (2015). *Arabidopsis* OR proteins are the major posttranscriptional regulators of phytoene synthase in controlling carotenoid

biosynthesis. Proceedings of the National Academy of Sciences USA **112**, 3558-3563.

Zhou, Z., Sun, L., Zhao, Y., An, L., Yan, A., Meng, X., and Gan, Y. (2013). Zinc Finger Protein 6 (ZFP6) regulates trichome initiation by integrating gibberellin and cytokinin signaling in *Arabidopsis thaliana*. New Phytologist **198**, 699-708.

Zhu, C., Naqvi, S., Capell, T., and Christou, P. (2009). Metabolic engineering of ketocarotenoid biosynthesis in higher plants. Archives of Biochemistry and Biophysics **483**, 182-190.

Zhu, C., Sanahuja, G., Yuan, D., Farré, G., Arjó, G., Berman, J., Zorrilla-López, U., Banakar, R., Bai, C., Pérez-Massot, E., Bassie, L., Capell, T., and Christou, P. (2013). Biofortification of plants with altered antioxidant content and composition: genetic engineering strategies. Plant Biotechnology Journal **11**, 129-141.

Zoratti, L., Karppinen, K., Luengo Escobar, A., Haggman, H., and Jaakola, L. (2014). Light-controlled flavonoid biosynthesis in fruits. Frontiers in Plant Science **5**, 1-16.

Zubo, Y.O., Yamburenko, M.V., Selivankina, S.Y., Shakirova, F.M., Avalbaev, A.M., Kudryakova, N.V., Zubkova, N.K., Liere, K., Kulaeva, O.N., Kusnetsov, V.V., and Borner, T. (2008). Cytokinin stimulates chloroplast transcription in detached barley leaves. Plant Physiology **148**, 1082-1093.